EMERGING INFECTIOUS DISEASES®

CDC
CENTERS FOR DISEASE CONTROL AND PREVENTION

High-Consequence Pathogens

April 2021

Johan Christian Dahl (1788–1857), Eruption of the Volcano Vesuvius, 1821. *Oil on canvas, 38.7 in × 54.1 in/98.3 cm × 137.5 cm.*
Public domain digital image courtesy of National Gallery of Denmark, Sølvgade 48–50, 1307 Copenhagen, Denmark.

EMERGING INFECTIOUS DISEASES®

Emerging Infectious Diseases is published monthly by the Centers for Disease Control and Prevention, 1600 Clifton Rd NE, Mailstop H16-2, Atlanta, GA 30329-4027, USA. Telephone 404-639-1960; email, eideditor@cdc.gov

EMERGING INFECTIOUS DISEASES®

High-Consequence Pathogens **April 2021**

On the Cover

Johan Christian Dahl (1788–1857), *Eruption of the Volcano Vesuvius,* 1821. Oil on canvas, 38.7 in × 54.1 in/98.3 cm × 137.5 cm. Public domain digital image courtesy of National Gallery of Denmark, Sølvgade 48–50, 1307 Copenhagen, Denmark.

About the Cover p. 1253

Synopses

Medscape EDUCATION ACTIVITY

Blastomycosis Surveillance in 5 States, United States, 1987–2018

The median time from symptom onset to diagnosis and the severity of illness suggest that surveillance underestimates the true number of cases.

K. Benedict et al. **999**

Reemergence of Human Monkeypox and Declining Population Immunity in the Context of Urbanization, Nigeria, 2017–2020

P.-Y. Nguyen et al. **1007**

Animal Reservoirs and Hosts for Emerging Alphacoronavirsuses and Betacoronaviruses

R.R. Ghai et al. **1015**

Difficulties in Differentiating Coronaviruses from Subcellular Structures in Human Tissues by Electron Microscopy

H.A. Bullock et al. **1023**

Characteristics of SARS-CoV-2 Transmission among Meat Processing Workers in Nebraska, USA, and Effectiveness of Risk Mitigation Measures

J.J. Herstein et al. **1032**

Medscape EDUCATION ACTIVITY

Systematic Review of Reported HIV Outbreaks, Pakistan, 2000–2019

In the absence of robust testing programs, timely and detailed outbreak reports are essential for HIV control.

E.M. Rabold et al. **1040**

Research

Medscape EDUCATION ACTIVITY

Infections with Tickborne Pathogens after Tick Bite, Austria, 2015–2018

Knowledge about outcomes of tick bites is crucial because infections with emerging pathogens might be underestimated.

M. Markowicz et al. **1048**

EMERGING INFECTIOUS DISEASES®
April 2021

Dispatches

Venezuelan Equine Encephalitis Complex Alphavirus in Bats, French Guiana
C. Fischer et al. **1141**

Stability of SARS-CoV-2 RNA in Nonsupplemented Saliva
I.M. Ott et al. **1146**

Rare Norovirus GIV Foodborne Outbreak, Wisconsin, USA
L. Barclay et al. **1151**

Persistence of SARS-CoV-2 N-Antibody Response in Healthcare Workers, London, UK
M. Shrotri et al. **1155**

Analysis of Asymptomatic and Presymptomatic Transmission in SARS-CoV-2 Outbreak, Germany, 2020
J.K. Bender et al. **1159**

Characteristics and Risk Factors of Hospitalized and Nonhospitalized COVID-19 Patients, Atlanta, Georgia, USA, March–April 2020
K. Pettrone et al. **1164**

Improving Treatment and Outcomes for Melioidosis in Children, Northern Cambodia, 2009–2018
A. Chandna et al. **1169**

Eastern Equine Encephalitis Virus in Mexican Wolf Pups at Zoo, Michigan, USA
K.A. Thompson et al. **1173**

Genomic Analysis of Novel Poxvirus Brazilian Porcupinepox Virus, Brazil, 2019
A.S. Hora et al. **1177**

Emergence of *Burkholderia pseudomallei* Sequence Type 562, Northern Australia
E.M. Muemann et al. **1057**

Histopathological Characterization of Cases of Spontaneous Fatal Feline Severe Fever with Thrombocytopenia Syndrome, Japan
Y. Sakai et al. **1068**

COVID-19–Associated Pulmonary Aspergillosis, March–August 2020
J. Salmanton-García et al. **1077**

Genomic Surveillance of a Globally Circulating Distinct Group W Clonal Complex 11 Meningococcal Variant, New Zealand, 2013–2018
Z. Yang et al. **1087**

Dynamic Public Perceptions of the Coronavirus Disease Crisis, the Netherlands, 2020
M. de Vries et al. **1098**

Evolution of Sequence Type 4821 Clonal Complex Hyperinvasive and Quinolone-Resistant Meningococci
M. Chen et al. **1110**

Epidemiologic and Genomic Reidentification of Yaws, Liberia
J.W.S. Timothy et al. **1123**

Sexual Contact as Risk Factor for *Campylobacter* Infection
K.G. Kuhn et al. **1133**

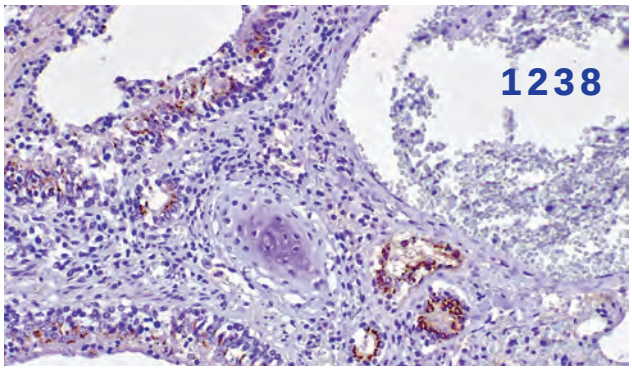

EMERGING INFECTIOUS DISEASES®
April 2021

Highly Pathogenic Avian Influenza Clade 2.3.4.4 Subtype H5N6 Viruses Isolated from Wild Whooper Swans, Mongolia, 2020
S. Jeong et al. **1181**

Increased SARS-Cov-2 Testing Capacity with Pooled Saliva Samples
A.E. Watkins et al. **1184**

SARS-CoV-2 Seropositivity among US Marine Recruits Attending Basic Training, United States, Spring–Fall 2020
A.G. Letizia et al. **1188**

Experimental SARS-CoV-2 Infection of Bank Voles
L. Ulrich et al. **1193**

Surveillance of COVID-19–Associated Multisystem Inflammatory Syndrome in Children, South Korea
Y.J. Choe et al. **1196**

Low-Level Middle East Respiratory Syndrome Coronavirus among Camel Handlers, Kenya, 2019
P.M. Munyua et al. **1201**

Emergence and Polyclonal Dissemination of OXA-244–Producing *Escherichia coli*, France
C. Emeraud et al. **1206**

Fatal Case of Crimean-Congo Hemorrhagic Fever Caused by Reassortant Virus, Spain, 2018
A. Negredo et al. **1211**

High Case-Fatality Rate for Human Anthrax, Northern Ghana, 2005–2016
J.K. Blackburn et al. **1216**

Postvaccination COVID-19 among Healthcare Workers, Israel
S. Amit et al. **1220**

Genomic Characterizations of Clade III Lineage of *Candida auris*, California, USA
T.K. Price et al. **1223**

Research Letters

Inguinal Ulceroglandular Tularemia Caused by *Francisella tularensis* Subspecies *holarctica*, Canada
C. Boodman et al. **1228**

Risk for Fomite-Mediated Transmission of SARS-CoV-2 in Child Daycares, Schools, Nursing Homes, and Offices
A.N.M. Kraay et al. **1229**

Tula Virus as Causative Agent of Hantavirus Disease in Immunocompetent Person, Germany
J. Hofmann et al. **1232**

Rapid Spread and Control of Multidrug-Resistant Gram-Negative Bacteria in COVID-19 Patient Care Units
A. Patel et al. **1234**

Cetacean Morbillivirus and *Toxoplasma gondii* Co-Infection in Mediterranean Monk Seal Pup, Italy
A. Petrella et al. **1237**

Increased Likelihood of Detecting Ebola Virus RNA in Semen by Using Sample Pelleting
C.M. Bozman et al. **1239**

Polytesistant *Mycobacterium bovis* Infection in Human and Sympatric Sheep, Spain, 2017–2018
B. Pérez de Val et al. **1241**

Novel SARS-CoV-2 Variant in Travelers from Brazil to Japan
T. Fujino et al. **1243**

Isolation of *Rickettsia rickettsii in* Rocky Mountain Spotted Fever Outbreak, Panama
Y. Zaldívar et al. **1245**

Co-infection with Severe Fever with Thrombocytopenia Syndrome Virus and *Rickettsia japonica* after Tick Bite
T. Fujikawa et al. **1247**

Imported SARS-CoV-2 Variant P.1 in Traveler Returning from Brazil to Italy
F. Maggi et al. **1249**

Books and Media

Understanding Coronavirus
X. Yin, N.M. Hackman **1252**

About the Cover

An Interesting and Horribly Wondrous Sight
B. Breedlove **1253**

Etymologia

Treponema
F.C. Pogliani, R.D. Ollhoff **1006**

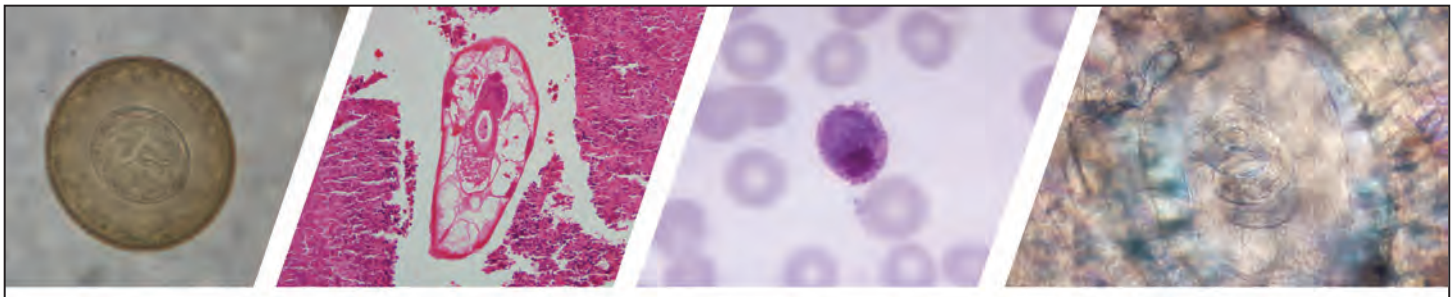

DPDx

Diagnostic Assistance and Training in Laboratory Identification of Parasites

A free service of CDC available to laboratorians, pathologists, and other health professionals in the United States and abroad

- Diagnosis from photographs of worms, histological sections, fecal, blood, and other specimen types
- Expert diagnostic review
- Formal diagnostic laboratory report
- Submission of samples via secure file share

Visit the DPDx website for information on laboratory diagnosis, geographic distribution, clinical features, parasite life cycles, and training via Monthly Case Studies of parasitic diseases.

www.cdc.gov/dpdx
dpdx@cdc.gov

U.S. Department of Health and Human Services
Centers for Disease Control and Prevention

CS272346-DE

Blastomycosis Surveillance in 5 States, United States, 1987–2018

Kaitlin Benedict, Suzanne Gibbons-Burgener, Anna Kocharian, Malia Ireland, Laura Rothfeldt, Natalie Christophe, Kimberly Signs, Brendan R. Jackson

Medscape EDUCATION ACTIVITY

In support of improving patient care, this activity has been planned and implemented by Medscape, LLC and Emerging Infectious Diseases. Medscape, LLC is jointly accredited by the Accreditation Council for Continuing Medical Education (ACCME), the Accreditation Council for Pharmacy Education (ACPE), and the American Nurses Credentialing Center (ANCC), to provide continuing education for the healthcare team.

Medscape, LLC designates this Journal-based CME activity for a maximum of 1.00 ***AMA PRA Category 1 Credit(s)™***. Physicians should claim only the credit commensurate with the extent of their participation in the activity.

Successful completion of this CME activity, which includes participation in the evaluation component, enables the participant to earn up to 1.0 MOC points in the American Board of Internal Medicine's (ABIM) Maintenance of Certification (MOC) program. Participants will earn MOC points equivalent to the amount of CME credits claimed for the activity. It is the CME activity provider's responsibility to submit participant completion information to ACCME for the purpose of granting ABIM MOC credit.

All other clinicians completing this activity will be issued a certificate of participation. To participate in this journal CME activity: (1) review the learning objectives and author disclosures; (2) study the education content; (3) take the post-test with a 75% minimum passing score and complete the evaluation at http://www.medscape.org/journal/eid; and (4) view/print certificate. For CME questions, see page 1255.

Release date: March 17, 2021; Expiration date: March 17, 2022

Learning Objectives

Upon completion of this activity, participants will be able to:

- Describe epidemiologic features of blastomycosis, according to an analysis of combined 1987–2018 surveillance data from the 5 states where it is reportable
- Determine clinical features of blastomycosis, according to an analysis of combined 1987–2018 surveillance data from the 5 states where it is reportable
- Identify public health and clinical implications of the epidemiologic and clinical features of blastomycosis, according to an analysis of combined 1987–2018 surveillance data from the 5 states where it is reportable

CME Editor

Amy J. Guinn, BA, MA, Copyeditor, Emerging Infectious Diseases. *Disclosure: Amy J. Guinn, BA, MA, has disclosed no relevant financial relationships.*

CME Author

Laurie Barclay, MD, freelance writer and reviewer, Medscape, LLC. *Disclosure: Laurie Barclay, MD, has disclosed no relevant financial relationships.*

Authors

Disclosures: ***Kaitlin Benedict, MPH; Suzanne Gibbons-Burgener, DVM, PhD; Anna Kocharian, MS; Malia Ireland, DVM, MPH; Laura K. Rothfeldt, DVM; Natalie Christophe, MPH; Kimberly Signs, BS, DVM;*** *and* ***Brendan R. Jackson, MD, MPH,*** *have disclosed no relevant financial relationships.*

Author affiliations: Centers for Disease Control and Prevention, Atlanta, Georgia, USA (K. Benedict, B.R. Jackson); Wisconsin Department of Health Services, Madison, Wisconsin, USA (S. Gibbons-Burgener, A. Kocharian); Minnesota Department of Health, St. Paul, Minnesota, USA (M. Ireland); Arkansas Department of Health, Little Rock, Arkansas, USA (L. Rothfeldt); Louisiana Department of Health, Lafayette, Louisiana, USA (N. Christophe); Michigan Department of Health and Human Services, Lansing, Michigan, USA (K. Signs)

DOI: https://doi.org/10.3201/eid2704.204078

Blastomycosis is caused by inhalation of *Blastomyces* spp. fungi. Limited data are available on the incidence and geographic range of blastomycosis in the United States. To better characterize its epidemiologic features, we analyzed combined surveillance data from the 5 states in which blastomycosis is reportable: Arkansas, Louisiana, Michigan, Minnesota, and Wisconsin. Surveillance identified 4,441 cases during 1987–2018, a mean of 192 cases per year. The mean annual incidence was <1 case/100,000 population in most areas but >20 cases/100,000 population in some northern counties of Wisconsin. Median patient age was 46 years, 2,892 (65%) patients were male, 1,662 (57%) were hospitalized, and 278 (8%) died. The median time from symptom onset to diagnosis was 33 days. The severity of illness and diagnostic delays suggest that surveillance underestimates the true number of cases. More in-depth surveillance in additional states could elucidate blastomycosis incidence and inform efforts to increase awareness.

Blastomycosis is a fungal infection caused primarily by inhalation of the environmental fungi *Blastomyces dermatitidis* and *B. gilchristii*. The incubation period varies from 2 to 15 weeks, and the clinical spectrum ranges from asymptomatic to life-threatening infections involving acute respiratory distress syndrome or extrapulmonary dissemination (*1*,*2*). Most identified cases involve pulmonary infection that manifests similarly to other causes of pneumonia (*1*,*2*). The clinical similarities between blastomycosis and other pulmonary infections often result in diagnostic delays and unnecessary empiric antimicrobial drug treatment for suspected bacterial pneumonia (*3*). Because acute illnesses can self-resolve before diagnosis, and because physician awareness of this generally uncommon disease probably is low in most parts of the United States, many blastomycosis cases likely go undetected.

In the United States, most blastomycosis cases are thought to occur in the midwestern, south-central, and southeastern states, in areas surrounding the Ohio and Mississippi River valleys, the Great Lakes, and the Saint Lawrence River. Cases also occur outside these regions, indicating that the infection's true range is broader than generally appreciated (*4*,*5*). *Blastomyces* spp. appear to have an affinity for moist soil and decomposing plant matter, but much remains unknown about its precise environmental niche (*6*,*7*). The fungus is difficult to isolate from the environment, making investigation of potential sources challenging.

Public health surveillance for blastomycosis in the United States is limited because it is currently reportable in only 5 US states: Arkansas, Louisiana, Michigan, Minnesota, and Wisconsin. Blastomycosis is not nationally notifiable, so the Centers for Disease Control and Prevention does not routinely receive case reports from states where it is reportable. Nevertheless, surveillance data represent some of the most comprehensive information about blastomycosis. Before the Council of State and Territorial Epidemiologists (CSTE) approved a standardized surveillance case definition in 2019 (*8*), state health departments used different case definitions (Appendix, https://wwwnc.cdc.gov/EID/article/27/4/20-4078-App1.pdf). However, state surveillance generally collected similar demographic, clinical, and laboratory data elements, enabling comparisons across states. We summarized available blastomycosis surveillance data to assess the overall burden of disease, geographic patterns and temporal trends, and factors associated with poor clinical outcomes.

Methods

We combined deidentified data on blastomycosis cases reported in Arkansas during January 1995–May 2018, Louisiana during January 1987–October 2018, Michigan during January 2007–December 2017, Minnesota during January 1999–December 2018, and Wisconsin during January 1990–December 2017. We also used the Louisiana Hospital Inpatient Discharge Database to identify additional cases among hospitalized patients in Louisiana during 1999–2014.

We included data elements that were collected by ≥3 states. We considered event date as the earliest date associated with the case; for example, symptom onset, or first healthcare visit, laboratory test order, or public health report. We considered all laboratory tests recorded as positive for blastomycosis to be positive, even without an explicitly stated qualitative or quantitative result. Negative blastomycosis test results were not routinely available; therefore, we did not include these in the analysis.

We used patients' state and county of residence to calculate annual state-specific incidence and county-level mean annual incidence per 100,000 persons by using yearly population estimates from the US Census Bureau, Population Division, Vintage 2015 Special Tabulation (https://www.census.gov). We used χ^2, Fisher exact, and *t*-tests to identify factors independently associated with hospitalization or death, the Cochran-Armitage test for trends in the proportion of patients who were hospitalized or died, and negative binomial regression to assess incidence trends, and we considered $p<0.05$ statistically significant. We also compared demographic features and outcomes among cases associated with outbreaks (outbreak cases) and those not associated with outbreaks

(nonoutbreak cases) for Minnesota and Wisconsin, the 2 states that reported outbreaks during the surveillance periods we examined. Human subjects review by the Centers for Disease Control and Prevention determined this project to be consistent with nonresearch public health surveillance.

Results

Descriptive Analysis

Data were available for 4,441 cases: 348 from Arkansas, 296 from Louisiana, 186 from Michigan, 671 from Minnesota, and 2,904 from Wisconsin. Most (2,892 [65%]) patients were male, and the median age was 46 years (range 0–97, interquartile range [IQR] 31–59) (Table 1). Most (64%, n = 2,778) cases were among persons of White race, 17% (740) were among persons of unknown race, 9% (406) were among persons of Black or African American races, and 5% (193) were among Asian, Native Hawaiian, or other Pacific Islander races. Most (2,828 [71%]) patients were not Hispanic or Latino; ethnicity was unknown for 1,015 (26%) patients.

Symptom data were available for 2,005 patients from Michigan, Minnesota, and Wisconsin beginning in 2005. The most common symptoms were cough in 79% (range by state 51%–83%) of patients, fever in 61% (range by state 38%–69%), shortness of breath in 55% (range by state 44%–85%), and weight loss in 54% (range by state 29%–62%).

Among 2,912 patients with hospitalization data, 57% (1,662) were hospitalized. The median length of hospitalization was 7 days (range 1–379 days, IQR 4–15 days; n = 1,231). Among 3,385 patients with mortality data, 278 (8%) died. The proportion of hospitalized patients did not change significantly during 2007–2017 (p = 0.252), but the proportion of patients who died increased from 9.9% to 12.4% (p = 0.017).

Data on positive blastomycosis laboratory tests were consistently available from Arkansas, Michigan, and Minnesota (Table 2). Among 1,241 reported cases from the 3 states, the most common test types were culture among 835 (67%) cases and microscopy among 333 (27%) cases. Less commonly reported tests included positive antigen tests for 206 (17%) cases and antibody tests for 59 (5%) cases.

Among 777 patients with available data, the median time from symptom onset to diagnosis was 33 days (range 1–2,996 days; IQR 16–75 days). We did not observe clear seasonal patterns by event month. Minnesota had 32 (5%) outbreak cases and Wisconsin had 181 (6%) outbreak cases. Outbreak cases were more frequent among younger persons (median age 25 years) than nonoutbreak cases (median age 45 years; p = 0.0092). Outbreak cases also more often occurred among female persons (41% vs. 34% of nonoutbreak cases; p = 0.0365) and non-White persons (28% vs. 19% of nonoutbreak cases; p = 0.002). In addition, persons with outbreak cases were less likely to be hospitalized (45% vs. 58% of nonoutbreak cases; p = 0.003) or to have died (2% vs. 9% of nonoutbreak cases; p = 0.001).

Bivariable Analysis

Age; female sex; non-White race; and positive antigen, culture, and microscopy tests had statistically significant associations with hospitalization (Table 3). The median age among hospitalized patients was 46 years compared with 44 years for nonhospitalized patients (p = 0.015). Female patients were more likely to be hospitalized (relative risk [RR] 1.13; 95% CI 1.06–1.21) than male patients. Persons of non-White races were more likely to be hospitalized (RR 1.13; 95% CI 1.05–1.21) than persons of White race. Patients with positive antigen tests (RR 1.25; 95% CI 1.13–1.37), positive culture (RR 1.28; 95% CI 1.20–1.36), and positive microscopy (RR 1.32; 95% CI 1.23–1.43) were more likely to be hospitalized than patients without positive results for those laboratory tests. Factors significantly associated with death were older age (median 61 years vs. 44 years; p<0.001) and positive microscopy test (RR 1.76; 95% CI 1.34–2.38).

Table 1. Patient characteristics of blastomycosis cases reported to public health, Arkansas, Louisiana, Michigan, Minnesota, and Wisconsin, USA, 1987–2018*

Characteristic	Value
Median age, y (range; IQR), n = 4,390	46 (0–97; 31–59)
Mean age, y, n = 4,390	45.3
Sex, n = 4,441	
M	2,892 (65.1)
F	1,533 (34.5)
Unknown	16 (0.4)
Race, n = 4,316	
White	2,778 (64.4)
Black or African American	406 (9.4)
Asian, Native Hawaiian, other Pacific Islander	193 (4.5)
American Indian or Alaska Native	152 (3.5)
Other or multiple races	47 (1.1)
Unknown	740 (17.2)
Ethnicity, n = 3,984	
Not Hispanic or Latino	2,828 (71.0)
Hispanic or Latino	141 (3.5)
Unknown	1,015 (25.5)
Hospitalized, n = 2,912	
Y	1,662 (57.1)
N	1,250 (42.9)
Died, n = 3,385	
Y	278 (8.2)
N	3,107 (91.8)

*Values are no. (%) except as indicated. IQR, interquartile range.

Incidence

During years for which data were available from all 5 states, 2007–2017, surveillance detected 2,111 cases, a mean of 192 cases per year. In Arkansas, incidence declined from 1.3 cases/100,000 population in 1995 to 0.4 cases/100,000 population in 2017 (p<0.001) (Figure 1). Incidence was stable during each state's surveillance period in Louisiana, Michigan, and Minnesota. Mean annual incidence was 0.2 cases/100,000 population in Louisiana, 0.2 cases/100,000 population in Michigan, and 0.6 cases/100,000 population in Minnesota. In Wisconsin, incidence peaked at >3 cases/100,000 population during 2006, 2010, and 2015. Mean annual county-level incidence in Wisconsin was highest in Menominee (42.1 cases/100,000 population), Lincoln (28.4 cases/100,000 population), and Vilas (26.5/100,000 population) counties (Figure 2).

Discussion

We summarize blastomycosis surveillance data from 5 states and provide a broad update on the basic epidemiology of this enigmatic and underrecognized disease. Many patients experienced severe outcomes and diagnostic delays. Our results show that blastomycosis is underdetected, even in states where it is reportable, and that more standardized and in-depth surveillance, ideally in additional states, would help public health professionals better identify highest-risk groups and emerging areas for targeted prevention messaging.

Blastomycosis often results in severe illness, even in previously healthy persons (*9*), but this observation might be influenced by underdetection of asymptomatic or milder, self-resolving disease. The high hospitalization rate of 57% noted in this analysis demonstrates that blastomycosis surveillance detects severe cases, which is typical for passive disease surveillance. We found an annual mean of <200 cases/year; a hospitalization rate of 57% suggests that ≈110 patients are hospitalized each year from states where blastomycosis is reportable. In contrast, ≈1,000 blastomycosis-associated hospitalizations occur nationwide (*10*,*11*), showing that the limited surveillance likely underdetects cases nationally.

Table 2. Positive laboratory tests among 1,241 blastomycosis cases reported to public health, Arkansas, Michigan, and Minnesota, United States, 1995–2018

Test type	No. (%)
Antibody	59 (4.8)
Immunodiffusion	18 (1.5)
Complement fixation	7 (0.6)
Enzyme immunoassay	30 (2.4)
Unspecified antibody test	17 (1.4)
Antigen	206 (16.6)
Confirmatory test	965 (77.8)
Culture	835 (67.3)
Microscopy*	333 (26.8)
DNA probe	40 (3.2)
PCR	2 (0.2)
Unspecified test type	166 (13.4)
Specimen type	
Culture	769 (100)
Bronchial specimen	372 (48.4)
Sputum	180 (23.4)
Other tissue besides lung	121 (15.7)
Lung tissue	21 (2.7)
Multiple specimen types	14 (1.8)
Other	61 (7.9)
Microscopy	342 (100)
Bronchoalveolar lavage	110 (32.2)
Sputum	78 (22.8)
Other tissue besides lung	52 (15.2)
Lung tissue	47 (13.7)
Multiple specimen types	24 (7.0)
Other	31 (9.1)

*Includes smear, histopathology, and unspecified microscopy tests.

The average time of >1 month from symptom onset to diagnosis indicates delays in seeking healthcare, delays in diagnosis, or both. This time interval is consistent with a previous report describing a median of 23 days between examination at a healthcare facility and a median of 2.5 courses of antibacterial medications for presumed bacterial infection before pulmonary blastomycosis was correctly diagnosed (*3*). Earlier diagnosis might reduce unnecessary antibacterial drug use, time, and resources invested in searching for alternative diagnoses and could potentially improve patient outcomes. Therefore, greater public and provider education about blastomycosis is needed, especially in areas where blastomycosis is less commonly recognized.

The high proportion of patients with positive confirmatory laboratory tests, such as culture and

Table 3. Factors associated with hospitalization or death among blastomycosis cases reported to public health, Arkansas, Louisiana, Michigan, Minnesota, and Wisconsin, United States, 1987–2018*

	Hospitalization		Death	
Characteristic	RR (95% CI)	p value	RR (95% CI)	p value
Older age	NA	0.015	NA	<0.001
Female sex	1.13 (1.05–1.21)	<0.001	1.05 (0.83–1.33)	0.681
Non-White race	1.13 (1.05–1.21)	0.002	1.08 (0.82–1.42)	0.588
Antigen test†	1.25 (1.13–1.37)	<0.001	1.27 (0.84–1.92)	0.255
Culture†	1.28 (1.20–1.36)	<0.001	1.02 (0.79–1.33)	0.864
Microscopy†	1.32 (1.23–1.43)	<0.001	1.76 (1.34–2.38)	<0.001

*NA, not applicable; RR, relative risk.
†Arkansas, Michigan, and Minnesota only.

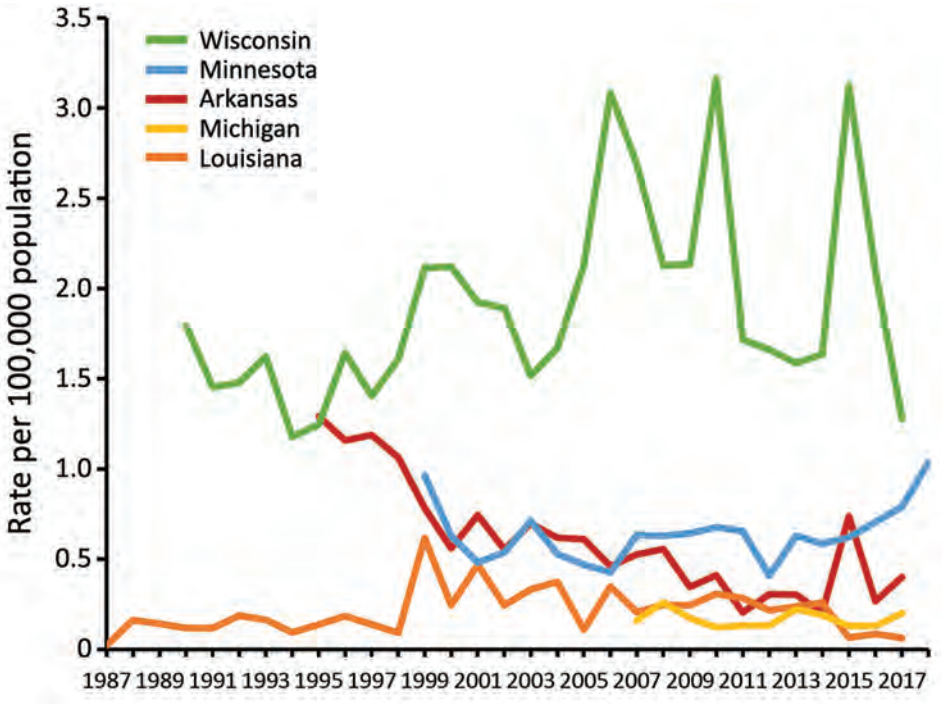

Figure 1. Annual state-specific incidence (no. cases/100,000 population) among 5 states in which blastomycosis is reportable, United States, 1987–2018. Cases reported during 2018 in Arkansas and Louisiana were excluded because data were not available for the entire year.

microscopy, likely reflects detection of more severe cases because serologic tests for blastomycosis offer only presumptive evidence of infection (*12*), and serologic tests were not included in most states' case definitions (Appendix). The associations between older age and confirmatory test types with hospitalization point to severe illness, and are unsurprising; however, why women were more likely to be hospitalized is unclear but could be related to delayed diagnosis or underdiagnosis of less severe disease in women. More blastomycosis hospitalizations typically occur among men (*10*,*13*), although a recent study found female sex was independently associated with death in blastomycosis patients with acute respiratory distress syndrome (*14*). The increased risk for hospitalization among persons of non-White races lends further evidence to the existence of blastomycosis-related health disparities, as previously suspected (*15*–*17*). Further studies could help determine whether these differences are related to genetic predisposition (*18*), involvement in outdoor activities resulting in exposures to *Blastomyces*, or access to medical care (*19*).

Reliance on often invasive and time-consuming tests such as culture and microscopy for diagnosis likely is a key factor in underdiagnosis of blastomycosis because these tests might not be ordered until tests for other diseases have been negative. Accordingly, most specimen types in our analysis were from bronchoalveolar lavage and lung and other tissue, which likely required biopsy. Given the prolonged time to diagnosis we identified, improved noninvasive diagnostic methods with high sensitivity and specificity for blastomycosis are needed for earlier and more frequent testing, which could prevent hospitalizations and deaths.

Consistent with previous reports, Wisconsin had the highest number of cases and incidence of the 5 states where blastomycosis is reportable, with mean annual incidence in several northern counties >20 cases/100,000 population. Peaks in incidence in Wisconsin corresponded to a known outbreak at a yard waste site in 2006 (*20*), an outbreak likely associated with multiple sources in 2010 (*21*), and an outbreak linked to recreational tubing on the Little Wolf River in 2015 (*22*). For case-patients in these outbreaks, younger age and higher likelihood of being non-White was consistent with our findings (*20*,*21*). In addition, the finding that patients with outbreak-associated cases had less severe outcomes could reflect detection of milder cases through enhanced case detection efforts during outbreak investigations. However, outbreaks comprised <6% of cases overall, suggesting that most cases occur sporadically, which also is true for histoplasmosis and coccidioidomycosis. Of note, most of northern Wisconsin is rich in soils classified as spodosols, which are characterized by high concentrations of organic matter in coarse, often sandy, particles (*23*). *Blastomyces* spp. are thought to dwell primarily in organic-rich soils. However, spodosols

also occur widely in northern Michigan, where disease incidence was not elevated, and are less common in northern Minnesota, where incidence was higher. Further study, including the role of soil types, could elucidate the natural habitat of these fungi.

For most states in this analysis, the relatively stable incidence and hospitalization rates over time were consistent with a previous analysis of blastomycosis-related hospitalizations during 2000–2011 (*10*). Another study found a decline in blastomycosis-associated deaths nationwide during 1990–2010 (*15*); the reasons for the increase in deaths we observed during 2007–2017 are unclear but could reflect improvements in case follow-up, a decline in reporting of less severe cases, or other surveillance changes over time.

The limitations of our study include that pooling surveillance data based on different blastomycosis case definitions is fundamentally problematic; however, few other data sources would enable analyses of thousands of cases, which is helpful for studying this uncommon disease. Furthermore, some states' case definitions changed over time. Although blastomycosis was reportable in each state during the years included in this analysis, Arkansas did not have a formal case definition, and Michigan did not have one until 2012. Wisconsin classified all cases as confirmed until September 2015, when their case definition changed to include confirmed and probable case classifications; for outbreaks in Wisconsin, a positive serologic blastomycosis test plus an epidemiologic link was sufficient to be considered a case. Moving forward, the standardized blastomycosis case definition from the Council of State and Territorial Epidemiologists will enable more robust comparisons between states and stratification of confirmed and probable cases.

Combining data from different times in each state is an additional potential limitation. Some states'

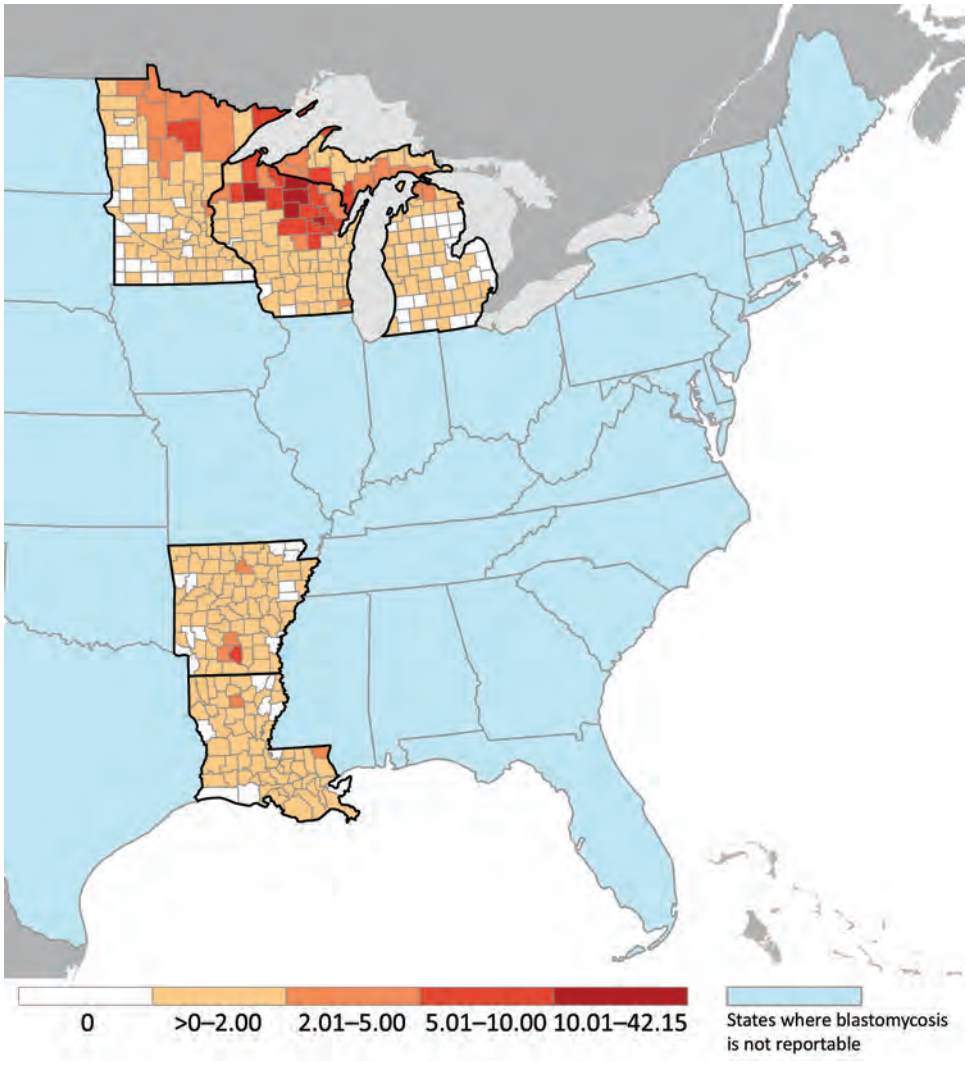

Figure 2. Mean annual county-specific incidence (no. cases/100,000 population) among 5 states in which blastomycosis is reportable, United States, 1987–2018. Cases reported during 2018 in Arkansas and Louisiana were excluded because data were not available for the entire year.

surveillance systems underwent changes during the analysis period; for example, data elements were added or removed, resulting in inconsistent denominators in the pooled analysis. For certain variables, such as race and ethnicity, missing data or values of "unknown" were common and demonstrate that information can be challenging to obtain because substantial time and resources often are needed to conduct case investigations (*24*). Data about environmental exposures, immunocompromised status, body site of infection, occupation, illness duration, and treatment were not available consistently from every state. Wisconsin and Minnesota conducted extensive follow-up on cases (*19*,*25*), providing deeper insight into state-specific features of blastomycosis. Collecting these types of data in a standardized way in additional states could help identify high-risk populations and activities and help inform prevention efforts.

In summary, blastomycosis remains a rarely reported but severe disease in most areas where it is under public health surveillance. Our findings indicate that blastomycosis likely is underdetected. Blastomycosis also can occur in areas outside those where it is commonly recognized (*4*) and might be emerging in new areas, such as east-central New York (*5*). Surveillance for blastomycosis in more areas and collection of more standardized, detailed data could help identify emerging geographic hotspots or clusters, new risk factors, and other epidemiologic patterns. Increased awareness among healthcare providers and the public could lead to faster diagnosis and treatment for blastomycosis patients.

Acknowledgments

We thank Jose Antonio Serrano and Stephanie McCracken for contributions to early study design and for coordinating blastomycosis data access; Racheal Odom for blastomycosis data collection; Jeff P. Davis (Wisconsin State Epidemiologist 1978–2018) for his tremendous contribution to the study of blastomycosis epidemiology and its surveillance; Nina D. Dutton for assistance with Figure 2; and Richard Bishop for coordinating access to US Census data.

About the Author

Ms. Benedict is an epidemiologist in the Mycotic Diseases Branch, Division of Foodborne, Waterborne, and Environmental Diseases, National Center for Emerging and Zoonotic Infectious Diseases, Centers for Disease Control and Prevention, Atlanta, Georgia, USA. Her research interests include the epidemiology and prevention of fungal infections.

References

1. Chapman SW, Dismukes WE, Proia LA, Bradsher RW, Pappas PG, Threlkeld MG, et al.; Infectious Diseases Society of America. Clinical practice guidelines for the management of blastomycosis: 2008 update by the Infectious Diseases Society of America. Clin Infect Dis. 2008;46:1801–12. https://doi.org/10.1086/588300
2. McBride JA, Gauthier GM, Klein BS. Clinical manifestations and treatment of blastomycosis. Clin Chest Med. 2017;38:435–49. https://doi.org/10.1016/j.ccm.2017.04.006
3. Alpern JD, Bahr NC, Vazquez-Benitez G, Boulware DR, Sellman JS, Sarosi GA. Diagnostic delay and antibiotic overuse in acute pulmonary blastomycosis. Open Forum Infect Dis. 2016;3:ofw078. https://doi.org/10.1093/ofid/ofw078
4. Benedict K, Thompson GR III, Deresinski S, Chiller T. Mycotic infections acquired outside areas of known endemicity, United States. Emerg Infect Dis. 2015;21:1935–41. https://doi.org/10.3201/eid2111.141950
5. McDonald R, Dufort E, Jackson BR, Tobin EH, Newman A, Benedict K, et al. Notes from the field: blastomycosis cases occurring outside of regions with known endemicity — New York, 2007–2017. MMWR Morb Mortal Wkly Rep. 2018;67:1077–8. https://doi.org/10.15585/mmwr.mm6738a8
6. Reed KD, Meece JK, Archer JR, Peterson AT. Ecologic niche modeling of *Blastomyces dermatitidis* in Wisconsin. PLoS One. 2008;3:e2034. https://doi.org/10.1371/journal.pone.0002034
7. McTaggart LR, Brown EM, Richardson SE. Phylogeographic analysis of *Blastomyces dermatitidis* and *Blastomyces gilchristii* reveals an association with North American freshwater drainage basins. PLoS One. 2016;11:e0159396. https://doi.org/10.1371/journal.pone.0159396
8. Council of State and Territorial Epidemiologists. Standardized surveillance case definition for blastomycosis 2019 [cited 2020 Mar 12]. https://cdn.ymaws.com/www.cste.org/resource/resmgr/2019ps/final/19-ID-02_Blastomycosis_final.pdf
9. McBride JA, Sterkel AK, Matkovic E, Broman AT, Gibbons-Burgener SN, Gauthier GM. Clinical manifestations and outcomes in immunocompetent and immunocompromised patients with blastomycosis. Clin Infect Dis. 2020;ciaa276. https://doi.org/10.1093/cid/ciaa276
10. Seitz AE, Younes N, Steiner CA, Prevots DR. Incidence and trends of blastomycosis-associated hospitalizations in the United States. PLoS One. 2014;9:e105466. https://doi.org/10.1371/journal.pone.0105466
11. Benedict K, Jackson BR, Chiller T, Beer KD. Estimation of direct healthcare costs of fungal diseases in the United States. Clin Infect Dis. 2019;68:1791–7. https://doi.org/10.1093/cid/ciy776
12. Saccente M, Woods GL. Clinical and laboratory update on blastomycosis. Clin Microbiol Rev. 2010;23:367–81. https://doi.org/10.1128/CMR.00056-09
13. Chu JH, Feudtner C, Heydon K, Walsh TJ, Zaoutis TE. Hospitalizations for endemic mycoses: a population-based national study. Clin Infect Dis. 2006;42:822–5. https://doi.org/10.1086/500405
14. Rush B, Lother S, Paunovic B, Mooney O, Kumar A. Outcomes with severe blastomycosis and respiratory failure in the United States. Clin Infect Dis. 2020;ciaa294. https://doi.org/10.1093/cid/ciaa294
15. Khuu D, Shafir S, Bristow B, Sorvillo F. Blastomycosis mortality rates, United States, 1990–2010. Emerg Infect Dis. 2014;20:1789–94. https://doi.org/10.3201/eid2011.131175
16. Lemos LB, Guo M, Baliga M. Blastomycosis: organ involvement and etiologic diagnosis. A review of 123

patients from Mississippi. Ann Diagn Pathol. 2000;4:391–406. https://doi.org/10.1053/adpa.2000.20755
17. Dworkin MS, Duckro AN, Proia L, Semel JD, Huhn G. The epidemiology of blastomycosis in Illinois and factors associated with death. Clin Infect Dis. 2005;41:e107–11. https://doi.org/10.1086/498152
18. Merkhofer RM Jr, O'Neill MB, Xiong D, Hernandez-Santos N, Dobson H, Fites JS, et al. Investigation of genetic susceptibility to blastomycosis reveals interleukin-6 as a potential susceptibility locus. MBio. 2019;10:e01224-19. https://doi.org/10.1128/mBio.01224-19
19. Gibbons-Burgener SN, Dieckman JL, Davis JP. Epidemiology of sporadic blastomycosis in Wisconsin, 2011–2015. Presented at: CSTE 2017 Annual Conference; Boise, Idaho, USA; June 4–8, 2017.
20. Pfister JR, Archer JR, Hersil S, Boers T, Reed KD, Meece JK, et al. Non-rural point source blastomycosis outbreak near a yard waste collection site. Clin Med Res. 2011;9:57–65. https://doi.org/10.3121/cmr.2010.958
21. Roy M, Benedict K, Deak E, Kirby MA, McNiel JT, Sickler CJ, et al. A large community outbreak of blastomycosis in Wisconsin with geographic and ethnic clustering. Clin Infect Dis. 2013;57:655–62. https://doi.org/10.1093/cid/cit366
22. Koske SE, Kocharian A, Kazmierczak JJ, Gibbons-Burgener SN, Dieckman JL, Klos RF, et al. Investigation of a large outbreak of blastomycosis caused by *Blastomyces gilchristii* among recreational river tubers, Wisconsin, 2015. Presented at: CSTE 2017 Annual Conference; Boise, Idaho, USA; June 4–8, 2017.
23. United States Department of Agriculture, Natural Resources Conservation Service. Spodosols map [cited 2020 Apr 22]. https://www.nrcs.usda.gov/wps/portal/nrcs/detail/soils/survey/class/maps/?cid=nrcs142p2_053608
24. McCracken S, Signs K, Stobierski M. Evaluating blastomycosis disease reporting in Michigan's disease surveillance system. Presented at: 2018 CSTE Annual Conference; West Palm Beach, Florida, USA; June 10–14, 2018.
25. Ireland M, Klumb C, Smith K, Scheftel J. Blastomycosis in Minnesota, USA, 1999–2018. Emerg Infect Dis J. 2020;26:866–75. https://doi.org/10.3201/eid2605.191074

Address for correspondence: Kaitlin Benedict, Centers for Disease Control and Prevention, 1600 Clifton Road NE, Mailstop H24-9, Atlanta, GA 30329-4027, USA; email: jsy8@cdc.gov

etymologia

Treponema [trep″o-ne′mə]

Fabio C. Pogliani,[1] Rüdiger D. Ollhoff[1]

From the Greek *trepo* (rotate, turn) and *ne¯ma* (thread), *Treponema* is a genus of gram-negative, anaerobic or microaerophilic bacteria. They are spiral-shaped and have flagella, which extend from motors at the pole, producing undulating movement through fluids, enabling tissue invasion and dissemination. In 1905, microbiologist Fritz Richard Schaudinn and dermatologist Paul Erich Hoffmann described *Treponema pallidum* subsp. *pallidum* as *Spirochaeta pallida* from a fresh human vulvar lesion.

Treponema spp. can invade the epidermis and oral, intestinal, and genital mucosa of humans and animals. They cause human diseases, such as syphilis, yaws, pinta, and bejel, and animal diseases, such as digital dermatitis. *T. phagedenis*, *T. pedis*, and *T. medium* infect mainly cattle. *T. paraluiscuniculi* can cause syphilis in rabbits.

Most *Treponema* spp. are not cultivable, except for *T. palllidum* subsp. *pallidum* and *T. phagedenis*. *T. pallidum* subsp. *pallidum* causative syphilis is a reemerging disease in industrialized countries. Digital dermatitis, a polytreponemal disease, is considered to be the major infectious claw disease in cattle worldwide.

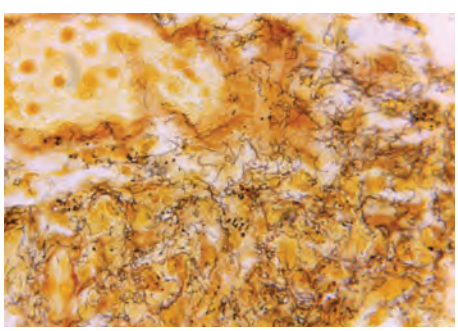

Tissue sample stained with Steiner silver stain. Image shows numerous, corkscrew-shaped, darkly-stained, *Treponema pallidum* spirochetes, which cause syphilis. Skip Van Orden, Centers for Disease Control, 1966.

Address for correspondence: Rüdiger D. Ollhoff, Programa de Pós-Graduação em Ciência Animal da Pontifícia Universidade Católica do Paraná, Rua Imaculada Conceição, 1155 Prado Velho, Curitiba 80215 901, Paraná, Brazil; email: daniel.ollhoff@pucpr.br

Sources

1. Dorland's illustrated medical dictionary. 32nd ed. Philadelphia: Elsevier Saunders; 2012.
2. Edmondson DG, Hu B, Norris SJ. Long-term in vitro culture of the syphilis spirochete *Treponema pallidum* subsp. *pallidum*. MBio. 2018;9:e01153. https://doi.org/10.1128/mBio.01153-18
3. Nally JE, Hornsby RL, Alt DP, Whitelegge JP. Phenotypic and proteomic characterization of treponemes associated with bovine digital dermatitis. Vet Microbiol. 2019;235:35–42. https://doi.org/10.1016/j.vetmic.2019.05.023
4. Oriel JD. The scars of Venus: a history of venereology. London: Springer-Verlag; 1994.
5. Šmajs D, Zobaníková M, Strouhal M, Čejková D, Dugan-Rocha S, Pospíšilová P, et al. Complete genome sequence of *Treponema paraluiscuniculi*, strain Cuniculi A: the loss of infectivity to humans is associated with genome decay. PLoS One. 2011;6:e20415. https://doi.org/10.1371/journal.pone.0020415

Author affiliations: Universidade de São Paulo, São Paulo, Brazil (F.C. Pogliani); Pontifícia Universidade Católica do Paraná, Curitiba, Brazil (R.D. Ollhoff)

DOI: https://doi.org/10.3201/eid2704.ET2704

[1]These authors contributed equally to this article.

Reemergence of Human Monkeypox and Declining Population Immunity in the Context of Urbanization, Nigeria, 2017–2020

Phi-Yen Nguyen, Whenayon Simeon Ajisegiri, Valentina Costantino, Abrar A. Chughtai, C. Raina MacIntyre

A monkeypox outbreak in Nigeria during 2017–2020 provides an illustrative case study for emerging zoonoses. We built a statistical model to simulate declining immunity from monkeypox at 2 levels. At the individual level, we used a constant rate of decline in immunity of 1.29% per year as smallpox vaccination rates fell. At the population level, the cohort of vaccinated residents decreased over time because of deaths and births. By 2016, only 10.1% of the total population in Nigeria was vaccinated against smallpox; the serologic immunity level was 25.7% among vaccinated persons and 2.6% in the overall population. The substantial resurgence of monkeypox in Nigeria in 2017 appears to have been driven by a combination of population growth, accumulation of unvaccinated cohorts, and decline in smallpox vaccine immunity. The expanding unvaccinated population means that entire households, not just children, are now more susceptible to monkeypox, increasing risk of human-to-human transmission.

Since September 2017, Nigeria has been experiencing the largest monkeypox outbreak in the country's history. As of November 2019, the country had reported 183 confirmed cases across 18 states (*1*). This outbreak is also the largest recorded that has been caused by the West Africa clade of the monkeypox virus (MPXV). Beyond its scale, this outbreak is an illustrative case study for emerging zoonosis because of its epidemiologic characteristics.

Preliminary genetic analysis suggests multiple zoonotic introductions from animal reservoirs into the human population (*2*). In 2018, an MPXV sample isolated from a case-patient in Cameroon was found to be genetically similar to a sample from Nigeria despite no epidemiologic linkage, raising the possibility of an epizootic event spanning the Nigeria-Cameroon border (*3*). This finding is uncharacteristic of the West Africa clade, which tends to cause temporally and geographically isolated outbreaks (*4*,*5*). Moreover, the 2017–2020 Nigeria outbreak showed a higher prevalence among adults; 78% of patients were 21–40 years of age (*1*), whereas historically, most case-patients were <15 years of age (*6*). The changing demographics of this outbreak may offer insights into reasons behind the reemergence of monkeypox in West Africa.

We hypothesized 2 main mechanisms to explain this resurgence after 40 years of no reported cases. First, residents have experienced increased exposure to and interactions with forest animals, driven by deforestation, armed conflicts, and population migration. Second, herd immunity from since-discontinued universal smallpox vaccination programs in the 1970s has declined over time (*7*). The 2 theories, not mutually exclusive, represent the loss of 2 different barriers to spillover (*8*). We aimed to examine the potential role of declining population immunity and how it interacts with the country's rapid urbanization to affect the reemergence of monkeypox in Nigeria. Whereas data on urbanization and land expansion are available, the dearth of data from recent serologic surveys makes it challenging to separate out changes in the levels of residual immunity from smallpox vaccination from the endemicity of monkeypox in the population. By using a statistical model to account for declining individual-level immunity, we aimed to quantify the fraction of the population that is susceptible to monkeypox and plot the growth of this population during 1970–2018.

Author affiliations: The Kirby Institute, Kensington, New South Wales, Australia (P.Y. Nguyen, V. Costantino, C.R. MacIntyre); The George Institute for Global Health, Sydney, New South Wales, Australia (W.S. Ajisegiri); University of New South Wales School of Population Health, Kensington (A.A. Chughtai)

DOI: https://doi.org/10.3201/eid2704.203569

Methods

Data Sources

We retrieved epidemiologic and demographic data from monthly situational reports and weekly epidemiologic reports from the Nigeria Centre for Disease Control and Prevention, as well as from published literature. Annual population data and crude death rates for 1970–2020 came from the World Bank data portal (*9*,*10*) and state population data and area size used to determine population density from the Nigeria National Bureau of Statistics (*11*).

Population Immunity Model

We sought to model declining immunity against monkeypox at 2 levels. At the individual level, we assumed that smallpox vaccination provides 85% effective cross-immunity against MPXV among all vaccinated persons (*12*) and that the level of serologic immunity to MPXV for each vaccinated person would decline at a constant rate until it reached 0%, at which point the person would be fully susceptible to MPXV. We set the rate of decline for serologic immunity levels at 1.29% (95% CI 0.56–2.71) per year, based on findings from a 2006 study in which the authors plotted the fraction of vaccinated case-patients protected against fatal or severe disease against the number of years since their most recent smallpox vaccination (*13*). At the population level, we assumed that 77.2% of the population in 1970 had received smallpox vaccination based on data from a series of surveys in 1969 that reported the proportion of populations in northern and western regions of Nigeria with evidence of smallpox vaccination by jet injectors (*14*). We used population sizes of these 2 regions to calculate a weighted country-level estimate of vaccination coverage, which we used in the model (Table 1). Because the surveys were conducted through 1969, we chose 1970 as the first year for the model.

In each subsequent year, we calculated that the size of the vaccinated population in the model would decline at a rate equivalent to that year's crude death rate. The difference between total population reported by World Bank and the living vaccinated population represented the immunologically naive population; this figure accounted for the number of newly born children and unvaccinated immigrant persons recruited into the subsequent year's unvaccinated population figure for the model. We calculated population immunity level by multiplying the proportion of the living vaccinated population in the total population by the individual immunity level. The model used countrywide population data, not state population data, because the latter became available only beginning with the 1991 census (*15*). We assumed that vaccination coverage was uniform across all states in 1970 and no subsequent vaccination campaigns occurred after 1970. To visualize the decline of immunity over time, we plotted the proportion of immunological-naive populations during 1970–2018 and superimposed individual- and population-level immunity levels onto this plot (Figure 1).

Geographic Distribution

We tabulated total confirmed and suspected or probable cases in each state through September 2020 based on case definitions (Table 2) and mapped these data as a chronopleth (Figure 2, panel A). We calculated population density and annual population growth rate during 2006–2016 for each state (Table 3) and mapped these data with Nigeria's 2018 road network overlaid as a chronopleth (*16*) (Figure 2, panel B). Risk ratios were calculated for states with population densities and annual growth rates higher than the national averages (Table 3). Only states with confirmed cases were considered for analysis because the definition of suspected or probable cases has low specificity and can lead to misdiagnosis with similar rash-like illnesses such as varicella zoster virus (*17*).

Results

Increase in Susceptible Population over Time

During 1970–2018, the overall population of Nigeria increased from 55.98 million to 195.87 million. The unvaccinated, immunologically naive population increased from 12.76 million (22.8% of total population) in 1970 to 177.62 million (90.7% of total population) in 2018. From 43.22 million (77.2% of total population) in 1970, the vaccinated population declined to ≈18.25 million (9.3% of total population) in 2018.

Table 1. Estimation of a weighted country-level estimate of smallpox vaccination coverage, Nigeria, 1969

Category	Northern Nigeria	Western Nigeria
Population assessed*	6.8 million	4.4 million
Weight assigned to region in calculation of overall coverage, %	60.7	39.3
Proportion of population with evidence of smallpox vaccination, %		
Region	88.4	60.0
Nation	77.2	

*Provided in the source study (*14*).

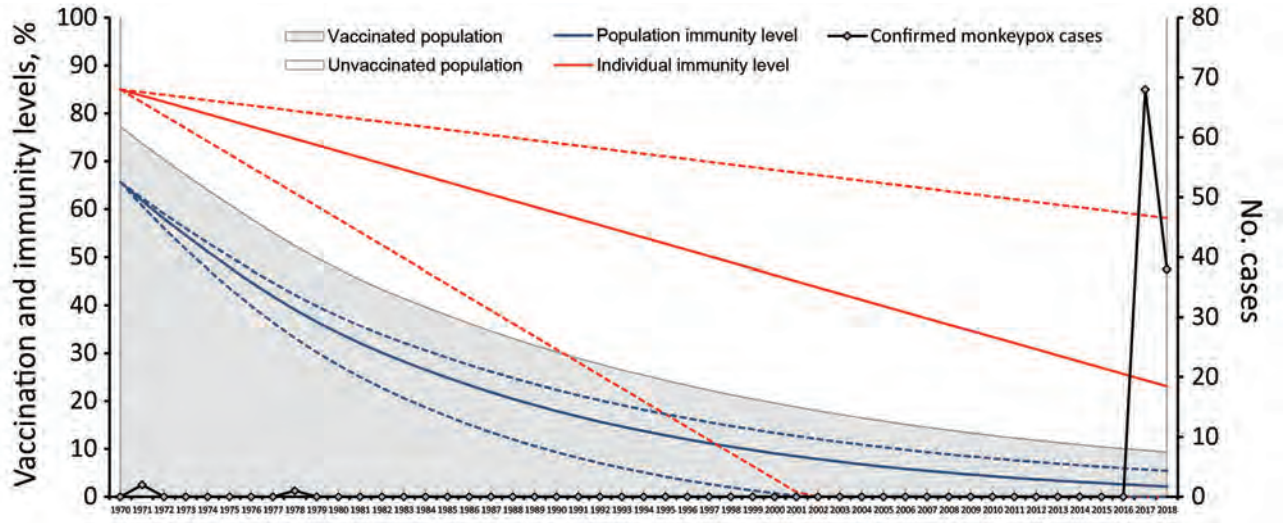

Figure 1. Relationship between population- and individual-level smallpox vaccination and immunity rates and resurgence of monkeypox cases in Nigeria, 1970–2018.

In addition, the cross-immunity protection of 85% conferred by smallpox vaccination for monkeypox, using the assumed linear rate of decline over time from vaccination, fell to only 23.1% (95% CI 0.0%–58.1%) among vaccinated persons. Combining the effects of declining immunity from these 2 factors, the overall population immunity, estimated to be 65.6% in 1970, declined to only 2.2% (95% CI 0.0%–5.4%) in 2018 (Figure 1). In 2016, the year preceding the outbreak, the percentage of the population vaccinated was 10.1% and estimated population immunity was 2.6% (95% CI 0.0%–6.0%).

Geographic Distribution

States that reported >10 confirmed cases within a year were Rivers (36), Bayelsa (31), Lagos (19), and Delta (17) (Table 3). Exported cases in the United Kingdom, Singapore, and Israel had epidemiologic linkages to clusters in these states with the highest numbers of monkeypox cases (*18*,*19*). Most states with confirmed cases were concentrated in the South-West (3), South-South (6), and South-East (4) zones, with sporadic spread to the North-West and North-Central zones, which include highly populated states such as the Federal Capital Territory (FCT), Nasawara, and Plateau (Table 3).

Among 17 states with confirmed cases, 4 (Rivers, Akwa Ibom, Oyo, and FCT) had annual population growth rates higher than the national average of 3.93%; Abuja (FCT), the capital city, increased 15.3% (Table 3). In 2016, the national population density was 421.1 persons/km^2, but 8 states had population densities >500 persons/km^2; Lagos state reported more than 3,500 persons/km^2 (Table 3). A dense network of roads converges in the South-South zone and Lagos state, an area with an overall population density of >1,000 persons/km^2 (Figure 2, panel B). States with population densities higher than the national average were 2.1 (95% CI 1.0–4.2) times more likely to report confirmed cases (p = 0.039). Higher risk (risk ratio 1.2, 95% CI 0.5–2.7; p = 0.65) was also observed among states with annual population growth higher than the national average, albeit without statistical significance.

Discussion

Our investigation shows that a large decline in estimated population immunity was observed before a 2017 increase in cases of monkeypox. On this basis, we postulate a relationship between decreased immunity to smallpox and resurgence of monkeypox in Nigeria. The potential role of declining population immunity in the resurgence of monkeypox has been raised in earlier studies (*4*,*6*,*7*,*20*). Epidemiologic evidence suggests previous smallpox vaccination

Table 2. Case definitions for monkeypox in Nigeria

Term	Definition
Suspected case	Acute illness with fever >38.3°C, intense headache, lymphadenopathy, back pain, myalgia, and intense asthenia followed 1–3 days later by a progressively developing rash often beginning on the face (most dense) then spreading elsewhere on the body, including soles of feet and palms of hand
Probable case	Meets the clinical case definition; not laboratory confirmed, but has an epidemiological link to a confirmed case
Confirmed case	Clinically compatible case that is laboratory confirmed by positive IgM, PCR, or virus isolation

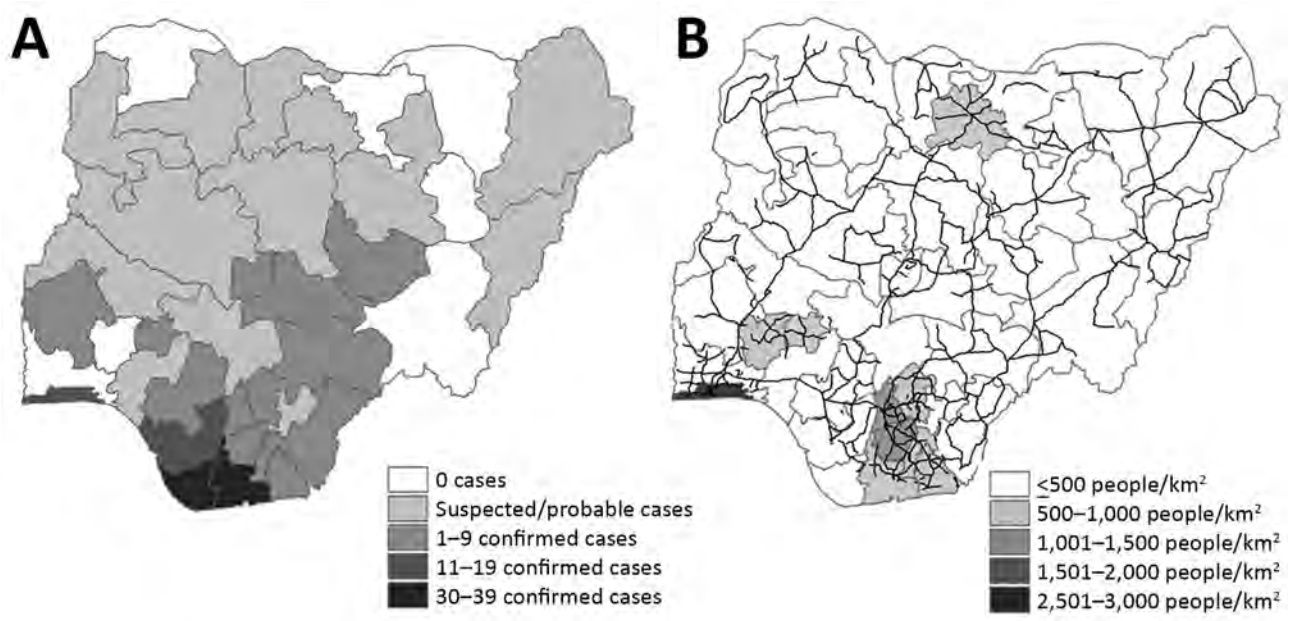

Figure 2. Monkeypox in Nigeria and factors affecting spread. A) Case distribution by state, September 2017–September 2020. B) Population density by state in 2016 (gray shading) and nationwide road network in 2018 (black lines).

provides at least partial protection against severe MPXV infections (*13*,*20*), further supported by immunologic studies of smallpox vaccine. Residual IgG and neutralizing antibodies were shown to persist in vaccinated persons (*21*–*23*) and have been associated with milder disease among infected patients (*24*). Among US monkeypox patients, those vaccinated for smallpox displayed evidence of vaccination immunity (orthopoxvirus [OPXV] IgG and memory B cells) after monkeypox exposure (24). Smallpox vaccine induces both humoral and cell-mediated response against OPXV, including MPXV, targeting a wide range of viral particles and preventing viral replication (*23*,*25*).

Our results show that the effect of a decline in individual-level immunity among vaccinated persons, as well as population growth in the postvaccination era, has substantially reduced the overall population immunity level within the past 45 years. The median age of the patients was 29 years old (*2*), notably higher than for previous outbreaks except from the 2017 outbreak in Central African Republic (median 27.5 years of age) and a single case in Sierra Leone in 1970 (27.5 years old) (*4*). This finding can be explained by the fact that children too young to get vaccinated in the 1970s have grown up and now form most of the contemporary susceptible population. The smallpox vaccination campaign officially ceased in 1980; by 2017, when the monkeypox outbreak in Nigeria occurred, the unvaccinated cohort would encompass all residents ≤37 years of age. This contemporary susceptible population is composed mainly of working adults who maintain wider social contact and are more likely to engage in activities that include risk of animal exposures, such as hunting, farming, or trading bush meat (*26*). In addition, the expanding unvaccinated population means that entire households are now susceptible to monkeypox instead of just children, which enhances the risk of human-to-human transmission. In fact, the index case in 2017 was part of a 5-member family cluster of cases (*27*).

Most confirmed cases were concentrated in the southern zones, which are characterized as natural ecologic niches of monkeypox because of swamps and rain forests (2,4). Satellite imagery during 2000–2016 shows a substantial increase in built-up areas and farmland in southern Nigeria, created at the expense of these forested areas (*28*). This expansion of developed areas increases the likelihood of reservoir animals, such as rodents, rabbits, and primates, being displaced from their natural habitat and living among humans, thus increasing interspecies contact (*29*). Past serologic surveys found higher seroprevalence of OPXV-specific IgG among residents of forested habitat, suggesting frequent exposure to MPXV and other OPXV (*5*,*30*,*31*). This evidence is further supported by the disproportionate prevalence among men in this outbreak (male:female ratio = 3:1), because predominantly men perform most

high-risk occupations dealing with wild animals, such as hunting and trading bush meat (*4*,*32*). In addition, expansion of urban transport networks may have contributed to widespread transmission in this outbreak, because states with >10 confirmed cases tended to be converging points for major roads (Figure 2, panel B).

Of note, an increasing number of cases were detected in drier savannahs in the northern zones, which are not typical ecologic niches of MPXV (*2*). This finding is possibly because more animal-human interfaces are occurring outside of MPXV natural habitats because of savannah being cleared for farming and settlement. In fact, savannah-to-agricultural land transition constituted the largest segment of land conversion in Nigeria during 1975–2013 (*33*). Moreover, interstate railway lines and highways may have enabled patients from monkeypox clusters to travel north from southern locations and subsequently infect local residents.

Several models have conceptualized zoonotic transmission as a multistage process with several bottlenecks that can influence the probability of spillover (*8*,*34*). In these models, host-specific and pathogen-specific factors determine how many pathogens are released into the environment and how long they survive. Individual human behaviors determine the probability and dose of exposure; individual human physiology and immunity determine the probability and severity of infection upon exposure (*8*). In other words, although urbanization and land conversion increase the frequency of animal exposure and the average exposure dose, human immunity potentially opposes this effect by lowering the probability of infection. At the same time, although smallpox vaccination may provide partial protection, sufficiently large infectious inoculum, through prolonged or frequent animal contact, can overcome such protection and manifest symptomatically (*24*,*35*).

Table 3. Annual population growth and number of cases, by state, Nigeria, 2006–2016*

State	Zone	Area, km^2	Population density, 2006, persons/km^2	Population density, 2016, persons/km^2	Annual population growth, %	No. cases
Abia	SE	4,900	580.7	760.7	3.1	1–9 confirmed cases
Adamawa	NE	38,700	82.1	109.8	3.4	Only suspected/probable cases
Akwa Ibom	SS	6,900	565.5	794.5	4.0	1–9 confirmed cases
Anambra	SE	4,865	858.8	1,136.2	3.2	1–9 confirmed cases
Bauchi	NE	49,119	94.7	133.1	4.0	Only suspected/probable cases
Bayelsa	SS	9,059	188.2	251.5	3.4	30–39 confirmed cases
Benue	NC	30,800	138.1	186.4	3.5	1–9 confirmed cases
Borno	NE	72,609	57.4	80.7	4.0	Only suspected/probable cases
Cross River	SS	21,787	132.8	177.5	3.4	1–9 confirmed cases
Delta	SS	17,108	240.4	331.0	3.8	11–19 confirmed cases
Ebonyi	SE	6,400	340.1	450.1	3.2	Only suspected/probable cases
Edo	SS	19,187	168.5	220.8	3.1	1–9 confirmed cases
Ekiti	SW	5,435	441.4	601.8	3.6	1–9 confirmed cases
Enugu	SE	7,534	433.7	585.5	3.5	1–9 confirmed cases
FCT	NC	7,607	184.9	468.5	15.3	1–9 confirmed cases
Gombe	NE	17,100	138.3	190.5	3.8	No cases
Imo	SE	5,288	742.7	1,022.8	3.8	1–9 confirmed cases
Jigawa	NW	23,287	187.3	250.3	3.4	No cases
Kaduna	NW	42,481	143.9	194.3	3.5	Only suspected/probable cases
Kano	NW	20,280	463.6	644.8	3.9	Only suspected/probable cases
Katsina	NW	23,561	246.2	332.4	3.5	Only suspected/probable cases
Kebbi	NW	36,985	88.1	120.1	3.6	Only suspected/probable cases
Kogi	NC	27,747	119.4	161.2	3.5	Only suspected/probable cases
Kwara	NC	35,705	66.2	89.4	3.5	Only suspected/probable cases
Lagos	SW	3,671	2,482.6	3,418.8	3.8	11–19 confirmed cases
Nasarawa	NC	28,735	65.1	87.8	3.5	1–9 confirmed cases
Niger	NC	68,925	57.4	80.6	4.0	Only suspected/probable cases
Ogun	SW	16,400	228.7	318.2	3.9	No cases
Ondo	SW	15,820	218.8	295.3	3.5	Only suspected/probable cases
Osun	SW	9,026	378.6	521.3	3.8	No cases
Oyo	SW	26,500	210.6	295.9	4.0	1–9 confirmed cases
Plateau	NC	27,147	118.1	154.7	3.1	1–9 confirmed cases
Rivers	SS	10,575	491.6	690.7	4.0	30–39 confirmed cases
Sokoto	NW	27,825	133.1	179.6	3.5	No cases
Taraba	NE	56,282	40.8	54.5	3.4	No cases
Yobe	NE	46,609	49.8	70.7	4.2	No cases
Zamfara	NW	37,931	86.4	119.0	3.8	Only suspected/probable cases
National average	NA	24,592	304.4	421.1	3.93	NA

*NA, not applicable; FCT, Federal Capital City; NC, North-Central; NE, North-East; NW, North-West; SE, South-East; SS, South-South; SW, South-West.

Although no cases were reported in Nigeria during 1978–2017, because of the high prevalence of smallpox vaccination among the 1970s cohort, mild and asymptomatic infections might have occurred but gone unreported. In addition, the West Africa clade is associated with lower virulence (*36*), which could have enabled the disease to spread through mild or asymptomatic cases not captured by passive surveillance. In fact, before the 2017 outbreak, monkeypox was not in the Integrated Disease Surveillance and Response system list of reportable diseases (*37*). Serologic surveys of West Africa populations revealed active levels of IgG suggestive of routine exposure to OPXV, albeit without patients recalling symptoms or having scars (*6*,*30*). The resurgence of monkeypox in Nigeria in 2017, although seemingly unprecedented, may be the result of alignment of several control gaps in the spillover process, driven by a combination of factors: modern urbanization, urban densification, waning of immunity among vaccinated residents, and accumulation of unvaccinated cohorts.

This study is subject to some limitations because our model was built on several assumptions. We assumed that the base population in 1970 started with a uniform immunity level of 85%; in reality, persons vaccinated before 1970 would have had a lower immunity level at the start of the model and persons vaccinated from 1970–1980 would have started with a higher immunity level at a later year. We assumed that 77.2% vaccination coverage was uniform across all states, but our uniform vaccination coverage and protection levels represent a simplified averaging of heterogeneous rates of coverage across states. Finally, for our model, we assumed that no vaccination campaigns occurred in Nigeria after 1970. In fact, several vaccination campaigns were conducted during 1969–1980 in Nigeria (*38*), but there was insufficient data on these campaigns' frequency and coverage to accurately quantify their effects on the population immunity level. The model also did not account for changing kinetics of antibodies and T-cells in persons receiving a booster dose (*39*).

Next, in the absence of state-specific population growth rates, we were unable to simulate rural-urban migration in the model, which resulted in an urban-rural growth differential and could lead to differential increase in the susceptible population between states (*40*,*41*). However, accurately estimating this effect would require expanding the parameters of a future model to account for population migration between states, data that are not publicly available. Last, the estimated rate of serologic immunity decline we used had a wide confidence interval in the source study (*13*); that would have increased the margin of error for our estimates of individual and population immunity levels. The model would benefit from future studies that more accurately estimate rates of immunity decline.

The wide geographic spread of the 2017 outbreak in Nigeria was likely driven by the lower level of residual OPXV immunity, population growth, an increase in the proportion of susceptible persons, and potential spillover events at the animal-human interfaces caused by human settlements encroaching into forested areas. The initial spillovers may have been followed by rapid human-to-human transmission enabled by high population density and a growing immunologically naive population fully susceptible to MPXV. High prevalence among working adults 21–40 years of age, born after universal vaccination programs were discontinued, suggests that declining population immunity plays a substantial role in the reemergence of monkeypox.

Fewer monkeypox cases were diagnosed in 2020, which other researchers have attributed to the self-limiting nature of MPXV human transmission (e.g., because of nonairborne mode of transmission, low probability of infection per contact) (*4*,*42*). However, we cannot rule out the possibility of future mutations that might enable sustained human-to-human transmission or adoption of more cosmopolitan animal reservoir hosts. Such occurrences would present substantial public health risks. These ongoing risks highlight the importance of serosurveillance to understand the extent of OPXV endemicity within the population. The role of vaccination in preventing monkeypox is being considered, and clinical trials for healthcare workers are underway (*43*,*44*). In the absence of seroprevalence data in Nigeria, this study provides an alternative method to estimate the residual level of vaccine immunity and adds another perspective to the discourse on monkeypox reemergence in West Africa.

This work was supported by a grant from the NHRMC Centre for Research Excellence in Integrated Systems for Epidemic Response (grant number 1107393).

About the Author

Ms. Nguyen was a Master of Public Health/International Public Health student at the University of New South Wales, Sydney, Australia, and was involved in COVID-19 research with The Kirby Institute at the time of this research. Her research interests are infectious disease surveillance, epidemic response, and predictive disease modelling.

References

1. Nigeria Centre for Disease Control and Prevention. Monkeypox monthly situational report, December 2019 [cited 2020 Oct 1]. https://ncdc.gov.ng/themes/common/files/sitreps/5a1a9820f21136842ba43f186b8d09e7.pdf
2. Yinka-Ogunleye A, Aruna O, Dalhat M, Ogoina D, McCollum A, Disu Y, et al.; CDC Monkeypox Outbreak Team. Outbreak of human monkeypox in Nigeria in 2017–18: a clinical and epidemiological report. Lancet Infect Dis. 2019;19:872–9. https://doi.org/10.1016/S1473-3099(19)30294-4
3. Sadeuh-Mba SA, Yonga MG, Els M, Batejat C, Eyangoh S, Caro V, et al. Monkeypox virus phylogenetic similarities between a human case detected in Cameroon in 2018 and the 2017–2018 outbreak in Nigeria. Infect Genet Evol. 2019;69:8–11. https://doi.org/10.1016/j.meegid.2019.01.006
4. Beer EM, Rao VB. A systematic review of the epidemiology of human monkeypox outbreaks and implications for outbreak strategy. PLoS Negl Trop Dis. 2019;13:e0007791. https://doi.org/10.1371/journal.pntd.0007791
5. Damon IK. Status of human monkeypox: clinical disease, epidemiology and research. Vaccine. 2011;29(Suppl 4):D54–9. https://doi.org/10.1016/j.vaccine.2011.04.014
6. Heymann DL, Szczeniowski M, Esteves K. Re-emergence of monkeypox in Africa: a review of the past six years. Br Med Bull. 1998;54:693–702. https://doi.org/10.1093/oxfordjournals.bmb.a011720
7. Simpson K, Heymann D, Brown CS, Edmunds WJ, Elsgaard J, Fine P, et al. Human monkeypox—after 40 years, an unintended consequence of smallpox eradication. Vaccine. 2020;38:5077–81. https://doi.org/10.1016/j.vaccine.2020.04.062
8. Plowright RK, Parrish CR, McCallum H, Hudson PJ, Ko AI, Graham AL, et al. Pathways to zoonotic spillover. Nat Rev Microbiol. 2017;15:502–10. https://doi.org/10.1038/nrmicro.2017.45
9. World Bank. Population, total—Nigeria [cited 2020 Sep 24]. https://data.worldbank.org/indicator/SP.POP.TOTL?locations=NG
10. World Bank. Death rate, crude (per 1,000 people)—Nigeria [cited 2020 Sep 20]. https://data.worldbank.org/indicator/SP.DYN.CDRT.IN?locations=NG
11. Nigeria National Bureau of Statistics. Annual abstract of statistics. 2010 [cited 2020 Oct 1]. http://ghdx.healthdata.org/record/nigeria-annual-abstract-statistics-2010
12. Fine PEM, Jezek Z, Grab B, Dixon H. The transmission potential of monkeypox virus in human populations. Int J Epidemiol. 1988;17:643–50. https://doi.org/10.1093/ije/17.3.643
13. Nishiura H, Eichner M. Estimation of the duration of vaccine-induced residual protection against severe and fatal smallpox based on secondary vaccination failure. Infection. 2006;34:241–6. https://doi.org/10.1007/s15010-006-6603-5
14. Henderson RH, Davis H, Eddins DL, Foege WH. Assessment of vaccination coverage, vaccination scar rates, and smallpox scarring in five areas of West Africa. Bull World Health Organ. 1973;48:183–94.
15. Nigeria Data Portal. Nigeria census: distribution of households, 2015 [cited 2020 Sep 24]. https://nigeria.opendataforafrica.org/xspplpb/nigeria-census
16. Humanitarian Data Exchange. Nigeria—roads. Updated 2018 Aug 15 [cited 2020 Oct 1]. https://data.humdata.org/dataset/nigeria-roads
17. Osadebe L, Hughes CM, Shongo Lushima R, Kabamba J, Nguete B, Malekani J, et al. Enhancing case definitions for surveillance of human monkeypox in the Democratic Republic of Congo. PLoS Negl Trop Dis. 2017;11:e0005857. https://doi.org/10.1371/journal.pntd.0005857
18. Kunasekaran MP. Report of monkeypox cases in 2018 in the United Kingdom. Global Biosecurity. 2019;1:140–9. https://doi.org/10.31646/gbio.22
19. Mauldin MR, McCollum AM, Nakazawa YJ, Mandra A, Whitehouse ER, Davidson W, et al. Exportation of monkeypox virus from the African continent. J Infect Dis. 2020 Sep 3 [Epub ahead of print]. https://doi.org/10.1093/infdis/jiaa559
20. Rimoin AW, Mulembakani PM, Johnston SC, Lloyd Smith JO, Kisalu NK, Kinkela TL, et al. Major increase in human monkeypox incidence 30 years after smallpox vaccination campaigns cease in the Democratic Republic of Congo. Proc Natl Acad Sci U S A. 2010;107:16262–7. https://doi.org/10.1073/pnas.1005769107
21. Hammarlund E, Lewis MW, Hansen SG, Strelow LI, Nelson JA, Sexton GJ, et al. Duration of antiviral immunity after smallpox vaccination. Nat Med. 2003;9:1131–7. https://doi.org/10.1038/nm917
22. Taub DD, Ershler WB, Janowski M, Artz A, Key ML, McKelvey J, et al. Immunity from smallpox vaccine persists for decades: a longitudinal study. Am J Med. 2008;121:1058–64. https://doi.org/10.1016/j.amjmed.2008.08.019
23. Gilchuk I, Gilchuk P, Sapparapu G, Lampley R, Singh V, Kose N, et al. Cross-neutralizing and protective human antibody specificities to poxvirus infections. Cell. 2016;167:684–694.e9. https://doi.org/10.1016/j.cell.2016.09.049
24. Karem KL, Reynolds M, Hughes C, Braden Z, Nigam P, Crotty S, et al. Monkeypox-induced immunity and failure of childhood smallpox vaccination to provide complete protection. Clin Vaccine Immunol. 2007;14:1318–27. https://doi.org/10.1128/CVI.00148-07
25. Kennedy RB, Ovsyannikova IG, Jacobson RM, Poland GA. The immunology of smallpox vaccines. Curr Opin Immunol. 2009;21:314–20. https://doi.org/10.1016/j.coi.2009.04.004
26. Quiner CA, Moses C, Monroe BP, Nakazawa Y, Doty JB, Hughes CM, et al. Presumptive risk factors for monkeypox in rural communities in the Democratic Republic of the Congo. PLoS One. 2017;12:e0168664. https://doi.org/10.1371/journal.pone.0168664
27. Ogoina D, Izibewule JH, Ogunleye A, Ederiane E, Anebonam U, Neni A, et al. The 2017 human monkeypox outbreak in Nigeria—report of outbreak experience and response in the Niger Delta University Teaching Hospital, Bayelsa State, Nigeria. PLoS One. 2019;14:e0214229. https://doi.org/10.1371/journal.pone.0214229
28. Izah LN, Majid Z, Mohd Ariff MF, Mohammed HI. Determining land use change pattern in southern Nigeria: a comparative study. IOP Conf Ser: Earth Environ Sci. 2018;169:012040. https://doi.org/10.1088/1755-1315/169/1/012040
29. Faust CL, McCallum HI, Bloomfield LSP, Gottdenker NL, Gillespie TR, Torney CJ, et al. Pathogen spillover during land conversion. Ecol Lett. 2018;21:471–83. https://doi.org/10.1111/ele.12904
30. Leendertz SAJ, Stern D, Theophil D, Anoh E, Mossoun A, Schubert G, et al. A cross-sectional serosurvey of anti-orthopoxvirus antibodies in central and western Africa. Viruses. 2017;9:278. https://doi.org/10.3390/v9100278
31. Reynolds MG, Carroll DS, Olson VA, Hughes C, Galley J, Likos A, et al. A silent enzootic of an orthopoxvirus in Ghana, West Africa: evidence for multi-species involvement in the absence of widespread human disease. Am J Trop Med Hyg. 2010;82:746–54. https://doi.org/10.4269/ajtmh.2010.09-0716

32. Ozioko KU, Okoye CI, Obiezue RN, Agbu RA. Knowledge, attitudes, and behavioural risk factors regarding zoonotic infections among bushmeat hunters and traders in Nsukka, southeast Nigeria. Epidemiol Health. 2018;40:e2018025. https://doi.org/10.4178/epih.e2018025
33. U.S. Geological Survey: Earth Resources Observation and Science Center. Land use, land cover, and trends in Nigeria [cited 2020 Oct 1]. https://eros.usgs.gov/westafrica/land-cover/land-use-land-cover-and-trends-nigeria
34. Kreuder Johnson C, Hitchens PL, Smiley Evans T, Goldstein T, Thomas K, Clements A, et al. Spillover and pandemic properties of zoonotic viruses with high host plasticity. Sci Rep. 2015;5:14830. https://doi.org/10.1038/srep14830
35. Mucker EM, Chapman J, Huzella LM, Huggins JW, Shamblin J, Robinson CG, et al. Susceptibility of marmosets () to monkeypox virus: a low dose prospective model for monkeypox and smallpox disease. PLoS One. 2015; 10:e0131742. https://doi.org/10.1371/journal.pone.0131742
36. Likos AM, Sammons SA, Olson VA, Frace AM, Li Y, Olsen-Rasmussen M, et al. A tale of two clades: monkeypox viruses. J Gen Virol. 2005;86:2661–72. https://doi.org/10.1099/vir.0.81215-0
37. Nigeria Centre for Disease Control and Prevention. Situation report: update of monkeypox outbreak in Nigeria, 2018 Feb 25 [cited 2020 Oct 2]. https://ncdc.gov.ng/themes/common/files/sitreps/7ba9ce49faf09f5212c1dbb48b31184b.pdf
38. Fenner F, Henderson DA, Arita I, Jezek Z, Ladnyi ID. Smallpox and its eradication. Geneva: World Health Organization; 1988.
39. Kennedy JS, Frey SE, Yan L, Rothman AL, Cruz J, Newman FK, et al. Induction of human T cell–mediated immune responses after primary and secondary smallpox vaccination. J Infect Dis. 2004;190:1286–94. https://doi.org/10.1086/423848
40. Sackey J, Liverpool-Tasie S, Salau S, Awoyemi T. Rural-urban transformation in Nigeria. J African Dev. 2012;14:131–68.
41. Farrell K. An inquiry into the nature and causes of Nigeria's rapid urban transition. Urban Forum. 2018;29:277–98
42. Jezek Z, Grab B, Dixon H. Stochastic model for interhuman spread of monkeypox. Am J Epidemiol. 1987;126:1082–92. https://doi.org/10.1093/oxfordjournals.aje.a114747
43. Public Health England. Cohort study of healthcare workers receiving Imvanex®. Clin Identifier NCT03745131. 2019. [cited 2020 Oct 1]. https://clinicaltrials.gov/ct2/show/NCT03745131
44. Petersen BW, Kabamba J, McCollum AM, Lushima RS, Wemakoy EO, Muyembe Tamfum JJ, et al. Vaccinating against monkeypox in the Democratic Republic of the Congo. Antiviral Res. 2019;162:171–7. https://doi.org/10.1016/j.antiviral.2018.11.004
45. Nigeria Centre for Disease Control and Prevention. Weekly epidemiological report, week 17, April 2019 [cited 2020 Oct 1]. https://ncdc.gov.ng/reports/257/2020-april-week-17

Address for correspondence: Phi-Yen Nguyen, UNSW Sydney, Kirby Institute, c/o Prof. Raina MacIntyre, Sydney, NSW 2052, Australia; email: phiyen.nguyen@protonmail.com

Animal Reservoirs and Hosts for Emerging Alphacoronaviruses and Betacoronaviruses

Ria R. Ghai, Ann Carpenter, Amanda Y. Liew, Krystalyn B. Martin, Meghan K. Herring, Susan I. Gerber, Aron J. Hall, Jonathan M. Sleeman, Sophie VonDobschuetz, Casey Barton Behravesh

The ongoing global pandemic caused by coronavirus disease has once again demonstrated the role of the family *Coronaviridae* in causing human disease outbreaks. Because severe acute respiratory syndrome coronavirus 2 was first detected in December 2019, information on its tropism, host range, and clinical manifestations in animals is limited. Given the limited information, data from other coronaviruses might be useful for informing scientific inquiry, risk assessment, and decision-making. We reviewed endemic and emerging infections of alphacoronaviruses and betacoronaviruses in wildlife, livestock, and companion animals and provide information on the receptor use, known hosts, and clinical signs associated with each host for 15 coronaviruses detected in humans and animals. This information can be used to guide implementation of a One Health approach that involves human health, animal health, environmental, and other relevant partners in developing strategies for preparedness, response, and control to current and future coronavirus disease threats.

Coronaviruses are a family of RNA viruses whose large genomes, propensity for mutation, and frequent recombination events have resulted in a diversity of strains and species that are capable of rapid adaptation to new hosts and ecologic environments (*1*). This viral plasticity has garnered widespread concern because of zoonotic potential and the consequences of new emergence events in both human and animal populations. The emergence of a new strain of severe acute respiratory syndrome coronavirus 2 (SARS-CoV-2), which causes coronavirus disease (COVID-19) has once again demonstrated the role of the family *Coronaviridae* in causing human disease outbreaks. SARS-CoV-2, a novel betacoronavirus, was identified in human patients from Wuhan, China, during December 2019 and has resulted in a global pandemic, an unprecedented public health emergency, and untold economic and societal repercussions worldwide. Similar to the 2002–2003 severe acute respiratory syndrome (SARS) epidemic, a live animal market where hundreds of animal species were sold is suspected to be associated with the emergence or early spread of COVID-19 in humans (*2*).

Although COVID-19 is novel in the breadth of the human outbreak, several pathogenic alphacoronaviruses and betacoronaviruses have shown similar patterns of emergence. As early as the 1930s, coronaviruses pathogenic to livestock, companion animals, and laboratory animals were identified (*3*). During the 1960s, 2 human coronaviruses, HCoV-229E and HCoV-OC43, were detected in patients who had common colds (*4*,*5*). Although it is speculated that HCoV-OC43 might also have emerged through a global pandemic in the late 1800s (*6*), the 2002–2003 SARS outbreak is the first known global epidemic caused by a coronavirus. The SARS epidemic triggered research within this viral family (*3*). This research led to detection of 2 new human coronaviruses, HCoV-NL63 and HCoV-HKU1 (*7*,*8*). HCoV-229E, HCoV-OC43, HCoV-NL63, and HCoV-HKU1 are now accepted as globally endemic common cold species that are typically associated with mild-to-moderate respiratory illness. In 2012, the most deadly human coronavirus to date was detected in the Arabian Peninsula: Middle East respiratory syndrome coronavirus (MERS-CoV) (*9*). A cumulative body of research on these and other coronaviruses has shown that most alphacoronaviruses and betacoronaviruses infecting humans have come from animal hosts and that both historic patterns and coronavirus biology establish an urgent ongoing threat to human and animal health (*10*).

Author affiliations: Centers for Disease Control and Prevention, Atlanta, Georgia, USA (R.R. Ghai, A. Carpenter, A.Y. Liew, K.B. Martin, M.K. Herring, S.I. Gerber, A.J. Hall, C. Barton Behravesh); Emory University, Atlanta (A.Y. Liew, K.B. Martin, M.K. Herring); US Geological Survey, Madison, Wisconsin, USA (J.M. Sleeman); Food and Agriculture Organization of the United Nations, Rome, Italy (S. VonDobschuetz)

DOI: https://doi.org/10.3201/eid2704.203945

Although coronaviruses are divided into 4 viral genera, namely alphacoronaviruses, betacoronaviruses, gammacoronaviruses, and deltacoronaviruses, we focus on alphacoronaviruses and betacoronaviruses because all known human coronaviruses are from these genera, and they may therefore pose an increased risk for causing future pandemics.

This review is intended to compile data to inform a One Health approach to combatting emerging alphacoronaviruses and betacoronaviruses. One Health is a collaborative, multisectoral, and transdisciplinary approach—working at the local, regional, national, and global levels—with the goal of achieving optimal health outcomes recognizing the interconnection between humans, animals, plants, and their shared environment (*11*). For example, in Qatar, a One Health approach for MERS-CoV prevention and control has been implemented since early in the outbreak, and is associated with improvements in coordination, joint outbreak response rates, and diagnostic capacity (*12*). Similarly, in the United States, establishment of the One Health Federal Interagency COVID-19 Coordination Group has been instrumental in ensuring an efficient and coordinated all-of-government response by creating a mechanism to communicate, share timely updates, and align messaging (*13*). More generally, the One Health approach is endorsed as an effective means of combatting zoonotic diseases internationally by the Tripartite international health organizations, consisting of the Food and Agriculture Organization of the United Nations, the World Health Organization, and the World Organisation for Animal Health (*14*).

As with other zoonotic diseases, effective implementation of a One Health approach for emerging coronaviruses requires an understanding of the transmission dynamics and human and animal hosts associated with the pathogen. Therefore, this review summarizes information from other coronavirus emergence events, which might be useful in identifying trends, establishing baselines, and informing decision-making by using a One Health approach around the current COVID-19 pandemic and future emerging coronavirus threats. Specifically, we provide information on the receptor used by each current or previously emerging coronavirus because tropism can help predict host susceptibility (Table 1) for all known hosts of each coronavirus and their host category (i.e., reservoir, intermediate, spillover, susceptible through experimental infection, or nonsusceptible through experimental infection) (Table 2, https://wwwnc.cdc.gov/EID/article/27/4/20-3945-T2.htm) and clinical signs associated with coronavirus infection (Table 3, https://wwwnc.cdc.gov/EID/article/27/4/20-3945-T3.htm)

Emerging Coronaviruses and Wildlife

More than 70% of zoonotic emerging infectious diseases in humans are caused by pathogens that have a wildlife origin (*11*). Several mammalian orders are now known to host coronaviruses, including carnivores, lagomorphs, nonhuman primates, ungulates and rodents (*3*). However, the attention has focused on Chiroptera (bats), which are hypothesized to be the origin host for all alphacoronaviruses and betacoronaviruses, and therefore all human coronaviruses (Table 2) (*1*,*3*).

After rodents, bats are the second most diverse and abundant mammalian order, comprising 20% of all mammalian biodiversity worldwide. In the past 2 decades, research has intensified to determine why bats harbor more zoonotic diseases than other mammalian taxa, including pathogens that result in high-consequence infectious diseases, such as Ebola and Marburg filoviruses; Nipah and Hendra paramyxoviruses; and SARS-CoV, SARS-CoV-2, and MERS-CoV, emerging in humans (*15*). Behavioral and ecologic traits, such as their gregariousness, sympatry with mixed species assemblages in roosts, and long lifespan relative to size, have been suggested explanations for why bats are reservoirs to many viral pathogens (*15*). Physiologically, bats have comparatively high metabolic rates and typically do not show clinical signs after viral infection. Recently, it has also been shown that bats have several immune characteristics that are unique among mammals and that cumulatively dampen their antiviral responses (*16*). Those factors also probably contribute to their effectiveness as viral reservoirs.

Coronavirus richness and diversity detected in bats far exceeds those of other mammalian orders; ≥11 of 18 chiropteran families across 6 continents have tested positive for ≥1 coronavirus species (*3*). A study surveying the diversity of wildlife coronaviruses across global disease hotspots identified 100 distinct viruses, of which 91 were detected in bats (*10*). This study reported that patterns of coronavirus diversity mirrored bat diversity and evolutionary history, reinforcing the idea that bats are the predominant reservoir of zoonotic and emerging coronaviruses (*10*). On the basis of extrapolations made in the same study, Anthony et al. predicted that bats harbor ≈3,204 coronaviruses, most of which remain undetected (*10*). Although much coronavirus diversity remains to be detected, several SARS-like coronaviruses have been detected already in bats,

Table 1. Current or previously emerging coronaviruses*

Pathogen (abbreviation)	Disease (abbreviation)	Viral genus	Receptor (abbreviation) [suspected]
Alphacoronavirus 1 (ACoV1); strain canine enteric coronavirus (CCoV)	Canine coronavirus infection (CCoV)	*Alphacoronavirus*	Aminopeptidase N (APN, CD13)
Alphacoronavirus 1 (ACoV1); strain feline infectious peritonitis virus (FIPV)	Feline infectious peritonitis virus (FIP)	*Alphacoronavirus*	Aminopeptidase N (APN, CD13)
Bat coronavirus HKU10	NA	*Alphacoronavirus*	Unknown
Ferret systemic coronavirus (FRSCV)	Ferret systemic coronavirus (FRSCV)–associated disease	*Alphacoronavirus*	Unknown
Human coronavirus NL63	Common cold	*Alphacoronavirus*	Angiotensin-converting enzyme 2 (ACE2)
Human coronavirus 229E	Common cold	*Alphacoronavirus*	Human aminopeptidase N (hAPN, CD13)
Porcine epidemic diarrhea virus (PEDV)	Porcine epidemic diarrhea (PED)	*Alphacoronavirus*	[Aminopeptidase N (APN, CD13)]
Rhinolophus bat coronavirus HKU2; strain swine acute diarrhea syndrome coronavirus (SADS-CoV)	Swine acute diarrhea syndrome (SADS)	*Alphacoronavirus*	Unknown
Betacoronavirus 1; strain bovine coronavirus	NA	*Betacoronavirus*	Human leukocyte antigen class I (HLA-1)
Betacoronavirus 1; strain canine respiratory coronavirus	Canine infectious respiratory disease (CIRD)	*Betacoronavirus*	Human leukocyte antigen class I (HLA-1)
Betacoronavirus1; strain human coronavirus OC43	Common cold	*Betacoronavirus*	Human leukocyte antigen class I (HLA-1)
Human coronavirus HKU1	Common cold	*Betacoronavirus*	Human leukocyte antigen class I (HLA-1)
Middle East respiratory syndrome coronavirus (MERS-CoV)	Middle East respiratory syndrome (MERS)	*Betacoronavirus*	Dipeptidyl peptidase 4 (DPP4, CD26)
Severe acute respiratory syndrome coronavirus (SARS-CoV)	Severe acute respiratory syndrome (SARS)	*Betacoronavirus*	Angiotensin-converting enzyme 2 (ACE2)
Severe acute respiratory syndrome coronavirus 2 (SARS-CoV-2)	Coronavirus disease (COVID-19)	*Betacoronavirus*	Angiotensin-converting enzyme 2 (ACE2)

*All coronaviruses are described in Tables 2 and 3, including the receptor used for viral entry. NA, not available.

including viruses that use the same human cellular receptor molecule as SARS-CoV and SARS-CoV-2, and might therefore pose an increased risk for future emergence from bats to humans (*17*).

Despite the risks associated with bat-origin coronaviruses, bats play integral roles in ecosystems, including insect suppression through predation, prey for numerous predators, pollinators for economically and ecologically useful plants, and seed dispersal for countless tropical trees and shrubs (*18*). Therefore, mitigating the risks of future emergence events from bats would benefit from minimizing close interaction between humans and bats and other wildlife, by reducing or stopping wildlife sales at wet markets, wildlife hunting, and encroachment on wildlife habitat.

Although further research on bats might help to understand the origins of coronaviruses, other wildlife species are intermediate hosts for human emerging coronaviruses. Intermediate hosts might not only add complexity to coronavirus transmission dynamics, but might also amplify viral spillover to new hosts by closing gaps in interaction frequency between species, and by increasing transmissibility and/or infectiousness through viral adaptation (*19*). A canonical example is SARS-CoV, whose intermediate host is accepted to be palm civets (Table 2; Appendix, https://wwwnc.cdc.gov/EID/article/27/4/20-3945-App1.pdf). In this instance, close interaction between humans and civets sold through wildlife markets probably facilitated transmission to humans, and passage and ongoing recombination in civet intermediate hosts is believed to have played a critical role in human receptor tropism (*19*,*20*) (Table 1).

Some wildlife species are at risk for human coronavirus spillover. Wild great apes, all species of which are endangered, are a taxonomic group vulnerable to spillover from humans, at least in part because they are our closest living relatives. Several documented respiratory outbreaks that resulted in clinical signs ranging from mild illness to death in chimpanzee and gorilla populations originated from a human source (*21*,*22*). The human betacoronavirus HCoV-OC43 was reported as the causative agent of mild-to-moderate respiratory illness among wild chimpanzees in Côte D'Ivoire in late 2016 and early 2017 (Table 2; Appendix), suggesting the susceptibility of these chimpanzees to human coronaviruses. As the COVID-19 pandemic continues, there is concern that susceptible wildlife, such as great apes, might be exposed to the virus through human contact, resulting in a new host reservoir, which could pose a risk for perpetuating

enzootic transmission and zoonotic transmission into recovering human populations.

Wildlife infections with SARS-CoV-2 have already occurred; the first natural infection of SARS-CoV-2 in a wild animal, and the first confirmed animal cases in the United States, were in tigers (n = 5) and lions (n = 3) at a zoo in New York, NY (Table 2; Appendix). Unlike most other asymptomatic animal cases reported previously, the large cats demonstrated respiratory signs that included coughing and wheezing but ultimately made a full recovery (Table 3). SARS-CoV-2 infection in wild felids in captivity highlights the complex interactions humans might have with wildlife, including the potential for human-to-wildlife transmission. Given these interlinkages, framing risk by using a One Health approach might more comprehensively address the socioeconomic and environmental drivers of disease emergence, leading to potentially novel, mutually beneficial solutions. For example, risks could be reduced by improving wildlife importation, trade and market regulations, and sanitary standards, which would not only protect public health and animal health but also result in positive wildlife conservation outcomes.

Emerging Coronaviruses and Livestock

Some coronaviruses naturally infect livestock and can have devastating economic consequences, such as swine acute diarrhea syndrome coronavirus (SADS-CoV), porcine epidemic diarrhea virus (PEDV), and betacoronavirus 1. Although recent studies suggest that pigs are not susceptible hosts for SARS-CoV-2 infection (*23*,*24*), pigs are a common host for alphacoronaviruses and betacoronaviruses; 6 viral species cause disease (*25*) (Table 2). Of these species, the enteric alphacoronavirus PEDV is considered reemerging, and the enteric alphacoronavirus SADS-CoV (a strain of the *Rhinolophus* bat coronavirus HKU2) is considered emerging (*25*). Although PEDV was detected in China in the 1970s, a highly pathogenic variant caused considerable losses to the United States pork industry in 2013–2014 (*26*). SADS-CoV is highly pathogenic in swine and was detected in Guangdong Province in China during 2016–2017, causing the death of nearly 25,000 piglets (*27*) (Table 3). SADS-CoV emerged within 100 km of the accepted locale of the SARS index case, and like SARS-CoV and SARS-CoV-2, SADS-CoV is suspected to originate in horseshoe bats (*Rhinolophus* spp.) (Table 2; Appendix). However, unlike SARS-CoV and SARS-CoV-2, SADS-CoV has not been detected outside China (*25*).

Among betacoronaviruses, a strain of betacoronavirus 1 also infects pigs (*25*). Porcine hemagglutinating encephalomyelitis virus has been circulating for decades and causes rapid death in piglets (*25*) (Table 3). Unlike other coronaviruses, betacoronavirus 1 is a unique species complex, in that its distinct strains are host-specific to a range of different species, including wild and domestic ungulates, rabbits, and canines (*19*,*28*) (Table 2; Appendix). Perhaps the most well-studied strain of betacoronavirus 1 is bovine coronavirus (BCoV), which has a major economic role because it can be associated with a suite of clinical disease in calves and cattle, including calf diarrhea, winter dysentery, and respiratory infection (*28*) (Table 3). BCoV also infects several other livestock species, including horses, sheep, and camels (*19*,*28*) (Table 2).

Livestock have also been intermediate hosts in the emergence of 3 human coronaviruses. An unknown ungulate species, speculated to be cattle, is accepted as the intermediate host of HCoV-OC43 (*6*,*29*), a strain of betacoronavirus 1 (Table 2). On the basis of molecular clock calculations, HCoV-OC43 is predicted to have jumped from livestock to humans around 1890, a timeframe coincident with pandemics of respiratory disease in cattle (which resulted in widespread culling) and humans (although this outbreak is historically attributed to influenza) (*6*). Dromedary camels are accepted as established hosts of MERS-CoV and are believed to be associated with the emergence of HCoV-229E in humans on the basis of closely related viruses found in camelids (Table 2; Appendix). Dromedary camels inhabit the Middle East and northern Africa and comprise 90% of extant camels on earth. In much of their range, dromedaries are a major livestock species that are used as racing and working animals, as well as for their milk, meat, and hides.

Livestock can also be spillover hosts of human coronavirus infection. After the 2002–2003 SARS outbreak, a study conducted on farms in Xiqing County, China, tested livestock (pigs, cattle, chickens, and ducks) and companion animals (dogs and cats), leading to detection of 1 pig that was positive for SARS-CoV by antibody test and reverse transcription PCR (*30*) (Table 2). A larger and more complex series of livestock outbreaks of SARS-CoV-2 has been unfolding since April 2020. Mink farms across Europe and North America have reported outbreaks of SARS-CoV-2 (Tables 2, 3). In most outbreaks, farmed mink were suspected to be initially infected by COVID-19–positive farm employees (*31*,*32*). Findings from the Netherlands have

also identified instances of spillback from mink to humans through ongoing investigations (*33*). National surveillance and control efforts have been implemented in several countries, many of which have subsequently identified other SARS-CoV-2–positive species living on or nearby mink farms, including cats, dogs, and escaped or wild mink (*32*). Several countries have implemented mandatory reporting of any virus-positive animals and depopulation or quarantine of affected farms (*32*). In Europe, several million mink have been culled, and a moratorium has been placed on the mink industry in some countries; such early and coordinated One Health actions are needed to prevent bidirectional transmission of zoonotic diseases (*32*).

Emerging Coronaviruses and Companion Animals

Companion animals are members of many households and can improve the physical and mental well-being of their owners (*34*). In the United States, ≈71.5 million households (57%) own ≥1 companion animal (*35*). Among households with companion animals, dogs (67%) and cats (44%) are the most commonly owned (*35*). Despite the many benefits of pet ownership, close interactions with pets pose risks for zoonotic disease transmission (*34*). Zoonotic diseases that are spread between humans and companion animals include rabies, salmonellosis, campylobacteriosis, and hookworm (*34*,*36*,*37*). Companion animals are estimated to be a source of >70 human diseases (*38*), and the burden of zoonotic diseases attributed to interactions with companion animals is substantial. For example, rabies kills ≈59,000 persons per year globally, and 99% of human rabies cases originate from rabid dogs (*37*).

Several common coronaviruses have been detected in companion animals, although none of the coronaviruses that are endemic to companion animal populations are zoonotic. One of the most common respiratory diseases in dogs is canine infectious respiratory disease, or kennel cough, which typically causes cough and nasal discharge in puppies and dogs (*39*,*40*). Although kennel cough can be caused by several pathogens, most frequently the bacterium *Bordetella bronchiseptica*, canine respiratory coronavirus (CRCoV) is a contributing pathogen to this syndrome (*39*,*41*) (Table 1). CRCoV is believed to originate from BCoV through a common ancestor, host variant, or a host species shift and is therefore considered a strain of betacoronavirus 1 (*39*,*41*). Regardless of how CRCoV and BCoV are genetically related, experimental studies have shown that dogs challenged with BCoV can become infected and transmit the virus to other dogs, although they do not exhibit clinical signs of disease (Tables 2, 3; Appendix).

Canine enteric coronavirus (CCoV) is an alphacoronavirus often associated with mild enteritis in puppies and dogs, especially in group housing situations (*42*). However, during 2005, a novel, highly pathogenic variant strain of CCoV-II, CB/05, was identified (*43*) (Table 2). This new variant is now pantropic, and results in a mortality rate up to 100% in isolated outbreaks in puppies (*43*) (Table 3). Because of its increased pathogenicity and changes in tissue tropism, CCoV is considered an emerging pathogen (*42*).

Although CCoV is generally considered to be specific to dogs, cats experimentally challenged with the virus can be infected with CCoV and mount an anamnestic response to further exposure, although they do not develop clinical signs of illness (Table 3; Appendix). In addition, although there are 2 serotypes of feline coronavirus (FCoV), FCoV type I and FCoV type II, type II is hypothesized to have originated from a recombination event between FCoV type I and CCoV, which suggests co-infections of coronaviruses among companion animals might yield opportunity for emergence of new disease (*44*).

Companion animals might also act as spillover hosts for human coronaviruses. A study after the 2002–2003 SARS outbreak showed that pet cats living in a Hong Kong, China, apartment complex were naturally infected with SARS during the epidemic (*45*). After the epidemic, challenge experiments in cats and ferrets found that both species could be experimentally infected and transmit the infection to immunologically naive animals of the same species they were housed with (*45*) (Table 2). In this experiment, cats did not show clinical signs of illness, although ferrets became lethargic, showed development of conjunctivitis, and died on days 16 and 21 postinfection. However, unlike human cases, there was no evidence that SARS-CoV–associated pneumonia was a cause of death (Table 3). Rather, the main findings in deceased ferrets were marked hepatic lipidosis and emaciation (*45*).

Companion animals, specifically dogs and cats, are among the most commonly infected groups of animals in the ongoing COVID-19 pandemic. Natural cases of suspected human-to-animal transmission have been confirmed in dogs and cats from several countries, and the earliest reports date back to March 2020 in Hong Kong (*32*). As of January 2021, there are ≈100 confirmed cases of SARS-CoV-2 infections in dogs and cats in the United States; most of those

cases resulted from exposure to owners who had COVID-19 (*46*). Experimental challenge studies additionally suggest that similar to SARS-CoV, several companion animals, including cats, ferrets, and golden hamsters, are all susceptible to SARS-CoV-2 infection under laboratory conditions (Table 2; Appendix). Furthermore, studies in cats, hamsters, and ferrets showed that they are capable of direct and indirect transmission to healthy animals of the same species in experimental settings (*23*,*24*,*47*,*48*), which underscores the need for infection prevention and control practices for humans and companion animals (*49*).

The global prevalence of companion animal ownership underscores the need for better understanding of pathogens, such as coronaviruses, that can infect pets. Because companion animals harbor endemic coronaviruses and might also be at risk for spillover for some human zoonotic coronaviruses, there is potential for coronavirus recombination events and new viral emergence to occur within these hosts. Therefore, ensuring that persons understand how to safely interact with their companion animals is essential for ensuring that persons and companion animals stay healthy while also protecting animal welfare.

Conclusions

A considerable number of mammalian species, including wildlife, livestock, and companion animals, are susceptible to infection with alphacoronaviruses and betacoronaviruses. The propensity of alphacoronaviruses and betacoronaviruses to jump to new hosts, coupled with their relatively large host ranges, suggests that a One Health approach could be used to develop strategies to mitigate the effects of current and future coronavirus emergence events. During the COVID-19 pandemic, One Health collaboration between public health and veterinary sectors has already bolstered critical healthcare resources and infrastructure, leading to improvements in diagnostic testing capacity and human resource availability (*50*). In the United States, the One Health Federal Interagency COVID-19 Coordination Group has developed risk communication and messaging for companion animals, livestock, and wildlife and has been instrumental in coordinating joint outbreak response and diagnostic testing in animals. As these examples highlight, integration of the One Health approach into preparedness planning, joint epidemiologic investigations, surveillance, laboratory diagnostics, risk assessment, and field research is not only beneficial but a useful approach to safeguard the health, welfare and safety of humans, animals, and their shared environment.

Acknowledgments

We thank members of the COVID-19 One Health Working Group of the Centers for Disease Control and Prevention, the One Health Federal Interagency Coordination Group, and state and local partners for providing valuable contributions and insights for this manuscript.

The opinions expressed by authors contributing to this journal do not necessarily reflect the opinions of the Centers for Disease Control and Prevention, Emory University, or the Food and Agriculture Organization of the United Nations, but do represent the views of the US Geological Survey.

About the Author

Dr. Ghai is an associate service fellow in the One Health Office, National Center for Emerging and Zoonotic Infectious Diseases, Centers for Disease Control and Prevention, Atlanta, GA. Her primary research interests include One Health, disease ecology, and zoonotic diseases.

References

1. Woo PC, Lau SK, Huang Y, Yuen K-Y. Coronavirus diversity, phylogeny and interspecies jumping. Exp Biol Med (Maywood). 2009;234:1117–27. https://doi.org/10.3181/0903-MR-94
2. Huang C, Wang Y, Li X, Ren L, Zhao J, Hu Y, et al. Clinical features of patients infected with 2019 novel coronavirus in Wuhan, China. Lancet. 2020;395:497–506. https://doi.org/10.1016/S0140-6736(20)30183-5
3. Drexler JF, Corman VM, Drosten C. Ecology, evolution and classification of bat coronaviruses in the aftermath of SARS. Antiviral Res. 2014;101:45–56. https://doi.org/10.1016/j.antiviral.2013.10.013
4. Hamre D, Procknow JJ. A new virus isolated from the human respiratory tract. Proc Soc Exp Biol Med. 1966;121:190–3. https://doi.org/10.3181/00379727-121-30734
5. McIntosh K, Dees JH, Becker WB, Kapikian AZ, Chanock RM. Recovery in tracheal organ cultures of novel viruses from patients with respiratory disease. Proc Natl Acad Sci U S A. 1967;57:933–40. https://doi.org/10.1073/pnas.57.4.933
6. Vijgen L, Keyaerts E, Moës E, Thoelen I, Wollants E, Lemey P, et al. Complete genomic sequence of human coronavirus OC43: molecular clock analysis suggests a relatively recent zoonotic coronavirus transmission event. J Virol. 2005;79:1595–604. https://doi.org/10.1128/JVI.79.3.1595-1604.2005
7. van der Hoek L, Pyrc K, Jebbink MF, Vermeulen-Oost W, Berkhout RJ, Wolthers KC, et al. Identification of a new human coronavirus. Nat Med. 2004;10:368–73. https://doi.org/10.1038/nm1024
8. Woo PC, Lau SK, Chu CM, Chan KH, Tsoi HW, Huang Y, et al. Characterization and complete genome sequence of a novel coronavirus, coronavirus HKU1, from patients with pneumonia. J Virol. 2005;79:884–95. https://doi.org/10.1128/JVI.79.2.884-895.2005
9. Zaki AM, van Boheemen S, Bestebroer TM, Osterhaus AD, Fouchier R. Isolation of a novel coronavirus from a man with pneumonia in Saudi Arabia. N Engl J Med. 2012;367:1814–20. https://doi.org/10.1056/NEJMoa1211721

10. Anthony SJ, Johnson CK, Greig DJ, Kramer S, Che X, Wells H, et al.; PREDICT Consortium. Global patterns in coronavirus diversity. Virus Evol. 2017;3:vex012. https://doi.org/10.1093/ve/vex012
11. Centers for Disease Control and Prevention. One Health. 2020 [cited 2020 Jul 15]. https://www.cdc.gov/onehealth/index.html
12. Farag E, Nour M, Islam MM, Mustafa A, Khalid M, Sikkema RS, et al. Qatar experience on One Health approach for Middle East respiratory syndrome coronavirus, 2012–2017: a viewpoint. One Health. 2019;7:100090. https://doi.org/10.1016/j.onehlt.2019.100090
13. Newman A, Smith D, Ghai RR, Wallace RM, Torchetti MK, Loiacono C, et al. First reported cases of SARS-CoV-2 infection in companion animals—New York, March–April 2020. MMWR Morb Mortal Wkly Rep. 2020;69:710–3. https://doi.org/10.15585/mmwr.mm6923e3
14. World Health Organization, Food and Agriculture Organization of the United Nations, World Organisation for Animal Health. Taking a multisectoral, One Health approach: a tripartite guide to addressing zoonotic diseases in countries. Geneva: The Organization; 2019.
15. Luis AD, Hayman DT, O'Shea TJ, Cryan PM, Gilbert AT, Pulliam JR, et al. A comparison of bats and rodents as reservoirs of zoonotic viruses: are bats special? Proc Biol Sci. 2013;280:20122753. https://doi.org/10.1098/rspb.2012.2753
16. Banerjee A, Baker ML, Kulcsar K, Misra V, Plowright R, Mossman K. Novel insights into immune systems of bats. Front Immunol. 2020;11:26. https://doi.org/10.3389/fimmu.2020.00026
17. Ge X-Y, Li J-L, Yang X-L, Chmura AA, Zhu G, Epstein JH, et al. Isolation and characterization of a bat SARS-like coronavirus that uses the ACE2 receptor. Nature. 2013;503:535–8. https://doi.org/10.1038/nature12711
18. Kasso M, Mundanthra B. Ecological and economic importance of bats (order Chiroptera). Int Sch Res Notices. 2013;2013:187415 [cited 2021 Jan 22]. https://www.hindawi.com/journals/isrn/2013/187415
19. Corman VM, Muth D, Niemeyer D, Drosten C. Hosts and sources of endemic human coronaviruses. In: Kielian M, Mettenleiter TC, Roossinck MJ, editors. Advances in Virus Research. New York: Academic Press; 2018. p. 163–88.
20. Song H-D, Tu C-C, Zhang G-W, Wang S-Y, Zheng K, Lei L-C, et al. Cross-host evolution of severe acute respiratory syndrome coronavirus in palm civet and human. Proc Natl Acad Sci U S A. 2005;102:2430–5. https://doi.org/10.1073/pnas.0409608102
21. Köndgen S, Schenk S, Pauli G, Boesch C, Leendertz FH. Noninvasive monitoring of respiratory viruses in wild chimpanzees. EcoHealth. 2010;7:332–41. https://doi.org/10.1007/s10393-010-0340-z
22. Scully EJ, Basnet S, Wrangham RW, Muller MN, Otali E, Hyeroba D, et al. Lethal respiratory disease associated with human rhinovirus C in wild chimpanzees, Uganda, 2013. Emerg Infect Dis. 2018;24:267–74. https://doi.org/10.3201/eid2402.170778
23. Shi J, Wen Z, Zhong G, Yang H, Wang C, Huang B, et al. Susceptibility of ferrets, cats, dogs, and other domesticated animals to SARS-coronavirus 2. Science. 2020;368:1016–20. https://doi.org/10.1126/science.abb7015
24. Schlottau K, Rissmann M, Graaf A, Schön J, Sehl J, Wylezich C, et al. Experimental transmission studies of SARS-CoV-2 in fruit bats, ferrets, pigs and chickens. Lancet Microbe. 2020;1:e218–25. https://doi.org/10.1016/S2666-5247(20)30089-6
25. Wang Q, Vlasova AN, Kenney SP, Saif LJ. Emerging and re-emerging coronaviruses in pigs. Curr Opin Virol. 2019;34:39–49. https://doi.org/10.1016/j.coviro.2018.12.001
26. Lee C. Porcine epidemic diarrhea virus: An emerging and re-emerging epizootic swine virus. Virol J. 2015;12:193. https://doi.org/10.1186/s12985-015-0421-2
27. Zhou P, Fan H, Lan T, Yang X-L, Shi W-F, Zhang W, et al. Fatal swine acute diarrhoea syndrome caused by an HKU2-related coronavirus of bat origin. Nature. 2018;556:255–8. https://doi.org/10.1038/s41586-018-0010-9
28. Amer HM. Bovine-like coronaviruses in domestic and wild ruminants. Anim Health Res Rev. 2018;19:113–24. https://doi.org/10.1017/S1466252318000117
29. Vijgen L, Keyaerts E, Lemey P, Maes P, Van Reeth K, Nauwynck H, et al. Evolutionary history of the closely related group 2 coronaviruses: porcine hemagglutinating encephalomyelitis virus, bovine coronavirus, and human coronavirus OC43. J Virol. 2006;80:7270–4. https://doi.org/10.1128/JVI.02675-05
30. Chen W, Yan M, Yang L, Ding B, He B, Wang Y, et al. SARS-associated coronavirus transmitted from human to pig. Emerg Infect Dis. 2005;11:446–8. https://doi.org/10.3201/eid1103.040824
31. Oreshkova N, Molenaar R-J, Vreman S, Harders F, Oude Munnink BB, Hakze-van der Honing RW, et al. SARS-CoV-2 infection in farmed minks, the Netherlands, April and May 2020. Euro Surveill. 2020;25:2001005. https://doi.org/10.2807/1560-7917.ES.2020.25.23.2001005
32. World Organisation for Animal Health. COVID 19 portal events in animals; 2020 [cited 2020 Jul 13]. : https://www.oie.int/en/scientific-expertise/specific-information-and-recommendations/questions-and-answers-on-2019novel-coronavirus/events-in-animals
33. Oude Munnink BB, Sikkema RS, Nieuwenhuijse DF, Molenaar RJ, Munger E, Molenkamp R, et al. Transmission of SARS-CoV-2 on mink farms between humans and mink and back to humans. Science. 2021;371:172–7. https://doi.org/10.1126/science.abe5901
34. Centers for Disease Control and Prevention. Healthy pets, healthy people, 2020 [cited 2020 Jul 13]. https://www.cdc.gov/healthypets/index.html
35. American Veterinary Medical Association. Pet ownership and demographics sourcebook. Schaumburg (IL): The Association; 2018.
36. Smith K, Boxrud D, Leano F, Snider C, Braden C, Montgomery S, et al.; Centers for Disease Control and Prevention (CDC). Outbreak of multidrug-resistant *Salmonella typhimurium* associated with rodents purchased at retail pet stores—United States, December 2003–October 2004. MMWR Morb Mortal Wkly Rep. 2005;54:429–33.
37. Hampson K, Coudeville L, Lembo T, Sambo M, Kieffer A, Attlan M, et al.; Global Alliance for Rabies Control Partners for Rabies Prevention. Estimating the global burden of endemic canine rabies. PLoS Negl Trop Dis. 2015;9:e0003709. https://doi.org/10.1371/journal.pntd.0003709
38. Stull JW, Brophy J, Weese JS. Reducing the risk of pet-associated zoonotic infections. CMAJ. 2015;187:736–43. https://doi.org/10.1503/cmaj.141020
39. Erles K, Toomey C, Brooks HW, Brownlie J. Detection of a group 2 coronavirus in dogs with canine infectious respiratory disease. Virology. 2003;310:216–23. https://doi.org/10.1016/S0042-6822(03)00160-0
40. Erles K, Brownlie J. Canine respiratory coronavirus: an emerging pathogen in the canine infectious respiratory disease complex. Vet Clin North Am Small Anim Pract.

2008;38:815–25, viii. https://doi.org/10.1016/j.cvsm.2008.02.008
41. Erles K, Shiu K-B, Brownlie J. Isolation and sequence analysis of canine respiratory coronavirus. Virus Res. 2007; 124:78–87. https://doi.org/10.1016/j.virusres.2006.10.004
42. Licitra BN, Duhamel GE, Whittaker GR. Canine enteric coronaviruses: emerging viral pathogens with distinct recombinant spike proteins. Viruses. 2014;6:3363–76. https://doi.org/10.3390/v6083363
43. Buonavoglia C, Decaro N, Martella V, Elia G, Campolo M, Desario C, et al. Canine coronavirus highly pathogenic for dogs. Emerg Infect Dis. 2006;12:492–4. https://doi.org/10.3201/eid1203.050839
44. Pratelli A. Genetic evolution of canine coronavirus and recent advances in prophylaxis. Vet Res. 2006;37:191–200. https://doi.org/10.1051/vetres:2005053
45. Martina BE, Haagmans BL, Kuiken T, Fouchier RA, Rimmelzwaan GF, Van Amerongen G, et al. Virology: SARS virus infection of cats and ferrets. Nature. 2003;425:915. https://doi.org/10.1038/425915a
46. US Department of Agriculture. Cases of SARS-CoV-2 in animals in the United States, 2020 [cited 2020 Dec 20]. https://www.aphis.usda.gov/aphis/ourfocus/animalhealth/sa_one_health/sars-cov-2-animals-us
47. Kim Y-I, Kim S-G, Kim S-M, Kim E-H, Park S-J, Yu K-M, et al. Infection and rapid transmission of SARS-CoV-2 in ferrets. Cell Host Microbe. 2020;27:704–709.e2. https://doi.org/10.1016/j.chom.2020.03.023
48. Halfmann PJ, Hatta M, Chiba S, Maemura T, Fan S, Takeda M, et al. Transmission of SARS-CoV-2 in domestic cats. N Engl J Med. 2020;383:592–4. https://doi.org/10.1056/NEJMc2013400
49. Centers for Disease Control and Prevention. Toolkit: One Health approach to address companion animals with SARS-CoV-2, 2020 [cited 2020 Dec 20]. https://www.cdc.gov/coronavirus/2019-ncov/animals/toolkit.html
50. Lorusso A, Calistri P, Mercante MT, Monaco F, Portanti O, Marcacci M, et al. A "One-Health" approach for diagnosis and molecular characterization of SARS-CoV-2 in Italy. One Health. 2020;10:100135. https://doi.org/10.1016/j.onehlt.2020.100135

Address for correspondence: Ria R. Ghai, Centers for Disease Control and Prevention, 1600 Clifton Rd NE, Mailstop H16-5, Atlanta, GA 30329-4027, USA; email: ofu9@cdc.gov

Difficulties in Differentiating Coronaviruses from Subcellular Structures in Human Tissues by Electron Microscopy

Hannah A. Bullock, Cynthia S. Goldsmith, Sherif R. Zaki, Roosecelis B. Martines, Sara E. Miller

Efforts to combat the coronavirus disease (COVID-19) pandemic caused by severe acute respiratory syndrome coronavirus 2 (SARS-CoV-2) have placed a renewed focus on the use of transmission electron microscopy for identifying coronavirus in tissues. In attempts to attribute pathology of COVID-19 patients directly to tissue damage caused by SARS-CoV-2, investigators have inaccurately reported subcellular structures, including coated vesicles, multivesicular bodies, and vesiculating rough endoplasmic reticulum, as coronavirus particles. We describe morphologic features of coronavirus that distinguish it from subcellular structures, including particle size range (60–140 nm), intracellular particle location within membrane-bound vacuoles, and a nucleocapsid appearing in cross section as dense dots (6–12 nm) within the particles. In addition, although the characteristic spikes of coronaviruses may be visible on the virus surface, especially on extracellular particles, they are less evident in thin sections than in negative stain preparations.

The *Coronaviridae* family of viruses contains several human pathogens, including severe acute respiratory syndrome coronavirus 2 (SARS-CoV-2), the causative agent of the coronavirus disease (COVID-19) pandemic. Since early 2020, the unprecedented collective response to the COVID-19 pandemic from the scientific and medical community has led to numerous SARS-CoV-2–related publications and underscored the urgent need to demonstrate and verify the presence of coronavirus directly in tissues. Among these publications are reports describing the pathology of SARS-CoV-2 infection in patient specimens, which have been scrutinized intensely by electron microscopy (EM) for evidence of the virus. Consequently, several articles have erroneously described the identification of coronavirus particles by EM in the lung (*1*–*6*), kidney (*6*–*13*; B. Diao et al., unpub. data, https://doi.org/10.1101/2020.03.04.20031120), heart (*14*,*15*), brain (*16*), liver (*17*), intestine (*6*,*18*), skin (*19*), and placenta (*20*–*22*) (Table). However, most of the presumed virus or virus-like particles shown in all of these reports either represent normal subcellular organelles previously demonstrated in cells (*23*) or, otherwise, lack sufficient ultrastructure and morphologic features to be conclusively identified as coronavirus. Since early May 2020, letters to the editors of several journals have refuted these descriptions (*24*–*30*), yet the misidentification of coronavirus particles continues. It is essential for our collective understanding of COVID-19 clinical pathology and pathogenesis as well as the field of diagnostic EM that these misidentifications of SARS-CoV-2 particles be addressed.

As of November 2020, only 2 articles and 1 letter to the editor had been published documenting clear EM evidence of SARS-CoV-2 directly in tissue samples (*30*–*32*), and another 2 articles showed rare viral particles (*33*,*34*). Here, we review published articles that used EM to search for SARS-CoV-2 in patient tissue samples. Our goal is to highlight the importance of coronavirus morphology and cellular localization in diagnosis and detection. In addition, we provide a side-by-side comparison of the subcellular structures that have been most frequently misinterpreted as SARS-CoV-2 along with actual viral particles that have been identified in COVID-19 autopsy tissues.

Coronavirus Structure

Knowledge of coronavirus ultrastructure and morphogenesis is paramount to avoiding errors in identification. The name coronavirus was coined by

Author affiliations: Synergy America, Inc., Atlanta, Georgia, USA (H.A. Bullock); Centers for Disease Control and Prevention, Atlanta (C.S. Goldsmith, S.R. Zaki, R.B. Martines); Duke Medical Center, Durham, North Carolina, USA (S.E. Miller)

DOI: https://doi.org/10.3201/eid2704.204337

June D. Almeida, who visualized the virus by EM in 1967 (*35*). The name was derived from the surface peplomers or spikes that give the viral particles the appearance of having a solar corona. These spikes are one of the more distinctive features for a coronavirus. For diagnostic EM, coronaviruses can be observed using 2 techniques, negative stain (*36*) and thin section (*36*,*37*). Negatively stained samples are prepared by adsorbing virus suspended in fluid onto a plastic-coated grid, wicking off excess liquid, and staining with a heavy-metal salt solution. The virus is coated with the stain, which penetrates

Table. Structures misidentified as coronavirus particles by transmission electron microscopy in publications, March–November 2020*

Original reference	Tissue	Structures misidentified as coronavirus (Figure no., panel)	Correct identification	Response
Yao et al. (*1*)	Lung	Spiked vesicles in the cytoplasm (1, A–C)	CCVs	NA
Pesaresi et al. (*2*)	Lung	Vacuole containing vesicles (1, A, B) Clusters of dark particles some associated with membranes (1, C, D) Clusters of dark particles (2, A, B, E)	MVB RER and possibly ribosomes Unidentifiable structures	NA
Grimes et al. (*3*)	Lung	Vacuole containing vesicles (2, A) Spiked vesicle in cytoplasm (2, B)	MVB Possible CCV	NA
Ackermann et al. (*4*)	Lung	Dark circular structures (3, D)	Unidentifiable structure	Scholkmann et al. (*29*)
Borczuk et al. (*5*)	Lung	Clusters of dark particles associated with membranes (6, E) Spiked vesicle in cytoplasm (7, F)	Vesiculating RER CCV	NA
Bradley et al. (*6*)	Lung	Collections of vesicles (5, A, D) Coated vesicles (5, B) Vacuole containing vesicles (5, C)	Unidentifiable structures CCVs MVB	Dittmayer et al. (*30*)
	Intestine	Circular membranes in cytoplasm (5, E) Extracellular spiked vesicles (5, F)	Unidentifiable structures Unidentifiable structures	NA
	Kidney	Spiked vesicles within a membrane (5, G) Membrane bound vesicles (5, H)	CCVs Unidentifiable structures	NA
Su et al. (*7*)	Kidney	Spiked vesicles in cytoplasm (2, A–D)	CCVs	Calomeni et al. (*24*); Miller et al. (*27*); Roufosse et al. (*28*)
Kissling et al. (*8*)	Kidney	Vacuole containing vesicles (1, E, F)	MVB	Calomeni et al. (*24*); Miller et al. (*27*); Roufosse et al. (*28*)
Varga et al. (*9*)	Kidney	Circular membrane structures with surrounding black dots (1, A, B)	Vesiculating RER	Goldsmith et al. (*26*); Roufosse et al. (*28*)
Farkash et al. (*10*)	Kidney	Spiked vesicles in cytoplasm (3, A–C) Vacuole containing vesicles (3, D)	CCVs MVB	Miller et al. (*25*); Roufosse et al. (*28*)
B. Diao et al., unpub. data, https://doi.org/10.1101/2020.03.04.20031120	Kidney	Spiked vesicles in cytoplasm (3)	CCVs	Roufosse et al. (*28*)
Abbate et al. (*11*)	Kidney	Spiked vesicle in cytoplasm (1)	CCV	NA
Menter et al. (*12*)	Kidney	Vacuoles containing vesicles (4, A–C) Collection of membrane bound particles (4, D)	MVB, Unidentifiable structure	NA
Werion et al. (*13*)	Kidney	Circular vesicles with internal black dots (3, A–C)	Outside-in RER	NA
Tavazzi et al. (*14*)	Heart	Spiked vesicles in cytoplasm (2, A–F)	CCVs	Dittmayer et al. (*30*)
Dolhnikoff et al. (*15*)	Heart	Roughly circular black structures (3, A, D) Clusters of dark particles, some associated with membranes (3, B, C)	Unidentifiable structures RER and clusters of ribosomes	Dittmayer et al. (*30*)
Paniz-Mondolfi et al. (*16*)	Brain	Vacuole containing circular particles (3, A, B) Vacuole containing vesicles (1, C, D)	Unidentifiable structures MVB	NA
Wang et al. (*17*)	Liver	Circular structures with surrounding black dots (1, M; 2, J)	Vesiculating RER	NA
Qian et al. (*18*)	Intestine	Spiked vesicles in cytoplasm (3, A, B)	CCVs	NA
Colmenero et al. (*19*)	Skin	Spiked vesicle in cytoplasm (4, D)	CCV	NA
Hosier et al. (*20*)	Placenta	Spiked vesicles in cytoplasm (4, C–F) Spherical particles (4, G–I)	CCVs Unidentifiable structures	NA
Algarroba et al. (*21*)	Placenta	Spiked vesicles in cytoplasm (2–6)	CCVs	NA
Sisman et al. (*22*)	Placenta	Vacuole containing circular particles (1, C)	Unidentifiable structures	NA

*CCV, clathrin or coatomer coated vesicles; MVB, multivesicular body; NA, not applicable; RER, rough endoplasmic reticulum.

between spikes protruding on the virus surface, making them visible. Thus, negative stain EM images readily show the prominent spikes that are associated with coronaviruses (Figure 1, panel A). For thin section EM, tissues or infected cell culture specimens are fixed in formalin or glutaraldehyde, stained with osmium, embedded in epoxy resin, baked to harden, and sectioned using an ultramicrotome. The resulting ultrathin sections show a cross-sectional view of the cells and viruses. In ultrathin sections of fixed tissues, coronavirus particles are ≈100 nm in diameter including their peplomer spikes and ≈80 nm in diameter excluding spikes (Figure 1, panel B). The spikes on coronavirus particles within cytoplasmic vacuoles (Figure 1, panel C) are not easily visible by thin section EM, unless the tissue is processed with tannic acid; instead, they usually appear as a fuzz on the surface of the virus. The difference in the appearance of the virus in negative stain versus thin section contributes to the confusion and misidentification of coronaviruses. Spikes are very rarely as clear in thin-sectioned specimens as they are when seen by negative stain EM.

Coronavirus Biology

Proper identification of coronaviruses within tissue samples requires understanding the biology of the virus and its replicative process (*37*–*39*); this knowledge ensures that the microscopist is searching for it in the correct cellular location, saving valuable time and helping to avoid misidentifying normal cellular structures as virus. In an infected cell, virus replication takes place within the host cell cytoplasm.

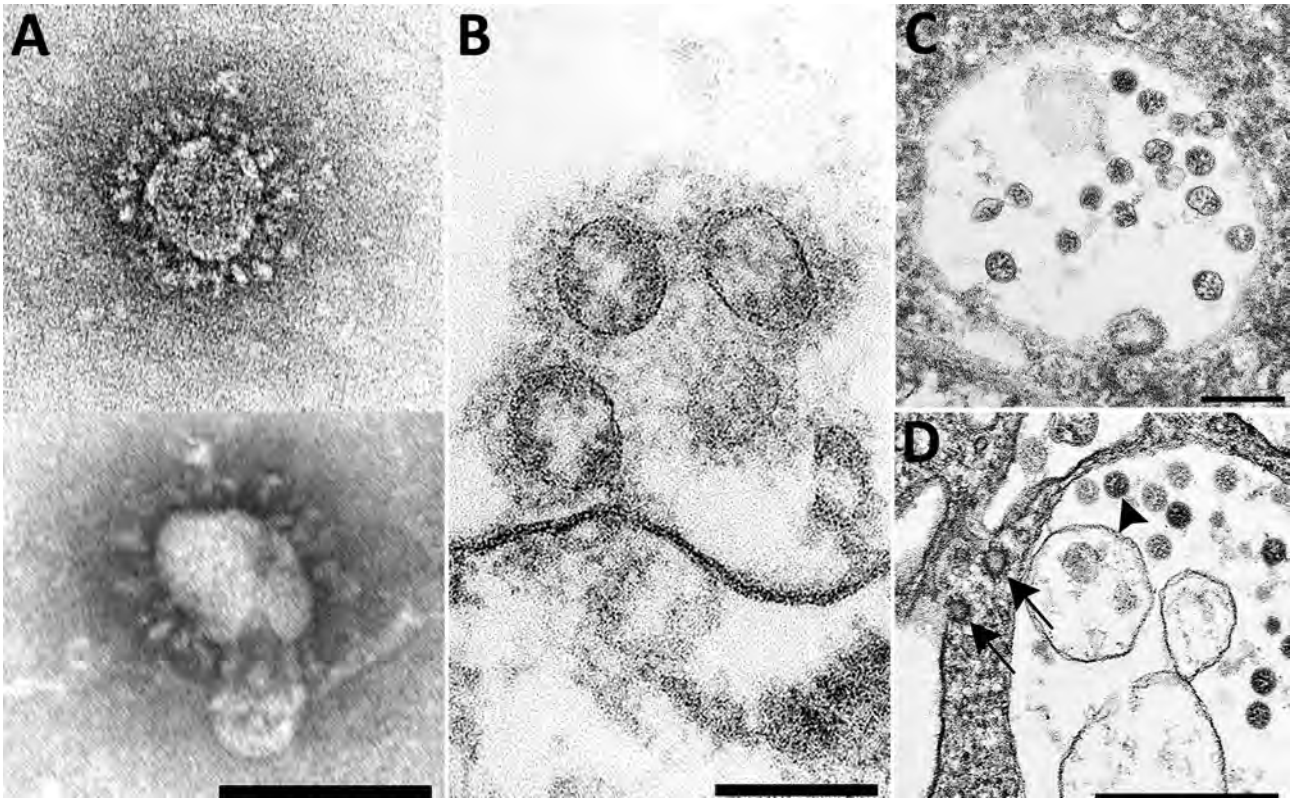

Figure 1. Overview of the ultrastructural features of coronavirus morphology as seen by negative stain and thin section. A) Extracellular viral particles ≈100 nm in diameter with prominent peplomers (spikes). Prepared from a cell culture sample by negative stain using heavy metal salt solutions to coat the outside of the virus. Scale bar indicates 100 nm. B) Extracellular viral particles ≈100 nm in diameter with clearly visible spikes. Cross sections through the helical nucleocapsid are visible on the interior of the particle as electron-dense black dots, 6–12 nm in diameter. Prepared by thin section from a formalin-fixed autopsy specimen. Scale bar indicates 100 nm. C) Intracellular viral particles ≈80 nm in diameter held within a membrane-bound vacuole. Cross sections through the helical nucleocapsid are visible inside the particles. Prepared by thin section from a formalin-fixed autopsy specimen. Scale bar indicates 200 nm. D) Intracellular viral particles (arrowhead) within a membrane-bound vacuole and nearby clathrin-coated vesicles (CCV) in the cytoplasm (arrows). CCV spikes directly contact the cell cytosol; viral spikes, barely visible as a faint fuzz, contact the vacuole contents. Cross sections through the helical nucleocapsid are visible inside the viral particles but not within the CCVs. Prepared by thin section from a glutaraldehyde-fixed cell culture sample. Scale bar indicates 500 nm.

Several studies have documented that the coronavirus replicative process induces formation of modified host cell membranes, including structures like double-membrane vesicles and convoluted membranes (*39*,*40*). Coronavirus structural components, including envelope, membrane, and spike proteins, are inserted into the endoplasmic reticulum (ER) and eventually move to the endoplasmic reticulum–Golgi intermediate compartment (ERGIC) (*37*,*41*). Complete virions are produced when the helical viral nucleocapsids bud through membranes of the ERGIC, taking with them ERGIC membrane, which pinches off to form spherical viral particles inside vesicles; the budding process provides the viral envelope (*37*,*38*). This region between the rough ER (RER) and the Golgi complex is known as the budding compartment. Virions then accumulate in the intracisternal space that forms a vacuole; if spikes were visible, they would be observed within the area of this membrane-bound vacuole (Figure 1, panels C, D). The vacuoles with viral particles migrate to the cell surface where the vacuolar and plasma membranes fuse, and the virus is extruded, resulting in extracellular particles in which spikes may be more apparent (*38*) (Figure 1, panel B). Of note, accumulations of coronavirus would not be found free within the cytoplasm of a cell, and at no point would the spikes of a coronavirus be in direct contact with the cytosol.

Structures Commonly Misidentified as Coronaviruses

We performed a literature search for reports published during March 1–November 30, 2020, that used EM to identify coronavirus directly in patient specimens. We used the keywords ultrastructure or electron microscopy in conjunction with COVID-19, SARS-CoV-2, or coronavirus when searching Google Scholar, PubMed, MEDLINE, Web of Science, and Scopus. We identified 27 reports with EM findings. Four of these reports and 1 letter to the editor included correctly identified coronavirus (*30*–*34*). The other 23 articles revealed a pattern of subcellular structures misidentified as virus (Table), including clathrin-coated and coatomer-coated vesicles (CCVs; 48%), multivesicular bodies (MVBs; 26%), circular cross-sections through vesiculated RER (19%), spherical invaginations of RER (4%), and other nonviral structures (30%). Figure 2 shows an overview of these subcellular components observed within autopsy tissues.

The most common structures erroneously identified as coronaviruses were CCVs (Table; Figure 2, panel A), which play essential roles in cellular transport. The clathrin protein is associated with vesicle formation and transport at the plasma membrane and trans-Golgi network. Coatomer proteins mediate transport within the Golgi complex and between the Golgi complex and ER (*42*). Although the sizes of the

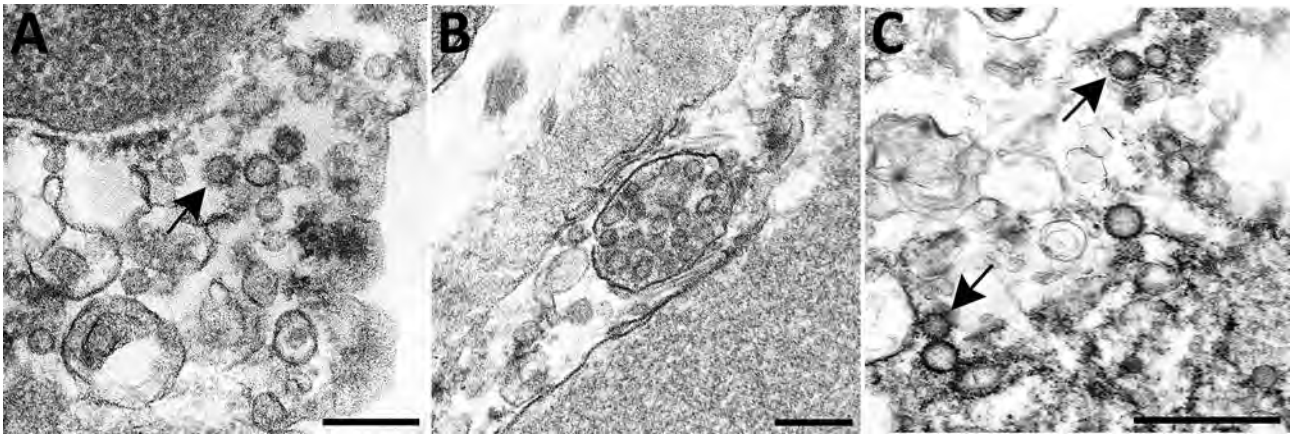

Figure 2. Overview of differential ultrastructural features of subcellular structures commonly misidentified as coronaviruses; all were prepared by thin section from formalin-fixed autopsy specimens. A) Clathrin-coated vesicles (CCVs), circular vesicles with a fringe of clathrin protein (arrow), in the cell cytoplasm range in size from 60 nm−100 nm. Differentiation: clathrin surrounding the vesicle may be misinterpreted as viral spikes, however, CCVs are free in the cell cytoplasm, and clathrin is in direct contact with the cytoplasm. Intracellular coronaviruses are found within membrane-bound vacuoles, and spikes, if visible, are in contact with the vacuolar contents. CCVs lack the internal black dots that signify cross sections through the viral nucleocapsid. Scale bar indicates 200 nm. B) Multivesicular body (MVB), a collection of membrane-bound roughly spherical vesicles formed by the inward budding of an endosomal membrane. Differentiation: MVBs may be confused with a vacuolar accumulation of coronavirus particles. Vesicles within multivesicular bodies do not have internal black dots that signify cross sections through the viral nucleocapsid. Scale bar indicates 200 nm. C) Circular cross sections through rough endoplasmic reticulum (RER) (arrows) found free within the cytoplasm. Differentiation: ribosomes along the endoplasmic reticulum may be confused with viral spikes. Ribosomes of vesiculating RER are in direct contact with the cell cytoplasm, unlike coronavirus spikes, which would be in contact with vacuolar contents. Vesiculating RER lacks cross sections through the viral nucleocapsid. Scale bar indicates 1 μm.

CCVs and the virus may be similar, the cellular location of each and the lack of cross sections through the viral nucleocapsid are key differentiating features (Figure 1, panel D). CCVs are found free in the cytoplasm, not within the membrane-bound vacuoles where intracellular coronavirus particles are found (Figure 1, panel D). The clathrin or coatomer projections protruding from the vesicles as a fringe can be easily misinterpreted as viral spikes. These clathrin and coatomer proteins, however, are in direct contact with the cell cytosol (Figure 1, panel D; Figure 2, panel A), whereas spikes on intracellular coronavirus particles, if visible, are within the vacuolar contents and not the cell fluid (Figure 1, panels C, D). An additional morphologic feature visible in coronaviruses in thin section EM is the helical nucleocapsid (*41*,*43*), which can be seen in cross sections as electron-dense black dots 6–12 nm in diameter on the inside of the viral particles (Figure 1 panels B-D). CCVs do not contain these black dots (Figure 1, panel D; Figure 2, panel A). The lack of these dots in a subcellular structure is a good indicator that it is not coronavirus.

Several reports have misidentified multivesicular bodies (MVBs) as coronavirus particles (Table). MVBs are a type of late endosome consisting of multiple vesicles within a membrane-bound structure formed from the inward budding of an outer endosomal membrane (Figure 2, panel B) and are part of standard cellular processes for protein degradation (*23*,*24*). MVBs may be confused with vacuolar accumulations of coronavirus; both have the appearance of a membrane-bound collection of spherical particles (Figure 1, panels C, D; Figure 2, panel B). The key differentiating feature is the lack of cross sections through the viral nucleocapsid within the spherical profiles of the MVB. Any purported membrane-bound accumulation of virus-like particles without the black dots signifying cross sections through the viral nucleocapsid is likely an MVB rather than a vacuole containing coronavirus. MVBs have also been misidentified as double-membrane vesicles, a part of the replication complex for coronaviruses. However, double-membrane vesicles are composed of 2 tightly apposed membranes, which is not the case with MVBs (*37*,*40*). In a letter to the editor of the journal *Kidney International*, Calomeni et al. discussed the prevalence of MVBs in kidney biopsies from the pre–COVID-19 era (*24*).

Circular cross sections through vesiculated RER, with its ribosome-studded membranes, have also been highlighted as viral particles in tissue samples (Table). The RER is the site of protein synthesis and plays a role in viral replication; however, it has been misidentified as virus itself in some recent publications. A thin section through an area of RER may give the appearance of a circular membrane with small dark spikes along the outside edge of the membrane (Figure 2, panel C). In this instance, the spikes along the membrane are in fact ribosomes, not viral peplomers. The substantial variability in size of circular cross sections through the RER indicate that these are not viral particles; coronavirus particles with spikes are typically around 80–100 nm in diameter. Vesiculating RER also lacks the interior black dots of cross sections through the viral nucleocapsid, and the ribosomes, mistaken for spikes, are in direct contact with the host cell cytoplasm, rather than the vacuolar content.

An additional structure that has misled investigators appears to be an invagination of RER that results in roughly spherical particles with ribosomes inside (*13*), referred to in one paper as outside-in RER (*44*). These virus-like particles are uniform and comparable in size to coronaviruses, ≈100 nm in diameter. The particles meet the morphological criteria for a coronavirus except that the dots inside are larger (≈20 nm) than those in cross sections through coronavirus nucleocapsids (≈6–12 nm). The exact nature of their composition or relationship to any cellular processes has not been determined.

Identifying Coronaviruses Using Formalin-Fixed Tissue and Formalin-Fixed, Paraffin-Embedded Samples

Although EM alone is a powerful tool, a multipronged approach for detecting and identifying viral particles can be key to the prompt and accurate diagnosis of the extent of infection and for further investigation into disease pathology. This fact is particularly true in rapidly developing situations, such as the COVID-19 pandemic, when transmission of high-quality scientific information is of paramount importance. Although formalin- or glutaraldehyde-fixed tissues embedded for EM are necessary for accurate classification of viral morphology and morphogenesis, the detection of virus within a tissue may require a more targeted approach to find the infected area, such as by working closely with a pathologist to select promising areas for EM from formalin-fixed tissues displaying evident disease pathology (e.g., areas of pulmonary consolidation) or by using formalin-fixed, paraffin-embedded (FFPE) blocks (*31*).

The benefit of using FFPE samples is the ability to perform a variety of diagnostic methodologies on serial sections from the same tissue, enabling comparison and correlation of test results. For example,

immunohistochemistry (IHC) tests using antibodies for a specific pathogen can be applied to sections of FFPE tissue on glass slides and, based on the IHC results, areas of interest that are likely to contain the antigen or virus can be identified for EM analysis. The selected areas can be prepared for EM by embedding a tissue section 4–6 μm thick affixed to a glass side in situ on the slide (on-slide), or the targeted tissue can be removed from the FFPE block using a biopsy punch, deparaffinized, and embedded in epoxy (*31*,*36*). However, processing and analyzing each of these sample types presents challenges; the foremost is the accurate identification of viral particles, because the ultrastructural morphology of the virus and the surrounding tissue may be degraded by the processing for light microscopy. Having an area of interest selected that is already positive for a virus by another test, such as IHC or in situ hybridization (ISH), aids in viral detection and identification by EM. For this approach to be successful, IHC and ISH assays must be rigorously evaluated and validated by using negative controls and by testing antibody cross-reactivities to prevent false positives and the misinterpretation of nonspecific staining.

An example of this approach in autopsy tissues is shown in Figure 3. We selected an area of interest for EM based on a positive IHC result for SARS-CoV-2 in ciliated epithelial cells from the trachea (Figure 3, panel A). Using FFPE samples leads to compromised ultrastructure and a reduction in viral particle size because of the additional processing these samples undergo, including embedding in paraffin, deparaffinizing, staining, and drying, before being dehydrated and embedded in epoxy for EM. This deteriorated ultrastructure is particularly evident in the on-slide sample (Figure 3, panel B). Although morphology is compromised, the presence of large numbers of intracellular and extracellular uniformly sized particles in areas corresponding to positive immunostaining or molecular labeling are clues to the presence of viruses. The extracellular viral particles are smaller than would be observed in a typical glutaraldehyde-fixed thin section sample due to shrinkage from processing, closer to 75 nm in diameter than 100 nm, but can still be differentiated from the surrounding ciliary structures. Closer examination of the FFPE biopsy punch sample (Figure 3, panel C) reveals apparent cross sections through the viral nucleocapsid as well as a surrounding fuzz which is suggestive of peplomers. Using a multifaceted approach such as this for SARS-CoV-2 detection enables accurate determination of the localization of the virus within tissues and correlation of histopathological with ultrastructural features of SARS-CoV-2 infection.

Conclusions

EM is powerful in its ability to provide a window into the ultrastructure, and thus function, of tissues and the infectious agents they may contain. It gives scientists a valuable tool to provide clear visual evidence of viral infection and disease pathology, unlike biochemical tests that require choosing a priori the correct reagent and may yield false positive or false negative results. However, knowledge of both viral morphogenesis and normal subcellular architecture is necessary to identify viruses correctly by EM. The

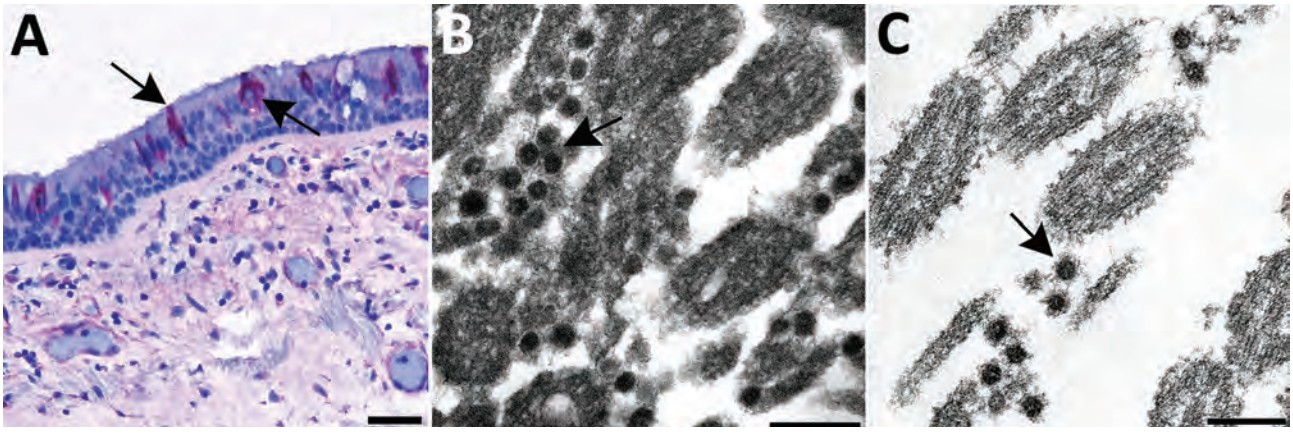

Figure 3. Use of immunohistochemistry and electron microscopy to detect severe acute respiratory syndrome coronavirus 2 (SARS-CoV-2) in formalin-fixed paraffin embedded (FFPE) autopsy tissues. A) Immunostaining (arrows) of SARS-CoV-2 in the epithelial cells of the trachea. Scale bar indicates 20 μm. B) Ultrastructural features of extracellular SARS-CoV-2 particles (arrow) in association with ciliated cells of the trachea from paraffin section in panel A, prepared using an FFPE on-slide method. Scale bar indicates 200 nm. C) Thin section of a biopsy punch from the original FFPE block in panel A showing viral particles (arrow) ≈75 nm. Scale bar indicates 200 nm.

issue of virus misidentification within tissue samples is not unique to coronaviruses or limited to those subcellular structures we addressed in this report; nuclear pores may be mistaken for herpesvirus, perichromatin granules for smaller DNA viruses such as parvoviruses or polyomaviruses, and ribosomes for picornaviruses. Neurosecretory granules and glycocalyceal bodies can also be misidentified as viruses (*23*,*45*,*46*). Before declaring the presence of viruses, particularly complex enveloped viruses with multiple appearances in different stages of maturation, we recommend consulting with a trained diagnostic EM professional who has extensive knowledge of viral ultrastructure. If, after such consultation, a definitive identification still cannot be made, a descriptive report may be used, including the size, morphology, and cellular location of the particles of interest. One should only use the term virus or a more specific term, such as coronavirus, when the particles in question can be positively identified. The term virus-like may be used when only some morphologic criteria for virus identification have been met or in cases of deteriorated ultrastructure.

The use of diagnostic EM for infectious diseases pathology research is at its best when it involves collaboration between specialists in pathology, microscopy, and microbiology. The scientific community's interest in diagnostic EM and the need for trained professionals in this field is highlighted by the number of recent articles seeking to identify SARS-CoV-2 particles in patient specimens. In each case of erroneously identified coronavirus particles, the structures mistaken for virus are common cellular organelles. These misinterpretations are easy to make without extensive training and are made easier by the publication of incorrectly identified viral structures. Articles with misidentified viral particles are used by others to verify the presence of viral particles in their own research, potentially wrongfully documenting the presence of the virus in damaged tissues. However, rather than actual virus infection of a failing organ, the damage could be due to lack of support of the infected organ due to the body's response to toxins, such as cytokines and circulating debris, or to clotting (*47*,*48*). These continued misinterpretations could have meaningful impacts on future publications about coronavirus detection and research.

Coronaviruses have been the cause of 3 life-threatening human disease outbreaks over the past 18 years: SARS-CoV in 2002, Middle East respiratory syndrome coronavirus in 2012, and finally, the 2020 SARS-CoV-2 pandemic. Given the abundance of coronaviruses in the natural environment, the scientific literature should accurately reflect the nature of SARS-CoV-2 infection, including the ultrastructure and cellular location within the cell of the virus. This need is important not only for our current understanding of SARS-CoV-2 infection but also as the public health community prepares for future outbreaks. Diagnostic EM has played a key role in previous outbreaks of Nipah virus, SARS-CoV, monkeypox virus, and Ebola viruses, as well as many others (*49*), and will continue to be a tool for detecting and characterizing new and emerging pathogens.

Acknowledgments

We thank Natalie Thornburg, Azaibi Tamin, and Jennifer Harcourt for providing SARS-CoV-2–infected Vero cell cultures. We also thank Brigid Bollweg, Luciana Flannery, and Pamela Fair for performing the SARS-CoV-2 immunohistochemistry assays.

Author contributions: H.B., C.G., R.M., S.Z., and S.M. contributed to the conceptualization of the manuscript. H.B., C.G., and S.M. drafted the manuscript. H.B., C.G., R.M., and S.M. performed the literature search and reviewed the literature. H.B., C.G., and R.M. contributed to the figure design and preparation. H.B., C.G., R.M., S.Z., and S.M. contributed to the proofing and revision of the manuscript and approved the final version for submission.

About the Author

Dr. Bullock works as an electron microscopist in the Infectious Diseases Pathology Branch, Division of High Consequences Pathogens and Pathology, National Center for Emerging and Zoonotic Infectious Diseases, Centers for Disease Control and Prevention. Her research interests include emerging infectious diseases and viral and bacterial ultrastructure.

References

1. Yao XH, He ZC, Li TY, Zhang HR, Wang Y, Mou H, et al. Pathological evidence for residual SARS-CoV-2 in pulmonary tissues of a ready-for-discharge patient. Cell Res. 2020;30:541–3. https://doi.org/10.1038/s41422-020-0318-5
2. Pesaresi M, Pirani F, Tagliabracci A, Valsecchi M, Procopio AD, Busardò FP, et al. SARS-CoV-2 identification in lungs, heart and kidney specimens by transmission and scanning electron microscopy. Eur Rev Med Pharmacol Sci. 2020;24:5186–8.
3. Grimes Z, Bryce C, Sordillo EM, Gordon RE, Reidy J, Paniz Mondolfi AE, et al. Fatal pulmonary thromboembolism in SARS-CoV-2 infection. Cardiovasc Pathol. 2020;48:107227. https://doi.org/10.1016/j.carpath.2020.107227
4. Ackermann M, Verleden SE, Kuehnel M, Haverich A, Welte T, Laenger F, et al. Pulmonary vascular endothelialitis,

thrombosis, and angiogenesis in Covid-19. N Engl J Med. 2020;383:120–8 https://doi.org/10.1056/NEJMoa2015432
5. Borczuk AC, Salvatore SP, Seshan SV, Patel SS, Bussel JB, Mostyka M, et al. COVID-19 pulmonary pathology: a multi-institutional autopsy cohort from Italy and New York City. Mod Pathol. 2020;33:2156–68. https://doi.org/10.1038/s41379-020-00661-1
6. Bradley BT, Maioli H, Johnston R, Chaudhry I, Fink SL, Xu H, et al. Histopathology and ultrastructural findings of fatal COVID-19 infections in Washington state: a case series. Lancet. 2020;396:320–32. https://doi.org/10.1016/S0140-6736(20)31305-2
7. Su H, Yang M, Wan C, Yi LX, Tang F, Zhu HY, et al. Renal histopathological analysis of 26 postmortem findings of patients with COVID-19 in China. Kidney Int. 2020;98:219–27. https://doi.org/10.1016/j.kint.2020.04.003
8. Kissling S, Rotman S, Gerber C, Halfon M, Lamoth F, Comte D, et al. Collapsing glomerulopathy in a COVID-19 patient. Kidney Int. 2020;98:228–31. https://doi.org/10.1016/j.kint.2020.04.006
9. Varga Z, Flammer AJ, Steiger P, Haberecker M, Andermatt R, Zinkernagel AS, et al. Endothelial cell infection and endotheliitis in COVID-19. Lancet. 2020;395:1417–8. https://doi.org/10.1016/S0140-6736(20)30937-5
10. Farkash EA, Wilson AM, Jentzen JM. Ultrastructural evidence for direct renal infection with SARS-CoV-2. J Am Soc Nephrol. 2020;31:1683–7. https://doi.org/10.1681/ASN.2020040432
11. Abbate M, Rottoli D, Gianatti A. COVID-19 attacks the kidney: ultrastructural evidence for the presence of virus in the glomerular epithelium. Nephron. 2020;144:341–2. https://doi.org/10.1159/000508430
12. Menter T, Haslbauer JD, Nienhold R, Savic S, Hopfer H, Deigendesch N, et al. Postmortem examination of COVID-19 patients reveals diffuse alveolar damage with severe capillary congestion and variegated findings in lungs and other organs suggesting vascular dysfunction. Histopathology. 2020;77:198–209. https://doi.org/10.1111/his.14134
13. Werion A, Belkhir L, Perrot M, Schmit G, Aydin S, Chen Z, et al.; Cliniques universitaires Saint-Luc (CUSL) COVID-19 Research Group. SARS-CoV-2 causes a specific dysfunction of the kidney proximal tubule. Kidney Int. 2020;98:1296–307. https://doi.org/10.1016/j.kint.2020.07.019
14. Tavazzi G, Pellegrini C, Maurelli M, Belliato M, Sciutti F, Bottazzi A, et al. Myocardial localization of coronavirus in COVID-19 cardiogenic shock. Eur J Heart Fail. 2020;22:911–5. https://doi.org/10.1002/ejhf.1828
15. Dolhnikoff M, Ferreira Ferranti J, de Almeida Monteiro RA, Duarte-Neto AN, Soares Gomes-Gouvêa M, Viu Degaspare N, et al. SARS-CoV-2 in cardiac tissue of a child with COVID-19–related multisystem inflammatory syndrome. Lancet Child Adolesc Health. 2020;4:790–4. https://doi.org/10.1016/S2352-4642(20)30257-1
16. Paniz-Mondolfi A, Bryce C, Grimes Z, Gordon RE, Reidy J, Lednicky J, et al. Central nervous system involvement by severe acute respiratory syndrome coronavirus-2 (SARS-CoV-2). J Med Virol. 2020;92:699–702. https://doi.org/10.1002/jmv.25915
17. Wang Y, Liu S, Liu H, Li W, Lin F, Jiang L, et al. SARS-CoV-2 infection of the liver directly contributes to hepatic impairment in patients with COVID-19. J Hepatol. 2020;73:807–16. https://doi.org/10.1016/j.jhep.2020.05.002
18. Qian Q, Fan L, Liu W, Li J, Yue J, Wang M, et al. Direct evidence of active SARS-CoV-2 replication in the intestine. Clin Infect Dis. 2020 Jul 8 [Epub ahead of print]. https://doi.org/10.1093/cid/ciaa925
19. Colmenero I, Santonja C, Alonso-Riaño M, Noguera-Morel L, Hernández-Martín A, Andina D, et al. SARS-CoV-2 endothelial infection causes COVID-19 chilblains: histopathological, immunohistochemical and ultrastructural study of seven pediatric cases. Br J Dermatol. 2020;183:729–37. https://doi.org/10.1111/bjd.19327
20. Hosier H, Farhadian SF, Morotti RA, Deshmukh U, Lu-Culligan A, Campbell KH, et al. SARS-CoV-2 infection of the placenta. J Clin Invest. 2020;130:4947–53. https://doi.org/10.1172/JCI139569
21. Algarroba GN, Rekawek P, Vahanian SA, Khullar P, Palaia T, Peltier MR, et al. Visualization of severe acute respiratory syndrome coronavirus 2 invading the human placenta using electron microscopy. Am J Obstet Gynecol. 2020;223:275–8. https://doi.org/10.1016/j.ajog.2020.05.023
22. Sisman J, Jaleel MA, Moreno W, Rajaram V, Collins RRJ, Savani RC, et al. Intrauterine transmission of SARS-CoV-2 infection in a preterm infant. Pediatr Infect Dis J. 2020;39:e265–7. https://doi.org/10.1097/INF.0000000000002815
23. Ghadially F. Ultrastructural pathology of the cell and matrix. 4th ed. Boston: Butterworth-Heinemann; 1997.
24. Calomeni E, Satoskar A, Ayoub I, Brodsky S, Rovin BH, Nadasdy T. Multivesicular bodies mimicking SARS-CoV-2 in patients without COVID-19. Kidney Int. 2020;98:233–4. https://doi.org/10.1016/j.kint.2020.05.003
25. Miller SE, Goldsmith CS. Caution in identifying coronaviruses by electron microscopy. J Am Soc Nephrol. 2020;31:2223–4. https://doi.org/10.1681/ASN.2020050755
26. Goldsmith CS, Miller SE, Martines RB, Bullock HA, Zaki SR. Electron microscopy of SARS-CoV-2: a challenging task. Lancet. 2020;395:e99. https://doi.org/10.1016/S0140-6736(20)31188-0
27. Miller SE, Brealey JK. Visualization of putative coronavirus in kidney. Kidney Int. 2020;98:231–2. https://doi.org/10.1016/j.kint.2020.05.004
28. Roufosse C, Curtis E, Moran L, Hollinshead M, Cook T, Hanley B, et al. Electron microscopic investigations in COVID-19: not all crowns are coronas. Kidney Int. 2020;98:505–6. https://doi.org/10.1016/j.kint.2020.05.012
29. Scholkmann F, Nicholls J. Letter to the editor: pulmonary vascular pathology in Covid-19. N Engl J Med. 2020;383:887–8. https://doi.org/10.1056/NEJMc2022068
30. Dittmayer C, Meinhardt J, Radbruch H, Radke J, Heppner BI, Heppner FL, et al. Why misinterpretation of electron micrographs in SARS-CoV-2-infected tissue goes viral. Lancet. 2020;396:e64–5. https://doi.org/10.1016/S0140-6736(20)32079-1
31. Martines RB, Ritter JM, Matkovic E, Gary J, Bollweg BC, Bullock H, et al.; COVID-19 Pathology Working Group. Pathology and pathogenesis of SARS-CoV-2 associated with fatal coronavirus disease, United States. Emerg Infect Dis. 2020;26:2005–15. https://doi.org/10.3201/eid2609.202095
32. Meinhardt J, Radke J, Dittmayer C, Franz J, Thomas C, Mothes R, et al. Olfactory transmucosal SARS-CoV-2 invasion as a port of central nervous system entry in individuals with COVID-19. Nat Neurosci. 2020 Nov 30 [Epub ahead of print]. https://doi.org/10.1038/s41593-020-00758-5 PMID: 33257876
33. Falasca L, Nardacci R, Colombo D, Lalle E, Di Caro A, Nicastri E, et al. Postmortem findings in Italian patients with COVID-19: A descriptive full autopsy study of cases with and without comorbidities. J Infect Dis. 2020;222:1807–15. https://doi.org/10.1093/infdis/jiaa578
34. Carsana L, Sonzogni A, Nasr A, Rossi RS, Pellegrinelli A, Zerbi P, et al. Pulmonary post-mortem findings in a series of COVID-19 cases from northern Italy: a two-centre

descriptive study. Lancet Infect Dis. 2020;20:1135–40. https://doi.org/10.1016/S1473-3099(20)30434-5
35. Almeida JD, Tyrrell DA. The morphology of three previously uncharacterized human respiratory viruses that grow in organ culture. J Gen Virol. 1967;1:175–8. https://doi.org/10.1099/0022-1317-1-2-175
36. Hayat M. Principles and techniques of electron microscopy: biological applications. 4th ed. Cambridge: Cambridge University Press; 2000.
37. Goldsmith CS, Tatti KM, Ksiazek TG, Rollin PE, Comer JA, Lee WW, et al. Ultrastructural characterization of SARS coronavirus. Emerg Infect Dis. 2004;10:320–6. https://doi.org/10.3201/eid1002.030913
38. Oshiro LS, Schieble JH, Lennette EH. Electron microscopic studies of coronavirus. J Gen Virol. 1971;12:161–8. https://doi.org/10.1099/0022-1317-12-2-161
39. Snijder EJ, Limpens RWAL, de Wilde AH, de Jong AWM, Zevenhoven-Dobbe JC, Maier HJ, et al. A unifying structural and functional model of the coronavirus replication organelle: tracking down RNA synthesis. PLoS Biol. 2020;18:e3000715. https://doi.org/10.1371/journal.pbio.3000715
40. Knoops K, Kikkert M, Worm SH, Zevenhoven-Dobbe JC, van der Meer Y, Koster AJ, et al. SARS-coronavirus replication is supported by a reticulovesicular network of modified endoplasmic reticulum. PLoS Biol. 2008;6:e226. https://doi.org/10.1371/journal.pbio.0060226
41. de Haan CAM, Rottier PJM. Molecular interactions in the assembly of coronaviruses. Adv Virus Res. 2005;64:165–230. https://doi.org/10.1016/S0065-3527(05)64006-7
42. Bonifacino JS, Lippincott-Schwartz J. Coat proteins: shaping membrane transport. Nat Rev Mol Cell Biol. 2003;4:409–14. https://doi.org/10.1038/nrm1099
43. Chang CK, Hou MH, Chang CF, Hsiao CD, Huang TH. The SARS coronavirus nucleocapsid protein—forms and functions. Antiviral Res. 2014;103:39–50. https://doi.org/10.1016/j.antiviral.2013.12.009
44. Hopfer H, Herzig MC, Gosert R, Menter T, Hench J, Tzankov A, et al. Hunting coronavirus by transmission electron microscopy—a guide to SARS-CoV-2-associated ultrastructural pathology in COVID-19 tissues. Histopathology. 2021;78:358–70. https://doi.org/10.1111/his.14264
45. Haguenau F. "Viruslike" particles as observed with the electron microscope. In: Dalton AJ, Haguenau F, editors. Ultrastructure of animal viruses and bacteriophages: an atlas. New York City: Academic Press, Inc; 1973. p. 391–7.
46. Miller SE. Detection and identification of viruses by electron microscopy. J Electron Microsc Tech. 1986;4:265–301. https://doi.org/10.1002/jemt.1060040305
47. Azkur AK, Akdis M, Azkur D, Sokolowska M, van de Veen W, Brüggen MC, et al. Immune response to SARS-CoV-2 and mechanisms of immunopathological changes in COVID-19. Allergy. 2020;75:1564–81. https://doi.org/10.1111/all.14364
48. Jose RJ, Manuel A. COVID-19 cytokine storm: the interplay between inflammation and coagulation. Lancet Respir Med. 2020;8:e46–7. https://doi.org/10.1016/S2213-2600(20)30216-2
49. Goldsmith CS, Ksiazek TG, Rollin PE, Comer JA, Nicholson WL, Peret TCT, et al. Cell culture and electron microscopy for identifying viruses in diseases of unknown cause. Emerg Infect Dis. 2013;19:886–91. https://doi.org/10.3201/eid1906.130173

Address for correspondence: Hannah Bullock, Centers for Disease Control and Prevention, 1600 Clifton Rd NE, Mailstop H18-SB, Atlanta, GA 30329-4027, USA; email: HBullock@cdc.gov

Characteristics of SARS-CoV-2 Transmission among Meat Processing Workers in Nebraska, USA, and Effectiveness of Risk Mitigation Measures

Jocelyn J. Herstein, Abraham Degarege, Derry Stover, Christopher Austin, Michelle M. Schwedhelm, James V. Lawler, John J. Lowe, Athena K. Ramos, Matthew Donahue

The coronavirus disease (COVID-19) pandemic has severely impacted the meat processing industry in the United States. We sought to detail demographics and outcomes of severe acute respiratory syndrome coronavirus 2 infections among workers in Nebraska meat processing facilities and determine the effects of initiating universal mask policies and installing physical barriers at 13 meat processing facilities. During April 1–July 31, 2020, COVID-19 was diagnosed in 5,002 Nebraska meat processing workers (attack rate 19%). After initiating both universal masking and physical barrier interventions, 8/13 facilities showed a statistically significant reduction in COVID-19 incidence in ≤10 days. Characteristics and incidence of confirmed cases aligned with many nationwide trends becoming apparent during this pandemic: specifically, high attack rates among meat processing industry workers, disproportionately high risk of adverse outcomes among ethnic and racial minority groups and men, and effectiveness of using multiple prevention and control interventions to reduce disease transmission.

In the early months of the coronavirus disease (COVID-19) pandemic, meat processing facilities became among the largest epicenters of COVID-19 outbreaks in the United States (*1*). Declared a critical infrastructure industry in April 2020 (*2*), meat processing facilities are particularly vulnerable to COVID-19 because of the high density of workers required for operations, prolonged close contact of personnel on the production line, indoor work environments with compact cafeteria and locker room areas, and a workforce with diverse cultural and linguistic backgrounds that make educational efforts more challenging (*3*). A Centers for Disease Control and Prevention (CDC) report found that, as of May 31, 2020, >16,000 workers in meat and poultry processing facilities in the United States had been diagnosed with COVID-19 and 86 had died (*4*); as of October 2020, those case counts and deaths had more than tripled (*5*).

Meat processing facilities in Nebraska employ ≈26,000 workers (*6*). The first COVID-19 illness among meat processing facility workers in Nebraska was identified March 9, 2020. As of July 2020, cases had been reported among workers in 23 Nebraska meat processing facilities. The University of Nebraska Medical Center (UNMC) and Nebraska Department of Health and Human Services partnered to mitigate COVID-19 risks in Nebraska among workers in this industry. Nebraska Department of Health and Human Services expanded case investigations and contact tracing teams and coordinated 2 mass testing events with participating meat processing facilities. UNMC created evidence-based guidelines for facilities (*7*) and assembled a team of infectious disease and infection prevention and control (IPC) experts to provide onsite and virtual technical assistance to facilities to evaluate gaps in IPC practices and provide facility-specific IPC recommendations.

Local and state health departments conducted case investigations to collect information on demographics, employer, occupation, industry, illness descriptions, medical history, and outcomes among Nebraska meat processing workers. Moreover, although industry-specific guidelines for mitigating COVID-19 transmission in meat processing facilities have been issued by CDC and other public health

Author affiliations: University of Nebraska Medical Center, Omaha, Nebraska, USA (J.J. Herstein, A. Degarege, J.V. Lawler, J.J. Lowe, A.K. Ramos); Nebraska Department of Health and Human Services, Lincoln, Nebraska, USA (D. Stover, C. Austin, M. Donahue); Nebraska Medicine, Omaha (M.M. Schwedhelm, J.V. Lawler)

DOI: https://doi.org/10.3201/eid2704.204800

organizations (*7*,*8*), the effectiveness of these measures among workers has not been reported. We present data on the effectiveness of initiating a universal mask policy and installing physical barriers (plexiglass or plastic partitions) between workstations and at cafeteria tables on reducing COVID-19 incidence at meat processing facilities in Nebraska.

Methods

Characteristics of Laboratory-Confirmed Cases

We used SAS version 9.4 (https://www.sas.com) to develop a keyword algorithm to identify meat processing facility workers by using occupation, industry, and employer data fields from case investigations conducted among Nebraska residents with laboratory-confirmed COVID-19. Specimens were collected from healthcare providers, work-sponsored testing events, state-sponsored testing events, and stationary state-sponsored testing sites during April 1–July 31, 2020. We used R 4.0.2 with dplyr version 1.0.2 (https://cran.r-project.org) to examine the duration of timelines between illness onset dates, specimen collection dates, and case investigation dates. Data from records with erroneous timelines were excluded from timeline analyses (Table 1), including records in which the same dates were recorded for illness onset, specimen collection, and investigation (not possible within the case investigation workflow) or if illness onset occurred after the case investigation.

We classified workers with laboratory-confirmed COVID-19 into 1 of 3 timeline categories based on the relationship between the illness onset date, specimen collection date, and case investigation date: primary timeline, probable timeline, or presymptomatic timeline. We classified workers into the primary timeline if they had an illness onset date followed by specimen collection date, followed by investigation date. We classified workers into the probable timeline if they were investigated before their positive test result was available. We further classified workers in the probable timeline into 3 subcategories: 1) illness onset occurring the same day as the investigation date, followed by specimen collection; 2) illness onset date followed by an investigation date, followed by specimen collection date; or 3) illness onset date followed by specimen collection date occurring on the same day the investigation began. We classified workers into the presymptomatic timeline if they had a specimen collection date followed by illness onset date, followed by an investigation date. We used the R package table1 version 1.2 to create frequency tables for demographics, illness descriptions, medical history, and outcomes.

Effects of Mask and Physical Barrier Interventions

The UNMC team provided technical assistance as voluntarily requested by meat processing facilities in the state to identify facility-specific recommendations on additional risk mitigation measures that could be implemented. We used a 4-page checklist summarizing primary IPC recommendations for meat processing facilities to guide technical assistance site visits or calls and subsequent debriefing with plant leadership (*7*). The checklist included recommendations for engineering controls (e.g., enhancing ventilation, installing physical barriers between workers on the production line and in cafeterias), administrative controls (e.g., cohorting of consistent work teams, education, environmental cleaning and disinfection policies), and personal protective equipment. Site visit personnel completed the checklist and gathered information on the workforce (e.g., number of employees, employee demographics) and dates of initiating a universal mask policy, installing physical barriers, or both. For each facility, the dates of initiating a universal mask policy and completing physical barrier installation were collated and used in the analyses.

Table 1. Timeline exclusions, subsets, and median durations for case investigations of severe acute respiratory syndrome coronavirus 2 infection among meat processing workers, Nebraska, April 1–July 31, 2020*

Category	Illness onset to specimen collection	Specimen collection to Investigation	Illness onset to investigation
Beginning total	3,695	4,834	3,817
Erroneous timelines excluded: onset date = collection date = investigation date	16	16	16
Erroneous timelines excluded: investigation → onset	39	39	40
Probable cases analyzed separately: onset = investigation → collection	29	29	31
Probable cases analyzed separately: onset → collection = investigation	76	116	76
Probable cases analyzed separately: onset → investigation → collection	19	55	19
Presymptomatic cases analyzed separately: collection → onset → investigation	214	214	214
Primary timeline totals: onset → collection → investigation	3,302	4,365	3,421
Median (range) for primary timeline, d	3 (0–53)	4 (1–109)	8 (1–110)

We used Stata version 16 (https://www.stata.com) to conduct a retrospective analysis of data on the incidence of severe acute respiratory syndrome coronavirus 2 (SARS-CoV-2) infection among employees in the meat processing facilities that received technical assistance during April–July 2020. To estimate when the effect of an intervention, measured by case counts, might be observed, we estimated the total duration from exposure through testing and diagnosis (positive test) at ≈10 days based on prior analyses (*9*). The main outcome variable we assessed was the incidence of SARS-CoV-2 infection.

For each plant, before-intervention incidence per 1,000 persons per day was calculated by dividing the number of cases reported before or <10 days after intervention by the product of the total number of employees and the number of days from baseline to 10 days after intervention. Postintervention incidence per 1,000 persons per day was calculated by dividing the number of new cases reported 10 days after intervention by the product of the total number of cases 10 days after intervention and the number of days from 10 days after intervention to the last day of the study period. Z-test of proportion was used to compare incidence per 1,000 persons per day before or <10 days after intervention with incidence 10 days after the intervention. Differences in the incidence of SARS-CoV-2 infection before and after the intervention were considered significant where p was <0.05.

Results

Characteristics of Laboratory-Confirmed and Probable Cases

During April 1–July 31, 2020, among Nebraska residents working at meat processing facilities, 5,002 of ≈26,000 received a diagnosis of COVID-19 (attack rate 19%). Of those, 3,817 (76%) had a recorded illness onset date, 4,834 (97%) had a recorded specimen collection date, and 5,002 (100%) had a recorded investigation date; 3,695 (74%) had both illness onset and specimen collection dates recorded, 4,834 (97%) had both specimen collection and investigation dates recorded, and 3,817 (76%) had both illness onset and investigation dates recorded. After excluding erroneous timelines, probable cases, and presymptomatic cases (Table 1), we used data from confirmed cases with illness onset followed by specimen collection followed by investigation to calculate durations for the primary timeline; we calculated durations independently for the probable and presymptomatic timelines.

For the primary timeline, the median duration from illness onset to specimen collection was 3 days (n = 3,302), from specimen collection to investigation was 4 days (n = 4,365), and from illness onset to investigation was 8 days (n = 3,421). For probable cases, the median duration from illness onset to specimen collection was 4 days (n = 124), from specimen collection to investigation was 0 days (n = 200), and from illness onset to investigation was 2.5 days (n = 124). For presymptomatic cases, median duration from specimen collection to illness onset was 3 days (n = 214), from specimen collection to investigation was 6 days (n = 214), and from illness onset to investigation was 4 days (n = 214).

Among the 5,002 total COVID-19 case-patients, the median age was 43 years (mean 42.7 years, range 13–81 years). Men accounted for 2,919 (58%) cases; 3,343 (67%) identified as Hispanic or Latino, 2,678 (54%) as White, 570 (11%) as Asian, 405 (8%) as Black or African American, 27 (<1%) as American Indian or Alaska Native, 16 (<1%) as Native Hawaiian or other Pacific Islander, and 1,306 (26%) as other race or unknown. Twenty-seven case-patients (<1%) were pregnant.

Symptoms were reported by 4,237 (85%) workers, 501 (10%) were asymptomatic, and 264 (5%) had unknown symptom status. Of those reporting symptoms, the average illness duration was 12.8 days (median 11 days). Headache (2,526; 60%), cough (2,442; 58%), and muscle pain (2,344; 55%) were most frequently reported symptoms. Smoking (124/4,237; 2%) was reported more frequently among workers not identifying as Hispanic or Latino (64; 5%) than among Hispanic or Latino workers (52; 2%). A preexisting medical condition was reported by 1,117 (22%) workers, most frequently diabetes (359; 32%) or cardiovascular disease (240; 21%). Diabetes was reported more frequently among workers identifying as Hispanic or Latino (277; 36%) than among non-Hispanic/Latino workers (72; 23%).

Among symptomatic case-patients, 225 (4%; median age 55 years, range 19–49 years) were hospitalized for an average duration of 8.4 days and 83 (2%; median age 57 years, range 21–79 years) required intensive care unit (ICU) admission; 21 (<1%; median age 63 years, range 39–79 years) workers died. Among the 225 hospitalized patients, 161 (72%) were men, as were 65 (78%) requiring ICU admission, and 17 (81%) who died. Hispanic or Latino ethnicity was reported for 164 (73%) hospitalized patients, 65 (78%) requiring ICU admission, and 18 (86%) who died.

Effects of Mask and Physical Barrier Interventions

We analyzed case counts and intervention initiation dates for 13 facilities for which data were available; technical assistance was provided onsite at 12 facilities and by telephone call to 1 facility. Facilities consisted

of primary processing plants for beef (n = 7), pork (n = 3), and poultry (n = 1), as well as 2 secondary processing plants. The number of workers employed at the 13 facilities ranged from <400 to several thousand (mean 1,675). Placement of physical barriers varied by facility, but they were generally located on the production line and at cafeteria tables; barriers consisted of plexiglass partitions, plastic wrap secured around PVC pipes, or plastic sheeting. Although the site visit teams recommended use of surgical masks, national shortages of personal protective equipment early in the pandemic led to the adoption of different masking requirements; some facilities allowed cloth masks, and other facilities acquired and provided surgical masks to workers. Of the 13 facilities, 5 (38%) initiated a universal mask policy ≥10 days before physical barriers were installed; 6 (46%) initiated a universal mask policy and installed physical barriers <10 days apart; and 2 (15%) had universal mask policies but no physical barriers in place at the time of technical assistance and whether physical barriers were installed later is unknown.

We analyzed the incidence of SARS-CoV-2 infection before and after the date the last intervention was initiated (e.g., date physical barriers were installed if universal mask policy began first). Ten days after the last intervention was initiated, 8 facilities (62%) showed a statistically significant ($p<0.05$) decrease in incidence and 3 (23%) showed a nonsignificant decrease; 1 (7%) facility showed a statistically significant ($p<0.05$) increase in incidence and 1 (7%) showed a nonsignificant increase in incidence (Table 2). Three facilities reported case counts from the time between initiating mask policy and physical barrier interventions that allowed us to compare incidence before mask intervention, between mask and physical barrier initiation, and after both were in place simultaneously (Table 3). All 3 facilities showed a significant reduction ($p<0.05$) in incidence, particularly with both interventions deployed.

Discussion

The meat processing industry in Nebraska employs ≈26,000 workers (*6*), of whom 5,002 were diagnosed with COVID-19 during March–July 2020. The attack rate during this time period (19%) was more than double the 9.1% attack rate that was reported in a multistate analysis of meat processing facilities across the United States through May 2020 (*4*). Cases in meat processing facilities have far-reaching effects, potentially fueling outbreaks within surrounding communities where workers and workers' families comprise a substantial proportion of area residents. In addition, plants are often located in rural communities with limited infrastructure and resources to respond to outbreaks. In Nebraska, the 8 counties with the highest COVID-19 case rates per capita (as of September 2020) are also home to large meat processing facilities (*10*).

This report supports the increasing body of evidence that the COVID-19 pandemic has disproportionately affected racial and ethnic minority groups (*11*). Although 67% of confirmed cases were among Nebraska meat processing workers reporting Hispanic or Latino ethnicity, they constituted 73% of hospitalized case-patients, 78% of ICU admissions, and 86% of deaths, indicating a higher proportion of poor outcomes (hospitalizations, ICU admissions, deaths) compared with other racial and ethnic groups. Likewise, data presented here

Table 2. Comparisons of the incidence of severe acute respiratory syndrome coronavirus 2 infection before and after mask or physical barrier interventions or both among employees in 13 meatpacking facilities in Nebraska, April–July 2020*

Facility	Incidence /1,000 persons /d		p value for difference
	≤10 d after final intervention	10 d after final intervention	
Facilities that initiated a universal mask policy ≥10 d before physical barriers			
A	7.27	0.33	<0.001
B	3.21	0.69	<0.001
C	3.46	0.27	<0.001
D	3.64	0.15	0.072
E	0.48	2.09	0.008
Facilities that initiated a universal mask policy and physical barriers <10 d of each other			
F	17.16	0.58	<0.001
G	2.49	1.27	0.002
H	4.08	0.78	<0.001
I	6.82	1.40	<0.001
J	2.19	0.059	<0.001
K	0.65	1.90	0.180
Facilities that only initiated a universal mask policy			
L	3.2	2.87	0.745
M	3.29	3.178	0.944

*For facilities that initiated both a universal mask policy and physical barriers, date of last intervention was defined as start date of latter intervention (i.e., if physical barriers were initiated first, final intervention date was date of mask policy initiation). For facilities that initiated only masking, final intervention date was the initiation date.

Table 3. Comparisons of the incidence of severe acute respiratory syndrome coronavirus 2 infection among meat processing workers before mask intervention, between mask and physical barrier intervention, and after physical barrier intervention in meatpacking facilities, Nebraska, April–July 2020

	Incidence /1,000 persons /d			
Facility	<10 d after mask intervention	Between day 10 after mask and day 10 after physical barrier intervention	≥10 d after physical intervention	p value for difference*
A	3.46	3.23	0.26	<0.001
B	11.13	42.2	0.58	<0.001
C	2.63	0.26	0.32	<0.001

*p value difference represents difference in incidence before initiation of mask intervention and after physical barrier intervention.

reflect emerging evidence suggesting disease manifestations are more severe in men (*12*,*13*). Despite comprising 58% of confirmed case-patients, men represented 72% of hospitalized case-patients, 78% of ICU admissions, and 81% of deaths. Higher risk of poor outcomes among men and ethnic and racial minority groups demands tailored prevention and education strategies to subgroups shown to be more affected by adverse outcomes, both for this specific work environment and for broader local, state, and federal public health policy applications. Plant or corporate management can work to address these disparities among their worker populations by engaging with language and culture experts to ensure appropriate and effective communication and educational materials (e.g., videos, infographics) by providing materials in all languages spoken by workers and partnering with respected local community leaders (e.g., religious and spiritual leaders, elders) and community organizations to educate and disseminate information to workers.

The proportion of SARS-CoV-2 infections that remain asymptomatic is uncertain, although some reports estimate it to be higher than 30% (*14*–*16*). The percentage of asymptomatic COVID-19 cases (10%) among Nebraska meat processing workers was lower than these estimates. However, because few Nebraska meat processing facilities completed mass testing events during the study period, it is likely that many asymptomatic cases went undetected and are not reflected in this report. Indeed, a mass testing event at 1 Nebraska facility found that nearly one third of workers confirmed with COVID-19 reported no symptoms (*17*). Data on the 214 presymptomatic case-patients described in this report suggest detectable levels of virus in these persons and therefore transmission potential (*18*–*20*) at a median of 3 days before onset. Mass and routine testing enables identification of asymptomatic and presymptomatic infections, leading to swifter isolation, fewer days of potential exposure, and faster identification, quarantine, and testing of close contacts. As detailed in this report, identifying presymptomatic cases shortened the duration from symptom onset to investigation by a median of 4 days. Facilitywide or corporationwide routine testing programs, with frequency of testing informed by both local community transmission rates and cases identified within the plant, can position meat processing plants to identify cases early and stem potential outbreaks.

Risk mitigation strategies based on symptoms, such as active screening protocols and paid sick leave policies, are limited by asymptomatic and presymptomatic transmission and emphasize the importance of multilayered IPC interventions. Industry-specific guidance released by the CDC and the Occupational Safety and Health Administration in late April (*8*) centered on the Hierarchy of Controls risk mitigation framework (https://www.cdc.gov/niosh/topics/hierarchy/default.html) to reduce transmission within facilities (*21*). Although many of these risk mitigation strategies are similar to those recommended for various other high-risk industries (e.g., schools, long-term care facilities), the effectiveness of these IPC measures in the meat processing work environment has not been reported.

Our results indicate significantly reduced incidence of COVID-19 cases in 62% of studied facilities following adoption of universal masking and physical barrier interventions. Several factors may explain why some facilities did not see incidence decrease and 1 saw incidence significantly increase after initiating these measures. First, as an engineering control, physical barriers are generally considered one of the most effective measures to reduce person-to-person transmission of a communicable disease because they do not rely on worker adherence (*21*). However, since the study period, evidence has mounted supporting the substantial role of aerosols in transmitting COVID-19 (*22*–*24*). Although physical barriers installed between meat processing workers on the production line and at cafeteria tables would block larger respiratory droplets, the primary mode of transmission according to the CDC (*22*), they would not fully protect against aerosol transmission. Moreover, low temperatures and limited fresh air supply combined with physically demanding work conditions could facilitate longer-range aerosol transmission (*25*). Enhancements in ventilation (e.g., increasing the number of air exchanges per hour, installing high efficiency particulate air [HEPA] filtration) should therefore be considered the most effective

engineering control for COVID-19. More study is needed on aerosol transmission dynamics in this setting.

Second, although masking is one of the most effective tools for reducing COVID-19 transmission (*26*,*27*), the effectiveness of a universal mask policy relies on workers being educated on and adhering to proper mask use. A previous study of Nebraska meat processing workers found that only 44% of workers had received information on how to wear and care for a mask properly (*28*). Observed adherence to proper mask use (e.g., wearing the mask over both mouth and nose, minimizing adjustment or touching of the front of the mask) varied during site visits; at some plants, nearly all workers exhibited proper use, but at other facilities nearly half of workers wore masks below their noses.

The IPC challenges inherent in meat processing facilities cannot be addressed with only 1 or 2 measures; multilayered interventions are more effective than any single measure (*29*). In addition to IPC-focused strategies to reduce transmission within the facility, such as reducing density, engineering controls, physical distancing, active screening, environmental cleaning and disinfection, and masking, workforce policies ensuring social protections such as paid sick leave and flexible absenteeism policies are critical tools to prevent the disease from entering the workplace. However, given the inherent IPC challenges faced by the industry (e.g., high density of workers, duration of shifts, indoor environment, crowded cafeterias where masks are removed), it is also possible that no combination of interventions will be completely effective at reducing transmission in meat processing facilities, particularly when high rates of local community transmission exist. Facilities that did not see a significant reduction in incidence after initiating mask policies and physical barriers may not have incorporated other strategies to the same degree as facilities that did see significantly reduced incidence. Alternatively, some facilities we assessed might have initiated key interventions well before cases among their workers were diagnosed, causing interventions to appear less effective in this study.

A limitation of this study is that, although we attempted to distinguish the effectiveness of a universal mask policy from that of physical barrier installation, only 3 facilities had enough cases between the initiation of the 2 interventions to evaluate the separate direct effects of the measures. Moreover, when it became apparent in mid-April that meat processing facilities were particularly vulnerable to and being affected by COVID-19, facilities scrambled to incorporate IPC strategies within a short timeline and requested simultaneous technical assistance from our team. In many cases, site visits were conducted <10 days after a universal mask policy or physical barrier installation was begun. Our site visits and incorporation of additional IPC measures beyond physical barriers and masking might have contributed to reduced incidence. In addition, we were not able to definitively separate out whether transmission to case-patients occurred in the workplace or in the community and therefore couldn't determine the exact effect risk mitigation measures had on incidence compared with trends in community transmission rates. However, COVID-19 cases among meat processing workers represented almost 1 in 5 cases in Nebraska during the study period (there were 27,036 total cases in Nebraska from the beginning of the pandemic through July 31, 2020) (*30*). In addition, Nebraska's first wave of COVID-19 cases peaked in early May and gradually declined from May to July; our findings indicate that mitigation measures had a more rapid effect on incidence than reductions reflected in community transmission trends.

In conclusion, we present a snapshot of the effect of COVID-19 among meat processing workers in facilities in Nebraska. Nearly 1 in 5 Nebraska meat processing workers were diagnosed with COVID-19 between March and July 2020, a profound burden of cases unparalleled in any other worker population. Many of the nationwide trends that have become apparent during this pandemic applied here, namely high attack rates among workers in the meat processing industry, a disproportionately high risk of adverse outcomes among ethnic and racial minority groups and men, and the effectiveness of IPC interventions at reducing person-to-person transmission. Increased multilayered IPC strategies, rapid contact tracing, and accessible testing are critical to identifying asymptomatic and presymptomatic cases and interrupting silent transmission. COVID-19 will be an enduring threat to the meat processing industry and its workers for the foreseeable future. Facilities must adopt and sustain multiple interventions to prevent, control, and rapidly identify transmission within facilities to protect this worker population.

About the Author

Dr. Herstein is director of the sub-Saharan Africa office for the Global Center for Health Security and an assistant professor for research in the College of Public Health at the University of Nebraska Medical Center. Her research interests include highly hazardous communicable diseases, global high-level isolation, infection control, and outbreak response and preparedness.

References

1. Taylor CA, Boulos C, Almond D. Livestock plants and COVID-19 transmission. Taylor CA, Boulos C, Almond D. Proc Natl Acad Sci U S A. 2020;117:31706–15. https://doi.org/10.1073/pnas.2010115117
2. US Department of Homeland Security Cybersecurity & Infrastructure Security Agency. Advisory memorandum on identification of essential critical infrastructure workers during COVID-19 response [cited 2020 Apr 17]. https://www.cisa.gov/sites/default/files/publications/Version_3.0_CISA_Guidance_on_Essential_Critical_Infrastructure_Workers_1.pdf
3. Dyal JW, Grant MP, Broadwater K, Bjork A, Waltenburg MA, Gibbins JD, et al. COVID-19 among workers in meat and poultry processing facilities—19 states, April 2020. MMWR Morb Mortal Wkly Rep. 2020;69:557–61. https://doi.org/10.15585/mmwr.mm6918e3
4. Waltenburg MA, Victoroff T, Rose CE, Butterfield M, Jervis RH, Fedak KM, et al. Update: COVID-19 among workers in meat and poultry facilities—United States, April–May 2020. MMWR Morb Mortal Wkly Rep. 2020;69:887–92. https://doi.org/10.15585/mmwr.mm6927e2
5. Food and Environment Reporting Network. Mapping COVID-19 outbreaks in the food system. 2020. [cited 2020 Oct 17] https://thefern.org/2020/04/mapping-covid-19-in-meat-and-food-processing-plants
6. National Institute of Occupational Safety and Health. Employed labor force query system, 2018 estimates (estimates from Bureau of Census, Bureau of Labor Statistics current population survey) [cited 2020 Sep 30]. https://www.bls.gov/cew/downloadable-data-files.htm
7. Herstein J, Schwedhelm M, Lowe A, Duysen E, Ramos A, Grimm B, et al. Meat processing facility COVID-19 Playbook. Prepared by the Global Center for Health Security and the Central States Center for Agricultural Safety and Health [cited 2020 Oct 5]. https://www.unmc.edu/healthsecurity/covid-19/meatprocessing/Meat-Processing-Playbook-Final.pdf
8. Centers for Disease Control and Prevention. Meat and poultry processing workers and employers: interim guidance from CDC and the Occupational Safety and Health Administration (OSHA) [cited 2020 Jun 18]. https://www.cdc.gov/coronavirus/2019-ncov/community/organizations/meat-poultry-processing-workers-employers.html
9. Wu Z, McGoogan JM. Characteristics of and important lessons from the coronavirus disease 2019 (COVID-19) outbreak in China: summary of a report of 72,314 cases from the Chinese Center for Disease Control and Prevention. JAMA. 2020;323:1239–42. https://doi.org/10.1001/jama.2020.2648
10. Nebraska COVID map and case count. New York Times [cited 2020 Sept 3] https://www.nytimes.com/interactive/2020/us/nebraska-coronavirus-cases.html
11. Centers for Disease Control and Prevention. Health equity considerations and racial and minority ethnic groups [cited 2020 Sep 30] https://www.cdc.gov/coronavirus/2019-ncov/community/health-equity/race-ethnicity.html
12. Petrilli CM, Jones SA, Yang J, Rajagopalan H, O'Donnell L, Chernyak Y, et al. Factors associated with hospital admission and critical illness among 5279 people with coronavirus disease 2019 in New York City: prospective cohort study. BMJ. 2020;369:m1966. https://doi.org/10.1136/bmj.m1966
13. Docherty AB, Harrison EM, Green CA, Hardwick HE, Pius R, Norman L, et al. Features of 20,133 UK patients in hospital with COVID-19 using the ISARIC WHO Clinical Characterisation Protocol: prospective observational cohort study. BMJ. 2020;369:m1985. https://doi.org/10.1136/bmj.m1985
14. Centers for Disease Control and Prevention. COVID-19 pandemic planning scenarios [cited 2020 Sep 30]. https://www.cdc.gov/coronavirus/2019-ncov/hcp/planning-scenarios.html
15. Buitrago-Garcia D, Egli-Gany D, Counotte MJ, Hossmann S, Imeri H, Ipekci AM, et al. Occurrence and transmission potential of asymptomatic and presymptomatic SARS-CoV-2 infections: a living systematic review and meta-analysis. PLoS Med. 2020;17:e1003346. https://doi.org/10.1371/journal.pmed.1003346
16. Oran DP, Topol EJ. Prevalence of asymptomatic SARS-CoV-2 infection: a narrative review. Ann Intern Med. 2020;173:362–7. https://doi.org/10.7326/M20-3012
17. Donahue M, Sreenivasan N, Stover D, Rajasingham A, Watson J, Bealle A, et al. Notes from the field: characteristics of meat processing facility workers with confirmed SARS-CoV-2 infection—Nebraska, April–May 2020. MMWR Morb Mortal Wkly Rep. 2020;69:1020–2. http://dx.doi.org/10.15585/mmwr.mm6931a3
18. Wei WE, Li Z, Chiew CJ, Yong SE, Toh MP, Lee VJ. Presymptomatic transmission of SARS-CoV-2—Singapore, January 23–March 16, 2020. MMWR Morb Mortal Wkly Rep. 2020;69:411–5. https://doi.org/10.15585/mmwr.mm6914e1
19. He X, Lau EHY, Wu P, Deng X, Wang J, Hao X, et al. Temporal dynamics in viral shedding and transmissibility of COVID-19. Nat Med. 2020;26:672–5. https://doi.org/10.1038/s41591-020-0869-5
20. Böhmer MM, Buchholz U, Corman VM, Hoch M, Katz K, Marosevic DV, et al. Investigation of a COVID-19 outbreak in Germany resulting from a single travel-associated primary case: a case series. Lancet Infect Dis. 2020;20:920–8. https://doi.org/10.1016/S1473-3099(20)30314-5
21. National Institute for Occupational Safety and Health (NIOSH). Hierarchy of controls. 2015 Jan 13 [cited 2020 Oct 11]. https://www.cdc.gov/niosh/topics/hierarchy/default.html
22. Centers for Disease Control and Prevention. Scientific brief: SARS-CoV-2 and potential airborne transmission. 2020 Oct 11 [cited 2020 Oct 11]. https://www.cdc.gov/coronavirus/2019-ncov/more/scientific-brief-sars-cov-2.html
23. Tang S, Mao Y, Jones RM, Tan Q, Ji JS, Li N, et al. Aerosol transmission of SARS-CoV-2? Evidence, prevention and control. Environ Int. 2020;144:106039. https://doi.org/10.1016/j.envint.2020.106039
24. Anderson EL, Turnham P, Griffin JR, Clarke CC. Consideration of the aerosol transmission for COVID-19 and public health. Risk Anal. 2020;40:902–7. https://doi.org/10.1111/risa.13500
25. Guenther T, Czech-Sioli M, Indenbirken D, Robitaille A, Tenhaken P, Exner M, et al. SARS-CoV-2 outbreak investigation in a German meat processing plant. EMBO Mol Med. 2020;12:e13296. https://doi.org/10.15252/emmm.202013296
26. Lyu W, Wehby GL. Community use of face masks and COVID-19: evidence from a natural experiment of state mandates in the US. Health Aff (Millwood). 2020;39:1419–25. https://doi.org/10.1377/hlthaff.2020.00818
27. Wang X, Ferro EG, Zhou G, Hashimoto D, Bhatt DL. Association between universal masking in a health care system and SARS-CoV-2 positivity among health care workers. JAMA. 2020;324:703–4. https://doi.org/10.1001/jama.2020.12897

28. University of Nebraska Medical Center. Concerns and perceptions of COVID-19 among meatpacking plant workers in Nebraska. 2020 [cited 2020 Oct 11] https://www.unmc.edu/healthsecurity/covid-19/meatprocessing/UNMC-Meatpacking-study-results-1-page-bilingual.pdf
29. Bruinen de Bruin Y, Lequarre AS, McCourt J, Clevestig P, Pigazzani F, Zare Jeddi M, et al. Initial impacts of global risk mitigation measures taken during the combatting of the COVID-19 pandemic. Saf Sci. 2020;128:104773. https://doi.org/10.1016/j.ssci.2020.104773
30. Nebraska Department of Health and Human Services. Coronavirus COVID-19 Nebraska cases [cited 2021 Jan 10] https://experience.arcgis.com/experience/ece0db09da4d4ca68252c3967aa1e9dd/page/page_0

Address for correspondence: Jocelyn J. Herstein, College of Public Health, University of Nebraska Medical Center, 984388 Nebraska Medical Center, Omaha, NE 68198, USA; email: jocelyn.herstein@unmc.edu

Systematic Review of Reported HIV Outbreaks, Pakistan, 2000–2019

Elizabeth M. Rabold,[1] Hammad Ali,[1] Danielle Fernandez, Martha Knuth, Karl Schenkel, Rana Jawad Asghar, Mirza Amir Baig, Saqib Shaikh, Oliver Morgan

Medscape EDUCATION ACTIVITY

In support of improving patient care, this activity has been planned and implemented by Medscape, LLC and Emerging Infectious Diseases. Medscape, LLC is jointly accredited by the Accreditation Council for Continuing Medical Education (ACCME), the Accreditation Council for Pharmacy Education (ACPE), and the American Nurses Credentialing Center (ANCC), to provide continuing education for the healthcare team.

Medscape, LLC designates this Journal-based CME activity for a maximum of 1.00 ***AMA PRA Category 1 Credit(s)™***. Physicians should claim only the credit commensurate with the extent of their participation in the activity.

Successful completion of this CME activity, which includes participation in the evaluation component, enables the participant to earn up to 1.0 MOC points in the American Board of Internal Medicine's (ABIM) Maintenance of Certification (MOC) program. Participants will earn MOC points equivalent to the amount of CME credits claimed for the activity. It is the CME activity provider's responsibility to submit participant completion information to ACCME for the purpose of granting ABIM MOC credit.

All other clinicians completing this activity will be issued a certificate of participation. To participate in this journal CME activity: (1) review the learning objectives and author disclosures; (2) study the education content; (3) take the post-test with a 75% minimum passing score and complete the evaluation at http://www.medscape.org/journal/eid; and (4) view/print certificate. For CME questions, see page 1256.

Release date: March 19, 2021; Expiration date: March 19, 2022

Learning Objectives

Upon completion of this activity, participants will be able to:

- Distinguish groups at highest risk for HIV infection in Pakistan
- Analyze causes of outbreaks of HIV infection in Pakistan
- Assess factors which might promote unsafe injection practices in Pakistan

CME Editor

Jude Rutledge, BA, Technical Writer/Editor, Emerging Infectious Diseases. *Disclosure: Jude Rutledge has disclosed no relevant financial relationships.*

CME Author

Charles P. Vega, MD, Health Sciences Clinical Professor of Family Medicine, University of California, Irvine School of Medicine, Irvine, California. *Disclosure: Charles P. Vega, MD, has disclosed the following relevant financial relationships: served as an advisor or consultant for GlaxoSmithKline.*

Authors

Disclosures: ***Elizabeth M. Rabold, MD, MPH; Hammad Ali, PhD; Danielle Fernandez, MPH; Martha Knuth, MLIS; Karl Schenkel, MD; Rana Jawad Asghar, MBBS, MPH; Mirza-Amir Baig, MBBS, MPH; Saqib Ali Shaikh, MSc, MBBS;*** *and* ***Oliver Morgan, PhD,*** *have disclosed no relevant financial relationships.*

Author affiliations: Centers for Disease Control and Prevention, Atlanta, Georgia, USA (E.M. Rabold, H. Ali, D. Fernandez, M. Knuth); World Health Organization, Geneva, Switzerland (K. Schenkel, O. Morgan); Global Health Strategists and Implementers, Karachi, Pakistan (R.J. Asghar); Pakistan Field Epidemiology and Laboratory Training Program, Karachi (M.A. Baig); Sindh AIDS Control Program, Larkana, Pakistan (S. Shaikh)

DOI: https://doi.org/10.3201/eid2704.204205

[1]These first authors contributed equally to this article.

Unsafe injection practices and injection drug use have been linked to multiple HIV outbreaks in Pakistan since 2003; however, few studies have systematically analyzed the causes of these outbreaks. We conducted a systematic review of published English-language literature indexed in bibliographic databases and search engines and a focused gray literature review to collate and analyze all reported HIV outbreaks in Pakistan during 2000–2019. Of 774 unique publications reviewed, we identified 25 eligible publications describing 7 outbreaks. More than half occurred during 2016–2019. The primary sources of transmission were iatrogenic transmission, affecting children, persons with chronic medical conditions, and the general population (4 outbreaks); injection drug use (2 outbreaks); and a combination of both (1 outbreak). In the absence of robust HIV testing and surveillance in Pakistan, timely and detailed outbreak reporting is important to understand the epidemiology of HIV in the country.

The first cases of HIV in Pakistan were reported in 1987, with epidemiologic evidence supporting the importation of cases by migrant workers from the Gulf States (*1*–*3*). Since that time, noncontinuous surveillance assessments have noted high prevalence of HIV in certain populations; the most recent 2016–2017 prevalence estimates were 38.4% among persons who inject drugs (PWID), 7.2% among transgender persons, and 5.6% among men who have sex with men (*4*–*8*). By comparison, the prevalence in the general population is 0.1%, representing ≈190,000 persons living with HIV (PLHIV), including 6,100 children <15 years of age, according to 2019 Joint United Nations Programme on HIV/AIDS (UNAIDS) estimates (*8*,*9*). Approximately 44,758 (24%) PLHIV were registered with the National AIDS Control Programme with a known diagnosis as of December 2020, and of these, only 24,362 (54%) were receiving antiretroviral therapy (ART) (*10*). These statistics are far below the UNAIDS 90–90–90 HIV treatment targets (90% of HIV-positive persons being aware of their status; of those, 90% receiving ART; and of those, 90% being virally suppressed) aimed at controlling the AIDS epidemic; most PLHIV (87%) in Pakistan are not receiving treatment (*11*).

In April 2019, a major HIV outbreak in Larkana District in Pakistan was identified by local and provincial public health officials (*12*). After several ill children with HIV-negative parents tested positive for HIV, the provincial Sindh AIDS Control Program began a voluntary district-wide testing campaign. During April 25–June 28, 2019, a total of 30,192 persons were tested for HIV; 876 (2.9%) were HIV positive, and 82% of those were children <15 years of age. A World Health Organization (WHO) report cited unsafe medical practices and poor infection control programs as key risk factors for infection (*12*) and noted that this outbreak was the fourth HIV outbreak in Larkana since 2003. A cursory review of the literature, however, did not identify peer-reviewed publications on all of these referenced outbreaks. The objective of our systematic review was to identify and collate data from all reported HIV outbreaks in Pakistan to describe overarching themes and aid in future prevention efforts.

Methods

We followed the PRISMA statement and the Cochrane Handbook to conduct this systematic review (Appendix Table 1, https://wwwnc.cdc.gov/EID/article/27/4/20-4205-App1.pdf) (*13*). We searched Medline, Embase, CAB Abstracts, Global Health, PsycInfo, Cochrane Library, Scopus, Academic Search Complete, Cumulative Index to Nursing and Allied Health Literature, ProQuest Central, PubMed Central, Virtual Health Library, and Google Scholar to identify English-language publications on reported HIV outbreaks in Pakistan during January 1, 2000–December 31, 2019. We limited the search to studies published after January 1, 2000, because the earliest reported HIV outbreak in Pakistan occurred in 2003 (*14*). To complement the published literature search, we conducted a comprehensive search of the gray literature (i.e., publications not published in indexed peer-reviewed journals), including UNAIDS reports, WHO reports, and International AIDS Society conference abstracts. In addition, we manually reviewed Pakistan's provincial and national Ministry of Health websites. The following search strategy was used for database and gray literature searches: (HIV or AIDS, any associated synonyms, or both) AND (outbreak, epidemic, pandemic, or cluster) AND (Pakistan [or all subnational units]). We omitted location criteria for manual review of Pakistan governmental websites. The full search strategy is detailed in Appendix Table 2. We used Endnote X9 (Clarivate Analytics, https://endnote.com) to import and manage retrieved records. To identify duplicate reports, we used the EndNote automated "find duplicates" function, with preferences set to match by title, author, and year; a second round of manual de-duplication was performed by using the same matching criteria. We grouped the remaining reports by database, search engine, and source, and authors reviewed these independently. We used a shared database to track the progress of the reviews.

We systematically screened and reviewed results from the published and gray literature search (Figure). We screened titles and abstracts, and we defaulted to reviewing the abstract if the title had an unclear focus and reviewing the full report if no abstract was available, counting it among the number of abstracts reviewed. We included publications that reported data on outbreaks of HIV or sudden increases in cases in Pakistan. For the purpose of this systematic review, we defined an outbreak as an unexpected number of HIV cases identified through targeted testing or key population surveillance, labeled and reported as an outbreak, and leading to an evaluation or investigation. We excluded abstracts without published final reports (unless identified in the gray literature), reports that provided prevalence or incidence data only (including key population surveys), opinion pieces without mention of a specific outbreak, mathematical modeling studies, epidemiologic analyses, reports without quantitative data, and preprint reports. We also excluded reports where the author did not define the described cases as an outbreak or did not provide a discrete geographic, temporal, or epidemiologic link. If identical reports were published in ≥1 journal, the earliest publication was included. Similarly, if identical or nearly identical reports were published in a journal and also included as a conference abstract, we included only the published report. If a report included outbreak data as well as a subset of data in a case control, cohort, or cross-sectional investigation, we included data on the larger outbreak and the study. We reviewed journal submission guidelines to determine whether a publication was peer-reviewed.

We organized eligible publications, gray literature, and government reports by geographic location and year of the reported outbreak. We included reports describing multiple outbreaks under each appropriate outbreak heading. We extracted year and type of report, investigating agency and source or reference for primary data, number of persons tested and diagnosed with HIV, case positivity rate (defined as the percentage of persons positive among the number tested within the period defined by the authors of the publication), notable demographic and behavioral characteristics of case-patients, major risk factors, and other relevant information (Appendix Table 3). We noted instances where articles used media reports as their primary citation. One author independently reviewed initial data extraction of all eligible reports for concurrence. If necessary, we reached out to corresponding authors of individual reports for clarification.

Results

Our initial search identified 1,653 records published during January 2000–December 2019. We removed 879 (53%) duplicate reports identified across multiple databases or search engines through automated and manual processes (Figure). Of the remaining 774 de-duplicated reports, 625 (81%) were excluded after review of the title and 108 (14%) were excluded after review of the abstract. We excluded 16 reports upon review of the full article, gray literature, or government report, leaving 25 (3%) reports eligible for inclusion.

The 25 reports identified by our search strategy described 7 outbreaks: 4 in Punjab Province (Sargodha, Sargodha District [2007]; Kot Imrana, Sargodha District [2018]; Jalalpur Jattan, Gujrat District [2008]; and Faisalabad, Faisalabad District [2019]) and 3 in Sindh Province (Larkana, Larkana District [2003 and 2016] and Ratodero, Larkana District [2019]) (Appendix Table 3). Six (24%) reports described ≥2 outbreaks.

Case-positivity rates ranged from 1.3% to 51.8%, varying in part because of sampling methods. The potential source of 4 of the 7 outbreaks was reported as iatrogenic transmission through unsafe healthcare practices at clinics, hospitals, and dialysis centers; 2 outbreaks were attributed to injection drug use, and 1 outbreak was attributed to both. Several reports described a potential association with unqualified healthcare providers (frequently designated as quacks in Pakistan [*15*]), in general, or with a specific provider. Some reports also reported cultural practices as a contributing factor to transmission. Populations most affected by the outbreaks varied by proposed etiology; iatrogenic causes affected the general community, including women and children, as well as persons living with specific medical conditions, such as end-stage renal disease. Recreational drug use affected primarily PWID, most frequently men.

Our review identified 5 reports in peer-reviewed literature, with the remaining reports published as letters to the editor or correspondence, nongovernmental organization and government reports, and conference abstracts. National or provincial AIDS control programs led the initial investigations of 4 of the 7 outbreaks; the National Institutes of Health-Pakistan and Field Epidemiology Training Program–Pakistan and district health departments provided data for the other 3 outbreaks. The Ratodero (2019) outbreak had additional support from WHO, other United Nations agencies, local universities, and other international and local partners. Of the

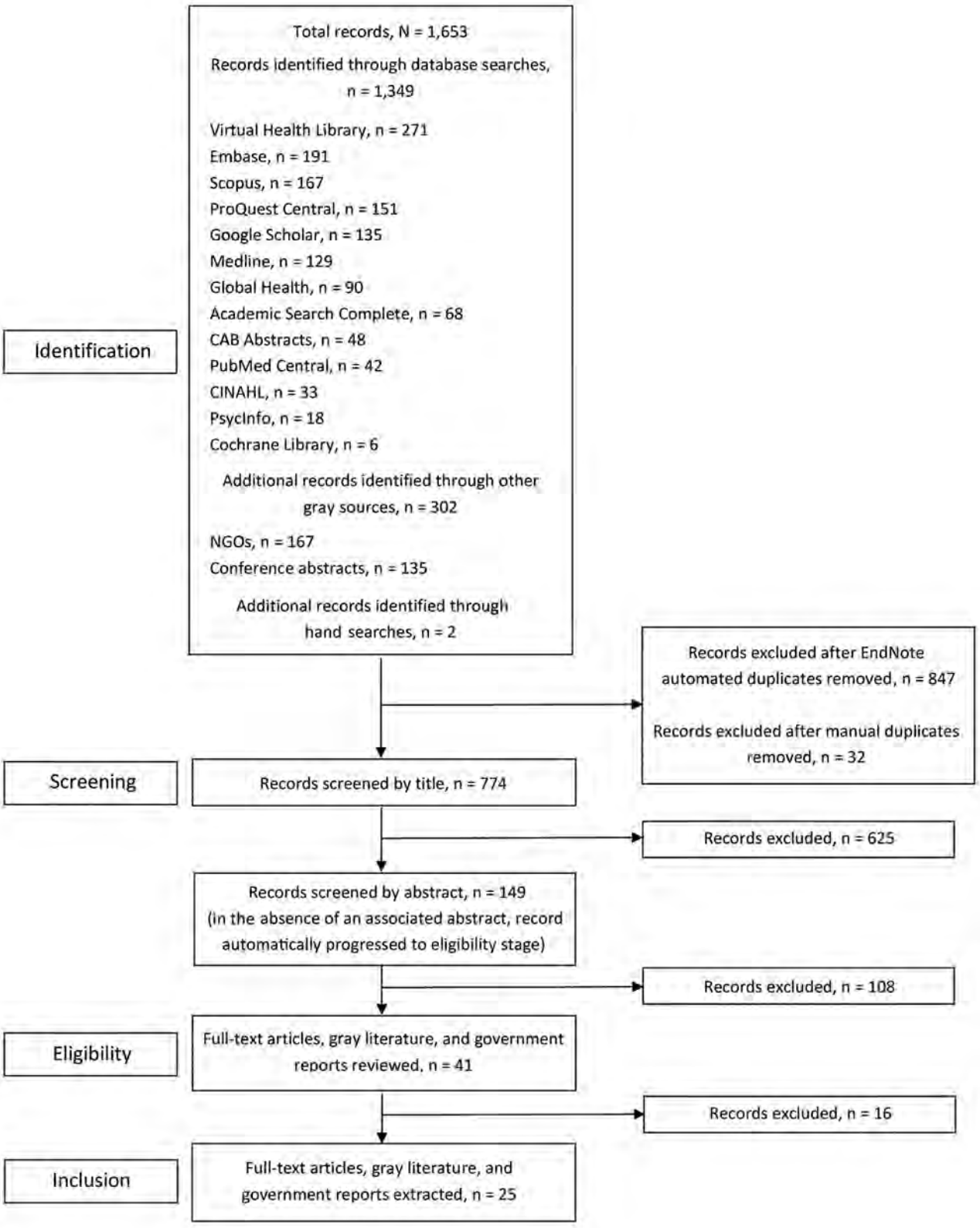

Figure. Identification and selection of studies reporting HIV outbreaks in Pakistan, January 2000–September 2019. CINAHL, Cumulative Index to Nursing and Allied Health Literature; NGOs, nongovernmental organizations.

25 reports, 17 (68%) describe this single outbreak. Other outbreaks had more limited data, often limited to case counts and affected population. Authors were often not directly affiliated with the primary data but rather briefly described testing statistics, demographic information, and risk factors obtained from investigations from government entities, media reports, and other sources. Some discrepancies were noted across reports pertaining to the same outbreak, and many reports did not provide complete information on case-positivity rates, study period, or method of data collection. Authors occasionally (4 [16%]) used media reports as the primary source of information. Though most outbreaks had at least 1 article citing primary data or data directly from a testing program, the single report found for the Faisalabad (2019) outbreak cited only a newspaper article. Of the 25 reports describing the 7 outbreaks, only 5 reports provided detailed outbreak investigation information. Despite more extensive investigations, these reports still had limited ability to draw conclusions or conduct statistical comparisons because of study design (e.g., no comparison group [*16*] or small sample size [*17*]). Only 1 of the 25 reports, describing an outbreak investigation in Jalalpar Jattan (2008), included phylogenetic information (*16*), which demonstrated that transmission likely occurred over a decade, reflecting endemic disease rather than an outbreak.

Discussion

Our review identified 25 reports describing 7 HIV outbreaks during 2000–2019 in Pakistan: 3 in Sindh Province and 4 in Punjab Province. Of these, 4 were identified during 2016–2019. In 2019, two outbreaks were reported: a large outbreak primarily affecting children in Ratodero in Larkana, a district with multiple prior outbreaks, and an outbreak in Faisalabad, primarily infecting PWID. Case-positivity rates ranged from 1.3% to 51.8%, and populations most affected varied by outbreak but included PWID; persons living with specific medical conditions; and the general population, including women and children. The level of detail pertaining to the description of data collection and investigation methods varied across the publications, and much of the data provided were collected not by authors but by national, provincial, and district health departments and other government entities. Iatrogenic transmission (57%), injection drug use (29%), or both (14%) were identified as the potential sources of the outbreaks; no outbreak solely attributable to sexual transmission was reported.

Iatrogenic transmission from unsafe healthcare practices and poor infection prevention and control was identified as the primary or contributing risk factor in 5 of the 7 HIV outbreaks (Jalalpur Jattan [2008], Kot Imrana [2018], Larkana [2016], Ratodero [2019], and Faisalabad [2019]). From a recent survey in Pakistan, researchers estimated that ≈38% of surveyed physicians likely reused syringes (*18*). Data from the latest Demographic Health Survey indicate that ≈9% of injections given to patients in Pakistan are unsafe, and every person receives an average of 4.1 therapeutic injections per year in Pakistan (*19*). Extrapolating from this frequency and safety data, approximately 1 in 3 persons might receive an unsafe injection every year in Pakistan (*19*). Furthermore, cross-sectional studies of persons with thalassemia in Pakistan have shown a high prevalence of bloodborne infections, including HIV, hepatitis B, and hepatitis C, suggestive of infection from blood transfusions (*20*,*21*). Nosocomial or iatrogenic transmission including unsafe blood transfusions and reuse of medical equipment has contributed to several HIV outbreaks in other countries, including ≈10,000 children in orphanages in Romania (*22*), >400 children in Libya with frequent co-infection with hepatitis B and C (*23*), and 242 adults and children in Cambodia (*24*).

Several factors might play a role in the propagation of unsafe injection practices in low-income countries. These factors include sociocultural factors such as healthcare providers' belief that compliance is better with injections than with oral medication and patients might seek healthcare elsewhere if not provided injections; financial incentives on the part of both patient and provider through fee-for-injection practices and contingent on provider ability to purchase and maintain a supply of injecting equipment; corruption, when money allocated for healthcare, such as disposable injecting equipment, is used elsewhere, leading to reuse of equipment; lack of policies and procedures around safe injection practices, such that policies forbidding the reuse of injecting equipment are not implemented nor enforced in low-income countries as they are in high-income countries; ready access to injectable medications without a prescription; and lack of awareness of risks associated with unsafe injection practices (*25*). Given these factors, developing a multi-strategy approach that might be adapted and tailored as necessary might help prevent future outbreaks of HIV and other bloodborne pathogens. These strategies include community and healthcare provider education to address excessive and unnecessary use

of therapeutic injections, implementation and monitoring of policies around single-use injecting equipment, and addressing gaps in infection prevention and control.

Injection drug use was reported as the primary or contributing cause of HIV transmission in 3 of the 7 outbreaks (Larkana [2003], Sargodha [2007], and Faisalabad [2019]). Periodic HIV surveillance data are available for key populations in specific cities from the National AIDS Control Programme Integrated Biologic and Behavioral Surveillance surveys, but they are not designed to measure prevalence for the general population or key populations in rural areas (*4*–*8*). The HIV prevalence among PWID documented by each survey increased from 10.8% to 38.4%; however, because the survey was expanded to new cities across the different reporting periods, direct comparison of the change in prevalence is not possible. Whether any change in prevalence might be attributable to sporadic outbreaks or a steady increase in HIV prevalence in this subpopulation is unknown. None of the literature describing outbreaks with injection drug use as the primary or contributing source of transmission reported a phylogenetic analysis, leaving timelines of infections in these outbreaks unclear.

Although the Integrated Biologic and Behavioral Surveillance surveys offer insight into HIV prevalence among key populations, the absence of routine HIV surveillance in the general population prevents understanding of the actual burden of the HIV epidemic in Pakistan. Considering the high prevalence of HIV in PWID, men who have sex with men, and female sex workers, as well as unsafe injection practices as we have described, spillover to the general population is only a matter of time. Widespread surveillance of HIV might be challenging and might yield little information given the low general population prevalence of 0.1% (*9*). However, adding surveillance of targeted populations at higher risk, such as pregnant women, patients at infectious disease or tuberculosis clinics, and persons requiring frequent transfusions, might provide early warning signs to changes in HIV prevalence. Likewise, systematic monitoring of the blood supply might represent an efficient, less costly approach to surveillance. Currently, routine surveillance is not conducted in any of these settings. Although phylogenetic analyses, which assist in understanding circulating strains and subtypes, might contribute to our understanding of a rise in cases, only 1 publication identified in this review reported a phylogenetic analysis; it showed that, despite preliminary data suggestive of a new outbreak, transmission occurred over a decade (*16*). Without comprehensive surveillance and phylogenetic data, ascertaining whether new HIV diagnoses or a sudden increase in diagnoses in an area represent an outbreak or simply missed HIV diagnoses with endemic transmission over time is difficult.

Outbreaks are underrepresented in the literature; those that are published have limited ability to characterize the full epidemiologic and phylogenetic footprint of an outbreak. Nonsystematic tracking of media reports identified at least 2 other potential outbreaks known to national or provincial AIDS control programs but not described by our systematic review (*26*,*27*). Given the frequency of media reports of HIV outbreaks, albeit without full epidemiologic data, and well-documented data on the widespread prevalence of unsafe injections across Pakistan, the paucity of systematic outbreak investigations is striking. Of the reports included in our systematic review, only 5 (20%) were peer-reviewed; the remaining were published as letters to the editor, editorials, general correspondence, abstracts, nongovernment organization publications, and government reports, without clear description of methods, study design, and data collection. Given the limited outbreak investigations and robust data reporting in peer-reviewed and gray literature, our systematic review likely underestimates the frequency of the problem and its associated burden of disease.

The main strength of our review is that we searched multiple bibliographic databases, with the addition of Google Scholar and the Virtual Health Library, nongovernmental organization and government websites, and conference abstracts to ensure all relevant publications were captured. However, we note several limitations. First, we recognize that the definition of an outbreak is challenging in the setting of limited phylogenetic and surveillance data. A study by Ansari et al. (*16*) determined that the observed increase in cases was likely a progression of endemic disease only after the results of phylogenetic analysis. As such, other outbreaks reported in this review might, if the same analyses were available, have been determined not to be outbreaks. Second, our literature review was limited to English-language publications. Although a potential exists for missing articles written in Urdu and other local languages, English is one of the official languages in the country and is the predominant language for scientific and medical research dissemination in Pakistan (*28*,*29*). Finally, although unlikely, a small chance exists that a unique outbreak might have been men-

tioned in a publication focusing on surveillance or other data and thus been missed by our tiered review approach. We also recognize that outbreak reports written by government entities might be for internal review only or might be posted online for a limited time, resulting in a possible bias towards availability of more recent outbreaks.

In summary, reported outbreaks in Pakistan suggest that the spread of HIV might continue if adequate prevention strategies are not adopted. Education campaigns to improve knowledge in the general public about unsafe injection practices, both therapeutic and recreational, might limit HIV transmission and occurrence of outbreaks. Assessing patient and provider misconceptions about the benefits of therapeutic injections could guide public health messaging and reduce demand for unnecessary medical interventions. Reviewing injection safety and infection prevention and control practices could inform healthcare reform efforts to limit iatrogenic exposures and the potential for HIV outbreaks. Last, developing and putting into place comprehensive HIV surveillance systems could assist in outbreak identification, prompting investigations that explore risk factors and underlying transmission sources. Reporting of outbreaks in peer-reviewed literature, including epidemiologic studies and phylogenetic analyses, might shed additional light on the etiologies of outbreaks and effective prevention strategies. Across the spectrum of reports identified by our systematic review, all reports had the consistent message of sounding an alarm and highlighting a potentially rapidly growing problem in Pakistan.

This project was supported by the President's Emergency Plan for AIDS Relief (PEPFAR) through the Centers for Disease Control and Prevention and by Cooperative Agreement no. U2GGH002093-01-00 through the Centers for Disease Control and Prevention and the Public Health Institute.

About the Author

Dr. Rabold is a medical officer in the Division of Global HIV and Tuberculosis, Center for Global Health, Centers for Disease Control and Prevention. Her research interests include prevention of mother-to-child transmission of HIV and comprehensive care of HIV-exposed infants. Dr. Ali is a medical epidemiologist in the Division of Global HIV and Tuberculosis, Center for Global Health, Centers for Disease Control and Prevention. His research interests include infectious disease epidemiology, surveillance, and global health.

References

1. Khanani RM, Hafeez A, Rab SM, Rasheed S. Human immunodeficiency virus-associated disorders in Pakistan. AIDS Res Hum Retroviruses. 1988;4:149–54. https://doi.org/10.1089/aid.1988.4.149
2. Abdul Mujeeb S, Hashmi MR. A study of HIV-antibody in sera of blood donors and people at risk. J Pak Med Assoc. 1988;38:221–2.
3. Shah SA, Khan OA, Kristensen S, Vermund SH. HIV-infected workers deported from the Gulf States: impact on southern Pakistan. Int J STD AIDS. 1999;10:812–4. https://doi.org/10.1258/0956462991913600
4. National AIDS Control Program. HIV Second Generation Surveillance in Pakistan: National Report Round 1, 2005. Islamabad: National AIDS Control Program; 2005.
5. National AIDS Control Program. HIV Second Generation Surveillance in Pakistan: National Report Round II, 2006–2007. Islamabad: National AIDS Control Program; 2007.
6. National AIDS Control Program. HIV Second Generation Surveillance in Pakistan: National Report Round III, 2008. Islamabad: National AIDS Control Program; 2008.
7. National AIDS Control Program. HIV Second Generation Surveillance in Pakistan: National Report Round IV, 2011. Islamabad: National AIDS Control Program; 2011.
8. National AIDS Control Program. Integrated biological and behavioral surveillance in Pakistan, 2016–2017: 2nd Generation HIV Surveillance in Pakistan, Round 5. Islamabad: National AIDS Control Program; 2017.
9. Joint United Nations Programme on HIV/AIDS (UNAIDS). Country factsheet—Pakistan. 2019 [cited 2021 Feb 16]. https://www.unaids.org/en/regionscountries/countries/pakistan
10. Ministry of National Health Services, Regulation & Coordination. National AIDS Control Programme. Current statistics.[cited 2021 Feb 16]. https://www.nacp.gov.pk
11. Joint United Nations Programme on HIV/AIDS (UNAIDS). 90–90–90: an ambitious treatment target to help end the AIDS epidemic. 2014 [cited 2021 Feb 16]. http://www.unaids.org/sites/default/files/media_asset/90-90-90_en.pdf
12. World Health Organization. HIV cases—Pakistan. 2019 [cited 2021 Feb 16]. https://www.who.int/csr/don/03-july-2019-hiv-cases-pakistan/en
13. Moher D, Liberati A, Tetzlaff J, Altman DG; PRISMA Group. Preferred reporting items for systematic reviews and meta-analyses: the PRISMA statement. Ann Intern Med. 2009;151:264–9, W64. https://doi.org/10.7326/0003-4819-151-4-200908180-00135
14. Shah SA, Altaf A, Mujeeb SA, Memon A. An outbreak of HIV infection among injection drug users in a small town in Pakistan: potential for national implications. Int J STD AIDS. 2004;15:209. https://doi.org/10.1258/095646204322916713
15. Afsar HA, Mahmood MA, Barney N, Ali S, Kadir MM, Bilgrami M. Community knowledge, attitude and practices regarding sexually transmitted infections in a rural district of Pakistan. J Pak Med Assoc. 2002;52:21–4.
16. Ansari JA, Salman M, Safdar RM, Ikram N, Mahmood T, Zaheer HA, et al. HIV/AIDS outbreak investigation in Jalalpur Jattan (JPJ), Gujrat, Pakistan. J Epidemiol Glob Health. 2013;3:261–8. https://doi.org/10.1016/j.jegh.2013.06.001
17. ur Rehman N, Emmanuel F, Akhtar S. HIV transmission among drug users in Larkana, Pakistan. Trop Doct. 2007;37:58–9. https://doi.org/10.1258/004947507779952096
18. Khan A, Altaf A, Qureshi H, Orakzai M, Khan A. Reuse of syringes for therapeutic injections in Pakistan: rethinking its definition and determinants. East Mediterr Health J. 2020;26:283–9. 2019;25.

19. National Institute of Population Studies and ICF. Pakistan Demographic and Health Survey, 2017–18 [cited 2021 Feb 16]. https://dhsprogram.com/pubs/pdf/FR354/FR354.pdf
20. Yasmeen H, Hasnain S. Epidemiology and risk factors of transfusion transmitted infections in thalassemia major: a multicenter study in Pakistan. Hematol Transfus Cell Ther. 2019;41:316–23. https://doi.org/10.1016/j.htct.2019.03.008
21. Al-Moshary M, Al-Mussaed E, Khan A. Prevalence of transfusion transmitted infections and the quality of life in β-thalassemia major patients. Cureus. 2019;11:e6129. https://doi.org/10.7759/cureus.6129
22. Dente K, Hess J. Pediatric AIDS in Romania—a country faces its epidemic and serves as a model of success. MedGenMed. 2006;8:11.
23. Yerly S, Quadri R, Negro F, Barbe KP, Cheseaux JJ, Burgisser P, et al. Nosocomial outbreak of multiple bloodborne viral infections. J Infect Dis. 2001;184:369–72. https://doi.org/10.1086/322036
24. Rouet F, Nouhin J, Zheng DP, Roche B, Black A, Prak S, et al. Massive iatrogenic outbreak of human immunodeficiency virus type 1 in rural Cambodia, 2014–2015. Clin Infect Dis. 2018;66:1733–41. https://doi.org/10.1093/cid/cix1071
25. Kermode M. Unsafe injections in low-income country health settings: need for injection safety promotion to prevent the spread of blood-borne viruses. Health Promot Int. 2004;19:95–103. https://doi.org/10.1093/heapro/dah110
26. Islam S. AIDS scare in a Chiniot village as 42 residents test positive for HIV. The Express Tribune. 2017 Jul 31 [cited 2021 Feb 16]. https://tribune.com.pk/story/1470850/aids-scare-chiniot-village-42-residents-test-positive-hiv
27. Khan MH. Surfacing of 140 HIV positive cases early this year in Hyderabad area goes unnoticed. Dawn. 2019 May 3 [cited 2021 Feb 16]. https://www.dawn.com/news/1479843
28. Journal of College of Physicians and Surgeons Pakistan. Instructions to authors [cited 2020 Oct 3]. https://jcpsp.pk/instructions-to-author.php
29. Journal of Pakistan Medical Association. Information for authors [cited 2021 Feb 16]. https://www.jpma.org.pk/view-instructions

Address for correspondence: Elizabeth M. Rabold, Centers for Disease Control and Prevention, 1600 Clifton Rd NE, Mailstop US1-1, Atlanta, GA 30329-4027, USA; email: nqo6@cdc.gov

Infections with Tickborne Pathogens after Tick Bite, Austria, 2015–2018

Mateusz Markowicz, Anna-Margarita Schötta, Dieter Höss, Michael Kundi, Christina Schray, Hannes Stockinger, Gerold Stanek

Medscape EDUCATION ACTIVITY

In support of improving patient care, this activity has been planned and implemented by Medscape, LLC and Emerging Infectious Diseases. Medscape, LLC is jointly accredited by the Accreditation Council for Continuing Medical Education (ACCME), the Accreditation Council for Pharmacy Education (ACPE), and the American Nurses Credentialing Center (ANCC), to provide continuing education for the healthcare team.

Medscape, LLC designates this Journal-based CME activity for a maximum of 1.00 ***AMA PRA Category 1 Credit(s)™***. Physicians should claim only the credit commensurate with the extent of their participation in the activity.

Successful completion of this CME activity, which includes participation in the evaluation component, enables the participant to earn up to 1.0 MOC points in the American Board of Internal Medicine's (ABIM) Maintenance of Certification (MOC) program. Participants will earn MOC points equivalent to the amount of CME credits claimed for the activity. It is the CME activity provider's responsibility to submit participant completion information to ACCME for the purpose of granting ABIM MOC credit.

All other clinicians completing this activity will be issued a certificate of participation. To participate in this journal CME activity: (1) review the learning objectives and author disclosures; (2) study the education content; (3) take the post-test with a 75% minimum passing score and complete the evaluation at http://www.medscape.org/journal/eid; and (4) view/print certificate. For CME questions, see page 1257.

Release date: March 18, 2021; Expiration date: March 18, 2022

Learning Objectives

Upon completion of this activity, participants will be able to:

- Assess characteristics of tick bites in the current study
- Analyze results of molecular screening of ticks in the current study
- Distinguish the rate of positive testing for Borrelia among patients in the current study
- Evaluate risk factors for a positive Borrelia infection in the current study.

CME Editor

Thomas J. Gryczan, MS, Technical Writer/Editor, Emerging Infectious Diseases. *Disclosure: Thomas J. Gryczan, MS, has disclosed no relevant financial relationships.*

CME Author

Charles P. Vega, MD, Health Sciences Clinical Professor of Family Medicine, University of California, Irvine School of Medicine, Irvine, California. *Disclosure: Charles P. Vega, MD, has disclosed the following relevant financial relationships: served as an advisor or consultant for GlaxoSmithKline.*

Authors

Disclosures: ***Mateusz Markowicz, MD; Anna-Margarita Schötta, BSc; Dieter Höss, MD; Christina Schray, MD;*** *and* ***Hannes Stockinger, PhD,*** *have disclosed no relevant financial relationships.* ***Michael Kundi, PhD,*** *has disclosed the following relevant financial relationships: served as an advisor or consultant for AVIR Green Hills Biotechnology AG; Valneva SE; Vivaldi Biosciences Inc.; received grants for clinical research from Pfizer Inc.* ***Gerold Stanek, MD,*** *has disclosed the following relevant financial relationships: served as an advisor or consultant for Valneva SE.*

Author affiliations: Medical University of Vienna, Vienna, Austria (M. Markowicz, A.-M. Schötta, M. Kundi, C. Schray, H. Stockinger, G. Stanek); Private Medical Office, Thiersee, Austria (D. Höss)

DOI: https://doi.org/10.3201/eid2704.203366

The aim of this prospective study was to assess the risk for tickborne infections after a tick bite. A total of 489 persons bitten by 1,295 ticks were assessed for occurrence of infections with *Borrelia burgdorferi* sensu lato, *Anaplasma phagocytophilum*, *Rickettsia* spp., *Babesia* spp., *Candidatus* Neoehrlichia mikurensis, and relapsing fever borreliae. *B. burgdorferi* s.l. infection was found in 25 (5.1%) participants, of whom 15 had erythema migrans. Eleven (2.3%) participants were positive by PCR for *Candidatus* N. mikurensis. One asymptomatic participant infected with *B. miyamotoi* was identified. Full engorgement of the tick (odds ratio 9.52) and confirmation of *B. burgdorferi* s.l. in the tick by PCR (odds ratio 4.39) increased the risk for infection. *Rickettsia helvetica* was highly abundant in ticks but not pathogenic to humans. Knowledge about the outcome of tick bites is crucial because infections with emerging pathogens might be underestimated because of limited laboratory facilities.

Ticks are vectors for a variety of tickborne pathogens that cause human disease (*1*). The diversity of tickborne pathogens has increased extensively in recent years, supported by progress in the molecular identification of microorganisms (*2*). Clinical studies on the health-related impact of many emerging tickborne pathogens are scarce and information on the epidemiology is limited.

We undertook a comprehensive observational study in Austria to assess the incidence of recognized tickborne infections by applying clinical, serologic, and microbiological endpoints. We conducted a detailed risk analysis of contracting Lyme borreliosis. Our objective was to investigate whether variables such as confirmation of *Borrelia burgdorferi* sensu lato in ticks, duration of tick attachment, engorgement of ticks, and number of simultaneous tick bites have an impact on the risk for infection. Furthermore, we wanted to know whether the localization of a given tick bite and any previous contact with *B. burgdorferi* s.l. can affect this risk.

Methods

Participants were enrolled prospectively during 2015–2018 at 2 centers in Austria (Vienna and Thiersee). The invitation to participate was announced in the local media. The analysis focused on infections with tickborne pathogens including *B. burgdorferi* s.l., *Anaplasma phagocytophilum*, *Rickettsia* spp., *Babesia* spp., *Candidatus* Neoehrlichia mikurensis, and relapsing fever borreliae. The study was approved by the ethics committee of the Medical University of Vienna (1064/2015) and of the Medical University of Innsbruck (AN2016-0043-359/4.16). Participants provided written informed consent.

Inclusion/Exclusion Criteria

Inclusion criteria were a minimum age of 18 years and the availability of the particular tick for testing. Persons bitten >7 days before assessment were excluded.

Questionnaire

A standardized questionnaire was used to collect information concerning tick bite location, history of erythema migrans, antimicrobial drug treatment within 4 weeks before the tick bite, estimated duration of tick attachment, number of ticks removed, and possible geographic region of tick attack. The feeding duration of the tick was reported in days by the difference of the estimated date of the tick bite and the date of tick removal.

Outcome Definition

Serologic testing and PCR for blood were conducted during the first week after the removal of the tick, with a follow-up scheduled 6 weeks thereafter. We defined infection as ≥1 of the following: occurrence of erythema migrans diagnosed by a medical professional (M.M. or D.H.), increase in *Borrelia*-specific antibodies in follow-up samples, and presence of the microorganism determined by PCR in the initial or follow-up blood samples.

Laboratory Analyses

Laboratory analyses were conducted at the Institute of Hygiene and Applied Immunology in Vienna. An experienced technician (A.-M.S.) identified ticks morphologically. If identification was inconclusive, we used molecular methods. Ten percent of the randomly selected *Ixodes ricinus* ticks underwent molecular identification to confirm the identification procedure. We documented the developmental stage of the ticks and recorded engorgement levels as not engorged, partially engorged, or fully engorged.

We extracted DNA from the ticks as described (*2*). Molecular identification of ticks was conducted by using the mitochondrial 16S rRNA gene (*3*), 12S rDNA gene (*4*), internal transcribed spacer 2 region (*5*), or cytochrome c oxidase subunit 1 gene (*6*). PCR products were purified and sent to Microsynth (https://www.microsynth.at) for bidirectional sequencing.

Molecular detection of *B. burgdorferi* s.l.; *Rickettsia* spp.; *Anaplasma*/*Ehrlichia* spp., including *Candidatus* N. mikurensis, *Babesia* spp., and *Coxiella burnetti*; was performed by using reverse line blot (RLB) hybridization (*2*). Sequencing was conducted if RLB failed to yield a species-specific signal. When *Rickettsia* spp. could not be identified by sequencing the 23S–5S intergenic spacer region used for RLB (*7*), we conducted

additional PCRs specific for the *gltA* gene (*8*,*9*). We used real-time PCRs to detect *B. miyamotoi* (*10*) and, in addition to RLB hybridization, for *Candidatus* N. mikurensis (*11*).

Molecular Analysis of Blood

We screened extracted DNA from blood containing EDTA for tickborne pathogens by using real-time PCR. The pathogens screened were *B. burgdorferi* s.l. (*12*), *Rickettsia* spp. (*12*), relapsing fever borreliae (*12*), *A. phagocytophilum* (*13*), *B. miyamotoi* (*10*), and *Candidatus* N. mikurensis (*11*).

Serologic Testing

We assessed infections with *B. burgdorferi* s.l. by comparing ELISA values for IgM and IgG at the first and the follow-up tests. The increase in antibody levels was observed when the first sample yielded a negative result by using the cutoff value provided by the manufacturer and the result was positive in the follow-up sample. For specimens with a value above the cutoff value in the initial sample, we defined the infection as a 25% increase. Positive and borderline ELISA results were confirmed by using immunoblot (Anti-Borrelia-EUROLINE-RN-AT; Euroimmun, https://www.euroimmun.com).

During this study, a change of test systems was necessary because of withdrawal of systems from the market. A *Borrelia* ELISA (Medac, https://international.medac.de) was used until the end of May 2018, followed by Anti-Borrelia-plusVlsE-ELISA (Euroimmun) after June 2018. In the instance that the first and the follow-up serum samples were analyzed by different ELISAs, we used a paired sample for retesting with the new ELISA.

We performed serologic testing for other tickborne pathogens by applying the following commercial tests: *A. phagocytophilum* and *Rickettsia* IgG immunofluorescence assays (Focus Diagnostics, https://www.focusdx.com) and the Weil-Felix agglutination assay (DiaMondiaL, https://www.diamondial.com) as an additional serologic test able to detect infections with *Rickettsia* spp. Infections were defined as a 4-fold change in the titer.

Determination of Sample Size

Human infection rates for *B. burgdorferi* s.l. after tick bites have been reported to be 2%–5% (*14*,*15*). Because high endemicity can be assumed for the covered regions, we determined the sample size on the basis of an upper limit of 5%. To have a power of 80% to detect an effect associated with an odds ratio (OR) ≥2, and considering covariates with a combined R^2 of 25%, a total of 411 participants were considered necessary to provide statistical significance at the (2-sided) 5% level.

Statistical Analysis

Because many participants had >1 tick on >1 occasion, we considered only ticks brought at the time of infection for infected persons. For noninfected persons who had >1 visit, 1 visit was chosen randomly, and the tick removed on that occasion was used for analysis. Similarly, if several ticks were available for the visit, 1 tick was randomly selected unless 1 of them was infected.

Preliminary comparisons of *Borrelia*-infected and noninfected participants were performed by using the Mann-Whitney test for metric data. We used the Fisher exact probability test for dichotomous data and the Fisher-Freeman-Halton test for categorical data. These data are reported as mean ± SD and median (interquartile range) with absolute and percent frequencies. Multiple logistic regression analysis was conducted to assess the risk for infection associated with attributes of the ticks, taking the age and sex of the participants into account. Seven persons did not complete follow-up testing and were excluded from the analyses. No imputation for missing data was applied. All analyses were performed by using Stata 13.1 (StataCorp LLC, https://www.stata.com).

Results

Study Population

A total of 489 participants were included in the study, of whom 7 were unavailable for follow-up. The number of ticks removed by the participants was 1,295. The final total of 482 study participants (255 women and 227 men) had a mean age of 49 years (range 19–83 years) and had been bitten by 1,279 ticks. A total of 433 (89.8%) participants were enrolled in Vienna and 49 (10.2%) were enrolled in Tyrol. At baseline, 120 (24.9%) participants were seropositive for *Borrelia* antibodies, 39 (8.1%) for *A. phagocytophilum* antibodies, and 13 (2.7%) for *Rickettsia* spp. antibodies. The mean time interval between the baseline and the follow-up test was 47 days (range 21–147 days).

Ticks Obtained from Participants

A total of 96% of the tick bites occurred in Austria. Most ticks were removed during the months of June (338, 26.4%) and May (303, 23.7%), followed by July (227, 17.7%) and August (115, 9.0%).

Of the 1,279 ticks, 1,277 (99.8%) were *I. ricinus*. The 2 remaining ticks were *H. concinna* and a nymphal

Haemaphysalis sp. tick imported from Cambodia. The most common developmental stage was the nymphal stage (922 ticks, 72.1%) followed by larvae (241 ticks, 18.8%), and adults (112 ticks [103 females and 9 males], 8.8%). For 4 ticks (0.3%), it was not possible to identify the developmental stage, but *I. ricinus* was confirmed by PCR.

We compiled an overview of tick collection (Figure 1). Of the 482 participants, 139 persons collected >1 tick. The highest number of ticks per person was 163. Nearly half of the ticks were removed on the first day (629, 49.2%) (Figure 2).

Molecular Screening of Ticks

B. burgdorferi s.l.was detected in 15.2% (194/1,279) of all ticks. The most common genospecies was *B. afzelii* in 66.5% (129/194), followed by *B. garinii*/*B. bavariensis* in 16.5% (32 ticks), *B. burgdorferi* sensu stricto in 7.7% (15 ticks), and other *Borrelia* spp. in 11.3% (22 ticks). Co-infections with >1 genospecies were detected in 4 ticks.

Rickettsia spp. was the second most frequent organism with 9.4% (120/1,279), and *R. helvetica* represented 86.7% (104/120) of all *Rickettsia*-positive ticks, followed by *R. monacensis* in 8 ticks (6.7%). Eight *Rickettsia*-positive samples yielded only genus-specific signals on the RLBs. Presence of *Candidatus* R. mendelii was confirmed by sequencing 4 of these ticks. Two were new species according to phylogenetic guidelines (*16*), of which 1 belonged to the spotted fever group *Rickettsiae* (*17*). For the remaining 2 *Rickettsia*-positive ticks, the species could not be identified. We provide an overview of the tickborne pathogens detected in the different life stages of the ticks (Table 1).

Of the 1,279 ticks included in the study, 380 (29.7%) harbored ≥1 tickborne pathogen. Dual infections with organisms of different genera occurred in 48 ticks (3.8%). Seven ticks (0.6%) harbored 3 different genera.

Human Infection

Borrelia infection was found in 25 (5.1%) participants. Fifteen patients had erythema migrans, of whom 9 also showed an increase in *Borrelia*-specific antibodies in the follow-up sample. All instances of erythema migrans except 1 were localized at the site of the tick bite. Moreover, in 10 persons, evidence of *Borrelia* infection was found by serologic testing, and these persons did not have erythema migrans or any other symptoms. Demonstration of *B. burgdoferi* s.l. by PCR in the blood was successful in only 1 participant who had erythema migrans in an early stage. Infection with *B. burgdorferi* s.l. occurred twice in 2 participants. One woman had an erythema migrans twice within 4 months. Another

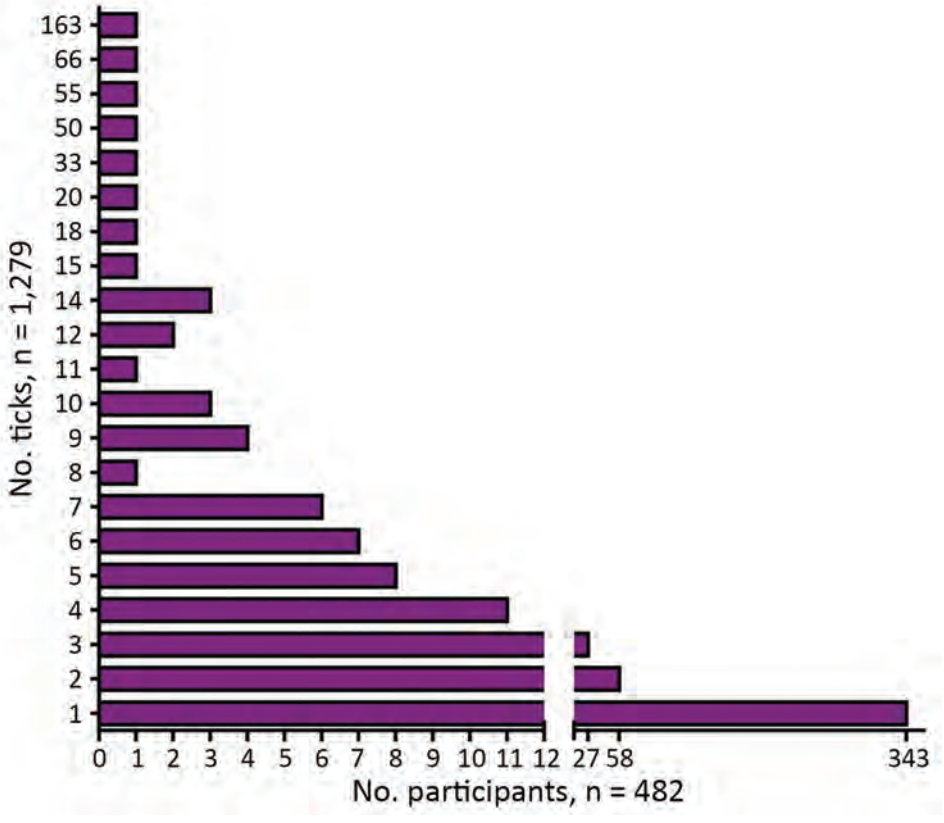

Figure 1. Number of ticks per study participant in study of infections with tickborne pathogens after tick bite, Austria, 2015–2018.

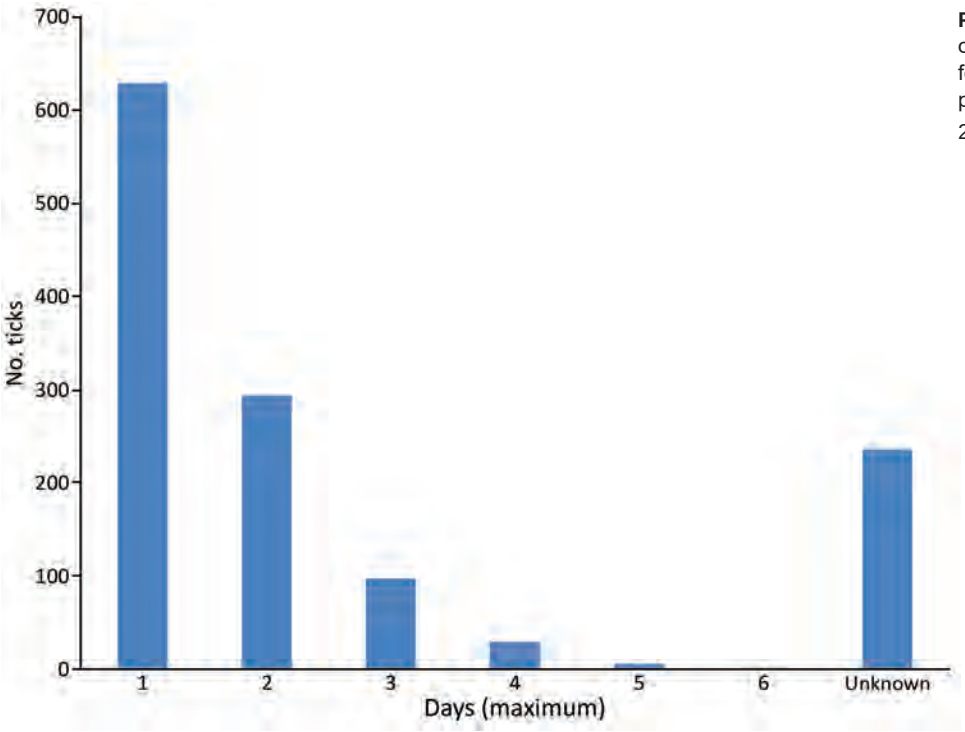

Figure 2. Estimated duration of tick attachment (n = 1,279) for infections with tickborne pathogens after tick bite, Austria, 2015–2018.

woman had an asymptomatic infection, followed by erythema migrans 3 weeks later. She had been bitten by 11 ticks and showed seroconversion. Thereafter, she had another tick bite, which caused also erythema migrans around the bite. Antimicrobial drugs were given to patients who had erythema migrans but not to those who had asymptomatic infections.

With regard to other infections, 11 (2.3%) participants were positive for *Candidatus* N. mikurensis. These participants reported no symptoms. For 3 participants, the presence of *Candidatus* N. mikurensis was identified at the first visit, as well as at the follow-up tests. The time intervals between the examinations for these 3 participants were 41, 44, and 86 days.

Table 1. Tickborne pathogens detected in different life stages of ticks after tick bite, Austria, 2015–2018

Pathogen or tick	Tick life stage					
	Adult females	Adult males	Nymphs	Larvae	Not identified	Total
Borrelia burgdorferi sensu lato	29	3	159	1	2	194
B. afzelii	10	1	115	1	2	132
B. garinii/B. bavariensis	7	1	24	0	0	32
B. burgdorferi sensu stricto	3	0	12	0	0	15
B. valaisiana	5	1	8	0	0	14
B. lusitaniae	1	0	1	0	0	2
B. spielmanii	3	0	3	0	0	6
Co-infections	0	0	4	0	0	4
Rickettsia spp.	14	0	69	37	0	120
R. helvetica	12	0	56	36	0	104
R. monacensis	1	0	6	1	0	8
Candidatus R. mendelii	1	0	3	0	0	4
New endosymbiont	0	0	1	0	0	1
Candidatus R. thierseensis	0	0	1	0	0	1
Not identified	0	0	2	0	0	2
Anaplasmataceae						
Candidatus Neoehrlichia mikurensis	5	1	46	1	1	54
Anaplasma phagocytophilum	1	0	29	0	0	30
Babesia spp.	3	0	20	5	0	28
B. microti	3	0	18	0	0	21
B. divergens	0	0	1	0	0	1
B.. venatorum	0	0	1	5	0	6
Relapsing fever borreliae						
B. miyamotoi	1	0	20	2	1	24

One study participant was positive for *B. miyamotoi* by PCR but reported no signs or symptoms. No infections with *A. phagocytophilum* or *Rickettsia* spp. were documented. No infections with *C. burnettii* or *Babesia* spp. were found by PCR; however, serologic testing was not used for these infections.

Risk for Infection with *B. burgdorferi* s.l.

We compared the demographic and other variables between the participants with *Borrelia* infection and noninfected participants (Table 2). In a multivariate model, the tick engorgement levels (OR 9.52) and confirmation of *B. burgdorferi* s.l. in ticks (OR 4.39) showed a major increase in the risk for infection (Table 3).

We also compared the differences in the distribution of ticks co-infected with multiple pathogens that had bitten participants with and without *Borrelia* infection. Of 37 ticks detached by 25 *Borrelia*-infected participants, 4 (10.8%) harbored >1 pathogen, whereas among 1,242 ticks from the noninfected group, 56 (4.5%) carried multiple pathogens (p = 0.07).

Discussion

We investigated 482 persons bitten by ticks for the occurrence of bacterial tickborne infections and *Babesia* spp. We demonstrated a high incidence of infections with the emerging pathogen, *Candidatus* N. mikurensis. Furthermore, our data clearly show that *R. helvetica*, though highly abundant in ticks in Austria, does not pose a risk for human health. We also conducted a detailed risk analysis for contracting Lyme borreliosis by analyzing numerous demographic and clinical parameters. This knowledge is needed for further research on the efficacy of specific interventions for preventing Lyme borreliosis, such as local or systemic antimicrobial drug prophylaxis after tick bite (*18*).

The risk for contracting *Borrelia* infection was 5.1%, which is consistent with published data for the Netherlands and Sweden (*14*,*15*), despite a different frequency of *B. burgdorferi* s.l. in ticks (15.2%) compared with previous reports (26% and 29.3%). This finding might be explained by the fact that more larvae were removed during the current study. *I. ricinus* larvae do not harbor *B. burgdorferi* s.l. because of lack of transovarial transmission of this pathogen. An investigation of ticks collected from vegetation throughout Austria showed that 25% of ticks were positive for *Borrelia* spp. (*2*), but no larvae were analyzed. Because male adult *I. ricinus* ticks rarely feed

Table 2. Comparison of persons infected and not infected with *Borrelia burgdorferi* sensu lato after tick bite, Austria, 2015–2018*

Variable	Not infected, n = 457		Infected, n = 25		p value
	No. or mean ± SD	Median, % (IQR)	No. or mean ± SD	Median, % (IQR)	
Sex					
M	214	46.8	12	48.0	1.000
F	243	53.2	13	52.0	NA
Age, y	48.7 ± 14.5	48.5 (36.8–59.1)	52.4 ± 14.0	54.0 (42.9–58.6)	0.216
Use of repellent	17	3.7	2	8.0	0.258
No. ticks	1.3 ± 1.2	1.0 (1.0–1.0)	2.4 ± 3.8	1.0 (1.0–2.0)	<0.001
Time, tick bite to blood test, d†	4.3 ± 4.0	4.0 (2.0–6.0)	3.9 ± 2.1	3.0 (2.0–5.0)	0.645
Duration of tick attachment, d	1.0 ± 2.9	1.0 (0.0–2.0)	1.2 ± 1.2	1.0 (0.0–2.0)	0.668
Tick location					
Left leg	119	26.0	15	60.0	<0.001
Right leg	130	28.4	13	52.0	0.022
Left arm	53	11.6	6	24.0	0.106
Right arm	55	12.0	4	16.0	0.530
Head/neck	21	4.6	1	4.0	1.000
Abdomen/chest	71	15.5	4	16.0	1.000
Genital/pelvic area	111	24.3	5	20.0	0.811
Back	46	10.1	4	16.0	0.314
Antimicrobial drug‡	30	6.6	0	0.0	0.39
PCR positive	62	13.6	11	44.0	<0.001
IgG§	57	12.5	6	24.0	0.08
IgM§	30	6.6	2	8.0	0.58
IgG and IgM§	23	5.0	2	8.0	0.37
History of erythema migrans	84	18.0	8	32.0	0.15
Tick engorgement					
None	180	39.5	4	16.0	<0.001
Slightly/partially	219	48.0	10	40.0	NA
Fully	57	12.5	11	44.0	NA

*IQR, interquartile range; NA, not applicable.
†Time between tick bite and first blood test.
‡Received within 4 weeks before tick bite.
§Presence of *Borrelia*-specific antibodies at the first visit.

Table 3. Multiple logistic regression analysis for assessing risk for infection with *Borrelia burgdorferi* sensu lato after tick bite, Austria, 2015–2018*

Parameter	p value	OR (95% CI)
Sex	0.818	0.90 (0.38–2.15)
Age	0.662	1.01 (0.98–1.04)
No. ticks	0.048	1.18 (1.00–1.39)
Tick PCR positive for *B. burgorferi*	0.001	4.39 (1.78–10.84)
Tick engorgement		
Fully	<0.001	9.52 (2.79–32.45)
Slightly/partially	0.229	2.09 (0.63–6.98)
Not engorged	NA	1 (NA)

*NA, not applicable; OR, odds ratio.

on humans, only 9 of 112 adult ticks detached by study participants were male.

The presence of *Borrelia* in ticks and the level of tick engorgement were the major predictors of infection. However, we did not find a correlation between infection and the time of attachment reported by the participants. Clinical trials on the relationship between infection risk and duration of tick feeding are scarce, and results are contradictory (*14*,*15*). Inconsistency might be attributed to the fact that self-assessment of the duration of tick attachment might be imprecise. We assume that if more granular time intervals (e.g., in hours instead of days) had been applied in our study, the results might have been different, particularly for the large group of persons who had removed their ticks within the first 24 hours (≈50% of the ticks in this study). Transmission of *B. burgdorferi* s.l. can occur ≤24 hours from tick attachment (*14*,*19*). Our study demonstrates that morphologic evaluation of tick engorgement is more reliable as a predictor for risk of infection. The risk was 10 times higher for fully engorged ticks than for nonengorged ticks. Limited correlation between self-reported duration of tick attachment and level of engorgement has been reported (*20*).

Our data suggest that a history of erythema migrans and presence of antibodies do not avert further *Borrelia* infections. The frequency of participants who had been seropositive at baseline and of those who had previous erythema migrans was higher in the infected group (Table 2). Although not statistically significant, these results suggest greater exposure to ticks.

Among other tickborne pathogens, *Candidatus* N. mikurensis was the most frequent agent identified in blood containing EDTA, and 2% of the participants had an asymptomatic infection with this emerging pathogen. Infection with *Candidatus* N. mikurensis can have a severe clinical picture. Life-threatening complications can occur not only for immunocompromised patients but also for immunocompetent patients (*21*,*22*). The pathogen was detected in blood samples of patients who had erythema migrans–like rashes in Norway; a total of 70 symptomatic patients were tested, and the pathogen was found in 10% of the patients (*23*). Asymptomatic infections are rare and they have been reported in healthy foresters from Poland (*24*), but no prospective data on the risk for acquiring the infection after tick bites are available. For 3 persons, we detected the pathogen in 2 consecutive samples. In 1 of these persons, the first positive sampling occurred during October, and the follow-up was performed 86 days later in January. Because no tick bites were documented in this study during the months of December–February, this finding suggests a long persistence of the pathogen in the blood in the absence of symptoms. However, there are no comparable reports on the persistence of *Candidatus* N. mikurensis in a human host.

B. miyamotoi is transmitted uniquely by *Ixodes* ticks and is an emerging pathogen causing febrile illness and meningitis in immunocompromised patients (*25*,*26*). With a prevalence of 2% in ticks, we expected a low incidence of infections in humans. We detected this spirochete in a healthy 79-year-old man. The incidence for infections with *A. phagocytophilum* was low, which corresponds to observations from Scandinavian countries (*27*). We did not document any case despite a relatively high level of background seroprevalence at study inclusion (8%). Severe cases of human granulocytic anaplasmosis sporadically occur in Austria (*28*), and a larger sample size might be necessary to detect such cases.

Rickettsia spp. was found in 9.4% of the ticks in our study. However, we did not identify any infections by using serologic or molecular methods. No study participant showed development of clinical signs of rickettsial infection, such as skin eschars or lymphadenopathy. The dominating species in ticks from Austria was *R. helvetica,* and only a few infections with this organism have been reported worldwide, suggesting its low pathogenicity (*16*,*29*).

We identified *Candidatus* R. mendelii in 4 ticks. This novel organism was initially identified in the Czech Republic during 2016 (*30*). Extensive data on its geographic distribution are missing. We also detected a new *Rickettsia* sp. of the spotted fever group in a tick from Tyrol, Austria (*17*).

We did not exclude patients who had received previous antimicrobial drug treatment. A total of 23 of these patients received antimicrobial drugs that

were active against tickborne pathogens starting 4 weeks before enrollment. Six participants were receiving antimicrobial drugs at study inclusion, and the time point for antimicrobial drug treatment was not known exactly for 7 participants. Two participants were receiving immunosuppressive treatment. For persons with multiple tick bites in the noninfected group, we randomly selected 1 tick for risk analysis because it would otherwise have been difficult to calculate a regression model. Finally, for some pathogens, we used PCR only to identify infections without additional serologic testing, including that for *Babesia* spp. and *B. miyamotoi*. Because of a low prevalence of these pathogens in ticks, it is unlikely that we would have found a substantial amount of infections by using serologic methods.

Acknowledgments

We thank Katharina Grabmeier-Pfistershammer and Julia Parzinger for their help in enrolling the study participants.

About the Author

Dr. Markowicz is a medical specialist in general medicine and hygiene and microbiology at the Medical University of Vienna, Vienna, Austria. He is also an unpaid member of the Executive Committee of the European Society of Clinical Microbiology and Infectious Diseases Study Group on Lyme Borreliosis. His primary research interests are Lyme borreliosis and other bacterial tickborne diseases.

References

1. Stanek G, Wormser GP, Gray J, Strle F. Lyme borreliosis. Lancet. 2012;379:461–73. https://doi.org/10.1016/S0140-6736(11)60103-7
2. Schötta A-M, Wijnveld M, Stockinger H, Stanek G. Approaches for reverse line blot-based detection of microbial pathogens in *Ixodes ricinus* ticks collected in Austria and impact of the chosen method. Appl Environ Microbiol. 2017;83:e00489-17. https://doi.org/10.1128/AEM.00489-17
3. Black WC IV, Piesman J. Phylogeny of hard- and soft-tick taxa (Acari: Ixodida) based on mitochondrial 16S rDNA sequences. Proc Natl Acad Sci U S A. 1994;91:10034–8. https://doi.org/10.1073/pnas.91.21.10034
4. Beati L, Keirans JE. Analysis of the systematic relationships among ticks of the genera *Rhipicephalus* and *Boophilus* (Acari: Ixodidae) based on mitochondrial 12S ribosomal DNA gene sequences and morphological characters. J Parasitol. 2001;87:32–48. https://doi.org/10.1645/0022-3395(2001)087[0032:AOTSRA]2.0.CO;2
5. Lv J, Wu S, Zhang Y, Chen Y, Feng C, Yuan X, et al. Assessment of four DNA fragments (COI, 16S rDNA, ITS2, 12S rDNA) for species identification of the Ixodida (Acari: Ixodida). Parasit Vectors. 2014;7:93. https://doi.org/10.1186/1756-3305-7-93
6. Chitimia L, Lin R-Q, Cosoroaba I, Wu XY, Song HQ, Yuan ZG, et al. Genetic characterization of ticks from southwestern Romania by sequences of mitochondrial *cox1* and *nad5* genes. Exp Appl Acarol. 2010;52:305–11. https://doi.org/10.1007/s10493-010-9365-9
7. Jado I, Escudero R, Gil H, Jiménez-Alonso MI, Sousa R, García-Pérez AL, et al. Molecular method for identification of *Rickettsia* species in clinical and environmental samples. J Clin Microbiol. 2006;44:4572–6. https://doi.org/10.1128/JCM.01227-06
8. Labruna MB, McBride JW, Bouyer DH, Camargo LM, Camargo EP, Walker DH. Molecular evidence for a spotted fever group *Rickettsia* species in the tick *Amblyomma longirostre* in Brazil. J Med Entomol. 2004;41:533–7. https://doi.org/10.1603/0022-2585-41.3.533
9. Labruna MB, Whitworth T, Horta MC, Bouyer DH, McBride JW, Pinter A, et al. *Rickettsia* species infecting *Amblyomma cooperi* ticks from an area in the state of São Paulo, Brazil, where Brazilian spotted fever is endemic. J Clin Microbiol. 2004;42:90–8. https://doi.org/10.1128/JCM.42.1.90-98.2004
10. Reiter M, Schötta A-M, Müller A, Stockinger H, Stanek G. A newly established real-time PCR for detection of *Borrelia miyamotoi* in *Ixodes ricinus* ticks. Ticks Tick Borne Dis. 2015;6:303–8. https://doi.org/10.1016/j.ttbdis.2015.02.002
11. Silaghi C, Woll D, Mahling M, Pfister K, Pfeffer M. *Candidatus* Neoehrlichia mikurensis in rodents in an area with sympatric existence of the hard ticks *Ixodes ricinus* and *Dermacentor reticulatus*, Germany. Parasit Vectors. 2012;5:285. https://doi.org/10.1186/1756-3305-5-285
12. Leschnik MW, Khanakah G, Duscher G, Wille-Piazzai W, Hörweg C, Joachim A, et al. Species, developmental stage and infection with microbial pathogens of engorged ticks removed from dogs and questing ticks. Med Vet Entomol. 2012;26:440–6. https://doi.org/10.1111/j.1365-2915.2012.01036.x
13. Pusterla N, Huder JB, Leutenegger CM, Braun U, Madigan JE, Lutz H. Quantitative real-time PCR for detection of members of the *Ehrlichia phagocytophila* genogroup in host animals and *Ixodes ricinus* ticks. J Clin Microbiol. 1999;37:1329–31. https://doi.org/10.1128/JCM.37.5.1329-1331.1999
14. Hofhuis A, Herremans T, Notermans DW, Sprong H, Fonville M, van der Giessen JW, et al. A prospective study among patients presenting at the general practitioner with a tick bite or erythema migrans in The Netherlands. PLoS One. 2013;8:e64361. https://doi.org/10.1371/journal.pone.0064361
15. Wilhelmsson P, Fryland L, Lindblom P, Sjöwall J, Ahlm C, Berglund J, et al. A prospective study on the incidence of *Borrelia burgdorferi* sensu lato infection after a tick bite in Sweden and on the Åland Islands, Finland (2008–2009). Ticks Tick Borne Dis. 2016;7:71–9. https://doi.org/10.1016/j.ttbdis.2015.08.009
16. Fournier PE, Grunnenberger F, Jaulhac B, Gastinger G, Raoult D. Evidence of *Rickettsia helvetica* infection in humans, eastern France. Emerg Infect Dis. 2000;6:389–92. https://doi.org/10.3201/eid0604.000412
17. Schötta AM, Wijnveld M, Höss D, Stanek G, Stockinger H, Markowicz M. Identification and characterization of "*Candidatus* Rickettsia thierseensis", a novel spotted fever group *Rickettsia* species detected in Austria. Microorganisms.2020;8:E1670. https://doi.org/10.3390/microorganisms 8111670
18. Schwameis M, Kündig T, Huber G, von Bidder L, Meinel L, Weisser R, et al. Topical azithromycin for the prevention of Lyme borreliosis: a randomised, placebo-controlled, phase 3 efficacy trial. Lancet Infect Dis. 2017;17:322–9. https://doi.org/10.1016/S1473-3099(16)30529-1

19. Nahimana I, Gern L, Blanc DS, Praz G, Francioli P, Péter O. Risk of *Borrelia burgdorferi* infection in western Switzerland following a tick bite. Eur J Clin Microbiol Infect Dis. 2004;23:603–8. https://doi.org/10.1007/s10096-004-1162-0
20. Sood SK, Salzman MB, Johnson BJ, Happ CM, Feig K, Carmody L, et al. Duration of tick attachment as a predictor of the risk of Lyme disease in an area in which Lyme disease is endemic. J Infect Dis. 1997;175:996–9. https://doi.org/10.1086/514009
21. Wennerås C. Infections with the tick-borne bacterium *Candidatus* Neoehrlichia mikurensis. Clin Microbiol Infect. 2015;21:621–30. https://doi.org/10.1016/j.cmi.2015.02.030
22. von Loewenich FD, Geissdörfer W, Disqué C, Matten J, Schett G, Sakka SG, et al. Detection of "*Candidatus* Neoehrlichia mikurensis" in two patients with severe febrile illnesses: evidence for a European sequence variant. J Clin Microbiol. 2010;48:2630–5. https://doi.org/10.1128/JCM.00588-10
23. Quarsten H, Grankvist A, Høyvoll L, Myre IB, Skarpaas T, Kjelland V, et al. *Candidatus* Neoehrlichia mikurensis and *Borrelia burgdorferi* sensu lato detected in the blood of Norwegian patients with erythema migrans. Ticks Tick Borne Dis. 2017;8:715–20. https://doi.org/10.1016/j.ttbdis.2017.05.004
24. Welc-Falęciak R, Siński E, Kowalec M, Zajkowska J, Pancewicz SA. Asymptomatic "*Candidatus* Neoehrlichia mikurensis" infections in immunocompetent humans. J Clin Microbiol. 2014;52:3072–4. https://doi.org/10.1128/JCM.00741-14
25. Platonov AE, Karan LS, Kolyasnikova NM, Makhneva NA, Toporkova MG, Maleev VV, et al. Humans infected with relapsing fever spirochete *Borrelia miyamotoi*, Russia. Emerg Infect Dis. 2011;17:1816–23. https://doi.org/10.3201/eid1710.101474
26. Henningsson AJ, Asgeirsson H, Hammas B, Karlsson E, Parke Å, Hoornstra D, et al. Two cases of *Borrelia miyamotoi* meningitis, Sweden, 2018. Emerg Infect Dis. 2019;25:1965–8. https://doi.org/10.3201/eid2510.190416
27. Henningsson AJ, Wilhelmsson P, Gyllemark P, Kozak M, Matussek A, Nyman D, et al. Low risk of seroconversion or clinical disease in humans after a bite by an *Anaplasma phagocytophilum*-–infected tick. Ticks Tick Borne Dis. 2015;6:787–92. https://doi.org/10.1016/j.ttbdis.2015.07.005
28. Hoepler W, Markowicz M, Schoetta AM, Zoufaly A, Stanek G, Wenisch C. Molecular diagnosis of autochthonous human anaplasmosis in Austria: an infectious diseases case report. BMC Infect Dis. 2020;20:288. https://doi.org/10.1186/s12879-020-04993-w
29. Parola P, Paddock CD, Raoult D. Tick-borne rickettsioses around the world: emerging diseases challenging old concepts. Clin Microbiol Rev. 2005;18:719–56. https://doi.org/10.1128/CMR.18.4.719-756.2005
30. Hajduskova E, Literak I, Papousek I, Costa FB, Novakova M, Labruna MB, et al. '*Candidatus* Rickettsia mendelii', a novel basal group rickettsia detected in *Ixodes ricinus* ticks in the Czech Republic. Ticks Tick Borne Dis. 2016;7:482–6. https://doi.org/10.1016/j.ttbdis.2016.02.004

Address for correspondence: Mateusz Markowicz, Institute for Hygiene and Applied Immunology, Center for Pathophysiology, Infectiology and Immunology, Medical University of Vienna, Kinderspitalgasse 15, Vienna A-1090, Austria, email: mateusz.markowicz@meduniwien.ac.at

Emergence of *Burkholderia pseudomallei* Sequence Type 562, Northern Australia

Ella M. Meumann, Mirjam Kaestli, Mark Mayo, Linda Ward, Audrey Rachlin, Jessica R. Webb, Mariana Kleinecke, Erin P. Price, Bart J. Currie

Since 2005, the range of *Burkholderia pseudomallei* sequence type 562 (ST562) has expanded in northern Australia. During 2005–2019, ST562 caused melioidosis in 61 humans and 3 animals. Cases initially occurred in suburbs surrounding a creek before spreading across urban Darwin, Australia and a nearby island community. In urban Darwin, ST562 caused 12% (53/440) of melioidosis cases, a proportion that increased during the study period. We analyzed 2 clusters of cases with epidemiologic links and used genomic analysis to identify previously unassociated cases. We found that ST562 isolates from Hainan Province, China, and Pingtung County, Taiwan, were distantly related to ST562 strains from Australia. Temporal genomic analysis suggested a single ST562 introduction into the Darwin region in ≈1988. The origin and transmission mode of ST562 into Australia remain uncertain.

The tropical disease melioidosis causes sepsis in persons with risk factors such as diabetes or hazardous alcohol consumption (*1*). The causative bacterium, *Burkholderia pseudomallei*, is found in soil and surface waters. Most reported cases of melioidosis occur in Southeast Asia and northern Australia during the monsoonal wet seasons (i.e., November–April in northern Australia and May–October in Southeast Asia) (*1*). Although melioidosis is increasingly found in China, the Pacific Islands, South Asia, Africa, and Central and South America (*2*), laboratory diagnostic constraints contribute to underreporting of cases. As a result, the true global distribution and prevalence of melioidosis remain uncertain (*3*).

Clinical manifestations are varied; however, pneumonia is the most common form, accounting for ≈50% of cases (*4*). The frequencies of these manifestations differ by region. For example, suppurative parotitis is common in children in Thailand and Cambodia but rare in Australia; manifestations such as prostate abscesses and brainstem encephalitis are reported rarely outside Australia (*1*,*4*). Death rates range from 9% in northern Australia to 40% in northeast Thailand (*1*,*4*). The extent to which transmission mode, host risk factors, access to diagnostic testing, appropriate antimicrobial drugs, and intensive care treatment account for differences in manifestations and outcomes remains uncertain. Clinical studies suggest that host risk factors are major contributors to disease severity and outcome (*1*).

Phylogeographic analyses suggest that *B. pseudomallei* emerged in ancient Australia and subsequently disseminated throughout Asia (*2*,*5*,*6*). Because of their ecologic niche, sensitivity to ultraviolet light, and rare transmission among humans, strains of *B. pseudomallei* in Australia have remained phylogenetically distinct from strains in Asia, Africa, and the Americas (*2*,*6*). Most reported instances of sequence type (ST) overlap between Asia and Australia are unrelated at the whole-genome level (*7*), with the exception of ST562 (*8*). Some STs in Southeast Asia occur over large geographic areas, such as along the Mekong and other rivers where erosion and washout from disturbed land might have contributed to *B. pseudomallei* dissemination (*2*,*9*,*10*).

Within Australia, most *B. pseudomallei* STs have a restricted geographic range (*11*). In the urban and rural areas of Darwin, STs have been found in the environment distributed across no more than 50 km (*12*). In Northern Australia, researchers have identified only 2 instances of long-range *B. pseudomallei* disper-

Author affiliations: Menzies School of Health Research, Darwin, Northern Territory, Australia (E.M. Meumann, M. Kaestli, M. Mayo, L. Ward, A. Rachlin, J.R. Webb, M. Kleinecke, E.P. Price, B.J. Currie); Charles Darwin University, Darwin (E.M. Meumann, M. Kaestli, M. Mayo, L. Ward, A. Rachlin, J.R. Webb, M. Kleinecke, E.P. Price, B.J. Currie); Royal Darwin Hospital, Darwin (E.M. Meumann, B.J. Currie); University of the Sunshine Coast, Sippy Downs, Queensland, Australia (E.P. Price)

DOI: https://doi.org/10.3201/eid2704.202716

sal, spanning distances of 90 km and 460 km (*13*,*14*). *B. pseudomallei* isolates in the Northern Territory of Australia are very diverse, belonging to at least 379 reported STs (*12*). In this region, strains found in clinical and environmental samples exhibit similar levels of diversity (*11*). High species diversity of *B. pseudomallei* exists in urban Darwin; however, several STs, including ST109, ST36, ST132, and in recent years, ST553, have dominated among clinical and environmental isolates (*7*,*15*).

The Darwin Prospective Melioidosis Study has documented every culture-confirmed melioidosis case in the Top End region of the Northern Territory since 1989. In 2005, we reported the emergence of *B. pseudomallei* ST562 in urban Darwin (*8*). Genomic analyses revealed limited diversity among isolates and a very narrow geographic range, suggesting a single, recent introduction event from Asia (*8*). We describe the clinical manifestations and genomic epidemiology of *B. pseudomallei* ST562, which is now well-established in urban Darwin and causes a large proportion of melioidosis cases in the region.

Methods

Melioidosis Cases

We conducted this study at Royal Darwin Hospital, the referral center for the Top End region. The Top End is in the wet-dry tropics, ≈245,000 km^2 in area, and sparsely populated. Darwin, the only city in the region, has a population of ≈122,000 persons; the remaining population lives in towns or remote communities separated by vast geographic distances. As part of the Darwin Prospective Melioidosis Study, we documented the demographic characteristics, risk factors, clinical features, and outcomes of 1,148 patients with culture-confirmed melioidosis during October 1, 1989–September 30, 2019 (*1*). We conducted multilocus sequence typing on isolates from 1,108 of 1,148 patients (https://pubmlst.org/organisms/burkholderia-pseudomallei) (*16*). Our study was approved by the Human Research Ethics Committee of the Northern Territory Department of Health and the Menzies School of Health Research, Darwin.

B. pseudomallei Isolates

We analyzed *B. pseudomallei* ST562 sequences from 61 humans (including 3 with recurrent infection), 3 animals, and 4 environmental samples in the Top End; 5 isolates from humans in Hainan Province, China; and 1 isolate from a human in Pingtung County, Taiwan. We conducted whole-genome sequencing using HiSeq 2000, HiSeq 2500, HiSeq 3000, MiSeq, or NovaSeq 6000 (Illumina, Inc., https://www.illumina.com). We also analyzed the genome of a ST562 strain isolated from a water source in Haikou city, Hainan Province, in 1975 (*17*). In addition, we conducted a global phylogenetic analysis using 281 non-ST562 *B. pseudomallei* genomes available in public sources (Appendix 1 Table, https://wwwnc.cdc.gov/EID/article/27/4/20-2716-App1.xlsx). We displayed the geographic distribution of Australia ST562 isolates using ArcGIS (https://www.arcgis.com/index.html) with shape files provided by the government of the Northern Territory.

Statistical Analyses

We conducted all analyses using R version 3.6.0 (http://www.r-project.org). We used a 2-tailed Fisher exact test to conduct a bivariate analysis of demographic characteristics, underlying conditions, clinical features, and outcomes of 53 patients with ST562 and 387 patients with non-ST562 *B. pseudomallei* infection during October 1, 2004–September 30, 2019 in urban Darwin. We considered significant characteristics (i.e., $p<0.05$ in bivariate analysis) in a binomial multivariable generalized linear model with ST562 infection as the outcome. Because of the strong temporal structure to the data, we also included year of diagnosis as a continuous variable (Appendix 2, https://wwwnc.cdc.gov/EID/article/27/4/20-2716-App2.pdf).

Bioinformatic Analyses

We conducted multiple sequence alignment and variant calling with Snippy version 4.3.6 (https://github.com/tseemann/snippy), using the closed ST562 MSHR5858 genome (*18*) (GenBank accession nos. CP008891–2) as the reference for ST562 phylogenetic analyses and the closed K96243 genome (*19*) (GenBank accession nos. BX571965–6) for the global analysis. We conducted maximum-likelihood phylogenetic analyses using IQ-TREE version 1.6.10 (*20*) and predicted regions of recombination using Gubbins version 2.3.4 (*21*). We used BEAST 2 (*22*) for temporal analysis of the core Australia ST562 alignment (Appendix 2).

Results

Australia *B. pseudomallei* ST562 Epidemiology

During 1989–2019, a total of 61 (5.5%) of 1,108 melioidosis cases were caused by *B. pseudomallei* ST562. After treatment completion, 3 (5%) patients had recurrent ST562 infection. Fifty-three (87%) ST562 patients resided in urban Darwin and 5 (8%) in an island community 81 km north of Darwin. In addition, 1 patient was

evacuated from a remote community in East Arnhem Land, Northern Territory, Australia, 6 days after returning from a visit in Darwin; 1 patient lived in a rural community 37 km from Darwin; and 1 patient with an unknown travel history sought treatment at Katherine District Hospital (Katherine, Northern Territory, Australia), 317 km south of Darwin.

During 2005–2019, the proportion of human melioidosis cases caused by ST562 in urban Darwin gradually increased (Figure 1). These cases mostly occurred in 2 hotspot regions: suburbs surrounding a creek where 17 (30%) of 57 melioidosis cases were caused by ST562 and a lagoon where 11 (38%) of 29 cases were caused by ST562. The geographic distribution of cases changed over the 15-year period, moving initially from the creek hotspot to other regions in Darwin and to the island community (Figure 2). Records showed 2 case clusters with known epidemiologic links; the first cluster comprised 5 patients at a hostel in the lagoon hotspot during January 2014–March 2019 and the second comprised 2 persons from separate apartments in the same complex who were each found dead in their apartments on the same day in January 2014. *B. pseudomallei* ST562 was isolated from the autopsy samples of the 2 persons.

In addition, ST562 infections developed in 2 sheep at a veterinary facility in 2009 and 2014 (*8*) and in a meerkat at a wildlife park in 2015 (*23*). These cases occurred in the lagoon hotspot. Environmental sampling at these facilities did not reveal *B. pseudomallei* ST562. Furthermore, despite extensive systematic sampling across Darwin in 2017–2018, researchers found ST562 on only 2 occasions, both at the creek hotspot (*15*). During the investigation of a 2011 melioidosis case in a human, we isolated ST562 from air and soil samples from the lagoon hotspot (*24*).

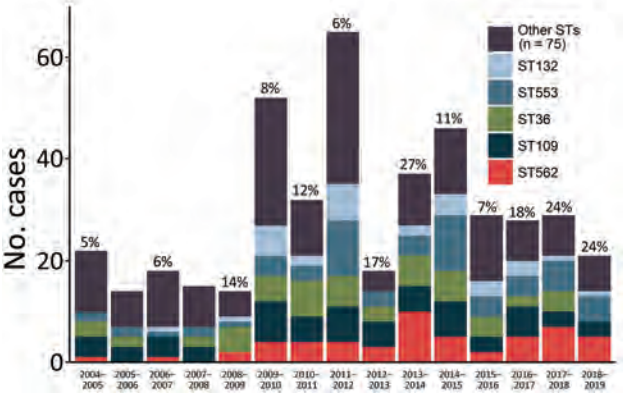

Figure 1. Distribution of melioidosis cases caused by various STs of *Burkholderia pseudomallei*, Darwin, Australia, 2004–2019. Twelve-month periods reflect the wet season then dry season and span October 1–September 30. ST, sequence type.

ST562 Risk Factors and Clinical Features

Among 440 melioidosis patients in urban Darwin during October 1, 2004–September 30, 2019, a significantly higher proportion of patients with ST562 were Aboriginal or Torres Strait Islander (66% vs. 44%; p<0.01), lived in the suburbs surrounding the creek hotspot (33% vs. 11%; p<0.01) or the lagoon hotspot (21% vs. 5%; p<0.01), or reported hazardous alcohol consumption (59% vs. 40%; p = 0.02) (Table 1). In a generalized linear model that included these predictors, only residence in either of the 2 hotspot locations was a significant predictor of infection (Table 1). Pneumonia was the most common manifestation among patients with ST562 (76%) and non-ST562 infections (68%) (Table 2). Among male patients, 10 (32%) with ST562 had a prostate abscess, compared with 33 (15%; p = 0.02) men with non-ST562 infections. In total, 3 patients with ST562 infection died before hospitalization. The proportion of patients with bacteremia, septic shock, or death from melioidosis was not different among those with ST562 versus non-ST562 infection (Table 2).

Australian *B. pseudomallei* ST562 Diversity

The 71 ST562 isolates from Australia were closely related with 141 single-nucleotide polymorphisms (SNPs) over a core alignment length of 7,071,987 nucleotides. These isolates were substantially less diverse than isolates of ST109, ST36, and ST132, which also are found in Darwin (*8*). The median pairwise difference among ST562 genomes was 5 SNPs (range 0–16 SNPs). We found a limited phylogenetic structure among the ST562 genomes, with multiple polytomies on maximum-likelihood analysis (Figure 3); we did not identify any recombination. The soil isolate collected from the lagoon hotspot, MSHR4681, differed by only 5 SNPs from the first soil isolate from the creek hotspot, MSHR10541, despite being collected 6 years and 12 km apart. Isolates from 3 patients (MSHR8799, MSHR9707, and MSHR11750) had no known epidemiologic links but were separated by 0 SNPs.

B. pseudomallei ST562 Genomic Clusters

The ST562 isolates from cases associated with the hostel were phylogenetically clustered (Figure 3). The first 2 cases occurred 1 day apart in January 2014 and the third occurred in March 2014; isolates from these 3 cases differed by 0 SNPs. A fourth case in December 2014 differed from the first 3 isolates by 1 SNP and a fifth case in March 2019 differed by an additional SNP. This clade also included an ST562 isolate from a patient not initially known to have resided at the hostel; further investigation revealed that this patient had checked

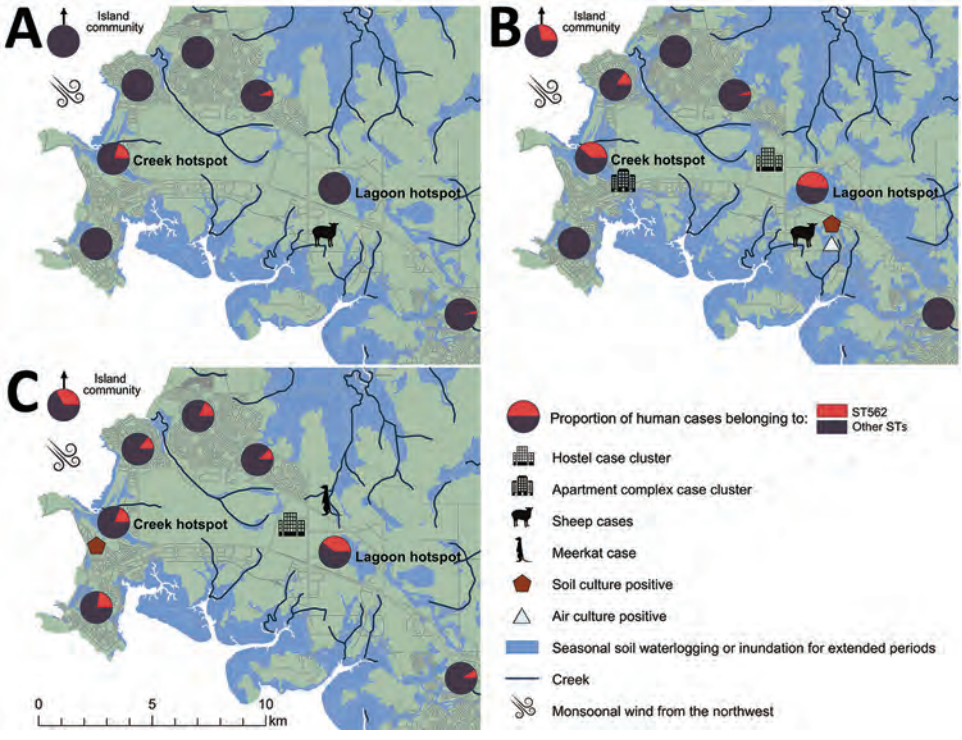

Figure 2. Proportion of melioidosis cases in humans caused by *Burkholderia pseudomallei* ST562, Darwin, Australia, 2004–2019. A) During October 2004–September 2009. B) During October 2009–September 2014. C) During October 2014–September 2019. ST, sequence type.

out of the hostel 6 days before being evacuated from a remote community for melioidosis treatment. Environmental sampling at the hostel did not detect ST562. We advised hostel staff regarding melioidosis prevention, including the importance of protective footwear and remaining indoors during storms.

The isolates from the 2 deceased persons from the apartment complex differed by 7 SNPs and did not fall within the same clade on the phylogenetic tree (Figure 3). However, an isolate from 1 of these patients was separated by 0 SNPs from a clinical isolate collected 10 months earlier from a patient who lived in the adjacent unit. Soil and water sampling of the apartment complex and its surroundings did not identify any *B. pseudomallei* ST562 isolates.

ST562 isolates from air and soil samples at a residence in the lagoon hotspot were separated by 0 SNPs. These isolates differed by 3 SNPs from a clinical isolate from a resident with bacteremic mediastinal melioidosis (24). Thirteen other clinical isolates were more closely related to the air and soil isolates than the clinical isolate from the resident; 1 isolate from a patient 8 years later was identical to the soil and air isolates. That patient lived 3.4 km downwind from the environmental sampling site.

Recurrent *B. pseudomallei* ST562 Infections

Of the 3 recurrent ST562 cases, genomic analysis confirmed that 1 case was a new infection and 2 were relapses (Figure 3). The first patient was treated for melioidosis pneumonia in January 2009 and March 2016; isolates from these 2 episodes differed by 9 SNPs and belonged to different phylogenetic clades, suggesting that these illnesses were caused by independent infection events (25). The second patient had *B. pseudomallei* isolated from urine in December 2017. This patient was treated with intravenous therapy for 4 weeks with ceftazidime then meropenem, then for 12 weeks with oral doxycycline. In October 2018, *B. pseudomallei* was again isolated from this patient's urine; the 2 isolates differed by 5 SNPs and belonged to the same clade, suggesting relapse. The third patient had acute pneumonia in January 2019 and was treated for 4 weeks with intravenous meropenem then ceftazidime, then for 12 weeks with oral trimethoprim/sulfamethoxazole. His symptoms improved and he returned to his community but was subsequently found dead in August 2019. His autopsy revealed pneumonia caused by an isolate differing from his original infection by only 1 SNP.

B. pseudomallei ST562 Origin and Dispersal

The mean estimated clock rate for the 71 Australia *B. pseudomallei* ST562 isolates was 4.11×10^{-8} substitutions/site/year (95% highest posterior density [HPD] $2.0–6.2 \times 10^{-8}$ substitutions/site/year) and the median estimate for the time to the most recent

Table 1. Demographic characteristics and risk factors for melioidosis caused by *Burkholderia pseudomallei* ST562, Darwin, Australia, October 1, 2004–September 30, 2019*

Characteristic	ST, no. (%)†		Bivariate model		Multivariable model	
	562, n = 53	Other, n = 387	OR (95% CI)	p value	OR (95% CI)	p value
Median age, y (range)	51 (13–85)	53 (1–97)	1.01 (0.99–1.02)	0.49		
Sex						
F	22 (42)	163 (42)	Referent			
M	31 (58)	224 (58)	0.98 (0.52–1.81)	>0.99		
Ethnicity						
Non-Indigenous persons	18 (34)	216 (56)	Referent			
Aboriginal or Torres Strait Islanders	35 (66)	171 (44)	2.45 (1.30−4.77)	<0.01	1.88 (0.94–3.77)	0.08
Hotspot‡						
Creek	17 (33)	40 (11)	3.83 (1.84–7.80)	<0.01	4.75 (2.22–10.19)	<0.01
Lagoon	11 (21)	18 (5)	5.02 (1.10–12.17)	<0.01	6.10 (2.39–15.54)	<0.01
Underlying condition						
Diabetes	28 (53)	177 (46)	1.33 (0.72–2.47)	0.38		
Hazardous alcohol consumption	31 (58)	156 (40)	2.08 (1.120–3.93)	0.02	1.72 (0.88–3.36)	0.11
Chronic lung disease	18 (34)	104 (27)	1.40 (0.71–2.67)	0.33		
Chronic kidney disease	9 (17)	53 (14)	1.29 (0.52–2.88)	0.53		
Congestive cardiac failure or rheumatic heart disease	3 (6)	34 (9)	0.62 (0.12–2.10)	0.60		
Malignancy	7 (13)	49 (13)	1.05 (0.39–2.52)	0.83		

*OR, odds ratio; ST, sequence type.
†Values are no. (%), except as indicated.
‡Values missing for 1 patient with ST562 and 30 patients with other STs.

common ancestor was 1988 (95% HPD 1961–2001) (Figure 4). Isolates from the creek hotspot predominated on the deepest branching clades and were distributed throughout the phylogeny, indicating initial establishment in and dispersal from the creek hotspot. Isolates from patients from the island community formed a clade estimated to have diverged from a common ancestor in 2010 (95% HPD 2004–2014). The 5 isolates from Hainan and the isolate from Taiwan were not included in the molecular dating analysis due to poor clock signal; these isolates were distantly related to ST562 isolates from Australia, differing by 6,252–7,786 SNPs (964–1,453 SNPs when excluding recombinogenic regions). In the global *B. pseudomallei* analysis, *B. pseudomallei* ST562 isolates from Australia were most closely related to isolates from East Asia (Figure 5). The ST562 clade belonged to the larger Asian clade in the global phylogeny (*8*).

Discussion

B. pseudomallei ST562 emerged in northern Australia in 2005, fifteen years after the Darwin Prospective Melioidosis Study began genomic surveillance (*1*,*8*). Initially, cases of ST562 in northern Australia mostly occurred in a creek hotspot before spreading across Darwin and to an island community to the north. A La Niña period of heavy rainfall during 2010–2012 was associated with increased melioidosis case

Table 2. Clinical features of melioidosis caused by *Burkholderia pseudomallei* ST562, Darwin, Australia, October 1, 2004–September 30, 2019*

Characteristic	ST, no. (%)		Bivariate	
	562, n = 53	Other, n = 387	OR (95% CI)	p value
Symptoms for <2 months	50 (94)	346 (89)	1.97 (0.59–10.32)	0.33
Localization				
Pulmonary	40 (75)	263 (68)	1.45 (0.73–3.06)	0.34
Abscess†				
Prostatic	10 (32)	33 (15)	2.73 (1.05–6.73)	0.02
Hepatic	1 (2)	13 (3)	0.55 (0.01–3.82)	>0.99
Splenic	2 (4)	25 (6)	0.57 (0.063–2.39)	0.76
Renal	3 (6)	9 (2)	2.51 (0.42–10.49)	0.17
Skin and/or soft tissue	3 (6)	51 (13)	0.40 (0.08–1.30)	0.17
Bone or joint	3 (6)	28 (7)	0.77 (0.14–2.64)	>0.99
Central nervous system	0	4 (1)	NA	>0.99
Severity				
Bacteremia¶	28 (55)	233 (61)	0.79 (0.42–1.49)	0.45
Septic shock	12 (23)	66 (17)	1.42 (0.64–2.94)	0.34
Death	7 (13)	35 (9)	1.53 (0.54–3.77)	0.32

*NA, not applicable; OR, odds ratio; ST, sequence type.
†Missing data for 1 patient with non-ST562 *B. pseudomallei* infection. Prostate abscess data is for 31 men with ST562 and 223 men with other STs.
¶Missing data for 2 patients with ST562 and 3 patients with other STs.

numbers in Darwin (*26*). After this period, the geographic distribution and proportion of cases attributable to ST562 rose. Increased connectivity of waterways and wet conditions might have contributed to ST562 spread in Darwin during this time.

The clinical manifestations, symptom duration, and severity of melioidosis caused by ST562 were similar to those caused by non-ST562 infections, suggesting that host risk factors and route of acquisition contributed to clinical features more than differences in virulence profiles (*1*,*27*). The only difference in clinical manifestations was a larger proportion of male ST562 patients with prostate abscesses. Compared with the rate in Asia, the greater melioidosis survival rates observed in Australia are probably improved by greater access to treatment, including intensive care (*1*,*4*).

Genomic analysis of ST562 strains from Australia demonstrated very little diversity, suggesting a single introduction event with a probable origin in Asia (*8*). The only other characterized ST562 isolates in this study are from Hainan Province, China, and from Pingtung County, Taiwan. Comparative genomic analysis showed that the strains from China and Taiwan strains belonged the same clade but were distantly related to strains in Australia. Researchers have not identified any close relatives of ST562 strains in Australia; their precise origin within Asia remains uncertain.

We estimated that the most recent common ancestor of the ST562 strains in Australia, which indicates the possible time of introduction, occurred in 1988; however, the 95% HPD for this estimate was wide (1961–2001). The estimated clock rate of 4.11 ×

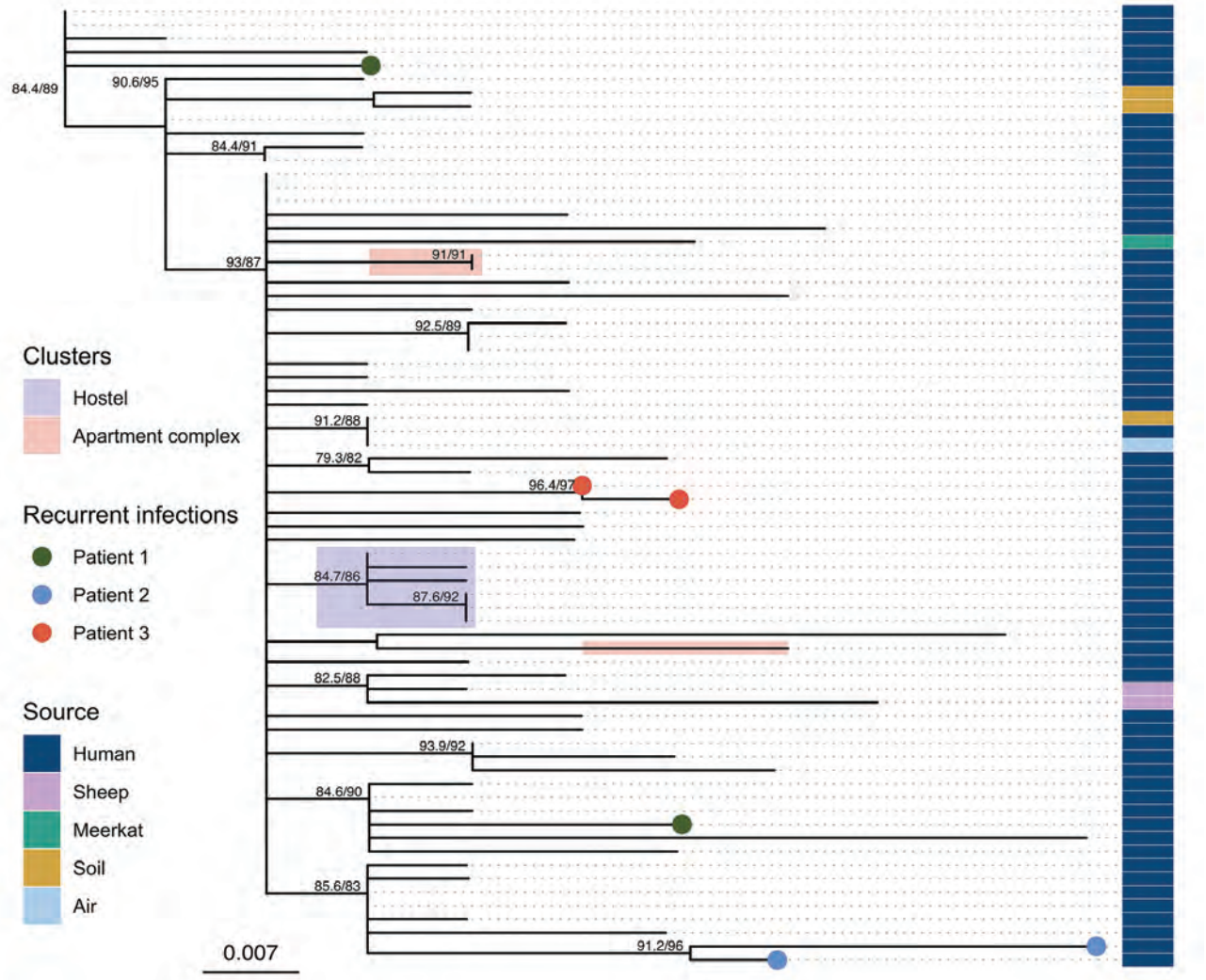

Figure 3. Maximum-likelihood phylogeny of *Burkholderia pseudomallei* sequence type 562 isolates from northern Australia, 2004–2019. Strain MSHR1967 (GenBank accession no. SRR2886997), the earliest sample, was used as the outgroup. Labels indicate nodes with approximate likelihood ratio >60 and ultrafast bootstrap >80. Scale bar indicates substitutions per site.

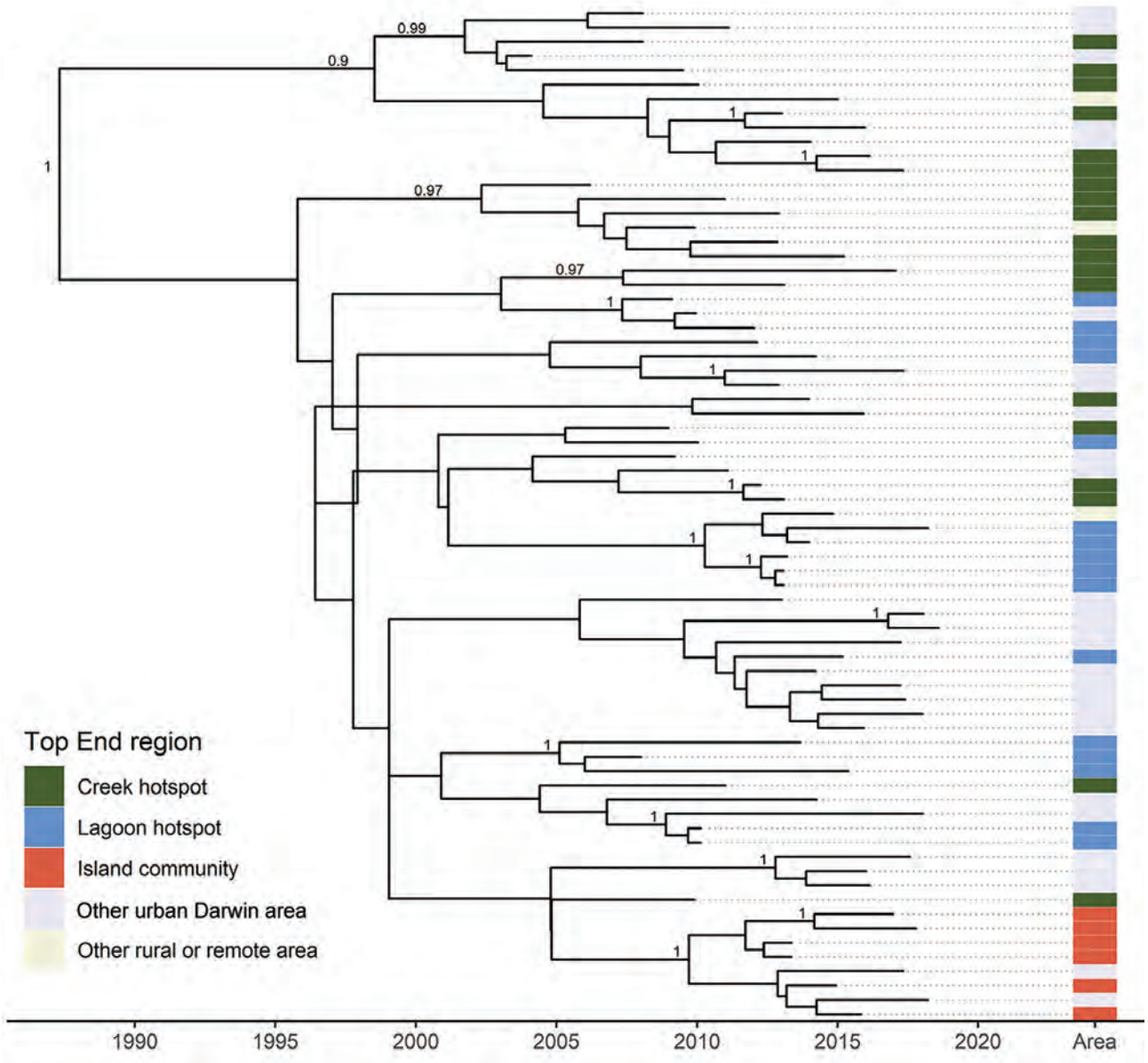

Figure 4. Maximum clade credibility tree of *Burkholderia pseudomallei* sequence type 562 isolates from northern Australia, 2004–2019. Labels indicate nodes with posterior support >0.8.

10^{-8} substitutions/site/year was lower than previously reported. For example, previous reports estimated the rate for serial isolates in patients with cystic fibrosis as 4.9×10^{-7} substitutions/site/year (*28*) and for isolates from a 16-year chronic lung infection as 1.7×10^{-7} substitutions/site/year (*29*). For *B. pseudomallei* groups in Asia and the Americas, the estimated mutation rates range from 1.12×10^{-6} to 9.22×10^{-7} substitutions/site/year (*2*). The variation in these estimates might reflect the difficulty in identifying and excluding SNPs resulting from recombination, the different ecologic conditions and selective pressures of isolates, and inadequate sampling.

B. pseudomallei can exist in a viable but nonculturable state (*30*) and can persist in the environment in suboptimal conditions outside of regions to which it is endemic; the slow replication rate during these periods might contribute to its slow accumulation of mutations. Cases have sporadically occurred in temperate Western Australia, where 2 isolates from animals on different farms collected 17 years apart differed by just 1 SNP (*31*). In contrast, the bacteria can evolve rapidly during acute infection; in 1 patient, 8 SNPs and 5 small insertions/deletions developed in a 12-day period (*32*). We observed similar variability; for example, environmental and clinical

samples collected 8 years apart differed by 0 SNPs, whereas isolates collected 10 months apart from the same patient differed by 5 SNPs. *B. pseudomallei* replication is probably greater in vivo, with the human host milieu placing the bacterium under greater selective pressure than the natural environment.

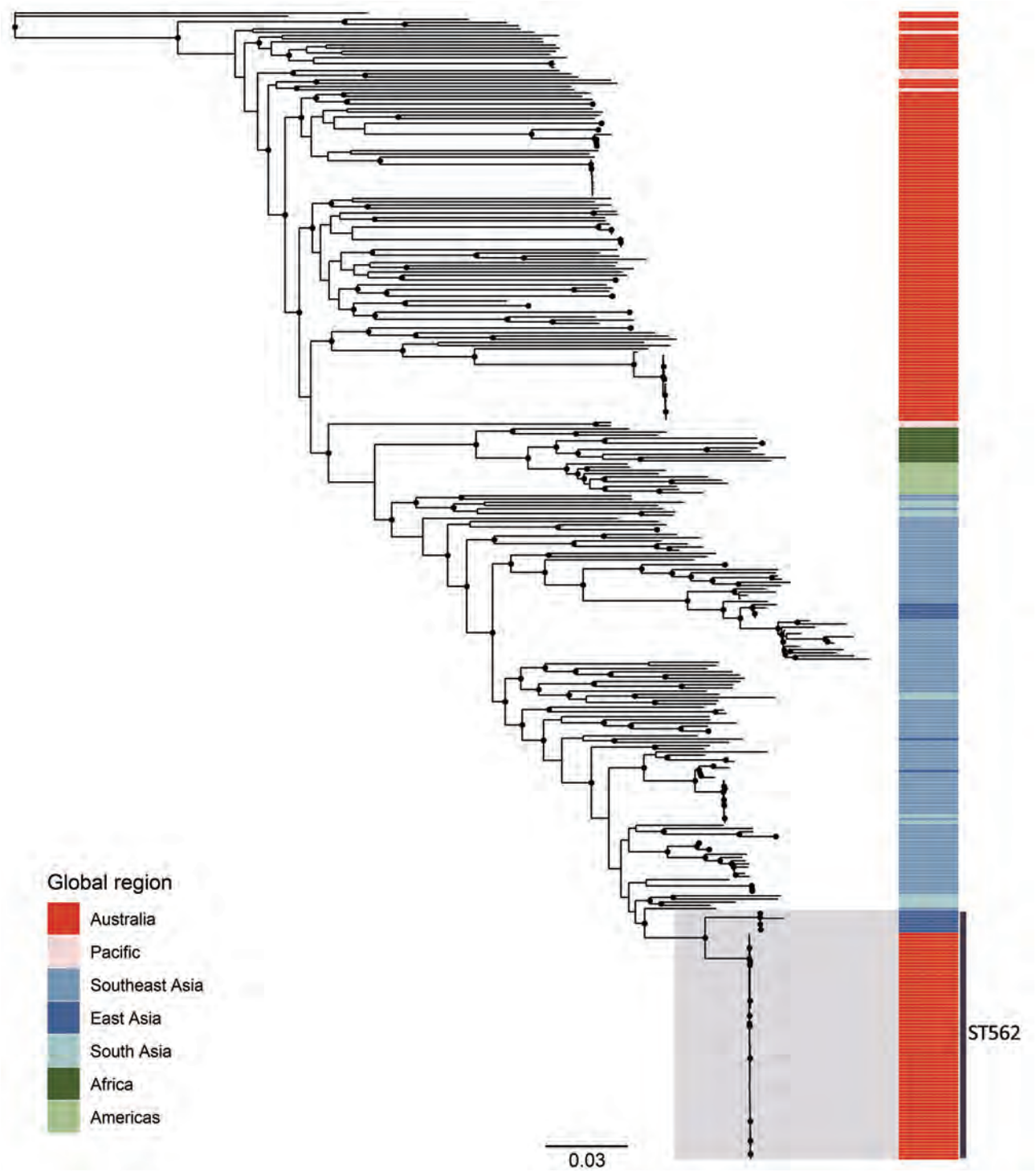

Figure 5. Maximum-likelihood global phylogeny of *Burkholderia pseudomallei* sequence type 562 isolates from northern Australia, 2004–2019, and genomes available in public sources (Appendix 1 Table, https://wwwnc.cdc.gov/EID/article/27/4/20-2716-App1.xlsx). Strain MSHR5619 (GenBank accession no. ERR298346), which had the most divergent genome, was used as the outgroup. Black circles indicate nodes with approximate likelihood ratio >95 and ultrafast bootstrap >95. Colors indicate geographic origin of samples. Scale bar indicates substitutions per site. ST, sequence type.

Previous epidemiologic investigations of melioidosis clusters in humans and animals suggest differences of ≤1 SNP from an implicated infecting source (*15*,*23*,*33*,*34*). In the investigation of 2 cases of infection with *B. pseudomallei* ST325 on the same rural property in northern Australian, there was 1 SNP difference between the 2 clinical isolates and the suspected environmental source, an unchlorinated water tank (*33*). In a fatal outbreak in a remote island community in northern Australia, 4 *B. pseudomallei* ST126 clinical isolates differed by ≤1 SNPs from an isolate from the town water supply (*34*). We confirmed case clusters at a hostel and an apartment complex by combining epidemiologic information and phylogenetic analysis, enabling the identification of previously unassociated cases. There was little diversity among *B. pseudomallei* ST562 isolates in northern Australia; many epidemiologically unrelated isolates differed by ≤1 SNP. Phylogenetic analysis was required for cluster identification.

Intercontinental dispersal of *B. pseudomallei* is an extremely unusual event, as demonstrated by the strong phylogeographic signal in the global phylogeny (*2*,*5*–*8*). The mode of ST562 transmission into northern Australia and then to an offshore island is unclear but could have been through soil, plants, animals, or humans (*8*) or through air during a severe weather event. The bacterium does not survive prolonged exposure to ultraviolet light, which probably limits aerial dispersal (*35*); many researchers consider long-range intercontinental spread through the air unlikely. However, *B. pseudomallei* has been isolated from air samples (*24*,*36*), suggesting that this route of transmission might be possible across relatively short distances. The dissemination of *B. pseudomallei* across islands in the Caribbean might have been mediated by hurricanes (*37*), and the dispersal of *B. pseudomallei* across northern Australia might be associated with tropical cyclones (*38*). Tropical cyclones occur every year in northern Australia, and melioidosis clusters can occur after these events (*31*,*39*). Clusters also have been associated with typhoons in Taiwan, where studies using multilocus sequence typing have suggested airborne dissemination from soil and an increase in human cases depending on the wind direction (*36*,*40*). The distance that *B. pseudomallei* can travel in such events remains uncertain.

Although *B. pseudomallei* colonization of humans is rare (*29*,*41*), the bacterium has been found in the feces of domestic and wild animals including wallabies, horses, and chickens (*42*,*43*), and in the beak of a healthy native peaceful dove (*Geopelia placida*) (*44*). A strong association exists between *B. pseudomallei* presence in soil and disturbance by horses, chickens, and pigs (*45*). *B. pseudomallei* has been imported into areas to which it is not endemic and that are associated with exotic animals (*46*,*47*), the most dramatic example of which was an outbreak in a zoo in Paris that caused the deaths of ≥2 humans and animals belonging to ≥10 different species (*43*,*48*). The outbreak spread from the Paris Zoological Park to the menagerie at the Paris Botanical Gardens and equestrian clubs across France. *B. pseudomallei* was isolated from horse manure in multiple gardens and from petri dishes placed near manure, suggesting aerosolization. Movement of horses for races contributed to the outbreak.

Animal importation and migratory birds are possible modes by which ST562 could have arrived in Darwin. In the lagoon hotspot, 2 facilities that housed imported animals were the sites of 3 cases in animals of melioidosis caused by *B. pseudomallei* ST562. A horse racetrack and multiple equestrian clubs are also in the creek and lagoon hotspots. Both hotspots are habitats for water birds, many of which migrate to the region every year through Asia's great flyways (*49*) and which could have carried *B. pseudomallei* ST562 to Darwin from Asia.

Although phylogenetic analysis confirms a single introduction event of Asian origin, how ST562 spread into northern Australia remains unknown. ST562 is now one of the most common *B. pseudomallei* STs in humans in urban Darwin. However, this ST rarely is isolated from the environment, including at sites associated with outbreaks. Further focused environmental sampling at key sites will help clarify ST562 epidemiology in northern Australia. The expanding capacity for genomic sequencing of *B. pseudomallei* will probably increase awareness of the ongoing global and regional dispersal of this bacterium and consequent melioidosis cases in humans and animals.

Acknowledgments

We thank Glenda Harrington and Vanessa Rigas for field sampling and laboratory support and Derek Sarovich for *Burkholderia pseudomallei* genome curation. We are grateful to Rob Baird and staff at Territory Pathology, Darwin, for clinical isolates and to Suresh Benedict and staff at Berrimah Veterinary Laboratory, Darwin, for animal isolates. We also thank Xiao Zheng, Ya-Lei Chen, and Jung-Jung Mu for sharing *B. pseudomallei* sequence type 562 isolates and genomes.

This research was funded by the Australian National Health and Medical Research Council (grant nos. 1046812, 1098337, and 1131932 [The HOT NORTH initiative]). E.M.M. was funded by a postgraduate scholarship from the Australian National Health and Medical Research Council (grant no. 1114696). E.P.P. was funded by an Advance Queensland fellowship (grant no. AQIRF0362018).

About the Author

Dr. Meumann is an infectious diseases physician at Royal Darwin Hospital, Darwin. Her research interests include genomic epidemiology of infectious diseases in northern Australia.

References

1. Currie BJ, Ward L, Cheng AC. The epidemiology and clinical spectrum of melioidosis: 540 cases from the 20 year Darwin prospective study. PLoS Negl Trop Dis. 2010;4:e900. https://doi.org/10.1371/journal.pntd.0000900
2. Chewapreecha C, Holden MT, Vehkala M, Välimäki N, Yang Z, Harris SR, et al. Global and regional dissemination and evolution of *Burkholderia pseudomallei*. Nat Microbiol. 2017;2:16263. https://doi.org/10.1038/nmicrobiol.2016.263
3. Limmathurotsakul D, Golding N, Dance DA, Messina JP, Pigott DM, Moyes CL, et al. Predicted global distribution of *Burkholderia pseudomallei* and burden of melioidosis. Nat Microbiol. 2016;1:15008. https://doi.org/10.1038/nmicrobiol.2015.8
4. Wiersinga WJ, Currie BJ, Peacock SJ. Melioidosis. N Engl J Med. 2012;367:1035–44. https://doi.org/10.1056/NEJMra1204699
5. Pearson T, Giffard P, Beckstrom-Sternberg S, Auerbach R, Hornstra H, Tuanyok A, et al. Phylogeographic reconstruction of a bacterial species with high levels of lateral gene transfer. BMC Biol. 2009;7:78. https://doi.org/10.1186/1741-7007-7-78
6. Sarovich DS, Garin B, De Smet B, Kaestli M, Mayo M, Vandamme P, et al. Phylogenomic analysis reveals an Asian origin for African *Burkholderia pseudomallei* and further supports melioidosis endemicity in Africa. MSphere. 2016;1:e00089–15. https://doi.org/10.1128/mSphere.00089-15
7. De Smet B, Sarovich DS, Price EP, Mayo M, Theobald V, Kham C, et al. Whole-genome sequencing confirms that *Burkholderia pseudomallei* multilocus sequence types common to both Cambodia and Australia are due to homoplasy. J Clin Microbiol. 2015;53:323–6. https://doi.org/10.1128/JCM.02574-14
8. Price EP, Sarovich DS, Smith EJ, MacHunter B, Harrington G, Theobald V, et al. Unprecedented melioidosis cases in Northern Australia caused by an Asian *Burkholderia pseudomallei* strain identified by using large-scale comparative genomics. Appl Environ Microbiol. 2016;82:954–63. https://doi.org/10.1128/AEM.03013-15
9. Zimmermann RE, Ribolzi O, Pierret A, Rattanavong S, Robinson MT, Newton PN, et al. Rivers as carriers and potential sentinels for *Burkholderia pseudomallei* in Laos. Sci Rep. 2018;8:8674. https://doi.org/10.1038/s41598-018-26684-y
10. Ribolzi O, Rochelle-Newall E, Dittrich S, Auda Y, Newton PN, Rattanavong S, et al. Land use and soil type determine the presence of the pathogen *Burkholderia pseudomallei* in tropical rivers. Environ Sci Pollut Res Int. 2016;23:7828–39. https://doi.org/10.1007/s11356-015-5943-z
11. McRobb E, Kaestli M, Price EP, Sarovich DS, Mayo M, Warner J, et al. Distribution of *Burkholderia pseudomallei* in northern Australia, a land of diversity. Appl Environ Microbiol. 2014;80:3463–8. https://doi.org/10.1128/AEM.00128-14
12. Chapple SNJ, Price EP, Sarovich DS, McRobb E, Mayo M, Kaestli M, et al. *Burkholderia pseudomallei* genotype distribution in the Northern Territory, Australia. Am J Trop Med Hyg. 2016;94:68–72. https://doi.org/10.4269/ajtmh.15-0627
13. Aziz A, Sarovich DS, Harris TM, Kaestli M, McRobb E, Mayo M, et al. Suspected cases of intracontinental *Burkholderia pseudomallei* sequence type homoplasy resolved using whole-genome sequencing. Microb Genom. 2017;3:3. https://doi.org/10.1099/mgen.0.000139
14. Rachlin A, Kleinecke M, Kaestli M, Mayo M, Webb JR, Rigas V, et al. A cluster of melioidosis infections in hatchling saltwater crocodiles (*Crocodylus porosus*) resolved using genome-wide comparison of a common north Australian strain of *Burkholderia pseudomallei*. Microb Genom. 2019;5:5. https://doi.org/10.1099/mgen.0.000288
15. Rachlin A, Mayo M, Webb JR, Kleinecke M, Rigas V, Harrington G, et al. Whole-genome sequencing of *Burkholderia pseudomallei* from an urban melioidosis hot spot reveals a fine-scale population structure and localised spatial clustering in the environment. Sci Rep. 2020;10:5443. https://doi.org/10.1038/s41598-020-62300-8
16. Godoy D, Randle G, Simpson AJ, Aanensen DM, Pitt TL, Kinoshita R, et al. Multilocus sequence typing and evolutionary relationships among the causative agents of melioidosis and glanders, *Burkholderia pseudomallei* and *Burkholderia mallei*. J Clin Microbiol. 2003;41:2068–79. https://doi.org/10.1128/JCM.41.5.2068-2079.2003
17. Song L, Yu Y, Feng L, He J, Wang T, Zhu H, et al. Draft genome sequence of *Burkholderia pseudomallei* strain 350105, isolated in Hainan, China, in 1976. Genome Announc. 2015;3:e01162–15. https://doi.org/10.1128/genomeA.01162-15
18. Daligault HE, Davenport KW, Minogue TD, Bishop-Lilly KA, Broomall SM, Bruce DC, et al. Whole-genome assemblies of 56 *Burkholderia* species. Genome Announc. 2014;2:2.
19. Holden MT, Titball RW, Peacock SJ, Cerdeño-Tárraga AM, Atkins T, Crossman LC, et al. Genomic plasticity of the causative agent of melioidosis, *Burkholderia pseudomallei*. Proc Natl Acad Sci U S A. 2004;101:14240–5. https://doi.org/10.1073/pnas.0403302101
20. Nguyen LT, Schmidt HA, von Haeseler A, Minh BQ. IQ-TREE: a fast and effective stochastic algorithm for estimating maximum-likelihood phylogenies. Mol Biol Evol. 2015;32:268–74. https://doi.org/10.1093/molbev/msu300
21. Croucher NJ, Page AJ, Connor TR, Delaney AJ, Keane JA, Bentley SD, et al. Rapid phylogenetic analysis of large samples of recombinant bacterial whole genome sequences using Gubbins. Nucleic Acids Res. 2015;43:e15. https://doi.org/10.1093/nar/gku1196
22. Bouckaert R, Heled J, Kühnert D, Vaughan T, Wu CH, Xie D, et al. BEAST 2: a software platform for Bayesian evolutionary analysis. PLOS Comput Biol. 2014;10:e1003537. https://doi.org/10.1371/journal.pcbi.1003537
23. Rachlin A, Shilton C, Webb JR, Mayo M, Kaestli M, Kleinecke M, et al. Melioidosis fatalities in captive slender-tailed meerkats (*Suricata suricatta*): combining epidemiology, pathology and whole-genome sequencing supports variable mechanisms of transmission with one health implications. BMC Vet Res. 2019;15:458. https://doi.org/10.1186/s12917-019-2198-9
24. Currie BJ, Price EP, Mayo M, Kaestli M, Theobald V, Harrington I, et al. Use of whole-genome sequencing to link

Burkholderia pseudomallei from air sampling to mediastinal melioidosis, Australia. Emerg Infect Dis. 2015;21:2052–4. https://doi.org/10.3201/eid2111.141802
25. Sarovich DS, Ward L, Price EP, Mayo M, Pitman MC, Baird RW, et al. Recurrent melioidosis in the Darwin Prospective Melioidosis Study: improving therapies mean that relapse cases are now rare. J Clin Microbiol. 2014;52:650–3. https://doi.org/10.1128/JCM.02239-13
26. Parameswaran U, Baird RW, Ward LM, Currie BJ. Melioidosis at Royal Darwin Hospital in the big 2009–2010 wet season: comparison with the preceding 20 years. Med J Aust. 2012;196:345–8. https://doi.org/10.5694/mja11.11170
27. Currie BJ. Melioidosis: evolving concepts in epidemiology, pathogenesis, and treatment. Semin Respir Crit Care Med. 2015;36:111–25. https://doi.org/10.1055/s-0034-1398389
28. Viberg LT, Sarovich DS, Kidd TJ, Geake JB, Bell SC, Currie BJ, et al. Within-host evolution of *Burkholderia pseudomallei* during chronic infection of seven Australasian cystic fibrosis patients. MBio. 2017;8:e00356–17. https://doi.org/10.1128/mBio.00356-17
29. Pearson T, Sahl JW, Hepp CM, Handady K, Hornstra H, Vazquez AJ, et al. Pathogen to commensal? Longitudinal within-host population dynamics, evolution, and adaptation during a chronic >16-year *Burkholderia pseudomallei* infection. PLoS Pathog. 2020;16:e1008298. https://doi.org/10.1371/journal.ppat.1008298
30. Inglis TJ, Sagripanti JL. Environmental factors that affect the survival and persistence of *Burkholderia pseudomallei*. Appl Environ Microbiol. 2006;72:6865–75. https://doi.org/10.1128/AEM.01036-06
31. Chapple SNJ, Sarovich DS, Holden MTG, Peacock SJ, Buller N, Golledge C, et al. Whole-genome sequencing of a quarter-century melioidosis outbreak in temperate Australia uncovers a region of low-prevalence endemicity. Microb Genom. 2016;2:e000067. https://doi.org/10.1099/mgen.0.000067
32. Limmathurotsakul D, Holden MT, Coupland P, Price EP, Chantratita N, Wuthiekanun V, et al. Microevolution of *Burkholderia pseudomallei* during an acute infection. J Clin Microbiol. 2014;52:3418–21. https://doi.org/10.1128/JCM.01219-14
33. McRobb E, Sarovich DS, Price EP, Kaestli M, Mayo M, Keim P, et al. Tracing melioidosis back to the source: using whole-genome sequencing to investigate an outbreak originating from a contaminated domestic water supply. J Clin Microbiol. 2015;53:1144–8. https://doi.org/10.1128/JCM.03453-14
34. Sarovich DS, Chapple SNJ, Price EP, Mayo M, Holden MTG, Peacock SJ, et al. Whole-genome sequencing to investigate a non-clonal melioidosis cluster on a remote Australian island. Microb Genom. 2017;3:e000117. https://doi.org/10.1099/mgen.0.000117
35. Sagripanti JL, Levy A, Robertson J, Merritt A, Inglis TJ. Inactivation of virulent *Burkholderia pseudomallei* by sunlight. Photochem Photobiol. 2009;85:978–86. https://doi.org/10.1111/j.1751-1097.2008.00518.x
36. Chen YL, Yen YC, Yang CY, Lee MS, Ho CK, Mena KD, et al. The concentrations of ambient *Burkholderia pseudomallei* during typhoon season in endemic area of melioidosis in Taiwan. PLoS Negl Trop Dis. 2014;8:e2877. https://doi.org/10.1371/journal.pntd.0002877
37. Hall CM, Jaramillo S, Jimenez R, Stone NE, Centner H, Busch JD, et al. *Burkholderia pseudomallei*, the causative agent of melioidosis, is rare but ecologically established and widely dispersed in the environment in Puerto Rico. PLoS Negl Trop Dis. 2019;13:e0007727. https://doi.org/10.1371/journal.pntd.0007727
38. Merritt AJ, Inglis TJJ. The role of climate in the epidemiology of melioidosis. Curr Trop Med Rep. 2017;4:185–91. https://doi.org/10.1007/s40475-017-0124-4
39. Kaestli M, Grist EPM, Ward L, Hill A, Mayo M, Currie BJ. The association of melioidosis with climatic factors in Darwin, Australia: a 23-year time-series analysis. J Infect. 2016;72:687–97. https://doi.org/10.1016/j.jinf.2016.02.015
40. Chen PS, Chen YS, Lin HH, Liu PJ, Ni WF, Hsueh PT, et al. Airborne transmission of melioidosis to humans from environmental aerosols contaminated with *B. pseudomallei*. PLoS Negl Trop Dis. 2015;9:e0003834. https://doi.org/10.1371/journal.pntd.0003834
41. Wuthiekanun V, Suputtamongkol Y, Simpson AJ, Kanaphun P, White NJ. Value of throat swab in diagnosis of melioidosis. J Clin Microbiol. 2001;39:3801–2. https://doi.org/10.1128/JCM.39.10.3801-3802.2001
42. Höger AC, Mayo M, Price EP, Theobald V, Harrington G, Machunter B, et al. The melioidosis agent *Burkholderia pseudomallei* and related opportunistic pathogens detected in faecal matter of wildlife and livestock in northern Australia. Epidemiol Infect. 2016;144:1924–32. https://doi.org/10.1017/S0950268816000285
43. Mollaret HH. "The case of the garden of plants" or how melioidosis appeared in France [in French]. Med Mal Infect. 1988;18:643–54. https://doi.org/10.1016/S0399-077X(88)80175-6
44. Hampton V, Kaestli M, Mayo M, Choy JL, Harrington G, Richardson L, et al. Melioidosis in birds and *Burkholderia pseudomallei* dispersal, Australia. Emerg Infect Dis. 2011;17:1310–2. https://doi.org/10.3201/eid1707.100707
45. Kaestli M, Mayo M, Harrington G, Ward L, Watt F, Hill JV, et al. Landscape changes influence the occurrence of the melioidosis bacterium *Burkholderia pseudomallei* in soil in northern Australia. PLoS Negl Trop Dis. 2009;3:e364. https://doi.org/10.1371/journal.pntd.0000364
46. Golledge CL, Chin WS, Tribe AE, Condon RJ, Ashdown LR. A case of human melioidosis originating in south-west Western Australia. Med J Aust. 1992;157:332–4. https://doi.org/10.5694/j.1326-5377.1992.tb137192.x
47. Dance DA, King C, Aucken H, Knott CD, West PG, Pitt TL. An outbreak of melioidosis in imported primates in Britain. Vet Rec. 1992;130:525–9. https://doi.org/10.1136/vr.130.24.525
48. Galimand M, Dodin A. Update on melioidosis in the world. Bull Soc Pathol Exot. 1982;75:375–83.
49. Sitters H, Minton C, Collins P, Etheridge B, Hassell C, O'Connor F. Extraordinary numbers of oriental pratincoles in NW Australia. Wader Study Group Bulletin. 2004;103:26–31.

Address for correspondence: Ella M. Meumann, Menzies School of Health Research, PO Box 41096, Casuarina, NT 0811, Australia; email: ella.meumann@menzies.edu.au

Histopathological Characterization of Cases of Spontaneous Fatal Feline Severe Fever with Thrombocytopenia Syndrome, Japan

Yusuke Sakai, Yuko Kuwabara, Keita Ishijima,[1] Saya Kagimoto, Serina Mura, Kango Tatemoto,[1] Ryusei Kuwata,[2] Kenzo Yonemitsu,[1] Shohei Minami, Yudai Kuroda,[1] Kenji Baba, Masaru Okuda, Hiroshi Shimoda, Masashi Sakurai, Masahiro Morimoto, Ken Maeda[1]

Severe fever with thrombocytopenia syndrome (SFTS) is an emerging tickborne infectious disease caused by SFTS virus (SFTSV). We report 7 cases of spontaneous fatal SFTS in felines. Necropsies revealed characteristic lesions, including necrotizing lymphadenitis in 5 cases and necrotizing splenitis and SFTSV-positive blastic lymphocytes in all cases. We detected hemorrhagic lesions in the gastrointestinal tract in 6 cases and lungs in 3 cases, suggesting a more severe clinical course of SFTS in felids than in humans. We noted necrotic or ulcerative foci in the gastrointestinal tract in 3 cases, the lung in 2 cases, and the liver in 4 cases. We clarified that blastic lymphocytes are predominant targets of SFTSV and involved in induction of necrotic foci. We also found that thymic epithelial cells were additional targets of SFTSV. These results provide insights for diagnosing feline SFTS during pathological examination and demonstrate the similarity of feline and human SFTS cases.

Severe fever with thrombocytopenia syndrome (SFTS) is an emerging infectious disease characterized by acute onset of high fever, hemorrhagic tendency, gastrointestinal and neurologic symptoms, thrombocytopenia, and leukocytopenia (*1*–*4*). The causative agent of SFTS is a novel *Dabie bandavirus*, SFTS virus (SFTSV), of the family *Phenuiviridae* (*5*). On the basis of epidemiologic evidence, SFTS is classified as a tickborne disease, and the main reservoir and vector involving human infection is thought to be the *Haemaphysalis longicornis* tick (*6*,*7*). In addition, various species of domestic and wild mammals, including goats, sheep, cattle, pigs, dogs, cats, boars, and deer, have been found to harbor SFTSV genomic RNA or SFTSV antibodies (*8*–*10*). These data demonstrate the infectivity of SFTSV in these animal species and circulation of SFTSV between ticks and animals in nature. Reported cases of SFTS in cheetahs and domestic cats have shown that nonhuman mammalian species can develop fatal disease similar to human SFTS (*11*,*12*). Susceptibility of cats to SFTSV also was confirmed by experimental SFTSV infection in cats, which caused a high incidence of severe hemorrhagic fever (*13*). Analyses of these cases confirmed shedding of viral particles from saliva and feces (*11*,*13*), which can cause transmission of SFTSV from diseased animals to humans (*14*).

Analysis of animals with SFTSV infection can inform the pathogenesis of SFTS in humans. Experimental infection in wild type and α/β interferon receptor knockout mice, rhesus macaques (*Macaca mulatta*), and signal transducer and activator of transcription-2 knockout hamsters have been reported (*15*–*19*), but hepatitis and splenitis have been reproduced only in hamster models (*19*). However, hemorrhagic and necrotic lesions in the liver, spleen, intestines, and lymph nodes have been reported only in fatal SFTS cases in humans and experimentally infected felines (*13*,*20*–*22*). Investigations of disease in animals that mimics human SFTS is crucial for informing prevention of animal-to-human transmission and controlling virus transmission among animals and ticks. Analysis of fatal cases in felines can clarify the pathology of SFTS and inform STFS diagnosis in animals. We provide evidence of characteristic macroscopic and microscopic lesions collected from 7 cases of spontaneous fatal SFTS in felines.

Authors affiliation: Yamaguchi University, Yamaguchi, Japan

DOI: https://doi.org/10.3201/eid2704.204148

[1]Current affiliation: National Institute of Infectious Diseases, Tokyo, Japan.

[2]Current affiliation: Okayama University of Science, Ehime, Japan.

Materials and Methods

Histology

We performed necropsies on 7 cats with SFTS symptoms, such as acute onset of thrombocytopenia, leukocytopenia, and lethargy (Table 1). We confirmed SFTSV infection by conventional reverse transcription PCR (RT-PCR) using 2 primer pairs targeting the small segment of the SFTSV genome (23). We collected and fixed tissue samples in 10% neutral buffered formalin and then processed the samples to create paraffin-embedded tissue sections. We cut tissue into sections 4-μm thick and stained sections with hematoxylin and eosin for histopathologic examination.

Immunohistochemistry

We subjected the 4-μm thick tissue sections to immunohistochemical staining. After deparaffinization, we performed antigen retrieval by incubating sections in 0.1% trypsin at 37°C for 20 min to obtain immunoglobulin (Ig) lambda chain; or by heating at 121°C for 5 min in pH 6.0 citrate buffer for SFTSV and CD3 staining; or pH 9.0 Tris-EDTA buffer for CD79a and Ki67 staining. After washing with phosphate-buffered saline (PBS), we inactivated endogenous peroxidase by immersion in 3% hydrogen peroxide in PBS. After treatment with 5% bovine serum albumin in PBS for 30 min, we incubated the sections with rabbit polyclonal anti-SFTSV antibody (diluted 1:1,000; gift from Shigeru Morikawa, Okayama University of Science, Okayama, Japan); FLEX Polyclonal Rabbit Anti-Human CD3 Ready-to-Use antibody (Dako, https://www.agilent.com); Monoclonal Mouse Anti-Human CD79a Antibody Clone HM57 (diluted 1:50; Dako); Mouse Monoclonal Anti-Ki67 Clone MIB-1 (diluted 1:1,000; eBioscience, https://www.thermofisher.com); or Polyclonal Rabbit Anti-Human Ig Lambda Light Chains (diluted 1:100; Dako). After washing with PBS, we incubated the sections with EnVision+/HRP Rabbit (Dako) horseradish peroxidase (HRP)–labeled polymer anti-rabbit or EnVision+/HRP Mouse (Dako) HRP-labeled polymer anti-mouse. We then visualized positive signals by peroxidase-diaminobenzidine reaction, and counterstained sections with hematoxylin stain.

Immunofluorescence

We performed double immunofluorescence labeling with cytokeratin-SFTSV and CD204-SFTSV on 4-μm thick tissue sections. We performed heat-mediated antigen retrieval for cytokeratin-SFTSV in pH 6.0 citrate buffer and for CD204-SFTSV antigen pH 9.0 Tris-EDTA buffer. After washing with PBS and blocking with 5% bovine serum albumin, we incubated the sections for 1 h at room temperature with a mixture of rabbit polyclonal anti-SFTSV antibody (diluted 1:1,000; TransGenic Inc., https://www.transgenic.co.jp) and mouse monoclonal anti-CD204 (diluted 1:400; TransGenic Inc.) or mouse monoclonal anti-cytokeratin clone AE1/AE3 (diluted 1:200; Dako). After washing with PBS, we incubated the sections in a mixture of Alexa Fluor 488 anti-rabbit IgG (diluted 1:400; Abcam, https://www.abcam.com), Alexa Fluor 594 anti-mouse IgG (diluted 1:400; Abcam), and DAPI (Dojindo, https://www.dojindo.com). We then analyzed the tissue sections by using an LSM 710 (Leica, https://www.leicabiosystems.com) confocal microscope.

Results

Gross Findings

Among the 7 cats with SFTS, gross lesions typically were characterized by changes in the lymphoid organs and hemorrhage (Table 2). In all the cases, we

Table 1. Clinicopathological findings in 7 cats with fatal severe fever with thrombocytopenia syndrome, Japan*

	Case no.						
Clinical findings	1	2	3	4	5	6	7
Clinical signs							
Anorexia	Y	Y	Y	Y	Y	Y	Y
Lethargy	Y	Y	Y	Y	Y	Y	Y
Neurologic signs	N	N	N	Y	N	N	N
Vomiting	N	Y	N	N	N	Y	N
Body temperature, °C	39.4	NA	NA	NA	39.3	39.9	39
Erythrocytes, 10^4 cells/μL	546	688	NA	364	718	820	593
Leukocytes, cells/μL	3,080	800	3,000	190	700	2,500	1,290
Platelets, cells/μL	38,000	7,000	0	0	<11,000	52,000	0
ALT, IU/L	105	NA	476	141	331	NA	58
AST, IU/L	51	NA	>1,000	4	1,010	NA	NA
ALP, IU/L	188	NA	NA	NA	NA	NA	<10
Total bilirubin, mg/dL	4.4	5.8	4.8	5.7	NA	NA	9.3
CPK, IU/L	NA	373	>2,000	>2,000	1,444	NA	NA

*ALP, alkaline phosphatase; ALT, alanine aminotransferase; AST, aspartate aminotransferase; CPK, creatine phosphokinase; NA, not available.

noted red enlarged lymph nodes from various regions. Although splenomegaly was unclear to mild, we noticed enlarged follicles appearing as multiple white spots in the spleen (Figure 1, panel A) in all cats. We detected hemorrhagic lesions in the gastrointestinal tract in 6 cats (Figure 1, panel B) and in the tracheal region of the lungs in 3 cats (Figure 1, panel C). In 3 cats, gastrointestinal lesions resulted in grossly obvious ulcers (Figure 1, panel D). Jaundice was detected in 5 cats.

Table 2. Gross lesions in 7 cats with fatal severe fever with thrombocytopenia syndrome, Japan

Lesions	Cases, no. (%)
Enteric hemorrhage	6 (85.7)
Gastrointestinal ulcer	3 (42.8)
Pulmonary hemorrhage	3 (42.8)
Jaundice	5 (71.4)

Lymphatic System Lesions

Histologically, characteristic SFTS lesions were observed in the lymphoid organs, such as the lymph nodes, spleen, and Peyer's patches. We noted lesions in the collected lymph nodes in all 7 cats (Table 3). In the cortex of SFTSV-affected lymph nodes, we observed an accumulation of the large blastic lymphocytes, as those described in a human case (*21*). The blastic lymphocyte cells were morphologically characterized by large, clear irregular-shaped nuclei with prominent central nucleoli and were similar to the morphology of the immature activated-B cells, called immunoblasts (Figure 2, panels A, B). Compatible with immunoblast-like cell morphology, these cells were considered cells of the B cell lineage because they were positive for CD79a expression (Figure 2, panel C). Immunohistochemistry also revealed that SFTSV antigens were exclusively detected in these blastic lymphocytes and SFTSV-positive blastic lymphocytes distributed in the cortex and paracortex area surrounding lymphoid follicles (Figure 2, panels D, E). Regardless of enlargement, some lymph nodes had neither SFTSV-positive cells nor necrotic lesions and were simply diagnosed as hyperplastic lymph nodes (Table 3; Figure 2, panel F). In some lymph nodes, the lesions proceeded to necrotizing lymphadenitis with SFTSV-positive blastic lymphocytes (Figure 2, panel G). In all cases, we detected SFTSV-positive blastic lymphocytes and necrotic foci in the spleen, mainly in the follicular area (Figure 2, panel H). We collected the thymus glands from 4 cats and observed infiltration of SFTSV-positive blastic lymphocytes mainly in the cortices of all specimens. Hemorrhagic and necrotic lesions also were observed in the thymus glands. As reported in humans (*20*–*22*), we observed numerous hemophagocytic macrophages in the lymphoid organs of all cases.

Intestinal Tract Lesions

We noted SFTSV-positive blastic lymphocytes in the intestinal tract in all cases (Figure 3), mainly in the Peyer's patches, the localized lymphoid follicular

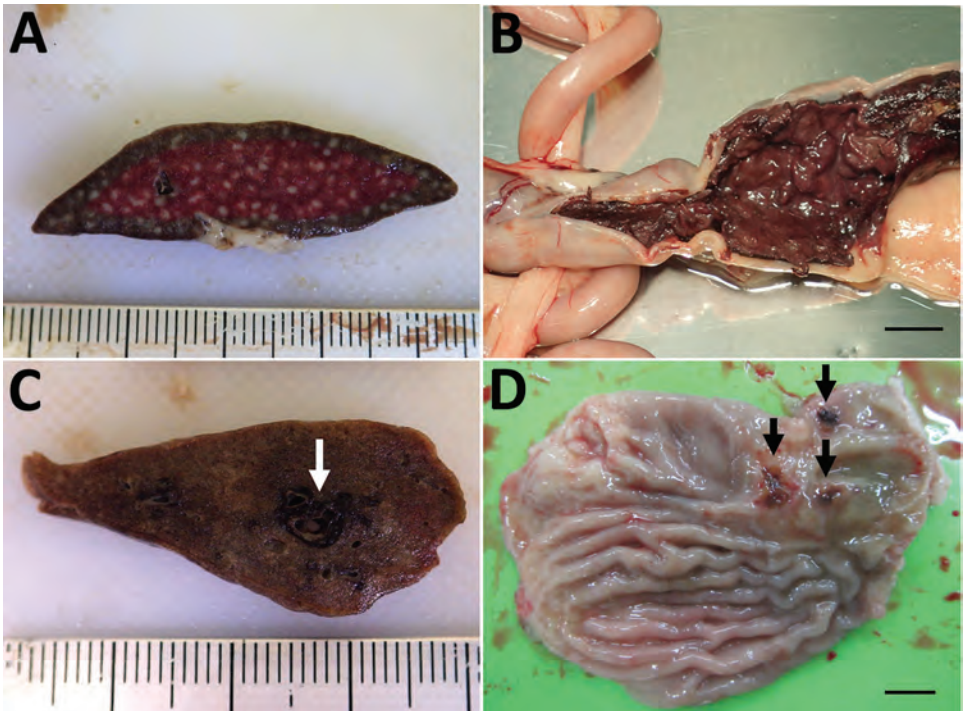

Figure 1. Gross pathology of lesions from cats with fatal severe fever with thrombocytopenia syndrome, Japan. A) Enlarged follicles (white spots) in the spleen. Ruler represents centimeters. B) Hemorrhage in the colon. Scale bar indicates 1 cm. C) Hemorrhage in the lung; white arrow indicates pulmonary hemorrhage around the trachea. Ruler represents centimeters. D) Gastrointestinal ulcers (black arrows) were also seen in some cases. Scale bar indicates 1 cm.

Table 3. Lesions in the lymphatic system from 7 cats with fatal severe fever with thrombocytopenia syndrome, Japan*

	Case no., n = no. lymph nodes assessed						
Lesions	1, n = 4	2, n = 1	3, n = 4	4, n = 9	5, n = 7	6, n = 4	7, n = 6
Hyperplasia without SFTSV-positive cells	0	0	3	0	2	2	0
SFTSV-positive blastic lymphocytes	3	1	1	6	2	1	2
Necrotizing lymphadenitis	1	0	0	3	3	1	4

*SFTSV, severe fever with thrombocytopenia syndrome virus.

structure in the intestinal submucosa; some of these cells infiltrated the lamina propria (Figure 3, panels A, B). We observed infiltration of these cells in all hemorrhage lesions and ulcers (Figure 3, panels C, D), suggesting a relationship between blastic lymphocytes and lesions.

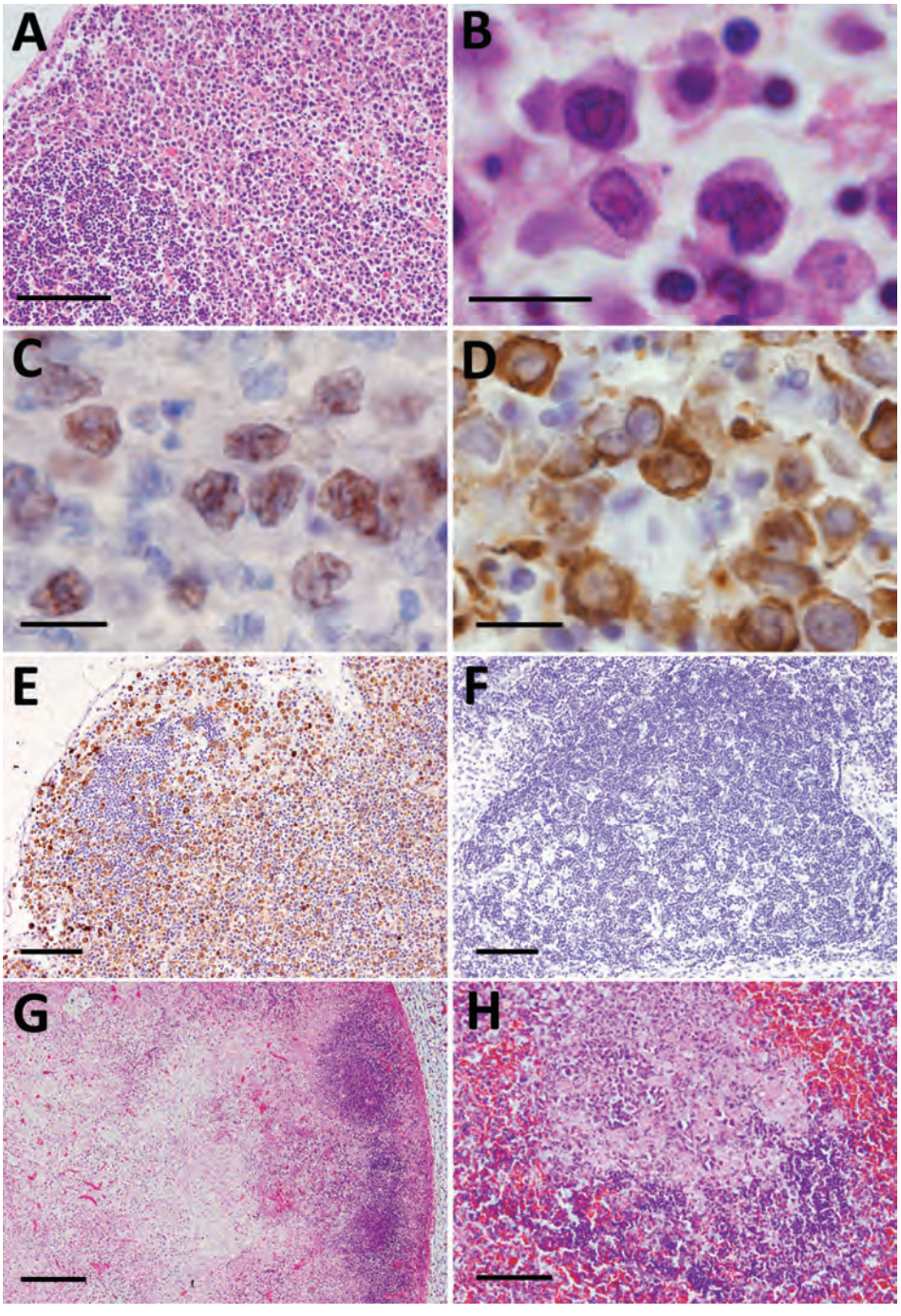

Figure 2. Histopathological lesions in the lymphoid organs from fatal cases of severe fever with thrombocytopenia syndrome (SFTS) in cats, Japan. A) Hematoxylin & eosin (HE)–stained lymph node demonstrating accumulation of blastic lymphocytes around the lymphoid follicle. Scale bar indicates 100 µm. B) HE-stained blastic lymphocytes from the lymph nodes demonstrating highly pleomorphic cells with large clear nuclei and prominent nucleoli, resembling immunoblasts. Scale bar indicates 10 µm. C, D) CD79a-stained (C) and immunohistochemistry-stained (D) blastic lymphocytes from the lymph nodes. Scale bar indicates 10 µm. E) Lymph node stained by immunohistochemistry revealing SFTS virus–positive blastic lymphocytes distributed around the follicle. Scale ar indicates 100 µm. F) Immunohistochemistry-stained hyperplastic lymph node demonstrating no SFTSV-positive cells or necrotic foci. Scale bar indicates 100 µm. G) Necrotic lymphadenitis in HE-stained lymph node. Scale bar indicates 200 µm. H) HE-stained spleen demonstrating necrotic lesions in the splenic follicle. Scale bar indicates 50 µm.

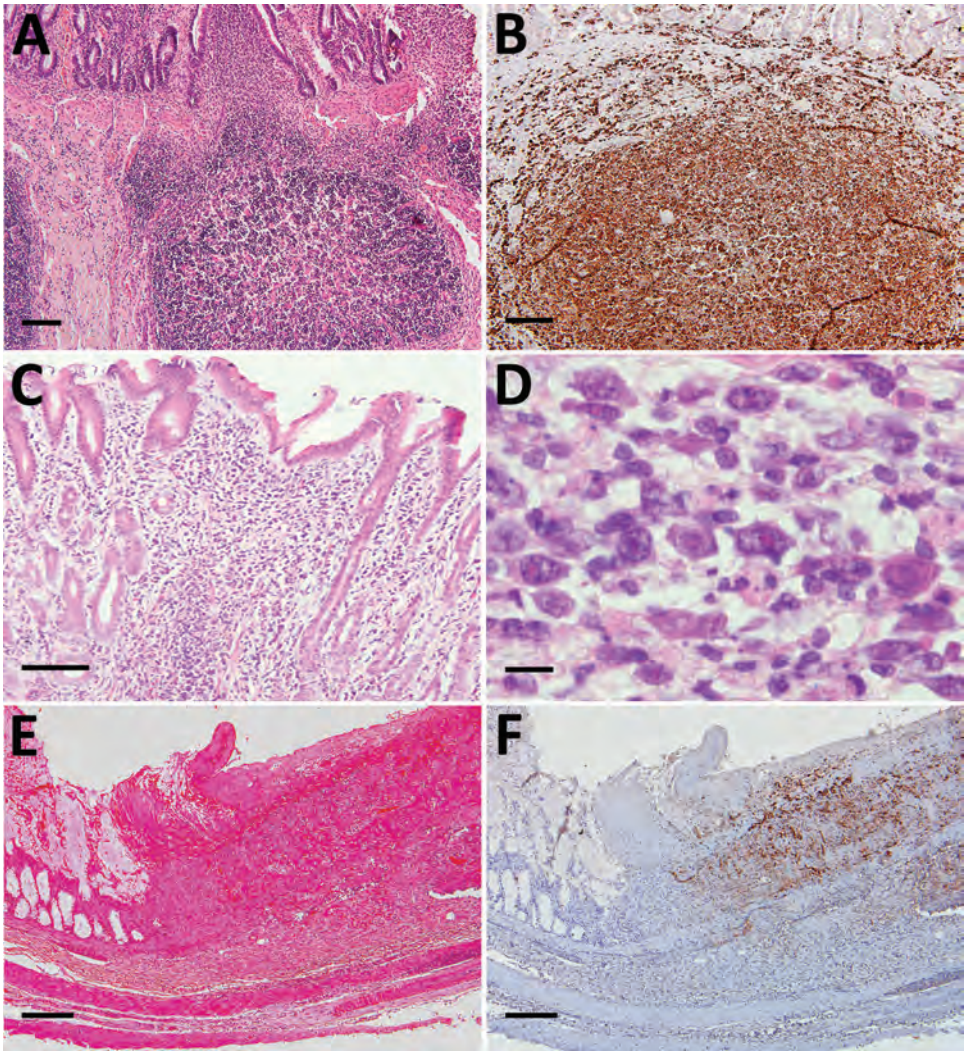

Figure 3. Histopathological lesions in the intestinal tracts from fatal cases of severe fever with thrombocytopenia syndrome (SFTS) in cats, Japan. A, B) Hematoxylin & eosin (HE)–stained (A) and immunohistochemistry-stained (B) ileum sections demonstrating enlargement of Peyer's patch and accumulation of SFTSV-positive blastic lymphocytes. Scale bars indicates 100 μm. C) HE-stained colon sections demonstrating infiltration of lymphocytes into the lamina propria. Scale bar indicates 100 μm. D) High power magnification of panel C demonstrating the infiltrating lymphocytes were blastic lymphocytes. Scale bar indicates 10 μm. E, F) HE stained (E) and immunohistochemistry-stained (F) ulcerative lesions in the cecum. Scale bars indicate 200 μm.

Liver and Lung Lesions

In the livers from 3 cats, we noted formation of small necrotic foci (Figure 4, panel A). The necrotic lesions always were surrounded by SFTSV-positive blastic lymphocytes (Figure 4, panel B), but the cells usually were distributed in the portal area. We also found bile pigmentation and hemophagocytic macrophages in the liver.

Feline SFTS pulmonary lesions consisted of hemorrhage in 3 cases and formation of necrotic foci in the interstitial tissues surrounding the trachea in 2 cases (Figure 4, panel C). Like hepatic necrotic foci, the pulmonary necrotic foci we observed in these cases also showed SFTSV-positive blastic lymphocytes (Figure 4, panel D).

SFTSV-Positive Blastic Lymphocyte Characterization

Immunohistochemistry revealed that SFTSV-positive signals were limited to the blastic lymphocytes, and these were of B cell lineage and expressed CD79a (Figure 2, panel C). We performed further characterization by using immunohistochemical stains against Ig lambda chain and Ki67. The results demonstrated that SFTSV-positive atypical lymphocytes expressed Ig lambda chain and Ki67 (Figure 4, panels E, F). Hence, we considered these cells plasmablasts, which are immature plasma cells retaining proliferation activities.

The presence of SFTSV antigens in macrophages has been reported (*15*,*24*). To investigate whether macrophages in our cases consisted of SFTSV-positive cells along with B cells, we performed double immunofluorescence analysis of the macrophage markers CD204 and SFTSV. The results demonstrated that SFTSV-positive cells were not CD204-positive (Figure 5).

SFTSV-Positive Cells in the Thymus

In addition to blastic lymphocytes, we found SFTSV-positive cells with spindle-to-polygonal morphology

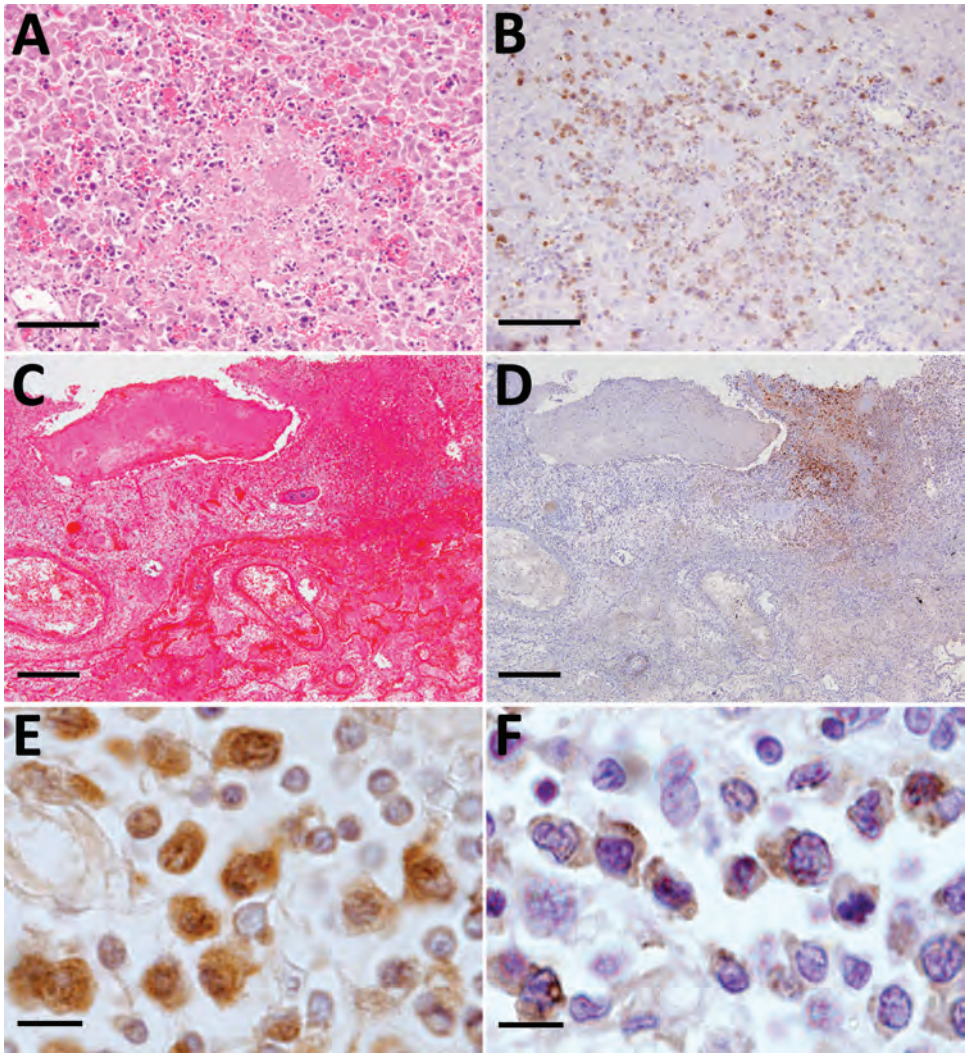

Figure 4. Necrotic foci in the liver and lung from fatal cases of severe fever with thrombocytopenia syndrome (SFTS) in cats, Japan. A, B) Hematoxylin & eosin (HE)–stained (A) and immunohistochemistry-stained (B) liver sections demonstrating SFTS virus–positive blastic lymphocytes in the necrotic foci. Scale bars indicate 100 μm. C, D) HE-stained (C) and immunohistochemistry-stained (D) lung sections demonstrating lymphocytes in the necrotic foci from the lungs. Scale bars indicates 200 μm. E, F) Ki67 (E) and Ig lambda chain (F) immunohistochemistry positively staining blastic lymphocytes. Scale bars indicates 10 μm.

in the thymus gland. Double immunofluorescence analysis of SFTSV and cytokeratin revealed that these cells were thymic epithelial cells (Figure 6).

Discussion

We analyzed the pathological changes in 7 fatal cases of SFTS in domestic felids. We detected characteristic lesions in the lymphoid organs, including the lymph nodes and spleen. We observed gross enlargement and hemorrhage of multiple lymph nodes and formation of white spots in the spleen in all 7 cases (Figure 1, panel D). Because these findings are highly suggestive of but not specific for feline SFTS, additional cases with these findings should be further examined to confirm viral infection by testing, such as RT-PCR.

Similar to human cases (*20*–*22*), we frequently observed necrotic lymphadenitis in this study and found accumulation of SFTSV-positive atypical lymphocytes in all 7 cases (Table 2). In addition, all 7 cats had necrotic splenitis, similar to human SFTS cases (*20*,*21*). Therefore, lesions in the lymphoid organs, or accumulation of atypical B cells can be considered characteristic and highly specific for lesions in SFTS for both humans and felines. Furthermore, these lesions can be useful indicators of whether experimental infection in laboratory animals appropriately reproduces spontaneous SFTS. In fact, feline cases of experimental infection showed necrotic lymphadenitis and splenitis (*13*).

Although some reports have detected SFTSV antigens in macrophages, our study demonstrated that SFTSV-positive cells mostly were blastic lymphocytes (Figure 2, panels B–D; Figure 4, panels E, F). Immunofluorescence revealed that only punctate signals were detected in the macrophages (Figure 5). This result indicates that macrophages can phagocytose SFTSV but do not support SFTSV replication. Our findings also showed that SFTSV targets the cells of B-cell lineage

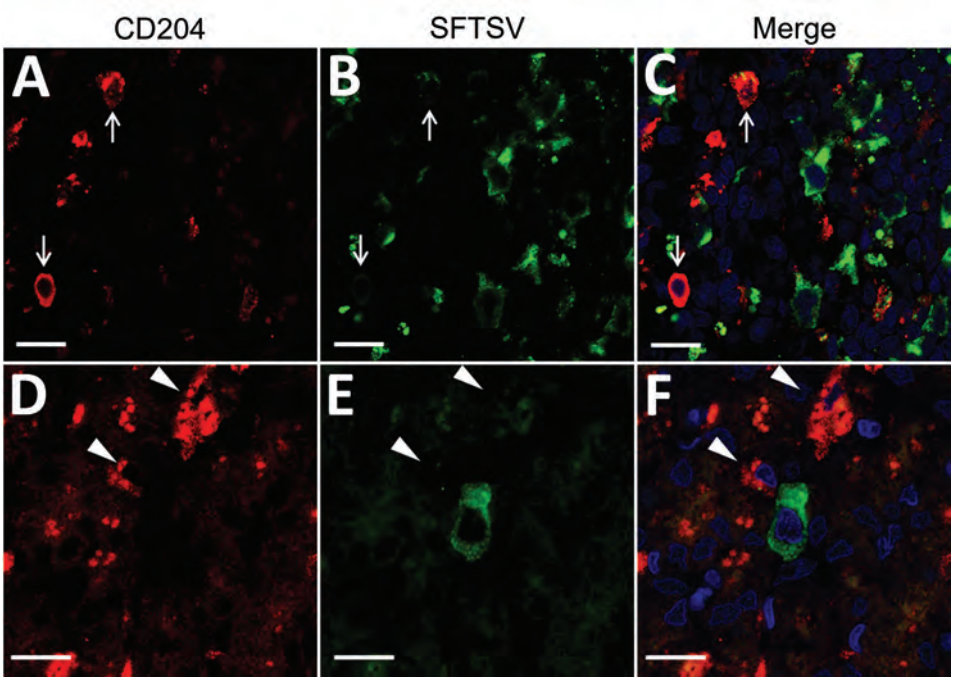

Figure 5. Double-labeling immunofluorescent staining of the lymph node (A–C) and the liver (D–F) from fatal cases severe fever with thrombocytopenia syndrome (SFTS) in cats, Japan. Red indicates signals of CD204. Green indicates signals of SFTS virus. Blue indicates nuclei labeled with DAPI. Arrows in panels A–C indicate CD204-positive macrophages in the lymph node. Arrows in panels D–F indicate CD204-positive kupffer cells in the liver. Scale bars indicate 10 μm.

and that plasmablasts were the predominant site of viral replication. Such tropism of SFTSV to plasmablast also has been reported in human cases and in vitro analysis clarified SFTSV targeted plasmablastic cell line, not B cell lymphoma cell lines (*25*). However, why large numbers of plasmablasts appeared and accumulated in the lymph nodes remains unclear. Dysregulated immunological response of plasmablasts to SFTSV infection and viral modulation of host-plasmablast dynamics are 2 possible causes of plasmablast accumulation in the lymph nodes. Furthermore, in all cases, we found SFTSV-positive blastic lymphocytes in and around the intestinal ulcerative lesions (Figure 3, panel F) and necrotic foci in the liver and lungs (Figure 4, panels A–D), suggesting a role of blastic lymphocytes in the pathogenesis of ulcers and necrotic lesions. Depositing of Ig in the necrotic foci and expression of death ligands in SFTSV-positive cells should be analyzed in future cases. Expression of cell death-inducing factors on SFTSV-positive blastic lymphocytes, such as self-reactive Ig and death ligands, could indicate a relationship between these cells and necrotic foci; further study is warranted. Our study demonstrated that the thymic epithelial cells can be another target of SFTSV. However, the significance of viral infection in the thymic epithelium is unclear.

Gastrointestinal manifestation is one of the clinical features of human SFTS (*1*–*4*). A lethal case of

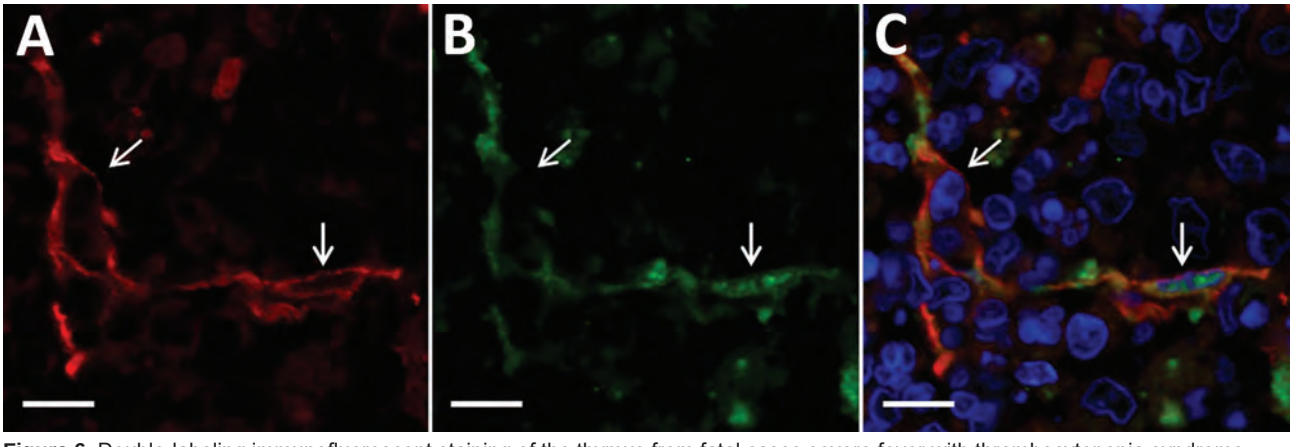

Figure 6. Double-labeling immunofluorescent staining of the thymus from fatal cases severe fever with thrombocytopenia syndrome (SFTS) in cats, Japan. Arrows indicate thymic epithelial cells. A, D) Red indicates signals of cytokeratin. B, E) Green indicates signals of SFTS virus. C, F) Blue indicates nuclei labeled with DAPI. Scale bars indicate 10 μm.

severe intestinal hemorrhage and another case of multiple gastrointestinal ulceration have been reported in humans (*20*,*26*). However, the incidence of these lesions is unclear because cases without obvious intestinal findings also have been reported (*21*). Experimental SFTSV infection in cats and our results have demonstrated a high rate of gastrointestinal hemorrhage (6/7 cases; Figure 1, panel A) and gastrointestinal ulcers (3/7 cases; Figure 3, panel E), which suggests that human and feline cases share a common pathogenesis and that feline cases show more severe gastrointestinal lesions than human cases (*13*). Pulmonary hemorrhage and necrotic foci also suggest the severity of feline SFTS. This severe pathogenesis in many tissues can cause high lethality, ≈70% (*27*), suggesting that feline SFTS is a typical lethal viral hemorrhagic fever.

Jaundice was frequently observed in our cases (Table 2) and in experimental infection in cats (*13*). Also, marked elevation of serum hepatic enzymes were detected in most cases (Table 1). However, in this study, morphologic lesions in the liver were only sporadic small necrotic foci, insufficient to cause systemic jaundice and marked elevation of serum hepatic enzymes. Microscopic lesions of the liver were also mild in human SFTS cases and in cats with experimental infection (*13*,*21*). These findings suggest microscopically undetectable hepatic damage or functional failure of the hepatobiliary system. Further analysis is needed to clarify the mechanism of liver damage in SFTS.

Other typical clinical manifestations of SFTS in humans include neurologic signs, thrombocytopenia, and leukocytopenia (*1*–*4*). Although neurologic signs were unclear in the cats in our study, thrombocytopenia and leukocytopenia were clinically detected. Analysis of the bone marrow and central nervous system in feline SFTS cases will help clarify pathogenesis.

Our study demonstrated typical lesions of spontaneous fatal cases of feline SFTS, consisting of similar pathological lesions and a more severe hemorrhagic tendency than in human SFTS cases. Information on disease in animals that mimics human SFTS can help prevent animal-to-human transmission. Thus, we believe feline models can be used to study the pathogenesis of SFTS.

Acknowledgments

We thank Shigeru Morikawa for providing the antibody against SFTSV. We also thank Shiho Hamada and Mari Shimizu for supporting the necropsy and laboratory work.

This research was supported by Japan Agency for Medical Research and Development under grant no. 20fk0108069.

About the Author

Dr. Sakai is an assistant professor in the Laboratory of Veterinary Pathology, Joint Faculty of Veterinary Medicine, Yamaguchi University. His research interests include the histopathology and molecular pathology of animal infectious diseases, especially zoonotic viral diseases.

References

1. Kato H, Yamagishi T, Shimada T, Matsui T, Shimojima M, Saijo M, et al.; SFTS Epidemiological Research Group–Japan. Epidemiological and clinical features of severe fever with thrombocytopenia syndrome in Japan, 2013–2014. PLoS One. 2016;11:e0165207. https://doi.org/10.1371/journal.pone.0165207
2. Kim YR, Yun Y, Bae SG, Park D, Kim S, Lee JM, et al. Severe fever with thrombocytopenia syndrome virus infection, South Korea, 2010. Emerg Infect Dis. 2018;24:2103–5. https://doi.org/10.3201/eid2411.170756
3. Li DX. Severe fever with thrombocytopenia syndrome: a newly discovered emerging infectious disease. Clin Microbiol Infect. 2015;21:614–20. https://doi.org/10.1016/j.cmi.2015.03.001
4. Saijo M. Pathophysiology of severe fever with thrombocytopenia syndrome and development of specific antiviral therapy. J Infect Chemother. 2018;24:773–81. https://doi.org/10.1016/j.jiac.2018.07.009
5. Yu XJ, Liang MF, Zhang SY, Liu Y, Li JD, Sun YL, et al. Fever with thrombocytopenia associated with a novel bunyavirus in China. N Engl J Med. 2011;364:1523–32. https://doi.org/10.1056/NEJMoa1010095
6. Robles NJC, Han HJ, Park SJ, Choi YK. Epidemiology of severe fever and thrombocytopenia syndrome virus infection and the need for therapeutics for the prevention. Clin Exp Vaccine Res. 2018;7:43–50. https://doi.org/10.7774/cevr.2018.7.1.43
7. Luo LM, Zhao L, Wen HL, Zhang ZT, Liu JW, Fang LZ, et al. *Haemaphysalis longicornis* ticks as reservoir and vector of severe fever with thrombocytopenia syndrome virus in China. Emerg Infect Dis. 2015;21:1770–6. https://doi.org/10.3201/eid2110.150126
8. Chen C, Li P, Li KF, Wang HL, Dai YX, Cheng X, et al. Animals as amplification hosts in the spread of severe fever with thrombocytopenia syndrome virus: A systematic review and meta-analysis. Int J Infect Dis. 2019;79:77–84. https://doi.org/10.1016/j.ijid.2018.11.017
9. Hwang J, Kang JG, Oh SS, Chae JB, Cho YK, Cho YS, et al. Molecular detection of severe fever with thrombocytopenia syndrome virus (SFTSV) in feral cats from Seoul, Korea. Ticks Tick Borne Dis. 2017;8:9–12. https://doi.org/10.1016/j.ttbdis.2016.08.005
10. Kimura T, Fukuma A, Shimojima M, Yamashita Y, Mizota F, Yamashita M, et al. Seroprevalence of severe fever with thrombocytopenia syndrome (SFTS) virus antibodies in humans and animals in Ehime prefecture, Japan, an endemic region of SFTS. J Infect Chemother. 2018;24:802–6. https://doi.org/10.1016/j.jiac.2018.06.007
11. Matsuno K, Nonoue N, Noda A, Kasajima N, Noguchi K, Takano A, et al. Fatal tickborne phlebovirus infection in captive cheetahs, Japan. Emerg Infect Dis. 2018;24:1726–9. https://doi.org/10.3201/eid2409.171667
12. Matsuu A, Momoi Y, Nishiguchi A, Noguchi K, Yabuki M, Hamakubo E, et al. Natural severe fever with thrombocytopenia syndrome virus infection in domestic cats

in Japan. Vet Microbiol. 2019;236:108346. https://doi.org/10.1016/j.vetmic.2019.06.019
13. Park ES, Shimojima M, Nagata N, Ami Y, Yoshikawa T, Iwata-Yoshikawa N, et al. Severe fever with thrombocytopenia syndrome phlebovirus causes lethal viral hemorrhagic fever in cats. Sci Rep. 2019;9:11990. https://doi.org/10.1038/s41598-019-48317-8
14. Kida K, Matsuoka Y, Shimoda T, Matsuoka H, Yamada H, Saito T, et al. A case of cat-to-human transmission of severe fever with thrombocytopenia syndrome virus. Jpn J Infect Dis. 2019;72:356–8. https://doi.org/10.7883/yoken.JJID.2018.526
15. Jin C, Liang M, Ning J, Gu W, Jiang H, Wu W, et al. Pathogenesis of emerging severe fever with thrombocytopenia syndrome virus in C57/BL6 mouse model. Proc Natl Acad Sci U S A. 2012;109:10053–8. https://doi.org/10.1073/pnas.1120246109
16. Liu Y, Wu B, Paessler S, Walker DH, Tesh RB, Yu XJ. The pathogenesis of severe fever with thrombocytopenia syndrome virus infection in alpha/beta interferon knockout mice: insights into the pathologic mechanisms of a new viral hemorrhagic fever. J Virol. 2014;88:1781–6. https://doi.org/10.1128/JVI.02277-13
17. Tani H, Fukuma A, Fukushi S, Taniguchi S, Yoshikawa T, Iwata-Yoshikawa N, et al. Efficacy of T-705 (favipiravir) in the treatment of infections with lethal severe fever with thrombocytopenia syndrome virus. MSphere. 2016;1: e00061–15. https://doi.org/10.1128/mSphere.00061-15
18. Jin C, Jiang H, Liang M, Han Y, Gu W, Zhang F, et al. SFTS virus infection in nonhuman primates. J Infect Dis. 2015;211:915–25. https://doi.org/10.1093/infdis/jiu564
19. Gowen BB, Westover JB, Miao J, Van Wettere AJ, Rigas JD, Hickerson BT, et al. Modeling severe fever with thrombocytopenia syndrome virus infection in golden Syrian hamsters: importance of STAT2 in preventing disease and effective treatment with favipiravir. J Virol. 2017;91: e01942–16. https://doi.org/10.1128/JVI.01942-16
20. Uehara N, Yano T, Ishihara A, Saijou M, Suzuki T. Fatal severe fever with thrombocytopenia syndrome: an autopsy case report. Intern Med. 2016;55:831–8. https://doi.org/10.2169/internalmedicine.55.5262
21. Hiraki T, Yoshimitsu M, Suzuki T, Goto Y, Higashi M, Yokoyama S, et al. Two autopsy cases of severe fever with thrombocytopenia syndrome (SFTS) in Japan: a pathognomonic histological feature and unique complication of SFTS. Pathol Int. 2014;64:569–75. https://doi.org/10.1111/pin.12207
22. Takahashi T, Maeda K, Suzuki T, Ishido A, Shigeoka T, Tominaga T, et al. The first identification and retrospective study of severe fever with thrombocytopenia syndrome in Japan. J Infect Dis. 2014;209:816–27. https://doi.org/10.1093/infdis/jit603
23. Yoshikawa T, Fukushi S, Tani H, Fukuma A, Taniguchi S, Toda S, et al. Sensitive and specific PCR systems for detection of both Chinese and Japanese severe fever with thrombocytopenia syndrome virus strains and prediction of patient survival based on viral load. J Clin Microbiol. 2014;52:3325–33. https://doi.org/10.1128/JCM.00742-14
24. Nakano A, Ogawa H, Nakanishi Y, Fujita H, Mahara F, Shiogama K, et al. Hemophagocytic lymphohistiocytosis in a fatal case of severe fever with thrombocytopenia syndrome. Intern Med. 2017;56:1597–602. https://doi.org/10.2169/internalmedicine.56.6904
25. Suzuki T, Sato Y, Sano K, Arashiro T, Katano H, Nakajima N, et al. Severe fever with thrombocytopenia syndrome virus targets B cells in lethal human infections. J Clin Invest. 2020;130:799–812. https://doi.org/10.1172/JCI129171
26. Kaneyuki S, Yoshikawa T, Tani H, Fukushi S, Taniguchi S, Fukuma A, et al. Ulcerative lesions with hemorrhage in a patient with severe fever with thrombocytopenia syndrome observed via upper gastrointestinal endoscopy. Jpn J Infect Dis. 2016;69:525–7. https://doi.org/10.7883/yoken.JJID.2015.404
27. Maeda K, Ishijima K, Tatemoto K, Sakai Y, Shimoda H, Takano A, et al. Animals that develop SFTS (mainly dogs and cats) [In Japanese]. Infect Agents Surveill Rep. 2019;40:118–9. https://www.niid.go.jp/niid/ja/allarticles/surveillance/2467-iasr/related-articles/related-articles-473/8988-473r06.html

Address for correspondence: Yusuke Sakai, Laboratory of Veterinary Pathology, Joint Faculty of Veterinary Medicine, Yamaguchi University, 1677-1 Yoshida, Yamaguchi-shi, Yamaguchi 753-8515, Japan; email: vsakai@yamaguchi-u.ac.jp

COVID-19–Associated Pulmonary Aspergillosis, March–August 2020

Jon Salmanton-García, Rosanne Sprute, Jannik Stemler, Michele Bartoletti, Damien Dupont, Maricela Valerio, Carolina Garcia-Vidal, Iker Falces-Romero, Marina Machado, Sofía de la Villa, Maria Schroeder, Irma Hoyo, Frank Hanses, Kennio Ferreira-Paim, Daniele Roberto Giacobbe, Jacques F. Meis, Jean-Pierre Gangneux, Azucena Rodríguez-Guardado, Spinello Antinori, Ertan Sal, Xhorxha Malaj, Danila Seidel, Oliver A. Cornely,[1] Philipp Koehler,[1] The FungiScope European Confederation of Medical Mycology/The International Society for Human and Animal Mycology Working Group[2]

Pneumonia caused by severe acute respiratory syndrome coronavirus 2 emerged in China at the end of 2019. Because of the severe immunomodulation and lymphocyte depletion caused by this virus and the subsequent administration of drugs directed at the immune system, we anticipated that patients might experience fungal superinfection. We collected data from 186 patients who had coronavirus disease–associated pulmonary aspergillosis (CAPA) worldwide during March–August 2020. Overall, 182 patients were admitted to the intensive care unit (ICU), including 180 with acute respiratory distress syndrome and 175 who received mechanical ventilation. CAPA was diagnosed a median of 10 days after coronavirus disease diagnosis. *Aspergillus fumigatus* was identified in 80.3% of patient cultures, 4 of which were azole-resistant. Most (52.7%) patients received voriconazole. In total, 52.2% of patients died; of the deaths, 33.0% were attributed to CAPA. We found that the cumulative incidence of CAPA in the ICU ranged from 1.0% to 39.1%.

Cases of pneumonia caused by severe acute respiratory syndrome coronavirus 2 (SARS-CoV-2) were first described in Wuhan, China, at the end of December 2019 (*1*). The infection rapidly spread, causing the coronavirus disease (COVID-19) pandemic (*2*).

Because SARS-CoV-2 and treatments such as dexamethasone or tocilizumab can impair the immune system, some researchers anticipated the possibility of fungal superinfection among COVID-19 patients (*3*–*6*). As of August 2020, researchers have documented COVID-19–associated pulmonary aspergillosis (CAPA) (*7*–*9*), invasive candidiasis (*10*), coccidioidomycosis (*11*), fusariosis (*12*), histoplasmosis (*13*), mucormycosis (*14*), pneumocystosis (*15*), and saccharomycosis (*16*). Varying cumulative rates of CAPA have been described, including rates of 0.7%–7.7% among COVID-19 patients (*17*,*18*), 2.5%–39.1% among ICU patients with COVID-19 (*19*,*20*), and 3.2%–29.6% among COVID-19 patients on mechanical

Author affiliations: University of Cologne, Cologne, Germany (J. Salmanton-García, R. Sprute, J. Stemler, E. Sal, X. Malaj, D. Seidel, O.A. Cornely, P. Koehler); L'Azienda Ospedaliero-Universitaria di Bologna Policlinico S. Orsola, Bologna, Italy (M. Bartoletti); Alma Mater Studiorum University of Bologna, Bologna (M. Bartoletti); Hospices Civils de Lyon, Lyon, France (D. Dupont); Université Claude Bernard Lyon 1, Lyon (D. Dupont); Centre de Recherche en Neurosciences de Lyon, Institut National de la Santé et de la Recherche Médicale, Centre National de la Recherche Scientifique, Lyon (D. Dupont); Instituto de Investigación Sanitaria Gregorio Marañón, Madrid, Spain (M. Valerio, M. Machado, S. de la Villa); Hospital Clinic, Institute of Biomedical Research August Pi i Sunyer, Barcelona, Spain (C. Garcia-Vidal); Hospital Universitario La Paz, Madrid (I. Falces-Romero); University Medical Center Hamburg-Eppendorf, Hamburg, Germany (M. Schroeder); Centro Médico ABC, Mexico City, Mexico (I. Hoyo); University Hospital Regensburg, Regensburg, Germany (F. Hanses); Federal University of Triângulo Mineiro, Uberaba, Brazil (K. Ferreira-Paim); Istituto di Ricovero e Cura a Carattere Scientifico San Martino Polyclinic Hospital, Genoa, Italy (D.R. Giacobbe); Canisius Wilhelmina Hospital, Nijmegen, the Netherlands (J.F. Meis); Federal University of Paraná, Curitiba, Brazil (J.F. Meis); University of Rennes I, Institut National de la Santé et de la Recherche Médicale, École des Hautes Études en Santé Publique, Institut de Recherche en Santé, Environnement et Travail, Rennes, France (J.-P. Gangneux); Hospital de Cabueñes, Gijón, Spain (A. Rodríguez-Guardado); Instituto de Investigación Sanitaria del Principado de Asturias, Oviedo, Spain (A. Rodríguez-Guardado); University of Milan, Milan, Italy (S. Antinori); German Centre for Infection Research, Cologne (O.A. Cornely)

DOI: https://doi.org/10.3201/eid2704.204895

[1]These senior authors contributed equally to this article.

[2]Members of this group are listed at the end of this article.

ventilation (*7*,*17*). Many of these patients lack the concurrent conditions usually associated with invasive pulmonary aspergillosis (IPA) such as malignancies, neutropenia, or history of allogeneic stem cell or solid organ transplantation (*21*). Admission to the ICU or severe influenza are also risk factors for IPA in non-neutropenic patients (*22*–*25*). Reports of CAPA have been mostly limited to a few single-center studies; therefore, a comprehensive analysis of international distribution currently is lacking (*4*).

We analyzed reports in the literature (*26*–*50*; references *51*–*54* in Appendix, https://wwwnc.cdc.gov/EID/article/27/4/20-4895-App1.pdf) and the FungiScope registry (reference *55* in Appendix) to describe baseline conditions, clinical management, and associated deaths in CAPA patients. This analysis also contextualizes the available cumulative incidences.

Methods

We conducted a retrospective analysis using clinical data of patients worldwide who received a CAPA diagnosis during March 1–August 31, 2020. Our analysis comprised data from the FungiScope registry and academic literature (Figure 1).

FungiScope (https://www.clinicaltrials.gov; National Clinical Trials identifier NCT01731353) is a global registry for emerging invasive fungal infections. FungiScope was approved by the local ethics committee of the University of Cologne, Cologne, Germany (study ID 05-102). The registry includes patients with invasive aspergillosis since 2019. FungiScope's methods have been described previously (reference *55* in Appendix).

In addition, we conducted a literature search using the PubMed database (https://pubmed.ncbi.nlm.nih.gov) for suspected CAPA cases occurring in March–August 2020. We used the search string "(Aspergill*) AND (invasive OR putative OR probable OR infection OR case OR patient OR report) AND (COVID* OR corona* OR SARS-CoV-2)," which identified 59 published articles. We reviewed and extracted relevant data from each of the publications. When necessary, we contacted authors for additional details (Appendix).

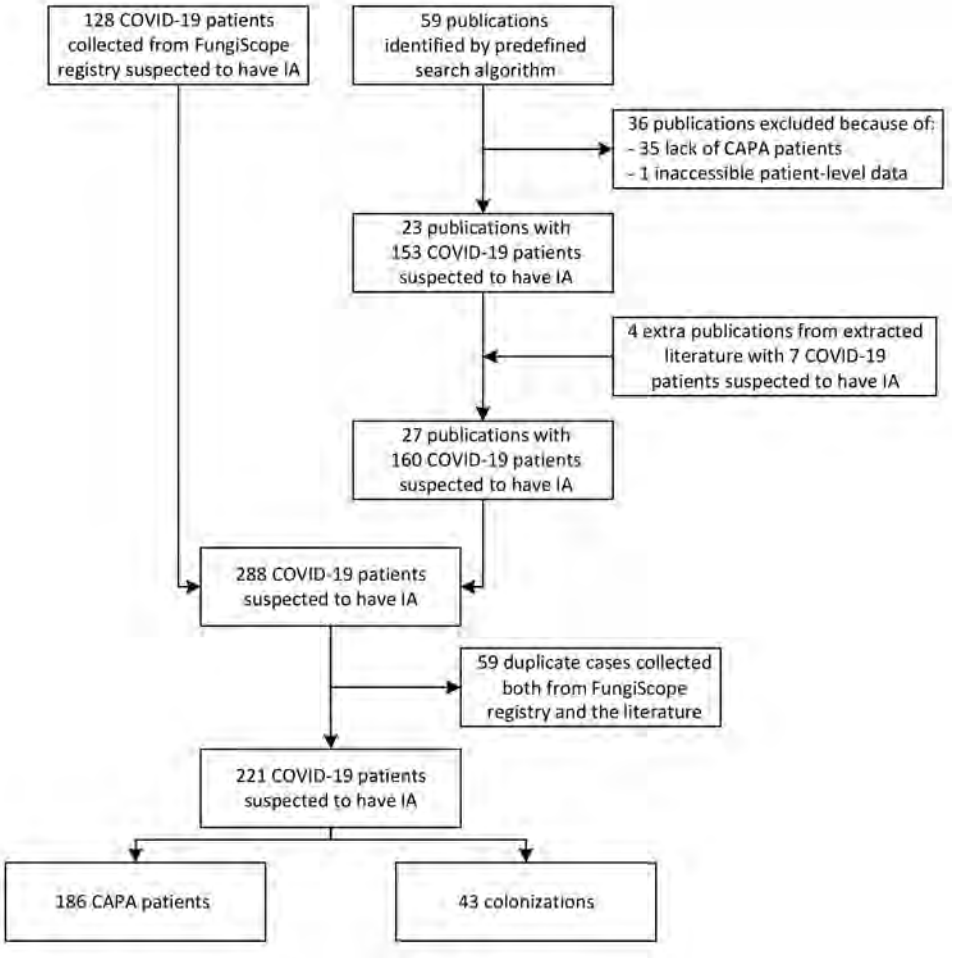

Figure 1. Enrollment process in study of patients with CAPA, March–August 2020. Patients were identified in the FungiScope registry and academic literature using the search string "(Aspergill*) AND (invasive OR putative OR probable OR infection OR case OR patient OR report) AND (COVID* OR corona* OR SARS-CoV-2) (Appendix Table 1, https://wwwnc.cdc.gov/EID/article/27/4/20-4895-App1.pdf). The initial 288 COVID-19 patients suspected to have IA were revised in a deduplication process; 59 double entries were identified. Only 1 report per patient was maintained. Thus, 221 individual COVID-19 patients suspected to have IA were assessed for CAPA. CAPA, COVID-19–associated pulmonary aspergillosis; COVID-19, coronavirus disease; EORTC/MSG, European Organization for Research and Treatment of Cancer/Mycoses Study Group; IA, invasive aspergillosis.

We reviewed each patient report using multiple diagnostic definitions. First, we evaluated the patients according to the consensus definition of Koehler et al. (reference *56* in Appendix); we classified the patients as having proven, probable, or possible CAPA. We used alternative definitions to evaluate patients who were nonclassifiable because of lack of essential information, such as the volume of saline recovered by nondirected bronchial lavage (NBL) fluid applied. We categorized the nonclassifiable patients as proven or probable according to the European Organization for Research and Treatment of Cancer/Invasive Fungal Infections Cooperative Group and the National Institute of Allergy and Infectious Diseases Mycoses Study Group criteria for invasive fungal infections (*21*) or as proven, putative, and colonized according to the AspICU algorithm for IPA in critically ill ICU patients by Blot et al. (*23*). We considered severe COVID-19 with acute respiratory distress syndrome (ARDS) to be a valid host criterion (i.e., acquired immunodeficiency) (*8*). We considered patients who met ≥1 definition to have CAPA; we categorized the rest as nonclassifiable.

We collected data on patients' demographic characteristics and baseline conditions. We also collected data on abnormal radiographic images, mycologic evidence, signs and symptoms at CAPA diagnosis, site of infection, antifungal susceptibility testing, antifungal treatment, death at 6 and 12 weeks after CAPA diagnosis, and absolute death. In addition, we calculated the length of time between COVID-19 and CAPA diagnoses, CAPA diagnosis and most recent healthcare contact with the patient, ICU admission and CAPA diagnosis, and installation of mechanical ventilation and CAPA diagnosis. The contribution of CAPA to patient death (i.e., attributable mortality) was assessed by the treating medical team (Appendix Table 2). To determine the cumulative incidence of CAPA in the facilities included in the analysis, we asked each institution for 3 different denominators: the total number of COVID-19 patients, the number of COVID-19 patients admitted to the ICU, and the number of COVID-19 patients admitted to the ICU who needed mechanical ventilation during March–August 2020.

Statistical Analysis

We did not calculate an a priori sample size for this exploratory study. To analyze the demographic and clinical characteristics of patients with CAPA, we describe categorical variables using frequencies and percentages; we describe continuous variables using medians and interquartile ranges (IQRs). We used SPSS Statistics 25.0 (IBM, https://www.ibm.com) for statistical analyses.

Results

We identified 186 CAPA cases during March 1–August 31, 2020, in 17 different countries, according to European Organization for Research and Treatment of Cancer/Invasive Fungal Infections Cooperative Group and the National Institute of Allergy and Infectious Diseases Mycoses Study Group criteria (*21*), Blot et al. algorithm (*23*), and Koehler et al. consensus definition (reference *56* in Appendix) (Figures 1, 2; Appendix Table 1). We identified 62 (33.3%) cases from literature, 45 (24.2%) from the FungiScope registry, and an additional 79 (42.5%) in both sources (Table 1). The median age among persons with CAPA was 68 years (IQR 59–73 years; range 15–87 years). Most (135; 72.6%) patients were men (Table 2).

Nearly all (182; 97.8%) patients were admitted to the ICU, most for ARDS (180; 96.8%) or mechanical ventilation (175; 94.1%). Other common baseline conditions and characteristics included corticosteroid administration (98; 52.7%), chronic cardiovascular disease (94; 50.5%), renal failure (74; 39.8%), diabetes mellitus (64; 34.4%), and obesity (47; 25.3%). Overall, 40 (21.5%) patients had chronic pulmonary disease (Table 2).

In total, 110 (59.1%) patients received either hydroxychloroquine (98; 52.7%) or chloroquine (12; 6.5%) for treatment of COVID-19. Sixty-eight (36.6%) patients received corticosteroids, mainly methylprednisolone monotherapy (26; 14.0%) or antivirals (67; 36.0%), especially lopinavir/ritonavir monotherapy (56; 30.1%). COVID-19 treatment had a median duration of 7 days before recovery or death (IQR 6–11 days; range 1–32 days) (Table 2; Appendix Table 3).

In 152 (81.7%) patients, CAPA was diagnosed a median of 10 days (IQR 5–16 days; range 0–51 days) after a positive respiratory sample for SARS-CoV-2 infection by reverse transcription PCR. Among all patients, *Aspergillus fumigatus* was the most frequently reported (122/152; 65.6%) pathogen. Six patients (3.2%) had cultures positive for >1 *Aspergillus* species. Samples mainly were from bronchoalveolar lavage (BAL) (50; 26.9%), tracheal aspirates (48; 25.8%), or bronchial aspirates (34; 18.3%). In 55 (29.6%) patients, culture was the only diagnostic tool that produced a positive result. Galactomannan (GM) levels were positive (i.e., optical density index ≥1.0) in samples from 113 (60.8%) patients, including BAL samples from 63 (33.9%) patients, serum or plasma from 29 (15.6%), and NBL from 22 (11.8%). Histologic techniques were used for diagnosis in 7

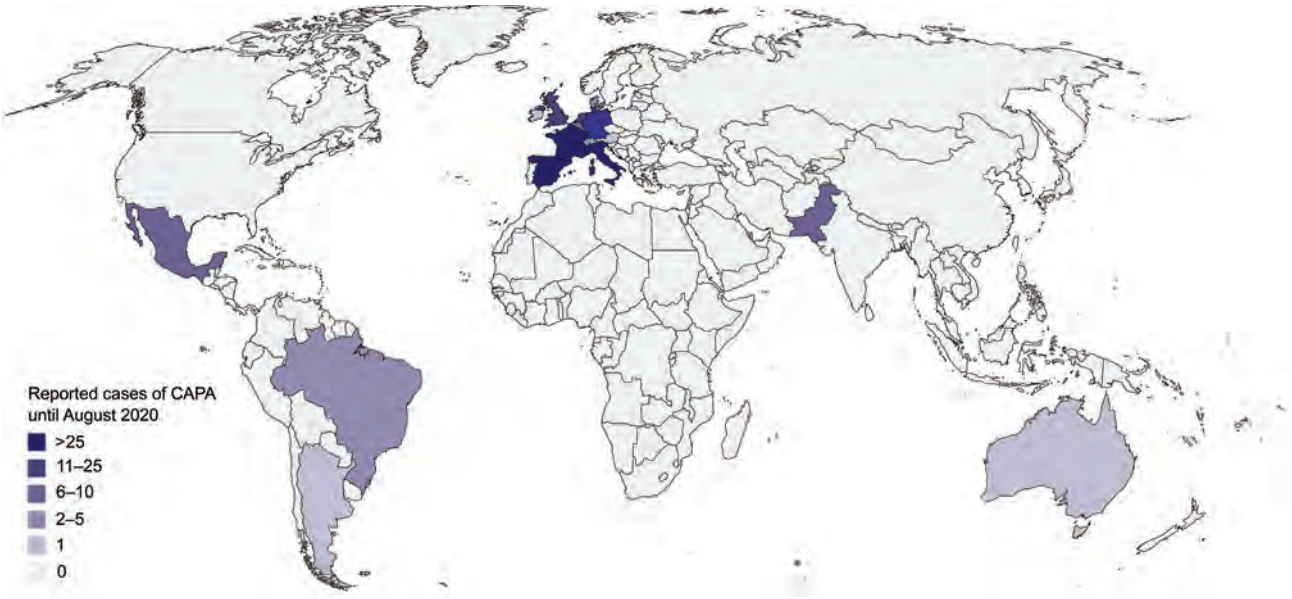

Figure 2. Global distribution of the 186 CAPA patients reported in the literature and FungiScope registry, March–August 2020. In total, 39 patients were from France, 36 from Italy, 26 from Spain, 23 from Germany, 14 from the Netherlands, 11 from the United Kingdom, 9 from Pakistan, 8 from Belgium, 6 from Mexico, 3 from Brazil, 3 from Switzerland, 2 from Denmark, 2 from Qatar, 1 from Argentina, 1 from Australia, 1 from Austria, and 1 from Ireland (Appendix Table 8, https://wwwnc.cdc.gov/EID/article/27/4/20-4895-App1.pdf). CAPA, COVID-19–associated pulmonary aspergillosis; COVID-19, coronavirus disease.

(3.8%) cases. Abnormal radiographic imaging was found in 182 (97.8%) patients, either in computed tomography scans (94; 50.5%), in chest radiographs (48; 25.8%), or both (40; 21.5%) (Table 2).

Overall, 30 (16.1%) patients provided samples for ≥1 antifungal susceptibility test, such as microdilution according to European Committee on Antimicrobial Susceptibility Testing guidelines (20; 10.8%) (reference *57* in Appendix), Etest (11; 5.9%), and Clinical and Laboratory Standards Institute microdilution procedures (1; 0.5%) (reference *58* in Appendix). The tests were predominantly performed on *A. fumigatus* (29; 15.6%) isolates, 3 of which had the TR34L98H resistance mutation in the *cyp51A* gene. One (0.5%) patient had voriconazole-resistant *A. lentulus* (MIC 2 μg/mL by EUCAST guidelines) (Appendix Table 4).

Of 186 CAPA patients, 49 (26.3%) patients did not receive mold-active antifungal therapy. The most common treatments were triazoles (117; 62.9%), especially voriconazole (98; 52.7%, including 79 patients for whom voriconazole was a first-line treatment) and isavuconazole (23; 12.4%). In total, 34 (19.4%) patients received amphotericin B, especially liposomal amphotericin B (23; 12.4%). Of the patients who received amphotericin B, 15 (65.2%) received it as first-line treatment. Antifungal treatment was administered for a median of 16 days before recovery or death (IQR 10–33 days; range 1–92 days) (Table 2; Appendix Table 5).

In total, 97 (52.2%) patients died, most (89; 47.8%) ≤6 weeks after CAPA diagnosis. In 32 (17.2%) patients, death was attributed to *Aspergillus*; including 25 (13.4%) patients who died of aspergillosis and COVID-19 infection. Patients were observed for a median of 22 days (IQR 7–42 days; range 0–144 days) after CAPA diagnosis; survivors were treated for a median of 40 days (IQR 28–50 days; range 1–144 days) and patients who died for a median of 9 days (IQR 3–18 days; range 0–144 days) (Table 2).

In total, 19 of 39 institutions provided denominators for cumulative incidence over the duration of the study period. The CAPA incidence among all COVID-19 patients ranged from 0.1%–9.7%. Among COVID-19 patients admitted to ICU, cumulative incidences ranged from 1.0%–39.1%. Among patients admitted to ICU who needed mechanical ventilation, cumulative incidences ranged from 1.1%–47.4% (Table 3).

Discussion

We described 62 CAPA cases in the literature, 45 in the FungiScope registry, and 79 in both that were diagnosed during March 1–August 31, 2020. Men had a higher (2.6:1) prevalence of CAPA than women. This finding corresponds with a meta-analysis of >3 million COVID-19 patients that showed that men were at increased risk for severe COVID-19

and therefore complications such as CAPA (reference *59* in Appendix).

Table 1. Pathogens of 186 patients with coronavirus disease–associated pulmonary aspergillosis, March–August 2020*

Characteristic	No. (%)
Pathogens†	
Aspergillus fumigatus	122 (65.6)
A. niger	13 (7.0)
A. flavus	10 (5.4)
A. terreus	6 (3.2)
A. calidoustus	1 (0.5)
A. lentulus	1 (0.5)
A. nidulans	1 (0.5)
A. penicillioides	1 (0.5)
A. versicolor	1 (0.5)
A. tubingensis	1 (0.5)
Aspergillus spp. (culture)‡	1 (0.5)
Aspergillus spp. (serologic techniques)	34 (18.3)
Other pathogens§	40 (21.5)
Case definition	
EORTC/MSG criteria (*21*)	
Proven	7 (3.8)
Probable	10 (5.4)
Nonclassifiable	169 (90.9)
AspICU algorithm (*23*)¶	
Proven	7 (3.8)
Putative	142 (76.3)
Colonization	34 (18.3)
Nonclassifiable	3 (1.6)
Consensus definition (reference 57 in Appendix)	
Proven	7 (3.8)
Probable	82 (44.1)
Possible	19 (10.2)
Nonclassifiable¶#	78 (41.9)
Mycologic evidence	
Culture**	152 (81.7)
Microscopy††	3 (1.6)
Histologic techniques‡‡	7 (3.8)
PCR§§	43 (23.1)
Galactomannan test¶¶	113 (60.8)

*Some patients had ≥1 pathogen or form of mycologic evidence. BAL, bronchoalveolar lavage; EORTC/MSG, European Organization for Research and Treatment of Cancer/Mycoses Study Group (*21*).
†A total of 2 patients had *A. fumigatus* and *A. niger* coinfection, 1 patient had *A. flavus* and *A. fumigatus* coninfection, 1 patient had *A. flavus* and *A. niger* coinfection, 1 patient had *A. fumigatus* and *A. terreus* coinfection, and 1 patient had *A. fumigatus* and *A. versicolor* coinfection.
‡One patient had an *Aspergillus* spp. infection diagnosed by culture. No species determination was provided. Other patient samples were diagnosed as *Aspergillus* spp, using serologic techniques.
§Small numbers of other pathogens were also retrieved from patient samples (Appendix Table 6, https://wwwnc.cdc.gov/EID/article/27/4/20-4895-App1.pdf).
¶AspICU method uses algorithm described by Blot et al. (*23*) for determining proven or putative aspergillosis in patients with influenza.
#Up to 78 cases (41.9%) were considered nonclassifiable according to the definition (reference *56* in Appendix) because of lack of specific details about the type of aspiration performed. Of these, 75 (96.2%) were classified as putative according to the Blot et al. algorithm (*23*) and 3 (3.8%) as probable according to EORTC/MSG criteria (*21*).
**Culture was used to analyze 50 BAL, 47 tracheal aspirate, 34 bronchial aspirate, 17 nondirected bronchial lavage, 3 sputum, 2 nonspecified lower respiratory tract, and 1 BAL and tracheal aspirate sample.
††Microscopy was used to analyze 1 BAL, 1 bronchial aspirate, and 1 tracheal aspirate sample.
‡‡Histologic techniques were used to analyze 7 lung tissue samples.
§§PCR was used to analyze 16 BAL, 12 tracheal aspirate, 10 nondirected bronchial lavage, 3 bronchial aspirate, 1 lung tissue, and 1 serum sample.
¶¶Galactomannan tests were used to analyze 63 BAL, 30 serum or plasma, 22 nondirected bronchial lavage, 9 tracheal aspirate, 3 bronchial aspirate, and 1 sputum sample.

Most (97.8%) patients were admitted to the ICU, mainly because of ARDS, need for mechanical ventilation, or both. We found that corticosteroid administration, chronic cardiovascular disease, renal failure, diabetes mellitus, and obesity were common characteristics among these patients. Approximately 1 in 5 patients had chronic pulmonary disease. Patients had many similarities to influenza-associated pulmonary aspergillosis (IAPA) patients from Schauwvlieghe et al. (*22*), including similar rates of mechanical ventilation (IAPA 90.0% vs. CAPA 94.1%), corticosteroid administration (IAPA 56.0% vs. CAPA 52.7%), baseline renal failure (IAPA 42.0% vs. CAPA 39.8%), obesity (IAPA 30.0% vs. CAPA 25.3%), and chronic pulmonary disease (IAPA 16.0% vs. CAPA 21.5%). IAPA patients had a higher proportion of malignancies (30.0% vs. 11.3%) and solid organ transplantation (13.0% vs. 2.7%); however, CAPA patients had a higher prevalence of diabetes mellitus (12.0% vs. 34.4%). In our study, 50.5% of patients had chronic cardiovascular disease. These differences in the distribution of baseline characteristics between IAPA and CAPA patients reflects the epidemiology of COVID-19, which is more common among those with chronic cardiovascular disease, whereas hematologic or oncologic malignancies (*22*) are more common among those with IAPA (reference *60* in Appendix). Only 2% of COVID-19 patients have cancer (reference *61* in Appendix).

Available guidelines for aspergillosis management recommend diagnostic procedures such as respiratory culture and galactomannan index of BAL samples (references *60*,*62* in Appendix). However, these procedures have a high risk for aerosolization; safety precautions should be used when handling samples from COVID-19 patients (references *63*,*64* in Appendix). The elevated risk for SARS-CoV-2 transmission and the initial recommendation against using bronchoscopy for COVID-19 diagnosis (references *63*,*64* in Appendix) might explain the low number of BAL tests used to diagnose CAPA in our study. Schauwvlieghe et al. (*22*) diagnosed IAPA by using BAL cultures in 63.0% of the patients and the galactomannan test in 88.0%. In the current study, BAL cultures tested positive for *Aspergillus* in 26.9% of COVID-19 patients; galactomannan tests were positive in 33.9% of patients. Alternative respiratory sample sources (e.g., bronchial aspirate, NBL, tracheal aspirate, and sputum) were used for cultures in 35.4% of IAPA patients (*22*) and 31.2% of CAPA patients. Alternative samples also were used for galactomannan tests in 17.2% of CAPA patients; if optical density index cutoff values were not standardized for alternative samples, clinicians used the values for BAL.

Table 2. Characteristics of 186 patients with coronavirus disease–associated pulmonary aspergillosis, March–August 2020*

Patient characteristic	No. (%)
Sex	
F	51 (27.4)
M	135 (72.6)
Median age, y (IQR)	68 (58–73)
COVID-19†	186 (100.0)
Median length of treatment, d (IQR)	7 (6–11)
Median time from COVID-19 diagnosis to CAPA, d (IQR)	10 (5–16)
Intensive care unit stay	182 (97.8)
Median length of stay before CAPA diagnosis, d (IQR)	8 (3–14)
Acute respiratory distress syndrome	180 (96.8)
Mechanical ventilation	175 (94.1)
Median time on ventilation before CAPA diagnosis, d (IQR)	7 (3–13)
Corticosteroid use	98 (52.7)
Concurrent conditions	
Chronic cardiovascular disease	94 (50.5)
Renal failure‡	74 (39.8)
Diabetes mellitus	64 (34.4)
Obesity	47 (25.3)
Chronic pulmonary disease	40 (21.5)
Hematologic or oncologic disease§	21 (11.3)
Hematologic malignancy	10 (5.4)
Solid tumor	9 (4.8)
Hematologic disease	2 (1.1)
Solid organ transplantation¶	4 (2.2)
Neutropenia	2 (1.1)
Other baseline conditions and characteristics#	70 (37.6)
Lung infection	186 (100.0)
Image abnormalities of the lungs	182 (97.8)
Computed tomography scan	134 (72.0)
Radiograph	88 (47.3)
Antifungal treatment	137 (73.7)
Median length of treatment, d (IQR)	16 (10–33)
Amphotericin B	36 (19.4)
Liposomal	23 (12.4)
Deoxycholate	11 (5.9)
Lipid complex	2 (1.1)
Echinocandins	24 (12.9)
Anidulafungin	10 (5.4)
Caspofungin	13 (7.0)
Micafungin	1 (0.5)
Ibrexafungerp	1 (0.5)
Triazoles	117 (62.9)
Voriconazole	98 (52.7)
Isavuconazole	23 (12.4)
Posaconazole	4 (2.2)
Fluconazole	1 (0.5)
Overall mortality	97 (52.2)
≤6 wks	89 (47.8)
≤12 wks	93 (50.0)
Median time to death, d (IQR)	9 (3–18)
Cause of death**	
CAPA	32 (17.2)
COVID-19	51 (27.4)
Other	36 (19.4)
Median length of observation from CAPA diagnosis, d (IQR)	22 (7–42)

*Values are no. (%), except as indicated. Some patients had ≥1 baseline condition or characteristic, image abnormality, or antifungal drug. CAPA, COVID-19–associated pulmonary aspergillosis; COVID-19, coronavirus disease.
†By definition, all CAPA patients had COVID-19 (Appendix Table 3, https://wwwnc.cdc.gov/EID/article/27/4/20-4895-App1.pdf).
‡In total, 54 patients had acute renal failure, 18 had chronic renal failure, and 2 had nonspecified renal failure.
§In total, 9 patients had hematologic malignancy: 3 had chronic leukemia, 3 had lymphoma, 2 had myelodysplastic syndrome, and 1 had acute leukemia. Eight patients had a solid tumor: 1 had breast cancer, 1 had carcinoma, 1 had cervical/uterine cancer, 1 had lung cancer, 1 had esophageal carcinoma, 1 had prostate cancer, 1 had testicular cancer, and 1 had urothelial carcinoma. Two patients had hematologic disease: 1 had acquired hemophilia type A and 1 had hemophagocytic lymphohistiocytosis.
¶In total, 3 patients had a kidney transplant, 1 had a liver transplant, and 1 had a lung transplant.
#Small numbers of patients had other concurrent conditions and characteristics (Appendix Table 7).
**In total, 32 patients died of CAPA or CAPA/COVID-19: 7 died of CAPA only; 25 died of CAPA and COVID-19. In addition, 26 died of COVID-19 only.

Table 3. Cumulative incidences of CAPA in 19 facilities, March–August 2020*

Country, site no.	CAPA cases, no.	Denominator, no. (% CAPA)			Timeframe
		COVID-19 patients	COVID-19 patients in ICU	COVID-19 patients on mechanical ventilation	
Argentina, I	2	673 (0.3)	163 (1.2)	69 (2.9)	Mar–Aug
Belgium, I	4	274 (1.5)	46 (8.7)	32 (12.5)	Mar–Aug
Belgium, II	4	NA	34 (11.8)	20 (20.0)	Mar–Apr
France, I	2	519 (0.4)	113 (1.8)	45 (4.4)	Mar–Aug
Germany, I	1	83 (1.2)	18 (5.6)	15 (6.7)	Mar–Aug
Germany, II	11	231 (4.8)	64 (17.2)	56 (19.6)	Mar–Aug
Germany, III	9	93 (9.7)	38 (23.7)	27 (33.3)	Mar–Aug
Germany, IV	7	123 (5.7)	76 (9.2)	57 (12.3)	Mar–Aug
Ireland, I	3	181 (1.7)	15 (20.0)	14 (21.4)	Mar–Aug
Italy, I	2	1,279 (0.2)	196 (1.0)	188 (1.1)	Mar–Aug
Italy, II	8	1,055 (0.8)	144 (5.6)	142 (5.6)	Mar–Aug
Mexico, I	6	312 (1.9)	131 (4.6)	115 (5.2)	Mar–Aug
Netherlands, I	9	NA	NA	53 (17.0)	Apr
Netherlands, II	6	483 (1.2)	118 (5.1)	NA	Mar–Aug
Pakistan, I	9	147 (6.1)	23 (39.1)	19 (47.4)	Mar–Apr
Spain, I	8	1,543 (0.5)	348 (2.3)	146 (5.5)	Mar–Aug
Spain, II	8	7,880 (0.1)	NA	NA	Mar–Aug
Spain, III	10	5,890 (0.2)	NA	NA	Mar–Aug
Switzerland, I	3	NA	118 (2.5)	80 (3.8)	Mar–May
United Kingdom, I	19	14,615 (0.1)	257 (7.4)	200 (9.5)	Mar–May
Total	131	35,381 (0.4)	1,902 (6.9)	1,278 (10.3)	Mar–Aug

*CAPA, COVID-19–associated pulmonary aspergillosis; COVID-19, coronavirus disease; ICU, intensive care unit; NA, not available.

Almost all (97.8%) patients had imaging abnormalities; however, many had only marginally typical features of aspergillosis, hampering the differential diagnosis of CAPA according to radiologic criteria.

Positive isolates were recovered from 81.7% of CAPA patients. Similar to IAPA patients, the most common (80.3%) pathogen was *A. fumigatus* (*22*). In total, 5 patients had azole-resistant infections: 4 *A. fumigatus* and 1 *A. lentulus* infection. We noted 2 patients who had a possible previous exposure to triazoles. The professions of these 2 patients involved exposure to fungicides and manipulated organic matter containing triazole-resistant *A. fumigatus*. Therefore, the treating teams hypothesized that workplace exposure might have contributed to these patients' illness. We found a similar proportion of patients with previous azole exposure as Verweij et al. (reference *65* in Appendix); however, the proportion found by Verweij et al. should be considered with caution because of small sample size.

Triazoles, especially voriconazole, were the most frequently administered antifungal drugs: 52.7% of the study cohort and 71.5% of the patients on antifungal treatment received voriconazole. We found that voriconazole use was associated with decreased death. The first-line use of voriconazole in 79 (80.6%) of 98 patients aligns with current recommendations (references *56*,*60*,*62* in Appendix).

We found a 50% mortality rate at 12 weeks after CAPA diagnosis. This finding is similar to the 51.0% mortality rate of IAPA patients in the same timeframe; however, these rates are almost 20 points higher than in other cohorts, such as aspergillosis patients with acute leukemia (33.8%) (reference *66* in Appendix). Nonetheless, in our study CAPA was attributed as the main reason for death in only 17.2% of the patients, whereas in Koehler et al. (reference *66* in Appendix), it was the main cause of death for 26.9% of patients with hematologic conditions.

We found an overall 6.9% cumulative incidence for CAPA among patients during the study period, although incidences varied by institution (1.0%–39.1% of CAPA patients admitted to ICU). In most facilities, the rates of CAPA were lower than those of IAPA (14%–19%) (reference *67* in Appendix). However, these ranges might vary according to diagnostic protocols in the different countries and healthcare facilities. Differences in screening practices for CAPA in COVID-19 patients might have affected detection rates and therefore our calculations of cumulative incidence (*8*). Further analyses are necessary to establish the geographic variance of this rate.

The first limitation of this study is that, because of the cross-sectional design of this study, we could not control for disease severity. Second, samples from the lower respiratory tract are the best way to differentiate between colonization and infection, but a low percentage of patients in this study had mycologic evidence from BAL culture or galactomannan tests. Third, we analyzed many cases from literature and could not contact certain authors for further details. In addition, institutions might not have documented all CAPA cases in the literature or FungiScope registry. Given the regional variability of the patient distribution,

longitudinal studies might be a more appropriate tool to determine rates. Finally, because of the retrospective nature of the study, we could not retrieve the necessary clinical and diagnostic details of all patients. As a result, many patients were not classifiable according to the definitions used in this article, possibly contributing to an underdiagnosis of CAPA.

In conclusion, we described a large cohort of CAPA patients using cases from the literature and the FungiScope registry. CAPA occurs mostly in ICU patients on mechanical ventilation. We found that CAPA patients had high rates of chronic cardiovascular disease, renal failure, diabetes mellitus, and corticosteroid use. We also found that CAPA substantially contributed to a high death rate in COVID-19 patients, although cumulative incidence varied by treatment site. We believe that improved screening can identify and enable early treatment of CAPA.

Members of the FungiScope European Confederation of Medical Mycology/the International Society for Human and Animal Mycology Working Group include Pilar Escribano, Mariana Chumbita, Martha Avilés-Robles, Julia Lanznaster, Mario Fernández-Ruiz, Guillaume Desoubeaux, Stefan Kluge, Matthias Kochanek, Norma B. Fernández, P. Lewis White, Kauser Jabeen, Florian Reizine, Stefaan van Biesen, Alexandre Alanio, Théo Ghelfenstein-Ferreira, Lynn Rutsaert, Jens T. van Praet, Emmanouil Glampedakis, Tobias Lahmer, Ali S. Omrani, Alida Fe Talento, Giuseppe Bruno, Andreas van Arkel, and Robbert Bentvelsen.

This work was carried out as part of routine duties. FungiScope is supported by unrestricted grants from Amplyx Pharmaceuticals, Inc.; Basilea Pharmaceuticals; Cidara Therapeutics, Inc.; F2G Ltd.; Matinas BioPharma; Mundipharma International; Pfizer Inc.; and Scynexis, Inc. FungiScope has been supported in the past by unrestricted grants from Astellas Pharma Inc., Gilead Sciences Inc., and MSD Sharp & Dohme GmbH.

J.S. has received research grants from Basilea Pharmaceuticals International Ltd. and travel grants from the Meta-Alexander Foundation and German Society for Infectious Diseases, outside the context of the submitted work. C.G.V. has received grants and speaker fees from Gilead Sciences, Inc. and Merck Sharp & Dohme Corp., and speaker fees from Janssen Pharmaceuticals, Lilly, Novartis, and Pfizer Inc., outside the context of the submitted work. M.S. receives funding from the Medical Faculty of the University of Hamburg, Hamburg, Germany for clinical leave. F.H. received lecture and other honoraria from Correvio Pharma Corp., InfectoPharm Arzneimittel und Consilium GmbH, and Novartis, outside the context of the submitted work. K.F.P. is financially supported by the Coordination for the Improvement of Higher Education Personnel Foundation and Ministry of Education of Brazil (proposal no. 09/2020) and a nonfinancial scientific grant from IMMY, outside the context of the submitted work. D.R.G. has received honoraria from Stepstone Pharma GmbH and unconditional grants from MSD Italia Srl and Correvio Pharma Corp. J.F.M. reports grants from F2G Ltd. and Pulmocide, consultancy fees from Scynexis, Inc., and speaker fees from Gilead Sciences Inc., United Medical, and Teva Pharmaceutical Industries Ltd., outside the context of the submitted work. J.P.G. has participated in advisory boards and received speaker honoraria from Pfizer Inc. and Gilead Sciences Inc., outside the context of the submitted work. E.S. has received grants from the Philipp Schwartz Initiative of the Alexander von Humboldt Foundation. O.A.C. is financially supported by the German Federal Ministry of Research and Education; is funded by the Deutsche Forschungsgemeinschaft under Germany's Excellence Strategy (CECAD, EXC 2030 – 390661388); has received research grants from Actelion Pharmaceuticals Global, Amplyx Pharmaceuticals, Inc., Astellas Pharma Inc., Basilea Pharmaceutica International Ltd., Cidara Therapeutics, Inc., Da Volterra, F2G Ltd., Gilead Sciences Inc., Janssen Pharmaceuticals, The Medicines Company, Melinta Therapeutics, Merck Sharp & Dohme Corp., Octapharma AG, Pfizer Inc., and Scynexis, Inc.; is a consultant to Actelion Pharmaceuticals Global, Allecra Therapeutics GmbH, Amplyx Pharmaceuticals, Inc., Astellas Pharma Inc., Basilea Pharmaceutica International Ltd., BIOSYS USA LLC, Cidara Therapeutics, Inc., Da Volterra, Entasis Therapeutics, F2G Ltd., Gilead Sciences Inc., Matinas BioPharma Holdings, Inc., MedPace, Inc., The Menarini Group, Merck Sharp & Dohme Corp., Mylan Inc., Nabriva Therapeutics plc, NOXXON Pharma, Octapharma AG, Paratek Pharmaceuticals, Inc., Pfizer Inc., Pharmaceutical Solutions Industry, Roche Diagnostics, Scynexis, Inc., and Shionogi Inc.; and received lecture honoraria from Al-Jazeera Pharmaceutical Industries, Astellas Pharma Inc., Basilea Pharmaceutica International Ltd., Gilead Sciences Inc., Grupo Biotoscana, Merck Sharp & Dohme Corp., and Pfizer Inc., outside the context of the submitted work. P.K. has received nonfinancial scientific grants from Miltenyi Biotec GmbH and the Cologne Excellence Cluster on Cellular Stress Responses in Aging-Associated Diseases, and lecture honoraria from or is advisor to Akademie für Infektionsmedizin e.V., Ambu GmbH, Astellas Pharma Inc., European Confederation of Medical Mycology, Gilead Sciences Inc., Gesundheits und Pflegezentrum Rüsselsheim gemeinnützige GmbH, Merck Sharp & Dohme Corp., and University Hospital, Ludwig Maximilian University of Munich, and is advisor to Gilead Sciences Inc. and NOXXON N.V. outside the context of the submitted work.

About the Author

Dr. Salmanton-García is an epidemiologist at University Hospital Cologne, Cologne. His primary research interests are invasive fungal infections, infectious diseases, epidemiology, and database management.

References

1. World Health Organization. Pneumonia of unknown cause. 2020 [cited 2021 Jun 23]. https://www.who.int/csr/don/05-january-2020-pneumonia-of-unkown-cause-china/en/.
2. Mahase E. Covid-19: WHO declares pandemic because of "alarming levels" of spread, severity, and inaction. BMJ. 2020;368:m1036. https://doi.org/10.1136/bmj.m1036
3. Koehler P, Meis JF, Ostrosky-Zeichner L, Böll B, Hoenigl M, Cornely OA, et al. COVID-19/influenza–associated pulmonary aspergillosis—management. 2020 [cited 2020 May 30]. https://repository.publisso.de/resource/frl%3A6421494.
4. Beer KD, Jackson BR, Chiller T, Verweij PE, Van de Veerdonk FL, Wauters J. Does pulmonary aspergillosis complicate coronavirus disease 2019? Crit Care Explor. 2020;2:e0211. https://doi.org/10.1097/CCE.0000000000000211
5. Costantini C, van de Veerdonk FL, Romani L. Covid-19–associated pulmonary aspergillosis: the other side of the coin. Vaccines (Basel). 2020;8:713. https://doi.org/10.3390/vaccines8040713
6. Arastehfar A, Carvalho A, van de Veerdonk FL, Jenks JD, Koehler P, Krause R, et al. COVID-19 associated pulmonary aspergillosis (CAPA)—from immunology to treatment. J Fungi (Basel). 2020;6:91. https://doi.org/10.3390/jof6020091
7. Alanio A, Dellière S, Fodil S, Bretagne S, Mégarbane B. Prevalence of putative invasive pulmonary aspergillosis in critically ill patients with COVID-19. Lancet Respir Med. 2020;8:e48–9. https://doi.org/10.1016/S2213-2600(20)30237-X
8. Koehler P, Cornely OA, Böttiger BW, Dusse F, Eichenauer DA, Fuchs F, et al. COVID-19 associated pulmonary aspergillosis. Mycoses. 2020;63:528–34. https://doi.org/10.1111/myc.13096
9. Dellière S, Dudoignon E, Fodil S, Voicu S, Collet M, Oillic PA, et al. Risk factors associated with COVID-19-associated pulmonary aspergillosis in ICU patients: a French multicentric retrospective cohort. Clin Microbiol Infect. 2020. https://doi.org/10.1016/j.cmi.2020.12.005
10. Chowdhary A, Tarai B, Singh A, Sharma A. Multidrug-resistant *Candida auris* infections in critically ill coronavirus disease patients, India, April–July 2020. Emerg Infect Dis. 2020;26:2694–6. https://doi.org/10.3201/eid2611.203504
11. Chang CC, Senining R, Kim J, Goyal R. An acute pulmonary coccidioidomycosis coinfection in a patient presenting with multifocal pneumonia with COVID-19. J Investig Med High Impact Case Rep. 2020;8:2324709620972244. https://doi.org/10.1177/2324709620972244
12. Poignon C, Blaize M, Vezinet C, Lampros A, Monsel A, Fekkar A. Invasive pulmonary fusariosis in an immunocompetent critically ill patient with severe COVID-19. Clin Microbiol Infect. 2020;26:1582–4. https://doi.org/10.1016/j.cmi.2020.06.026
13. Messina FA, Marin E, Caceres DH, Romero M, Depardo R, Priarone MM, et al. Coronavirus disease 2019 (COVID-19) in a patient with disseminated histoplasmosis and HIV—a case report from Argentina and literature review. J Fungi (Basel). 2020;6:275. https://doi.org/10.3390/jof6040275
14. Werthman-Ehrenreich A. Mucormycosis with orbital compartment syndrome in a patient with COVID-19. Am J Emerg Med. 2020. https://doi.org/10.1016/j.ajem.2020.09.032
15. Menon AA, Berg DD, Brea EJ, Deutsch AJ, Kidia KK, Thurber EG, et al. A case of COVID-19 and *Pneumocystis jirovecii* coinfection. Am J Respir Crit Care Med. 2020;202:136–8. https://doi.org/10.1164/rccm.202003-0766LE
16. Ventoulis I, Sarmourli T, Amoiridou P, Mantzana P, Exindari M, Gioula G, et al. Bloodstream infection by *Saccharomyces cerevisiae* in two COVID-19 patients after receiving supplementation of *Saccharomyces* in the ICU. J Fungi (Basel). 2020;6:98. https://doi.org/10.3390/jof6030098
17. van Arkel ALE, Rijpstra TA, Belderbos HNA, van Wijngaarden P, Verweij PE, Bentvelsen RG. COVID-19-associated pulmonary aspergillosis. Am J Respir Crit Care Med. 2020;202:132–5. https://doi.org/10.1164/rccm.202004-1038LE
18. Zhang SY, Lian JS, Hu JH, Zhang XL, Lu YF, Cai H, et al. Clinical characteristics of different subtypes and risk factors for the severity of illness in patients with COVID-19 in Zhejiang, China. Infect Dis Poverty. 2020;9:85. https://doi.org/10.1186/s40249-020-00710-6
19. Nasir N, Farooqi J, Mahmood SF, Jabeen K. COVID-19-associated pulmonary aspergillosis (CAPA) in patients admitted with severe COVID-19 pneumonia: an observational study from Pakistan. Mycoses. 2020;63:766–70. https://doi.org/10.1111/myc.13135
20. Lamoth F, Glampedakis E, Boillat-Blanco N, Oddo M, Pagani JL. Incidence of invasive pulmonary aspergillosis among critically ill COVID-19 patients. Clin Microbiol Infect. 2020;26:1706–8. https://doi.org/10.1016/j.cmi.2020.07.010
21. Donnelly JP, Chen SC, Kauffman CA, Steinbach WJ, Baddley JW, Verweij PE, et al. Revision and update of the consensus definitions of invasive fungal disease from the European Organization for Research and Treatment of Cancer and the Mycoses Study Group Education and Research Consortium. Clin Infect Dis. 2020;71:1367–76. https://doi.org/10.1093/cid/ciz1008
22. Schauwvlieghe AFAD, Rijnders BJA, Philips N, Verwijs R, Vanderbeke L, Van Tienen C, et al.; Dutch-Belgian Mycosis Study Group. Invasive aspergillosis in patients admitted to the intensive care unit with severe influenza: a retrospective cohort study. Lancet Respir Med. 2018;6:782–92. https://doi.org/10.1016/S2213-2600(18)30274-1
23. Blot SI, Taccone FS, Van den Abeele AM, Bulpa P, Meersseman W, Brusselaers N, et al.; AspICU Study Investigators. A clinical algorithm to diagnose invasive pulmonary aspergillosis in critically ill patients. Am J Respir Crit Care Med. 2012;186:56–64. https://doi.org/10.1164/rccm.201111-1978OC
24. Koehler P, Bassetti M, Kochanek M, Shimabukuro-Vornhagen A, Cornely OA. Intensive care management of influenza-associated pulmonary aspergillosis. Clin Microbiol Infect. 2019;25:1501–9. https://doi.org/10.1016/j.cmi.2019.04.031
25. Verweij PE, Rijnders BJA, Brüggemann RJM, Azoulay E, Bassetti M, Blot S, et al. Review of influenza-associated pulmonary aspergillosis in ICU patients and proposal for a case definition: an expert opinion. Intensive Care Med. 2020;46:1524–35. https://doi.org/10.1007/s00134-020-06091-6
26. Fernández NB, Cáceres DH, Beer KD, Irrazabal C, Delgado G, Farias L, et al. Ventilator-associated pneumonia

involving *Aspergillus flavus* in a patient with coronavirus disease 2019 (COVID-19) from Argentina. Med Mycol Case Rep. 2020 Jul 5 [Epub ahead of print]. https://doi.org/10.1016/j.mmcr.2020.07.001
27. Sharma A, Hofmeyr A, Bansal A, Thakkar D, Lam L, Harrington Z, et al. COVID-19 associated pulmonary aspergillosis (CAPA): An Australian case report. Med Mycol Case Rep. 2020 Jun 18 [Epub ahead of print]. https://doi.org/10.1016/j.mmcr.2020.06.002
28. Prattes J, Valentin T, Hoenigl M, Talakic E, Reisinger AC, Eller P. Invasive pulmonary aspergillosis complicating COVID-19 in the ICU - A case report. Med Mycol Case Rep. 2020 May 11 [Epub ahead of print]. https://doi.org/10.1016/j.mmcr.2020.05.001
29. Rutsaert L, Steinfort N, Van Hunsel T, Bomans P, Naesens R, Mertes H, et al. COVID-19-associated invasive pulmonary aspergillosis. Ann Intensive Care. 2020;10:71. https://doi.org/10.1186/s13613-020-00686-4
30. Sarrazyn C, Dhaese S, Demey B, Vandecasteele S, Reynders M, Van Praet JT. Incidence, risk factors, timing and outcome of influenza versus Covid-19 associated putative invasive aspergillosis. Infect Control Hosp Epidemiol. 2020 Sept 9;1–7 [Epub ahead of print]. https://doi.org/10.1017/ice.2020.460
31. Lemos DRQ, D'Angelo SM, Farias LABG, Almeida MM, Gomes RG, Pinto GP, et al. Health system collapse 45 days after the detection of COVID-19 in Ceará, Northeast Brazil: a preliminary analysis. Rev Soc Bras Med Trop. 2020;53:e20200354. https://doi.org/10.1590/0037-8682-0354-2020
32. Helleberg M, Steensen M, Arendrup MC. Invasive aspergillosis in patients with severe COVID-19 pneumonia. Clin Microbiol Infect. 2021;27:147–8. https://doi.org/10.1016/j.cmi.2020.07.047
33. Alanio A, Dellière S, Fodil S, Bretagne S, Mégarbane B. Prevalence of putative invasive pulmonary aspergillosis in critically ill patients with COVID-19. Lancet Respir Med. 2020;8:e48–9. https://doi.org/10.1016/S2213-2600(20)30237-X
34. Blaize M, Mayaux J, Nabet C, Lampros A, Marcelin AG, Thellier M, et al. Fatal invasive aspergillosis and coronavirus disease in an immunocompetent patient. Emerg Infect Dis. 2020;26:1636–7. https://doi.org/10.3201/eid2607.201603
35. Dupont D, Menotti J, Turc J, Miossec C, Wallet F, Richard JC, et al. Pulmonary aspergillosis in critically ill patients with Coronavirus Disease 2019 (COVID-19). Med Mycol. 2021;59:110–4. https://doi.org/10.1093/mmy/myaa078
36. Gangneux JP, Bougnoux ME, Dannaoui E, Cornet M, Zahar JR. Invasive fungal diseases during COVID-19: We should be prepared. J Mycol Med. 2020;30:100971. https://doi.org/10.1016/j.mycmed.2020.100971
37. Ghelfenstein-Ferreira T, Saade A, Alanio A, Bretagne S, Araujo de Castro R, Hamane S, et al. Recovery of a triazole-resistant *Aspergillus fumigatus* in respiratory specimen of COVID-19 patient in ICU—a case report. Med Mycol Case Rep. 2020 Jul 2 [Epub ahead of print]. https://doi.org/10.1016/j.mmcr.2020.06.006
38. Lescure FX, Bouadma L, Nguyen D, Parisey M, Wicky PH, Behillil S, et al. Clinical and virological data of the first cases of COVID-19 in Europe: a case series. Lancet Infect Dis. 2020;20:697–706. https://doi.org/10.1016/S1473-3099(20)30200-0
39. Schein F, Muñoz-Pons H, Mahinc C, Grange R, Cathébras P, Flori P. Fatal aspergillosis complicating severe SARS-CoV-2 infection: a case report. J Mycol Med. 2020;30:101039. https://doi.org/10.1016/j.mycmed.2020.101039
40. Lahmer T, Rasch S, Spinner C, Geisler F, Schmid RM, Huber W. Invasive pulmonary aspergillosis in severe coronavirus disease 2019 pneumonia. Clin Microbiol Infect. 2020;26:1428–9. https://doi.org/10.1016/j.cmi.2020.05.032
41. Mohamed A, Hassan T, Trzos-Grzybowska M, Thomas J, Quinn A, O'Sullivan M, et al. Multi-triazole-resistant *Aspergillus fumigatus* and SARS-CoV-2 co-infection: a lethal combination. Med Mycol Case Rep. 2020 Jun 26 [Epub ahead of print]. https://doi.org/10.1016/j.mmcr.2020.06.005
42. Antinori S, Rech R, Galimberti L, Castelli A, Angeli E, Fossali T, et al. Invasive pulmonary aspergillosis complicating SARS-CoV-2 pneumonia: a diagnostic challenge. Travel Med Infect Dis. 2020;38:101752. https://doi.org/10.1016/j.tmaid.2020.101752
44. Bartoletti M, Pascale R, Cricca M, Rinaldi M, Maccaro A, Bussini L, et al.; PREDICO Study Group. Epidemiology of invasive pulmonary aspergillosis among COVID-19 intubated patients: a prospective study. Clin Infect Dis. 2020 Jul 28 [Epub ahead of print]. https://doi.org/10.1093/cid/ciaa1065
44. Bruno G, Fabrizio C, Buccoliero GB. COVID-19–associated pulmonary aspergillosis: adding insult to injury. Lancet Microbe. 2020;1:e106. https://doi.org/10.1016/S2666-5247(20)30063-X
45. Meijer EFJ, Dofferhoff ASM, Hoiting O, Buil JB, Meis JF. Azole-resistant COVID-19–associated pulmonary aspergillosis in an immunocompetent host: a case report. J Fungi (Basel). 2020;6:79. https://doi.org/10.3390/jof6020079
46. van Arkel ALE, Rijpstra TA, Belderbos HNA, van Wijngaarden P, Verweij PE, Bentvelsen RG. COVID-19–associated pulmonary aspergillosis. Am J Respir Crit Care Med. 2020;202:132–5. https://doi.org/10.1164/rccm.202004-1038LE
47. Van Biesen S, Kwa D, Bosman RJ, Juffermans NP. Detection of invasive pulmonary aspergillosis in COVID-19 with non-directed BAL. Am J Respir Crit Care Med. 2020;202:1171–3. https://doi.org/10.1164/rccm.202005-2018LE
48. Nasir N, Farooqi J, Mahmood SF, Jabeen K. COVID-19–associated pulmonary aspergillosis (CAPA) in patients a dmitted with severe COVID-19 pneumonia: an observational study from Pakistan. Mycoses. 2020;63:766–70. https://doi.org/10.1111/myc.13135
49. Abdalla S, Almaslamani MA, Hashim SM, Ibrahim AS, Omrani AS. Fatal coronavirus disease 2019–associated pulmonary aspergillosis; a report of two cases and review of the literature. IDCases. 2020;22:e00935. https://doi.org/10.1016/j.idcr.2020.e00935
50. Falces-Romero I, Ruiz-Bastián M, Díaz-Pollán B, Maseda E, García-Rodríguez J; SARS-CoV-2 Working Group. Isolation of *Aspergillus* spp. in respiratory samples of patients with COVID-19 in a Spanish tertiary care hospital. Mycoses. 2020;63:1144–8. https://doi.org/10.1111/myc.13155

Address for correspondence: Jon Salmanton-García, University of Cologne, Herderstrasse 52-54, Cologne 50931, Germany; email: jon.salmanton-garcia@uk-koeln.de

Genomic Surveillance of a Globally Circulating Distinct Group W Clonal Complex 11 Meningococcal Variant, New Zealand, 2013–2018

Zuyu Yang,[1] Xiaoyun Ren,[1] Heather Davies, Timothy Wood, Liza Lopez, Jill Sherwood, Audrey Tiong, Philip E. Carter

Genomic surveillance is an essential part of effective disease control, enabling identification of emerging and expanding strains and monitoring of subsequent interventions. Whole-genome sequencing was used to analyze the genomic diversity of all *Neisseria meningitidis* isolates submitted to the New Zealand Meningococcal Reference Laboratory during 2013–2018. Of the 347 isolates submitted for whole-genome sequencing, we identified 68 sequence types belonging to 18 clonal complexes (CC). The predominant CC was CC41/44; next in predominance was CC11. Comparison of the 45 New Zealand group W CC11 isolates with worldwide representatives of group W CC11 isolates revealed that the original UK strain, the 2013 UK strain, and a distinctive variant (the 2015 strain) were causing invasive group W meningococcal disease in New Zealand. The 2015 strain also demonstrated increased resistance to penicillin and has been circulating in Canada and several countries in Europe, highlighting that close monitoring is needed to prevent future outbreaks around the world.

Neisseria meningitidis, a gram-negative bacterium, is the causative agent for meningococcal meningitis and septicemia and has been associated with isolated cases, outbreaks, and epidemics worldwide (*1*). The rapid progression of invasive meningococcal disease (IMD) and its high incidence of severe illness and death make IMD a feared and closely monitored disease. *N. meningitidis* is classified into 12 groups on the basis of capsular polysaccharide structure, but 6 groups (A, B, C, W, X, and Y) cause most life-threatening IMD (*2*). Most meningococcal disease is caused by hyperinvasive lineages belonging to specific clonal complexes (CC) as defined by multilocus sequence typing (MLST) (*3*), including CC32, CC41/44, CC11, and CC5 (*4*). Obtaining complete genetic information and resolving the evolutionary relationships of invasive pathogens are vital for identifying the origins and expansion of new pathogenic strains.

Group W CC11 (W:CC11) meningococci emerged as a global cause of IMD after an outbreak in Mecca, Saudi Arabia, in 2000 (*5*). High levels of group W disease have recently occurred in many countries and regions, including the United Kingdom (*6*), Sweden (*7*), Australia (*8*), and North America (*9*,*10*), and whole-genome sequencing (WGS) has been used to investigate its spread. Core-genome MLST found that group W:CC11 isolates were distinct from groups B and C sequence type (ST) 11 isolates (*11*). Currently, 4 major W:CC11 strains belonging to 2 major lineages are circulating globally: the Hajj strain sublineage, including the Hajj strain (*12*), and the South America strain sublineage, which includes the South America strain that emerged in 2003 in southern Brazil (*13*); the UK strain, a variant of the South America strain; and the 2013 UK strain (*14*), which has expanded into several countries (*8*,*9*,*15*).

During 1991–2008, New Zealand experienced a prolonged epidemic of IMD; most cases were caused by a single *N. meningitidis* group B strain (NZMenB), defined by PorA type P1.7–2,4 and belonging to CC41/44 (*16*,*17*). A strain-specific vaccine, MeNZB, was introduced in 2004 (*18*) and withdrawn in 2008 after rates of IMD decreased (*19*). The NZMenB strain continues to cause about one third of meningococcal infections in New Zealand, but other group B, C, W, and Y strains are also circulating (*20*). Recently, incidence of IMD caused by W:CC11 has increased in New Zealand. To learn more about

Author affiliation: Institute of Environmental Science and Research, Porirua, New Zealand

DOI: https://doi.org/10.3201/eid2704.191716

[1]These authors contributed equally to this article.

the genetic diversity associated with IMD after the epidemic, we used WGS to analyze 347 isolates collected during 2013–2018. We determined their clonal relationship and compared the genomes of the New Zealand W:CC11 isolates with global representatives of W:CC11 lineages.

Methods

Surveillance and Epidemiologic Analysis

Meningococcal disease is a notifiable disease in New Zealand; all IMD cases are referred to the Meningococcal Reference Laboratory at the Institute of Environmental Science and Research (ESR) for routine grouping using slide agglutination or PCR (*21*). For this study, disease incidence and case demographics were derived from notification data extracted from the national notifiable disease surveillance database. Annual population denominators were taken from Statistics New Zealand. We used R version 3.4.4 (https://www.r-project.org) to perform all statistical tests. Shannon–Wiener diversity index was calculated by using vegan version 2.5.6 (*22*).

WGS

We analyzed all available meningococcal isolates from 2013–2018 in New Zealand by WGS (Appendix 1 Table 1, https://wwwnc.cdc.gov/EID/article/27/4/19-1716-App1.xlsx). Genomic DNA was purified by using the Gentra Puregene Yeast/Bact. Kit (QIAGEN, https://www.qiagen.com) or High Pure PCR Template Preparation Kit (Roche, https://www.roche.com) according to the manufacturer's protocols. A 10-μL loop of bacteria, grown overnight on Columbia blood agar plates (Fort Richard Laboratories, Auckland, NZ), was suspended in 300 μL of lysis buffer and heat-killed at 56°C for 1 h. We then quantified DNA by using the Quant-iT PicoGreen dsDNA assay kit (Thermo Fisher Scientific, https://www.thermofisher.com) and constructed libraries by using Nextera-XT DNA Library Preparation Kit (Illumina, https://www.illumina.com). Paired-end sequencing of 2 × 150 bp was performed on the Illumina platform at ESR. Read data are available for download from the National Center for Biotechnology Information Sequence Read Archive (Bioproject accession no. PRJNA592848) and from PubMLST (https://pubmlst.org).

Genomic Analysis

Raw reads were quality trimmed by using Trimmomatic version 0.32 (*23*) to remove adapters, low quality bases (<Q20), and reads shorter than 60 bp. SPAdes version 3.10.1 (*24*) was used for assembly, and contigs >200 bp were kept. Assembled contigs were used for in silico MLST, capsular grouping, and antigen typing by using meningotype version 0.82-β (*25*). Single-nucleotide polymorphisms (SNPs) were identified by aligning quality-trimmed paired-end reads to the *N. meningitidis* reference sequence FAM18 (GenBank accession no. AM421808.1) and using Bowtie2 version 2.2.5 (*26*). Alignments were processed with Picard-tools (*27*) to remove duplicated reads and assessed with Qualimap version 2.2.1 (*28*) (Appendix 1 Table 2). We used FreeBayes version 1.2.0–2-g29c4002 (E. Garrison, unpub. data, https://arxiv.org/abs/1207.3907) to detect sequence variations among isolates with these settings: ploidy = 1, at 20× minimum depth and 70% minimum variant allele frequency. We filtered variants by using vcflib (*29*) and vcftools version 0.1.12b (*30*) and removed sites located in the tandem repeat regions by using the intersect function from BEDTools version 2.23.0 (*31*). For datasets that included only assembled genomes, we used Parsnp version 1.1.2 (*32*) to perform core-genome alignment and FAM18 (AM421808.1) as reference.

Phylogenetic Analysis

We constructed phylogenetic analyses from core SNP alignment by using the maximum-likelihood method under the general time reversible substitution model with RAxML version 8.2.12 (*33*) and estimated the relative robustness of the clades with 200 bootstrap replicates (*34*). We used ClonalFrameML version 1.25 (*35*) to construct recombination-corrected phylogeny on the basis of core SNP tree topology. For datasets that included only assembled genomes, we generated a maximum-likelihood phylogenetic tree by using RAxML on the basis of the core-genome alignment with 200 bootstrap replicates. Phylogenies were annotated by using iTOL (*36*).

Selection of Global Group W:CC11 Isolates

We compared New Zealand group W:CC11 isolates with 153 short-read datasets and 30 draft assemblies. Short-read data in the European Nucleotide Archive were selected to represent all major lineages of group W:CC11. We followed studies by Lucidarme et al. (*14*) and Tsang et al. (*9*) and randomly chose 1–3 isolates per year per country. We selected 153 datasets including 151 group W isolates and 2 group C isolates (ERR557598 and ERR976806), which were used as an outgroup to study the genetic relationship within group W:CC11.

We used the PubMLST *Neisseria* database to identify other isolates closely related to the New Zealand

ST11 isolates (*37*). As of February 18, 2019, a total of 30 isolates were within the 50 mismatch thresholds to NZ17MI0022 based on comparison of the *N. meningitidis* core-genome MLST (*38*). Draft assemblies of these 30 isolates were downloaded from PubMLST. Short-read data were available for 3 of these 30 isolates. We compiled detailed information on sequences used for phylogenetic analysis (Appendix 1 Table 3).

Antimicrobial Susceptibility Testing of New Zealand Group W:CC11 Isolates

Of the 45 New Zealand invasive group W:CC11 isolates, 42 were assessed for susceptibility to penicillin, ciprofloxacin, ceftriaxone, and rifampin. MICs were determined by gradient strip on Mueller-Hinton agar with 5% sheep blood and interpreted according to the Clinical and Laboratory Standards Institute breakpoints (*39*). Assembled contigs were used for in silico penA typing by using the PubMLST *Neisseria* database.

Results

Epidemiology of Meningococcal Disease in New Zealand, 2013–2018

During 2013–2018, a total of 484 cases of meningococcal disease were reported, including 456 confirmed and 28 probable cases, for a confirmation rate of 94.2% (Figure 1, panel A; Appendix 1 Table 4). Rates of IMD (Figure 1, panel B) continued to fall after the end of the group B epidemic in 2008 (coefficient = −2.619, R^2 = 0.6947; p = 0.0245) but increased during 2014–2018 (coefficient = 2.481, R^2 = 0.9567; p = 0.0025). Inflection point of the time series was identified by breakpoint analysis and using the R package strucchange (*40*) and tested by the Chow test in R by using monthly disease rates (cases/100,000) during January 2008–December 2018 (Appendix 1 Table 5). The test identified the inflection point as October 2013 (95% CI January–December 2013).

Group B meningococci continue to be responsible for most IMD cases in New Zealand. Among the 438 confirmed cases analyzed by ESR during 2013–2018 were 265 (54.7%) group B (100 NZMenB and 165 other group B) cases, 58 (13.2%) group C cases, 61 (13.9%) group W cases, and 47 (10.7%) group Y cases (Figure 1, panel C; Appendix 1 Table 6). To compare whether significant changes occurred during 2013–2018, we used a 2-proportion Z-test in R to compare the proportion of diseases caused by each group. We found that the proportion of group W disease in 2018 (33/133) was significantly greater than that in 2013 (5/58, χ^2 = 8.2415; p = 0.002047). In contrast, the proportion of disease caused by group C in 2018 (10/133) is significantly less than that of 2013 (17/58, χ^2 = 10.578; p = 0.00057).

The rate of IMD continues to be highest among patients <1 year of age (from 10.2/100,000 population in 2014 to 23.1/100,000 population in 2017); rates are second highest among children 1–4 years of age (from 5.2/100,000 population in 2014 to 9.8/100,000 population in 2017). Adults >60 years of age are more affected by group W and Y disease (Figure 2; Appendix 1 Table 7).

Clonal Distribution of Circulating Meningococci

We performed WGS and in silico typing on the 347 New Zealand meningococcal isolates (288 invasive and 59 noninvasive) collected during 2013–2018. The WGS dataset includes 175 group B isolates (65 NZMenB and 110 other group B), 48 group C isolates, 2 group E isolates, 64 group W isolates, 47 group Y isolates, 1 group X isolate, and 8 nongroupable isolates. MLST analysis showed that the 347 isolates contained 49 known STs. The 10 most common STs were ST11 (85), ST154 (43), ST23 (21), ST42 (17), ST32 (16), ST213 (15), ST1655 (15), ST1572 (11), ST6058 (8), and ST22 (7). There were 39 other STs with a single isolate and 19 unassigned STs (submitted through this project). The STs identified belonged to 18 clonal complexes. A total of 93 unique strains were defined by combination of group:PorA-variable region (VR)1, PorA-VR2:FetA:CC, with a Shannon–Wiener diversity index of 3.516. Bexsero antigen sequence types analysis showed 69 unique types with 23 isolates in which type could not be determined because of the absence of required loci (Appendix 1 Table 1).

Maximum-likelihood phylogeny constructed from 75,187 core SNP alignments (by using *N. meningitidis* FAM18 as the reference genome) showed 17 highly supported clades (with ≥90% bootstrap value), 15 of which were consistent with the CC definition (Figure 3). One clade of group B isolates could not be assigned to a CC because its ST had not been assigned a CC designation; it is noted as N1 on the phylogenetic tree. CC11 is the predominant CC consisting of 40 group C and 54 group W isolates; the second most common was CC41/44, consisting of 90 group B and 1 nongroupable isolates.

Since the NZMenB epidemic, New Zealand has used a combination of PorA subtype with group information to define *N. meningitidis* strains. We integrated the PorA and CC information to identify the strains currently circulating in New Zealand (Figure 4).

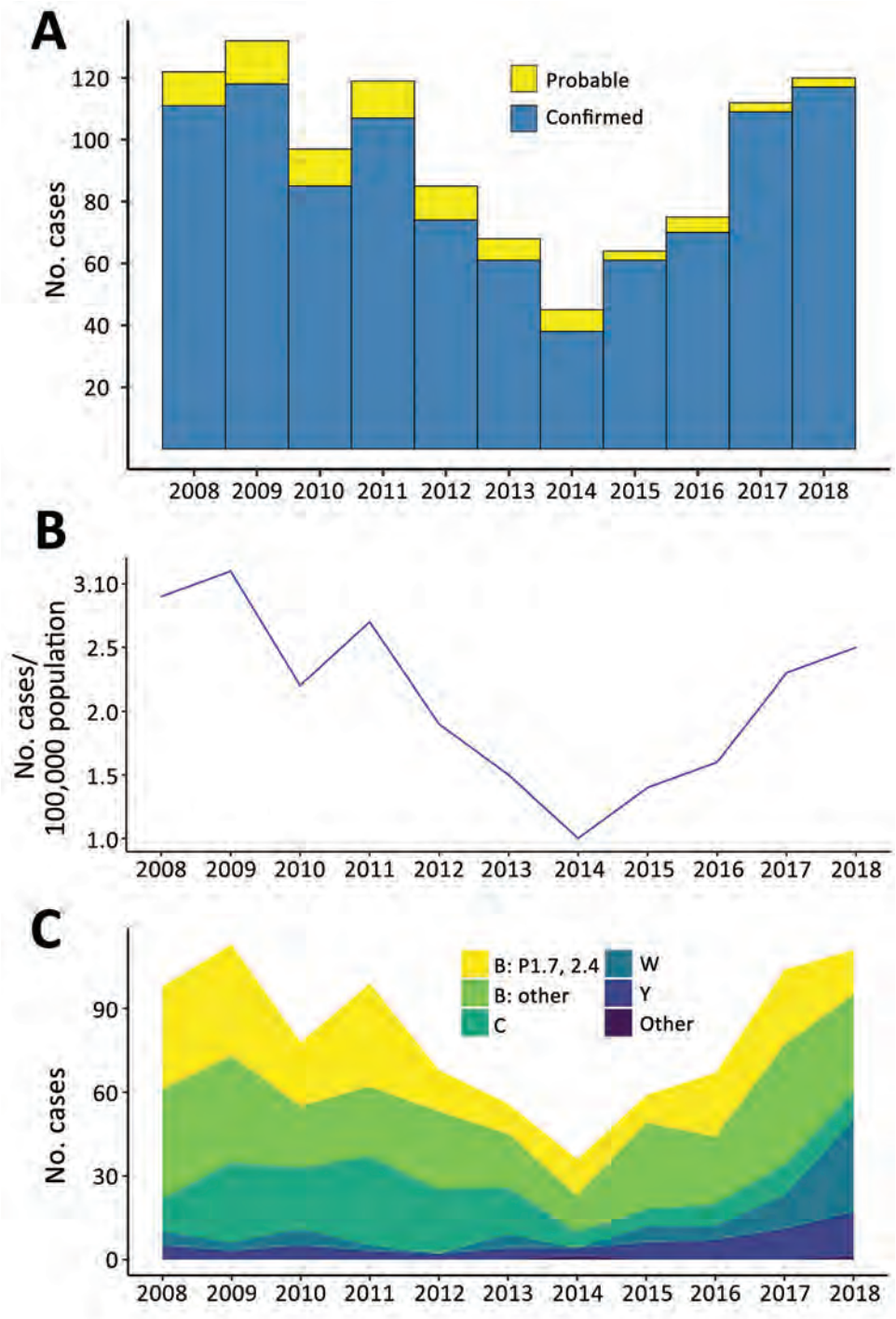

Figure 1. Epidemiology of meningococcal disease, New Zealand, 2013–2018. A) Number of confirmed and probable cases. B) Number of cases per 100,000 population of meningococcal disease. C) Meningococcal disease by group.

Phylogenetic Analysis of New Zealand W:CC11 Isolates

Rates of group W disease in 2018 were higher than in 2013. Most sequenced group W isolates in 2018 (30/35) belonged to CC11. To understand how New Zealand W:CC11 isolates relate to the global group W lineages, we analyzed New Zealand W:CC11 in the context of major W:CC11 lineages. We included 196 CC11 isolates in this analysis (151 downloaded from public databases and 45 invasive isolates from New Zealand). The mapping rate was 92.4%–99.3% when *N. meningitidis* FAM18 (AM421808.1), a representative of CC11, was used as a reference. The mean genome depth was 152X, with 84.8%–97.7% of loci covered at >20-fold (Appendix 1 Table 2).

We used core SNP (48,507 bps) alignment to construct the phylogenetic relationship of New Zealand

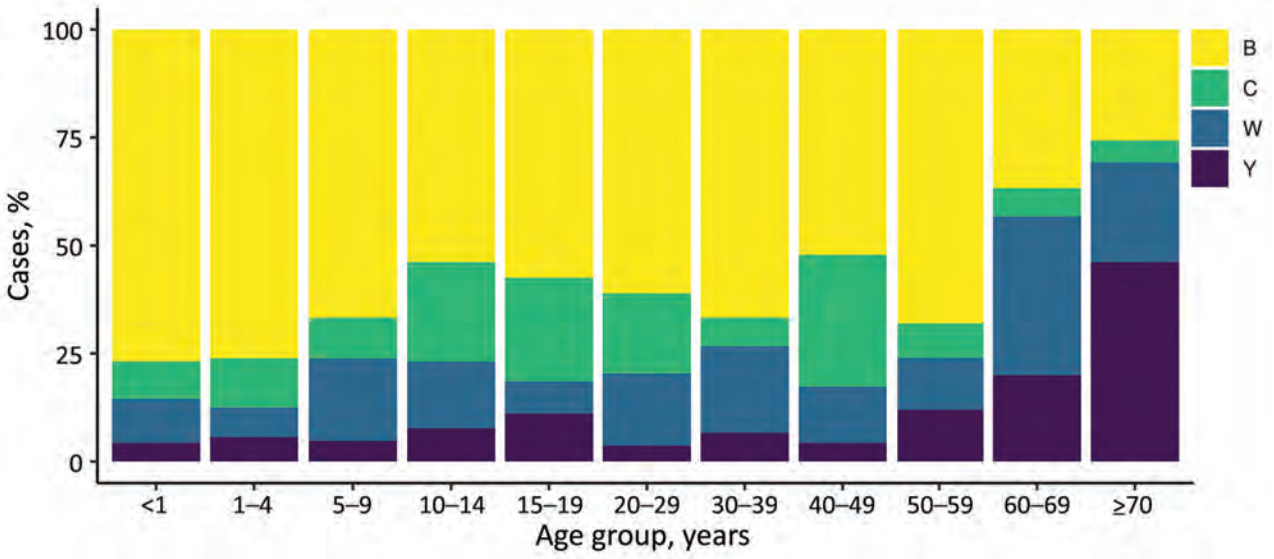

Figure 2. Age group distribution of meningococcal disease, by isolate group, New Zealand, 2013–2018

W:CC11 isolates within the global W:CC11 (Figure 5). Phylogeny was rooted with 2 group C CC11 isolates. An unrooted neighbor-net phylogeny from the same dataset is shown in Appendix 2 Figure 1 (https://wwwnc.cdc.gov/EID/article/27/4/19-1716-App2.pdf). Recombination-corrected phylogeny from the same dataset is shown in Appendix 2 Figure 2. Excluding the basal older sublineages, all other isolates formed 2 strongly supported clades. Clade I corresponds to the previously identified Hajj sublineage, and clade II corresponds to the previously identified South America sublineage. All New Zealand CC11 isolates were located within clade II: 4 clustered with the original UK strains, 12 clustered with the 2013 UK strain, and the other 29 formed a separate cluster with the 2 isolates from the United Kingdom and 1 isolate from Ireland (Figure 5).

To determine whether other isolates are closely related to the new New Zealand cluster, we searched PubMLST and found 27 additional isolates within 50 allele (the cgMLST 0.1 scheme) differences to NZ17MI0022. Because only assembled contigs were available for these isolates, we used a core-genome alignment approach to analyze their relationship within clade II of the W:CC11 isolates. All additional 27 W:CC11 isolates clustered with the New Zealand cluster with high bootstrap support (Appendix 2 Figure 3). The 27 isolates are from Canada and 6 countries in Europe (Appendix 1 Table 3).

Both phylogenetic analyses suggest that the new New Zealand cluster is part of the W:CC11 South America strain sublineage derived from the original UK strain. Because the earliest isolate of the new variant was identified in 2015, we named it the 2015 strain of the W:CC11 South America strain sublineage (the 2015 strain).

Epidemiology of the 2015 Strain

Similar to the 2013 UK strain, the 2015 strain is associated with higher death rates. During 2017–2018, the 2015 strain was associated with a death rate of 17.8% (6/34 cases) in New Zealand, higher than the rate of 5.9% (10/170 cases) for other groups in the same period ($p = 0.03$ by Fisher exact test). The 2015 strain also disproportionally affected older adults; 26% of total 2015-strain cases affected adults >60 years of age (9/34), whereas 5.8% (7/121) of total group B cases affected adults in that age group ($p = 0.01466$ by Fisher exact test).

2015 Strain and Penicillin Susceptibility

In 2016, Mowlaboccus et al. (*41*) described a W:CC11 variant circulating in Australia that demonstrated intermediate resistance or was resistant to penicillin and had penA allele 253. To examine whether the New Zealand 2015-strain isolates were also resistant to penicillin, we tested the antimicrobial susceptibility of 42 invasive New Zealand W:CC11 isolates in this study. All 42 isolates were susceptible to ciprofloxacin (MIC ≤0.03 mg/L), ceftriaxone (≤0.12 mg/L), and rifampin (≤0.5 mg/L) (Appendix 1 Table 8). We observed variation in penicillin susceptibility among the 42 isolates (Appendix 1 Table 8) by using Clinical and Laboratory Standards Institute breakpoints. Of the 15 isolates belonging to either the original UK strain or the 2013 UK strain, all were susceptible to penicillin (≤0.06 mg/L). Of the 27 isolates belonging to the new 2015 strain, 12 displayed intermediate

resistance (0.12–0.25 mg/L) and 15 were resistant (≥0.5 mg/L). The 2015-strain isolates were significantly more resistant to penicillin ($p<0.00001$ by Fisher exact test). All 27 New Zealand 2015-strain isolates had penA allele 253, the same allele described in the Australia study (*41*). In the larger dataset that included 30 international 2015-strain isolates, all but 1 isolate had penA allele 253 (Appendix 1 Table 3).

Discussion

We comprehensively analyzed *N. meningitidis* in New Zealand during 2013–2018 to describe its population structure after the NZMenB epidemic. We examined the rate of IMD and clonal distribution of circulating isolates. We also offer evidence that a distinct variant of W:CC11 is circulating globally and has been causing IMD since 2015.

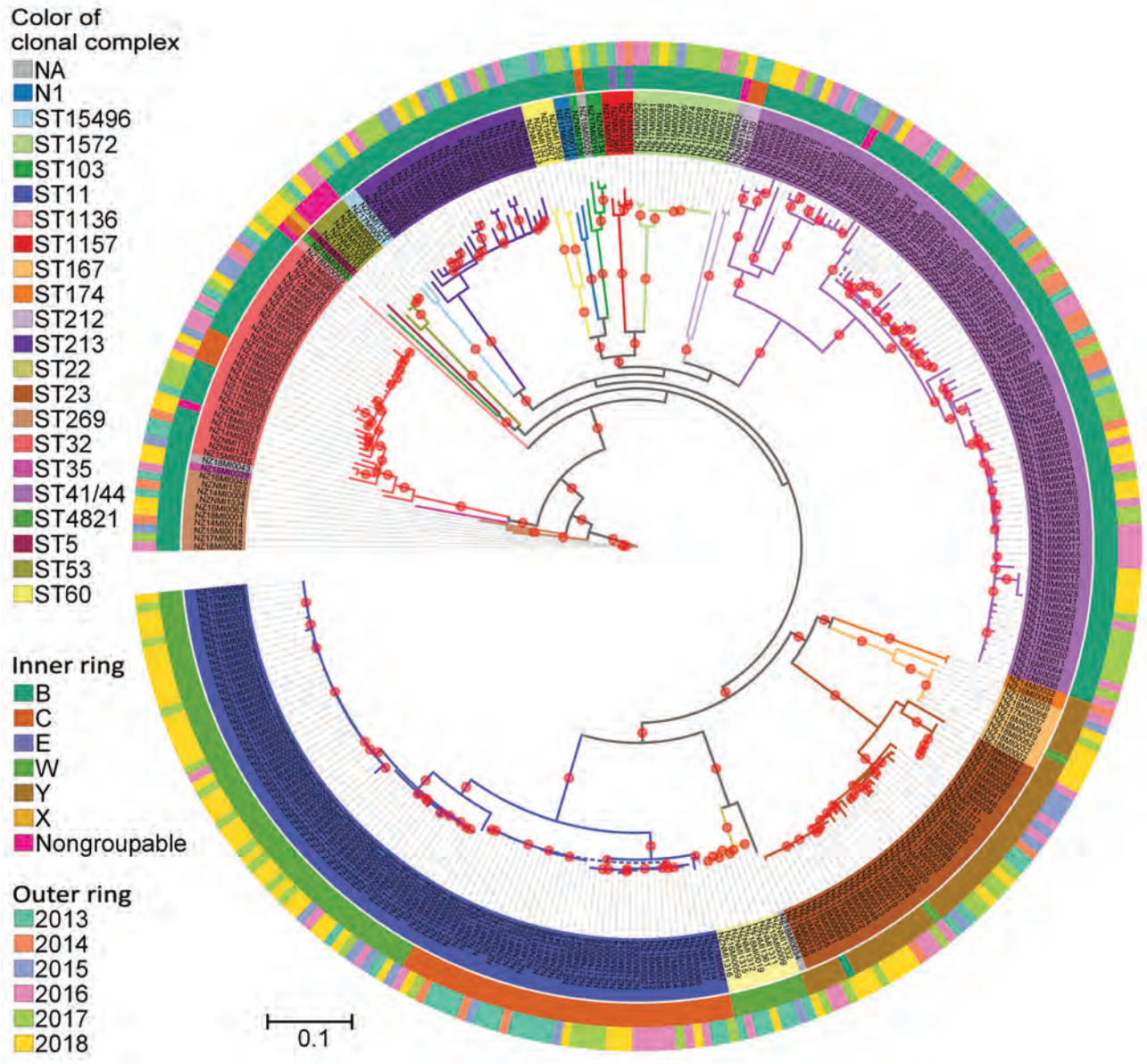

Figure 3. Phylogenetic analysis of New Zealand *Neisseria meningitidis* isolates, 2013–2018. Maximum-likelihood phylogeny was constructed by using a generalized time reversible substitution model and core single-nucleotide polymorphism alignments with RAxML version 8.2.12 (*33*). Branches with >90% bootstrap consensus (200 bootstrap replications) are highlighted with a red dot. Isolate names and clades are colored according to their clonal complex designation. The inner ring indicates the group and outer ring designates the year of isolation of the isolates. N1 lineage corresponds to sequence type that does not have clonal complex designation. NA corresponds to individual isolates where clonal complex is not assigned. Scale bar indicates average number of substitutions per site.

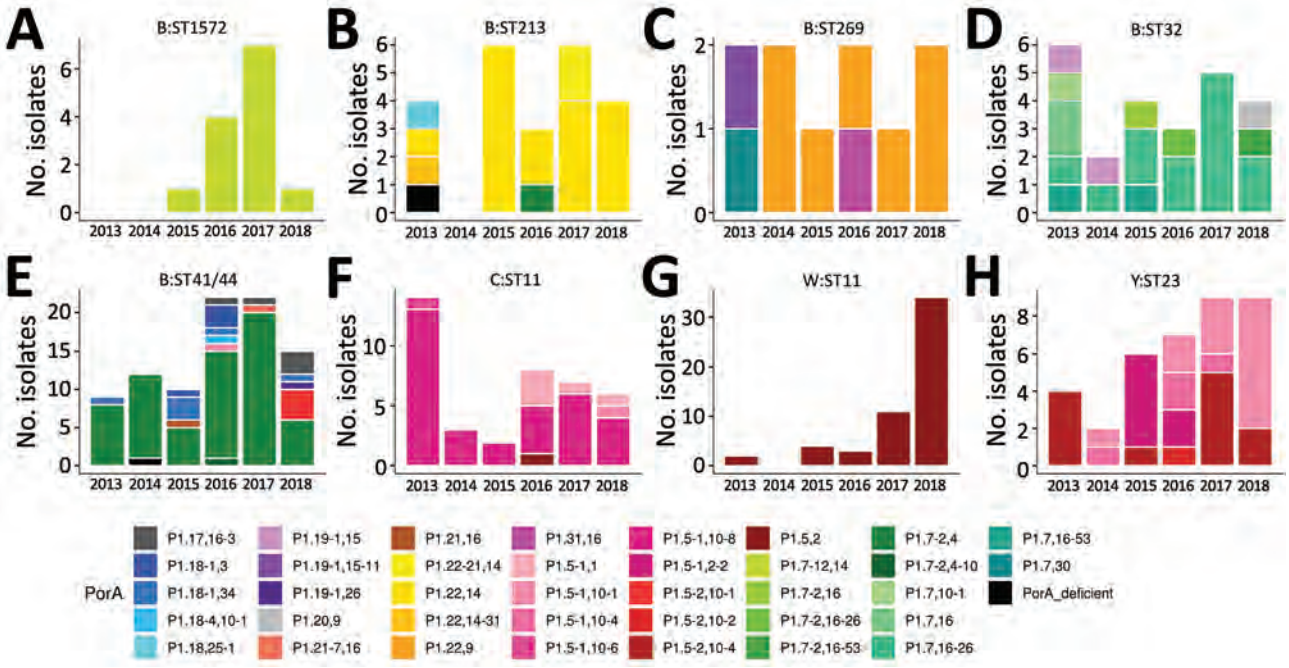

Figure 4. Diversity and prevalence of PorA variable region (VR) variants in common *Neisseria meningitidis* strains in New Zealand, 2013–2018. PorA VR1 and VR2 variant diversity and numbers of common strains are depicted. Strain is defined by group and clonal complex. Only strains with >10 isolates were analyzed.

Meningococcal disease continues to substantially affect the health of persons in New Zealand. In comparison with other developed countries (such as the United States, the United Kingdom, and the Netherlands, which have reported ≤1 case/100,000 population) (*42*–*45*), New Zealand still has a high rate of IMD notification. Although the rate of meningococcal disease in 2018 (2.5 cases/100,000 population) was substantially lower than the peak rate observed during the epidemic (17.4 cases/100,000 population in 2001), rates of IMD in New Zealand have increased since 2014 (Appendix 2 Figure 1).

The distribution of group Y disease and group W disease has changed over the past decade. Incidence of group Y disease has been increasing since the late 1990s in the Americas and since 2010 in Europe (*46*,*47*). The number and proportion of group Y disease in New Zealand began to increase in 2013 (2/85 [2%] in 2012 to 4/68 [6%] in 2013). The increase in group W:CC11 disease here was not significant until 2017 and 2018, when the number of group W cases more than tripled, from 10 to 33. In the United Kingdom, the original UK strain emerged in 2009; the descendant 2013 strain emerged in 2013 and expanded to other countries thereafter (*15*). These data suggest that IMD trends in New Zealand follow global trends with some delay, possibly because of geographic isolation. Therefore, for IMD monitoring in New Zealand, continued detailed typing of meningococcal isolates is critical for obtaining comparable data for participation in global meningococcal surveillance.

By using group and PorA type for strain definition, the diversity index for 2013–2018 period meningococci is slightly higher (Shannon–Wiener index 2.98) than that for 2008–2012, the 5-year period followingthe end of the epidemic (Shannon–Wiener index 2.81; data not shown). Since 2012, nonepidemic group B cases have regularly surpassed epidemic cases; 47% of group B cases were caused by nonepidemic strains during 2008–2011, and 63% were caused by nonepidemic strains during 2012–2018. The top 3 strains circulating within the nonepidemic group B cases were B:P1.22,14:F5–5:CC213 (13 isolates), B:P1.7,16–26:F3–3:CC32 (13 isolates), and B:P1.7–12,14:F1–7:CC1572 (12 isolates). All 3 strains are present in PubMLST. B:P1.22,14:CC213 is a common strain, however, only 2 isolates contain the FetA-VR:5–5 allele. PubMLST has 41 B: P1.7,16–26:F3–3:CC32 isolates and 6 B:P1.7–12,14:F1–7:CC1572 isolates (accessed November 3, 2020). Taken together, these data suggest that the meningococcal population in New Zealand has become more diverse after the group B epidemic. Comparison of New Zealand with other countries is challenging because no comprehensive public database exists that contains all

IMD cases with fine-typing information. The United Kingdom, however, has been depositing most of their IMD typing information into PubMLST since July 2010, and for 2013–2017, the dataset contains 2,790 records and 649 unique strains (group:PorA-VR1,PorA-VR2:FetA:CC, Shannon–Wiener index 4.45). This information suggests that the isolates that cause IMD are less diverse in New Zealand, which may reflect its smaller and more distributed population structure.

The clonal expansion of a new penicillin-resistant clade of W:CC11 was first identified in Australia in 2016 (*41*). Four isolates (PubMLST identification nos. 41966, 42206, 42409, 50313) that were found to be closely related to the Australia clade (cluster B) (*42*) are part of the 2015-strain cluster (Appendix 2 Figure 3), suggesting that the Western Australia clone belongs in the 2015-strain cluster. In our study, the New Zealand 2015-strain isolates were significantly less susceptible to penicillin compared with New Zealand isolates belonging to the original UK or the 2013 UK strain (Appendix 1 Table 8). The penA 253 allele was hypothesized to play a role in decreasing penicillin susceptibility in the new clade of W:CC11 found in Australia (*41*). All isolates in the 2015 variant cluster, except ERR1994517 from the United Kingdom, have the penA 253 allele (Appendix 1 Table 3), suggesting that penicillin resistance is a common characteristic of the 2015 strain. The presence of the penA 253 allele has consequences for the choice of antimicrobial drug to

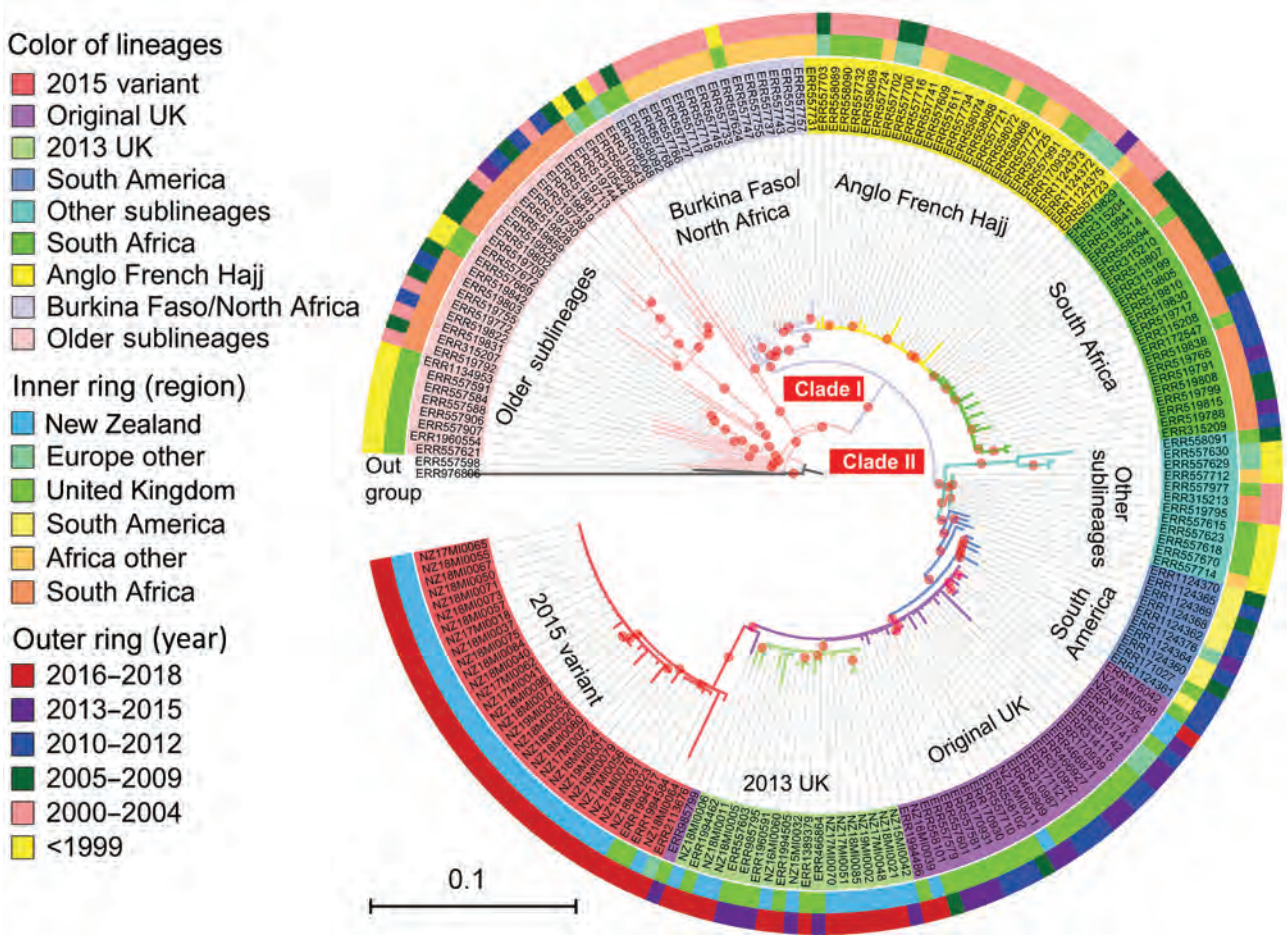

Figure 5. Phylogenetic position of New Zealand group W clonal complex 11 (W:CC11) *Neisseria meningitidis* isolates within the global W:CC11 major lineages. Maximum-likelihood phylogeny was generated by RAxML version 8.2.12 (*33*) on the basis of the core single-nucleotide polymorphism alignment of 198 W:CC11 isolates. Branches with a bootstrap (200 replications) value >90% are indicated with a red dot. Excluding the basal older sublineages, all other isolates form 2 strongly supported clades marked as clade I and clade II, which correspond to the Hajj strain sublineage and the South America strain sublineage. All the major defined lineages of W:CC11 are marked and indicated by consistent background color of isolate's identification number and branches. The inner ring and outer ring designate the region and year of isolation for each isolate. Scale bar indicates average number of substitutions per site.

treat IMD. At the end of 2018, a high rate of W:CC11 disease in the Northland area of New Zealand triggered a local vaccination campaign against the disease. Most of these cases were caused by the 2015 strain. Partly because of the increased penicillin resistance of the 2015 strain, in 2018 the New Zealand Ministry of Health recommended ceftriaxone as the first-choice antimicrobial drug for patients with suspected meningococcal disease (*48*).

W:CC11 meningococci are emerging as a diversifying lineage with several new strains occurring in different geographic locations (*10*,*11*,*41*). Phylogenetic analyses suggest that the 2015 strain is part of the major South America–UK (clade II) lineage (Figure 3; Appendix 2 Figure 3), most likely representing a clonal expansion from a single variant within the original UK strain. The increase in New Zealand group W cases is mainly attributable to the 2015 strain identified in this study. In contrast, the 2013 UK strain was largely responsible for the increases seen in Europe (*15*). We found the 2013 UK strain circulating in New Zealand but in low numbers (3/10 cases in 2017 and 6/33 cases in 2018). For reasons unknown, the 2015 strain, rather than the 2013 UK strain, is expanding in New Zealand. Invasive disease provides no selective advantage for meningococcal bacteria, and a strain must remain in carriage in order to expand in a population. The 2015 strain might have originated in the Australia or New Zealand region and is therefore better adapted to the population, either because of more favorable host immunity or climate and living conditions. Its carriage may have precluded expansion of the 2013 UK strain.

Genomic surveillance of *N. meningitidis* has revealed in great detail the genetic diversity and population structure of circulating meningococci in New Zealand; this more refined surveillance enables the tracking of specific strains that are identifiable only by high-resolution phylogenetic analysis. By using this approach, we identified a distinct globally circulating W:CC11 strain, which would not have been possible without genomic information. Our results emphasize the value of obtaining complete genetic information for invasive pathogens and resolving their global evolutionary relationship for identifying the origin and expansion of new pathogenic variants or strains. Such information will benefit surveillance and can be used to help prevent and control future epidemics.

Acknowledgments

We thank Yoryea Mantziou for her assistance in DNA sequencing; the staff of the Antibiotic Reference Laboratories, Institute of Environmental Science and Research, for antimicrobial susceptibility testing; and Kristin Dyet and Joanne Hewitt for their thoughtful comments and feedback.

This study was funded by Health Research Council grant no. 17-364, New Zealand.

This study used data from routine meningococcal surveillance activities conducted by the Institute of Environmental Science and Research under contract to the New Zealand Ministry of Health.

About the Author

Dr. Yang is a postdoctoral researcher at the Institute of Environmental Science and Research investigating the population genomics and evolution of the bacterial pathogen *N. meningitidis*. She is interested in using genome sequencing to address evolutionary questions such as tracing evolutionary history and population dynamics, as well as understanding genetic determinants of phenotypic variation.

References

1. Halperin SA, Bettinger JA, Greenwood B, Harrison LH, Jelfs J, Ladhani SN, et al. The changing and dynamic epidemiology of meningococcal disease. Vaccine. 2012;30 (Suppl 2):B26–36. https://doi.org/10.1016/j.vaccine.2011.12.032
2. Harrison LH, Trotter CL, Ramsay ME. Global epidemiology of meningococcal disease. Vaccine. 2009;27(Suppl 2):B51–63. https://doi.org/10.1016/j.vaccine.2009.04.063
3. Maiden MCJ, Bygraves JA, Feil E, Morelli G, Russell JE, Urwin R, et al. Multilocus sequence typing: a portable approach to the identification of clones within populations of pathogenic microorganisms. Proc Natl Acad Sci U S A. 1998;95:3140–5. https://doi.org/10.1073/pnas.95.6.3140
4. Waśko I, Hryniewicz W, Skoczyńska A. Significance of meningococcal hyperinvasive clonal complexes and their influence on vaccines development. Pol J Microbiol. 2015;64:313–21. https://doi.org/10.5604/17331331.1185912
5. Mustapha MM, Marsh JW, Krauland MG, Fernandez JO, de Lemos APS, Dunning Hotopp JC, et al. Genomic epidemiology of hypervirulent serogroup W, ST-11 *Neisseria meningitidis*. EBioMedicine. 2015;2:1447–55. https://doi.org/10.1016/j.ebiom.2015.09.007
6. Ladhani SN, Beebeejaun K, Lucidarme J, Campbell H, Gray S, Kaczmarski E, et al. Increase in endemic *Neisseria meningitidis* capsular group W sequence type 11 complex associated with severe invasive disease in England and Wales. Clin Infect Dis. 2015;60:578–85. https://doi.org/10.1093/cid/ciu881
7. Eriksson L, Hedberg ST, Jacobsson S, Fredlund H, Mölling P, Stenmark B. Whole-genome sequencing of emerging invasive *Neisseria meningitidis* serogroup W in Sweden. J Clin Microbiol. 2018;56:e01409–17. https://doi.org/10.1128/JCM.01409-17
8. Martin NV, Ong KS, Howden BP, Lahra MM, Lambert SB, Beard FH, et al.; Communicable Diseases Network Australia MenW Working Group. Rise in invasive serogroup W meningococcal disease in Australia 2013-2015. Commun Dis Intell Q Rep. 2016;40:E454–9.

9. Tsang RSW, Ahmad T, Tyler S, Lefebvre B, Deeks SL, Gilca R, et al. Whole genome typing of the recently emerged Canadian serogroup W *Neisseria meningitidis* sequence type 11 clonal complex isolates associated with invasive meningococcal disease. Int J Infect Dis. 2018;69:55–62. https://doi.org/10.1016/j.ijid.2018.01.019
10. Potts CC, Joseph SJ, Chang HY, Chen A, Vuong J, Hu F, et al. Population structure of invasive *Neisseria meningitidis* in the United States, 2011-15. J Infect. 2018;77:427–34. https://doi.org/10.1016/j.jinf.2018.06.008
11. Lucidarme J, Hill DMC, Bratcher HB, Gray SJ, du Plessis M, Tsang RSW, et al. Genomic resolution of an aggressive, widespread, diverse and expanding meningococcal group B, C and W lineage. J Infect. 2015;71:544–52. https://doi.org/10.1016/j.jinf.2015.07.007
12. Taha MK, Achtman M, Alonso JM, Greenwood B, Ramsay M, Fox A, et al. Serogroup W135 meningococcal disease in Hajj pilgrims. Lancet. 2000;356:2159. https://doi.org/10.1016/S0140-6736(00)03502-9
13. Weidlich L, Baethgen LF, Mayer LW, Moraes C, Klein CC, Nunes LS, et al. High prevalence of *Neisseria meningitidis* hypervirulent lineages and emergence of W135:P1.5,2:ST-11 clone in Southern Brazil. J Infect. 2008;57:324–31. https://doi.org/10.1016/j.jinf.2008.07.014
14. Lucidarme J, Scott KJ, Ure R, Smith A, Lindsay D, Stenmark B, et al. An international invasive meningococcal disease outbreak due to a novel and rapidly expanding serogroup W strain, Scotland and Sweden, July to August 2015. Euro Surveill. 2016;21:15–23. https://doi.org/10.2807/1560-7917.ES.2016.21.45.30395
15. Krone M, Gray S, Abad R, Skoczyńska A, Stefanelli P, van der Ende A, et al. Increase of invasive meningococcal serogroup W disease in Europe, 2013 to 2017. Euro Surveill. 2019;24:24. https://doi.org/10.2807/1560-7917.ES.2019.24.14.1800245
16. Devoy AF, Dyet KH, Martin DR. Stability of PorA during a meningococcal disease epidemic. J Clin Microbiol. 2005 ;43:832–7. https://doi.org/10.1128/JCM.43.2.832-837.2005
17. Dyet KH, Martin DR. Clonal analysis of the serogroup B meningococci causing New Zealand's epidemic. Epidemiol Infect. 2006;134:377–83. https://doi.org/10.1017/S0950268805004954
18. Sexton K, Lennon D, Oster P, Crengle S, Martin D, Mulholland K, et al. The New Zealand Meningococcal Vaccine Strategy: a tailor-made vaccine to combat a devastating epidemic. N Z Med J. 2004;117:U1015.
19. Loring BJ, Turner N, Petousis-Harris H. MeNZB vaccine and epidemic control: when do you stop vaccinating? Vaccine. 2008;26:5899–904. https://doi.org/10.1016/j.vaccine.2008.08.062
20. Institute of Environmental Science and Research Limited. Notifiable Diseases in New Zealand: Annual Report 2016. Porirua, New Zealand [cited 2020 Nov 3]. https://surv.esr.cri.nz/surveillance/annual_surveillance.php?we_objectID=4656
21. Bennett DE, Cafferkey MT. Consecutive use of two multiplex PCR-based assays for simultaneous identification and determination of capsular status of nine common *Neisseria meningitidis* serogroups associated with invasive disease. J Clin Microbiol. 2006;44:1127–31. https://doi.org/10.1128/JCM.44.3.1127-1131.2006
22. Oksanen G, Blanchet FG, Friendly M, Kindt R, Legendre P, McGlinn D, et al. Vegan: community ecology package [cited 2020 Nov 3]. https://CRAN.R-project.org/package=vegan
23. Bolger AM, Lohse M, Usadel B. Trimmomatic: a flexible trimmer for Illumina sequence data. Bioinformatics. 2014;30:2114–20. https://doi.org/10.1093/bioinformatics/btu170
24. Bankevich A, Nurk S, Antipov D, Gurevich AA, Dvorkin M, Kulikov AS, et al. SPAdes: a new genome assembly algorithm and its applications to single-cell sequencing. J Comput Biol. 2012;19:455–77. https://doi.org/10.1089/cmb.2012.0021
25. Kwong JC, Gonçalves da Silva A, Stinear TP, Howden BP, Seemann T. Meningotype: [cited 2020 Nov 3]. https://github.com/MDU-PHL/meningotype
26. Langmead B, Trapnell C, Pop M, Salzberg SL. Ultrafast and memory-efficient alignment of short DNA sequences to the human genome. Genome Biol. 2009;10:R25. https://doi.org/10.1186/gb-2009-10-3-r25
27. Picard toolkit. 2019 [cited 2020 Nov 3]. http://broadinstitute.github.io/picard
28. Okonechnikov K, Conesa A, García-Alcalde F. Qualimap 2: advanced multi-sample quality control for high-throughput sequencing data. Bioinformatics. 2016;32:292–4.
29. Garrison E. Vcflib [cited 2020 Nov 3]. https://github.com/vcflib/vcflib
30. Danecek P, Auton A, Abecasis G, Albers CA, Banks E, DePristo MA, et al.; 1000 Genomes Project Analysis Group. The variant call format and VCFtools. Bioinformatics. 2011;27:2156–8. https://doi.org/10.1093/bioinformatics/btr330
31. Quinlan AR, Hall IM. BEDTools: a flexible suite of utilities for comparing genomic features. Bioinformatics. 2010;26:841–2. https://doi.org/10.1093/bioinformatics/btq033
32. Treangen TJ, Ondov BD, Koren S, Phillippy AM. The Harvest suite for rapid core-genome alignment and visualization of thousands of intraspecific microbial genomes. Genome Biol. 2014;15:524. https://doi.org/10.1186/s13059-014-0524-x
33. Stamatakis A. RAxML version 8: a tool for phylogenetic analysis and post-analysis of large phylogenies. Bioinformatics. 2014;30:1312–3. https://doi.org/10.1093/bioinformatics/btu033
34. Felsenstein J. Confidence-limits on phylogenies—an approach using the bootstrap. Evolution. 1985;39:783–91. https://doi.org/10.1111/j.1558-5646.1985.tb00420.x
35. Didelot X, Wilson DJ. ClonalFrameML: efficient inference of recombination in whole bacterial genomes. PLOS Comput Biol. 2015;11:e1004041. https://doi.org/10.1371/journal.pcbi.1004041
36. Letunic I, Bork P. Interactive tree of life (iTOL) v3: an online tool for the display and annotation of phylogenetic and other trees. Nucleic Acids Res. 2016;44(W1):W242-5. https://doi.org/10.1093/nar/gkw290
37. Jolley KA, Bray JE, Maiden MCJ. Open-access bacterial population genomics: BIGSdb software, the PubMLST.org website and their applications. Wellcome Open Res. 2018;3:124. https://doi.org/10.12688/wellcomeopenres.14826.1
38. Bratcher HB, Corton C, Jolley KA, Parkhill J, Maiden MC. A gene-by-gene population genomics platform: de novo assembly, annotation and genealogical analysis of 108 representative *Neisseria meningitidis* genomes. BMC Genomics. 2014;15:1138. https://doi.org/10.1186/1471-2164-15-1138
39. Clinical and Laboratory Standards Institute. Performance standards for antimicrobial susceptibility testing: 28th edition (informational supplement M100). Wayne (PA): The Institute; 2018.
40. Zeileis A, Leisch F, Hornik K, Kleiber C, Hansen B, Zeileis MA. Package 'strucchange' [cited 2020 Nov 3]. https://CRAN.R-project.org/package=strucchange
41. Mowlaboccus S, Jolley KA, Bray JE, Pang S, Lee YT, Bew JD, et al. Clonal expansion of new penicillin-resistant

clade of *Neisseria meningitidis* serogroup W clonal complex 11, Australia. Emerg Infect Dis. 2017;23:1364–7. https://doi.org/10.3201/eid2308.170259
42. Whaley MJ, Joseph SJ, Retchless AC, Kretz CB, Blain A, Hu F, et al. Whole genome sequencing for investigations of meningococcal outbreaks in the United States: a retrospective analysis. Sci Rep. 2018;8:15803. https://doi.org/10.1038/s41598-018-33622-5
43. Public Health England. Invasive meningococcal disease in England: annual laboratory confirmed reports for epidemiological year 2017 to 2018. London: Public Health England; 2018 [cited 2020 Nov 3]. https://assets.publishing.service.gov.uk/government/uploads/system/uploads/attachment_data/file/751821/hpr3818_IMD.pdf
44. Knol MJ, de Melker HE, Berbers GAM, van Ravenhorst MB, Ruijs WLM, van Vliet JA. Meningococcal disease in the Netherlands: background information for the Health Council. RIVM Report 2017–0031. 2017 [cited 2020 Nov 03]. https://www.rivm.nl/bibliotheek/rapporten/2017-0031.pdf
45. Knol MJ, Hahné SJM, Lucidarme J, Campbell H, de Melker HE, Gray SJ, et al. Temporal associations between national outbreaks of meningococcal serogroup W and C disease in the Netherlands and England: an observational cohort study. Lancet Public Health. 2017;2:e473–82. https://doi.org/10.1016/S2468-2667(17)30157-3
46. Leimkugel J, Racloz V, Jacintho da Silva L, Pluschke G. Global review of meningococcal disease. A shifting etiology. J Bacterial Res. 2009;1:6–18.
47. Bröker M, Jacobsson S, Kuusi M, Pace D, Simões MJ, Skoczynska A, et al. Meningococcal group Y emergence in Europe: update 2011. Hum Vaccin Immunother. 2012;8:1907–11. https://doi.org/10.4161/hv.21794
48. Ministry of Health Manatū Hauora. Change to treatment recommendations for meningococcal disease. 2018 Nov 30 [cited 2020 Nov 3]. https://www.health.govt.nz/news-media/news-items/change-treatment-recommendations-meningococcal-disease

Address for correspondence: Philip E. Carter, Invasive Pathogens Laboratory, Institute of Environmental Science and Research, 34 Kenepuru Dr, Porirua, New Zealand; email: Philip.Carter@esr.cri.nz

Dynamic Public Perceptions of the Coronavirus Disease Crisis, the Netherlands, 2020

Marion de Vries, Liesbeth Claassen, Margreet J.M. te Wierik, Susan van den Hof, Anne E.M. Brabers, Judith D. de Jong, Danielle R.M. Timmermans,[1] Aura Timen[1]

A key component of outbreak control is monitoring public perceptions and public response. To determine public perceptions and public responses during the first 3 months of the coronavirus disease (COVID-19) outbreak in the Netherlands, we conducted 6 repeated surveys of ≈3,000 persons. Generalized estimating equations analyses revealed changes over time as well as differences between groups at low and high risk. Overall, respondents perceived the risks associated with COVID-19 to be considerable, were positive about the mitigation measures, trusted the information and the measures from authorities, and adopted protective measures. Substantial increases were observed in risk perceptions and self-reported protective behavior in the first weeks of the outbreak. Individual differences were based mainly on participants' age and health condition. We recommend that authorities constantly adjust their COVID-19 communication and mitigation strategies to fit public perceptions and public responses and that they tailor the information for different groups.

Since December 2019, the world has been facing a new and severe threat to public health. Severe acute respiratory syndrome coronavirus 2 (SARS-CoV-2), which causes mild to severe respiratory illness (coronavirus disease [COVID-19]), was first found in humans in Wuhan, China (*1*). The virus spread rapidly over the world, and on March 11, 2020, the World Health Organization declared a COVID-19 pandemic (*2*). Globally, by January 23, 2021, a total of 96,877,399 cases had been confirmed, including 2,098,879 deaths (*3*). The risks associated with COVID-19 are not equally distributed; some regions (within and between countries) are more strongly affected than others, health workers are at increased risk for infection, and elderly persons with certain chronic underlying conditions and men are at increased risk for severe COVID-19 illness and death (*4*).

During the COVID-19 pandemic, countries all over the world rapidly adopted various measures to counter the spread of the virus. In the initial (containment) stage, the measures were aimed at identifying and isolating new cases. As the number of cases started to rise quickly, countries announced additional social distancing measures. Many countries undertook stringent mitigation measures, such as closing schools and restaurants, restraining domestic and foreign travel, and, for some, implementing a total lockdown of the society (*5*). For these measures to be effective, governments rely strongly on the support and compliance of the general public.

To maintain support for the protective measures for a longer period, governments need insights into the dynamics of public perceptions (regarding the risks associated with COVID-19 and the recommended protective measures) and the trust in the authorities who imposed these measures. These perceptions and trust influence the public's compliance with the measures (*6*) and are essential indicators for public sentiments and information needs. Such insights enable optimal adaptation and tailoring of risk and crisis communication (*7*–*10*). The first publications about public perceptions of and responses to the COVID-19 pandemic are, to our knowledge, all cross-sectional and do not provide insights into the dynamics (*11*–*19*). Previous studies about the 2009 influenza A(H1N1) pandemic showed considerable changes in, among other things, perceptions of risk, trust in authorities, and self-reported protective behavior over a longer crisis period (*20*–*25*).

Author affiliations: National Institute for Public Health and the Environment (RIVM), Bilthoven, the Netherlands (M. de Vries, L. Claassen, M.J.M. te Wierik, S. van den Hof, A. Timen); Netherlands Institute for Health Services Research, Utrecht, the Netherlands (A.E.M. Brabers, J.D. de Jong); Maastricht University, Maastricht, the Netherlands (J.D. de Jong); Amsterdam UMC, Amsterdam, the Netherlands (D.R.M. Timmermans); Vrije Universiteit Amsterdam, Amsterdam (A. Timen)

DOI: https://doi.org/10.3201/eid2704.203328

[1]These authors contributed equally to this article.

Our study focused on public perceptions, trust, and behavior in the first 3 months of the COVID-19 crisis in the Netherlands. Our main research question asked about the evolution of public perceptions of COVID-19, perceptions of control measures, trust in authorities, and self-reported protective behavior between the onset of the outbreak and the first relaxations of government measures. We discuss these findings in light of the epidemiologic curve of COVID-19 in the Netherlands and the government outbreak response during February–May 2020 (Figure 1). In addition, we explored differences in perceptions, trust, and self-reported behavior between groups of persons at different levels of risk. Therefore, our second research question asked whether persons differ in their perceptions of COVID-19, perceptions of the control measures, trust in authorities, and self-reported protective behavior on the basis of their age, sex, region of residence, health condition, and health sector employment.

Methods

Case Study

The first COVID-19 case in the Netherlands was identified on February 27, 2020 (*26*). In the following weeks, the number of confirmed cases increased rapidly (*27*,*28*) and the number of cases between regions differed considerably. The 12 provinces in the Netherlands can be roughly divided into 4 regions: north, east, south, and west. Through May 17, the region most strongly affected by the COVID-19 outbreak was the southern region (58–63 deaths/100,000 residents), especially compared with the northern region (3–9 deaths/100,000 residents). The eastern region reported 19–31 deaths/100,000 residents and the western region 16–30 deaths/100,000 residents (*29*).

After the first case of COVID-19 was reported, the government issued various measures that increased in stringency through March 23, 2020. When a sustained

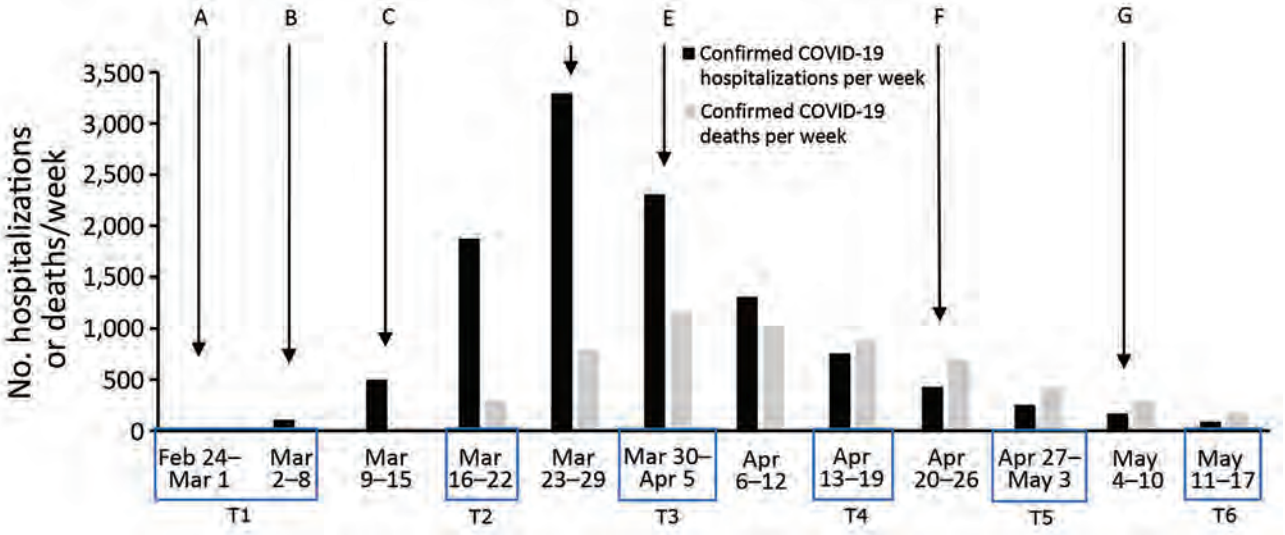

Figure 1. Course of COVID-19 in the Netherlands, February 24–May 17, 2020. COVID-19 hospitalizations and deaths are shown by week (data from https://www.rivm.nl/coronavirus-covid-19/grafieken). Blue boxes labeled T1–T6 along baseline indicate timing of data collection for this study. Letters indicate implementations and relaxations of COVID-19 protective measures announced by the Netherlands government in press conferences on national television (data from https://www.acaps.org/covid19-government-measures-dataset and https://www.rijksoverheid.nl/onderwerpen/coronavirus-covid-19; a selection of the measures is shown): A) All residents asked to self-isolate after receiving a COVID-19 diagnosis or if living in a household with a confirmed COVID-19 patient. B) Residents of Noord-Brabant Province (southern Netherlands) asked to self-isolate when experiencing symptoms. C) All residents experiencing symptoms asked to self-isolate, work at home as much as possible, keep distance from others. Gatherings of >100 persons prohibited; various public places closed, including (pre) schools and universities, restaurants and bars, sports clubs. D) All residents asked to stay at home as much as possible, self-quarantine when someone in the household has a fever or dyspnea. All gatherings prohibited; professions that require direct contact, such as hairdressers and masseurs, prohibited; visiting nursing homes prohibited. In some areas, mayors can prohibit groups of >3 persons who do not maintain 1.5-m distance from each other (except members of the same household). Law-enforcement allowed to fine those who do not adhere to the measures. E) All measures extended through April 28. F) Children allowed to play sports outside in groups starting April 29. Preschools and primary schools reopen (partly) starting May 11. All other measures extended through May 19. G) Starting May 11, the advice "stay at home as much as possible" replaced with the advice "avoid crowds"; gatherings up to 30 persons allowed (with 1.5-m distance); most professions that require direct contact can resume working, with extra precautions. Not indicated: Starting June 1, restaurants and bars reopen (maximum 30 persons/establishment and with 1.5-m distance); primary schools reopen (all days of the week); gatherings up to 100 persons allowed (with 1.5-m distance). COVID-19, coronavirus disease.

decrease in the number of cases, hospitalizations, and deaths was reached (May 11, 2020), the government gradually relaxed measures (Figure 1).

Study Population and Procedure

We conducted 6 repeated online surveys among members of the Dutch Health Care Consumer Panel (*30*). The panel consists of ≈11,000 residents of the Netherlands (≥18 years of age) who had been invited to participate on the panel on the basis of a random selection of name and address data or were invited to participate by their general practitioner. The panel population is regularly renewed, and persons cannot enroll themselves without an invitation. As a result of oversampling of persons >65 years of age for other research purposes and underparticipation of persons <30 years of age, the median age of the panel population is 65 years (range 19–101 years).

The 6 repeated surveys were added to a weekly online survey that monitors influenza-like symptoms. The invitations for the first survey (time 1 [T1]) of the weekly monitor was sent to all 10,993 active panel members, who could complete the survey from February 24 through March 9, 2020. In the first survey, respondents could indicate whether they wanted to be invited for the consequent weekly surveys; those who indicated "yes" received a weekly invitation for all follow-up surveys. Participation in each survey was voluntary and did not depend on participation in previous surveys. The follow-up surveys with the variables addressed in this study were completed during March 16–23 (T2), March 30–April 5 (T3), April 14–19 (T4), April 28–May 3 (T5), and May 11–17 (T6) (Figure 1).

Before joining the panel population, potential panel members actively consented to participation and data sharing; they were informed about the

Table 1. An overview of the survey questions and corresponding measurements used to assess dynamic public perceptions of the coronavirus disease crisis, the Netherlands, 2020*

Topic, variable	Survey question (answer category)
Perceptions of COVID-19	
Perceived probability COVID-19	In your opinion, how likely is it that you will become ill due to the new coronavirus in the next 12 months? (1. very unlikely—5. very likely)
Perceived severity of	How severe would it be to you if you develop one of the following diseases in the next 12 months? (1. Not severe at all—5. Very severe)†
Flu	Flu
COVID-19	Disease due to the novel coronavirus
Ebola	Ebola
Concerns about	Are you concerned due to the new coronavirus … (1. Not at all concerned—5. Very concerned)
Own health	About your own health?
Health of family members	About the health of your family members?
Perceptions of control measures	
Perception that sufficient measures are taken	Do you think that the Netherlands is currently taking sufficient measures to control the spread of the new coronavirus? (1. Certainly not—5. Certainly yes)‡
Perceptions of the recommended measures§	Below there are several statements about the measures advised by the government to control the spread of the coronavirus. Please state what you think about these statements. (1. Certainly not—5. Certainly yes)
Measures are effective	I think the recommended measures help to control the spread of the coronavirus
Most others adhere to measures	Most people close to me adhere to the recommended measures.
Difficult to adhere to measures	I find it difficult to adhere to the recommended measures.
Trust in authorities	
Trust in information from the National Institute for Public Health and the Environment (RIVM)§	How much trust do you have in the information from the National Institute for Public Health and the Environment (RIVM) about the new coronavirus? (1. No trust—5. A lot of trust)
Trust in government measures§	How much trust do you have in the measures that the government is taking to control the spread of the new corona virus? (1. No trust—5. A lot of trust)
Self-reported protective behavior	
Adopted protective measures	Have you taken measures to protect yourself or your family members from the new coronavirus? (1. No / 2. Yes, namely…)
Adherence to recommended measures§	Do you adhere to the guidelines advised by the government to control the spread of the new coronavirus? (1. Yes / 2. Partly / 3. No / 4. Don't know)¶

*COVID-19, coronavirus disease; Flu, influenza; T1–T6, surveys 1–6.
†Adapted from previous studies on public responses to influenza A(H1N1) (*25*) and Ebola (*32*) to allow for comparison with previous crises and to place the perceived severity of COVID-19 into context with other diseases. These are, from an expert's perspective, less severe (flu) and more severe (Ebola) infectious diseases than COVID-19.
‡Formulated in T1 and T2 as "Do you think that the Netherlands is currently taking sufficient measures to prevent the spread of the new coronavirus?"
§Not assessed at T1 and T2.
¶The answer categories "partly," "no," and "don't know" were merged into 1 value next to the value "yes" because of low response frequencies to the categories "no" and "don't know."

purpose and content of the survey and that they could skip questions or stop participating at any time. Completing the survey, including answering questions about influenza-like symptoms, took an average of 8 minutes. The Clinical Expertise Centre at the National Institute for Public Health and the Environment (RIVM; Bilthoven, the Netherlands) determined that this research was exempt from needing further approval from an ethics research committee (reference no. LCI-451). The gathered data were analyzed and processed according the General Data Protection Regulation. More elaborate descriptions of the data collection are published elsewhere (*31*) and provided in the Appendix (https://wwwnc.cdc.gov/EID/article/27/4/20-3328-App1.pdf).

Variables

The survey questions addressed public perceptions of COVID-19, perceptions of control measures, trust in authorities, and self-reported protective behavior. The T3 survey and subsequent surveys were supplemented with extra questions about control measures and about trust in authorities (Table 1).

The factors that put persons at increased risk for COVID-19 were operationalized as sex (male/female), age group (<50, 50–69, or ≥70 years of age), region of residence (north, east, west, south; variable determined on the basis of postal codes), employment in healthcare (assessed at T1 with the question "Do you currently work in the healthcare sector?: no/yes"), and underlying health condition [assessed at T1 with the question "Please mark the disease(s) or condition(s) you have below. (Multiple answers possible): A) chronic respiratory disease; B) serious heart disease or myocardial infarction; C) diabetes; D) an allergy such as hay fever, dust mite allergy, or pet allergy; E) other long-term or chronic condition, namely: … F). I don't have any diseases or conditions)."]. The last variable was recoded as "underlying health condition" if respondents answered A, B, C, or E; all others were coded as "no underlying health condition."

Analyses

We computed descriptive statistics for each variable in T1–T6 (Table 1). To study changes over time and differences between persons in these variables, we performed generalized estimating equation (GEE) analyses (with exchangeable correlation matrix). We performed linear (for dependent variables with a 5-point Likert scale) and logistic (for dependent variables with binary outcomes) GEE analyses. The independent variables were time (T1–T6), sex, age group, region of residence, underlying health condition, and employment in healthcare. All GEE analyses were controlled for education level and income. To observe all changes between the subsequent waves, we repeated all GEE analyses with different reference groups for time (T1, T3, and T5). We excluded from analysis respondents who participated in T1 but did not consent to be invited to participate in the follow-up surveys.

Table 2. Characteristics of respondents to the first survey who consented to participation and were invited to participate in successive surveys used to assess dynamic public perceptions of the coronavirus disease crisis, the Netherlands, 2020*

Characteristic	No. (%)
Sex	
M	1,644 (50)
F	1,624 (50)
Age, y	
<30	24 (1)
30–49	530 (16)
50–69	1,220 (37)
≥70	1,494 (46)
Education level*	
Low	336 (10)
Middle	1,528 (47)
High	1,352 (41)
Unknown	52 (2)
Monthly household income, €	
<1,750	661 (20)
1,750–2,700	1,078 (33)
>2,700	1,399 (43)
Unknown	130 (4)
Region of residence	
North	539 (16)
East	738 (23)
South	655 (20)
West	1,320 (40)
Unknown	16 (1)
Underlying health condition	
Present	1,567 (48)
Absent	1,649 (50)
Unknown	52 (2)
Work in healthcare	
Yes	359 (11)
No	2,886 (88)
Unknown	23 (1)
Total	3,268 (100)

*Operationalization (*33*).

Results

Study Population

Of the 10,993 persons invited to participate, 4,325 (39%) completed the first survey. Of note, 2,052 respondents completed the first survey before February 27, 2020 (when the first COVID-19 case in the Netherlands was confirmed). A total of 3,268 (30%) consented to be invited for the follow-up surveys, of which 2,592 participated in T2 (79%), 2,710 in T3 (83%), 2,726 in T4 (83%), 2,654 in T5 (81%), and 2,705 in T6 (83%) (*33*) (Table 2; Appendix).

Perceptions of COVID-19

Overall, respondents perceived acquiring COVID-19 as probable and considerably severe (Figure 2). The perceived severity of COVID-19 was more similar to that of Ebola than that of influenza. Concerns about their own health were substantial, and concerns about the health of family members were even more so.

The most considerable change in the perceptions of COVID-19 was seen between T1 and T2; the mean perceived probability of COVID-19, concerns about one's own health, and concerns about family members increased considerably. Perceived severity of COVID-19 increased (significantly) only between T2 and T3. Between T3 and T6, perceptions of COVID-19 were largely stable, except for a slight but significant decrease in concerns.

Perceptions of Control Measures

Overall, respondents thought that the Netherlands undertook sufficient measures to control the spread of COVID-19, perceived the recommended measures as effective, thought that most others adhered to the measures, and did not perceive adhering to the measures as difficult (Figure 3). The perception that the Netherlands was taking sufficient measures changed nonlinearly between T1 and T6. Perception of measure effectiveness followed a pattern similar to the perception that sufficient measures were taken; it slightly increased between T3 and T4 and slightly decreased between T5 and T6. The perception that most others adhere to the measures decreased gradually between T3 and T6, and the perceived difficulty of adhering to the measures increased slightly between T3 and T5.

Trust in Authorities

Overall, trust in the information from RIVM and in the measures taken by the government was fairly high (Figure 4). A slight decrease in trust in the information from RIVM was observed between T4 and T5. Trust in the measures from the government slightly increased between T3 and T4 and slightly decreased between T5 and T6.

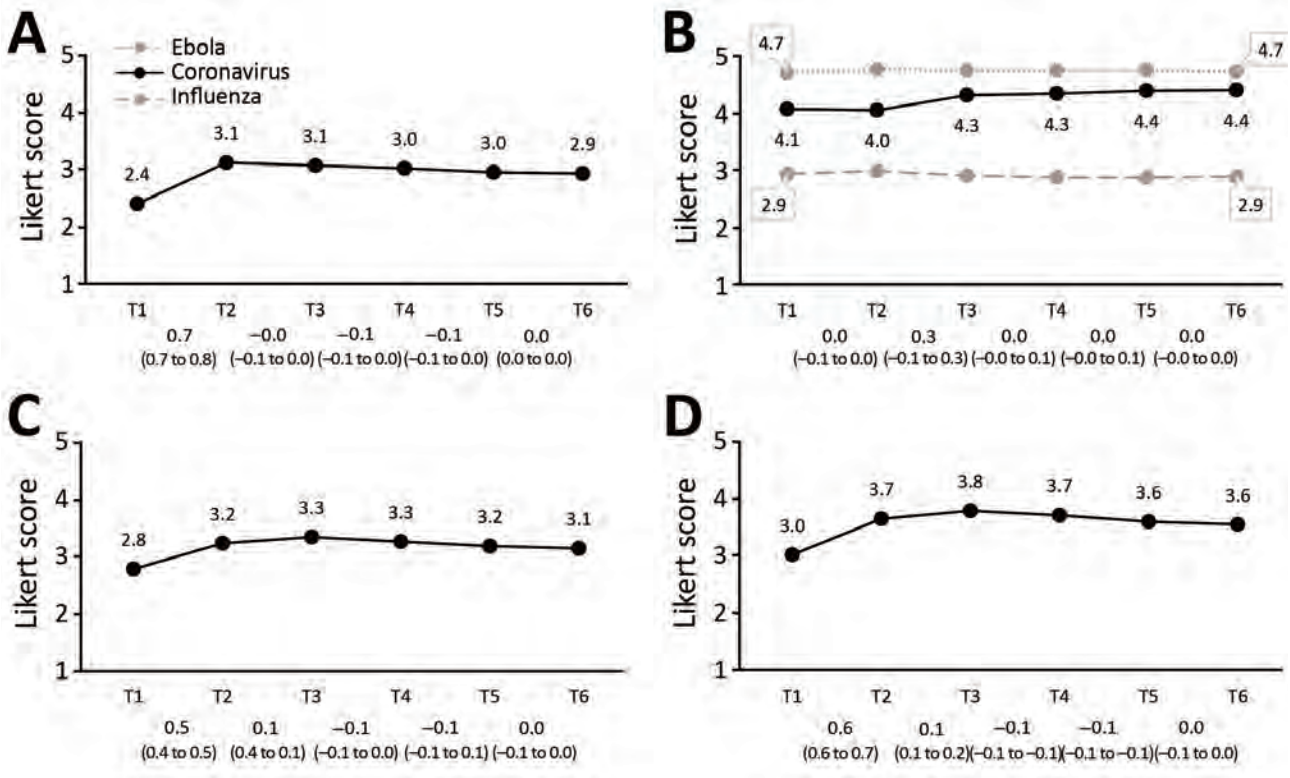

Figure 2. Perceptions of COVID-19 in the Netherlands. A) Perceived probability of COVID-19; B) perceived severity of influenza, coronavirus disease, Ebola; C) concerns about own heath; D) concerns about health of family members. Mean values per survey are shown above the graph line. Note that the 95% CIs around the mean estimates could not be shown on the figure because the 95% CIs are very close to the mean estimates (upper values of <mean + 0.1 and lower values of >mean – 0.1). All 95% CIs around the mean estimates are shown in Appendix Table 2 (https://wwwnc.cdc.gov/EID/article/27/4/20-3328-App1.pdf). Changes between subsequent surveys, based on generalized estimating equation analyses, are shown below the baselines as β and 95% CIs. The coefficients and 95% CIs shown in Figure 3, panel B, are generalized estimating equation results with perceived severity of coronavirus disease as the dependent variable. COVID-19, coronavirus disease.

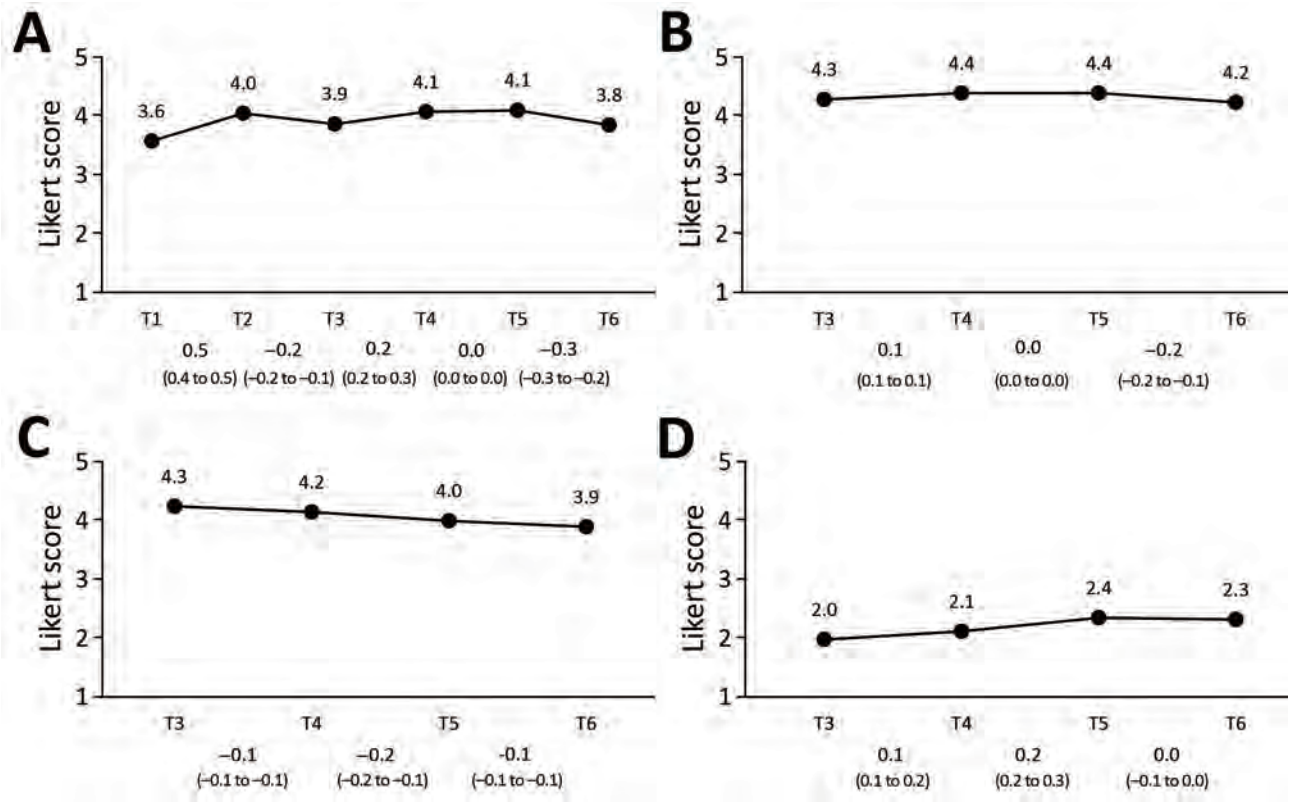

Figure 3. Perceptions of coronavirus disease control measures in the Netherlands. A) Sufficient measures are taken; B) measures are effective; C) most others adhere to measures; D) difficult to adhere to measures. Mean values per survey are shown above the graph line. Note that the 95% CIs around the mean estimates could not be shown in the figure because the 95% CIs are very close to the mean estimates (upper values of <mean + 0.1 and lower values of >mean – 0.1). All 95% CIs around the mean estimates are shown in Appendix Table 2 (https://wwwnc.cdc.gov/EID/article/27/4/20-3328-App1.pdf). Changes between subsequent surveys, based on generalized estimating equation analyses, are shown below the baselines as β and 95% CIs.

Self-Reported Protective Behavior

From T1 through T2, the proportion of respondents who indicated that they took measures to protect themselves or their family members against SARS-CoV-2 increased drastically, from 17% to 79% (Figure 5). From T2 through T3, this percentage increased further, to 88%, and consequently decreased to 80% at T6. Likewise, from T3 through T6, the proportion of respondents who indicated that they (fully) adhered to the recommended guidelines declined gradually from 94% to 85%.

Differences Based on Risk Factors

The most notable differences between persons in terms of perceptions (Tables 3, 4), trust in authorities (Table 5), and self-reported protective behavior (Table 6) were based on age. Compared with persons <50 years of age, those 50–69 and ≥70 years of age perceived acquisition of COVID-19 as being less probable and COVID-19 as more severe and were more concerned about their own health. In addition, respondents ≥70 years of age were also more likely to perceive the government's measures as sufficient, effective, and adhered to by most others and were less likely to perceive adhering to the measures as difficult. That difference in perceived difficulty was also observed for those 50–69 compared with those <50 years of age. Participants ≥70 years of age also experienced more trust in authorities and were more likely to adhere to the guidelines.

We observed several differences between respondents with and without an underlying health condition. Respondents with an underlying health condition perceived acquisition of COVID-19 as being more probable and COVID-19 as being more severe, and they were more concerned about their own health and that of family members. These respondents also perceived that measures taken were less sufficient, had less trust in authorities, and were slightly more likely to have adopted protective measures.

Some additional small differences were observed on the basis of sex, region, and employment.

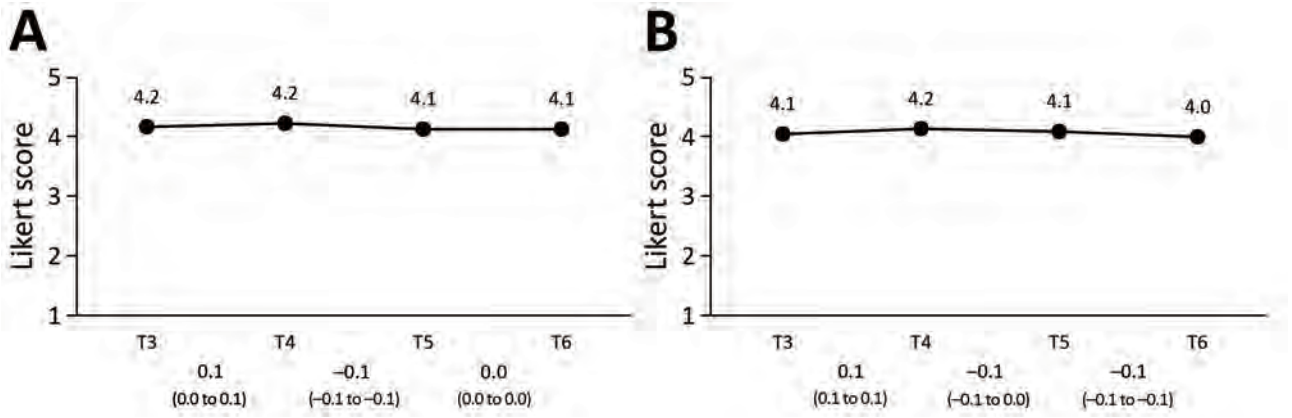

Figure 4. Trust in authorities in the Netherlands. A) Trust information from National Institute for Public Health and the Environment (RIVM), Bilthoven, the Netherlands; B) trust government measures. Mean values per survey are shown above the graph line. Note that the 95% CIs around the mean estimates could not be shown in the figure because the 95% CIs are very close to the mean estimates (upper values of <mean + 0.1 and lower values of >mean – 0.1). All 95% CIs around the mean estimates are shown in Appendix Table 2 (https://wwwnc.cdc.gov/EID/article/27/4/20-3328-App1.pdf). Changes between subsequent surveys, based on generalized estimating equation analyses, are shown below the baselines as β and 95% CIs.

Women perceived the probability of acquiring and severity of COVD-19 as being somewhat greater than did men and were slightly more concerned about family members. In addition, women were somewhat more positive about the measures (sufficient, effective, and adhered to by others) and were more likely to have adopted protective measures. Compared with residents from the northern region of the Netherlands, residents from the southern region were slightly more concerned about their own health, and residents from the eastern region had somewhat more trust in authorities. The only difference based on employment in the healthcare sector was seen in perceived probability of a SARS-CoV-2 infection (slightly higher among healthcare workers).

Discussion

Our results suggest that during the first wave of COVID-19, persons in the Netherlands generally perceived the risks posed by COVID-19 as considerable, were positive about the measures taken by the government to control the spread of COVID-19, trusted the information and the measures from the authorities in charge of the control policy, and adopted protective behavior. Public perceptions and behavior changed between the onset of the crisis and the initial relaxation of measures, particularly in the first phase of the outbreak. Differences between persons were mostly seen on the basis of age and underlying health conditions.

The changes in public perceptions, trust, and behavior need to be interpreted in light of the rapid

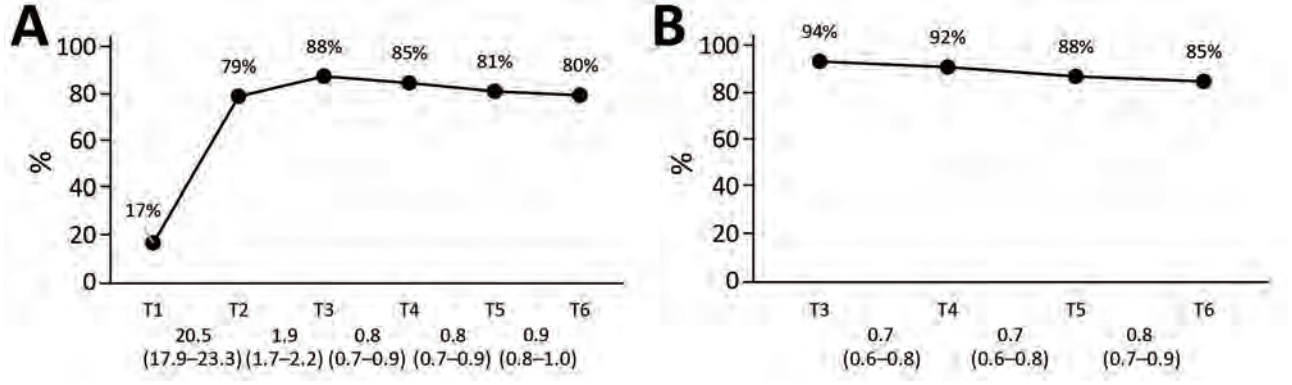

Figure 5. Self-reported coronavirus disease protective behavior in the Netherlands. A) Self-reported protective measures taken; B) self-reported adherence to guidelines. Mean values per survey are shown above the graph line. Note that the 95% CIs around the mean estimates could not be shown in the figure because the 95% CIs are very close to the mean estimates (upper values of <mean + 0.1 and lower values of >mean – 0.1). All 95% CIs around the mean estimates are shown in Appendix Table 2 (https://wwwnc.cdc.gov/EID/article/27/4/20-3328-App1.pdf). Changes between subsequent surveys, based on generalized estimating equation analyses, are shown below the baselines as odds ratios and 95% CIs.

Table 3. Differences in perceptions of COVID-19 based on sex, age, region of residence, health condition, and healthcare employment determined in assessment of dynamic public perceptions of the coronavirus disease crisis, the Netherlands, 2020*

Independent variable	Perceived probability of COVID-19, β (95% CI)	Perceived severity of COVID-19, β (95% CI)	Concerns about own health, β (95% CI)	Concerns about health of family members, β (95% CI)
Female vs. male	**0.1 (0.1 to 0.1)**	**0.1 (0.1 to 0.2)**	0.1 (0 to 0.1)	**0.2 (0.1 to 0.2)**
Age, y				
≥70 vs. <50	**–0.3 (–0.4 to –0.3)**	**0.6 (0.5 to 0.7)**	**0.4 (0.3 to 0.4)**	0 (−0.1 to 0)
50–69 vs. <50	**–0.2 (–0.3 to –0.2)**	**0.4 (0.3 to 0.4)**	**0.2 (0.1 to 0.2)**	−0.1 (−0.2 to 0)
Region				
Southern vs. northern	0 (−0.1 to 0.1)	0.1 (0 to 0.2)	**0.1 (0.1 to 0.2)**	0.1 (0 to 0.2)
Western vs. northern	0 (−0.1 to 0.1)	0.1 (0 to 0.1)	0.1 (0 to 0.1)	0 (0 to 0.1)
Eastern vs. northern	0 (0 to 0.1)	0 (0 to 0.1)	0 (−0.1 to 0.1)	0 (−0.1 to 0.1)
Health condition vs. no health condition	**0.2 (0.1 to 0.2)**	**0.1 (0.1 to 0.2)**	**0.4 (0.3 to 0.4)**	**0.2 (0.2 to 0.3)**
Work in healthcare vs. not in healthcare	**0.1 (0.1 to 0.2)**	−0.1 (−0.2 to 0)	−0.1 (−0.2 to 0)	0 (−0.1 to 0.1)

*Survey questions shown in Table 1. Boldface indicates 95% CIs that do not include 0. COVID-19, coronavirus disease.

developments in the epidemiologic curve of COVID-19 and the outbreak response during this study (Figure 1). After the first confirmed COVID-19 case (February 27, 2020), the outbreak unfolded rapidly and stringent control measures were issued during live press conferences on national television (March 12 and 15). These developments are probably reflected in the observed increases in the respondents' perceived probability of acquiring COVID-19, concerns, and self-reported protective behavior in this period. Up to the end of March/beginning of April, the number of COVID-19 cases rose rapidly, as did the number of hospitalizations, intensive care unit admissions, and deaths. The increased visibility of severe COVID-19 illness and death during this period might have increased perceptions of severity (which had remained stable in the first weeks).

As the number of cases, hospitalizations, intensive care unit admissions, and deaths gradually declined at the beginning of May, the government announced gradual relaxations of the control measures. During this period, the number of respondents who reported having taken protective measures and adhered to the recommended guidelines declined. This change in protective behavior is not likely to be explained by a change in risk perception, perception of the efficacy of the measures, or trust in authorities (factors shown to influence behavior during disease outbreaks [*6*,*9*,*13*]) because these factors were stable during this period. This change in behavior might be partly explained by a decrease in the public's perceived self-efficacy (*6*,*34*) because during this period we observed an increase in the public's perceived difficulty of adhering to the measures.

More recent research in the Netherlands has shown that in the months after our study, persons perceived it to be increasingly difficult to adhere to several of the control measures (*35*). Although the perceived difficulty of not shaking hands and practicing proper handwashing remained relatively stable, the perceived difficulty of maintaining a 1.5-m distance from others increased considerably from mid-April through mid-July 2020. Another study also found fairly high compliance with hygiene measures during the COVID-19 pandemic, along with limited compliance on social distancing measures (*36*). This finding might be explained by the assumed negative effect of social distancing on mental health and loneliness

Table 4. Differences in perceptions of control measures based on sex, age, region of residence, health condition, and healthcare employment determined in assessment of dynamic public perceptions of the coronavirus disease crisis, the Netherlands, 2020*

Independent variable	Sufficient measures are taken, β (95% CI)	Measures are effective, β (95% CI)	Most others adhere to measures, β (95% CI)	Difficult to adhere to measures, β (95% CI)
Female vs. male	**0.1 (0.1 to 0.2)**	**0.1 (0.1 to 0.2)**	**0.2 (0.2 to 0.2)**	−0.1 (−0.1 to 0)
Age, y				
≥70 vs. <50	**0.2 (0.2 to 0.3)**	**0.2 (0.1 to 0.2)**	**0.2 (0.2 to 0.3)**	**–0.2 (–0.3 to –0.1)**
50–69 vs. <50	0.1 (0 to 0.2)	0.1 (0 to 0.1)	0.1 (0 to 0.2)	**–0.3 (–0.4 to 0.2)**
Region				
Southern vs. northern	0 (−0.1 to 0.1)	0 (−0.1 to 0.1)	−0.1 (−0.1 to 0)	0 (−0.1 to 0.1)
Western vs. northern	0 (−0.1 to 0.1)	0 (−0.1 to 0.1)	−0.1 (−0.1 to 0)	0 (−0.1 to 0.1)
Eastern vs. northern	0.1 (0 to 0.2)	0.1 (0 to 0 1)	0 (−0.1 to 0)	0 (−0.1 to 0.1)
Health condition vs. no health condition	**–0.2 (–0.2 to –0.1)**	−0.1 (−0.1 to 0)	−0.1 (−0.1 to 0)	0 (−0.1 to 0.1)
Work in healthcare vs. not in healthcare	0.1 (0 to 0.1)	0 (−0.1 to 0.1)	0 (−0.1 to 0.1)	0.1 (0 to 0.2)

*Actual survey questions shown in Table 1. Boldface indicates 95% CIs that do not include 0. COVID-19, coronavirus disease.

Table 5. Differences in trust in authorities based on sex, age, region of residence, health condition, and healthcare employment determined in assessment of dynamic public perceptions of the coronavirus disease crisis, the Netherlands, 2020*

Independent variable	Trust RIVM information, β (95% CI)	Trust government measures, β (95% CI)
Female vs. male	0.1 (0 to 0.1)	0.1 (0 to 0.2)
Age, y		
≥70 vs. <50	**0.3 (0.2 to 0.4)**	**0.3 (0.2 to 0.4)**
50–69 vs. <50	0.1 (0 to 0.2)	0.1 (0 to 0.2)
Region		
Southern vs. northern	0 (−0.1 to 0.1)	0.1 (0 to 0.1)
Western vs. northern	0.1 (0 to 0.1)	0 (0 to 0.1)
Eastern vs. northern	**0.2 (0.1 to 0.2)**	**0.1 (0.1 to 0.2)**
Health condition vs. no health condition	**–0.1 (–0.2 to –0.1)**	**–0.1 (–0.2 to –0.1)**
Work in healthcare vs. not in healthcare	0.1 (0 to 0.2)	0 (−0.1 to 0.1)

*Actual survey questions shown in Table 1. Boldface indicates 95% CIs that do not include 0. RIVM, National Institute for Public Health and the Environment.

(*37*–*39*). It is understandable that persons find it (increasingly) hard to be apart from others, specifically from their loved ones. Other factors, such as more practical barriers (e.g., difficult to keep distance in small corridors in the supermarket) (*40*) and perceived social norms (*41*), might also play a role.

Trust in the information and the measures from authorities was relatively high and stable throughout the first wave of the COVID-19 crisis. Other studies from New Zealand (*42*) and South Korea (*43*) have shown increased trust in government during the spring of 2020 compared with earlier years, which the authors attributed to the decisive and rapid governmental crisis response. A study in the United Kingdom suggests that trust can also rapidly decline, which was observed after government announcements to relax lockdown measures and news of misconduct by a high government official (*44*). Of note, recent research has also shown a decrease in public trust in the government's approach to the COVID-19 crisis in the Netherlands from the end of May through the beginning of October (*45*). Whether this decreased trust is explained by relaxations of measures or other events/processes needs further investigation.

In our study, the differences in perceptions, trust, and self-reported behavior between subgroups were rather small. Overall, the largest observed differences were based on age and health condition. Older persons perceived COVID-19 as more severe and had more concerns about their own health than did younger persons. At the same time, older persons perceived the probability of their getting infected with the virus to be lower. A similar result was found in an earlier study on COVID-19 risk perceptions, which showed increased perceived risk for death among elderly persons but lower perceived risk for infection (*14*). An explanation for the lower perceived risk is that older persons might have adopted more stringent social distancing measures than younger persons and therefore perceived their risk for infection as being smaller. In formal communications, maintaining strict social distancing was recommended for persons >70 years of age, and it was recommended that everyone avoid visiting elderly persons (*46*). Respondents with a chronic health condition also perceived their risk of becoming infected to be more probable and the infection to be more severe, and they were more concerned than those with no underlying health condition.

In line with risk-perception literature and previous research on behavior during disease outbreaks (*6*), we also found small differences on the basis of sex. Although the risk for severe COVID-19 illness is higher for men (*4*), women in our study indicated slightly

Table 6. Differences in self-reported protective behavior based on sex, age, region of residence, health condition, and healthcare employment determined in assessment of dynamic public perceptions of the coronavirus disease crisis, the Netherlands, 2020*

Independent variable	Self-reported protective measures taken, odds ratio (95% CI)	Self-reported adherence to guidelines, odds ratio (95% CI)
Female vs. male	**1.8 (1.6 to 2.1)**	1.2 (1.0 to 1.5)
Age, y		
≥70 vs. <50	1.2 (1.0 to 1.5)	**1.7 (1.3 to 2.2)**
50–69 vs. <50	1.1 (0.9 to 1.4)	1.2 (0.9 to 1.6)
Region		
Southern vs. northern	1.1 (0.9 to 1.4)	0.9 (0.6 to 1.2)
Western vs. northern	0.9 (0.7 to 1.1)	1.0 (0.8 to 1.3)
Eastern vs. northern	1.1 (0.9 to 1.3)	1.2 (0.9 to 1.7)
Health condition vs. no health condition	**1.3 (1.1 to 1.4)**	1.0 (0.8 to 1.2)
Work in healthcare vs. not in healthcare	0.9 (0.7 to 1.2)	0.8 (0.6 to 1.0)

*Actual survey questions shown in Table 1. Boldface indicates 95% CIs that do not include 1.0.

higher risk perceptions and were more likely to adopt measures to protect themselves and their family. Despite the considerable differences in infection rates between the different regions in the Netherlands and the increased risk to healthcare workers (*4*) and in contrast to previous perception study findings (*15*,*19*), we found few differences between persons on the basis of region of residence and healthcare employment.

One study limitation is that the study sample is not perfectly representative of the population of the Netherlands at large; specifically, our study included few respondents <30 years of age. Another limitation is that our operationalization of the variable "underlying health condition" includes all self-reported chronic or long-term conditions (except for allergies). At the start of this study, little was known about the specific underlying health conditions associated with increased risk for COVID-19, and these underlying conditions have therefore not been separately added to the survey as answer categories. In addition, the behaviors reported in our study are self-reported and might be subject to social desirability bias.

Our findings emphasize the need to monitor public perceptions and public responses among different groups during crises because these perceptions can change considerably over time and can differ among persons. Such insights are needed to be able to respond to changes in public perceptions and public responses with timely and accurate risk and crisis communication. To maintain public compliance with protective measures during the COVID-19 crisis, we also need to understand why persons struggle with adhering to these measures and what they need to help them overcome these difficulties. Consulting and collaborating with communities to understand their difficulties and needs during this unprecedented crisis is pivotal. When differences between perceptions, responses, and needs in certain groups are large (e.g., between younger and older persons), targeting or tailoring information to specific groups is advisable. Such group-targeted information should be well-adapted to common views in a specific group and should reach the group through various accessible channels (e.g., social media or postal mail) or intermediaries (e.g., schoolteachers, general practitioners).

Acknowledgments

We thank all respondents for their participation in our study as well as Rosa Joosten for her contribution to Figure 1.

This research was funded by the National Institute for Public Health and the Environment (RIVM).

About the Author

Ms. de Vries is a PhD candidate at the National Institute for Public Health and the Environment (RIVM) in the Netherlands. Her academic background is in sociology and global health, and her PhD study focuses on the analysis of public perceptions of health risks and media coverage during public health crises.

References

1. Tan W, Zhao X, Ma X, Wang W, Niu P, Xu W, et al. A novel coronavirus genome identified in a cluster of pneumonia cases—Wuhan, China 2019− 2020. China CDC Weekly. 2020;2:61–2. https://doi.org/10.46234/ccdcw2020.017
2. World Health Organization. WHO announces COVID-19 outbreak a pandemic [cited 2020 Apr 10]. http://www.euro.who.int/en/health-topics/health-emergencies/coronavirus-covid-19/news/news/2020/3/who-announces-covid-19-outbreak-a-pandemic
3. World Health Organization. WHO coronavirus disease (COVID-19) dashboard [cited 2021 Jan 24]. https://covid19.who.int
4. European Centre for Disease Prevention and Control. Coronavirus disease 2019 (COVID-19) pandemic: increased transmission in the EU/EEA and the UK—ninth update. Stockholm; The Centre; 2020. p. 1–50.
5. Hale T, Petherik A, Phillips T, Webster S. Variation in government responses to COVID-19: version 2.0 [2020 Jun 05]. https://www.bsg.ox.ac.uk/sites/default/files/2020-03/BSG-WP-2020-031-v2.0.pdf
6. Bish A, Michie S. Demographic and attitudinal determinants of protective behaviours during a pandemic: a review. Br J Health Psychol. 2010;15:797–824. https://doi.org/10.1348/135910710X485826
7. World Health Organization. Risk Communication and Community Engagement (RCCE) action plan guidance COVID-19 preparedness and response [cited 2021 Jan 13]. https://www.who.int/publications/i/item/risk-communication-and-community-engagement-(rcce)-action-plan-guidance
8. Brug J, Aro AR, Richardus JH. Risk perceptions and behaviour: towards pandemic control of emerging infectious diseases. Int J Behav Med. 2009;16:3.
9. Gilles I, Bangerter A, Clémence A, Green EG, Krings F, Staerklé C, et al. Trust in medical organizations predicts pandemic (H1N1) 2009 vaccination behavior and perceived efficacy of protection measures in the Swiss public. Eur J Epidemiol. 2011;26:203–10. https://doi.org/10.1007/s10654-011-9577-2
10. Betsch C, Böhm R, Chapman GB. Using behavioral insights to increase vaccination policy effectiveness. Policy Insights Behav Brain Sci. 2015;2:61–73. https://doi.org/10.1177/2372732215600716
11. Geldsetzer P. Knowledge and perceptions of COVID-19 among the general public in the United States and the United Kingdom: a cross-sectional online survey. Ann Intern Med. 2020;173:157–60. https://doi.org/10.7326/M20-0912
12. Roy D, Tripathy S, Kar SK, Sharma N, Verma SK, Kaushal V. Study of knowledge, attitude, anxiety & perceived mental healthcare need in Indian population

during COVID-19 pandemic. Asian J Psychiatr. 2020;51:102083. https://doi.org/10.1016/j.ajp.2020.102083
13. Plohl N, Musil B. Modeling compliance with COVID-19 prevention guidelines: the critical role of trust in science. Psychol Health Med. 2021;26:1–12. https://doi.org/10.1080/13548506.2020.1772988
14. Bruine de Bruin W. Age differences in COVID-19 risk perceptions and mental health: Evidence from a national US survey conducted in March 2020. J Gerontol B Psychol Sci Soc Sci. 2020 May 29 [Epub ahead of print]. https://doi.org/10.1093/geronb/gbaa074
15. Peres D, Monteiro J, Almeida M, Ladeira R. Risk perception of COVID-19 among the Portuguese healthcare professionals and general population. J Hosp Infect. 2020;105:434–7. https://doi.org/10.1016/j.jhin.2020.05.038
16. Zhong B-L, Luo W, Li HM, Zhang QQ, Liu XG, Li WT, et al. Knowledge, attitudes, and practices towards COVID-19 among Chinese residents during the rapid rise period of the COVID-19 outbreak: a quick online cross-sectional survey. Int J Biol Sci. 2020;16:1745–52. https://doi.org/10.7150/ijbs.45221
17. McFadden SM, Malik AA, Aguolu OG, Willebrand KS, Omer SB. Perceptions of the adult US population regarding the novel coronavirus outbreak. PLoS One. 2020;15:e0231808. https://doi.org/10.1371/journal.pone.0231808
18. Niepel C, Kranz D, Borgonovi F, Emslander V, Greiff S. The coronavirus (COVID-19) fatality risk perception of US adult residents in March and April 2020. Br J Health Psychol. 2020;25:883–8. https://doi.org/10.1111/bjhp.12438
19. Czeisler MÉ, Tynan MA, Howard ME, Honeycutt S, Fulmer EB, Kidder DP, et al. Public attitudes, behaviors, and beliefs related to COVID-19, stay-at-home orders, nonessential business closures, and public health guidance—United States, New York City, and Los Angeles, May 5–12, 2020. MMWR Morb Mortal Wkly Rep. 2020;69:751–8. https://doi.org/10.15585/mmwr.mm6924e1
20. Reintjes R, Das E, Klemm C, Richardus JH, Keßler V, Ahmad A. "Pandemic Public Health Paradox": time series analysis of the 2009/10 influenza A/H1N1 epidemiology, media attention, risk perception and public reactions in 5 European countries. PLoS One. 2016;11:e0151258. https://doi.org/10.1371/journal.pone.0151258
21. van der Weerd W, Timmermans DR, Beaujean DJ, Oudhoff J, van Steenbergen JE. Monitoring the level of government trust, risk perception and intention of the general public to adopt protective measures during the influenza A (H1N1) pandemic in the Netherlands. BMC Public Health. 2011;11:575. https://doi.org/10.1186/1471-2458-11-575
22. Bults M, Beaujean DJ, Richardus JH, Voeten HA. Perceptions and behavioral responses of the general public during the 2009 influenza A (H1N1) pandemic: a systematic review. Disaster Med Public Health Prep. 2015;9:207–19. https://doi.org/10.1017/dmp.2014.160
23. Bangerter A, Krings F, Mouton A, Gilles I, Green EG, Clémence A. Longitudinal investigation of public trust in institutions relative to the 2009 H1N1 pandemic in Switzerland. PLoS One. 2012;7:e49806. https://doi.org/10.1371/journal.pone.0049806
24. Mayor E, Eicher V, Bangerter A, Gilles I, Clémence A, Green EG. Dynamic social representations of the 2009 H1N1 pandemic: shifting patterns of sense-making and blame. Public Underst Sci. 2013;22:1011–24. https://doi.org/10.1177/0963662512443326
25. Bults M, Beaujean DJ, de Zwart O, Kok G, van Empelen P, van Steenbergen JE, et al. Perceived risk, anxiety, and behavioural responses of the general public during the early phase of the influenza A (H1N1) pandemic in the Netherlands: results of three consecutive online surveys. BMC Public Health. 2011;11:2. https://doi.org/10.1186/1471-2458-11-2
26. World Health Organization (WHO). Coronavirus disease 2019 (COVID-19): situation report—39 [cited 2021 Jan 13]. https://www.who.int/docs/default-source/coronaviruse/situation-reports/20200228-sitrep-39-covid-19.pdf?sfvrsn=5bbf3e7d_4
27. Reusken CB, Buiting A, Bleeker-Rovers C, Diederen B, Hooiveld M, Friesema I, et al. Rapid assessment of regional SARS-CoV-2 community transmission through a convenience sample of healthcare workers, the Netherlands, March 2020. Euro Surveill. 2020;25:2000334. https://doi.org/10.2807/1560-7917.ES.2020.25.12.2000334
28. Government of the Netherlands. Dutch measures against coronavirus [cited 2021 Jan 13]. https://www.government.nl/topics/coronavirus-covid-19/tackling-new-coronavirus-in-the-netherlands
29. National Institute for Public Health and the Environment (RIVM). COVID-19 dataset [cited 2021 Jan 13]. https://data.rivm.nl/covid-19
30. Brabers AEM, Reitsema-van Rooijen M, de Jong JD. Consumentenpanel Gezondheidszorg: Basisrapport met informatie over het panel (2015) [cited 2021 Jan 13]. https://www.nivel.nl/nl/publicatie/consumentenpanel-gezondheidszorg-basisrapport-met-informatie-over-het-panel-2015
31. Brabers A, Meijer M, Hooiveld M, de Jong J. Monitor griepachtige klachten en uitbraak van het coronavirus: het perspectief van de burger [cited 2021 Jan 13]. https://www.nivel.nl/nl/publicatie/monitor-griepachtige-klachten-en-uitbraak-van-het-coronavirus-het-perspectief-van-de
32. Schol LGC, Mollers M, Swaan CM, Beaujean DJMA, Wong A, Timen A. Knowledge, perceptions and media use of the Dutch general public and healthcare workers regarding Ebola, 2014. BMC Infect Dis. 2018;18:18. https://doi.org/10.1186/s12879-017-2906-7
33. Centraal Bureau voor de Statistiek (CBS), Standaard Onderwijsindeling 2006 [cited 2021 Jan 13]. https://www.cbs.nl/nl-nl/onze-diensten/methoden/classificaties/onderwijs-en-beroepen/standaard-onderwijsindeling--soi--/standaard-onderwijsindeling-2006
34. Rosenstock IM. The health belief model and preventive health behavior. Health Educ Monogr. 1974;2:354–86. https://doi.org/10.1177/109019817400200405
35. National Institute for Public Health and the Environment (RIVM). Waarom wel of niet naleven van de gedragsregels? [cited 2020 Nov 27]. https://www.rivm.nl/gedragsonderzoek/maatregelen-welbevinden/verklaringen-gedrag
36. Tong KK, Chen JH, Yu EW, Wu AMS. Adherence to COVID-19 precautionary measures: applying the health belief model and generalised social beliefs to a probability community sample. Appl Psychol Health Well-Being. 2020;12:1205–23. https://doi.org/10.1111/aphw.12230
37. Venkatesh A, Edirappuli S. Social distancing in covid-19: what are the mental health implications? BMJ. 2020;369:m1379. https://doi.org/10.1136/bmj.m1379
38. Tyrrell CJ, Williams KN. The paradox of social distancing: implications for older adults in the context of COVID-19. Psychol Trauma. 2020;12(S1):S214–6. https://doi.org/10.1037/tra0000845
39. Abel T, McQueen D. The COVID-19 pandemic calls for spatial distancing and social closeness: not for social

distancing! Int J Public Health. 2020;65:231. https://doi.org/10.1007/s00038-020-01366-7
40. Coroiu A, Moran C, Campbell T, Geller AC. Barriers and facilitators of adherence to social distancing recommendations during COVID-19 among a large international sample of adults. PLoS One. 2020;15:e0239795. https://doi.org/10.1371/journal.pone.0239795
41. Andrews JL, Foulkes L, Blakemore S-J. Peer influence in adolescence: public-health implications for COVID-19. Trends Cogn Sci. 2020;24:585–7. https://doi.org/10.1016/j.tics.2020.05.001
42. Sibley CG, Greaves LM, Satherley N, Wilson MS, Overall NC, Lee CHJ, et al. Effects of the COVID-19 pandemic and nationwide lockdown on trust, attitudes toward government, and well-being. Am Psychol. 2020;75:618–30. https://doi.org/10.1037/amp0000662
43. Kye B, Hwang S-J. Social trust in the midst of pandemic crisis: implications from COVID-19 of South Korea. Res Soc Stratif Mobil. 2020;68:100523. https://doi.org/10.1016/j.rssm.2020.100523
44. Fancourt D, Steptoe A, Wright L. The Cummings effect: politics, trust, and behaviours during the COVID-19 pandemic. Lancet. 2020;396:464–5. https://doi.org/10.1016/S0140-6736(20)31690-1
45. National Institute for Public Health and the Environment (RIVM). Communicatie en vertrouwen: vertrouwen in Nederlandse aanpak [cited 2020 Nov 27]. https://www.rivm.nl/gedragsonderzoek/maatregelen-welbevinden/communicatie-en-vertrouwen
46. Government of the Netherlands. Coronavirus: what does it mean to 'keep your distance'? [cited 2020 Jun 22]. https://www.government.nl/latest/news/2020/03/16/coronavirus-what-does-it-mean-to-%E2%80%98keep-your-distance%E2%80%99

Address for correspondence: Marion deVries, National Institute of Public Health and the Environment (RIVM), Centre for Infectious Disease Control, P.O. Box 1, 3720 BA Bilthoven, the Netherlands; email: marion.de.vries@rivm.nl

etymologia revisited

Zika [zēkə] Virus

Zika virus is a mosquito-borne positive-sense, single-stranded RNA virus in the family *Flaviviridae*, genus *Flavivirus* that causes a mild, acute febrile illness similar to dengue. In 1947, scientists researching yellow fever placed a rhesus macaque in a cage in the Zika Forest (*zika* meaning "overgrown" in the Luganda language), near the East African Virus Research Institute in Entebbe, Uganda. A fever developed in the monkey, and researchers isolated from its serum a transmissible agent that was first described as Zika virus in 1952. It was subsequently isolated from a human in Nigeria in 1954. From its discovery until 2007, confirmed cases of Zika virus infection from Africa and Southeast Asia were rare. In 2007, however, a major epidemic occurred in Yap Island, Micronesia. More recently, epidemics have occurred in Polynesia, Easter Island, the Cook Islands, and New Caledonia.

Sources

1. Dick GW, Kitchen SF, Haddow AJ. Zika virus. I. Isolations and serological specificity. Trans R Soc Trop Med Hyg. 1952;46:509–20. http://dx.doi.org/10.1016/ 0035-9203(52)90042-4
2. Hayes EB. Zika virus outside Africa. Emerg Infect Dis. 2009; 15:1347–50. http://dx.doi.org/10.3201/eid1509.090442
3. MacNamara FN. Zika virus: a report on three cases of human infection during an epidemic of jaundice in Nigeria. Trans R Soc Trop Med Hyg. 1954;48:139–45. http://dx.doi.org/10.1016/0035-9203(54)90006-1
4. Murphy JD. Luganda–English dictionary. Washington (DC): The Catholic University of America Press; 1972.

Originally published in June 2014

https://wwwnc.cdc.gov/eid/article/20/6/et-2014_article

Evolution of Sequence Type 4821 Clonal Complex Hyperinvasive and Quinolone-Resistant Meningococci

Mingliang Chen,[1] Odile B. Harrison,[1] Holly B. Bratcher, Zhiyan Bo, Keith A. Jolley, Charlene M.C. Rodrigues, James E. Bray, Qinglan Guo, Xi Zhang, Min Chen, Martin C.J. Maiden

Expansion of quinolone-resistant *Neisseria meningitidis* clone China$^{CC4821\text{-}R1\text{-}C/B}$ from sequence type (ST) 4821 clonal complex (CC4821) caused a serogroup shift from serogroup A to serogroup C invasive meningococcal disease (IMD) in China. To determine the relationship among globally distributed CC4821 meningococci, we analyzed whole-genome sequence data from 173 CC4821 meningococci isolated from 4 continents during 1972–2019. These meningococci clustered into 4 sublineages (1–4); sublineage 1 primarily comprised of IMD isolates (41/50, 82%). Most isolates from outside China (40/49, 81.6%) formed a distinct sublineage, the Europe–USA cluster, with the typical strain designation B:P1.17-6,23:F3-36:ST-3200(CC4821), harboring mutations in penicillin-binding protein 2. These data show that the quinolone-resistant clone China$^{CC4821\text{-}R1\text{-}C/B}$ has expanded to other countries. The increasing distribution worldwide of serogroup B CC4821 raises the concern that CC4821 has the potential to cause a pandemic that would be challenging to control, despite indirect evidence that the Trumenba vaccine might afford some protection.

Neisseria meningitidis, a leading cause of bacterial meningitis and septicemia globally, causes ≈1.2 million invasive meningococcal disease (IMD) cases annually and a case-fatality rate of 11% (*1*). Meningococci are classified into 12 serogroups based on capsular polysaccharides (*1*); genetic relationships among isolates are defined by clonal complexes (CCs) identified by multilocus sequence typing (MLST), which are surrogates for lineages (2). The relationship among serogroups, CCs (lineages), and IMD fluctuates over time and by location, but IMD isolates are dominated by CCs known as hyperinvasive lineages, usually associated with one of the 6 disease-causing serogroups (MenA, MenB, MenC, MenW, MenX, and MenY).

In China, the national dissemination of hyperinvasive sequence type (ST) 4821 clonal complex (CC4821) meningococci led to a shift in IMD epidemiology from mostly MenA to predominantly MenC (*3*,*4*). Although no quinolone resistance was identified in CC4821 in China during 1965–1985, high-frequency resistance (79%) occurred from 2005 onward due to expansion of the quinolone-resistant clone China$^{CC4821\text{-}R1\text{-}C/B}$ (*5*). Previous studies discovered that CC4821 can be divided into 2 groups, with group 1 associated with IMD (*6*,*7*). Peng et al. identified 6 strain-specific genome regions resulting from horizontal gene transfer (HGT) in isolate 053442 (*8*); this finding was consistent with the emergence of the China$^{CC4821\text{-}R1\text{-}C/B}$ clone associated with multiple HGT events within genes encoding surface antigens (*6*), although the donors of these events were not identified.

Globally, the number of CC4821 IMD isolates has increased. At the time CC4821 was identified, isolates were confined to China (*4*,*9*); however, by June 2020, a total of 59 CC4821 isolates had been identified in 19 countries worldwide (Figure 1). Moreover, 3 IMD cases caused by quinolone-resistant CC4821 isolates were reported in Canada (n = 2) and Japan (n = 1) after 2013 (*10*,*11*); 3 other CC4821 isolates were found to colonize the anorectal tract of men who have sex with men (MSM) (*12*). We investigated the genomic events leading to the emergence and expansion of hyperinvasive CC4821 meningococci by describing the phylogenetic relationships among meningococci with different serogroups (MenC, MenB, MenW, and nongroupable), sources (IMD, carriage, and MSM), locations (China or other countries),

Author affiliations: Shanghai Municipal Center for Disease Control and Prevention, Shanghai, China (M. Chen, X. Zhang, M. Chen); University of Oxford, Oxford, UK (O.B. Harrison, H.B. Bratcher, Z. Bo, K.A. Jolley, C.M.C. Rodrigues, J.E. Bray, M.C.J. Maiden); Fudan University Huashan Hospital, Shanghai (Q. Guo)

DOI: https://doi.org/10.3201/eid2704.203612

[1]These authors contributed equally to this article.

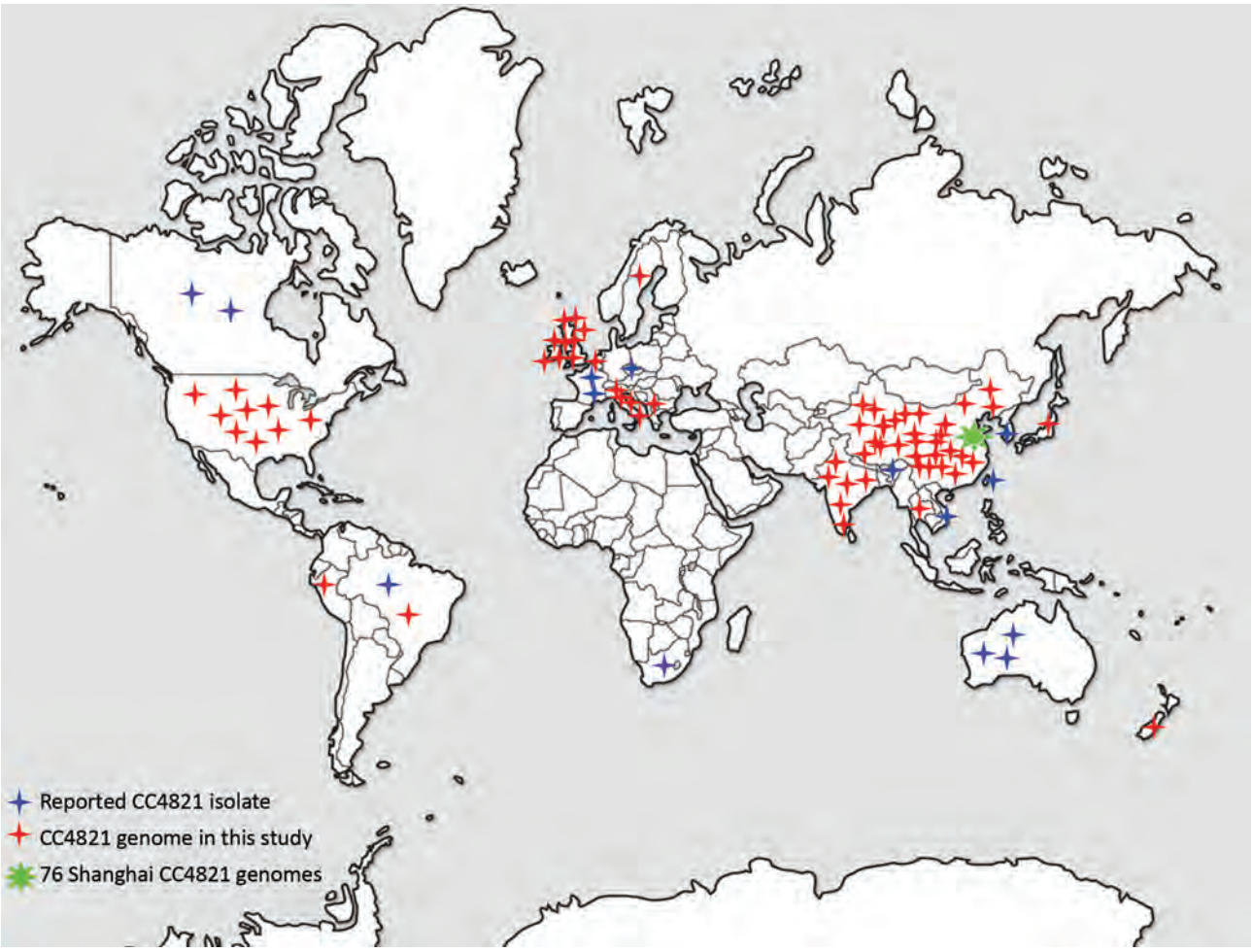

Figure 1. Distribution of CC4821 *Neisseria meningitidis* isolates worldwide. CC4821 isolates were identified in China and in 19 countries of Europe, Africa, North America, South America, Oceania, and Asia. CC, clonal complex.

and dates of isolation (1972–1978 vs. 2004–2019). We assessed genes encoding key antigens and antimicrobial resistance phenotypes, identified putative donors of HGT events unique to the epidemic and quinolone-resistant clone China$^{CC4821\text{-}R1\text{-}C/B}$, and characterized isolates outside of China.

Materials and Methods

Isolate Collection and Whole-Genome Sequencing

A total of 173 CC4821 genomes were collected dating from 1972–1978 (n = 19) and 2004–2019 (n = 154), including isolates from IMD (66/173, 38.2%), genitourinary sites (6/173, 3.5%), asymptomatic carriage (86/173, 49.7%), and unknown sources (15/173, 8.7%) (Appendix 1 Table 1, https://wwwnc.cdc.gov/EID/article/27/4/20-3612-App1.xlsx). Shanghai CDC sequenced 76 CC4821 isolates with Illumina HiSeq (Illumina, https://www.illumina.com) using paired-end 150 base reads as previously described (*13*). An additional 97 publicly available CC4821 genomes consisted of 48 genomes from 14 provinces of China, including the reference strain 053442 (*6*–*8*) and 49 genomes from countries outside of China, including the United Kingdom (n = 20), United States (n = 8), and 11 other countries (n = 21) (Figure 1; Appendix 1 Table 1) (*10*,*12*,*14*–*17*). The completeness and contamination of the genomes were evaluated using CheckM (*18*).

Antigenic and Antimicrobial Resistance Characteristics of CC4821 Genomes

To describe the antigenic and antimicrobial resistance characteristics of CC4821 genomes, we extracted from genomes nucleotides of 9 antigen coding genes (*porA*, *fHbp*, *nhba*, *porB*, *fetA*, *opcA*, *nspA*, *tbpA*, and *NMB0315*) (*19*–*22*) and 5 resistance-associated genes (*gyrA*, *parC*, *penA*, *ponA*, and *rpoB*) (*23*,*24*) for analysis. We annotated and analyzed deduced

encoding factor H–binding protein (fHbp), *Neisseria* heparin-binding antigen (NHBA), *Neisseria* adhesion antigen (NadA), and outer membrane protein (PorA) peptides and deduced meningococcal vaccine antigen reactivity (MenDeVAR) index from the PubMLST *Neisseria* database (*25*).

Identifying CC4821 (L44) Sublineages

In the *Neisseria* PubMLST database, a lineage-specific core genome MLST typing scheme containing loci found in 95% of CC4821 isolates was established and designated L44 cgMLST consistent with the previously described CC4821 lineage 44 (*26*). We compared the 173 CC4821 genomes using Genome Comparator (*27*) and the L44 cgMLST scheme, identifying distinct sublineages. To characterize each sublineage, we visualized a FASTA output from the Genome Comparator Tool using all 2,860 defined loci (NEIS0001–NEIS3173, not contiguous) using MEGA version 5 (*28*). We used Z2491 (GenBank accession no. NC_003116) as outgroup in accordance with previous studies (*6*,*8*). Assembled contigs and annotation information of 173 genomes in this study can be accessed at https://pubMLST.org/neisseria (Appendix 1 Table 1).

Identifying and Characterizing Unique Alleles in Sublineages

We determined shared and unique alleles using outputs from Genome Comparator. An allele was defined as unique to a sublineage if it was present in >90% of the genomes in that sublineage but absent in other sublineages. Genes with unique alleles were functionally characterized according to the Kyoto Encyclopedia of Genes and Genomes Orthology groupings of its database (*29*).

Identifying HGT Events and Putative Donors

Inputting the aligned sequences generated from Parsnp (*30*), we predicted putative HGT events using Gubbins (*31*). To search for potential donors, we blasted alleles and sequences of contiguous loci that were predicted to originate from HGT against the PubMLST database. We identified potential donors as previously described (*32*). We labeled recombination areas with unique loci on the circular genome map of genome 053442 by BLAST (https://blast.ncbi.nlm.nih.gov/Blast.cgi) comparisons to strains of other sublineages, as generated using BRIG (*33*).

Screening Molecular Markers of MSM Infection Strains from Europe

In addition to the lineage of 11.2 possessing PorA P1.5–1,10–8, 3 other molecular features have been identified in meningococci causing infections among MSM in Europe during 2012–2014; these features were functional nitrite reductase (AniA); frameshifted *fHbp* allele found mostly in urethritis and proctitis isolates; and *penA327* that had reduced susceptibility to penicillin and third-generation cephalosporins (*34*). These 3 molecular markers were screened among all the 173 CC4821 genomes.

Results

Isolate Characterization

The 173 CC4821 isolates represented 46 different STs; ST4821 (n = 41, 23.7%) and ST3200 (n = 30, 17.3%) were the most prevalent. We identified 43 PorA subtypes, of which P1.7-2,14 (n = 25, 14.5%) and P1.17-6,23 (n = 18, 10.4%) were the most frequent. We identified 27 FetA variants; F3-3 (n = 47, 27.2%) and F3-36 (n = 37, 21.4%) were the most prevalent (Appendix 1 Table 1).

Identifying 4 Sublineages

We identified 2,161 loci in reference genome 053442, including 1,699 core genes. Most (1,527/1,699, 89.9%) of the core loci had *p*-distance values of 0–0.1; 0.8% (14/1,699) showed high *p*-distance values of 0.50–0.68. On the basis of the L44 cgMLST scheme, we divided the CC4821 isolates into 4 sublineages (Figure 2): L44.1, identical to the China$^{CC4821\text{-}R1\text{-}C/B}$ clone (n = 50, 28.9%), composed of isolates from China (n = 44) and other countries (n = 6) during 2004–2019 that were very closely related (Figure 3); L44.2 (n = 29, 16.8%), composed of isolates from China (n = 28) and the United Kingdom (n = 1) during 2005–2019; L44.3 (n = 58, 33.5%), composed of isolates from China (n = 18) and countries outside China (n = 40) during 1977–2019; and L44.4 (n = 32, 18.5%), composed of isolates from China (n = 30) and India (n = 2) during 1972–2017. Four additional isolates from China were not assigned to any sublineages.

Features of the 4 Sublineages

The percentage of IMD isolates was significantly higher in L44.1 (41/50, 82%) than the other 3 sublineages (17.2%–22.4%; p<0.001) (Figure 2). L44.1, containing the reference strain 053442, was mainly composed of MenC isolates (44/50, 88%) and had ST4821 as its central ST. L44.2, was mainly composed of MenB isolates (27/29, 93.1%) and its central ST was ST5664. L44.3 was mainly composed of MenB (55/58, 94.8%) with ST3200 as its central ST. L44.4 was mainly composed of MenC (14/32, 43.8%) and MenW (11/32, 34.4%) with its central ST3436

(Appendix 2 Figure 1, https://wwwnc.cdc.gov/EID/article/27/4/20-3612-App2.pdf).

Analysis of the 5 antimicrobial resistance genes revealed that both *gyrA*-71 (with T91I) and *parC*-12 were specific to L44.1; *parC*-275 and *penA*-9 (with 5 mutations) were both specific to L44.3, and *gyrA*-294 (with T91I) was discovered only in L44.4 (Table 1; Appendix 2 Figures 2–6). In L44.1, all of the isolates possessed the quinolone resistance–associated mutation T91I in GyrA (Figure 4). In L44.3, 40/58 (69.0%) harbored PBP2 mutations, almost always from countries outside of China (38/40, 95%) (Figures 5, 6).

Vaccine Antigens among the 4 Sublineages

Analysis of 9 antigenic genes identified several alleles unique to a certain sublineage (Table 2; Appendix 2 Figures 7–17). For example, FetA-VR F3-3 was found in L44.1, F1-91 in L44.2, F3-36 and F3-9 in L44.3, and F1-7 in L44.4 isolates (Appendix 2 Figure 11). In L44.1, most isolates had the same antigenic gene profile (*nhba*-124, *porB*-29, *fetA*-64, *opcA*-4, *nspA*-4, *tbpA*-7, and *NMB0315*-21) (Figure 4), and 25/50 (50%) had the PorA subtype of P1.7-2,14 (Figure 3). In L44.3, most had the same gene profile (*fHbp*-16, *nhba*-553, *porB*-265, *fetA*-1069, *opcA*-100, *nspA*-26, and *NMB0315*-194), with *porA* and *tbpA* showing high genetic diversity (Figure 5).

We analyzed deduced peptide sequences for vaccine antigen constituents among MenB isolates (n = 97). We identified 16 fHbp peptides, of which peptide 16 (variant 2/subfamily A) was present in 70/97 (72.2%) isolates, including 31/70 isolates from China. There were 20 NHBA peptides, of which alleles 669 (46/95, 48.4%), 901 (11/95, 11.6%), and 668 (10/95, 10.5%) occurred most frequently. The *nadA* gene was absent in all isolates (including other serogroups). Of 31 PorA VR1/VR2 combinations, the most frequently occurring was P1.20,23 (11/97, 11.3%).

MenDeVAR Index values were assigned for MenB disease isolates (n = 29, including the 6 isolates from genitourinary sites), but 27/29 (93.1%) isolates had insufficient data from experimental studies to estimate the coverage of the MenB vaccine Bexsero (Appendix 2 Table 2). We predicted cross-reactivity to the MenB vaccine Trumenba for 18/29 (62.1%) isolates. For the MenB disease isolates from China, 7/17 (41.2%) were deemed cross-reactive with Trumenba;

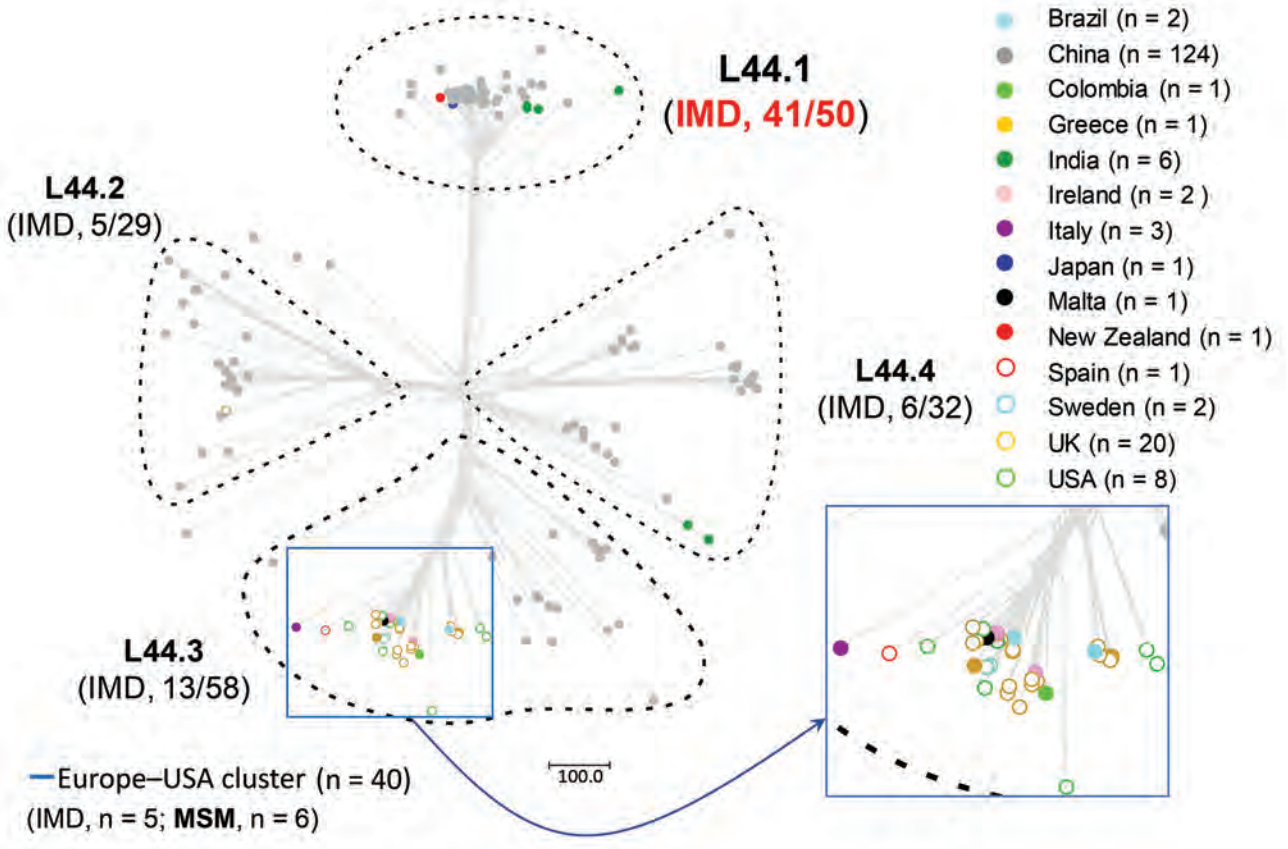

Figure 2. Allele-based sublineages of clonal complex 4821 *Neisseria meningitidis* identified using lineage 44 core genome multilocus sequence typing scheme. The inset shows the country distribution of the 40 genomes constituting the Europe–USA cluster. IMD, invasive meningococcal disease; MSM, men who have sex with men.

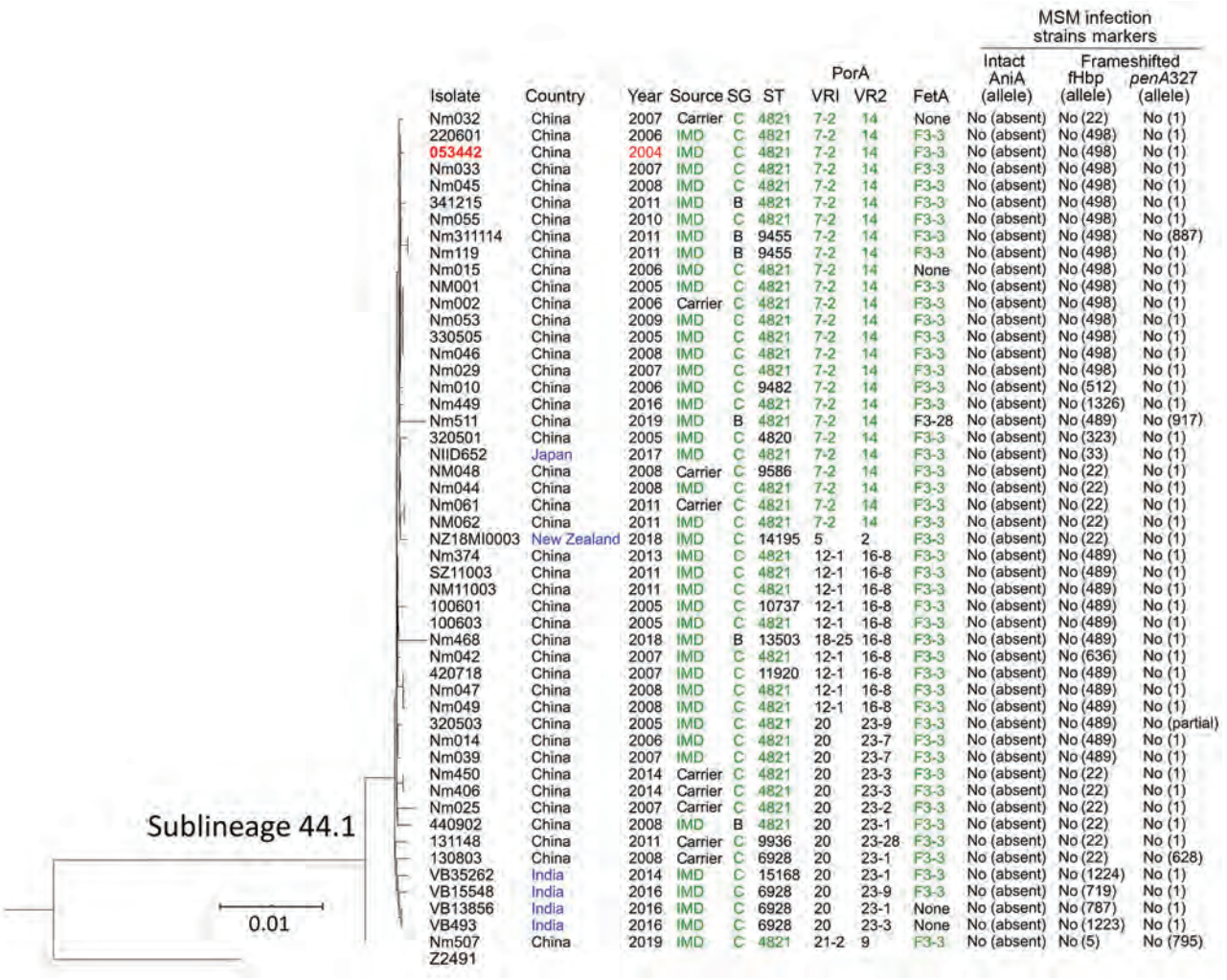

Isolate	Country	Year	Source	SG	ST	PorA VR1	PorA VR2	FetA	MSM infection strains markers: Intact AniA (allele)	Frameshifted fHbp (allele)	Frameshifted *penA*327 (allele)
Nm032	China	2007	Carrier	C	4821	7-2	14	None	No (absent)	No (22)	No (1)
220601	China	2006	IMD	C	4821	7-2	14	F3-3	No (absent)	No (498)	No (1)
053442	China	2004	IMD	C	4821	7-2	14	F3-3	No (absent)	No (498)	No (1)
Nm033	China	2007	IMD	C	4821	7-2	14	F3-3	No (absent)	No (498)	No (1)
Nm045	China	2008	IMD	C	4821	7-2	14	F3-3	No (absent)	No (498)	No (1)
341215	China	2011	IMD	B	4821	7-2	14	F3-3	No (absent)	No (498)	No (1)
Nm055	China	2010	IMD	C	4821	7-2	14	F3-3	No (absent)	No (498)	No (1)
Nm311114	China	2011	IMD	B	9455	7-2	14	F3-3	No (absent)	No (498)	No (887)
Nm119	China	2011	IMD	B	9455	7-2	14	F3-3	No (absent)	No (498)	No (1)
Nm015	China	2006	IMD	C	4821	7-2	14	None	No (absent)	No (498)	No (1)
NM001	China	2005	IMD	C	4821	7-2	14	F3-3	No (absent)	No (498)	No (1)
Nm002	China	2006	Carrier	C	4821	7-2	14	F3-3	No (absent)	No (498)	No (1)
Nm053	China	2009	IMD	C	4821	7-2	14	F3-3	No (absent)	No (498)	No (1)
330505	China	2005	IMD	C	4821	7-2	14	F3-3	No (absent)	No (498)	No (1)
Nm046	China	2008	IMD	C	4821	7-2	14	F3-3	No (absent)	No (498)	No (1)
Nm029	China	2007	IMD	C	4821	7-2	14	F3-3	No (absent)	No (498)	No (1)
Nm010	China	2006	IMD	C	9482	7-2	14	F3-3	No (absent)	No (512)	No (1)
Nm449	China	2016	IMD	C	4821	7-2	14	F3-3	No (absent)	No (1326)	No (1)
Nm511	China	2019	IMD	B	4821	7-2	14	F3-28	No (absent)	No (489)	No (917)
320501	China	2005	IMD	C	4820	7-2	14	F3-3	No (absent)	No (323)	No (1)
NIID652	Japan	2017	IMD	C	4821	7-2	14	F3-3	No (absent)	No (33)	No (1)
NM048	China	2008	Carrier	C	9586	7-2	14	F3-3	No (absent)	No (22)	No (1)
Nm044	China	2008	IMD	C	4821	7-2	14	F3-3	No (absent)	No (22)	No (1)
Nm061	China	2011	Carrier	C	4821	7-2	14	F3-3	No (absent)	No (22)	No (1)
NM062	China	2011	IMD	C	4821	7-2	14	F3-3	No (absent)	No (22)	No (1)
NZ18MI0003	New Zealand	2018	IMD	C	14195	5	2	F3-3	No (absent)	No (22)	No (1)
Nm374	China	2013	IMD	C	4821	12-1	16-8	F3-3	No (absent)	No (489)	No (1)
SZ11003	China	2011	IMD	C	4821	12-1	16-8	F3-3	No (absent)	No (489)	No (1)
NM11003	China	2011	IMD	C	4821	12-1	16-8	F3-3	No (absent)	No (489)	No (1)
100601	China	2005	IMD	C	10737	12-1	16-8	F3-3	No (absent)	No (489)	No (1)
100603	China	2005	IMD	C	4821	12-1	16-8	F3-3	No (absent)	No (489)	No (1)
Nm468	China	2018	IMD	B	13503	18-25	16-8	F3-3	No (absent)	No (489)	No (1)
Nm042	China	2007	IMD	C	4821	12-1	16-8	F3-3	No (absent)	No (636)	No (1)
420718	China	2007	IMD	C	11920	12-1	16-8	F3-3	No (absent)	No (489)	No (1)
Nm047	China	2008	IMD	C	4821	12-1	16-8	F3-3	No (absent)	No (489)	No (1)
Nm049	China	2008	IMD	C	4821	12-1	16-8	F3-3	No (absent)	No (489)	No (1)
320503	China	2005	IMD	C	4821	20	23-9	F3-3	No (absent)	No (489)	No (partial)
Nm014	China	2006	IMD	C	4821	20	23-7	F3-3	No (absent)	No (489)	No (1)
Nm039	China	2007	IMD	C	4821	20	23-7	F3-3	No (absent)	No (489)	No (1)
Nm450	China	2014	Carrier	C	4821	20	23-3	F3-3	No (absent)	No (22)	No (1)
Nm406	China	2014	Carrier	C	4821	20	23-3	F3-3	No (absent)	No (22)	No (1)
Nm025	China	2007	Carrier	C	4821	20	23-2	F3-3	No (absent)	No (22)	No (1)
440902	China	2008	IMD	B	4821	20	23-1	F3-3	No (absent)	No (22)	No (1)
131148	China	2011	Carrier	C	9936	20	23-28	F3-3	No (absent)	No (22)	No (1)
130803	China	2008	Carrier	C	6928	20	23-1	F3-3	No (absent)	No (22)	No (628)
VB35262	India	2014	IMD	C	15168	20	23-1	F3-3	No (absent)	No (1224)	No (1)
VB15548	India	2016	IMD	C	6928	20	23-9	F3-3	No (absent)	No (719)	No (1)
VB13856	India	2016	IMD	C	6928	20	23-1	None	No (absent)	No (787)	No (1)
VB493	India	2016	IMD	C	6928	20	23-3	None	No (absent)	No (1223)	No (1)
Nm507	China	2019	IMD	C	4821	21-2	9	F3-3	No (absent)	No (5)	No (795)
Z2491											

Figure 3. Phylogenetic tree and data of clonal complex 4821 *Neisseria meningitidis* sublineage L44.1 (China$^{CC4821\text{-}R1\text{-}C/B}$) isolates. Red text indicates the oldest isolate of the sublineage; blue text, the isolates from countries outside of China; and green text, the dominant type or allele. Scale bar indicates substitutions per site. IMD, invasive meningococcal disease; MSM, men who have sex with men; SG, serogroup; ST, sequence type; VR, variable region.

however, we had insufficient data for the remaining 10/17 (58.8%) to determine reactivity.

Molecular Markers of Strains from Europe Infecting MSM

None of the CC4821 isolates harbored frameshifted *fHbp* allele or *penA327*, but the distribution of putatively functional AniA proteins was diverse. The *aniA* gene was absent in all L44.1 isolates (Figure 3) but was present in all of the other 123 CC4821 isolates, of which 96.7% (119/123) isolates harbored putatively functional AniA proteins (Figure 5; Appendix 2 Figures 16–17).

Evolution of Sublineage L44.1 (China$^{CC4821\text{-}R1\text{-}C/B}$ Clone)

Five specific loci were present in >90% of L44.1 but in <10% of other sublineages. These loci were involved in signaling and cellular processes (n = 2), metabolism (n = 1), and genetic information processing (n = 1) (Table 3). No loci were specific to any of other 3 sublineages.

Prediction of HGT events contributing to the emergence of L44.1 using Gubbins discovered 126 events involving 686 loci shared by the 50 L44.1 isolates (Appendix 2 Figure 18). These events included 216 loci with alleles specific to L44.1. We discovered an additional 83 unique loci based on analysis of the accessory genome. Therefore, a total of 299 unique loci were identified in L44.1; of those, 139 (46.5%) were involved in metabolic function (Appendix 1 Table 3). These 299 unique loci were distributed across the chromosome; we observed 44 areas (216 loci) harboring contiguous loci with unique alleles (Figure 7), among which the exact donors of 36 areas across 149

Table 1. Specific alleles of antimicrobial resistance genes in 4 sublineages of clonal complex 4821 of *Neisseria meningitidis*

Sublineage	Resistant, allele no. (no. isolates)				
	gyrA	*parC*	*penA*	*ponA*	*rpoB*
L44.1, n = 50	71 (50)	12 (43)	None	None	None
L44.2, n = 29	None	None	None	None	None
L44.3, n = 58	None	275 (41)	9 (35)	None	None
L44.4, n = 32	294 (11)	None	None	None	None

loci were identified in 46 putative HGT events. The total length of these putative recombination fragments was ≈225 kb, including 87 kb (38.7%) originating from the C:ST-9514 cluster isolates in China during 1966–1977, followed by 25 kb (11.1%) from MenA isolates (CC5 and CC1) in China during 1966–1984 (Table 4, https://wwwnc.cdc.gov/EID/article/27/4/20-3612-T4.htm).

Evolution of CC4821 Isolates from Outside China

We identified 49 CC4821 isolates from countries outside of China, and most (40/49, 81.6%) were assigned to L44.3, of which there were 39 MenB and 1 MenC, constituting the distinct Europe–USA cluster (Figures 2, 5). The representative molecular characteristics of the Europe–USA cluster was B:P1.17-6,23:F3-36:ST-3200(CC4821); its antigen gene profile was *porA*-423, *fHbp*-16, *nhba*-553, *porB*-265, *fetA*-1069, *opcA*-100, *nspA*-26, *tbpA*-1333, and *NMB0315*-194 and antimicrobial resistance profile *gyrA*-12, *parC*-275, *penA*-9 with PBP2 mutations, *ponA*-7, and *rpoB*-85 (Figure 6). In Gubbins analysis, 33 events involving 193 loci were shared by all the Europe–USA cluster isolates (Appendix 2 Figure 18); we discovered 60 unique loci for which we could not identify their potential donors. These unique loci were involved in functions mainly associated with metabolism (23/60, 38.3%) and genetic information processing (18/60, 30%) (Appendix 1 Table 4).

In addition to the 40 Europe–USA cluster isolates, there were 6 MenC invasive isolates from India (n = 4, identified 2014–2016), Japan (n = 1, identified in 2017),

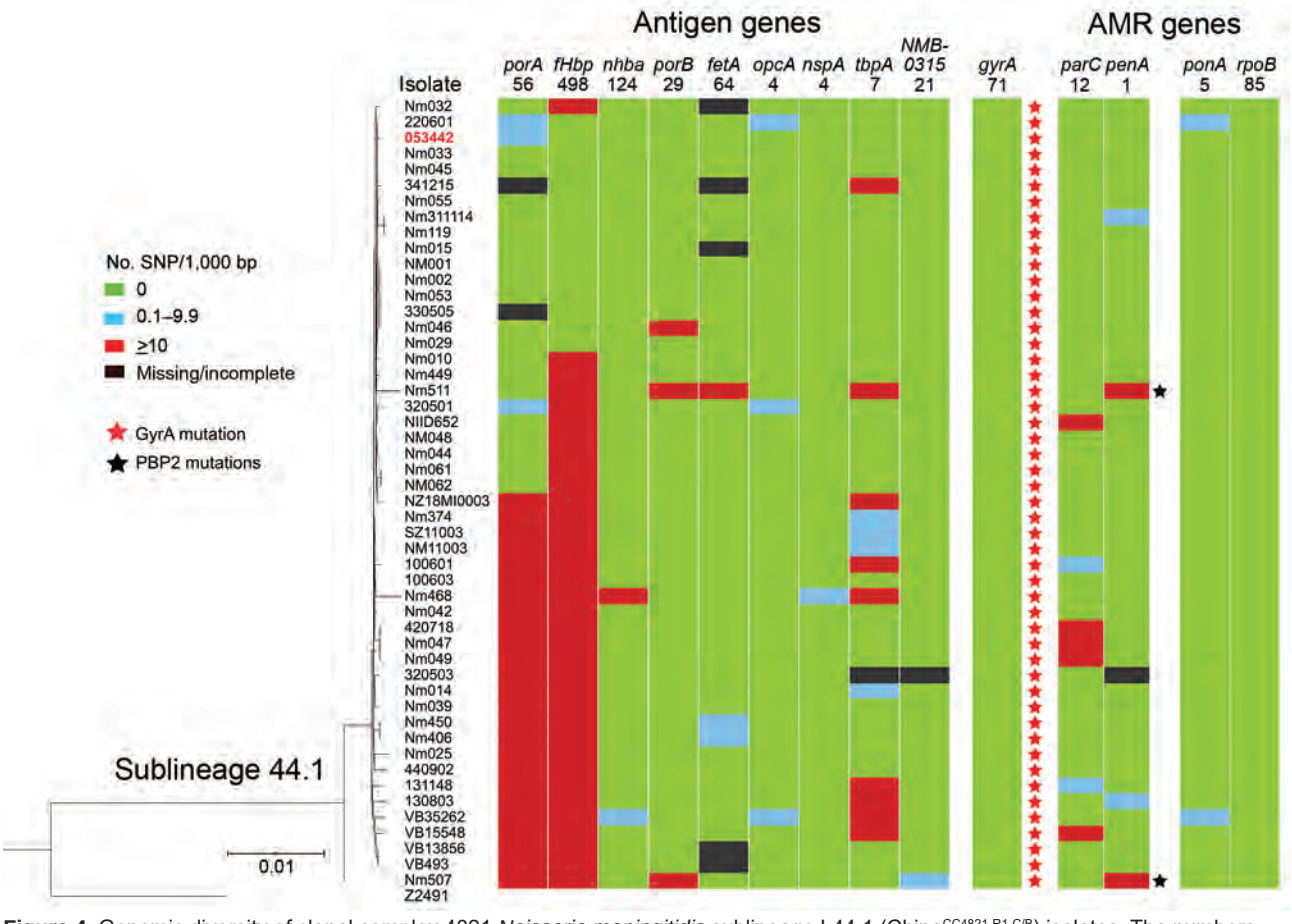

Figure 4. Genomic diversity of clonal complex 4821 *Neisseria meningitidis* sublineage L44.1 (China$^{CC4821\text{-}R1\text{-}C/B}$) isolates. The numbers underneath the antigen genes and AMR genes are the dominant alleles for that particular gene, and the colored blocks for SNPs/1,000 bp were determined using the allele number labeled above each column as the reference allele. AMR, antimicrobial resistance; SNP, single-nucleotide polymorphism.

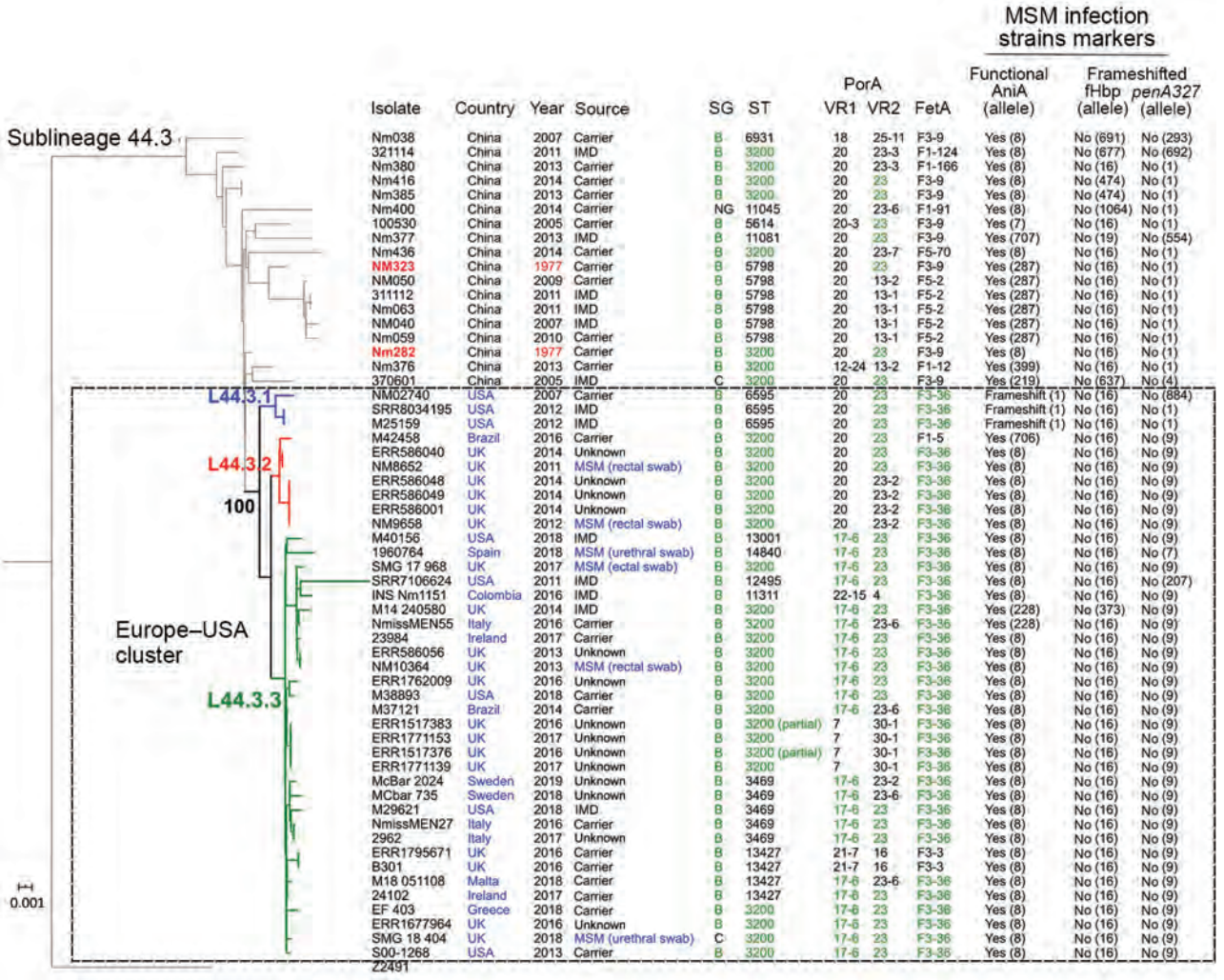

Figure 5. Phylogenetic tree and data of clonal complex 4821 *Neisseria meningitidis* sublineage L44.3 isolates. Red text indicates the oldest isolates of the sublineage; blue text, the isolates from countries outside of China and the isolates from genitourinary swabs from MSM; and green text, the dominant type or allele. The Europe–USA cluster can be further divided into 3 subclusters: subcluster L44.3.1, composed of 3 ST6595 isolates from the United States, all of which contained putatively nonfunctional AniA; L44.3.2, composed of 7 ST3200 isolates from the United Kingdom (n = 6) and Brazil (n = 1); and L44.3.3, composed of 30 isolates with multiple geographic locations. All the isolates from urethral (n = 2) and rectal (n = 4) swabs were assigned to L44.3.2 and L44.3.3, both of which comprised isolates with putatively functional AniA. Scale bar indicates substitutions per site. IMD, invasive meningococcal disease; MSM, men who have sex with men; NG, nongroupable; SG, serogroup; ST, sequence type; VR, variable region.

and New Zealand (n = 1, identified in 2018). These 6 isolates were clustered together and were closely related with 44 isolates from China within sublineage L44.1 (Figures 2–3). Only the isolate from Japan showed the typical molecular feature of Anhui outbreak strain (C:P1.7-2,14:F3-3:ST-4821[CC4821]).

Features and Evolution of Serogroup W CC4821 Isolates

A total of 11 MenW isolates from China were identified; the representative strain designation was W:P1.5-3,10-2:F1-7:ST-8491(CC4821), with similar gene profiles of antigen-encoding loci (*porA*-1804, *fHbp*-474, *nhba*-966, *fetA*-37, *opcA*-4, *nspA*-117, and *NMB0315*-21) and antimicrobial resistance loci (*gyrA*-294 with T91I, *parC*-779, *ponA*-7, and *rpoB*-85). These MenW isolates constituted a distinct cluster in L44.4; they were more closely related to NM193 (C:P1.20-3,23-1:F1-5:ST-3436[CC4821], dating from 1972) than to NM205 (C:P1.20,23-2:F5-135:ST-4821[CC4821], dating from 1973) (Appendix 2 Figure 17).

Discussion

The meningococci can cause IMD, leading to endemic disease in most if not all human populations. Several

genotypes belonging to hyperinvasive lineages, in combination with the disease-associated capsular serogroups, can cause elevated levels of disease; some of which also possess epidemic and pandemic potential. In the past 100 years, notable epidemics and pandemics have included meningococci such as A:CC1, A:CC5, B:CC41/44, C:CC11, and W:CC11 (*35*). Here, we employed a genomic analysis of MenB, MenC, and MenW CC4821 isolates dating from 1972–2019 to assess their epidemic and pandemic potential. Of special concern are the expansion of the quinolone-resistant clone China$^{CC4821\text{-}R1\text{-}C/B}$ from China to other countries; the potential possession of universal resistance to penicillin in Europe–USA cluster isolates; and the uncertainty over the potential efficacy of existing vaccines to prevent B:CC4821 diseases.

CC4821, which corresponds to lineage 44, shares several properties in common with the hyperinvasive CC11 meningococci (lineage 11): its ability to express several serogroups, global distribution, colonization of urogenital and anorectal tracts, and separation into distinct sublineages. CC11 has caused well-documented epidemics and pandemics on several occasions, including US military outbreaks in the 1960s; Hajj-associated outbreaks in 2000s; and the global epidemics from 2010, especially outbreaks among MSM (*34*–*38*). These similar characteristics raise the concern that the CC4821 may have the potential to cause similar global pandemics.

Consistent with the presence of the epidemic CC4821 clone in countries outside of China, 6 CC4821 IMD meningococci from India, Japan, and New Zealand, isolated during 2014–2018, clustered with China$^{CC4821\text{-}R1\text{-}C/B}$ meningococci in L44.1 (Figure 3). IMD cases caused by these 6 isolates were all found in native inhabitants (*10*,*15*,*39*); all 6 isolates shared

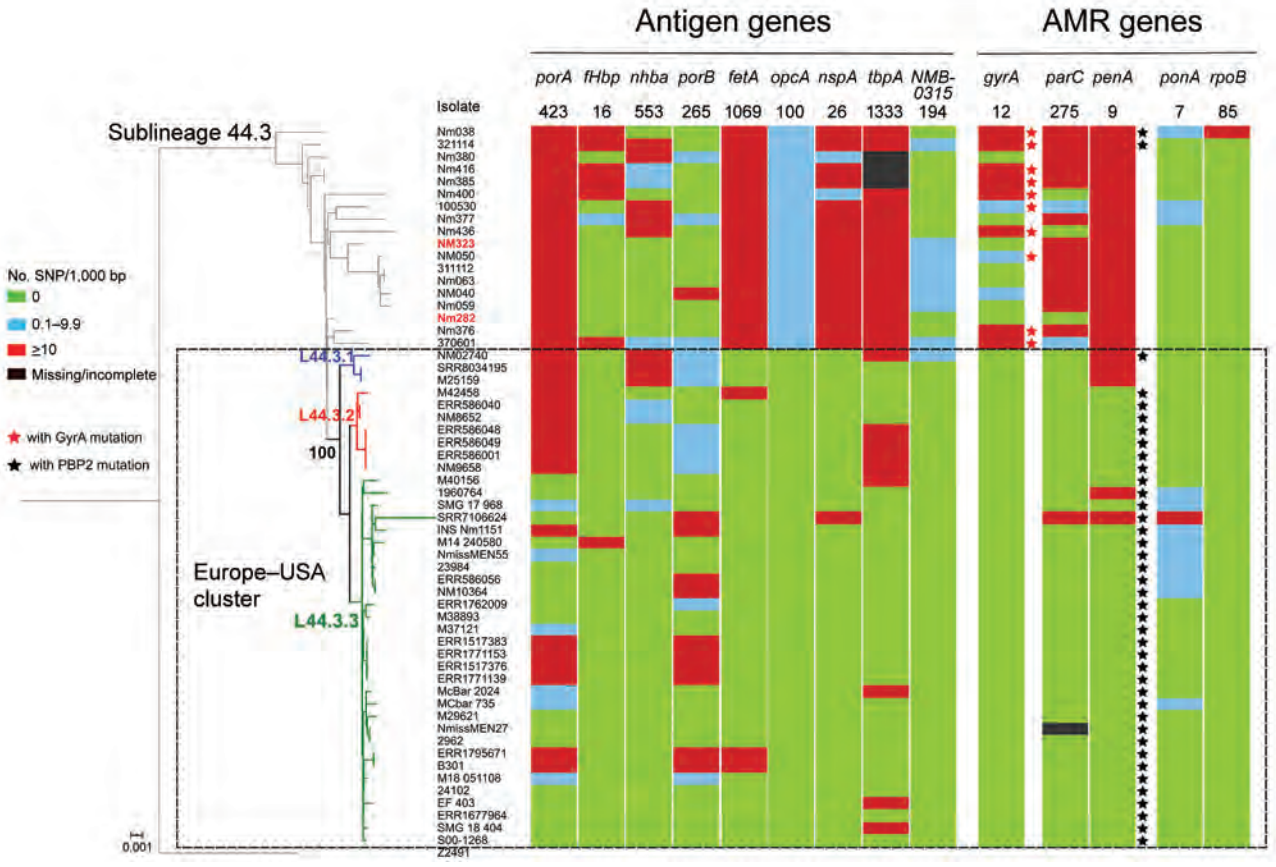

Figure 6. Genomic diversity of clonal complex 4821 *Neisseria meningitidis* sublineage L44.3 isolates. The numbers underneath the antigen genes and AMR genes are the dominant alleles for that particular gene, and the color blocks for SNPs/1,000 bp were determined using the allele number labeled above each column as the reference allele. The Europe–USA cluster can be further divided into 3 subclusters: subcluster L44.3.1, composed of 3 ST6595 isolates from the United States, all of which contained putatively nonfunctional AniA; L44.3.2, composed of 7 ST3200 isolates from the United Kingdom (n = 6) and Brazil (n = 1); and L44.3.3, composed of 30 isolates with multiple geographic locations. All the isolates from urethral (n = 2) and rectal (n = 4) swabs were assigned to L44.3.2 and L44.3.3, both of which comprised isolates with putatively functional AniA. Scale bar indicates substitutions per site. AMR, antimicrobial resistance; SNP, single-nucleotide polymorphism.

Table 2. Specific alleles of antigenic genes in 4 sublineages of clonal complex 4821 of *Neisseria meningitidis*

Sublineage	Antigen allele no. (no. isolates)								
	PorA	*fHbp*	*nhba*	PorB	FetA-VR	*opcA*	*nspA*	*tbpA*	*NMB-0315*
L44.1, n = 50	P1.7–2,14 (25) P1.12–1,16–8 (9)	22 (12) 489 (13) 498 (15)	124 (48)	3–48 (47)	F3–3 (45)	None	4 (49)	7 (36)	None
L44.2, n = 29	None	None	965 (10) 967 (12)	3–81 (15)	F1–91 (20)	None	None	None	335 (26)
L44.3, n = 58	P1.17–6,23-x* (23)	None	None	3–229 (35)	F3–9 (8) F3–36 (37)	100 (40)	26 (39)	1,333 (31)	194 (49)
L44.4, n = 32	P1.5–3,10–2 (8)	None	None	3–460 (7)	F1–7 (11)	None	117 (20)	None	None

*23-x refers to 23, 23–2, and 23–6.

similar serogroup, antibiotic, and antigen (except *porA* and *fHbp*) gene characteristics with isolates from China in this sublineage. In particular, all 6 isolates harbored the T91I mutation in GyrA, the molecular marker of quinolone resistance, compatible with their quinolone-resistant phenotype (*10*,*15*,*39*). These isolates also had strain-specific features, which suggested that they resulted from transmission from the China$^{CC4821\text{-}R1\text{-}C/B}$ clone. The isolate from Japan, which had the typical molecular features of the Anhui outbreak strain (C:P1.7-2,14:F3-3:ST-4821[CC4821]) (*4*), became the earliest-reported quinolone-resistant meningococcus harboring ParC mutation (S87I, allele 1538) to cause IMD worldwide (*10*). In contrast, none of the China$^{CC4821\text{-}R1\text{-}C/B}$ clone isolates from China had ParC mutations conferring antimicrobial resistance. The isolate from Japan was more closely related to the reference strain 053442 than were the 4 India and 1 New Zealand isolates, which had different STs, *porA*, *fHbp*, and *tbpA* alleles (Figure 4).

Although we did not identify a putative ancestor of the quinolone-resistant clone China$^{CC4821\text{-}R1\text{-}C/B}$ in this study, we found 299 loci with alleles unique to this sublineage. Approximately half of these loci were associated with metabolic pathways, suggesting that divergence in metabolic genes may play a role in the emergence of epidemic meningococci. Several studies have indicated that metabolic genes can influence the pathogenesis and virulence of the meningococcus, for example by allowing alternative host resources to be exploited in invasive disseminated infections (*40*). Changes in the hyperinvasive A:CC5 meningococci circulating in Africa have been associated with HGT of core genes involved in metabolic processes (*41*). The putative donors of these unique alleles included lineages from different serogroups and dates of isolation, such as C:ST-9514 cluster, 1960s–1970s; A:CC5 and A:CC1, 1960s–1980s; B:CC32, 1960s; B:CC41/44, 1970s; and E:CC178, 1980s (Table 4). The C:ST-9514 cluster, STs that do not presently form part of a clonal complex documented in PubMLST, has ST9514 as the central ST and was predominant in MenC carriage isolates during 1965–1980 in Shanghai, China (*42*). Therefore, the emergence of China$^{CC4821\text{-}R1\text{-}C/B}$ clone was perhaps associated with accumulation of these unique alleles, which accounted for the separation from other sublineages in the allele-based phylogeny (Figure 2).

In the PubMLST database, >60% of the CC4821 isolates from outside China were MenB. Of these, 49 genomes were available in this study, including isolates from IMD (n = 15) and urogenital and rectal tracts (n = 6). Most of these genomes clustered in sublineage L44.3 and constituted a distinct cluster, the Europe–USA cluster, showing the typical strain designation: B:P1.17-6,23-x:F3-36:ST-3200(CC4821), wherein 23-x refers to 23, 23-2, and 23-6. The PorA and FetA types P1.17-6,23-x and F3-36 were only found in this cluster. The *Neisseria* PubMLST database had no genome data for 24 CC4821 isolates from other countries (United States, Brazil, France, Czech Republic, Spain, Italy, Australia, and Vietnam), but included PorA or FetA variants for the 24 isolates (Appendix 1 Table 5). Of these, 19 (79.2%) exhibited P1.17-6,23-x or F3-36, suggesting they might belong to the Europe–USA cluster. This cluster was distinct from the epidemic clone China$^{CC4821\text{-}R1\text{-}C/B}$. For example, the antigen profile characteristic of the Europe–USA cluster was P1.17-6,23-x, F3-36, PorB-3-229, *fHbp* -16, *nhba*-553, *opcA*-100, *nspA*-26, and *tbpA*-1333, compared with P1.7-2,14, F3-3, PorB-3-48, *fHbp*-498, 22 and 489, *nhba*-124, *opcA*-4, *nspA*-4, and *tbpA*-7 in the China$^{CC4821\text{-}R1\text{-}C/B}$ clone. In addition, all the China$^{CC4821\text{-}R1\text{-}C/B}$ isolates harbored the mutation T91I in GyrA, whereas almost all of the Europe–USA cluster isolates possessed mutations in PBP2 (F504L, A510V, I515V, H541N, and I566V). This may reflect different antibiotic selective pressures experienced by the Europe–USA and the China$^{CC4821\text{-}R1\text{-}C/B}$ meningococci. Penicillins were the most-used antimicrobial drugs in outpatients in Europe, whereas China has the second largest global increases of fluoroquinolone consumption (*43*,*44*). A high frequency (>70%) of quinolone resistance has been reported in China since 2005 (*5*), whereas 65% of meningococci

in Europe showed reduced susceptibility to penicillin G during 1945–2006 (*45*). In the 2 oldest isolates of the sublineage L44.3, Nm282 (B:P1.20,23:F3-36:ST-3200[CC4812]) was much closer to the Europe–USA cluster isolates than Nm323 (B:P1.20,23:F3-36:ST-5798[CC4821]) (Figure 5), and it seemed more likely to be the ancestor of the Europe–USA cluster isolates.

Urogenital and rectal meningococci have raised increasing public health concerns (*34*). In 2017, CC4821 anorectal isolates were identified in the United Kingdom (*12*). In this study, we identified CC4821 isolates from urethral and rectal tracts that clustered with isolates from IMD specimens and oropharyngeal carriage (Figure 5). With the exception of L44.1 isolates, most of the CC4821 isolates contained a putatively functional nitrite reductase (AniA), required for growth in anaerobic environments. The CC4821 isolates acquired quinolone resistance alleles from *N. lactamica* and *N. subflava* (*46*); the ability to grow in anaerobic environments will facilitate acquisition of gonococcal alleles, including antimicrobial resistance alleles. Such events seem to have already occurred in a sublineage of CC11, which was responsible for several IMD outbreaks and urethritis among MSM (*34*). They shared the same *penA* allele (*penA327/penAXXX-IV*) with gonococcal bacteria and showed decreased susceptibility to third-generation cephalosporins (*47*). Although PubMLST is the largest global repository of meningococcal genomes (>22,000), a paucity of genomic data were available from isolates originating from the genitourinary or respiratory tract, suggesting an underestimation of the global dissemination of CC4821. Therefore, we recommend WGS for urogenital-, rectal-, and respiratory-derived meningococci if they are exhibiting antimicrobial resistance.

CC4821 lineage 44 includes isolates from different serogroups, including MenB, MenC, and MenW. In China, MenC and MenW isolates can be prevented

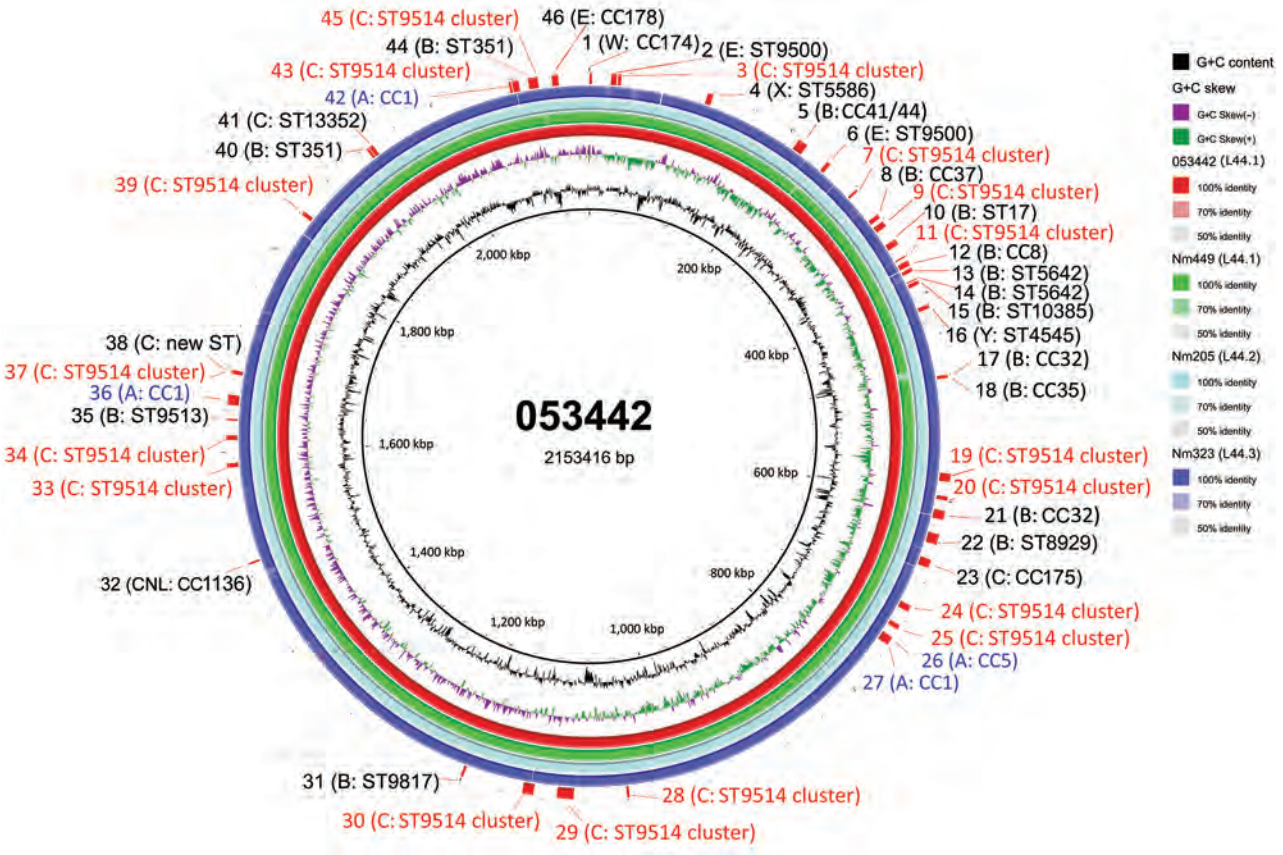

Figure 7. Circular genome map of CC4821 *Neisseria meningitidis* genome 053442 with BLAST (https://blast.ncbi.nlm.nih.gov/Blast.cgi) comparisons to the genomes of other sublineages. The innermost rings show guanine and cytosine (G+C) content (black) and G+C skew (negative in purple, positive in green) of genome 053442. The 4 outer rings show BLAST comparisons (using BLASTn and an E-value cutoff of 10.0) to the complete genome sequence of 053442 (red), Nm449 (green), Nm205 (pale blue), and Nm323 (blue); shading on rings indicates percentage identity as indicated in the key. Labels around the outer ring refer to the 46 HGT events involving 149 unique loci that are labeled with their possible donor strain. Red text indicates loci related to most common donors; blue text indicates those with serogroup A hyperinvasive lineage donors. CC, clonal complex; HGT, horizontal gene transfer; Nm, *N. meningitidis*; ST, sequence type.

Table 3. Loci present only in sublineage L44.1 of clonal complex 4821 of *Neisseria meningitidis**

Locus	Gene ID	Product	KEGG pathway
NEIS0364	NMCC_0368	Conserved hypothetical protein	Genetic information processing
NEIS0365	NMCC_0369	Competence protein ComFC	Signaling and cellular processes
NEIS0632	NMCC_0638	Lipoprotein	Signaling and cellular processes
NEIS2493	NMBG2136_1300	Hypothetical integral membrane protein	Not included
NEIS3165	NMCC_2037	Histone macro-H2A1-related protein	Metabolism

*KEGG, Kyoto Encyclopedia of Genes and Genomes.

by vaccines, such as group A and C meningococcal polysaccharide vaccine (MPV-AC) and MPV-ACYW, but no routinely administered vaccine is available to prevent MenB IMD (*48*). Two protein-based vaccines, targeting MenB meningococci 4CMenB (Bexsero) and rLP2086 (Trumenba), have been licensed in several countries (*49*–*50*; reference *51* in Appendix 2), but limited data are available on the bacterial coverage of these vaccines to CC4821 isolates directly from serum bactericidal activity assays, the Meningococcal Antigen Typing System (MATS) for Bexsero, or meningococcal antigen surface expression for Trumenba. One B:CC4821 isolate (M14-240580, UK) was reported to be tested using the MATS assay and showed no potential protection (reference *52* in Appendix 2). Using systems to index complex genotypic and phenotypic data, such as the MenDeVAR Index, we predicted that ≈60% of B:CC4821 disease-causing isolates might be prevented through vaccination with Trumenba; data are insufficient to infer Bexsero reactivity. Further testing of globally diverse meningococci is needed with these experimental assays to analyze potential vaccine impact in settings outside Europe.

In summary, we have undertaken a comprehensive genomic analysis of a hyperinvasive meningococcal CC4821 expressing MenB, MenC, and MenW with expansion from China to other global geographic locations with currently available genomic data. We identified key genomic factors and putative evolutionary changes that might have led to the emergence and persistence of the epidemic quinolone-resistant clone in China. Vaccine coverage for MenB CC4821 isolates needs further evaluation. Enhanced laboratory surveillance for CC4821 isolates from IMD cases and from oropharyngeal, urethral, and rectal carriage is needed to monitor global trends of expansion, which will be essential for local immunization policies.

Acknowledgments

We thank the MRF Meningococcus Genome Library, Sharif Shaaban, and Bingqing Zhu for providing CC4821 genomes through the *Neisseria* MLST Database. We thank Don Weiss of New York City Department of Health and Mental Hygiene for sharing with us the epidemiologic information of isolate S00-1268. We thank Xin Wang, Henju Marjuki, and Nadav Topaz of US Centers for Disease Control and Prevention for sharing with us the epidemiological information of isolates M29621, M38893, and M40156. We thank Zhaoyi Jia of Hebei CDC for checking the epidemiological information of isolate 130644. We thank Jay Lucidarme and Ray Borrow of Public Health England for sharing with us the epidemiological information of isolate M14 240580. We thank Hongyou Chen of Shanghai CDC for assistance of Gubbins analysis.

This study made use of *Neisseria* genomic data deposited in the *Neisseria* PubMLST Database (https://pubmlst.org/neisseria/) sited at the University of Oxford (Jolley & Maiden 2018, Wellcome open research, 3:124); the development of this database has been funded by the Wellcome Trust and European Union. This work was supported by National Natural Science Foundation of China under grant 81872909 and 81601801, Shanghai Rising-Star Program from Shanghai Municipal Science and Technology Commission (grant 17QA1403100), a Municipal Human Resources Development Program for Outstanding Young Talents in Medical and Health Sciences in Shanghai (grant 2017YQ039), and the 13th Five-Year Project of National Health and Family Planning Commission of the People's Republic of China (grants 2017ZX10303405004 and 2017ZX10103009-003). The funders had no role in the study design, data collection and interpretation, or the decision to submit the work for publication.

About the Author

Dr. Chen is an associate professor in Department of Microbiology, Shanghai Municipal Center for Disease Control and Prevention. His research interests include mechanisms of antimicrobial resistance in clinical isolates responsible for respiratory tract infections.

References

1. Jafri RZ, Ali A, Messonnier NE, Tevi-Benissan C, Durrheim D, Eskola J, et al. Global epidemiology of invasive meningococcal disease. Popul Health Metr. 2013;11:17. https://doi.org/10.1186/1478-7954-11-17
2. Maiden MC, Bygraves JA, Feil E, Morelli G, Russell JE, Urwin R, et al. Multilocus sequence typing: a portable approach to the identification of clones within populations

of pathogenic microorganisms. Proc Natl Acad Sci U S A. 1998;95:3140–5. https://doi.org/10.1073/pnas.95.6.3140
3. Zhou H, Gao Y, Xu L, Li M, Li Q, Li Y, et al. Distribution of serogroups and sequence types in disease-associated and carrier strains of *Neisseria meningitidis* isolated in China between 2003 and 2008. Epidemiol Infect. 2012;140:1296–303. https://doi.org/10.1017/S0950268811001865
4. Shao Z, Li W, Ren J, Liang X, Xu L, Diao B, et al. Identification of a new *Neisseria meningitidis* serogroup C clone from Anhui province, China. Lancet. 2006;367:419–23. https://doi.org/10.1016/S0140-6736(06)68141-5
5. Chen M, Guo Q, Wang Y, Zou Y, Wang G, Zhang X, et al. Shifts in the antibiotic susceptibility, serogroups, and clonal complexes of *Neisseria meningitidis* in Shanghai, China: a time trend analysis of the pre-quinolone and quinolone eras. PLoS Med. 2015;12:e1001838, discussion e1001838. https://doi.org/10.1371/journal.pmed.1001838
6. Guo Q, Mustapha MM, Chen M, Qu D, Zhang X, Chen M, et al. Evolution of sequence type 4821 clonal complex meningococcal strains in China from prequinolone to quinolone era, 1972–2013. Emerg Infect Dis. 2018;24:683–90. https://doi.org/10.3201/eid2404.171744
7. Zhu B, Xu Z, Du P, Xu L, Sun X, Gao Y, et al. Sequence type 4821 clonal complex serogroup B *Neisseria meningitidis* in China, 1978–2013. Emerg Infect Dis. 2015;21:925–32. https://doi.org/10.3201/eid2106.140687
8. Peng J, Yang L, Yang F, Yang J, Yan Y, Nie H, et al. Characterization of ST-4821 complex, a unique *Neisseria meningitidis* clone. Genomics. 2008;91:78–87. https://doi.org/10.1016/j.ygeno.2007.10.004
9. Chiou CS, Liao JC, Liao TL, Li CC, Chou CY, Chang HL, et al. Molecular epidemiology and emergence of worldwide epidemic clones of *Neisseria meningitidis* in Taiwan. BMC Infect Dis. 2006;6:25. https://doi.org/10.1186/1471-2334-6-25
10. Kawasaki Y, Matsubara K, Takahashi H, Morita M, Ohnishi M, Hori M, et al. Invasive meningococcal disease due to ciprofloxacin-resistant *Neisseria meningitidis* sequence type 4821: The first case in Japan. J Infect Chemother. 2018 2018;24:305–8.
11. Tsang RS, Law DK, Deng S, Hoang L. Ciprofloxacin-resistant *Neisseria meningitidis* in Canada: likely imported strains. Can J Microbiol. 2017;63:265–8. https://doi.org/10.1139/cjm-2016-0716
12. Harrison OB, Cole K, Peters J, Cresswell F, Dean G, Eyre DW, et al. Genomic analysis of urogenital and rectal *Neisseria meningitidis* isolates reveals encapsulated hyperinvasive meningococci and coincident multidrug-resistant gonococci. Sex Transm Infect. 2017;93:445–51. https://doi.org/10.1136/sextrans-2016-052781
13. Chen M, Wang W, Tu L, Zheng Y, Pan H, Wang G, et al. An *emm*5 Group A streptococcal outbreak among workers in a factory manufacturing telephone accessories. Front Microbiol. 2017;8:1156. https://doi.org/10.3389/fmicb.2017.01156
14. Topaz N, Boxrud D, Retchless AC, Nichols M, Chang HY, Hu F, et al. BMScan: using whole genome similarity to rapidly and accurately identify bacterial meningitis causing species. BMC Infect Dis. 2018;18:405. https://doi.org/10.1186/s12879-018-3324-1
15. Veeraraghavan B, Neeravi AR, Devanga Ragupathi NK, Inbanathan FY, Pragasam AK, Verghese VP. Whole-genome shotgun sequencing of the first observation of *Neisseria meningitidis* sequence type 6928 in India. Genome Announc. 2016; 4:e01232-16. https://doi.org/10.1128/genomeA.01232-16
16. Moura ARSS, Kretz CB, Ferreira IE, Nunes AMPB, de Moraes JC, Reis MG, et al. Molecular characterization of *Neisseria meningitidis* isolates recovered from 11-19-year-old meningococcal carriers in Salvador, Brazil. PLoS One. 2017;12:e0185038. https://doi.org/10.1371/journal.pone.0185038
17. Ezeoke I, Galac MR, Lin Y, Liem AT, Roth PA, Kilianski A, et al. Tracking a serial killer: integrating phylogenetic relationships, epidemiology, and geography for two invasive meningococcal disease outbreaks. PLoS One. 2018;13:e0202615. https://doi.org/10.1371/journal.pone.0202615
18. Parks DH, Imelfort M, Skennerton CT, Hugenholtz P, Tyson GW. CheckM: assessing the quality of microbial genomes recovered from isolates, single cells, and metagenomes. Genome Res. 2015;25:1043–55. https://doi.org/10.1101/gr.186072.114
19. Wu X, Li K, Xie M, Yu M, Tang S, Li Z, et al. Construction and protective immunogenicity of DNA vaccine pNMB0315 against *Neisseria meningitidis* serogroup B. Mol Med Rep. 2018;17:3178–85.
20. Lewis LA, Ngampasutadol J, Wallace R, Reid JE, Vogel U, Ram S. The meningococcal vaccine candidate neisserial surface protein A (NspA) binds to factor H and enhances meningococcal resistance to complement. PLoS Pathog. 2010;6:e1001027. https://doi.org/10.1371/journal.ppat.1001027
21. Poolman JT, Richmond P. Multivalent meningococcal serogroup B vaccines: challenges in predicting protection and measuring effectiveness. Expert Rev Vaccines. 2015;14:1277–87. https://doi.org/10.1586/14760584.2015.1071670
22. Fegan JE, Calmettes C, Islam EA, Ahn SK, Chaudhuri S, Yu RH, et al. Utility of hybrid transferrin binding protein antigens for protection against pathogenic *Neisseria* species. Front Immunol. 2019;10:247. https://doi.org/10.3389/fimmu.2019.00247
23. Unemo M, Shafer WM. Antimicrobial resistance in *Neisseria gonorrhoeae* in the 21st century: past, evolution, and future. Clin Microbiol Rev. 2014;27:587–613. https://doi.org/10.1128/CMR.00010-14
24. Acevedo R, Bai X, Borrow R, Caugant DA, Carlos J, Ceyhan M, et al. The Global Meningococcal Initiative meeting on prevention of meningococcal disease worldwide: epidemiology, surveillance, hypervirulent strains, antibiotic resistance, and high-risk populations. Expert Rev Vaccines. 2019;18:15–30. https://doi.org/10.1080/14760584.2019.1557520
25. Rodrigues CMC, Jolley KA, Smith A, Cameron JC, Feavers IM, Maiden MCJ. Meningococcal deduced vaccine antigen reactivity (MenDeVAR) index: a rapid and accessible tool that exploits genomic data in public health and clinical microbiology applications. J Clin Microbiol. 2020;59:e02161-20. https://doi.org/10.1128/JCM.02161-20
26. Bratcher HB, Corton C, Jolley KA, Parkhill J, Maiden MCJ. A gene-by-gene population genomics platform: de novo assembly, annotation and genealogical analysis of 108 representative *Neisseria meningitidis* genomes. BMC Genomics. 2014;15:1138. https://doi.org/10.1186/1471-2164-15-1138
27. Jolley KA, Bray JE, Maiden MCJ. Open-access bacterial population genomics: BIGSdb software, the PubMLST.org website and their applications. Wellcome open research. 2018;3:124. https://doi.org/10.12688/wellcomeopenres.14826.1
28. Tamura K, Peterson D, Peterson N, Stecher G, Nei M, Kumar S. MEGA5: molecular evolutionary genetics analysis using maximum likelihood, evolutionary distance, and maximum parsimony methods. Mol Biol Evol. 2011;28:2731–9. https://doi.org/10.1093/molbev/msr121

29. Kanehisa M, Goto S, Sato Y, Furumichi M, Tanabe M. KEGG for integration and interpretation of large-scale molecular data sets. Nucleic Acids Res. 2012;40(D1):D109–14. https://doi.org/10.1093/nar/gkr988
30. Treangen TJ, Ondov BD, Koren S, Phillippy AM. The Harvest suite for rapid core-genome alignment and visualization of thousands of intraspecific microbial genomes. Genome Biol. 2014;15:524. https://doi.org/10.1186/s13059-014-0524-x
31. Croucher NJ, Page AJ, Connor TR, Delaney AJ, Keane JA, Bentley SD, et al. Rapid phylogenetic analysis of large samples of recombinant bacterial whole genome sequences using Gubbins. Nucleic Acids Res. 2015;43:e15. https://doi.org/10.1093/nar/gku1196
32. Mustapha MM, Marsh JW, Krauland MG, Fernandez JO, de Lemos AP, Dunning Hotopp JC, et al. Genomic investigation reveals highly conserved, mosaic, recombination events associated with capsular switching among invasive *Neisseria meningitidis* serogroup W sequence type (ST)-11 strains. Genome Biol Evol. 2016;8:2065–75. https://doi.org/10.1093/gbe/evw122
33. Alikhan NF, Petty NK, Ben Zakour NL, Beatson SA. BLAST Ring Image Generator (BRIG): simple prokaryote genome comparisons. BMC Genomics. 2011;12:402. https://doi.org/10.1186/1471-2164-12-402
34. Ladhani SN, Lucidarme J, Parikh SR, Campbell H, Borrow R, Ramsay ME. Meningococcal disease and sexual transmission: urogenital and anorectal infections and invasive disease due to *Neisseria meningitidis*. Lancet. 2020;395:1865–77. https://doi.org/10.1016/S0140-6736(20)30913-2
35. Harrison LH, Trotter CL, Ramsay ME. Global epidemiology of meningococcal disease. Vaccine. 2009; Suppl 2:B51-63. https://doi.org/10.1016/j.vaccine.2009.04.063
36. Krone M, Gray S, Abad R, Skoczyńska A, Stefanelli P, van der Ende A, et al. Increase of invasive meningococcal serogroup W disease in Europe, 2013 to 2017. Euro Surveill. 2019;24. https://doi.org/10.2807/1560-7917.ES.2019.24.14.1800245
37. Lucidarme J, Hill DM, Bratcher HB, Gray SJ, du Plessis M, Tsang RS, et al. Genomic resolution of an aggressive, widespread, diverse, and expanding meningococcal serogroup B, C, and W lineage. J Infect. 2015;71:544–52. https://doi.org/10.1016/j.jinf.2015.07.007
38. Mayer LW, Reeves MW, Al-Hamdan N, Sacchi CT, Taha MK, Ajello GW, et al. Outbreak of W135 meningococcal disease in 2000: not emergence of a new W135 strain but clonal expansion within the electophoretic type-37 complex. J Infect Dis. 2002;185:1596–605. https://doi.org/10.1086/340414
39. Veeraraghavan B, Lal B, Devanga Ragupathi NK, Neeravi IR, Jeyaraman R, Varghese R, et al. First genome report on novel sequence types of *Neisseria meningitidis*: ST12777 and ST12778. J Glob Antimicrob Resist. 2018;12:117–8. https://doi.org/10.1016/j.jgar.2017.11.014
40. Schoen C, Kischkies L, Elias J, Ampattu BJ. Metabolism and virulence in *Neisseria meningitidis*. Front Cell Infect Microbiol. 2014;4:114. https://doi.org/10.3389/fcimb.2014.00114
41. Watkins ER, Maiden MC. Metabolic shift in the emergence of hyperinvasive pandemic meningococcal lineages. Sci Rep. 2017;7:41126. https://doi.org/10.1038/srep41126
42. Chen M, Rodrigues CMC, Harrison OB, Zhang C, Tan T, Chen J, et al. Invasive meningococcal disease in Shanghai, China from 1950 to 2016: implications for serogroup B vaccine implementation. Sci Rep. 2018;8:12334. https://doi.org/10.1038/s41598-018-30048-x
43. Adriaenssens N, Coenen S, Versporten A, Muller A, Minalu G, Faes C, et al.; ESAC Project Group. European Surveillance of Antimicrobial Consumption (ESAC): systemic antiviral use in Europe. J Antimicrob Chemother. 2011;66(Suppl 6):vi3–12. https://doi.org/10.1093/jac/dkr190
44. Van Boeckel TP, Gandra S, Ashok A, Caudron Q, Grenfell BT, Levin SA, et al. Global antibiotic consumption 2000 to 2010: an analysis of national pharmaceutical sales data. Lancet Infect Dis. 2014;14:742–50. https://doi.org/10.1016/S1473-3099(14)70780-7
45. Taha MK, Vázquez JA, Hong E, Bennett DE, Bertrand S, Bukovski S, et al. Target gene sequencing to characterize the penicillin G susceptibility of *Neisseria meningitidis*. Antimicrob Agents Chemother. 2007;51:2784–92. https://doi.org/10.1128/AAC.00412-07
46. Chen M, Zhang C, Zhang X, Chen M. meningococcal quinolone resistance originated from several commensal *Neisseria* species. Antimicrob Agents Chemother. 2020; 64:e01494–19.
47. Deghmane AE, Hong E, Taha MK. Emergence of meningococci with reduced susceptibility to third-generation cephalosporins. J Antimicrob Chemother. 2017;72:95–8. https://doi.org/10.1093/jac/dkw400
48. Li J, Shao Z, Liu G, Bai X, Borrow R, Chen M, et al. Meningococcal disease and control in China: findings and updates from the Global Meningococcal Initiative (GMI). J Infect. 2018;76:429–37. https://doi.org/10.1016/j.jinf.2018.01.007
49. Ladhani SN, Ramsay M, Borrow R, Riordan A, Watson JM, Pollard AJ. Enter B and W: two new meningococcal vaccine programmes launched. Arch Dis Child. 2016;101:91–5. https://doi.org/10.1136/archdischild-2015-308928
50. Ostergaard L, Vesikari T, Absalon J, Beeslaar J, Ward BJ, Senders S, et al.; B1971009 and B1971016 Trial Investigators. A bivalent meningococcal B vaccine in adolescents and young adults. N Engl J Med. 2017;377:2349–62. https://doi.org/10.1056/NEJMoa1614474

Address for correspondence: Mingliang Chen or Min Chen, Shanghai Municipal Center for Disease Control and Prevention, 1380 West ZhongShan Rd, Shanghai 200336, China; email: cmlbright@126.com or chenmin@scdc.sh.cn; Martin C.J. Maiden, University of Oxford, South Parks Rd, Oxford, OX1 3SY, UK; email: martin.maiden@zoo.ox.ac.uk

Epidemiologic and Genomic Reidentification of Yaws, Liberia

Joseph W.S. Timothy, Mathew A. Beale, Emerson Rogers, Zeela Zaizay, Katherine E. Halliday, Tarnue Mulbah, Romeo K. Giddings, Stephen L. Walker, Nicholas R. Thomson, Karsor K. Kollie,[1] Rachel L. Pullan,[1] Michael Marks[1]

We confirmed endemicity and autochthonous transmission of yaws in Liberia after a population-based, community-led burden estimation (56,825 participants). Serologically confirmed yaws was rare and focal at population level (24 cases; 2.6 [95% CI 1.4–3.9] cases/10,000 population) with similar clinical epidemiology to other endemic countries in West Africa. Unsupervised classification of spatially referenced case finding data indicated that yaws was more likely to occur in hard-to-reach communities; healthcare-seeking was low among communities, and clinical awareness of yaws was low among healthcare workers. We recovered whole bacterial genomes from 12 cases and describe a monophyletic clade of *Treponema pallidum* subspecies *pertenue*, phylogenetically distinct from known TPE lineages, including those affecting neighboring nonhuman primate populations (Taï Forest, Côte d'Ivoire). Yaws is endemic in Liberia but exhibits low focal population prevalence with evidence of a historical genetic bottleneck and subsequent local expansion. Reporting gaps appear attributable to challenging epidemiology and low disease awareness.

Yaws, caused by the bacterium *Treponema pallidum* subspecies *pertenue* (TPE), is an infection of skin and soft tissues, affecting primarily children, with transmission driven by direct human-to-human contact (*1*). TPE disseminates through the bloodstream and lymphatic system and can lead to extensive ulcerative or papillomatous lesions and progressive damage to cartilage or bone. In eradication campaigns that ran during 1948–1964, >300 million persons were assessed for yaws and >50 million were treated with injectable benzathine penicillin, reducing global prevalence by as much as 95% (*2*). Despite this achievement, interest in yaws eradication waned and the disease resurged in several countries in Africa, the Pacific, and Southeast Asia by the 1970s. In 2012 the World Health Organization (WHO) relaunched eradication efforts based on total community and targeted treatment with single-dose azithromycin, termed the Morges strategy (*3*).

Historically, 103 countries have reported cases of yaws, but as of 2018 only 14 continued to report confirmed cases to WHO (*4*). It remains unclear whether this reflects true absence of disease or rather inadequate surveillance and loss of disease-specific expertise (*5*). A recent modeling study suggested that more than two thirds of countries without recent data would be highly unlikely to report yaws without dedicated active surveillance (*4*). Furthermore, since the launch of the Morges strategy, the Philippines remains the only country that previously reported cases to subsequently confirm autochthonous transmission (*6*). Surveillance activities are challenging because of low population-level prevalence with cases clustered (*7*,*8*) among poor rural populations with low accessibility (*9*), although there is a lack of objective data on yaws-endemic communities. Consequently, no standardized approaches exist to efficiently identify cases in areas of unknown burden (*10*,*11*). One approach proposed by WHO to is to integrate active surveillance for multiple neglected tropical diseases (NTDs) that affect the skin (skin NTDs) (*12*), including yaws, an approach recently adopted by several countries in West Africa (*13*).

For *T. pallidum* subspecies *pallidum*, genetic epidemiology has informed understanding on global transmission patterns and macrolide resistance (*14*,*15*). Despite their close genetic relationship, few whole-genome sequences are currently available for TPE.

Author affiliations: London School of Hygiene and Tropical Medicine, London, UK (J.W.S. Timothy, K.E. Halliday, S.L. Walker, N.R. Thomson, R.L. Pullan, M. Marks); Wellcome Sanger Institute, Hinxton, UK (M.A. Beale, N.R. Thomson); Ministry of Health, Monrovia, Liberia (E. Rogers, Z. Zaizay, T. Mulbah, R.K. Giddings, K.K. Kollie); University College London Hospitals NHS Foundation Trust, London (S.L. Walker, M. Marks)

DOI: https://doi.org/10.3201/eid2704.204442

[1]These senior authors contributed equally to this article.

Furthermore, yaws-like disease caused by TPE has now been detected in nonhuman primate species in several countries in sub-Saharan Africa, including Côte d'Ivoire (*16*,*17*). The direct role of nonhuman primate species as a potential reservoir for zoonotic infection is currently unknown, but it may prove critical to guiding eradication strategies (*16*). Yaws eradication efforts will be supported through improved genomic analyses of human and nonhuman primate TPE at different spatiotemporal scales to inform understanding of transmission and antimicrobial resistance.

Yaws was previously highly endemic to Liberia; active clinical prevalence was estimated to be as high as 30% during the first eradication era (*18*). National surveillance systems, however, ceased reporting cases by the mid-1970s, and no yaws cases have been confirmed in subsequent decades (*5*,*19*). Several countries in the region do continue to report high numbers of yaws cases (*5*), including neighboring Côte d'Ivoire, and there have been anecdotal reports of unconfirmed cases in Liberia in recent years. As part of an integrated project on skin NTDs, we undertook an exhaustive population-based burden estimation in Maryland County, Liberia, and identified 24 cases of serologically confirmed yaws. We present detailed epidemiologic and whole-genome characterization of these cases and their affected communities.

Methods

Setting and Survey Design

We conducted a population-based cross-sectional integrated survey for skin NTDs (Buruli ulcer, leprosy, lymphatic filariasis–associated morbidity, and yaws) during June–October 2018 in Maryland County, Liberia (census population 165,456) (Appendix 1, https://wwwnc.cdc.gov/EID/article/27/4/20-4442-App1.pdf). Maryland County is in the far southeast part of Liberia and borders known yaws-endemic regions in Côte d'Ivoire. All communities and residents were eligible for inclusion. We defined community health worker catchment areas as primary sampling units (PSUs), stratified them across all 24 health facilities, and systematically selected them using probability proportional to size. The study protocol was approved by the University of Liberia (PIRE) Institutional Review Board (no. 18-02-088) and the Ethics Committee of the London School of Hygiene and Tropical Medicine (no. 14698).

Procedures

Community health workers undertook exhaustive screening for skin NTDs by visiting all households, door to door, in their selected PSUs. The community health workers showed photographs of common skin NTD lesions to household members who verbally reported whether they, or other household members, currently exhibited skin lesions similar to those in the photographs. Suspected skin lesions identified by community health workers were subsequently verified by specially trained nonphysician healthcare workers during follow-up surveys. For the purpose of this survey, we focused on the typical lesions of primary yaws, namely ulcerative lesions and papillomas. All persons with lesions compatible with yaws or tropical ulcer, and any child (<18 years of age) with any form of ulcer were tested using a rapid treponemal test (SD Bioline, https://www.globalpointofcare.abbott); if that result was positive, then they were tested with the syphilis dual path platform (DPP) lateral flow assay (ChemBio, https://chembio.com). During clinical diagnosis, details of healthcare-seeking behaviors and previous diagnoses were recorded, then confirmed at health facilities. For clinically suspicious cases of yaws or any other ulcers, swab specimens were collected from the largest lesion. Lesion samples were shipped to the London School of Hygiene and Tropical Medicine, where a multiplex quantitative PCR (qPCR) assay for both TPE (targeting *polA*) and *Haemophilus ducreyi* (*hhdA*), and a separate qPCR for *Mycobacterium ulcerans*, the causative agent of Buruli ulcer (*IS2404*), were performed. All serologically confirmed yaws cases (DPP positive) were referred for immediate treatment with azithromycin.

Outcome

We defined yaws infection as being positive for both treponemal and nontreponemal antibodies on testing with the DPP assay. We defined active yaws as a clinically suspicious lesion in which TPE was detected by qPCR from a lesion sample. Survey activities also included measurement of other skin NTDs (Appendix).

Data Analysis

We estimated prevalence through design-based inference as a stratified 1-stage cluster design with variance estimated using jackknife repeated replication (R version 4.0.1, survey version 3.36; https://www.r-project.org). The intraclass correlation coefficient (ICC) of PSUs was estimated from intercept-only binomial mixed effects models (lme4 version 1.1–23) (*20*). We extracted community accessibility data from all household GPS point locations (n = 9,375) collected by community health workers during screening from open-source GIS layers (raster version 3.1–5). Locations with missing data (n = 489) following extraction

were removed and median values aggregated by PSU for analysis. We used unsupervised classification to objectively define subpopulations of PSUs with lowest accessibility in Maryland County. We classified PSUs using nested (K-means) or partitioning (hierarchical agglomerative and divisive) clustering methods (cluster version 2.1.0). We used Euclidean distance as a standard measure and limited cluster number between 2 and 5. We applied Ward's method for hierarchical agglomerative classification. We chose the optimal approach using weighted rank aggregation across 3 measures of internal validity: Dunn index, silhouette width, and adjusted connectivity (optCluster version 1.3.0) (*21*) leading to selection of divisive hierarchical classification for final analysis.

Whole-Genome Sequencing

From all TPE PCR-positive swabs in the study, we submitted samples with a qPCR threshold of <Cq 32 for whole-genome sequencing using the pooled sequence capture method described previously (*14*,*22*). We mapped *Treponema*-specific sequencing reads to the Samoa D reference genome (bwa mem version 0.7.15), as previously described (*15*), to infer a whole genome multiple sequence alignment (samtools version 1.6, bcftools version 1.6, http://www.htslib.org), contextualized by 33 high-quality publicly available TPE genomes (and 1 *T. pallidum* subsp. *endemicum* as outgroup) from around the world. We used Gubbins version 2.4.1 (https://github.com/sanger-pathogens/gubbins) to mask recombination and generated a maximum likelihood phylogeny (IQ-Tree version 1.6.10, http://www.iqtree.org). Macrolide resistance-associated alleles were inferred as previously described (*15*). We inferred pairwise single nucleotide polymorphism distances between samples using pairsnp (https://github.com/gtonkinhill/pairsnp). We performed joint ancestral reconstruction using pyjar (https://github.com/simonrharris/pyjar).

Results

After exhaustive screening of 56,825 persons from 92 clusters in Maryland County, we assessed 81 persons with ulcerative or papillomatous lesions meeting testing criteria for yaws, using an SD Bioline rapid treponemal test. We identified 28 treponemal seropositive persons who were subsequently tested using the ChemBio DPP. Among this group, we identified 24 cases of serologically confirmed yaws infection; of these, 17 were PCR-confirmed active yaws lesions. We estimated the design-adjusted population prevalence of serologically-confirmed yaws infection as 2.6 (95% CI 1.4–3.9) cases/10,000 population (Table). Of note, the first case of yaws was not confirmed until 36,621 persons had been screened (Figure 1), emphasizing the sampling effort in confirmation of the first case. The spatial distribution of cases was highly focal, with occurrence in only 8/92 (8.7%) survey clusters and an intraclass correlation coefficient estimated at 0.93 (Figure 2). Maryland County is divided into 6 health districts; confirmed cases were identified in 3 districts, including a single, isolated case within the most populated district, Pleebo (Figure 2). Spatial clustering was also evident from the concentration of 15 cases (62.5%) among clusters served by a single health facility, where the maximum cluster-level prevalence of 2.0% was observed.

Aside from 1 case in a 32-year-old person, all confirmed cases were in persons ≤18 years of age, most of whom were male (Table). The most common clinical presentation was a solitary skin lesion. The morphology of the skin lesions was either papillomatous (12/24; 50.0%) or ulcerated (12/24; 50.0%). A total of 11/12 (91.7%) papillomas had a positive PCR for TPE (a specimen was missing for 1 sample), compared with 6/12 (50%) yaws-like ulcers that had a positive PCR for TPE. In addition, 12 persons identified with clinically suspicious yaws lesions tested negative by yaws serology. Among this group, we detected *H. ducreyi* in 3 persons and *IS2404* from *M. ulcerans* in 2 persons. Most persons with yaws cases (15/24; 62.5%) reported having symptoms for <6 months, although 3 reported persistence of symptoms for >3 years.

Active healthcare seeking for treatment of yaws among users of the Maryland health system appeared low, as did clinical awareness among providers. Fewer than half of persons with confirmed cases reported seeking formal healthcare for lesions before survey activities (Table). Among those seeking care (n = 11), only 1 person received any formal diagnosis (tropical ulcer) although 6 (54.5%) received prescription pharmaceuticals. Use of traditional medicine providers was rarely reported for persons with confirmed yaws (2/24, 8.3% of cases) despite the common use of these pathways for other skin NTDs reported in our project (data not shown). Only 1/7 (14.3%) nonphysician healthcare workers recruited for validation survey activities reported prior awareness of the clinical diagnosis of yaws during presurvey knowledge assessments. Despite this lack of awareness, the positive predictive value (PPV) of confirmed yaws among clinically suspicious cases was promising after a tailored training program for healthcare workers (64.5%, 95% CI 46.5%–80.3%). When broken down by major clinical forms, yaws papillomas demonstrated notably higher clinical PPV than ulcers (Table). Clinical teams

were also trained to differentiate between multiple forms of ulcers. The negative predictive value (NPV) among all ulcers clinically diagnosed with non-yaws etiology was high (98.0%, 95% CI 93.1%–99.8%). NPV remained high (94.4%, 95% CI 81.3%–99.3%) when limited to only tropical ulcers, the major differential diagnosis of yaws ulcers.

To objectively classify the accessibility of survey communities in Maryland County, we used a divisive hierarchical classification algorithm that defined 3 distinct population groups, which we described as high accessible (65 clusters), low accessible (26 clusters), and very low accessible (1 cluster; Appendix 1). Yaws cases were identified in all 3 population groups (Figure 2); the proportion of yaws-endemic communities was inversely correlated with accessibility (high access: 3/65, 4.6%; low access: 3/26, 11.5%; very low access: 1/1, 100%; p = 0.041). Four cases of active yaws were identified in the single very–low-access cluster (Figure 3, cluster A, prevalence 1.3%). This community exhibited similar population density to low-access clusters, but estimated travel times to cities, calculated using friction surface data, were 2.6 times higher and estimated travel times to health facilities were 3.6 times higher. More than half the confirmed cases (14/24; 58.3%) were identified in high-access clusters, including 1 community with 10 cases and prevalence of 2.0% (Figure 3, cluster B). Among the high-access communities, no cases were identified in clusters a priori defined as urban or periurban.

Table. Descriptive epidemiological characteristics of serologically confirmed yaws cases, Liberia*

Characteristic	Value
Total serologically confirmed cases	24
Total PCR-positive lesions	17 (70.8)
Whole genome recovered	12 (50.0)
Prevalence of serologically confirmed yaws, cases/10,000 population (95% CI)	
Crude prevalence in survey population	4.2 (2.5–5.9)
Design-adjusted population prevalence	2.6 (1.4–3.9)
Clinical diagnostic accuracy, % (95% CI)	
Positive predictive value of all suspected yaws	64.7 (46.5–80.3)
Positive predictive value of yaws ulcers	47.6 (25.7–70.2)
Negative predictive value of tropical ulcers	94.4 (81.3–99.3)
Positive predictive value of yaws papilloma	92.3 (64.0–99.8)
Case demographics	
Median age, y(interquartile range)†	10 (8.2–12.0)
Sex‡	
M	17 (73.9)
F	6 (26.1)
Clinical presentation	
Ulcer	12 (50.0)
Papilloma	12 (50.0)
No. active lesions‡	
1	17 (73.9)
2	3 (13.0)
3	2 (8.7)
10	1 (4.4)
Patient-reported duration of lesion	
<8 wk	9 (37.5)
8–26 wk	6 (25.0)
27 wk–1 y	5 (20.8)
1–3 y	0
>3 y	3 (12.5)
Unknown	1 (4.2)
Sought formal healthcare for lesion(s)	
Yes	11 (45.8)
No	13
Provided with any diagnosis from health provider	
Yes	1 (4.2)
No	23
Treated lesion(s) with prescription pharmaceuticals	
Yes	6 (25.0)
No	18
Sought traditional medicine for lesion(s)	
Yes	2 (8.3)
No	22

*Values are no. (%) except as indicated.
†Missing data for 2 cases.
‡Missing data for 1 case.

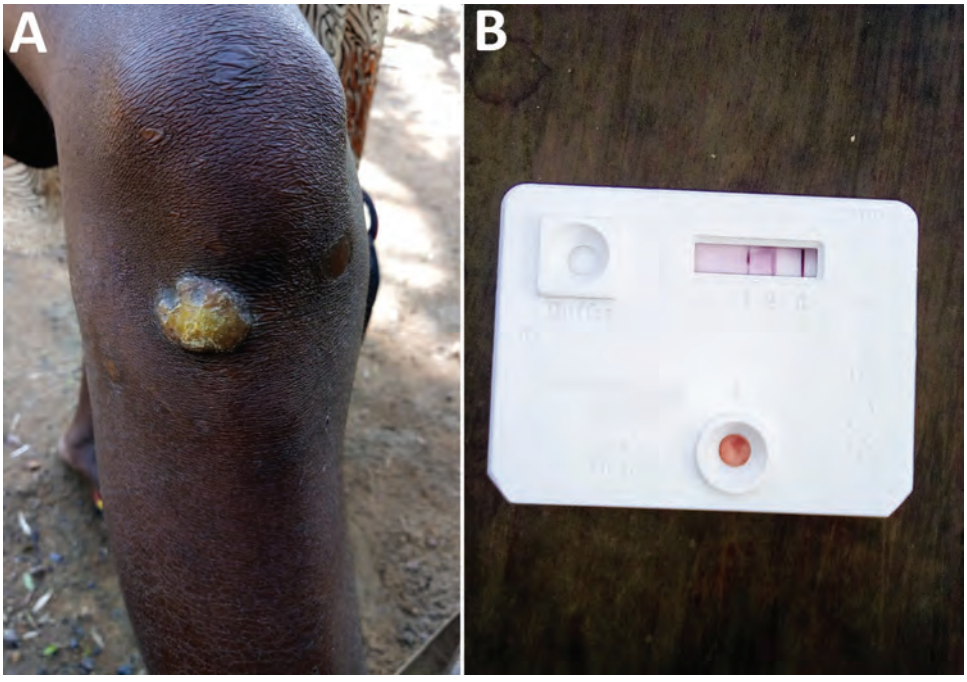

Figure 1. Clinical presentation and serological results of the first confirmed case of yaws since the 1970s and first whole *Treponema pallidum* subspecies *pertenue* (TPE) genome from Liberia. A) Papillomatous yaws lesion below the right knee. B) Paired serological results from this case. Dual path platform syphilis lateral flow assay (ChemBio, https://chembio.com) shows antibody binding to treponemal and nontreponemal antigen indicative of active yaws infection. A complete genome sequence was recovered from this case (Figure 3).

We conducted a sensitivity analysis using alternative clustering algorithms (k-means and agglomerative hierarchical). Both outputs failed to define a very–low-access group, yet delineated low-access populations with strong concordance to the original grouping. Yaws cases were similarly distributed across these 2 groups but lacked statistical evidence of a difference (agglomerative; high, 4/66, 6.1%; low, 4/26, 15.4%; p = 0.22). We also repeated classification analysis with leprosy-endemic communities (Appendix 1). This showed that leprosy did not follow the same patterns as yaws, with cases most frequent in high-access clusters (22/65, 33.8%; low access, 5/26, 19.2%; very low access, 0/1; p = 0.38).

We were able to recover whole genomes from 12 of the 17 PCR-positive lesion samples (Appendix 1 Table 1). We identified a novel monophyletic TPE clade in Maryland County (Figure 3) in which all sequences were phylogenetically distinct relative to publicly available TPE genomes isolated from humans and nonhuman primates (Figure 4). This distinction includes clear separation from the geographically related TPE genomes isolated in nonhuman primates from nearby Taï National Park (Côte d'Ivoire). All Liberia genomes were extremely closely related; 10 variable genome positions described the entire Liberia subtree, and a maximum of 7 pairwise single-nucleotide polymorphisms exist between any 2 TPE genomes. Ancestral reconstruction on the phylogeny inferred that the maximum number of substitutions from the common ancestor of all genomes sequenced from Maryland County was 4. Contextualized by previous estimates that the molecular clock rate of *T. pallidum* is 4–9 years/substitutions/genome (*14*,*23*), which suggests a recent common ancestor within the past 16–36 years. Despite low overall diversity, there remained evidence of local geographic separation within Maryland County genomes, particularly among 2 northernmost communities (Figure 3, clusters A, B). All sequences were predicted to be azithromycin sensitive based on in silico analysis of the 2 known azithromycin resistance loci (A2058G, A2059G) in the 23S ribosomal regions previously reported for syphilis or yaws.

Discussion

We have demonstrated through deployment of comprehensive serologic and molecular tools that yaws remains endemic to Liberia and have provided detailed epidemiologic description of the cases and the affected communities. Our results also provide novel insight into the genetic epidemiology of yaws in West Africa and the operational challenges of identifying yaws cases in countries with unknown disease distribution.

The clinical profile of yaws in Liberia is similar to those from other endemic countries in West Africa: the disease is predominantly detected in male children who have a high proportion of papillomatous lesions (*24*). We showed that TPE genomes in Maryland County form a monophyletic clade that is clearly distinct from other publicly available TPE genomes. The

low genomic diversity within samples from Liberia is consistent with previous observations regarding low mutation rates of TPE and TPA (*14*,*23*) yet contrasts the genetic and geographic structuring observed in the broader global phylogeny. This finding suggests evolution and expansion of local TPE strains from a common ancestor subsequent to the benzathine penicillin-based eradication campaigns conducted until the 1960s, rather than recent importation from elsewhere. This information contrasts with a recent study on highly endemic Lihir Island, Papua New Guinea, where TPE was polyphyletic and exhibited ≥3 distinct phylogenetic clades (*15*). These observations were made despite a smaller geographic area and population and may reflect both higher TPE transmission rates and mobility among island inhabitants. Repeated events similar to those observed in Liberia occurring across the West Africa region may also explain the broader geographic structuring (Figure 4). Under this scenario, circulating TPE populations may have undergone historic collapse as a consequence of previous eradication efforts, leading to genetic bottlenecks and subsequent expansion of isolated residual cases. Characterization of genomes from other spatially contiguous locations

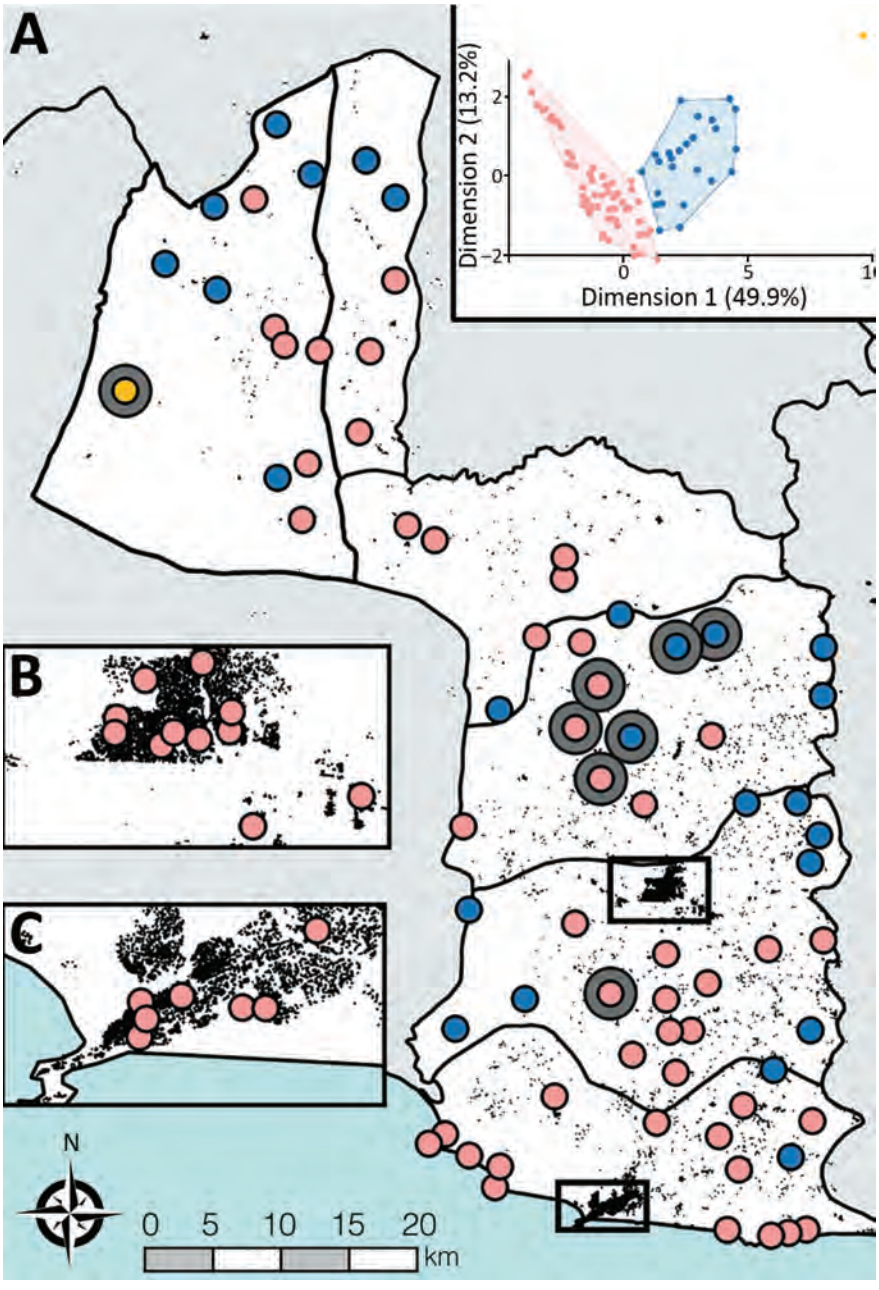

Figure 2. Spatial occurrence and accessibility of yaws endemic communities in Maryland County, Liberia. A) All survey cluster centroids (n = 92). Yaws endemic clusters are shown by large gray circles. All survey clusters were classified based on accessibility criteria into high access (pink), low access (blue), and very low access (yellow) using open-source GIS datasets. Black features are OpenStreetMap defined buildings (©OSM Contributors) to provide indication of structural density. B, C) Main urban centers of Maryland County: Pleebo (B) and Harper (C). Inset: Results of divisive hierarchical classification. The axes of this plot show the principal components and proportion of variance explained by each component.

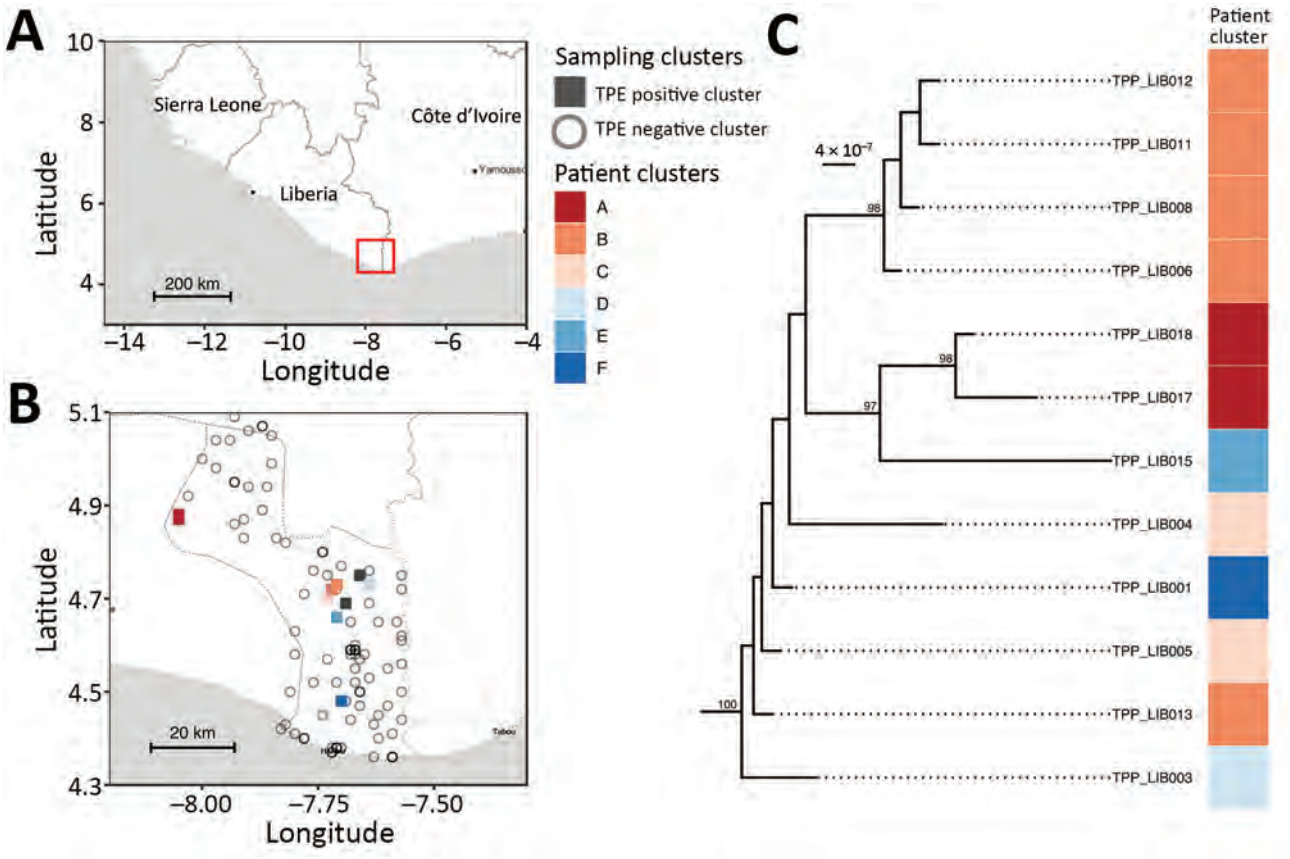

Figure 3. Spatial and phylogenetic distribution of 12 whole genome TPE sequences isolated from serologically confirmed yaws cases in Maryland County, Liberia. Genomes are extremely closely related but show evidence of geographical separation. A) Regional map with study area highlighted in red. B) Maryland County, indicating sampling location of *Treponema* genome (colored by survey cluster). C) Maximum-likelihood whole genome phylogeny of Liberia genomes, scaled by substitutions per site, showing phylogenetic relationships of patient samples. Ultra-fast bootstrap values >95% are indicated on the tree. Map tiles by Stamen Design (CC-BY 3.0), map data by OpenStreetMap (ODbl). TPE, *Treponema pallidum* subspecies *pertenue*.

will, however, be required to better understand fine-scale transmission in this region.

The bacterial genomes we describe were recovered from human patients with yaws who were <200 km from Taï National Park and represent the closest geospatial overlap with nonhuman primate TPE genomes currently available (*16*). These human-derived TPE genomes appearing completely unrelated to those from nonhuman primates, coupled with our detection of only a single monophyletic clade, highlight the importance of geography on TPE population structure. This finding is also inconsistent with recent zoonotic transmission between humans and the nonhuman primates in this area (*17*), although more intensive, localized sampling is needed to affirm our understanding of TPE as a potential zoonosis.

Recent implementation of azithromycin mass drug administration (MDA) in Papua New Guinea led to the emergence of azithromycin-resistant strains of TPE (*25*). We found no evidence of azithromycin-resistant alleles in any TPE genomes in Liberia. To our knowledge, these genomes represent the western limit of human TPE genomes described in Africa and suggest low prevalence or selection pressure for resistance alleles in Maryland. The absence of azithromycin MDA programs across Liberia (*26*) for either yaws or trachoma is a key consideration for low selection pressure.

Given the sampling methods used during this study, exhaustive screening among a large population fraction, our findings provide useful insight into the process of confirming yaws cases in areas of unknown distribution. In light of the extensive screening, the low observed prevalence and highly focal nature of the disease were particularly striking, reinforcing the limited feasibility of stand-alone survey-based approaches for detecting yaws. Surveys and case-finding activities for yaws should instead be

considered when integrated alongside those for other skin NTDs to maximize efficiency (*12*,*27*). Our findings also support the use of larger implementation units for MDA at the county level, equivalent to the WHO definition of districts, following confirmation of an active yaws case, given the evident difficulty in excluding occurrence within smaller implementation units. We also sought only cases with active clinical symptoms of yaws disease, which means that our estimate of yaws infection is likely a substantial underestimate, given that the ratio of active to latent infection can be as high as 1:6 (*28*).

Although standalone surveys for yaws may be unsuitable, our results suggest that community-led case finding activities should be considered, including photo-based screening. Our accessibility analysis also provides some support for WHO guidance of purposively selecting remote communities for these activities (*11*). Our data suggested that the proportion of communities with yaws cases was greater among those classified as low or very low access. Our approach identified a single very-low-access cluster with high prevalence of confirmed yaws, thus supporting the idea that extremely remote settings may be at highest risk. The need for targeted case finding in areas of unknown distribution was further emphasized by the large sampling effort before identification of the first case in our survey process. Of note,

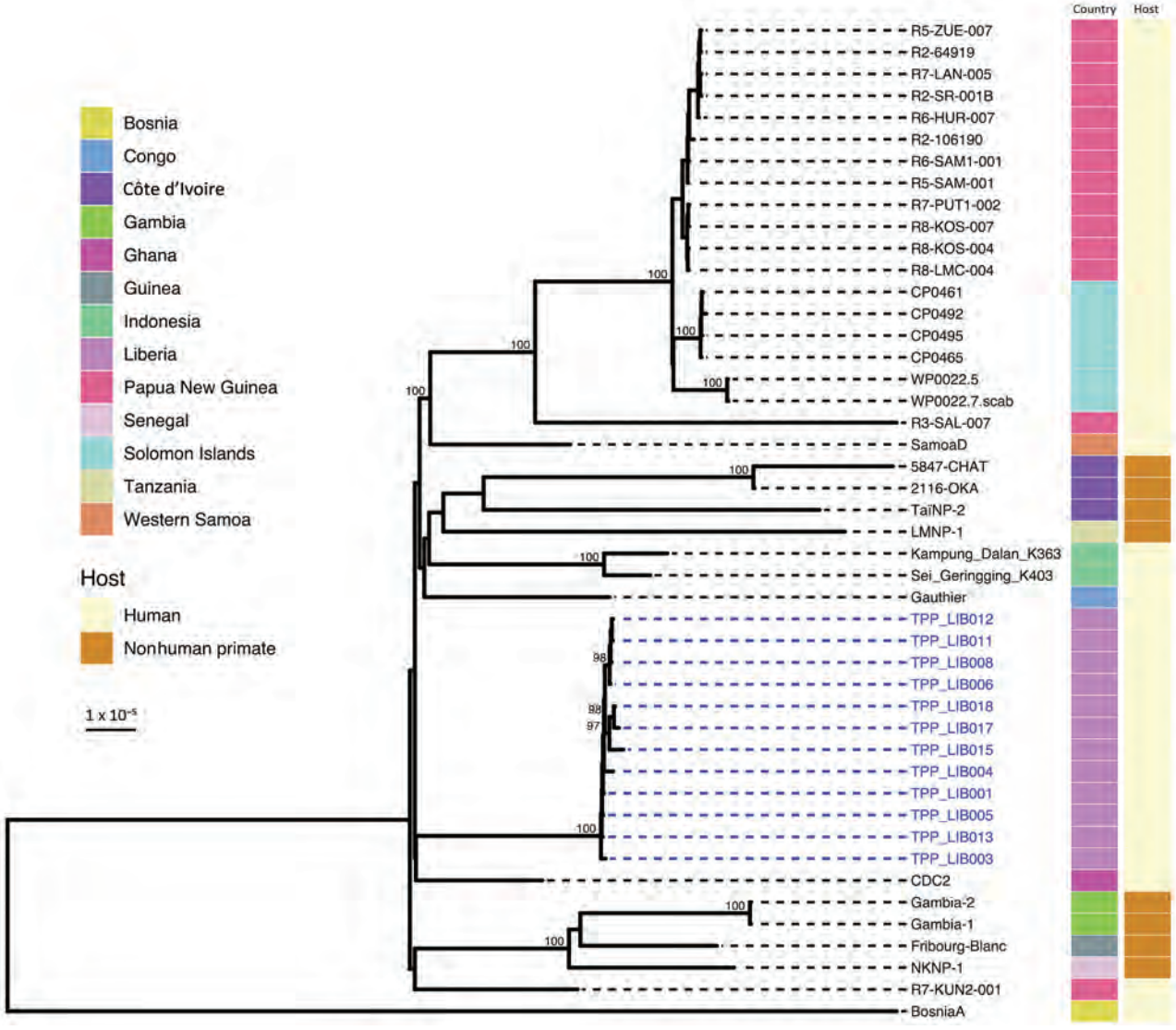

Figure 4. Global context of whole *Treponema pallidum* subspecies *pertenue* (TPE) genomes from Liberia. Liberia genomes form a monophyletic clade, genetically distant from publicly available genomes including 3 isolated from nonhuman primates in nearby Taï National Park (Côte d'Ivoire). Plot shows a maximum-likelihood phylogeny of 12 Liberia genomes contextualized with 34 published global genomes, scaled by substitutions per site. Ultra-fast bootstrap values >95% are indicated on the tree. Colored tracks show country of sampling and original host organism. Novel Liberia genomes from this study are indicated with blue labels.

however, half of all yaws-endemic communities in Maryland were defined as high access. Even though no cases were found in periurban or urban settings, these data show that if activities were focused solely on the most remote communities, most cases would be missed, a crucial point in light of eradication goals.

A recent modeling analysis indicated that, on the basis of several epidemiologic and structural factors, Liberia was unlikely to report yaws cases, even if present (*4*). Our findings indicate that knowledge and healthcare seeking for yaws among both healthcare workers and communities appeared low. Coupled with both our epidemiologic and accessibility findings, this contextual information highlights the challenges of yaws surveillance. We did, however, demonstrate that nonphysician healthcare workers could be trained to provide reliable clinical diagnoses of suspicious lesions despite limited prior awareness. These results are promising, given that the PPV and NPV of yaws can be low because of differential diagnoses (*29*,*30*). The high PPV attributable to papillomatous lesions also highlights that a clinical case definition of a yaws-like papilloma may be an effective tool in settings where serologic or molecular diagnostics are not available.

Our study's limitations include the potential for missed yaws infections or cases of active disease. We did not screen every community in Maryland County, and community healthcare workers may have missed cases during case finding, nor did we train community healthcare workers to screen for the less common clinical manifestations of yaws. To reduce selection and classification bias, we administered rigorous training, real-time data monitoring, and quality control surveys in all community healthcare worker–surveyed clusters. Despite these efforts, both the prevalence of active yaws and genomic diversity of TPE in Maryland County could be greater than we report. In addition, we did not characterize latent yaws through widespread serologic testing; therefore, we cannot provide indications of the prevalence of latent infection. The inherent limitations of high host and bacterial contamination, combined with low *Treponema* load in swab specimens, permitted us to recover genomes from only 12 of 17 PCR-confirmed cases, meaning that we may have missed unsampled diversity.

Our use of exhaustive, rigorously validated sampling methods provides an unusual level of insight into the epidemiology of yaws and the public health challenges associated with confirming cases in areas of unknown burden. Coupled with the genomic characterization of TPE, we provide key details of TPE diversity in this region, which expands and reinforces understanding of TPE spatiotemporal diversity in West Africa. Other previously yaws-endemic countries can use our approaches and findings to inform surveillance activities and to support global yaws eradication efforts.

Acknowledgments

We thank Anna Wickenden and Paul Saunderson for their crucial support in conception and implementation. We are indebted to the community health workers and front-line health workers who supported survey implementation, and to the tireless work of our team of verifiers: Stanley Duwor, William Govergo, Emmanuel Johnson, Tina Hampey, Aloysius Geekor Johnson, and Lawrence Kollie. We specifically acknowledge Lawrence Kollie from our verification team and community healthcare worker Antony Toe, who identified and confirmed the first case of yaws in our survey. We also thank Amos Ballah and Jonathan C. Willie for their outstanding logistical support of the project. We thank WHO for donation of yaws rapid diagnostic tools to this project. We thank Benn Sartorius for providing data for accessibility analyses. We thank the Sequencing Pipelines teams, and Christoph Puethe and the Pathogen Informatics team at the Wellcome Sanger Institute, for assistance with sequencing and bioinformatic data handling support respectively. Finally, we thank the communities of Maryland County and the Maryland County health team for their participation and support of the project from inception to conclusion.

Raw sequencing reads from whole genome sequencing were deposited at the European Nucleotide Archive under BioProject PRJEB40752. All accession numbers used in the project are listed in Appendix 2 (https://wwwnc.cdc.gov/EID/article/27/4/20-4442-App2.xlsx) with the appropriate sample identifier and related metadata. Data collected from this study, including de-identified aggregated data, will be made available in Data Compass, the London School of Hygiene and Tropical Medicine digital data repository.

This work was supported by funding from American Leprosy Missions/AIM Initiative and Wellcome funding (grant no. 206194) to the Sanger Institute.

About the Author

Dr. Timothy is an epidemiologist based at the London School of Hygiene and Tropical Medicine and the UK Public Health Rapid Support Team. His major research interests are the epidemiology and control of neglected tropical diseases and emerging infectious diseases.

References

1. Marks M, Mitjà O, Solomon AW, Asiedu KB, Mabey DC. Yaws. Br Med Bull. 2015;113:91–100. https://doi.org/10.1093/bmb/ldu037
2. Asiedu K, Amouzou B, Dhariwal A, Karam M, Lobo D, Patnaik S, et al. Yaws eradication: past efforts and future perspectives. Bull World Health Organ. 2008;86:499–499A. https://doi.org/10.2471/BLT.08.055608
3. World Health Organization Department of Control of Neglected Tropical Diseases. Summary report of a consultation on the eradication of yaws. Geneva: The Organization; 2012.
4. Fitzpatrick C, Asiedu K, Solomon AW, Mitja O, Marks M, Van der Stuyft P, et al. Prioritizing surveillance activities for certification of yaws eradication based on a review and model of historical case reporting. PLoS Negl Trop Dis. 2018; 12:e0006953. https://doi.org/10.1371/journal.pntd.0006953
5. World Health Organization (WHO). Results of the 2017 global WHO survey on yaws. Wkly Epidemiol Rec. 2018;93:417–28.
6. Dofitas BL, Kalim SP, Toledo CB, Richardus JH. Yaws in the Philippines: first reported cases since the 1970s. Infect Dis Poverty. 2020;9:1–16. https://doi.org/10.1186/s40249-019-0617-6
7. Marks M, Vahi V, Sokana O, Puiahi E, Pavluck A, Zhang Z, et al. Mapping the epidemiology of yaws in the Solomon Islands: a cluster randomized survey. Am J Trop Med Hyg. 2015;92:129–33. https://doi.org/10.4269/ajtmh.14-0438
8. Mitjà O, Hays R, Ipai A, Gubaila D, Lelngei F, Kirara M, et al. Outcome predictors in treatment of yaws. Emerg Infect Dis. 2011;17:1083–5. https://doi.org/10.3201/eid/1706.101575
9. Fitzpatrick C, Asiedu K, Jannin J. Where the road ends, yaws begins? The cost-effectiveness of eradication versus more roads. PLoS Negl Trop Dis. 2014;8:e3165. https://doi.org/10.1371/journal.pntd.0003165
10. World Health Organization Department of Control of Neglected Tropical Diseases. Eradication of yaws—a guide for programme managers. Geneva: The Organization; 2018.
11. World Health Organization Department of Control of Neglected Tropical Diseases. Report of a global meeting on yaws eradication surveillance, monitoring and evaluation. Geneva: The Organization; 2018.
12. Mitjà O, Marks M, Bertran L, Kollie K, Argaw D, Fahal AH, et al. Integrated control and management of neglected tropical skin diseases. PLoS Negl Trop Dis. 2017;11:e0005136. https://doi.org/10.1371/journal.pntd.0005136
13. Yotsu RR. Integrated management of skin NTDs—lessons learned from existing practice and field research. Trop Med Infect Dis. 2018;3:120. https://doi.org/10.3390/tropicalmed3040120
14. Beale MA, Marks M, Sahi SK, Tantalo LC, Nori AV, French P, et al. Genomic epidemiology of syphilis reveals independent emergence of macrolide resistance across multiple circulating lineages. Nat Commun. 2019;10:3255. https://doi.org/10.1038/s41467-019-11216-7
15. Beale M, Noguera-Julian M, Godornes C, Casadellà M, González-Beiras C, Parera M, et al. Yaws re-emergence and bacterial drug resistance selection after mass administration of azithromycin: a genomic epidemiology investigation. Lancet Microbe. 2020;1:e263–71. https://doi.org/10.1016/S2666-5247(20)30113-0
16. Knauf S, Gogarten JF, Schuenemann VJ, De Nys HM, Düx A, Strouhal M, et al. Nonhuman primates across sub-Saharan Africa are infected with the yaws bacterium *Treponema pallidum* subsp. *pertenue*. Emerg Microbes Infect. 2018;7:1–4. https://doi.org/10.1038/s41426-018-0156-4
17. Mubemba B, Gogarten JF, Schuenemann VJ, Düx A, Lang A, Nowak K, et al. Geographically structured genomic diversity of non-human primate-infecting *Treponema pallidum* subsp. *pertenue*. Microb Genom. 2020;6:mgen000463. https://doi.org/10.1099/mgen.0.000463
18. World Health Organization Department of Communicable Disease Prevention, Control and Eradication. International work in endemic treponematoses and venereal infections 1948–1963. Geneva: The Organization; 1965.
19. Widy-Wirski R. Surveillance and control of resurgent yaws in the African region. Rev Infect Dis. 1985;7(Suppl 2):S227–32. https://doi.org/10.1093/clinids/7-Supplement_2.S227
20. Nakagawa S, Johnson PCD, Schielzeth H. The coefficient of determination R^2 and intra-class correlation coefficient from generalized linear mixed-effects models revisited and expanded. J R Soc Interface. 2017;14:20170213. https://doi.org/10.1098/rsif.2017.0213
21. Sangkaew S, Tan LK, Ng LC, Ferguson NM, Dorigatti I. Using cluster analysis to reconstruct dengue exposure patterns from cross-sectional serological studies in Singapore. Parasit Vectors. 2020;13:32. https://doi.org/10.1186/s13071-020-3898-5
22. Marks M, Fookes M, Wagner J, Butcher R, Ghinai R, Sokana O, et al. Diagnostics for yaws eradication: insights from direct next-generation sequencing of cutaneous strains of *Treponema pallidum*. Clin Infect Dis. 2018;66:818–24. https://doi.org/10.1093/cid/cix892
23. Majander K, Pfrengle S, Kocher A, Neukamm J, du Plessis L, Pla-Díaz M, et al. Ancient bacterial genomes reveal a high diversity of *Treponema pallidum* strains in early modern Europe. Curr Biol. 2020;30:3788–3803.e10. https://doi.org/10.1016/j.cub.2020.07.058
24. Marks M, Mitjà O, Bottomley C, Kwakye C, Houinei W, Bauri M, et al.; study team. Comparative efficacy of low-dose versus standard-dose azithromycin for patients with yaws: a randomised non-inferiority trial in Ghana and Papua New Guinea. Lancet Glob Health. 2018;6:e401–10. https://doi.org/10.1016/S2214-109X(18)30023-8
25. Mitjà O, Godornes C, Houinei W, Kapa A, Paru R, Abel H, et al. Re-emergence of yaws after single mass azithromycin treatment followed by targeted treatment: a longitudinal study. Lancet. 2018;391:1599–607. https://doi.org/10.1016/S0140-6736(18)30204-6
26. Liberia Ministry of Health. The Republic of Liberia Ministry of Health master plan for neglected tropical diseases 2016–2020; 2016 [cited 2020 Aug 31] https://espen.afro.who.int/system/files/content/resources/LIBERIA_NTD_Master_Plan_2016_2020.pdf
27. Marks M, Mitja O. Prevalence surveys for podoconiosis and other neglected skin diseases: time for an integrated approach. Lancet Glob Health. 2019;7:e554–5. https://doi.org/10.1016/S2214-109X(19)30158-5
28. Mitjà O, Asiedu K, Mabey D. Yaws. Lancet. 2013;381:763–73. https://doi.org/10.1016/S0140-6736(12)62130-8
29. Mitjà O, Lukehart SA, Pokowas G, Moses P, Kapa A, Godornes C, et al. *Haemophilus ducreyi* as a cause of skin ulcers in children from a yaws-endemic area of Papua New Guinea: a prospective cohort study. Lancet Glob Health. 2014;2:e235–41. https://doi.org/10.1016/S2214-109X(14)70019-1
30. González-Beiras C, Kapa A, Vall-Mayans M, Paru R, Gavilán S, Houinei W, et al. Single-dose azithromycin for the treatment of *Haemophilus ducreyi* skin ulcers in Papua New Guinea. Clin Infect Dis. 2017;65:2085–90. https://doi.org/10.1093/cid/cix723

Address for correspondence: Joseph Timothy, London School of Hygiene and Tropical Medicine, Keppel Street, London, WC1E 7HT, UK; email: joseph.timothy@lshtm.ac.uk

Sexual Contact as Risk Factor for *Campylobacter* Infection, Denmark

Katrin Gaardbo Kuhn, Anne Kathrine Hvass, Annette Hartvig Christiansen, Steen Ethelberg, Susan Alice Cowan

Campylobacteriosis is a disease of worldwide importance, but aspects of its transmission dynamics, particularly risk factors, are still poorly understood. We used data from a matched case-control study of 4,269 men who have sex with men (MSM) and 26,215 controls, combined with national surveillance data on *Campylobacter* spp., *Salmonella* spp., and *Shigella* spp., to calculate matched odds ratios (mORs) for infection among MSM and controls. MSM had higher odds of *Campylobacter* (mOR 14, 95% CI 10–21) and *Shigella* (mOR 74, 95% CI 27–203) infections, but not *Salmonella* (mOR 0.2, 95% CI 0–13), and were less likely than controls to have acquired *Campylobacter* infection abroad (χ^2 = 21; p<0.001). Our results confirm that sexual contact is a risk factor for campylobacteriosis and also suggest explanations for unique features of *Campylobacter* epidemiology. These findings provide a baseline for updating infection risk guidelines to the general population.

Foodborne diseases are a global cause of illness and death, imposing an economic burden on not only the food industry but also the public health sector. *Campylobacter* is the most frequently reported gastrointestinal bacterial pathogen in high-income countries (*1*), responsible for an estimated 166 million diarrheal illnesses worldwide and 3.7 million disability-adjusted life years (*2*). The disease is usually self-limiting, with symptoms manifesting as acute watery or bloody diarrhea; treatment is only required for severe cases. *Campylobacter* infection is a causal factor for Guillain-Barré syndrome, a peripheral nerve disorder, which can potentially cause paralysis. Incidence of *Campylobacter* infection is higher in men and boys than in women and girls, and several countries report high incidence in children <5 years of age and in young adults (*1*,*3*). In most high-income countries, infection with *Campylobacter* is notifiable as part of national surveillance programs for infectious diseases.

Campylobacteriosis is a zoonotic disease; poultry, wild birds, pets, and farm animals are the main reservoirs. Transmission to humans occurs primarily through unsafe handling or consumption of raw or undercooked chicken, consumption of raw milk, or contact with domestic animals (*4*–*6*). However, a large proportion of cases cannot be easily explained by these factors and it has been suggested that other infection routes (e.g., the environment) are equally important in explaining transmission of this disease (*4*,*7*). Some zoonotic pathogens such as *Shigella* spp., *Giardia lamblia*, and *Entamoeba histolytica* have been associated with high risk for infection among men who have sex with men (MSM) because of anal–oral contact (*8*–*12*). Even though several outbreaks have been reported and observational studies have described a high incidence of *Campylobacter* infection among MSM (*8*,*13*,*14*,*15*–*21*), sexual contact is not officially considered among its risk factors for MSM or heterosexual partners in general. However, the transmission potential and incidence of gastrointestinal illnesses among MSM and heterosexual partners engaging in anal–oral sexual contact is difficult to evaluate based on laboratory data only, which does not contain sexual exposure information.

In Denmark, some infectious diseases, including all foodborne and most sexually transmitted infections, must be reported to Statens Serum Institut (SSI; https://en.ssi.dk), the national institute for infectious diseases of Denmark, through the national surveillance and notification system. The surveillance system comprises 2 parts: clinical notifications and laboratory notifications. Clinical notifications cover diseases that must be reported (Appendix, https://wwwnc.cdc.gov/EID/article/27/4/20-2337-App1.pdf), including serious infectious diseases (e.g.,

Author affiliations: University of Oklahoma Health Sciences Center, Oklahoma City, Oklahoma, USA (K.G. Kuhn); Statens Serum Institut, Copenhagen, Denmark (K.G. Kuhn, A.K. Hvass, A.H. Christiansen, S. Ethelberg, S.A. Cowan); University of Copenhagen Department of Public Health, Copenhagen (S. Ethelberg)

DOI: https://doi.org/10.3201/eid2704.202337

meningitis and tuberculosis), sexually transmitted diseases, and *Shigella* spp. infections. These notifications include relevant patient information, primarily the unique individual Civil Registration System (CPR) number (22) and circumstances possibly affecting transmission of the infection, such as sexual contact, foreign travel, and contact with hospitals. General practitioners and hospital physicians fill out details on paper forms that are sent to SSI for manual entry into the database of the national clinical reporting system for infectious diseases. While MSM sexual contact is listed as a possible factor related to transmission, notifications do not include information on anal-oral contact between heterosexual partners.

The laboratory notification system receives reports of all gastrointestinal infections from certain microorganisms, including campylobacteriosis, salmonellosis, and shigellosis, for which clinical microbiological laboratories are obliged to report findings; reports also include the patient's CPR number. Laboratory notifications can include information on travel but this is not mandatory. Notifications of gastrointestinal infections are registered and stored in the Denmark Register of Enteric Pathogens. By using each patient's unique CPR number, duplication of patient records can be avoided and multiple reports for individual patients from the clinical infectious disease and enteric infections databases can be coupled. These data can then be used to generate linked datasets of notifiable diseases and possible explanatory or risk factors. We used these high-quality national surveillance data in an individually matched case–control study undertaken to investigate the frequency of *Campylobacter* infections among MSM in Denmark.

Methods

Study Design and Participants

We undertook a national retrospective, individually matched case-control study, with a 9-year study period, 2010–2018, among men ≥18 years of age residing in Denmark. Using an inverted case-control design, we considered MSM as case-patients and infections with *Campylobacter* spp., *Shigella* spp., or *Salmonella* spp. as exposures (Figure 1). We defined an MSM case-patient as a man ≥18 years of age, with ≥1 notification of any infectious disease (Appendix) acquired through MSM contact reported to SSI in a clinical notification during the study period. However, for men identified by CPR number in >1 notification during the study period, we included data from only 1 report. We excluded those <18 years of age at the time of the notification or with an incomplete CPR number. For the control group, we randomly selected men ≥18 years of age from CPR digital records. We individually matched each MSM case-patient to (ideally) 3–5 controls by age (by year and month of birth) and municipality of residence. To determine exposures, we drew information on laboratory-confirmed infections with *Campylobacter* spp., nontyphoidal *Salmonella* spp., and *Shigella* spp. from the enteric infections database.

Extraction of Data

From the clinical infectious disease database, we extracted clinical notifications of men with an infectious disease acquired through MSM contact during 2010–2018, and from the enteric infections database, laboratory notifications of *Campylobacter* spp., *Salmonella* spp., and *Shigella* spp. infections over the same

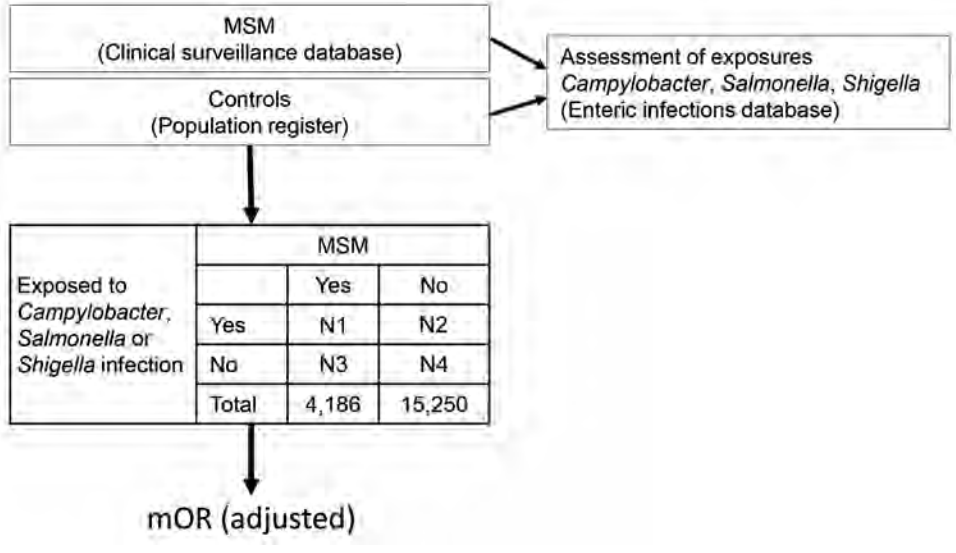

Figure 1. Inverted case-control study design in study of sexual contact as risk factor for *Campylobacter* infection, Denmark, 2010–2018. mOR adjusted for foreign travel, year of notification, infection with any of the other pathogens, and recurrent infections. mOR, matched odds ratio; MSM, men who have sex with men.

period. For each disease notification, we obtained the CPR number of the MSM case-patient, year of notification, and whether the infection was assumed to have been acquired in Denmark or abroad. We included notifications for all species of the 3 pathogens. Data on campylobacteriosis, salmonellosis, and shigellosis were extracted for both sexes and all age groups but only reports for men ≥18 years of age at the time of notification were included in the study. For calculation of age-specific incidence of the pathogens, we used national population data available from Statistics Denmark (https://www.statistikbanken.dk).

Calculations and Statistical Analysis

To illustrate the age distribution of infection, we divided case-patients and controls into 2 groups: those <40 years of age and those ≥40 years of age. We analyzed the difference between the frequency of travel-acquired and recurrent infections in the MSM and control groups, age distributions of infections, and the geographic distribution of MSM case-patients in comparison to the general population using χ^2 tests. We calculated unadjusted and adjusted matched odds ratios (mORs) with 95% CIs for the 3 exposures, *Campylobacter*, *Salmonella*, and *Shigella* infections, in MSM case-patients and controls using conditional logistic regression. The analysis was adjusted for foreign travel, year of notification, infection with any of the other pathogens included in the study, and recurrent infections. We analyzed the distribution of MSM notifications and gastrointestinal diseases over time using a simple regression for trend. We performed all data analyses using Stata version 14 (StataCorp, https://www.stata.com).

This study was approved under the general agreement for noninterventional database studies between the Danish Data Protection Agency and Statens Serum Institut (reference number 2008-54-0474). According to regulations in Denmark, ethics committee approval is not required for studies that do not involve analysis of biologic material from human subjects.

Results

From the clinical infectious disease database, we extracted 4,269 individual reports (only 1 per person) of men who had acquired a notifiable disease through MSM contact during January 1, 2010–December 31, 2018. Of these, 83 (1.9%) men were excluded because they did not have either a valid CPR number or an address in Denmark. For the control group, we extracted 15,250 randomly selected matched male controls from the CPR registry. The mean age was 41 years (median 40 years, range 18–88 years) for both the case-patients and the controls. Case-patients and controls were geographically distributed throughout Denmark, but a significantly larger proportion of the study population than the general population resided in the Capital Region (χ^2 = 1,400; p<0.0001).

From the Register of Enteric Pathogens, we extracted 49,321 notifications of infections with ≥1 of the 3 bacterial pathogens (exposures); 748 patients had registrations for ≥2 recurrent infections with the same pathogen during the study period (Table 1). Most (76%) notifications were for *Campylobacter* infections: 55% *C. jejuni*, 4% *C. coli*, and 40% other *Campylobacter* spp. with no species reported. In the MSM group, a total of 132 *Campylobacter*, 3 *Salmonella*, and

Table 1. Gastrointestinal diseases reported to Statens Serum Institut, Denmark, 2010–2018*

Pathogen	Patients with enteric infection exposures, n = 49,321	MSM, n = 4,186	Controls, n = 15,250
Campylobacter	37,602	132 (3)	74 (0.5)
Annual incidence	7.4‡	35§	5.4§
Recurrent infections	524 (1.4)	4 (3)	0
Foreign travel†	7,252 (19)	15 (11)	24 (32)
Age <40 y	19,930 (53)	79 (60)	35 (47)
Salmonella	10,450	3 (0.1)	44 (0.3)
Annual incidence	2.1‡	7.2§	3.2§
Recurrent infections	109 (1)	0	0
Foreign travel†	3,916 (37)	1 (33)	9 (20)
Age <40 y	3,380 (32)	1 (33)	15 (34)
Shigella	1,269	64 (1.5)	4 (0.03)
Annual incidence	0.2‡	17§	0.3§
Recurrent infections	15 (1.2)	0	0
Foreign travel†	527 (42)	7 (11)	1 (25)
Age <40 y	838 (66)	39 (61)	3 (75)

*Values are no. () except as indicated, except incidence, which is given as cases/10,000 population. MSM, men who have sex with men.
†Travel information was unknown for 57 of patients with *Campylobacter* infections, 25 of patients with *Salmonella* infections, and 55 of patients with *Shigella* infections (both MSMs and controls).
‡Annual incidence refers to incidence in the population of Denmark.
§Annual incidence refers to incidence in the sample population.

64 *Shigella* infections were reported during the study period (Table 1). In the control group, we observed 74 *Campylobacter*, 44 *Salmonella*, and 4 *Shigella* infections (Table 1). Compared with controls, a higher proportion of MSM case-patients <40 years of age had *Campylobacter* infections (Table 1), although this difference was not statistically significant ($\chi^2 = 3$; p = 0.08).

Overall, we found that the odds of a *Campylobacter* infection were 14 times higher among MSM than controls (Table 2). MSM case-patients also had 74 times higher odds than controls of being infected with *Shigella*, a pathogen known to be transmitted by sexual contact (Table 2). However, we found no significant difference between *Salmonella* infection rates in MSM case-patients and controls (Table 2). MSM case-patients who were infected with *Campylobacter* were significantly less likely to have acquired their infection abroad compared with controls ($\chi^2 = 21$; p<0.001), which was not the case for *Salmonella* or *Shigella*. Over the study period, there were 4 (3%) recurrent *Campylobacter* infections in the MSM group compared with none in the control group (statistical analysis not possible); there were no recurrent *Salmonella* or *Shigella* infections in the MSM or control groups. During the study period, we observed an increase among MSM case-patients in clinical infections acquired through MSM contact and *Campylobacter* or *Shigella* infections (Figure 2, t = 5–11; p<0.001). We did not observe any change in the proportion of *Salmonella* among MSM case-patients (t = −2; p = 0.1) or for any of the 3 pathogens in the control group (Figure 2, t = −1 to 2; p = 0.1–0.4).

Discussion

We present surveillance data–driven evidence that campylobacteriosis can be transmitted through sexual contact. Among our study group of MSM case-patients, the odds of being infected with *Campylobacter* was 14 times higher than among controls. We observed a similar pattern for shigellosis, which is known to be transmitted by sexual contact, but not for *Salmonella* infection. In Denmark, *Salmonella* infections are considered almost exclusively foodborne whereas domestic *Shigella* infections are regarded as primarily sexually transmitted and secondarily as foodborne or transmitted through general person-to-person contact. *Campylobacter* infection is linked to several different transmission routes (*4*), handling or consuming of poultry long considered the most notable.

However, our results reinforce information from many reports suggesting *Campylobacter* can be transmitted through sexual contact; these reports provide explanations for unique aspects of *Campylobacter* epidemiology supported by biologic facts from other foodborne bacteria. Reported outbreaks among MSM in Canada (*14*,*19*,*23*,*24*) and previous observations of higher infection rates in homosexual men and HIV-positive patients (*8*,*13*,*17*,*20*,*21*,*25*,*26*) indicate the likelihood that *Campylobacter* can be transmitted through sexual contact. In spite of this, sexual contact has not traditionally been considered a possible transmission route in sporadic campylobacteriosis cases and therefore has been excluded as a possible risk factor in published case-control studies (*4*). We were unable to assess the risk of *Campylobacter* transmission through anal–oral contact between heterosexual partners because only MSM sexual contact is reported on notifications. However, it is highly likely that the risk of infection through this type of sexual contact is equally relevant for heterosexual and MSM partners.

Several aspects of *Campylobacter* epidemiology remain to be clarified, such as why the disease is more common among men (*3*,*13*,*27*–*29*). Many explanations have been proposed, including differences in food handling and preparation, healthcare-seeking behaviors, and physiologies. We provide an additional explanation: adult men practicing sex with other men are at significantly higher risk (p<0.001) of campylobacteriosis. In this study, *Campylobacter* incidence in the MSM group was almost 5 times higher than in the general population, which could be a partial driver for higher incidence in men.

Another feature observed in surveillance statistics from several countries was the biphasic age distribution of *Campylobacter* infections, showing pronounced peaks in children <5 years of age and young adults 20–40 years of age (*3*,*30*–*33*). In the 20–40-year age group, these peaks have also been observed for *Shigella* (*34*,*35*), but not for other foodborne bacteria

Table 2. Matched odds ratios by gastrointestinal infection among MSM and controls in study of sexual contact as risk factor for *Campylobacter* infection, Denmark, 2010–2018*

Pathogen	MSM, no. (%), n = 4,186	Controls, no. (%), n = 15,250	Unadjusted comparison		Adjusted comparison†	
			mOR (95% CI)	p value	mOR (95% CI)	p value
Campylobacter	132 (3)	74 (0.5)	16 (11–23)	<0.001	14 (10–21)	<0.001
Salmonella	3 (0.07)	5 (0.03)	3 (0.7–13)	0.132	0.2 (0.02–1.3)	0.09
Shigella	64 (1.5)	4 (0.03)	105 (37–307)	<0.001	74 (27–203)	<0.001

*mOR, matched odds ratio; MSM, men who have sex with men.
†Adjusted for foreign travel, year of notification/infection, infection with any of the other pathogens and recurrent infections.

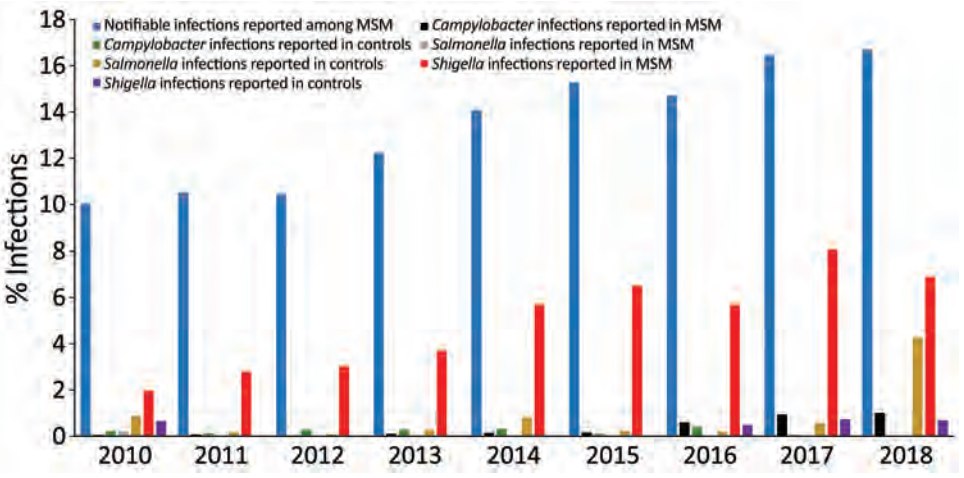

Figure 2. Percentages of clinical notifications of infections acquired through MSM contact (notifiable infections) and *Campylobacter*, *Salmonella*, and *Shigella* infections reported among MSM and controls in study of sexual contact as risk factor for *Campylobacter* infection, Denmark, 2010–2018. MSM were men ≥18 years of age notified of any infectious disease acquired through sexual contact with another man. Controls were men ≥18 years randomly selected from the Denmark population register. MSM and controls <18 years of age or who did not have a valid national civil registration number were excluded from the study. MSM, men who have sex with men.

such as *Salmonella*. These findings have been explained by the secondary weaning phase, meaning that young adults away from home are less aware of proper hygiene practices, secondary infections from caring for young children at home, or hormonal and behavioral factors. When comparing different age groups, we saw higher *Campylobacter* infection rates in MSM <40 years of age compared with controls, although this difference was not statistically significant because of the small sample size. On the basis of our results, we suggest that, in countries with a clear biphasic *Campylobacter* age distribution, some of the high infection frequency among young adults might be explained by sexual transmission among persons in this very sexually active age group.

Bacterial pathogens can be transmitted through fecal–oral contact during sex, either directly, through anal–oral contact or anal–penile–oral contact, or indirectly, such as through the use of sex toys or fingers. In 1974, sexual contact was recognized as a risk factor for infection with *Shigella* spp. (*11*), and such contact is now widely acknowledged as one of the most important transmission routes for shigellosis. The probability of infection with a foodborne bacterium from fecal–oral contact is directly related to the infectious dose. For *Shigella* spp. this dose can be as low as 10–1,000 organisms, and for *Campylobacter*, 500–10,000 organisms (*36*). The infectious dose for *Salmonella* spp. varies (*37*) but might be as high as 1 million bacterial cells. Pathogens with a low infectious dose are easier to transmit from person to person, including through sexual contact; on the basis of our findings, we tentatively propose that this might be the case for *Shigella* and *Campylobacter*, but not *Salmonella*.

In Denmark and the rest of Europe, campylobacteriosis and shigellosis are often acquired abroad; 30%–50% of infections are reported as travel related (*3*,*33*). This possibility was reflected in our control group, but *Campylobacter* infections among MSM were significantly less likely to have been travel related (p<0.001). Assuming that many *Campylobacter* and *Shigella* cases in the MSM group have been acquired by sexual contact, this domestic pattern is not surprising because MSM contact is most commonly not a holiday experience and infection is more likely to happen at home.

During the study period, there was a significant (p<0.001) increase in the proportion of MSM case-patients infected with *Shigella* or *Campylobacter*, but not with *Salmonella*; we found no increase in the control group. Incidence of campylobacteriosis in Denmark has increased recently (*3*), reflecting a combination of actual increases in cases of the disease, changes in diagnostic techniques, and improved electronic notification. During the study period, laboratory diagnosis of gastrointestinal pathogens has transitioned from culturing to more sensitive PCR testing of feces. This change could explain some of the increase in recorded *Shigella* and *Campylobacter* infections; however, similar increases would be expected for *Salmonella* and for the number of infections in the control group. An increasing trend over time would also be observed if there had been larger outbreaks of *Shigella* and *Campylobacter* among MSM case-patients later in the study period, but only 1 outbreak of shigellosis was reported, and none of campylobacteriosis among MSM during this time (*38*). The most likely explanation for the observed increase in *Shigella* and *Campy-*

lobacter among MSM case-patients is the concurrent increase in the proportion of infections transmitted through MSM contact reported to SSI. More extensive reporting has increased the amount of data available in the electronic databases, in turn increasing the likelihood of discovering infections in the MSM group.

Our study had 2 major strengths: use of routinely collected high-quality national surveillance data for our analyses and results supported by biologic evidence and demographic information, such as the infectious doses and the low level of travel-related infections in the MSM group that explain some of the unique characteristics of *Campylobacter* transmission. The first limitation is that, although clinical notifications of diseases in Denmark can include MSM contact as possibly associated with the circumstances of the infection, such inclusions are based on patient statements, and only HIV, syphilis, gonorrhea, and hepatitis infections must be reported. Therefore, the MSM population group probably did not include all men with an infection acquired through MSM contact during the study period. It is also very likely that the control group included some MSM and that some reported *Campylobacter*, *Shigella*, or *Salmonella* infections in the control group were acquired through MSM contact. However, such an underestimation would tend to lower the estimates of association toward 1 and, in fact, approximate the odds ratios to risk ratios. Differences between case-patients and controls concerning how exposure was determined (i.e., from a notification to SSI about infection with an enteric pathogen) could have affected the results. However, because physicians and laboratories in Denmark operate under the same guidelines and procedures and the notification records are uniformly registered, such differences are unlikely to have had an effect.

The results in this study provide a measure of the risk associated with a notifiable infectious disease among a specific group of MSM and not among a general MSM population. However, considering the robust mORs and corresponding CIs combined with published reports about high *Campylobacter* incidence in MSM populations, we believe that our findings can be extrapolated to MSM in general. The case-patient group might overrepresent risk-taking persons more likely to practice unsafe sex, and if that is the case, the increased risk for *Campylobacter* infection through sexual contact would primarily apply to this high-risk group. However, it can also be argued that this risk applies to the wider MSM population because condom use would not eliminate the infection risk associated with several fecal–oral transmission routes. The case-patients we selected might also have a high frequency of known risk factors, such as use of proton pump inhibitors, certain occupations, or increased contact with animals, that we could not account for in this study.

Another limitation of the data used in our study was the incomplete travel information for persons with reported infections. Travel history was unknown for patients with 25% of *Salmonella*, 55% of *Shigella*, and 57% of *Campylobacter* infections because of incomplete registration and lack of follow-up interviews. This proportion was similar between case-patients and controls. In spite of this, our results still indicated that MSM are less likely to have acquired *Campylobacter* or *Shigella* infections abroad. Also, although our data covered all infections reported as acquired through MSM contact and all confirmed cases of campylobacteriosis, salmonellosis, and shigellosis, these do not account for all cases. Notifications are based on passive surveillance and underestimate the true incidence because persons with infections who do not seek medical attention are not captured (*39*). However, because our system enabled linkage of individual data collected, we believe that these results are as accurate as possible and could be generalized to similar settings. Lack of association between MSM contact and *Salmonella* infection might reflect the true situation or that a larger sample size is needed.

The cycle of transmission through sexual contact among adults contributes substantially to the burden of disease in highly industrialized countries, but likely not in low-middle income settings where limited hygiene and sanitation constitute greater risk factors. Therefore, the external validity of the results in some locations should be considered and we encourage public health agencies in other countries to replicate this study to corroborate the findings. Finally, as we did not directly measure *Campylobacter* infection transmitted through anal-oral contact, the association is speculative and our conclusions are derived from surveillance data analyses in combination with knowledge gained from studies of other bacteria.

Our findings indicate a strong likelihood that *Campylobacter* can be transmitted during sexual contact. Given previous reports of outbreaks and high incidence of *Campylobacter* among MSM, this is not surprising. Combining this theory with high-quality national surveillance data, our results offer additional reasonable explanations for why surveillance statistics from some countries show that adult men are more frequently infected with *Campylobacter* than are women and why *Campylobacter* incidence peaks among young adults. Overall, our findings not only

address epidemiologic questions but also highlight a need to inform the public about the risk of infection through sexual activity in regions where *Campylobacter* incidence exhibits patterns similar to those in Denmark. These results are primarily applicable to adults in high-income settings in some countries; further studies are warranted among the general MSM population rather than only those with a reported notifiable disease. However, considering the high burden of campylobacteriosis in Europe, the United States, and Australia, incorporating knowledge from these findings into general information campaigns might encourage the use of precautionary measures during sexual contact, which could, in turn, lead to lower infection rates and reduced overall costs to society.

Acknowledgments

We are grateful to Kåre Mølbak and Tyra Grove Krause for feedback on the study.

About the author

Dr. Kuhn is a senior infectious disease epidemiologist working as a professor at the University of Oklahoma Health Sciences Center. Her research interests include foodborne and waterborne infections, climate change, and research related to One Health collaborations.

References

1. Kaakoush NO, Castaño-Rodríguez N, Mitchell HM, Man SM. Global epidemiology of *Campylobacter* infection. Clin Microbiol Rev. 2015;28:687–720. https://doi.org/10.1128/CMR.00006-15
2. Havelaar AH, Kirk MD, Torgerson PR, Gibb HJ, Hald T, Lake RJ, et al.; World Health Organization Foodborne Disease Burden Epidemiology Reference Group. World Health Organization global estimates and regional comparisons of the burden of foodborne Disease in 2010. PLoS Med. 2015;12:e1001923. https://doi.org/10.1371/journal.pmed.1001923
3. Kuhn KG, Nielsen EM, Mølbak K, Ethelberg S. Epidemiology of campylobacteriosis in Denmark 2000-2015. Zoonoses Public Health. 2018;65:59–66. https://doi.org/10.1111/zph.12367
4. Kuhn KG, Nielsen EM, Mølbak K, Ethelberg S. Determinants of sporadic *Campylobacter* infections in Denmark: a nationwide case-control study among children and young adults. Clin Epidemiol. 2018;10:1695–707. https://doi.org/10.2147/CLEP.S177141
5. MacDonald E, White R, Mexia R, Bruun T, Kapperud G, Lange H, et al. Risk factors for sporadic domestically acquired *Campylobacter* infections in Norway 2010–2011: a national prospective case-control study. PLoS One. 2015;10:e0139636. https://doi.org/10.1371/journal.pone.0139636
6. Mughini Gras L, Smid JH, Wagenaar JA, de Boer AG, Havelaar AH, Friesema IHM, et al. Risk factors for campylobacteriosis of chicken, ruminant, and environmental origin: a combined case-control and source attribution analysis. PLoS One. 2012;7:e42599. https://doi.org/10.1371/journal.pone.0042599
7. Hansson I, Sandberg M, Habib I, Lowman R, Engvall EO. Knowledge gaps in control of *Campylobacter* for prevention of campylobacteriosis. Transbound Emerg Dis. 2018;65(Suppl 1):30–48. https://doi.org/10.1111/tbed.12870
8. Narayan S, Galanis E; BC STEI Group. Are enteric infections sexually transmitted in British Columbia? Can Commun Dis Rep. 2016;42:24–9. https://doi.org/10.14745/ccdr.v42i02a01
9. Escobedo AA, Almirall P, Alfonso M, Cimerman S, Chacín-Bonilla L. Sexual transmission of giardiasis: a neglected route of spread? Acta Trop. 2014;132:106–11. https://doi.org/10.1016/j.actatropica.2013.12.025
10. Fletcher SM, Stark D, Harkness J, Ellis J. Enteric protozoa in the developed world: a public health perspective. Clin Microbiol Rev. 2012;25:420–49. https://doi.org/10.1128/CMR.05038-11
11. Tauxe RV, McDonald RC, Hargrett-Bean N, Blake PA. The persistence of *Shigella flexneri* in the United States: increasing role of adult males. Am J Public Health. 1988;78:1432–5. https://doi.org/10.2105/AJPH.78.11.1432
12. Mildvan D, Gelb AM, William D. Venereal transmission of enteric pathogens in male homosexuals. Two case reports. JAMA. 1977;238:1387–9. https://doi.org/10.1001/jama.1977.03280140065022
13. Mook P, Gardiner D, Kanagarajah S, Kerac M, Hughes G, Field N, et al. Use of gender distribution in routine surveillance data to detect potential transmission of gastrointestinal infections among men who have sex with men in England. Epidemiol Infect. 2018;146:1468–77. https://doi.org/10.1017/S0950268818001681
14. Marchand-Senécal X, Bekal S, Pilon PA, Sylvestre J-L, Gaudreau C. *Campylobacter fetus* cluster among men who have sex with men, Montreal, Quebec, Canada, 2014–2016. Clin Infect Dis. 2017;65:1751–3. https://doi.org/10.1093/cid/cix610
15. Gaudreau C, Rodrigues-Coutlée S, Pilon PA, Coutlée F, Bekal S. Long-lasting outbreak of erythromycin- and ciprofloxacin-resistant *Campylobacter jejuni* subspecies *jejuni* from 2003 to 2013 in men who have sex with men, Quebec, Canada. Clin Infect Dis. 2015;61:1549–52. https://doi.org/10.1093/cid/civ570
16. Allos BM, Allos BM. *Campylobacter jejuni* infections: update on emerging issues and trends. Clin Infect Dis. 2001;32:1201–6. https://doi.org/10.1086/319760
17. Sorvillo FJ, Lieb LE, Waterman SH. Incidence of campylobacteriosis among patients with AIDS in Los Angeles County. J Acquir Immune Defic Syndr (1988). 1991;4:598–602.
18. Quinn TC, Goodell SE, Fennell C, Wang SP, Schuffler MD, Holmes KK, et al. Infections with *Campylobacter jejuni* and *Campylobacter*-like organisms in homosexual men. Ann Intern Med. 1984;101:187–92. https://doi.org/10.7326/0003-4819-101-2-187
19. Gaudreau C, Michaud S. Cluster of erythromycin- and ciprofloxacin-resistant *Campylobacter jejuni* subsp. *jejuni* from 1999 to 2001 in men who have sex with men, Québec, Canada. Clin Infect Dis. 2003;37:131–6. https://doi.org/10.1086/375221
20. Newman KL, Newman GS, Cybulski RJ, Fang FC. Gastroenteritis in men who have sex with men in Seattle, Washington, 2017–2018. Clin Infect Dis. 2020;71:17. https://doi.org/10.1093/cid/ciz783

21. Gerninger AL, Addetia A, Starr K, Cybulski RJ, Stewart MK, Salipante SJ, et al. International spread of multidrug-resistant *Campylobacter coli* in men who have sex with men in Washington state and Quebec, 2015–2018. Clin Infect Dis. 2020;71:29. https://doi.org/10.1093/cid/ciz1060
22. Pedersen CB. The Danish Civil Registration System. Scand J Public Health. 2011;39(7 Suppl):22–5. https://doi.org/10.1177/1403494810387965
23. Gaudreau C, Pilon PA, Sylvestre J-L, Boucher F, Bekal S. Multidrug-resistant *Campylobacter coli* in men who have sex with men, Quebec, Canada, 2015. Emerg Infect Dis. 2016;22:1661–3. https://doi.org/10.3201/eid2209.151695
24. Gaudreau C, Helferty M, Sylvestre J-L, Allard R, Pilon PA, Poisson M, et al. *Campylobacter coli* outbreak in men who have sex with men, Quebec, Canada, 2010–2011. Emerg Infect Dis. 2013;19:764–7. https://doi.org/10.3201/eid1905.121344
25. Hughes G, Silalang P, Were J, Patel H, Childs T, Alexander S, et al. Prevalence and characteristics of gastrointestinal infections in men who have sex with men diagnosed with rectal chlamydia infection in the UK: an 'unlinked anonymous' cross-sectional study. Sex Transm Infect. 2018;94:518–21. https://doi.org/10.1136/sextrans-2016-053057
26. Larsen IK, Gradel KO, Helms M, Hornstrup MK, Jürgens G, Mens H, et al. Non-typhoidal *Salmonella* and *Campylobacter* infections among HIV-positive patients in Denmark. Scand J Infect Dis. 2011;43:3–7. https://doi.org/10.3109/00365548.2010.517780
27. Walter F, Ott JJ, Claus H, Krause G. Sex- and age patterns in incidence of infectious diseases in Germany: analyses of surveillance records over a 13-year period (2001–2013). Epidemiol Infect. 2018;146:372–8. https://doi.org/10.1017/S0950268817002771
28. Moffatt CRM, Glass K, Stafford R, D'Este C, Kirk MD. The campylobacteriosis conundrum – examining the incidence of infection with *Campylobacter* sp. in Australia, 1998–2013. Epidemiol Infect. 2017;145:839–47. https://doi.org/10.1017/S0950268816002909
29. Strachan NJC, Watson RO, Novik V, Hofreuter D, Ogden ID, Galán JE. Sexual dimorphism in campylobacteriosis. Epidemiol Infect. 2008;136:1492–5. https://doi.org/10.1017/S0950268807009934
30. Gillespie IA, O'Brien SJ, Penman C, Tompkins D, Cowden J, Humphrey TJ. Demographic determinants for *Campylobacter* infection in England and Wales: implications for future epidemiological studies. Epidemiol Infect. 2008;136:1717–25. https://doi.org/10.1017/S0950268808000319
31. Schielke A, Rosner BM, Stark K. Epidemiology of campylobacteriosis in Germany—insights from 10 years of surveillance. BMC Infect Dis. 2014;14:30. https://doi.org/10.1186/1471-2334-14-30
32. Geissler AL, Bustos Carrillo F, Swanson K, Patrick ME, Fullerton KE, Bennett C, et al. Increasing *Campylobacter* infections, outbreaks, and antimicrobial resistance in the United States, 2004–2012. Clin Infect Dis. 2017;65:1624–31. https://doi.org/10.1093/cid/cix624
33. Nichols GL, Richardson JF, Sheppard SK, Lane C, Sarran C. *Campylobacter* epidemiology: a descriptive study reviewing 1 million cases in England and Wales between 1989 and 2011. BMJ Open. 2012;2:e001179. https://doi.org/10.1136/bmjopen-2012-001179
34. Haley CC, Ong KL, Hedberg K, Cieslak PR, Scallan E, Marcus R, et al. Risk factors for sporadic shigellosis, FoodNet 2005. Foodborne Pathog Dis. 2010;7:741–7. https://doi.org/10.1089/fpd.2009.0448
35. European Centre for Disease Prevention and Control. Shigellosis—annual epidemiological report 2016 (2014 data). Stockholm: The Centre; 2016 [cited 2019 May 3]. http://ecdc.europa.eu/en/publications-data/shigellosis-annual-epidemiological-report-2016-2014-data
36. Kothary MH, Babu US. Infective dose of foodborne pathogens in volunteers: a review. J Food Saf. 2001;21:49–68. https://doi.org/10.1111/j.1745-4565.2001.tb00307.x
37. Blaser MJ, Newman LS. A review of human salmonellosis: I. infective dose. Rev Infect Dis. 1982;4:1096–106. https://doi.org/10.1093/clinids/4.6.1096
38. Statens Serum Institut. Epi-News: week 48—2017. Shigellose 2014–2016. Copenhagen: Statens Serum Institut [cited 2021 Jan 1]. https://www.ssi.dk/Aktuelt/Nyhedsbreve/EPI-NYT/2017/Uge%2048%20-%202017
39. Haagsma JA, Geenen PL, Ethelberg S, Fetsch A, Hansdotter F, Jansen A, et al.; Med-Vet-Net Working Group. Community incidence of pathogen-specific gastroenteritis: reconstructing the surveillance pyramid for seven pathogens in seven European Union member states. Epidemiol Infect. 2013;141:1625–39. https://doi.org/10.1017/S0950268812002166

Address for correspondence: Katrin Gaardbo Kuhn, Hudson College of Public Health, University of Oklahoma Health Sciences Center, 801 NE 13th St, Oklahoma City, OK 73104, USA; email: katrin-kuhn@ouhsc.edu

Venezuelan Equine Encephalitis Complex Alphavirus in Bats, French Guiana

Carlo Fischer,[1] Dominique Pontier,[1] Ondine Filippi-Codaccioni, Jean-Batiste Pons, Ignacio Postigo-Hidalgo, Jeanne Duhayer, Sebastian Brünink, Jan Felix Drexler

Although essential for control strategies, knowledge about transmission cycles is limited for Venezuelan equine encephalitis complex alphaviruses (VEEVs). After testing 1,398 bats from French Guiana for alphaviruses, we identified and isolated a new strain of the encephalitogenic VEEV species Tonate virus (TONV). Bats may contribute to TONV spread in Latin America.

Venezuelan equine encephalitis complex alphaviruses (VEEVs) are arthropod-borne viruses (arboviruses) (*1*,*2*). Most VEE complex viruses can infect livestock and humans, causing predominantly acute febrile illness; some VEE complex viruses, including Tonate virus (TONV), which is the predominant VEE complex virus in French Guiana, also cause lethal encephalitis in humans (*3*). Clarifying the enzootic transmission cycles of VEEVs is essential for developing control strategies. Some VEEVs infect a broad range of invertebrate and vertebrate hosts, including horses, birds, rodents, and bats (*4*). Other than humans, only birds have been identified as naturally infected vertebrate hosts for TONV by direct virus detection and characterization (*5*,*6*). Bats are particularly relevant hosts of zoonotic viruses (*7*) and are potential hosts of selected VEEV subtypes in Mexico and Trinidad (*4*,*8*). To gain more insights into the ecology of VEEVs in French Guiana, we sampled bats and tested them for alphavirus infections using molecular, serologic, and cell-culture–based tools.

Author affiliations: Charité-Universitätsmedizin Berlin, corporate member of Freie Universität Berlin, Humboldt-Universität zu Berlin and Berlin Institute of Health, Institute of Virology, Berlin, Germany (C. Fischer, I. Postigo-Hidalgo, S. Brünink, J.F. Drexler); Université de Lyon, Villeurbanne, France (D. Pontier, O. Filippi-Codaccioni, J.-B. Pons, J. Duhayer); Sechenov University, Martsinovsky Institute of Medical Parasitology, Tropical and Vector-Borne Diseases, Moscow, Russia (J.F. Drexler); German Centre for Infection Research, Berlin, Germany (J.F. Drexler)

DOI: https://doi.org/10.3201/eid2704.202676

The Study

We screened serum samples from 1,398 individual animals representing 25 different bat species collected during 2010–2018 in French Guiana using a broadly reactive alphavirus-specific reverse transcription PCR (RT-PCR) for viral RNA (Table 1) (*9*). All animals were released unharmed after sampling.

The overall TONV detection rate among all tested animals was 0.07% (95% CI −0.07% to 0.21%). Only 1 apparently healthy fringe-lipped bat (*Trachops cirrhosus*) sampled in 2011 was PCR-positive; we classified the virus as TONV (also known as VEEV subtype IIIB) upon amplicon sequencing (*6*). Among 11 individual fringe-lipped bats, the detection rate was 9.1% (95% CI −11.2% to 29.3%) (Figure 1, panel A). The TONV-positive sample was quantified by real-time RT-PCR using strain-specific oligonucleotides and an in vitro transcribed RNA standard (Table 2). Although the concentration of viral RNA in this sample was low, 78.5 genome copies/μL of blood, the virus was isolated on Vero E6 cells, suggesting potential to infect cells of primate origin. Successful isolation was consistent with highly efficient replication in cell culture, reaching 10^7 copies/μL of supernatant within 24 hours at different multiplicities of infection (Figure 2, panel A).

The complete viral genome was generated from the original isolate by high-throughput sequencing (MiSeq V3 chemistry; Illumina, https://www.illumina.com). In a complete genome-based maximum likelihood phylogeny, the bat-associated TONV (GenBank accession no. MW809725) clustered with the only available TONV strain, which was isolated in 1973 from a bird (Figure 2, panel B). Despite ≈40 years between the 2 TONV isolations and despite the divergent vertebrate hosts, the nucleotide identity between the bat-associated and the bird-associated TONVs was 98.1%, averaged over the whole genome. The high rate of genomic conservation is probably

[1]These authors contributed equally to this article.

Table 1. Bats tested for Tonate virus infection by PCR and PRNT, French Guiana*

Species	Animals screened by RT-PCR							PRNT screening, positive/tested
	2010	2011	2012	2015	2016	2017	Total	
Anoura geoffroyi	48	29	74	40	50	13	254	1/13
Artibeus lituratus	0	0	0	0	3	1	4	0
A. obscurus	0	0	0	0	2	8	10	0/10
A. planirostris	0	0	0	0	21	35	56	1/10
Carollia perspicillata	3	6	14	6	97	119	245	1/17
Cynomops planirostris	0	0	0	0	0	4	4	0
Dermanura cinerea	0	0	0	0	9	16	25	0
Desmodus rotundus	1	1	5	13	0	2	22	1/13
Lonchorhina inusitata	0	0	0	0	3	3	6	0
Molossus molossus	0	0	0	0	56	35	91	0/20
M. rufus	0	0	0	0	9	1	10	0
Noctilio albiventris	0	0	0	0	2	3	5	0
N. leporinus	0	0	0	0	1	25	26	0/20
Phyllostomus latifolius	5	1	2	1	0	0	9	0
P. hastatus	0	0	0	20	16	30	66	0
Platyrrhinus brachycephalus	0	0	0	0	3	8	11	0
P. fusciventris	0	0	0	0	0	9	9	0
P. incarum	0	0	0	0	3	1	4	0
Pteronotus gymnonotus	0	0	0	0	0	11	11	0
Pteronotus sp.	61	79	33	119	85	81	458	0/45
Sturnira lilium	0	0	0	0	6	20	26	0/8
S. tildae	0	0	0	0	17	8	25	0
Tonatia saurophila	1	0	0	0	0	3	4	0
Trachops cirrhosus	2	**1**	0	0	6	2	11	0/11
Uroderma bilobatum	0	0	0	0	2	4	6	0
Total	121	117	128	199	391	442	1398	4/167

*PCR-positive bat species and sample are highlighted in bold. PRNT screening was conducted using a screening dilution of 1:50 only because sample volumes were limited. PRNT, plaque reduction neutralization test; RT-PCR, reverse transcription PCR.

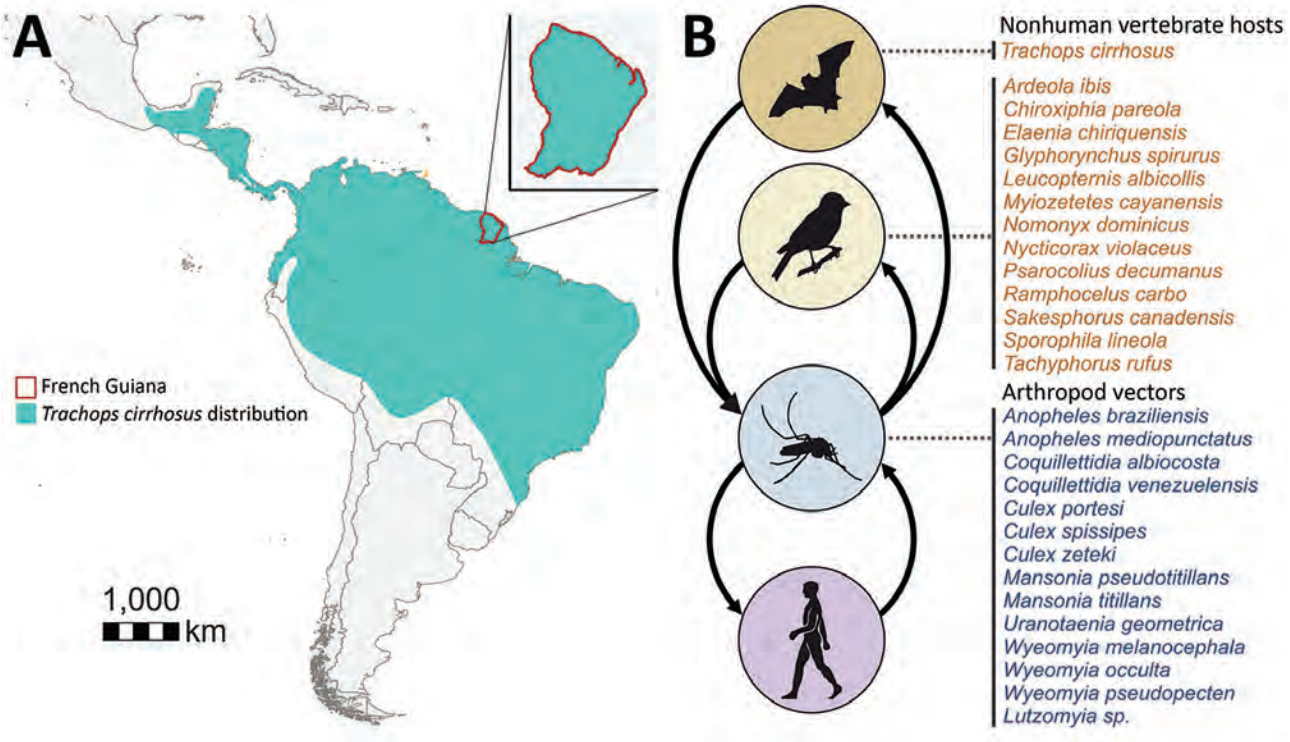

Figure 1. Tonate virus hosts and cycles for study of Venezuelan equine encephalitis complex alphavirus in bats, French Guiana. A) Geographic location of French Guiana in South America and distribution of fringe-lipped bats according to the International Union for Conservation of Nature Red List (https://www.iucnredlist.org/). B) Schematic transmission cycles of TONV according to data from this study and preliminary studies (*5*,*6*).

Table 2. Oligonucleotides for quantification of TONV, French Guiana*

Name	Sequence, 5′ → 3′	Concentration
Forward primer	CATTGTCATAGCCAGCAGAGTTCT	400 nM
Reverse primer	GACTTGATACCTTTGACGATGTTGTC	400 nM
Probe (FAM-labeled)	CGCGAACGTCTGACCAACTCACCCT	200 nM

*We carried out 25 μL real-time RT-PCR reactions using the Superscript III one-step RT-PCR system with Platinum Taq polymerase (Thermo Fisher Scientific, https://www.thermofisher.com). Reactions were set up with 5 μL extracted RNA; 12.5 μL of 2× reaction buffer; 0.4 μL of a 50 mM magnesium sulfate solution; 1 μg of nonacetylated bovine serum albumin; and 1 μL enzyme. Amplification was conducted at 50°C for 15 min, followed by 95°C for 3 min and 45 cycles of 95°C for 15 s and 58°C for 30 s with fluorescence, read at the 58° annealing/extension step on a LightCycler 480 thermocycler (Roche, https://www.roche.com). FAM, fluorescein amidite; RT-PCR, reverse transcription PCR.

a consequence of purifying selection that is a predominant evolutionary force acting on arboviruses because of their need to infect both vertebrate and arthropod cells (*10*). Nucleotide identity was <90% only within the hypervariable region (HVR) located in the alphaviral genomic region encoding the nonstructural protein 3 (nsP3) (Figure 2, panel C). In total, 31 aa substitutions or deletions were present in the bat-associated TONV compared with the bird-associated TONV, of which 14 were located within the nsP3 HVR ($p<0.0001$ by χ^2 test comparing the HVR to other genomic regions) (Figure 2, panel C). At the 5′ end of the HVR, the bat-associated TONV showed a larger in-frame deletion of 9 nt compared with the bird-associated TONV. This genomic region was covered by roughly 8,000 reads, supporting the deletion not being caused by technical mistakes during sequencing (Appendix Figure, https://wwwnc.cdc.gov/EID/article/27/4/20-2676-App1.pdf). The nsP3 HVR is assumed to play a crucial role for vector adaptation of VEEVs (*11*), supported by experimental evidence showing that exchanging the nsP3 of the alphaviruses chikungunya virus and o'nyong nyong virus dramatically affects the ability of chimeras to infect *Anopheles* and *Aedes* mosquito cells (*12*). The nsP3 deletion may therefore hypothetically reflect viral

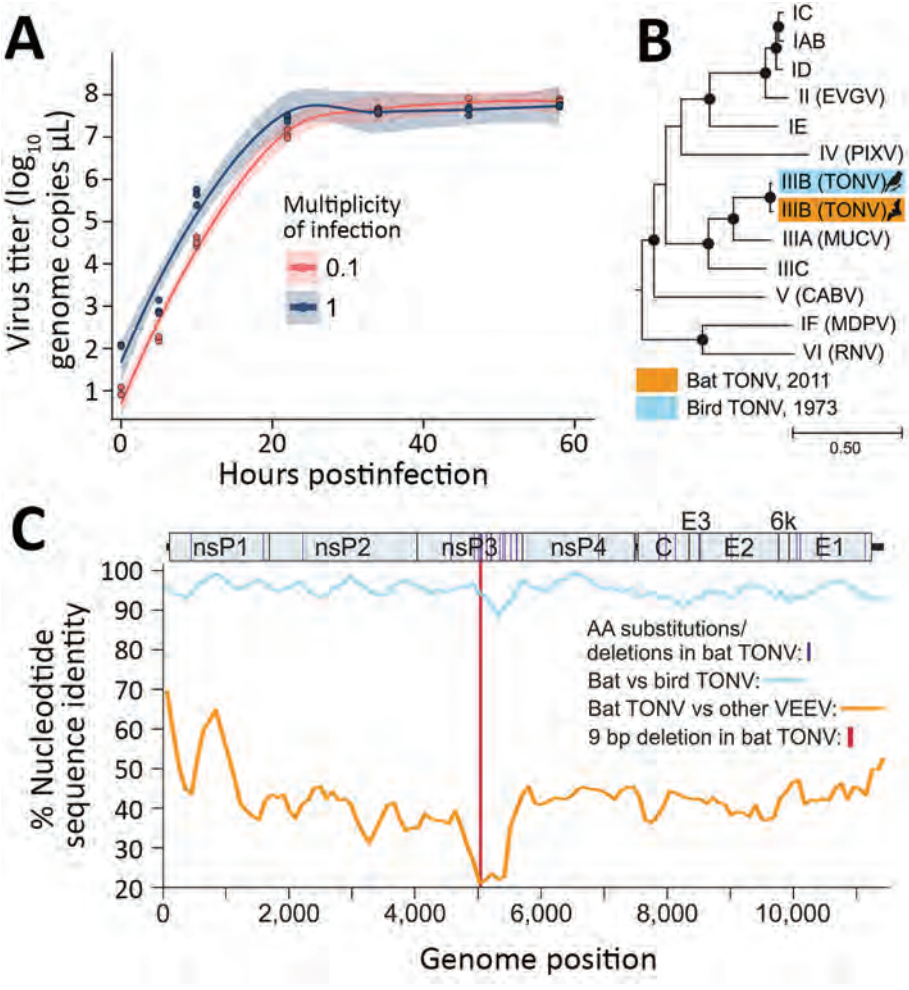

Figure 2. Characterization of bat TONV in study of VEE complex alphavirus in bats, French Guiana. (For additional discussion of Methods, see Appendix, https://wwwnc.cdc.gov/EID/article/27/4/20-2676-App1.pdf.) A) Growth kinetics of the new bat TONV on Vero E6 cells in 24-well plates. B) Maximum-likelihood phylogeny of TONV and members of the VEEV antigenic complex based on full genome nucleotide sequences. Eastern equine encephalitis virus (NC_003899) was included as an outgroup. Viruses are named according to the VEEV subtype classification: IAB/IC/ID/IE/IIIC, Venezuelan equine encephalitis virus; IF, Mosso das Pedras virus; II, Everglades virus; IIIA, Mucambo virus; IIIB, Tonate virus; IV, Pixuna virus; V, Cabassou virus; VI, Rio Negro virus. Bootstrap support above 90% is highlighted by filled circles. C) Percentage nucleotide sequence identity between TONV isolates and other viruses of the VEE antigenic complex. The median coverage for consensus preparation was 5,504 (range 5–11,605). TONV, Tonate virus; VEE, Venezuelan equine encephalitis.

adaptation to different invertebrate, and potentially also vertebrate, hosts. Cell culture–based experiments including mosquito, bat, and bird cell lines, as well as in vivo infections, comparing the growth of both TONV isolates and chimeric viruses will be needed to yield definite assessments on the potential effect of the observed HVR deletion on the viral phenotype.

Detection of acute TONV infection in only 1 fringe-lipped bat was not surprising because alphaviral viremia is typically short-lived (*13*). To examine the frequency of past TONV infections in bats, we tested 167 bat serum samples for TONV-specific neutralizing antibodies by 50% plaque reduction neutralization test ($PRNT_{50}$). We selected the sample set on the basis of availability of sufficient sample volumes; a preference for fringe-lipped bats, the attempt to represent the most abundant bat species investigated in this study; and a focus on bat genera in which VEEV-specific neutralizing antibodies had been detected previously in other countries (*4*,*8*). Four bats were seropositive, resulting in an overall TONV seroprevalence of 2.4% (95% CI 0.1%–4.7%) among tested samples. Limited reduction of PFUs at a serum dilution of 1:50 spoke against high antibody titers in those 4 animals and, indeed, no neutralization was observed when those 4 serum samples were tested at a dilution of 1:500. The 4 seropositive bats belonged to the species *Anoura geoffroyi* (1/13 animals, 7.7%; 95% CI −9.1% to 24.5%), *Artibeus planirostris* (1/10 animals, 10%; 95% CI −12.6% to 32.6%), *Carollia perspicillata* (1/17 animals, 5.9%; 95% CI −6.6% to 18.4%), and *Desmodus rotundus* (1/13 animals, 7.7%; 95% CI −9.1% to 24.5%). All 11 fringe-lipped bats, including the acutely infected PCR-positive animal, showed no detectable neutralization of TONV.

Our serologic data are limited by testing only 1 relatively high serum dilution, and by the inability to differentiate between the neutralization of TONV and of other VEEVs such as Cabassou or Mucambo virus, which occur in geographic proximity to TONV (*14*). The serologic data therefore support low-level circulation of TONV or of antigenically related VEEVs in different bat species. Low prevalence of antibodies neutralizing TONV is consistent with the detection of VEEV antibodies in *Desmodus rotundus* (4.9%), *Carollia perspicillata* (6.9%), *Artibeus* spp. (4.4%), and *Noctilio leporinus* (7.1%) bats in Trinidad by epitope-blocking ELISA and hemagglutination inhibition tests (*8*).

Conclusion

The breadth of the VEEV host range remains unknown for most VEEV species or subtypes (*1*). This lack of information is particularly true for TONV, which has been found only in birds and humans so far. Identifying bats as naturally infected TONV hosts is thus a key finding, indicating a broad vertebrate host range for TONV. The TONV host range may hypothetically include other vertebrates, such as rodents, that are naturally infected by other VEEVs closely related to TONV (*4*) and by preliminary data on TONV infections in sentinel mice in the 1970s (*5*) (Figure 1, panel B). In French Guiana, 12% of the overall human population shows serologic evidence for prior TONV infection, but the regions of highest risk for TONV infection remained unclear. One serosurvey reported highest seroprevalence in the coastal regions (35%) (*5*), whereas another serosurvey reported highest seroprevalence in inland savannah areas (53%) (*15*). The broad distribution of TONV might be explained by a broad vertebrate host range adding to the previously known broad invertebrate host range (*2*,*5*). Bats are extraordinary species and hosts for many zoonotic viruses and may thus also play a major role in TONV maintenance (*7*). Future research addressing TONV transmission cycles should include sampling of a broad range of vertebrate animals in ecologically different habitats, ideally including bats and analyses of TONV-competent mosquito bloodmeals.

Acknowledgments

We are grateful to all volunteers and field workers who have helped us during the field sessions.

Authorization for bat capture in French Guiana was provided by the Ministry of Ecology, Environment, and Sustainable Development during 2015–2020 (approval no. C692660703 from the Departmental Direction of Population Protection (DDPP, Rhône, France). All methods (capture and animal handling) were approved by the Muséum national d'Histoire naturelle, Société française pour l'étude et la protection des mammifères, and the Direction de l'environnement, de l'aménagement et du logement (DEAL), Guyane.

This work was supported by European Union's Horizon 2020 research and innovation program through the ZIKAlliance project (grant agreement no. 734548) and Laboratoire d'Excellence Dynamiques éco-évolutives des maladies infectieuses (ANR-11-LABX-0048) of Université de Lyon, within the program Investissements d'Avenir (ANR-11-IDEX-0007).

About the Author

Mr. Fischer is a PhD student at the Institute of Virology at Charité-Universitätsmedizin, Berlin, Germany. His primary research interests are diagnostics and epidemiology of emerging viruses.

References

1. Forrester NL, Wertheim JO, Dugan VG, Auguste AJ, Lin D, Adams AP, et al. Evolution and spread of Venezuelan equine encephalitis complex alphavirus in the Americas. PLoS Negl Trop Dis. 2017;11:e0005693. https://doi.org/10.1371/journal.pntd.0005693
2. Degallier N, Digoutte J, Pajot F. Épidémiologie de deux arbovirus du complexe VEE en Guyane Francaise: données préliminaires sur les relations virus-vecteurs. Cahiers ORSTOM Série Entomologie Médicale et Parasitologie. 1978;16:209–21.
3. Hommel D, Heraud JM, Hulin A, Talarmin A. Association of Tonate virus (subtype IIIB of the Venezuelan equine encephalitis complex) with encephalitis in a human. Clin Infect Dis. 2000;30:188–90. https://doi.org/10.1086/313611
4. Sotomayor-Bonilla J, Abella-Medrano CA, Chaves A, Álvarez-Mendizábal P, Rico-Chávez Ó, Ibáñez-Bernal S, et al. Potential sympatric vectors and mammalian hosts of Venezuelan equine encephalitis virus in southern Mexico. J Wildl Dis. 2017;53:657–61. https://doi.org/10.7589/2016-11-249
5. Digoutte J. Ecologie des Arbovirus et Leur Rôle Pathogène chez L'Homme en Guyane Française. Cayenne, French Guiana: Institut Pasteur de la Guyane Française—Groupe I.N.S.E.R.M. U79; 1975.
6. Mutricy R, Djossou F, Matheus S, Lorenzi-Martinez E, De Laval F, Demar M, et al. Discriminating tonate virus from dengue virus infection: a matched case-control study in French Guiana, 2003-2016. Am J Trop Med Hyg. 2020;102:195–201. https://doi.org/10.4269/ajtmh.19-0156
7. Olival KJ, Hosseini PR, Zambrana-Torrelio C, Ross N, Bogich TL, Daszak P. Host and viral traits predict zoonotic spillover from mammals. Nature. 2017;546:646–50. https://doi.org/10.1038/nature22975
8. Thompson NN, Auguste AJ, Travassos da Rosa AP, Carrington CV, Blitvich BJ, Chadee DD, et al. Seroepidemiology of selected alphaviruses and flaviviruses in bats in Trinidad. Zoonoses Public Health. 2015;62:53–60.
9. Grywna K, Kupfer B, Panning M, Drexler JF, Emmerich P, Drosten C, et al. Detection of all species of the genus *Alphavirus* by reverse transcription-PCR with diagnostic sensitivity. J Clin Microbiol. 2010;48:3386–7. https://doi.org/10.1128/JCM.00317-10
10. Woelk CH, Holmes EC. Reduced positive selection in vector-borne RNA viruses. Mol Biol Evol. 2002;19:2333–6. https://doi.org/10.1093/oxfordjournals.molbev.a004059
11. Götte B, Liu L, McInerney GM. The enigmatic alphavirus non-structural protein 3 (nsP3) revealing its secrets at last. Viruses. 2018;10:105. https://doi.org/10.3390/v10030105
12. Saxton-Shaw KD, Ledermann JP, Borland EM, Stovall JL, Mossel EC, Singh AJ, et al. O'nyong nyong virus molecular determinants of unique vector specificity reside in non-structural protein 3. PLoS Negl Trop Dis. 2013;7:e1931. https://doi.org/10.1371/journal.pntd.0001931
13. Bozza FA, Moreira-Soto A, Rockstroh A, Fischer C, Nascimento AD, Calheiros AS, et al. Differential shedding and antibody kinetics of Zika and chikungunya viruses, Brazil. Emerg Infect Dis. 2019;25:311–5. https://doi.org/10.3201/eid2502.180166
14. Aguilar PV, Estrada-Franco JG, Navarro-Lopez R, Ferro C, Haddow AD, Weaver SC. Endemic Venezuelan equine encephalitis in the Americas: hidden under the dengue umbrella. Future Virol. 2011;6:721–40. https://doi.org/10.2217/fvl.11.50
15. Talarmin A, Trochu J, Gardon J, Laventure S, Hommel D, Lelarge J, et al. Tonate virus infection in French Guiana: clinical aspects and seroepidemiologic study. Am J Trop Med Hyg. 2001;64:274–9. https://doi.org/10.4269/ajtmh.2001.64.274

Address for correspondence: Jan Felix Drexler, Charité-Universitätsmedizin Berlin, Institute of Virology, Helmut-Ruska-Haus Charitéplatz 1, 10098 Berlin, Germany; email: felix.drexler@charite.de

Stability of SARS-CoV-2 RNA in Nonsupplemented Saliva

Isabel M. Ott,[1] Madison S. Strine,[1] Anne E. Watkins, Maikel Boot, Chaney C. Kalinich, Christina A. Harden, Chantal B.F. Vogels, Arnau Casanovas-Massana, Adam J. Moore, M. Catherine Muenker, Maura Nakahata, Maria Tokuyama, Allison Nelson, John Fournier, Santos Bermejo, Melissa Campbell, Rupak Datta, Charles S. Dela Cruz, Shelli F. Farhadian, Albert I. Ko, Akiko Iwasaki, Nathan D. Grubaugh,[2] Craig B. Wilen,[2] Anne L. Wyllie,[2] the Yale IMPACT Research team[3]

The expense of saliva collection devices designed to stabilize severe acute respiratory syndrome coronavirus 2 RNA is prohibitive to mass testing. However, virus RNA in nonsupplemented saliva is stable for extended periods and at elevated temperatures. Simple plastic tubes for saliva collection will make large-scale testing and continued surveillance easier.

Despite increased diagnostic testing capacity for severe acute respiratory syndrome coronavirus 2 (SARS-CoV-2), testing in many countries, including the United States, is still inadequate for slowing the coronavirus disease (COVID-19) pandemic. Many persons still do not have access to SARS-CoV-2 testing, and for some that do, an imbalance between supply and demand at large testing centers leads to long delays before results are received. The demand for testing will only increase as many schools, colleges, and workplaces reopen. Ideally, specialized population surveillance–oriented testing would require minimal diversion of resources from clinical diagnostic testing, be affordable and scalable, and enable rapid and reliable virus identification for persons with asymptomatic or subclinical infections. Thus, simplifying the sample collection and testing workflow is critical.

A simple solution is saliva collection. Saliva is a sensitive source for SARS-CoV-2 detection (*1*–*3*) and an alternative sample type for antigen and antibody testing (*4*,*5*). In addition, saliva collection is noninvasive, can be reliably performed without trained health professionals, and does not rely on a sometimes-limited swab supply. However, almost all saliva-based tests approved by the US Food and Drug Administration require specialized collection tubes containing stabilization or inactivation buffers that are costly and not always available. Moreover, as saliva continues to gain popularity as a potential specimen to aid testing demands, standardized collection methods have not been defined for saliva collection as they have for swab-based specimen collection. When true saliva is not collected (e.g., if it contains sputum), which can happen with COVID-19 inpatients when saliva is difficult to produce, specimens can be difficult to pipette (*6*). Combined with untested concerns regarding SARS-CoV-2 RNA stability in saliva, using supplements to reduce degradation and improve sample processing has become common. Previous work with saliva samples, however, has indicated that some buffers optimized for host nucleic acid stabilization may actually inhibit viral RNA detection (*7*) (S.B. Griesemer et al., unpub. data, https://doi.org/10.1101/2020.06.16.20133041), particularly in extraction-free PCRs (D.R.E. D.R.E. Ranoa et al., unpub. data, https://doi.org/10.1101/2020.06.18.159434). Thus, if true saliva (relatively easy to pipette) is being tested, the utility of collecting saliva in expensive tubes containing purported stabilization buffers comes into question. To explore the viability of broadly deploying affordable saliva-based surveillance approaches (*8*), we characterized SARS-CoV-2 RNA stability and virus infectivity in saliva samples stored in widely

Author affiliations: Yale School of Public Health, New Haven, Connecticut, USA (I.M. Ott, A.E. Watkins, C.C. Kalinich, C.A. Harden, C.B.F. Vogels, A. Casanovas-Massana, A.J. Moore, M.C. Muenker, M. Nakahata, A.I. Ko, N.D. Grubaugh, A.L. Wyllie); Yale School of Medicine, New Haven (M.S. Strine, M. Boot, M. Tokuyama, A. Nelson, J. Fournier, S. Bermejo, M. Campbell, R. Datta, C.S. Dela Cruz, S.F. Farhadian, A.I. Ko, A. Iwasaki, C. Wilen); Howard Hughes Medical Institute, New Haven (A. Iwasaki)

DOI: https://doi.org/10.3201/eid2704.204199

[1]These first authors contributed equally to this article.

[2]These senior authors contributed equally to this article.

[3]Team members team are listed at the end of this article.

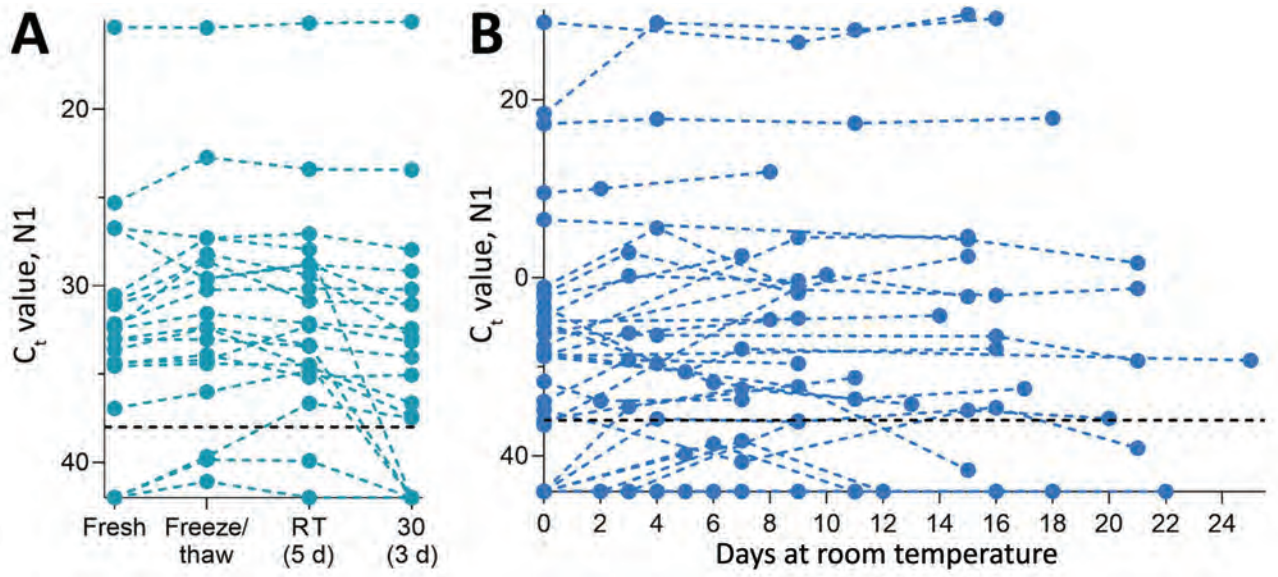

Figure 1. Stability of severe acute respiratory syndrome coronavirus 2 (SARS-CoV-2) RNA (N1) detection in saliva. A) Detection of SARS-CoV-2 RNA in 20 saliva samples on day of sample collection (fresh) did not significantly change after storage at −80°C (to assess the effect of a freeze/thaw cycle), 3 days at 30°C, or 5 days at RT (recorded as ≈19°C). Detection of N1 remained similar to that of freshly collected samples, regardless of starting C_t value (Pearson r = −0.085, p = 0.518). B) At RT, detection remained stable for up to 25 days. Colored dashed lines track the same sample through different storage conditions. Black horizontal dashed lines represent C_t 38, which we applied as the cutoff to determine sample positivity. Samples that remained not detected after 45 cycles are depicted on the x-axis. C_t, cycle threshold; RT, room temperature.

available, sterile, nuclease-free laboratory plastic (polypropylene) tubes.

The Study

We used saliva collected from COVID-19 inpatients and at-risk healthcare workers into sterile wide-mouth containers (*3*) without preservatives (nonsupplemented) to evaluate the temporal stability of SARS-CoV-2 RNA at different holding temperatures (−80°C, 4°C, ≈19°C, 30°C) (Appendix, https://wwwnc.cdc.gov/EID/article/27/4/20-4199-App1.pdf). SARS-CoV-2 RNA from saliva was consistently detected at similar levels regardless of the holding time and temperatures tested. After RNA extraction and quantitative reverse transcription PCR (qRT-PCR) testing for SARS-CoV-2 on the day of saliva collection (*3*), we aliquoted and stored the remaining 20 sample volumes at −80°C, room temperature (≈19°C), and 30°C. Whether stored at −80°C, room temperature (5 days), or 30°C (3 days), the qRT-PCR cycle threshold (C_t) values for the N1 region of the nucleocapsid protein did not differ significantly from those for samples tested on the day of collection (Figure 1, panel A). After the freeze/thaw cycle or storage at room temperature, we observed C_t decreases of 1.058 (95% CI 2.289 to 0.141) for freeze/thaw and 0.960 (95% CI −2.219 to 0.266) for room temperature; however, the strength of this effect was low. We saw a similar effect after incubation at 30°C, with a C_t increase of 0.973 (95% CI −0.252 to 2.197). Moreover, SARS-CoV-2 RNA remained relatively stable in saliva samples left at room temperature for up to 25 days (C_t 0.027, 95% CI −0.019 to 0.071 C_t) (Figure 1, panel B). Regardless of starting C_t value (viral load), this prolonged stability of SARS-CoV-2 RNA was also observed when samples were stored for longer periods at −80°C (maximum 92 days), 4°C (maximum 21 days), and 30°C (maximum 16 days) (Appendix Figure 1).

Although SARS-CoV-2 RNA from saliva remained stable over time, we observed a decrease in human ribonuclease P at higher temperatures (room temperature, C_t 1.837, 95% CI 0.468 to 3.188 C_t; 30°C, C_t 3.526, 95% CI 1.750 to 5.349 C_t; Appendix Figure 2); the change in concentration was greater than that observed for SARS-CoV-2 RNA (Appendix Figure 3). Thus, although human RNA from saliva degrades without stabilization buffers, SARS-CoV-2 RNA remains protected even at warm temperatures suitable for nuclease activity.

Because saliva has antiviral properties (*9*,*10*), we explored the infectiousness of SARS-CoV-2 in saliva samples. We inoculated Vero-E6 cells with 49 saliva samples with higher virus RNA titers (C_t range 13.57–35.32, median 26.01; Appendix Figure 4) because others have shown that SARS-CoV-2 isolation is uncommon from samples with low virus RNA titers (*11*,*12*;

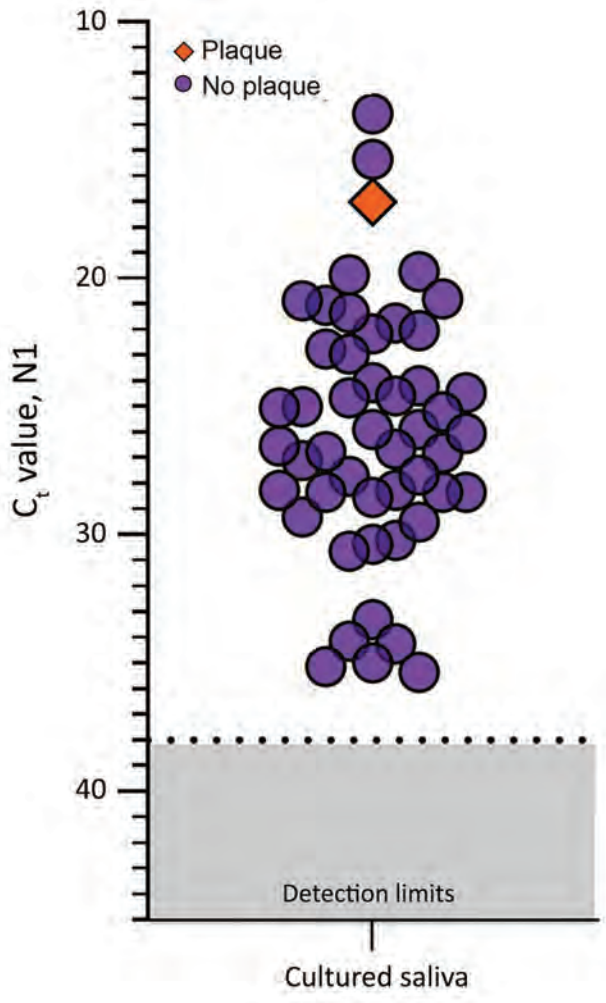

Figure 2. Detection of severe acute respiratory syndrome coronavirus 2 (SARS-CoV-2) in saliva samples tested for infectious SARS-CoV-2. SARS-CoV-2 N1 detection (C_t values) measured by quantitative reverse transcription PCR for each saliva sample incubated with Vero-E6 cells for 72 hours. The orange diamond depicts the only sample that produced plaque-forming units (titer increase of 3.79×10^4 PFU/mL; purple circles indicate samples that did not produce plaque-forming units by 72 h after inoculation; dashed lines indicate C_t 38 (the cutoff for sample positivity); gray shading indicates C_ts below the limit of detection. C_t, cycle threshold.

M.D. Folgueira, unpub. data, https://www.medrxiv.org/content/10.1101/2020.06.10.20127837v1). By 72 hours after inoculation, C_t values were reduced in 9 (18.7%) of the 49 cultured saliva samples tested by qRT-PCR (−12.90, −11.53, −4.30, −3.68, −3.49, −2.88, −2.81, −2.66, −2.40). Although these findings suggest an increased number of SARS-CoV-2 RNA copies by 72 hours, they may not definitively demonstrate active virus replication. For instance, C_t reductions could also result from sampling artifacts or assay variations (disparities in inoculation, RNA extraction, and qRT-PCR). To determine whether this amplification resulted from detectable, active virus replication, we performed plaque assays in triplicate with cellular lysate from 72 hours after inoculation. Only 1 of these 9 samples produced plaque-forming units; titer increased 3.79×10^4 PFU/mL at 1 hour and at 72 hours after inoculation (Figure 2). This finding suggests that increased SARS-CoV-2 genome copies identified by qRT-PCR may fall below the limit of detection in plaque assay sensitivity (100 PFU/mL) until a certain reduction in C_t is reached (e.g., C_t reduction ≤12.90) or that components of saliva possibly inhibit active viral particle production and release in vitro. A similar result has been observed when attempting to perform plaque assays of virus from the colon (*13*), despite studies showing that SARS-CoV-2 infects gut enterocytes (*14*).

Conclusions

The cost of commercial tubes specialized for saliva collection and SARS-CoV-2 RNA stabilization (>$7/tube) (Table) can be prohibitive for mass testing. Inexpensive saliva-based testing methods are urgently needed to help reach the capacity required to safely reopen schools and workplaces. We demonstrate the stability of SARS-CoV-2 RNA detection in saliva stored for prolonged periods in a variety of settings, which indicates that saliva can be simply collected without the need for additives.

Previous studies have demonstrated the ease with which saliva can be collected into simple, wide-mouth containers (*3*,*15*) and that buffers marketed for RNA stabilization may be detrimental to SARS-CoV-2 detection (S.B. Griesemer et al., unpub data, https://doi.org/10.1101/2020.06.16.20133041). Although some of these buffers are also marketed for virus inactivation, SARS-CoV-2 is still considered a Biosafety Level 2 hazard, meaning that with or without buffer, any saliva sample should still be handled with care. Without the need for RNA stabilization and given the limited evidence of virus replication in saliva samples, affordable alternatives to making testing accessible throughout the country are simple, sterile, nuclease-free plastic containers.

SARS-CoV-2 stability at room temperature and at 30°C permits more affordable collection and transport strategies without the need for expensive cooling strategies. Absence of the requirement for cold chain handling also makes saliva testing easier in regions with limited resources. Thus, one key for meeting mass testing demands is collection of saliva in simple, sterile, nuclease-fee tubes, negating the high costs associated with specialized collection devices.

Table. Possible saliva collection devices for severe acute respiratory virus coronavirus 2 RNA testing

Tube type	Collection	Buffer type	Cost per sample, USD	Manufacturer
Oragene•Dx collection device (OGD-510)*	Funnel	Ethanol <24%; Tris 1%–5% (host DNA stabilization)	28.00	Genotek, https://www.dnagenotek.com
Samplify SD-3000	Funnel	Dry preservative; sodium dodecyl sulfate <1%	24.00	Samplify (URL not available)
Saliva collection kit	Funnel	Unknown	22.47	IBI Scientific, https://www.ibisci.com
SDNA-1000 small tubes*	Wide-mouth tube	Ethanol 10%–25%; Tris 1%–5%; thiocyanic acid:guanidine (1:1) 25%–50%; pH 7.9–8.3	17.99	Spectrum Solutions, https://spectrumsolution.com
Saliva RNA Collection and Preservation Device	Wide-mouth tube	Unknown liquid, colorless, odorless	18	Norgen (Biotek), https://norgenbiotek.com
Liquid biopsy/spit devices	Complicated unit (various)	Unknown	9–12 each	Oasis Diagnostics, https://4saliva.com
OMNIgene•ORAL saliva collection device (OM-505)*	Funnel	Sodium dodecyl sulfate 1%–5%; glycine,N,N′-trans-1,2-cyclohexanediylbis [N-(carboxymethyl)-,hydrate 1%–5%; lithium chloride 0.5%–1.5%	9.50	Genotek
GeneFix Saliva DNA/RNA Collection	Funnel	Unknown liquid, colorless	9	Isohelix, https://isohelix.com
DNA/RNA Shield saliva collection kit*	Wide-mouth tube	Unknown liquid, colorless, pH 5.0–7	7.25	Zymo Research, https://www.zymoresearch.com
Saliva collection system	Small beaker	Unknown	Unavailable	Greiner Bio-One, ttps://www.gbo.com
Pedia•SAL Infant/Toddler Salivary Collection	Soother + collector	None	Unavailable	Oasis Diagnostics
Oral swab	Swab	None	1.76	Salimetrics, https://salimetrics.com
Saliva collection aid + cryovial	Straw + 2 mL collection vial	None	1.36/straw, 0.76/vial	Salimetrics
Urine collection cups	Wide-mouth cup	None	0.47	ThermoFisher, https://www.thermofisher.com
Sterile tube, large volume	Wide-mouth tube	None	0.46 (25 mL), 0.38 (5 mL)	Eppendorf, https://www.eppendorf.com
Sterile tube, small volume	Narrow-mouth tube	None	0.16 (2 mL)	ThermoFisher

*Approved by US Food and Drug Administration Emergency Use Authorization for saliva-based diagnostics.

Yale IMPACT Research Team authors (in alphabetical order): Kelly Anastasio, Michael H. Askenase, Maria Batsu, Sean Bickerton, Kristina Brower, Molly L. Bucklin, Staci Cahill, Yiyun Cao, Edward Courchaine, Giuseppe DeIuliis, Rebecca Earnest, Renata Filler, Bertie Geng, Benjamin Goldman-Israelow, Ryan Handoko, William Khoury-Hanold, Daniel Kim, Lynda Knaggs, Maxine Kuang, Eriko Kudo, Sarah Lapidus, Joseph Lim, Melissa Linehan, Peiwen Lu, Alice Lu-Culligan, Amyn A. Malik, Anjelica Martin, Irene Matos, David McDonald, Maksym Minasyan, Nida Naushad, Jessica Nouws, Abeer Obaid, Camila Odio, Ji Eun Oh, Saad Omer, Annsea Park, Hong-Jai Park, Xiaohua Peng, Mary Petrone, Sarah Prophet, Tyler Rice, Kadi-Ann Rose, Lorenzo Sewanan, Lokesh Sharma, Denise Shepard, Mikhail Smolgovsky, Nicole Sonnert, Yvette Strong, Codruta Todeasa, Jordan Valdez, Sofia Velazquez, Arvind Venkataraman, Pavithra Vijayakumar, Elizabeth B. White, Yexin Yang.

Acknowledgments

We gratefully acknowledge the study participants for their time and commitment to the study. We thank all members of the clinical team at Yale New Haven Hospital for their dedication and work, which made this study possible. We also thank S. Taylor and P. Jack for technical discussions.

This study was supported by the Huffman Family Donor Advised Fund (N.D.G.), Fast Grant funding support from the Emergent Ventures at the Mercatus Center, George Mason University (N.D.G.), the Yale Institute for Global Health (N.D.G.), and the Beatrice Kleinberg Neuwirth Fund (A.I.K.). C.B.F.V. is supported by NWO Rubicon 019.181EN.004.

About the Author

Ms. Ott is a research assistant in the Department of Epidemiology of Microbial Diseases at the Yale School

of Public Health, New Haven CT. Her work focuses on developing diagnostic tools for and analyzing functional evolution of viral pathogens, with particular focus on SARS-CoV-2 and endemic arboviruses.

References

1. Hanson KE, Barker AP, Hillyard DR, Gilmore N, Barrett JW, Orlandi RR, et al. Self-collected anterior nasal and saliva specimens versus health care worker-collected nasopharyngeal swabs for the molecular detection of SARS-CoV-2. J Clin Microbiol. 2020;58:e01824-20.
2. Byrne RL, Kay GA, Kontogianni K, Aljayyoussi G, Brown L, Collins AM, et al. Saliva alternative to upper respiratory swabs for SARS-CoV-2 diagnosis. Emerg Infect Dis. 2020;26:2770–1.
3. Wyllie AL, Fournier J, Casanovas-Massana A, Campbell M, Tokuyama M, Vijayakumar P, et al. Saliva or nasopharyngeal swab specimens for detection of SARS-CoV-2. N Engl J Med. 2020;383:1283–6. https://doi.org/10.1056/NEJMc2016359
4. Isho B, Abe KT, Zuo M, Jamal AJ, Rathod B, Wang JH, et al. Persistence of serum and saliva antibody responses to SARS-CoV-2 spike antigens in COVID-19 patients. Sci Immunol. 2020;5:eabe5511.
5. Pisanic N, Randad PR, Kruczynski K, Manabe YC, Thomas DL, Pekosz A, et al. COVID-19 serology at population scale: SARS-CoV-2-specific antibody responses in saliva. J Clin Microbiol. 2020;59:e02204–20. https://doi.org/10.1128/JCM.02204-20
6. Landry ML, Criscuolo J, Peaper DR. Challenges in use of saliva for detection of SARS CoV-2 RNA in symptomatic outpatients. J Clin Virol. 2020;130:104567. https://doi.org/10.1016/j.jcv.2020.104567
7. Jones TH, Muehlhauser V. Effect of handling and storage conditions and stabilizing agent on the recovery of viral RNA from oral fluid of pigs. J Virol Methods. 2014;198:26–31. https://doi.org/10.1016/j.jviromet.2013.12.011
8. Vogels CBF, Watkins AE, Harden CA, Brackney DE, Shafer J, Wang J, et al. SalivaDirect: a simplified and flexible platform to enhance SARS-CoV-2 testing capacity. Med. 2020 Dec 26 [Epub ahead of print]. https://doi.org/10.1016/j.medj.2020.12.010
9. Lieleg O, Lieleg C, Bloom J, Buck CB, Ribbeck K. Mucin biopolymers as broad-spectrum antiviral agents. Biomacromolecules. 2012;13:1724–32. https://doi.org/10.1021/bm3001292
10. Malamud D, Abrams WR, Barber CA, Weissman D, Rehtanz M, Golub E. Antiviral activities in human saliva. Adv Dent Res. 2011;23:34–7. https://doi.org/10.1177/0022034511399282
11. Wölfel R, Corman VM, Guggemos W, Seilmaier M, Zange S, Müller MA, et al. Virological assessment of hospitalized patients with COVID-2019. Nature. 2020;581:465–9. https://doi.org/10.1038/s41586-020-2196-x
12. Bullard J, Dust K, Funk D, Strong JE, Alexander D, Garnett L, et al. Predicting infectious SARS-CoV-2 from diagnostic samples. Clin Infect Dis. 2020 May 22 [Epub ahead of print]. https://doi.org/10.1093/cid/ciaa638
13. Zang R, Gomez Castro MF, McCune BT, Zeng Q, Rothlauf PW, Sonnek NM, et al. TMPRSS2 and TMPRSS4 promote SARS-CoV-2 infection of human small intestinal enterocytes. Sci Immunol. 2020;5:eabc3582. https://doi.org/10.1126/sciimmunol.abc3582
14. Lamers MM, Beumer J, van der Vaart J, Knoops K, Puschhof J, Breugem TI, et al. SARS-CoV-2 productively infects human gut enterocytes. Science. 2020;369:50–4. https://doi.org/10.1126/science.abc1669
15. Wyllie AL, Chu MLJN, Schellens MHB, van Engelsdorp Gastelaars J, Jansen MD, van der Ende A, et al. *Streptococcus pneumoniae* in saliva of Dutch primary school children. PLoS One. 2014;9:e102045. https://doi.org/10.1371/journal.pone.0102045

Address for correspondence: Anne L. Wyllie and Nathan D. Grubaugh, Yale School of Public Health, 60 College St, New Haven, CT 06511, USA; email: anne.wyllie@yale.edu and nathan.grubaugh@yale.edu

Rare Norovirus GIV Foodborne Outbreak, Wisconsin, USA

Leslie Barclay, Tim Davis, Jan Vinjé

We report a norovirus GIV outbreak in the United States, 15 years after the last reported outbreak. During May 2016 in Wisconsin, 53 persons, including 4 food handlers, reported being ill. The outbreak was linked to individually prepared fruit consumed as a fruit salad. The virus was phylogenetically classified as a novel GIV genotype.

Norovirus is the leading cause of epidemic and endemic acute gastroenteritis globally. The virus can be transmitted through person-to-person contact, consumption of fecally contaminated food or water, or self-contamination after touching contaminated environmental surfaces (*1*,*2*). Noroviruses are divided into at least 10 genogroups (G), and viruses in GI, GII, GIV, GVIII, and GIX cause illness in humans (*3*). More than 99% of all norovirus outbreaks are caused by GI and GII viruses in the United States (*4*). GVIII includes 2 strains that have been detected in Japan during 2004 and 2011 (*3*), and GIX has caused 11 reported outbreaks in the United States since 2013 (https://www.cdc.gov/norovirus/reporting/calicinet/data.html).

GIV is divided into 2 recognized genotypes: GIV.1, which infects humans (*5*), and GIV.2, which infects canines and felines (*6*). GIV viruses were reported in humans in the Netherlands during 1998 and the United States during 1999 (*7*,*8*) and have since been sporadically reported in clinical and environmental samples (*5*,*9*–*11*). An outbreak linked to a GIV norovirus in the United States has not been reported since 2001 (*4*,*8*). In this article, we describe a 2016 foodborne norovirus outbreak associated with a novel GIV strain (tentatively GIV.NA).

The Study

On May 6, 2016, the Wisconsin Department of Public Health was notified of a possible norovirus outbreak. The outbreak occurred at a breakfast event held at a restaurant on May 3, 2016, for local business owners (Figure 1). According to interviews of the affected group, 49 attendees and 4 food handlers reported being ill, and the first case was reported on May 4, 2016. The peak of illness occurred 48 hours after the breakfast event. Symptoms included diarrhea, vomiting, and nausea (Table 1). Duration of illness was 1–5 days (median 2 days), and incubation time range was 15–57 hours (median 38 hours).

On the basis of the epidemiologic investigation, pathogen transmission occurred through foodborne exposure, and the highest risk ratio was linked to individually eaten fruit from a fruit salad served at the breakfast (risk ratio 2.17–3.29) (Table 2). The epidemiologic curve and risk ratios were calculated by using Microsoft Excel (https://www.microsoft.com) and R software (http://www.r-project.org). The food handlers prepared the fruit, which was served as a fruit salad during the meal on May 2, the day before the breakfast. Reportedly, the strawberries and grapes were washed, whereas the melons were not. There was no leftover fruit available for laboratory testing.

Nucleic acid was extracted from stool samples collected from 6 ill persons and tested for norovirus GI/GII by real-time quantitative reverse transcription PCR (qRT-PCR), and 5 GII-positive samples (from 3 attendees and 2 food handlers) with high cycle threshold values (range 28–37) were amplified by conventional RT-PCR targeting a partial region of the 5′ end of open reading frame 2 (*4*). The sequences did not cluster with any GI or GII norovirus reference sequences and closely matched GIV viruses (*4*).

Next-generation sequencing (NGS) was performed on 3 samples and verification of final consensus sequences was performed by using Geneious version 11.1.2 (Biomatters Inc., https://www.newjerseybids.us) (*4*). Sequences for all 3 near complete genomes (≈7,490 nt) were identical (GenBank accession no. NC_044855). The closest polymerase gene sequence in GenBank had a 79% nt similarity (Figure 2, panel A), and the capsid sequence matched partial

Author affiliations: Centers for Disease Control and Prevention, Atlanta, Georgia, USA (L. Barclay, J. Vinjé); Wisconsin State Laboratory of Hygiene, Madison, Wisconsin, USA (T. Davis)

DOI: https://doi.org/10.3201/eid2704.204521

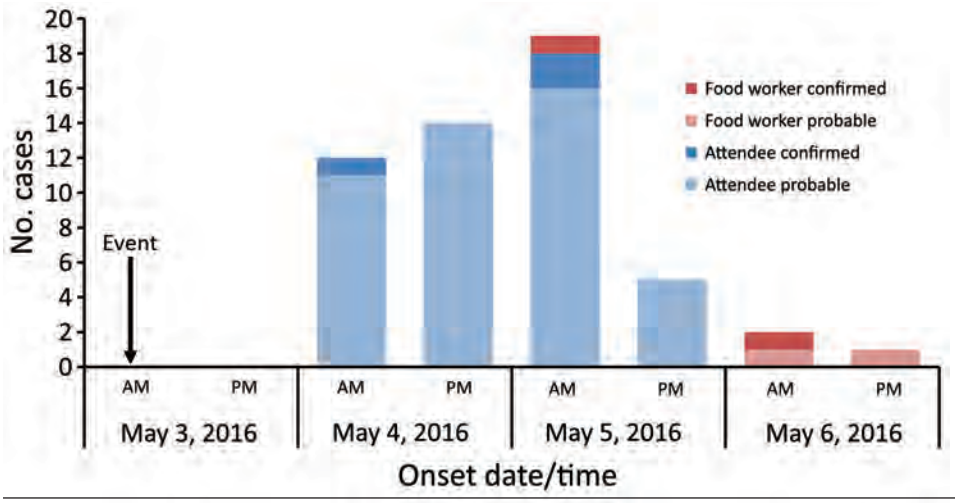

Figure 1. Epidemiologic curve of attendees and food handlers by date of illness onset for event during rare norovirus GIV foodborne outbreak, Wisconsin, USA. Arrow indicates event date and time period event occurred. AM indicates 12:00 AM–11:59 AM and PM indicates 12:00 PM–11:59 PM. Dark red indicates laboratory-confirmed food workers, light red indicates probable food workers, dark blue indicates laboratory-confirmed attendees, and light blue indicates probable attendees.

Table 1. Clinical and demographic characteristics of attendees associated with a norovirus GIV foodborne outbreak, Wisconsin, USA*

Characteristic	Value
Onset of illness	2016 May 4
Total no. ill	49
Hospitalized	0
Died	0
Duration of illness, d	2
Primary case-patients	49
Laboratory confirmed	3
Probable	46
Secondary case-patients	0
Laboratory confirmed	0
Probable	0
Sex	
M	13 (26.5)
F	34 (69.4)
Unknown	2 (4.1)
Age range, y (median)	17–77 (47)
Age group, y	
<1	0 (0)
1–4	0 (0)
5–9	0 (0)
10–19	2 (4.1)
20–49	24 (49.0)
50–74	14 (28.6)
≥75	1 (2.0)
Unknown	8 (16.3)
Case-patients with known illness duration	35
Duration range, d	1–5
Duration median, d	2
Case-patients with known incubation period	49
Incubation range, h	15–57
Incubation median, h	38
Symptom	
Diarrhea	44 (89.8)
Nausea	41 (83.7)
Fatigue	41 (83.7)
Headache	35 (71.4)
Abdominal pain	34 (69.4)
Chills	31 (63.3)
Vomiting	30 (61.2)
Body ache	30 (61.2)

*Values are no. or no. (%) except as indicated. Clinical and demographic characteristics for the 4 food handlers associated with this outbreak are not available.

capsid sequences derived from wastewater in Brazil, Japan, and the United States with a 98% nt identity. The closest complete major capsid sequence in GenBank (accession no. AF414426) had a 76% aa identity (Figure 2, panel B).

Conclusions

We report a novel norovirus GIV genotype as the causative agent of a foodborne norovirus outbreak. Norovirus GIV outbreaks are rare and were reported in the Netherlands during 1998, the United States during 1999, and in Australia during 2010 (*5*,*7*,*8*) and have since been detected sporadically in clinical samples (*9*–*11*). However, seroprevalence studies in Italy, the Netherlands, and the United States have shown that 19%–31% of these populations have antibodies against GIV (*12*–*14*). Possible explanations include that most laboratories do not test for norovirus GIV or most infections are asymptomatic or do not lead to a visit to a physician. However, 3 young children who were positive for GIV in a study in Italy had severe endemic acute gastroenteritis symptoms (*10*).

Several studies have detected norovirus GIV in rivers and wastewater (*9*–*11*,*15*); the number of positive samples ranged from 8.2% to 34%, further supporting that norovirus GIV is circulating in the general population. Several short sequences detected in wastewater collected in Brazil, Japan, and the United States match the capsid sequence in our study (*9*,*15*). However, new norovirus genotypes require ≥2 nonidentical complete capsid sequences from different geographic locations that form a separate phylogenetic cluster (*3*) Therefore, the virus detected in this outbreak cannot officially be assigned as GIV.3 yet but is assigned GIV.NA1[PNA1].

Table 2. Analysis of implicated food and drink in a norovirus GIV outbreak, Wisconsin, USA*

	Persons who ate food or drink		Persons who did not eat food or drink			
Food and drink items implicated	Total	% Ill	Total	% Ill	RR (95% CI)	p value
Any quiche	74	58	5	60	0.95 (0.32–2.89)	0.934
Ham and cheese quiche	51	63	23	48	1.40 (0.83–2.38)	0.229
Vegetable quiche	21	48	54	63	0.71 (0.41–1.21)	0.226
Any fruit	71	65	7	0	2.84 (2.07–3.89)	<0.05
Cantaloupe	55	67	12	25	2.29 (1.39–3.78)	<0.05
Honeydew melon	52	65	12	25	2.17 (1.32–3.56)	<0.05
Grapes	58	69	9	0	3.22 (2.20–4.73)	<0.05
Strawberries	56	70	10	0	3.29 (2.22–4.90)	<0.05
Potato pancakes	63	63	16	38	1.71 (1.04–2.82)	0.060
Applesauce	41	68	35	46	1.71 (1.00–2.95)	<0.05
Muffins	50	62	25	52	1.26 (0.74–2.17)	0.407
Butter	9	78	64	56	1.97 (0.56–6.90)	0.219
Orange juice	60	63	17	47	1.44 (0.83–2.52)	0.227
Coffee	58	60	20	55	1.13 (0.64–2.03)	0.675
Creamer	21	67	53	55	1.36 (0.69–2.66)	0.348
Water	67	61	7	43	1.47 (0.73–3.00)	0.347

*RR, relative risk.

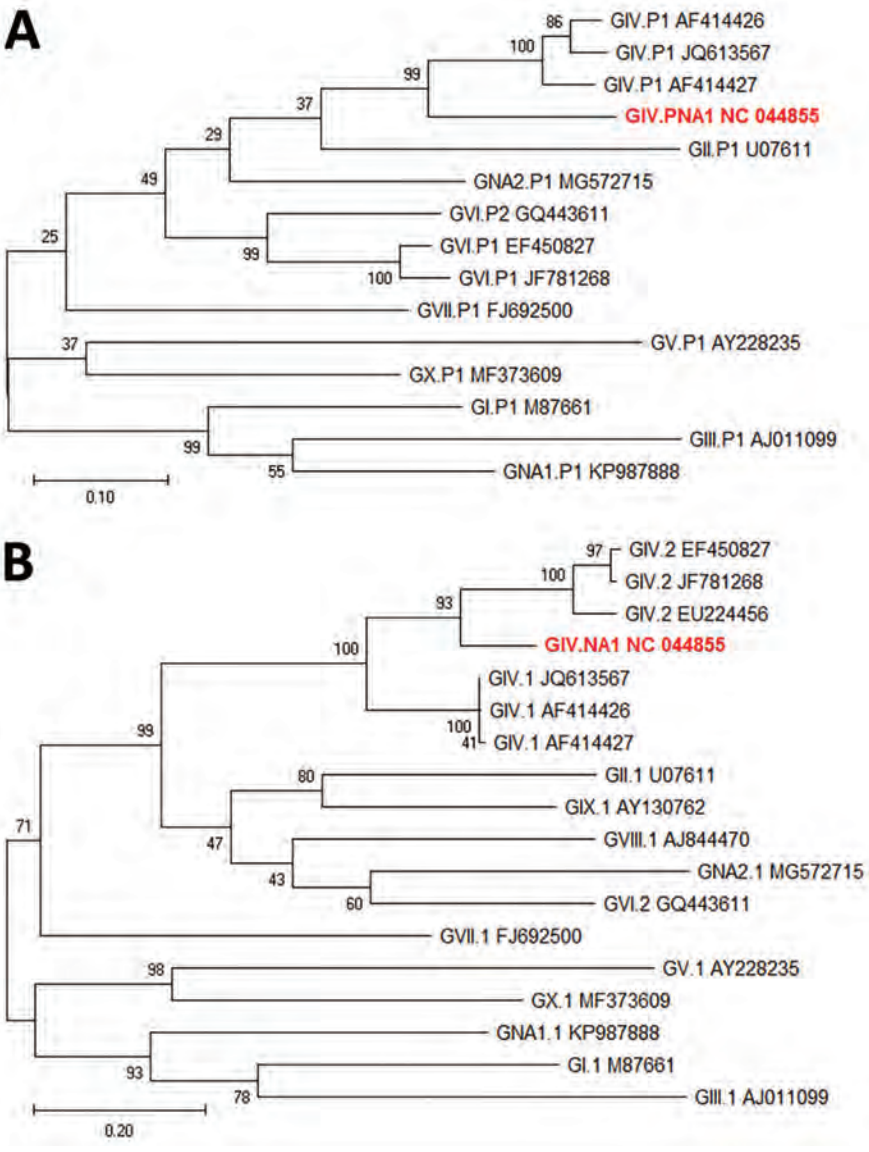

Figure 2. Maximum-likelihood phylogenetic analysis of rare norovirus GIV isolated during foodborne outbreak, Wisconsin, USA (red text), and reference strains. A) Partial polymerase gene (762 nt); B) complete capsid (VP1) gene (554 aa). Bootstrap support for 500 replicates is indicated on branches. For polymerase analysis, evolutionary distances were inferred by the Tamura-Nei model. For VP1 analysis, evolutionary distances were inferred by using the Jones-Taylor-Thornton matrix-based model. Reference strains are represented by type and GenBank accession number. Scale bar in panel A indicates nucleotide substitutions per site, and scale bar in panel B indicates amino acid substitutions per site.

Detection of a norovirus GIV strain associated with a foodborne outbreak shows that despite the absence of reported GIV norovirus outbreaks over the past 15 years in the United States, these viruses continue to circulate in the human population. Because samples from endemic acute gastroenteritis outbreaks are typically tested only for noroviruses GI and GII, including testing of norovirus-negative samples for GIV might improve determining endemic acute gastroenteritis outbreaks of unknown etiology.

Acknowledgments

We are grateful to Rachel Klos for providing epidemiologic data as part of the outbreak investigation, Kshama Aswath and Anna Montmayeur for performing NGS and sequence analysis of full-length genomes, and Preeti Chhabra for quality checking the NGS sequences and uploading the final sequence to GenBank.

About the Author

Ms. Barclay is a microbiologist at the National Calicivirus Laboratory, Division of Viral Diseases, National Center for Immunization and Respiratory Diseases, Centers for Disease Control and Prevention, Atlanta, GA. Her primary research interest is surveillance of noroviruses and other viral gastroenteritis viruses.

References

1. Ahmed SM, Hall AJ, Robinson AE, Verhoef L, Premkumar P, Parashar UD, et al. Global prevalence of norovirus in cases of gastroenteritis: a systematic review and meta-analysis. Lancet Infect Dis. 2014;14:725–30. https://doi.org/10.1016/S1473-3099(14)70767-4
2. Wikswo ME, Kambhampati A, Shioda K, Walsh KA, Bowen A, Hall AJ; Centers for Disease Control and Prevention (CDC). Outbreaks of acute gastroenteritis transmitted by person-to-person contact, environmental contamination, and unknown modes of transmission—United States, 2009–2013. MMWR Surveill Summ. 2015;64:1–16. https://doi.org/10.15585/mmwr.ss6412a1
3. Chhabra P, de Graaf M, Parra GI, Chan MC, Green K, Martella V, et al. Updated classification of norovirus genogroups and genotypes. J Gen Virol. 2019;100:1393–406. https://doi.org/10.1099/jgv.0.001318
4. Cannon JL, Barclay L, Collins NR, Wikswo ME, Castro CJ, Magaña LC, et al. Genetic and epidemiologic trends of norovirus outbreaks in the United States from 2013 to 2016 demonstrated emergence of novel GII.4 recombinant viruses. J Clin Microbiol. 2017;55:2208–21. https://doi.org/10.1128/JCM.00455-17
5. Eden JS, Lim KL, White PA. Complete genome of the human norovirus GIV.1 strain Lake Macquarie virus. J Virol. 2012;86:10251–2. https://doi.org/10.1128/JVI.01604-12
6. Martella V, Campolo M, Lorusso E, Cavicchio P, Camero M, Bellacicco AL, et al. Norovirus in captive lion cub (*Panthera leo*). Emerg Infect Dis. 2007;13:1071–3. https://doi.org/10.3201/eid1307.070268
7. Vinjé J, Koopmans MP. Simultaneous detection and genotyping of "Norwalk-like viruses" by oligonucleotide array in a reverse line blot hybridization format. J Clin Microbiol. 2000;38:2595–601. https://doi.org/10.1128/JCM.38.7.2595-2601.2000
8. Zheng DP, Widdowson MA, Glass RI, Vinjé J. Molecular epidemiology of genogroup II-genotype 4 noroviruses in the United States between 1994 and 2006. J Clin Microbiol. 2010;48:168–77. https://doi.org/10.1128/JCM.01622-09
9. Fioretti JM, Fumian TM, Rocha MS, Dos Santos IA, Carvalho-Costa FA, de Assis MR, et al. Surveillance of noroviruses in Rio de Janeiro, Brazil: occurrence of new GIV genotype in clinical and wastewater samples. Food Environ Virol. 2018;10:1–6. https://doi.org/10.1007/s12560-017-9308-2
10. La Rosa G, Pourshaban M, Iaconelli M, Muscillo M. Detection of genogroup IV noroviruses in environmental and clinical samples and partial sequencing through rapid amplification of cDNA ends. Arch Virol. 2008;153:2077–83. https://doi.org/10.1007/s00705-008-0241-4
11. Muscillo M, Fratini M, Graffeo R, Sanguinetti M, Martella V, Green KY, et al. GIV noroviruses in wastewaters and in stool specimens from hospitalized patients. Food Environ Virol. 2013;5:194–202. https://doi.org/10.1007/s12560-013-9121-5
12. Di Martino B, Di Profio F, Ceci C, Di Felice E, Green KY, Bok K, et al. Seroprevalence of norovirus genogroup IV antibodies among humans, Italy, 2010–2011. Emerg Infect Dis. 2014;20:1828–32. https://doi.org/10.3201/eid2011.131601
13. Kirby AE, Kienast Y, Zhu W, Barton J, Anderson E, Sizemore M, et al. Norovirus seroprevalence among adults in the United States: analysis of NHANES serum specimens from 1999–2000 and 2003–2004. Viruses. 2020;12:179. https://doi.org/10.3390/v12020179
14. van Beek J, de Graaf M, Xia M, Jiang X, Vinjé J, Beersma M, et al. Comparison of norovirus genogroup I, II and IV seroprevalence among children in the Netherlands, 1963, 1983 and 2006. J Gen Virol. 2016;97:2255–64. https://doi.org/10.1099/jgv.0.000533
15. Kitajima M, Rachmadi AT, Iker BC, Haramoto E, Gerba CP. Genetically distinct genogroup IV norovirus strains identified in wastewater. Arch Virol. 2016;161:3521–5. https://doi.org/10.1007/s00705-016-3036-z

Address for correspondence: Leslie Barclay, Centers for Disease Control and Prevention, 1600 Clifton Rd NE, Mailstop H18-7, Atlanta, GA, 30329-4027; email: lbarclay@cdc.gov

Persistence of SARS-CoV-2 N-Antibody Response in Healthcare Workers, London, UK

Madhumita Shrotri, Ross J. Harris, Alison Rodger, Timothy Planche, Frances Sanderson, Tabitha Mahungu, Alastair McGregor, Paul T. Heath, The LondonCOVID Group, Colin S. Brown, Jake Dunning, Susan Hopkins, Shamez Ladhani, Meera Chand

Prospective serosurveillance of severe acute respiratory syndrome coronavirus 2 in 1,069 healthcare workers in London, UK, demonstrated that nucleocapsid antibody titers were stable and sustained for ≤12 weeks in 312 seropositive participants. This finding was consistent across demographic and clinical variables and contrasts with reports of short-term antibody waning.

The durability of antibody responses to severe acute respiratory syndrome coronavirus 2 (SARS-CoV-2), the virus responsible for coronavirus disease (COVID-19), is of scientific and strategic interest for public health systems worldwide. After SARS-CoV-2 infection, antibodies are produced against multiple viral epitopes, including the nucleocapsid (N) protein, which is highly immunogenic and abundantly expressed (*1*). A key concern is the potential for rapid waning of antibodies and seroreversion (loss of detectable antibodies), as seen with other novel betacoronaviruses (*2*), which might represent declining immunity and could compromise serosurveillance.

Frontline healthcare workers are a vital population for serosurveillance because they are at greater risk than the general population. We describe findings from a serosurveillance study conducted in London, UK, by Public Health England (PHE).

Author affiliations: Public Health England, London, UK (M. Shrotri, R.J. Harris, C.S. Brown, J. Dunning, S. Hopkins, S. Ladhani, M. Chand); University College London, London (A. Rodger); Royal Free NHS Foundation Trust, London (A. Rodger, T. Mahungu, C.S. Brown); St. George's University Hospitals NHS Foundation Trust, London (T. Planche); St. George's University of London (T. Planche, P.T. Heath, S. Ladhani); Imperial College Healthcare NHS Trust, London (F. Sanderson); London North West University Healthcare NHS Trust, London (A. McGregor)

DOI: https://doi.org/10.3201/eid2704.204554

The Study

We conducted prospective serosurveillance of healthcare professionals in secondary care settings across London beginning March 30, 2020. Healthcare workers were recruited by hospital research teams and provided written informed consent. Demographic, occupational, and clinical data were collected at baseline, including self-reported previous laboratory-confirmed COVID-19. Participants provided blood samples and completed symptom surveys at baseline and 2-weekly intervals until July 21, 2020, reporting any new illness or COVID-19 diagnosis. Blood samples were centrifuged and frozen locally; PHE then tested serum samples by using the Elecsys Anti-SARS-CoV-2 total antibody assay (Roche, https://www.roche.com), according to the manufacturer's instructions. This test is an electrochemiluminescence immunoassay for antibodies targeting the N protein (IgG, IgM, or IgA) and produces a numeric cutoff index derived from comparison of the sample and calibrator signals (*3*). The surveillance protocol was approved by the PHE Research Ethics Governance Group (R&D REGG Ref: NR0192, March 31, 2020).

We compared differences in seropositivity between groups by using χ^2 tests and multivariable logistic regression to provide adjusted odds ratios (aORs). We estimated biweekly seroconversion and seroreversion rates and binomial 95% CIs. We analyzed trends in individual-level antibody responses beginning 4 weeks after the first positive antibody test, which allowed time for responses to stabilize. We used mixed effects regression to analyze trends in log antibody titers and assessed fixed effects for differences in antibody response through likelihood ratio tests.

Surveillance involved 1,069 participants from 4 hospitals: Charing Cross (n = 192), Northwick Park (n = 217), Royal Free (n = 126), and St. George's (n = 534).

Of these, 850 participants had ≥4 sampling visits and 395 ≥6 sampling visits (over 10–12 weeks of follow-up). Overall, 312 (29%) participants had ≥1 positive antibody test (95% CI 26%–32%); of those, 181 (58%) had ≥8 weeks and 42 (13%) 12 weeks of follow-up after the first positive test (Appendix Table 1, https://wwwnc.cdc.gov/EID/article/27/4/20-4554-App1.pdf). Seropositivity varied between hospitals (p = 0.042), from 25% to 35%. In total, 109 (10.2%) participants self-reported laboratory-confirmed COVID-19, 407 (32%) reported respiratory illness, 5 (0.47%) reported hospitalization, and 794 (61%) did not report illness.

We observed no difference in seropositivity by sex, profession, performance of aerosol-generating procedures, employment in the emergency department, or immunocompromised status (Appendix

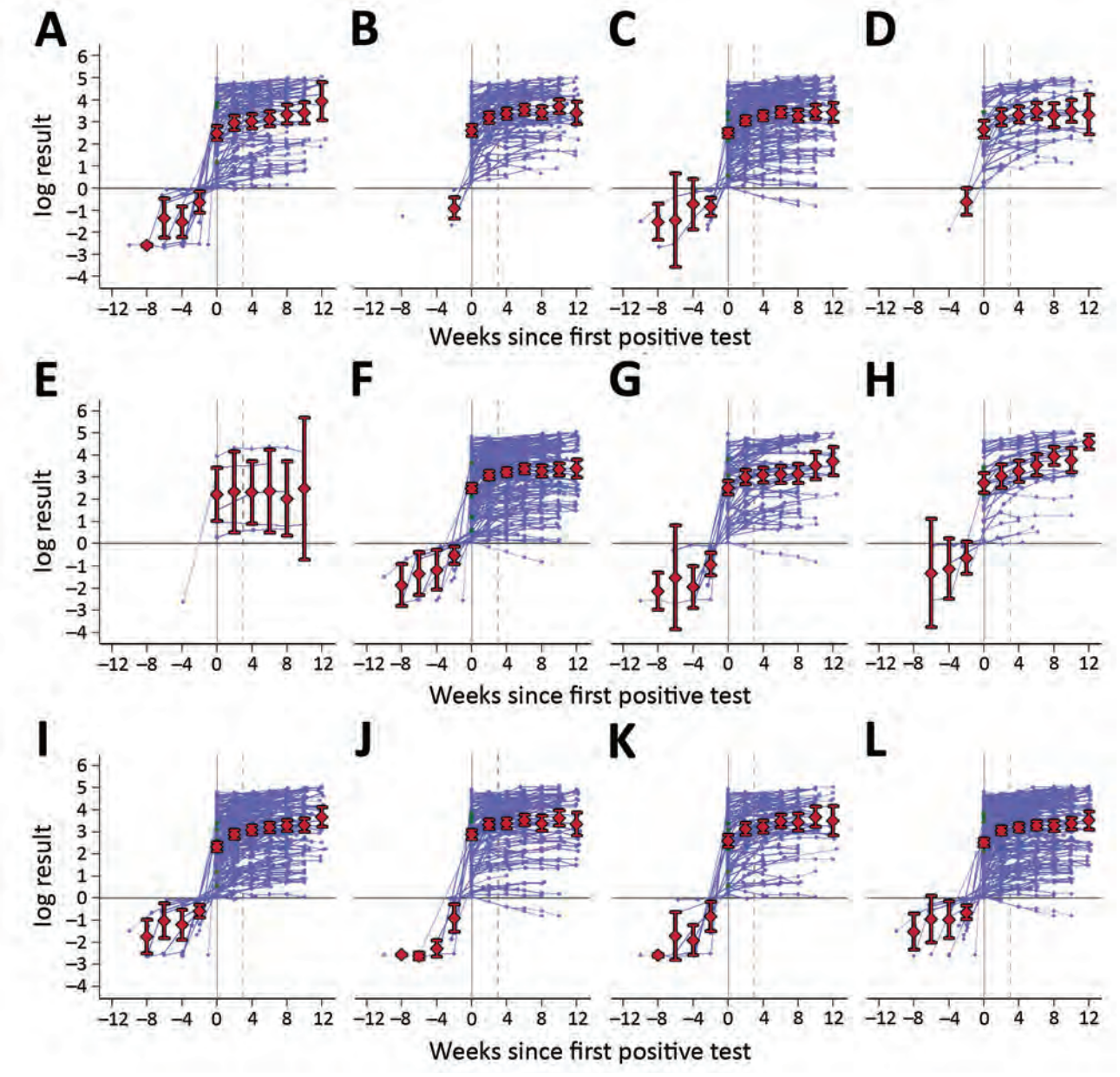

Figure. log antibody titers over time in participants with ≥1 positive test result by subgroups in study of nucleocapsid-antibody response in healthcare workers, London, UK. Subgroups are as follows: A) no self-reported illness (n = 99), B) coronavirus disease (COVID-19) diagnosis (n = 94), C) respiratory illness (n = 175), D) other illness (n = 43), E) immunocompromised (n = 6), F) general hospital employee (n = 204), G) emergency department employee (n = 71), H) intensive care unit employee (n = 38), I) age <40 years (n = 185), J) age ≥40 years (n = 127), K) male sex (n = 95), L) female sex (n = 217). Times are with respect to the date of the first positive test (week 0), and week 4 is indicated by dashed lines; previous negative results are also included. Individual responses are indicated by blue lines; mean titers with 95% CI for the mean are shown in red.

Table 2). Participants 25–34 years of age had higher odds of seropositivity than those 35–44 years of age (aOR 1.57, 95% CI 1.09–2.26), but little difference was seen among older age groups. Those working in intensive care units had lower odds of seropositivity than participants from other hospital departments (aOR 0.58, 95% CI 0.38–0.91).

Most seropositive participants tested positive at baseline (279/312, 89%). Only 33 participants seroconverted during follow-up, corresponding to a biweekly rate of 1.2% (95% CI 0.8%–1.7%). We observed 4 seroreversions, corresponding to a biweekly rate of 0.4% (95% CI 0.1%–0.9%).

log antibody titers remained stable over time in seropositive participants, and little within-individual variability was observed (Figure). The general trend across all subgroups was a slight increase over time, although data are sparse for some groups.

We modeled trends beginning 4 weeks after the first positive antibody test. The mean weekly change was a 3.9% increase (95% CI 3.2%–4.6%). The model enables individual variability and thus estimates a distribution in trends, which ranged from a 0.5% decrease to an 8.5% increase per week, at 1 SD below/above the mean.

Baseline response or subsequent trend did not differ by work setting, clinical symptoms, or laboratory-confirmed COVID-19; minimum likelihood ratio p value was 0.46. Participants ≥40 years of age had 30% higher antibody titers at baseline (p = 0.08) but less increase over time; weekly increase was 2.9% (95% CI 1.8%–4.0%) compared with 4.5% (95% CI 3.6%–5.4%) in those <40 years of age (p = 0.028). We observed similar baseline titers between women and men (p = 0.61) but different trends; women demonstrated a weekly increase of 3.4% (95% CI 2.6%–4.2%) compared with 5.2% (95% CI 3.8%–6.6%) in men (p = 0.035).

Conclusions

In this study, N-antibody seropositivity was 29% among healthcare workers, and a small, sustained rise in antibody titers occurred over 12 weeks. The increase could be explained by the natural boosting of antibodies through repeated SARS-CoV-2 exposure; however, we saw no evidence of sporadic, sharp increases in antibodies in seropositive participants, and we observed little deviation from an overall linear trend. High initial seroprevalence and low subsequent seroconversion rates (Appendix Figures 1, 2) indicate that most exposures occurred before surveillance began. The low seroincidence after April might be attributable to changes in hospital infection control practices and national lockdown.

These findings demonstrate the short-term stability of N-antibody titers in healthcare staff, regardless of demographic or clinical differences. Seropositive participants not reporting any COVID-19 diagnosis or previous illness (even mild or atypical symptoms) demonstrated the same antibody trends as those who reported symptoms or laboratory-confirmed COVID-19, thereby supporting N-antibody testing as a reliable surveillance indicator. Although seroreversion was uncommon, such rates, if sustained, might be concerning in the long term.

Although cross-reactivity against the N protein has been observed and appears more prevalent than cross-reactivity against the spike (S) protein (E.M. Anderson, unpub. data, https://doi.org/10.1101/2020.11.06.20227215; C.F. Houlihan, unpub. data, https://doi.org/10.1101/2020.06.08.20120584), the risk for false positives because of preexisting human coronavirus antibodies seems low on the basis of available data. The Elecsys assay demonstrated >99.5% specificity in 2 independent evaluations using large numbers of prepandemic control samples (*3*,*4*) and demonstrated high positive predictive value at an estimated 10% seroprevalence. Nonetheless, this study is limited by use of a single immunoassay, by self-reported data on COVID-19 diagnosis, and by limited testing early in the pandemic.

Several studies have demonstrated substantial declines in antibody titers over 3–5 months by using anti-S or anti–receptor-binding domain immunoassays (*5*–*9*). Although findings are not consistent across all reports (*6*,*10*), disparities could be explained by shorter follow-up periods that missed later decline. In contrast, the few studies conducting serial testing for ≥3 months by using N-antibody assays, particularly the Elecsys assay, report that titers remained steady (*9*) or increased (*11*; F. Muecksch, unpub. data, https://doi.org/10.1101/2020.08.05.20169128). These studies were limited by small sample sizes, single-site recruitment, and few time points with long sampling intervals. Our study replicates these findings in a large, multicenter cohort with frequent sampling and focuses on healthcare workers with mostly asymptomatic or mild disease, with robust statistical analysis to demonstrate consistent findings across all groups. These data can usefully inform serosurveillance strategies during the second wave.

For unknown reasons, N-antibodies appear highly stable in the short term, despite demonstrating no functional role; whether this stability would persist over longer follow-up periods remains to be answered. Although less useful as correlates of

immunity, N-antibodies could serve a critical role in serosurveillance as S-based vaccines are deployed, helping to distinguish infection-induced seroconversion from vaccine-induced seroconversion.

Acknowledgments

We thank the whole LondonCOVID Group, which includes research colleagues at Northwick Park Hospital, Charing Cross Hospital, St. George's Hospital, the Royal Free Hospital, and Public Health England Colindale; and laboratory colleagues at Public Health England Porton Down and the Sero-Epidemiology Unit for their vital contributions to this work.

This study was internally funded by Public Health England.

About the Author

Dr. Shrotri is a specialty registrar in public health medicine based in London and holds an honorary contract with Public Health England. Her research interests include epidemiology of communicable diseases and vaccinology.

References

1. Liu W, Liu L, Kou G, Zheng Y, Ding Y, Ni W, et al. Evaluation of nucleocapsid and spike protein-based enzyme-linked immunosorbent assays for detecting antibodies against SARS-CoV-2. J Clin Microbiol. 2020;58:1–7. https://doi.org/10.1128/JCM.00461-20
2. Kellam P, Barclay W. The dynamics of humoral immune responses following SARS-CoV-2 infection and the potential for reinfection. J Gen Virol. 2020;101:791–7. https://doi.org/10.1099/jgv.0.001439
3. Public Health England. Evaluation of Roche Elecsys Anti-SARS-CoV-2 serology assay for the detection of anti-SARS-CoV-2 antibodies. London: Public Health England; 2020 [cited 2020 Dec 21]. https://assets.publishing.service.gov.uk/government/uploads/system/uploads/attachment_data/file/891598/Evaluation_of_Roche_Elecsys_anti_SARS_CoV_2_PHE_200610_v8.1_FINAL.pdf
4. Ainsworth M, Andersson M, Auckland K, Baillie JK, Barnes E, Beer S, et al. National SARS-CoV-2 Serology Assay Evaluation Group. Performance characteristics of five immunoassays for SARS-CoV-2: a head-to-head benchmark comparison. Lancet Infect Dis. 2020;20:1390–400. https://doi.org/10.1016/S1473-3099(20)30634-4
5. Ibarrondo FJ, Fulcher JA, Goodman-Meza D, Elliott J, Hofmann C, Hausner MA, et al. Rapid decay of anti–SARS-CoV-2 antibodies in persons with mild Covid-19. N Engl J Med. 2020;383:1085–7. https://doi.org/10.1056/NEJMc2025179
6. Bölke E, Matuschek C, Fischer JC. Loss of Anti-SARS-CoV-2 Antibodies in Mild Covid-19. N Engl J Med. 2020;383:1694–8. https://doi.org/10.1056/NEJMc2027051
7. Wajnberg A, Amanat F, Firpo A, Altman DR, Bailey MJ, Mansour M, et al. Robust neutralizing antibodies to SARS-CoV-2 infection persist for months. Science. 2020;370:1227–30. https://doi.org/10.1126/science.abd7728
8. Perreault J, Tremblay T, Fournier MJ, Drouin M, Beaudoin-Bussières G, Prévost J, et al. Waning of SARS-CoV-2 RBD antibodies in longitudinal convalescent plasma samples within 4 months after symptom onset. Blood. 2020;136:2588–91. https://doi.org/10.1182/blood.2020008367
9. Seow J, Graham C, Merrick B, Acors S, Pickering S, Steel KJA, et al. Longitudinal observation and decline of neutralizing antibody responses in the three months following SARS-CoV-2 infection in humans. Nat Microbiol. 2020;5:1598–607. https://doi.org/10.1038/s41564-020-00813-8
10. Wang Y, Zhang L, Sang L, Ye F, Ruan S, Zhong B, et al. Kinetics of viral load and antibody response in relation to COVID-19 severity. J Clin Invest. 2020;130:5235–44. https://doi.org/10.1172/JCI138759
11. Fill Malfertheiner S, Brandstetter S, Roth S, Harner S, Buntrock-Döpke H, Toncheva AA, et al. Immune response to SARS-CoV-2 in health care workers following a COVID-19 outbreak: A prospective longitudinal study. J Clin Virol. 2020;130:104575. https://doi.org/10.1016/j.jcv.2020.104575

Address for correspondence: Madhumita Shrotri, Public Health England, Wellington House, 133-155 Waterloo Rd, London, SE1 8UG, UK; email: Madhumita.shrotri@phe.gov.uk

Analysis of Asymptomatic and Presymptomatic Transmission in SARS-CoV-2 Outbreak, Germany, 2020

Jennifer K. Bender,[1] Michael Brandl,[1] Michael Höhle, Udo Buchholz, Nadine Zeitlmann

We determined secondary attack rates (SAR) among close contacts of 59 asymptomatic and symptomatic coronavirus disease case-patients by presymptomatic and symptomatic exposure. We observed no transmission from asymptomatic case-patients and highest SAR through presymptomatic exposure. Rapid quarantine of close contacts with or without symptoms is needed to prevent presymptomatic transmission.

During the ongoing coronavirus disease (COVID-19) pandemic, worldwide, >85 million severe acute respiratory syndrome coronavirus 2 (SARS-CoV-2) infections had been reported as of January 7, 2021 (https://covid19.who.int). Although it was clear from the beginning of the pandemic that symptomatic transmission of SARS-CoV-2 occurs, presymptomatic transmission has also been described (*1*–*6*). Furthermore, transmission from asymptomatic cases was deemed possible on the basis of findings that viral load of asymptomatic cases was similar to that of symptomatic cases (*7*). Understanding how transmission occurs from asymptomatic cases and from symptomatic cases in their presymptomatic and symptomatic phase, as well as the frequency of transmission, is essential for public health management. We assessed asymptomatic, presymptomatic, and symptomatic transmission during an outbreak investigation of 59 COVID-19 cases by determining secondary attack rates (SAR) according to the respective exposure periods. In addition, we estimated key parameters such as serial interval and incubation period.

Author affiliations: Robert Koch Institute, Wernigerode, Germany (J.K. Bender); European Centre for Disease Prevention and Control, Stockholm, Sweden (J.K. Bender, M. Brandl); Robert Koch Institute, Berlin, Germany (M. Brandl, M. Höhle, U. Buchholz, N. Zeitlmann); Stockholm University, Stockholm (M. Höhle); Federal Institute for Quality Assurance and Transparency in Healthcare, Berlin (M. Höhle)

DOI: https://doi.org/10.3201/eid2704.204576

The Study

On February 29, 2020, a COVID-19 case was notified to the local public health authority (LPHA) of a rural district in southern Germany without previously observed community transmission. During the infectious period, the case-patient had attended several carnival events in the district. The LPHA immediately initiated contact tracing, identifying all close contacts; they were quarantined and tested irrespective of symptoms. By the end of March 2020, a cluster of 59 cases had been identified through successive contact tracing activities.

We interviewed the case-patients of the cluster by phone regarding symptoms developed during SARS-CoV-2 infection; potential source cases or events; and household contacts (HCs) and close nonhousehold or other contacts (OCs) in their infectious period (Appendix, https://wwwnc.cdc.gov/EID/article/27/4/20-4576-App1.pdf). We obtained an empirical distribution of the serial interval from the average over all possible transmission trees of the cluster. We obtained generation time and incubation period by averaging over the estimates as described by Reich et al. (*8*) (Appendix).

To estimate SAR and relative risks (RRs) we conducted a retrospective cohort study, including all HCs and OCs as recalled by the case-patients that met inclusion criteria (Appendix). We calculated pooled SAR of HCs and OCs for 2 outcomes, laboratory confirmation (SAR_{lab}) and development of respiratory symptoms (SAR_{res}) in the following groups: HCs and OCs of asymptomatic case-patients who never experienced symptoms; HCs and OCs of

[1]These first authors contributed equally to this article.

Table 1. Demographics of coronavirus disease case-patients and their contacts in a district in southern Germany*

Case type	No. (%) asymptomatic	No. (%) symptomatic			Total
		Phase not specified or both†	Presymptomatic phase only	Symptomatic phase only	
Case-patients					
Total	7 (13.2)	46 (86.8)	NA	NA	53 (100)
Female	3 (11.5)	23 (88.5)	NA	NA	26 (100)
Male	4 (14.8)	23 (85.2)	NA	NA	27 (100)
Median age	36 (IQR 6–68)	40 (IQR 29–50)	NA	NA	39.5 (IQR 29–50)‡
Contact persons by type of exposure					
HC	7 (16.7)	35 (83.3)	NA	NA	42 (100)
OC	52 (24.5)	48 (22.6)	81 (38.2)	31 (14.6)	212 (100)

*HC, household contact; IQR, interquartile range; NA, not applicable; OC, nonhousehold or other contact.
†The phase in which the contact occurred was not specified, or contact occurred in both phases.
‡Three of 53 cases were children <15 y of age.

symptomatic case-patients in which the phase with contact could not be specified by the case-patient or with contact in both phases; OCs of symptomatic case-patients with contact only in the presymptomatic phase; and OCs of symptomatic case-patients with contact only in the symptomatic phase.

We were able to contact 53/59 (90%) case-patients. Three case-patients were children <15 years of age (Table 1). Forty-six (87%) were symptomatic, and 7 (13%) were asymptomatic (Appendix Figure 1). The cluster resulted in 144 possible transmission trees, which span over 5 generations (Figure). No secondary transmission resulted from asymptomatic cases. We determined a median serial interval of 3.0 (IQR 1.0–6.0) days and a median incubation period of 4.3 (IQR 2.5–6.5) days (Appendix Table 1).

In total, 42 HCs and 212 OCs were included in the cohort study (Table 1). The overall SAR_{lab} was 13% (4/32) for HCs and 14% (20/148) for OCs. The overall SAR_{res} was 29% (12/42) for HCs and 17% (29/170)

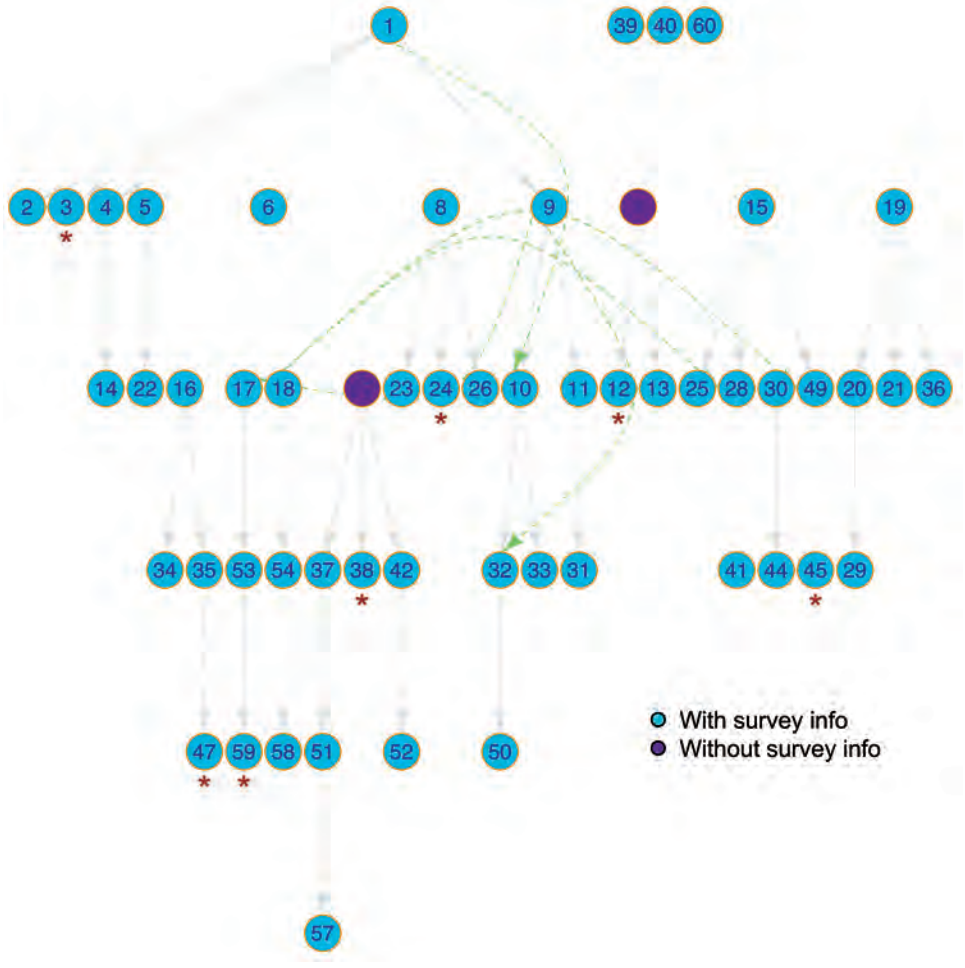

Figure. Transmission tree of the investigated cluster of coronavirus disease that evolved in a district in southern Germany. Cases 39, 40, and 60 participated in the survey but were not included in the analysis because we had no information on source case. Cases 7 and 27 did not participate in the survey and thus, no information on source case was available. Dashed lines represent source case–infectee pairs in which the infectee reported >1 possible source case; solid lines represent source case–infectee pairs in which only 1 source case was mapped to the infectee. Asterisks (*) indicate asymptomatic cases. Implausible transmissions (e.g., ID 6) were omitted.

Table 2. Secondary attack rates among contacts of coronavirus disease case-patients in a district in southern Germany*

Clinical symptoms of source case	No. contacts tested positive or experienced respiratory symptoms	Total no. contacts	SAR, %	RR (95% CI)
Household contacts SAR_{lab}				
Asymptomatic	0	4	0	Reference
Symptomatic, phase not specified or both†	4	28	14.3	0.8 (0.09–∞)
Total	4	32	12.5	
Household contacts SAR_{res}				
Asymptomatic	0	7	0	Reference
Symptomatic, phase not specified or both	12	35	34.3	3.4 (0.56–∞)
Total	12	42	28.6	
Other contacts SAR_{lab}				
Asymptomatic cases	0	22	0	Reference
Symptomatic, phase not specified or both	3	25	12.0	3.4 (0.36–∞)
Symptomatic, presymptomatic phase only	15	72	20.8	6.5 (1.1–∞)
Symptomatic, symptomatic phase only	2	29	6.9	1.8 (0.14–∞)
Total	20	148	13.5	
Other contacts SAR_{res}				
Asymptomatic cases	2	52	3.8	Reference
Symptomatic, phase not specified or both	4	22	18.2	4.7 (0.68–52)
Symptomatic, presymptomatic phase only	22	67	32.8	8.5 (2.1–75)
Symptomatic, symptomatic phase only	1	29	3.5	0.90 (0.02–17)
Total	29	170	17.1	

*RR relative risk; SAR, secondary attack rate; SAR_{lab} secondary attack rate for laboratory-confirmed SARS-CoV-2–positive contact persons; SAR_{res}, secondary attack rate for contact persons who experienced respiratory symptoms after contact.
†The phase in which the contact occurred was not specified, or contact occurred in both phases.

for OCs (Table 2). We did not identify any HC who tested positive or experienced respiratory symptoms after contact with asymptomatic case-patients. Neither SAR_{lab} nor SAR_{res} of HCs of symptomatic case-patients were significantly higher compared with HCs of asymptomatic cases (SAR_{lab} p = 1.0; SAR_{res} p = 0.23). We observed no laboratory-confirmed SARS-CoV-2 transmission from asymptomatic case-patients to any of the 22 OCs (Table 2; Appendix Figure 2). SAR_{lab} was highest for OCs with contact during the case-patients' presymptomatic phases (21%; 15/72) yielding a RR of 6.5 (95% CI 1.1–∞) when compared with contacts of asymptomatic case-patients. Adjusting for case-patients' age, sex, and number of contact persons showed no substantial changes in the magnitude of estimates (data not shown). Presymptomatic transmission accounted for ≥75% of all transmissions to OCs in the cohort (Appendix).

Conclusions

In this cluster of COVID-19 cases, little to no transmission occurred from asymptomatic case-patients. Presymptomatic transmission was more frequent than symptomatic transmission. The serial interval was short; very short intervals occurred.

The fact that we did not detect any laboratory-confirmed SARS-CoV-2 transmission from asymptomatic case-patients is in line with multiple studies (*9*–*11*). However, Oran et al. have speculated that asymptomatic cases contribute to the rapid progression of the pandemic (*12*). Some studies may be prone to misclassify presymptomatic cases as asymptomatic, leading to heterogeneous reporting of SAR of asymptomatic cases, because of different case definitions or differential duration of follow-up. In our study we used a very sensitive case definition for symptomatic cases that did not require specific symptoms (e.g. fever) to be present. Also, timing of our study would have enabled detection of late onset of symptoms, which gives us confidence in our classification of exposure groups.

The 75% of SARS-CoV-2 transmissions in our cohort from case-patients in their presymptomatic phase exceeds reported transmission rates from other investigations (*1*,*13*,*14*). Possible reasons are the prior evidence that infectiousness peaks around the date of symptom onset, declining thereafter (*15*), and that case-patients probably reduced social contacts themselves once they experienced symptoms or when ordered to self-isolate. A large proportion of cases with presymptomatic transmission in our cluster is further supported by the median serial interval of 3 days.

Of note are the consequences for public health management: first, the need for early detection of COVID-19 cases and for initiation of contact tracing as soon as possible to quarantine close contacts, particularly because short serial intervals may lead to further transmission chains. Second, suspect case-patients or persons with any respiratory illness should immediately self-isolate and inform their contacts met in the presymptomatic and symptomatic phases.

A limitation of our study is that evidence was obtained from a single outbreak and might not be

applicable to other settings. We used only information as recalled by the case-patients, which is imperfect and may introduce errors or bias. Because we used development of respiratory symptoms as a proxy for possible SARS-CoV-2 infections among contacts, and because incidence of respiratory illnesses was still high in this winter timeframe, SAR_{res} may be overestimated. However, this possible source of misclassification should be nondifferential between groups. We excluded many HCs because of uncertainties about the potential simultaneous introduction of SARS-CoV-2 in the household, which may have led to an underestimation of SAR among HCs. In the transmission tree, we had to omit various source case–infectee pairs because case-patients' recalled symptom onset differed substantially from surveillance data and was not plausible (Appendix). Finally, although community transmission of SARS-CoV-2 was deemed unlikely in the affected district at the time, we cannot rule out that some cases acquired infections from other sources.

In conclusion, our study suggests that asymptomatic cases are unlikely to contribute substantially to the spread of SARS-CoV-2. COVID-19 cases should be detected and managed early to quarantine close contacts immediately and prevent presymptomatic transmissions.

Acknowledgments

As J.K.B. is a fellow of the European Public Health Microbiology Training at the European Centre for Disease Prevention and Control (ECDC) Fellowship Programme (and supported financially by this program) and M.B. is a fellow of the European Programme for Intervention Epidemiology Training at the ECDC and the Postgraduate Training for Applied Epidemiology at the Robert Koch Institute, we first acknowledge these programs. We also thank the local public health authority of the district for its continuous efforts fighting the COVID-19 pandemic as well as for providing us with information about the cluster and corresponding data for subsequent analysis. We thank the team of researchers assisting with the case interviews: Johannes Zeiher, Nora-Katharina Küpke, Sandra Niendorf, Sangeeta Banerji, and Susann Dupke. Furthermore, we especially thank all COVID-19 case-patients of this cluster for their participation in the study.

About the Author

Dr. Bender is a fellow of the European Public Health Microbiology Training Programme of the European Centre for Disease Prevention and Control. She is a microbiologist affiliated with the Nosocomial Pathogens and Antibiotic Resistances Unit, Department of Infectious Diseases of the Robert Koch Institute. Her research interest focuses on the emergence of multidrug-resistant nosocomial pathogens.

References

1. Wei WE, Li Z, Chiew CJ, Yong SE, Toh MP, Lee VJ. Presymptomatic transmission of SARS-CoV-2—Singapore, January 23–March 16, 2020. MMWR Morb Mortal Wkly Rep. 2020;69:411–5. https://doi.org/10.15585/mmwr.mm6914e1
2. Böhmer MM, Buchholz U, Corman VM, Hoch M, Katz K, Marosevic DV, et al. Investigation of a COVID-19 outbreak in Germany resulting from a single travel-associated primary case: a case series. Lancet Infect Dis. 2020;20:920–8. https://doi.org/10.1016/S1473-3099(20)30314-5
3. Tong ZD, Tang A, Li KF, Li P, Wang HL, Yi JP, et al. Potential presymptomatic transmission of SARS-CoV-2, Zhejiang Province, China, 2020. Emerg Infect Dis. 2020;26:1052–4. https://doi.org/10.3201/eid2605.200198
4. Huang L, Zhang X, Zhang X, Wei Z, Zhang L, Xu J, et al. Rapid asymptomatic transmission of COVID-19 during the incubation period demonstrating strong infectivity in a cluster of youngsters aged 16–23 years outside Wuhan and characteristics of young patients with COVID-19: A prospective contact-tracing study. J Infect. 2020;80:e1–13. https://doi.org/10.1016/j.jinf.2020.03.006
5. Yu P, Zhu J, Zhang Z, Han Y. A familial cluster of infection associated with the 2019 novel coronavirus indicating possible person-to-person transmission during the incubation period. J Infect Dis. 2020;221:1757–61. https://doi.org/10.1093/infdis/jiaa077
6. Arons MM, Hatfield KM, Reddy SC, Kimball A, James A, Jacobs JR, et al.; Public Health–Seattle and King County and CDC COVID-19 Investigation Team. Presymptomatic SARS-CoV-2 infections and transmission in a skilled nursing facility. N Engl J Med. 2020;382:2081–90. https://doi.org/10.1056/NEJMoa2008457
7. Zou L, Ruan F, Huang M, Liang L, Huang H, Hong Z, et al. SARS-CoV-2 viral load in upper respiratory specimens of infected patients. N Engl J Med. 2020;382:1177–9. https://doi.org/10.1056/NEJMc2001737
8. Reich NG, Lessler J, Cummings DA, Brookmeyer R. Estimating incubation period distributions with coarse data. Stat Med. 2009;28:2769–84. https://doi.org/10.1002/sim.3659
9. Park SY, Kim Y-M, Yi S, Lee S, Na B-J, Kim CB, et al. Coronavirus disease outbreak in call center, South Korea. Emerg Infect Dis. 2020;26:1666–70. https://doi.org/10.3201/eid2608.201274
10. Cheng HY, Jian SW, Liu DP, Ng TC, Huang WT, Lin HH; Taiwan COVID-19 Outbreak Investigation Team. Contact tracing assessment of COVID-19 transmission dynamics in Taiwan and risk at different exposure periods before and after symptom onset. JAMA Intern Med. 2020;180:1156–63. https://doi.org/10.1001/jamainternmed.2020.2020
11. Luo L, Liu D, Liao X, Wu X, Jing Q, Zheng J, et al. Contact settings and risk for transmission in 3,410 close contacts of patients with COVID-19 in Guangzhou, China. Ann Intern Med. 2020;173:879–87. https://doi.org/10.7326/M20-2671
12. Oran DP, Topol EJ. Prevalence of asymptomatic SARS-CoV-2 infection: a narrative review. Ann Intern Med. 2020;173:362–7. https://doi.org/10.7326/M20-3012

13. Ferretti L, Wymant C, Kendall M, Zhao L, Nurtay A, Abeler-Dörner L, et al. Quantifying SARS-CoV-2 transmission suggests epidemic control with digital contact tracing. Science. 2020;368:eabb6936. https://doi.org/10.1126/science.abb6936
14. Ganyani T, Kremer C, Chen D, Torneri A, Faes C, Wallinga J, et al. Estimating the generation interval for coronavirus disease (COVID-19) based on symptom onset data, March 2020. Euro Surveill. 2020;25. https://doi.org/10.2807/1560-7917.ES.2020.25.17.2000257
15. He X, Lau EHY, Wu P, Deng X, Wang J, Hao X, et al. Temporal dynamics in viral shedding and transmissibility of COVID-19. Nat Med. 2020;26:672–5. https://doi.org/10.1038/s41591-020-0869-5

Address for correspondence: Jennifer K. Bender, Department of Infectious Diseases, Robert Koch Institute, Burgstrasse 37, 38855 Wernigerode, Germany; email: benderj@rki.de

Characteristics and Risk Factors of Hospitalized and Nonhospitalized COVID-19 Patients, Atlanta, Georgia, USA, March–April 2020

Kristen Pettrone, Eleanor Burnett, Ruth Link-Gelles, Sarah C. Haight, Caroline Schrodt, Lucinda England, Danica J. Gomes, Mays Shamout, Kevin O'Laughlin, Anne Kimball, Erin F. Blau, Chandresh N. Ladva, Christine M. Szablewski, Melissa Tobin-D'Angelo, Nadine Oosmanally, Cherie Drenzek, Sean D. Browning, Beau B. Bruce, Juliana da Silva, Jeremy A.W. Gold, Brendan R. Jackson, Sapna Bamrah Morris, Pavithra Natarajan, Robyn Neblett Fanfair, Priti R. Patel, Jessica Rogers-Brown, John Rossow, Karen K. Wong, David J. Murphy, James M. Blum, Julie Hollberg, Benjamin Lefkove, Frank W. Brown, Tom Shimabukuro, Claire M. Midgley, Jacqueline E. Tate, Marie E. Killerby

We compared the characteristics of hospitalized and nonhospitalized patients who had coronavirus disease in Atlanta, Georgia, USA. We found that risk for hospitalization increased with a patient's age and number of concurrent conditions. We also found a potential association between hospitalization and high hemoglobin A1c levels in persons with diabetes.

Information about care-seeking behavior, symptom duration, and risk factors for progression to severe illness in nonhospitalized patients with coronavirus disease (COVID-19) aids in resource planning, disease identification, risk stratification, and clinical management of nonhospitalized patients (*1*–*6*). We built on a previous analysis comparing hospitalized and nonhospitalized COVID-19 patients, which found that hospitalized patients were more likely to be ≥65 years of age, men, Black, diabetic, or obese (*7*). We describe symptom patterns, duration of illness, and care-seeking behavior among nonhospitalized patients and explore the relationships between hospitalization and the number, control, and interaction of concurrent medical conditions and age. We defined control as how well a disease is managed in the patient, as measured by hemoglobin A1c levels in diabetics, number of classes of hypertension medication being taken by patients with hypertension, and BMI among patients with obesity.

Author affiliations: Centers for Disease Control and Prevention, Atlanta, Georgia, USA (K. Pettrone, E. Burnett, R. Link-Gelles, S.C. Haight, C. Schrodt, L. England, D.J. Gomes, M. Shamout, K. O'Laughlin, A. Kimball, E.F. Blau, C.N. Ladva, C.M. Szablewski, S.D. Browning, B.B. Bruce, J. da Silva, J.A.W. Gold, B.R. Jackson, S.B. Morris, P. Natarajan, R.N. Fanfair, P.R. Patel, J. Rogers-Brown, J. Rossow, K.K. Wong, T. Shimabukuro, C.M. Midgely, J.E. Tate, M.E. Killerby); Commissioned Corps of the U.S. Public Health Service, Rockville, Maryland, USA (R. Link-Gelles, R.N. Fanfair, J. Rossow, J.E. Tate); Georgia Department of Public Health, Atlanta (C.M. Szablewski, M. Tobin-D'Angelo, N. Oosmanally, C. Drenzek); Emory University School of Medicine, Atlanta (D.J. Murphy, J.M. Blum, J. Hollberg, F.W. Brown); Emory Decatur Hospital, Decatur, Georgia, USA (B. Lefkove, F.W. Brown)

DOI: https://doi.org/10.3201/eid2704.204709

The Study

We enrolled hospitalized and nonhospitalized patients ≥18 years of age with laboratory-confirmed COVID-19 (defined as a positive real-time reverse transcription PCR result for severe acute respiratory syndrome coronavirus 2) treated at 6 acute care hospitals and outpatient clinics affiliated with a single academic hospital system in the Atlanta, Georgia, USA, metropolitan area during March 1–April 7, 2020, as previously described (*7*). In this investigation, we compared characteristics and symptoms of hospitalized and nonhospitalized persons using χ^2, Fisher exact, or *t*-test as appropriate.

We conducted univariable and multivariable logistic regression analyses to explore the associations between age group and number of underlying conditions on risk for hospitalization. We conducted separate analyses to model the associations and interactions of diabetes, hypertension, and obesity

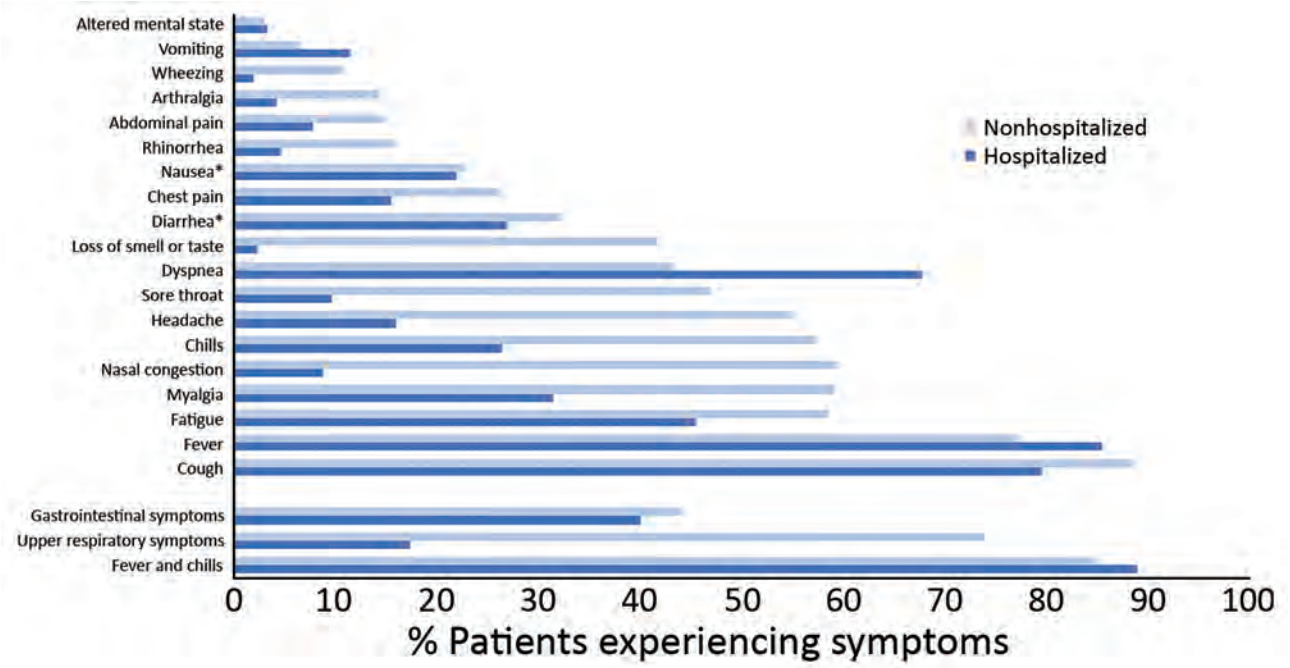

Figure. Symptoms of coronavirus disease among hospitalized and nonhospitalized patients, Atlanta, Georgia, USA, 2020. Gastrointestinal symptoms include vomiting, nausea, diarrhea, and abdominal pain. Upper respiratory symptoms include sore throat, rhinorrhea, and nasal congestion. *p≥0.01.

with hospitalization for COVID-19. We then used univariable and multivariable logistic regression to investigate whether the severity or control of concurrent conditions was associated with increased risk for hospitalization. We modeled the association between body mass index (BMI) and hospitalization. Further, we investigated whether use of multiple classes of hypertension medication was associated with hospitalization among patients with hypertension and the association of elevated levels (≥7%) of hemoglobin A1c (HbA1c) and hospitalization among patients with diabetes. This level was chosen because a value <7% is considered an indicator of adequate blood glucose control in patients with diabetes (*8*). Multivariable models were adjusted for characteristics previously associated with hospitalization in these populations (*7*) (Appendix, https://wwwnc.cdc.gov/EID/article/27/4/20-4709-App1.pdf).

We enrolled 311 nonhospitalized and 220 hospitalized patients in this study (Appendix Tables 1–3). We reviewed patient medical records and found that upper respiratory system symptoms including rhinorrhea, nasal congestion, and pharyngitis were more common among nonhospitalized patients than hospitalized patients (74% vs. 17%; p = 0.01). In contrast, hospitalized patients had dyspnea more frequently than did nonhospitalized patients (68% vs. 43%; p = 0.01) (Figure 1). Of 147 nonhospitalized patients with available information on symptom duration, 67 (46%) reported symptoms lasting ≥21 days.

Of 311 nonhospitalized patients, 135 (43%) had their first contact with the healthcare system for their COVID-19 illness on a telephone triage line, 23 (7%) at the emergency department, and 141 (45%) at an ambulatory care clinic (Table 1). Of nonhospitalized patients, 85% sought in-person care (i.e., ambulatory care, emergency department, or urgent care) a single time for their COVID-19 illness. A subset of 188 non-

Table 1. Treatment settings of 311 nonhospitalized patients with coronavirus disease, Atlanta, Georgia, USA, 2020*

Treatment setting	Value
First interaction	
Ambulatory care	141 (45)
Telephone triage line	135 (43)
Emergency department	23 (7)
Other†	12 (4)
All interactions	
Ambulatory care	269 (87)
Telephone triage line	210 (68)
Emergency department	45 (15)
Other†	22 (7)
Median no. visits (IQR)	1 (1–1)
Ambulatory care	1 (1–1)
Telephone triage line	1 (1–2)
Emergency department	1 (1–1)

*Values are no. (%) patients except as indicated. IQR, interquartile range.
†Includes retail health, telehealth, and urgent care.

hospitalized patients had information in their medical records about all their COVID-19 healthcare visits. These 188 patients had 400 documented healthcare visits: 188 (47%) ambulatory care, 167 (42%) telehealth, 39 (10%) in-person emergency department, and 6 (2%) urgent care visits. Within this subset, 57% of visits among those patients with symptoms lasting ≥21 days were telehealth appointments; 56% of visits among those with symptoms <21 days were in-person primary care visits.

Odds of hospitalization increased with advancing age (50–59 years of age, adjusted odds ratio [aOR] 2.1, 95% CI 0.7–6.6; 60–69 years, aOR 4.1, 95% CI 1.3–13.3; ≥70 years, aOR 9.2, 95% CI 2.7–31.0). The aOR of hospitalization demonstrated a dose-dependent relationship with number of concurrent conditions (1 condition, aOR 1.8, 95% CI 0.8–3.7; 2 conditions, aOR 2.3, 95% CI 1.1–4.8; ≥3 conditions, aOR 4.2, 95% CI 1.9–9.1) (Table 2).

Among patients with hypertension, the odds of hospitalization demonstrated a possible dose-dependent increase among patients taking multiple classes of hypertension medications; however, precision of estimates was limited by small sample size (Table 2). Among patients with diabetes, those with a recent HbA1c score ≥7% had an increased risk for hospitalization (aOR 4.1, 95% CI 0.9–19.1); however, precision of estimates was limited by small sample size. Among obese patients (BMI ≥30), BMI was not associated with increasing odds of hospitalization (Table 2). In the multivariable analyses, we did not detect significant additive or multiplicative interaction between diabetes and obesity, hypertension and obesity, or hypertension and diabetes (Appendix Table 4).

Conclusions

Symptoms lasting ≥21 days were common among nonhospitalized patients in this investigation; however, <20% of these patients had >1 in-person healthcare visit for COVID-19 during acute illness. These extended symptom durations, in conjunction with limited care-seeking behavior, suggest that many mildly ill COVID-19 patients can self-manage

Table 2. Risk factors for hospitalization among patients with coronavirus disease, Atlanta, Georgia, USA, 2020*

Characteristic	Hospitalized, no. (%)	Nonhospitalized, no. (%)	Crude OR (85% CI)	Adjusted OR (95% CI)
Age, y				
Total	220 (100)	311 (100)		
18–29	5 (2)	52 (17)	Referent	Referent†
30–39	24 (11)	79 (25)	3.0 (1.1–8.2)	1.4 (0.4–4.6)
40–49	36 (16)	54 (17)	6.3 (2.3–16.8)	3.0 (0.9–9.5)
50–59	41 (19)	63 (20)	6.4 (2.4–16.9)	2.1 (0.7–6.6)
60–69	56 (26)	41 (13)	13.9 (5.2–37.2)	4.1 (1.3–13.3)
≥70	58 (26)	22 (7)	25.7 (9.2–71.4)	9.2 (2.7–31.0)
No. concurrent conditions				
Total	220 (100)	311 (100)		
0	21 (10)	122 (39)	Referent	Referent‡
1	48 (22)	80 (26)	3.5 (1.9–6.3)	1.8 (0.8–3.7)
2	71 (32)	68 (22)	6.0 (3.4–10.6)	2.3 (1.1–4.8)
≥3	80 (36)	41 (13)	12.2 (6.6–22.4)	4.2 (1.9–9.1)
Hemoglobin A1c§				
Total	81 (100)	30 (100)		
<7%	17 (21)	17 (57)	Referent	Referent¶
≥7%	38 (47)	7 (23)	3.3 (1.2–9.4)	4.1 (0.9–19.1)
Missing data	26 (32)	6 (20)		
Obesity				
Total	220 (100)	311 (100)		
<30	86 (39)	123 (40)	Referent	Referent#
30–34	65 (30)	52 (17)	1.8 (1.2–3.0)	2.6 (1.3–5.0)
35–40	34 (16)	26 (8)	1.9 (1.0–3.5)	2.2 (1.0–4.8)
>40	25 (11)	26 (8)	1.6 (0.8–2.9)	1.8 (0. 7–4.5)
Missing data	10 (5)	84 (27)		
No. classes of hypertension medications**				
Total	142 (100)	101 (100)		
0	20 (14)	13 (13)	Referent	Referent#
1	38 (27)	42 (42)	0.7 (0.3–1.6)	0.7 (0.3–2.0)
2	48 (34)	33 (33)	1.0 (0.5–2.4)	1.6 (0.6–4.5)
≥3	36 (25)	13 (13)	1.9 (0.7–5.0)	1.8 (0.5–6.0)

*OR, odds ratio.
†Adjusted for number of underlying conditions, race, sex, insurance, and smoking (including current or former smoking).
‡Adjusted for age, race, sex, insurance, and smoking (including current or former smoking).
§Among patients with diabetes.
¶Adjusted for age, race, sex, healthcare personnel status, and hypertension.
#Adjusted for age, race, sex, healthcare personnel status, and diabetes.
**Among patients with hypertension.

their symptoms. Because telemedicine was the second most common healthcare delivery method in our investigation, we hypothesize that it might have provided ongoing patient support and decreased the need for in-person healthcare visits (*9*). These findings can assist healthcare providers with anticipatory guidance for patients and caregivers and can inform decisions about allocation of resources for healthcare delivery.

We found that age and number of underlying conditions were associated with a dose-dependent increase in likelihood of hospitalization. Elderly COVID-19 patients frequently have multiple conditions that increase risk for hospitalization and serious infection (*10*). However, we did not find a significant additive or multiplicative interaction between the 3 most common underlying conditions among study participants: hypertension, diabetes, and obesity.

We hypothesized that degree of control of underlying conditions would affect risk for hospitalization. We found that the aORs for hospitalization were higher among patients with diabetes who had elevated mean levels of HbA1c and among patients with hypertension taking an increasing number of hypertension medications. Although not statistically significant, these findings may suggest an association between the management of concurrent conditions and COVID-19 disease severity. Despite obesity's association with increased risk for severe illness and death from COVID-19 (*11*,*12*), we did not find an increasing risk for hospitalization with increasing BMI among persons with obesity.

A limitation of our study is that, because of small sample sizes, our analyses might have lacked power to detect a significant association between degree of control of underlying conditions and hospitalization. In addition, our sample comprised patients at a single hospital system during a limited timeframe, and thus our results might not be generalizable to other populations. Because this hospital system prioritized certain persons (e.g., older patients, patients with underlying conditions, and healthcare personnel) for outpatient SARS-COV-2 testing, these persons might be overrepresented among the nonhospitalized patients in our sample. We were also not able to assess symptom resolution among all patients during the timeframe of this investigation and therefore might not have accounted for all follow-up healthcare visits for COVID-19.

In conclusion, although many nonhospitalized patients in this study reported symptoms lasting ≥21 days, most cases of COVID-19 among nonhospitalized patients were managed with a single ambulatory care visit and telehealth follow-up appointments. Patients of increasing age, with a greater number of underlying conditions, and with poor management of those conditions might be at higher risk for hospitalization and severe disease from COVID-19.

About the Author

Dr. Pettrone is an Epidemic Intelligence Service Officer in the Division of Vital Statistics, National Center for Health Statistics, Centers for Disease Control and Prevention. Her research interests include infectious disease and public health.

References

1. Jain V, Yuan JM. Predictive symptoms and comorbidities for severe COVID-19 and intensive care unit admission: a systematic review and meta-analysis. Int J Public Health. 2020;65:533–46. https://doi.org/10.1007/s00038-020-01390-7
2. Fang X, Li S, Yu H, Wang P, Zhang Y, Chen Z, et al. Epidemiological, comorbidity factors with severity and prognosis of COVID-19: a systematic review and meta-analysis. Aging (Albany NY). 2020;12:12493–503. https://doi.org/10.18632/aging.103579
3. Pascarella G, Strumia A, Piliego C, Bruno F, Del Buono R, Costa F, et al. COVID-19 diagnosis and management: a comprehensive review. J Intern Med. 2020;288:192–206. https://doi.org/10.1111/joim.13091
4. Tenforde MW, Kim SS, Lindsell CJ, Billig Rose E, Shapiro NI, Files DC, et al.; IVY Network Investigators; CDC COVID-19 Response Team; IVY Network Investigators. Symptom duration and risk factors for delayed return to usual health among outpatients with COVID-19 in a multistate health care systems network—United States, March–June 2020. MMWR Morb Mortal Wkly Rep. 2020;69:993–8. https://doi.org/10.15585/mmwr.mm6930e1
5. Czeisler M, Marynak K, Clarke K, Salah Z, Shakya I, Thierry J, et al. Delay or avoidance of medical care because of COVID-19–related concerns—United States, June 2020. MMWR Morb Mortal Wkly Rep. 2020;69:1250–7.
6. Desai R, Singh S, Parekh T, Sachdeva S, Sachdeva R, Kumar G. COVID-19 and diabetes mellitus: a need for prudence in elderly patients from a pooled analysis. Diabetes Metab Syndr. 2020;14:683–5. https://doi.org/10.1016/j.dsx.2020.05.021
7. Killerby ME, Link-Gelles R, Haight SC, Schrodt CA, England L, Gomes DJ, et al.; CDC COVID-19 Response Clinical Team. Characteristics associated with hospitalization among patients with COVID-19—metropolitan Atlanta, Georgia, March–April 2020. MMWR Morb Mortal Wkly Rep. 2020;69:790–4. https://doi.org/10.15585/mmwr.mm6925e1
8. Sherwani SI, Khan HA, Ekhzaimy A, Masood A, Sakharkar MK. Significance of HbA1c test in diagnosis and prognosis of diabetic patients. Biomark Insights. 2016;11:95–104. https://doi.org/10.4137/BMI.S38440
9. Contreras CM, Metzger GA, Beane JD, Dedhia PH, Ejaz A, Pawlik TM. Telemedicine: patient-provider clinical engagement during the COVID-19 pandemic and beyond.

J Gastrointest Surg. 2020;24:1692–7. https://doi.org/10.1007/s11605-020-04623-5
10. Piccirillo JF, Vlahiotis A, Barrett LB, Flood KL, Spitznagel EL, Steyerberg EW. The changing prevalence of comorbidity across the age spectrum. Crit Rev Oncol Hematol. 2008;67:124–32. https://doi.org/10.1016/j.critrevonc.2008.01.013
11. Palaiodimos L, Kokkinidis DG, Li W, Karamanis D, Ognibene J, Arora S, Southern WN, Mantzoros CS. Severe obesity, increasing age and male sex are independently associated with worse in-hospital outcomes, and higher in-hospital mortality, in a cohort of patients with COVID-19 in the Bronx, New York. Metabolism. 2020;108:154262
12. Yang J, Tian C, Chen Y, Zhu C, Chi H, Li J, et al. Obesity aggravates COVID-19: an updated systematic review and meta-analysis. J Med Virol. 2020;jmv.26677. https://doi.org/10.1002/jmv.26677

Address for correspondence: Kristen Pettrone, Centers for Disease Control and Prevention, 1600 Clifton Rd NE, Mailstop V25-1, Atlanta, GA 30329-4027, USA; email: pho3@cdc.gov

Improving Treatment and Outcomes for Melioidosis in Children, Northern Cambodia, 2009–2018

Arjun Chandna,[1] Moritz Bonhoeffer,[1] Thyl Miliya, Keang Suy, Sena Sao, Paul Turner

We report trends in manifestations, treatment, and outcomes of 355 children with culture-confirmed melioidosis over 10 years at a pediatric hospital in northern Cambodia. Bacteremia and presentation with pneumonia were risk factors for death. A total of 39 children recovered after being given only oral antimicrobial drug treatment.

Melioidosis, an infection caused by *Burkholderia pseudomallei*, remains an underrecognized disease, especially in children, in many locations to which it is endemic (*1*,*2*). Diverse clinical manifestations and intrinsic resistance to many antimicrobial drugs used for empirical treatment of sepsis contribute to high mortality rates (*2*–*4*).

Conventionally, antimicrobial drug therapy for melioidosis comprises 2 phases: intravenous treatment for ≥10 days, followed by a prolonged, oral, eradication phase for a minimum of 12 weeks (*5*,*6*). Localized cutaneous disease might be treatable with oral agents alone, but adherence with eradication therapy is often difficult to achieve (*4*,*5*,*7*–*9*). We report trends in management and outcomes of melioidosis over 10 years at a nongovernmental pediatric hospital in northern Cambodia.

The Study

This study was approved by the hospital institutional review board (AHC IRB 979-14; 1044-15) and the Oxford Tropical Medicine Research Ethics Committee (OxTREC 550-14). Data on all culture-confirmed case-patients who had *B. pseudomallei* infection during January 1, 2009–December 31, 2018, were collected retrospectively (2009–2013) and prospectively as part of an invasive bacterial infection surveillance study. Retrospective case-patients (the first 173 case-patients) have previously been described and are included to illustrate trends over the decade (*2*).

Retrospective case-patients were identified by searching laboratory logbooks and databases, which were cross-checked against the hospital electronic patient information system. Data were extracted onto a standardized case report form, which was also adapted for contemporaneous capture of prospective case-patients. Repeat searches of the databases were conducted at the end of the study (Appendix Figure 1, https://wwwnc.cdc.gov/EID/article/27/4/20-1683-App1.pdf). The study site, microbiology specimen processing, and case definitions have been described elsewhere (*2*,*8*). We provide the statistical methods used (Appendix). Severe undernutrition was defined as a weight-for-age z-score <–3.

Approximately half (57.5%, 255/355) the children with melioidosis were male, and most (82.8%, 294/355) were brought for treatment during the wet season (Appendix Figure 2). Median age was 5.7 years (interquartile range 3.1–9.5 years). Concurrent conditions were infrequent (14/355, 3.9%). Parotitis was the most common manifestation (27.3%, 97/355) (Table 1).

Hospital guidelines (introduced in 2012) recommend obtaining blood, throat swab and urine specimens for culture for all patients who have suspected melioidosis. However, blood was collected for culture for only 157 (44.2%) of 355 case-patients, a throat swab specimen for 31 (8.7%) of 355, and a urine sample for 16 (4.5%) of 355. Use of microbiological testing improved over time (Appendix Table 5, Figure 3). Of those who had blood cultured, 46.5% (73/157) were

Author affiliations: Angkor Hospital for Children, Siem Reap, Cambodia (A. Chandna, M. Bonhoeffer, T. Miliya, K. Suy, S. Sao, P. Turner); University of Oxford, Oxford, UK (A. Chandna, P. Turner)

DOI: https://doi.org/10.3201/eid2704.201683

[1]These authors contributed equally to this article.

Table 1. Characteristics for 355 children who had culture-confirmed melioidosis, northern Cambodia, 2009–2018*

Characteristic	Value
Median age, y (IQR)	5.7 (3.1–9.5)
Sex	
M	255 (57.5)
F	100 (42.5)
Concurrent condition, n = 355	14 (3.9)
Thalassemia	4
Systemic lupus erythematosus	2
Suspected underlying immunodeficiency	2
Asthma	1
Epilepsy	1
Acute lymphoblastic leukemia	1
Congenital heart disease	1
Chronic kidney disease	1
Pure red cell aplasia	1
Clinical manifestations, n = 355	
Parotitis	97 (27.3)
Skin or soft tissue infection	96 (27.0)
Pneumonia	69 (19.4)
Lymphadenitis	58 (16.3)
Meningitis	1 (0.3)
Multifocal infection	12 (3.4)
Other†	8 (2.3)
Unknown‡	15 (4.5)
Management strategy, n = 355	
Admitted case-patients	212 (59.7)
Case-patients admitted at first presentation	145 (40.8)
Empiric treatment with effective intensive-phase therapy	51
Treatment with effective intensive-phase therapy within 48 h	38
Treatment with effective intensive-phase therapy after 48 h	40
No effective intensive-phase therapy received§	11
Treatment information not available	5
Admitted to intensive care unit, n = 212	52 (24.5)
Surviving patients completing 12 weeks of eradication therapy, n = 306	102 (33.3)
No. patients treated successfully with only oral antimicrobial drugs	39

*Values are no. (%) except as indicated. IQR, interquartile range.
†Clinical manifestations for patients classified as Other included mandibular osteomyelitis (2), diarrheal disease (2), vaginitis (2), mastoiditis (1), and septic arthritis (1).
‡Clinical manifestations were unknown for 15 patients: 10 were bacteremic and 5 had *Burkholderia pseudomallei* isolated from pus swabs.
§A total of 9 children died within 24 h (before culture results were available), and 2 were switched directly to oral treatment.

bacteremic. The proportion of bacteremic children remained consistent over the study period (Appendix Figure 4). For 12 children who were evaluated during 2017–2018, the only positive microbiological specimen was a throat swab specimen.

Treatment data were available for 344 (96.9%) of 355 children. Of these, 140 were admitted when care was initially sought; 89 (63.6%) received an intravenous antimicrobial drug (ceftazidime, meropenem, or imipenem) that had activity against *B. pseudomallei* within 48 hours (Table 1). Eleven children did not receive an effective intravenous drug; 9 died within 24 hours (before culture results were available), and 2 were switched directly to an oral treatment. The time to effective antimicrobial drug therapy did not change over the study period.

The in-hospital case-fatality rate (CFR) was 11.5% (41/355). Median time to death was 2.5 days (interquartile range 1–8 days). Two deaths occurred after discharge for children who had completed 14 days of intensive therapy.

Pneumonia, female sex, and age <5 years were risk factors for death. Among children who had a blood culture, bacteremia was strongly associated with death, as was severe undernutrition in children <10 years of age. Adjusted analyses, including only children <10 years of age who had a blood culture (n = 128), confirmed that bacteremia (odds ratio 57.09, 95% CI 10.80–1,063.54; p<0.001) and pneumonia (odds ratio 3.95, 95% CI 1.22–14.43; p = 0.027) were independently associated with death (Table 2). The annual CFR remained stable, although a nonsignificant decrease was observed for bacteremic children (Appendix Figure 5). This decrease occurred in the context of major reductions in the prevalence of undernutrition (Figure 1).

Of 312 surviving case-patients, postdischarge information was available for 306 (98.1%), of whom 102 (33.3%) completed ≥12 weeks of eradication therapy. The proportion of children completing eradication therapy increased substantially during the study period (Figure 2), and trimethoprim/sulfamethoxazole

Table 2. Risk factors for death of children who had culture-confirmed *Burkholderia pseudomallei* infection, northern Cambodia, 2009–2018*

Characteristic	Survivors	Nonsurvivors	Unadjusted OR (95% CI); p value	Adjusted OR (95% CI); p value
Whole population, n = 355	n = 312	n = 43		
Female sex	126/312 (40.4)	25/43 (58.1)	2.05 (1.07–3.91); 0.03	1.58 (0.71–3.53); 0.26
Age <5 y	126/312 (40.4)	25/43 (58.1)	2.05 (1.07–3.91); 0.03	0.69 (0.28–1.60); 0.39
Pneumonia†	34/312, (10.9)	35/43 (81.4)	35.77 (15.34–83.41); <0.001	38.99 (16.46–104.01); <0.001
Bacteremia‡	31/114 (27.2)	42/43 (97.7)	112.45 (14.83–852.47); <0.001	70.24 (13.73–1,289.14); <0.001
Severe undernutrition§	32/225 (14.2)	12/37 (32.4)	2.90 (1.32–6.34); 0.008	1.36 (0.51–3.52); 0.53
Children ≤10 y of age who had blood culture, n = 128	n = 91	n = 37		
Female sex	39/91 (42.9)	20/37 (54.1)	1.57 (0.73–3.38); 0.25	1.24 (0.44–3.46); 0.679
Age <5 y	54/91 (59.3)	23/37 (62.2)	1.13 (0.51–2.47); 0.77	0.70 (0.21–2.18); 0.542
Pneumonia†	31/91 (34.1)	30/37 (81.1)	8.29 (3.27–21.02); <0.001	3.97 (1.22–14.43); 0.027
Bacteremia	29/91 (31.9)	36/37 (97.3)	76.97 (10.05–589.16); <0.001	57.09 (10.80–1,063.54); <0.001
Severe undernutrition	17/91 (18.7)	12/37 (32.4)	2.09 (0.88–4.97); 0.09	2.08 (0.62–7.72); 0.247

*Values are no. positive/no. tested (%) except as indicated. OR, odds ratio.
†Pneumonia was defined according to the working diagnosis of the treating clinical team, taking into consideration clinical, laboratory, and radiologic information. A total of 89.9% (62/69) of children who were given a diagnosis of pneumonia had a chest radiograph.
‡Risk for bacteremia assessed in children who had a blood culture collected (n = 157).
§Risk for severe undernutrition (weight-for-age z score <–3) assessed in children <10 y of age (n = 262; a weight measurement was available for 95.6% [262/274] of children <10 y of age). Multivariate analyses adjusted for sex, age <5 years, and pneumonia. Subgroup analysis (n = 128). Includes only children <10 y of age who had a blood culture collected.

was increasingly likely to be selected as the eradication agent of choice (Appendix Figure 6). Thirty-nine children recovered after receiving only oral antimicrobial drug treatment, including 17 who had lymphadenitis, 14 who had with localized cutaneous disease, and 4 who had parotitis. No culture-confirmed relapses have been reported.

Conclusions

Our study illustrates the challenges associated with providing care for children who have melioidosis at a pediatric hospital in northern Cambodia. Unlike many hospitals in the region, there was access to level 3 care in a pediatric intensive care unit and an on-site diagnostic microbiology laboratory supported by an active clinical microbiology liaison service (*10*). Nevertheless, 2/10 children admitted because they had melioidosis did not survive to leave the hospital, and only one third of those discharged alive were confirmed as having completed eradication therapy.

Few easily identifiable features exist to alert clinicians to a possible diagnosis of melioidosis. Given the necessity of early and appropriate antimicrobial drug therapy and the intrinsic resistance of *B. pseudomallei* to many first-line antimicrobial drugs, clinicians have the difficult task of maintaining a high index of suspicion while balancing the need for effective antimicrobial stewardship.

Our study might have underestimated the burden associated with melioidosis due to suboptimal

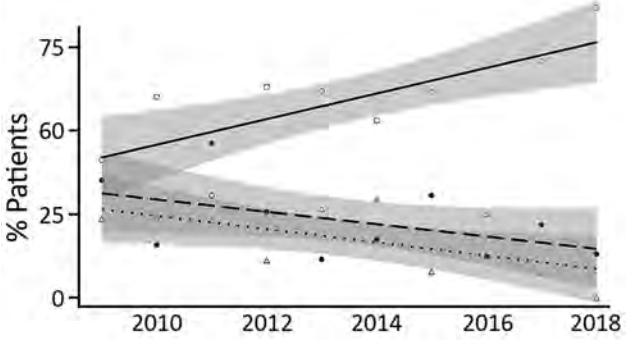

Figure 1. Prevalence of undernutrition for 262 children <10 years of age who had culture-confirmed melioidosis, northern Cambodia, 2009–2018. Linear trend lines indicate nonunderweight children (solid line, open circles: R = 0.76; p = 0.011), children with moderate undernutrition (weight for age z-score [WAZ] <–2) (dashed line, solid circles: R = −0.49; p = 0.150), and children with severe nutrition (WAZ <–3) (dotted line, open triangles: R = −0.59; p = 0.074). Shaded areas indicate 95% CIs for linear trend lines.

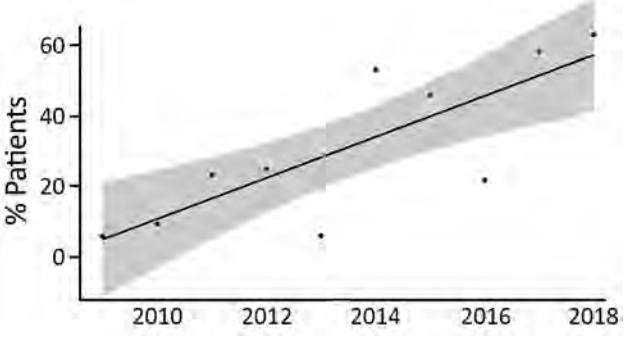

Figure 2. Proportion of 306 surviving children who had culture-confirmed melioidosis and completed ≥12 weeks of eradication therapy, northern Cambodia, 2009–2018. Shaded area indicates 95% CIs for the linear trend line (R = 0.8; p = 0.006).

diagnostic testing, particularly at the beginning of the study period. The hospital's clinical microbiology liaison service has expanded over time and now includes 3 weekly infection rounds, invasive bacterial and hospital-acquired infection surveillance, and antimicrobial drug and diagnostic stewardship training as part of the hospital induction program. During 2015, the antimicrobial treatment guidelines became accessible by a mobile application (*10*). In the final 2 years of the study period, 12 children received a confirmed diagnosis only because the clinical team sent a throat swab specimen specifically for *B. pseudomallei* culture.

We observed a slight decrease in the CFR for bacteremic children. Although not significant, this trend cannot be explained by changes in case-mix severity (proportion of bacteremic children) or time to effective antimicrobial therapy. However, it did occur in the context of substantial gains in the nutritional status of the population. Malnutrition might potentiate severity of melioidosis in children and is a well-recognized risk factor in other pediatric infections (*4*,*11*).

The fact that only one third of children surviving to hospital discharge went on to successfully complete 12 weeks of eradication therapy illustrates both the challenge associated with ambulatory care in resource-constrained settings and the gains that can be achieved over time. During 2009, only 5% of case-patients completed 12 weeks of eradication therapy, compared with 52% during 2018. Furthermore, by the end of the study period, amoxicillin/clavulanic acid had been replaced by trimethoprim/sulfamethoxazole acid as the eradication drug of choice, consistent with current recommendations (*5*,*6*).

This study lends support to the idea that certain *B. pseudomallei* infections might be treatable with oral agents alone (*5*). The 39 cases described herein add to ≥26 previously reported case-patients for whom successful outcomes have been achieved in the absence of parenteral therapy (*4*,*8*,*9*).

In summary, melioidosis remains a major disease in children in Cambodia. Proactive microbiological specimen collection is critical to confirming the diagnosis. Although adherence with prolonged eradication therapy is challenging, over time, improvements can be realized. Adherence will become increasingly essential if outpatient oral treatment regimens are to be considered in resource-limited settings, as they are in some high-income, disease-endemic locations (*4*).

The Cambodia Oxford Medical Research Unit is part of the Wellcome Trust Thailand Africa and Asia Programme and receives core support (grant 106698Z/14/Z) from the UK Wellcome Trust.

About the Author

Dr. Chandna is a Wellcome Trust Doctoral Training Fellow at the Cambodia Oxford Medical Research Unit, Angkor Hospital for Children, Siem Reap, Cambodia. His primary research interest is the syndromic management of febrile illness and sepsis in resource-limited settings.

References

1. Limmathurotsakul D, Golding N, Dance DA, Messina JP, Pigott DM, Moyes CL, et al. Predicted global distribution of *Burkholderia pseudomallei* and burden of melioidosis. Nat Microbiol. 2016;1:15008. https://doi.org/10.1038/nmicrobiol.2015.8
2. Turner P, Kloprogge S, Miliya T, Soeng S, Tan P, Sar P, et al. A retrospective analysis of melioidosis in Cambodian children, 2009–2013. BMC Infect Dis. 2016;16:688. https://doi.org/10.1186/s12879-016-2034-9
3. Stoesser N, Pocock J, Moore CE, Soeng S, Chhat HP, Sar P, et al. Pediatric suppurative parotitis in Cambodia between 2007 and 2011. Pediatr Infect Dis J. 2012;31:865–8. https://doi.org/10.1097/INF.0b013e318258873b
4. McLeod C, Morris PS, Bauert PA, Kilburn CJ, Ward LM, Baird RW, et al. Clinical presentation and medical management of melioidosis in children: a 24-year prospective study in the Northern Territory of Australia and review of the literature. Clin Infect Dis. 2015;60:21–6. https://doi.org/10.1093/cid/ciu733
5. Dance D. Treatment and prophylaxis of melioidosis. Int J Antimicrob Agents. 2014;43:310–8. https://doi.org/10.1016/j.ijantimicag.2014.01.005
6. Lipsitz R, Garges S, Aurigemma R, Baccam P, Blaney DD, Cheng AC, et al. Workshop on treatment of and postexposure prophylaxis for *Burkholderia pseudomallei* and *B. mallei* Infection, 2010. Emerg Infect Dis. 2012;18:e2. https://doi.org/10.3201/eid1812.120638
7. Pitman MC, Luck T, Marshall CS, Anstey NM, Ward L, Currie BJ. Intravenous therapy duration and outcomes in melioidosis: a new treatment paradigm. PLoS Negl Trop Dis. 2015;9:e0003586. https://doi.org/10.1371/journal.pntd.0003586
8. Pagnarith Y, Kumar V, Thaipadungpanit J, Wuthiekanun V, Amornchai P, Sin L, et al. Emergence of pediatric melioidosis in Siem Reap, Cambodia. Am J Trop Med Hyg. 2010;82:1106–12. https://doi.org/10.4269/ajtmh.2010.10-0030
9. Lumbiganon P, Chotechuangnirun N, Kosalaraksa P, Teeratakulpisarn J. Localized melioidosis in children in Thailand: treatment and long-term outcome. J Trop Pediatr. 2011;57:185–91. https://doi.org/10.1093/tropej/fmq078
10. Fox-Lewis S, Pol S, Miliya T, Day NPJ, Turner P, Turner C. Utilization of a clinical microbiology service at a Cambodian paediatric hospital and its impact on appropriate antimicrobial prescribing. J Antimicrob Chemother. 2018;73:509–16. https://doi.org/10.1093/jac/dkx414
11. Walson JL, Berkley JA. The impact of malnutrition on childhood infections. Curr Opin Infect Dis. 2018;31:231–6. https://doi.org/10.1097/QCO.0000000000000448

Address for correspondence: Arjun Chandna, Cambodia Oxford Medical Research Unit, Angkor Hospital for Children, Tep Vong Rd and Oum Chhay St, Svay Dangkum, PO Box 50, Siem Reap, Cambodia; email: arjun@tropmedres.ac

Eastern Equine Encephalitis Virus in Mexican Wolf Pups at Zoo, Michigan, USA

Kimberly A. Thompson, Eileen Henderson, Scott D. Fitzgerald, Edward D. Walker, Matti Kiupel

During the 2019 Eastern equine encephalitis virus (EEEV) outbreak in Michigan, two 2-month old Mexican wolf pups experienced neurologic signs, lymphohistiocytic neutrophilic meningoencephalitis with neuronal necrosis and neuronophagia, and acute death. We identified EEEV by reverse transcription real-time PCR and in situ hybridization. Vector mosquitoes were trapped at the zoo.

In North America, Eastern equine encephalitis virus (EEEV; family *Togaviridae*, genus *Alphavirus*) occurs as an enzootic cycle between mosquitoes (primarily *Culiseta melanura*) and passerine birds within freshwater hardwood swamps (*1*–*3*). When favorable ecologic conditions occur, EEEV prevalence increases via amplification until spillover transmission occurs into humans and equids, and less commonly other species (*1*). Other mosquito species, such as *Coquilettidia perturbans* and *Aedes vexans*, act as bridge vectors by preferentially feeding on mammals; they may be responsible for the epizootic cases among mammalian hosts (*2*). Outbreaks of EEEV in the northern United States occur intermittently between years but during a predictable time of the year, late summer through early fall (*3*).

Among the naturally occurring encephalitic alphaviruses, EEEV has the highest mortality rate in humans (50%–75%) and equids (70%–90%) (*4*). Additional reports exist of clinical disease in a wide variety of mammalian and avian species, including swine, cattle, white-tailed deer, alpacas, seals, domestic canids, pheasants, emus, penguins, and cassowary birds (*5*–*10*). Clinical signs of EEEV range from asymptomatic infection to severe and often fatal neurologic disease; signs may include pyrexia, anorexia, recumbency, diarrhea, ataxia, seizures, nystagmus, and head pressing. Previous reports of EEEV in domestic canids have been rare and have mainly been in young puppies <6 months of age (*9*,*10*). Serologic evidence suggests that exposure to EEEV in free-ranging gray wolves (*Canis lupus*) is low (0% of pups and 3% of adults) in Minnesota (*11*), where EEEV is uncommon.

Author affiliations: Binder Park Zoo, Battle Creek, Michigan, USA (K.A. Thompson); Michigan State University Veterinary Diagnostic Laboratory, Lansing, Michigan, USA (E. Henderson, S.D. Fitzgerald, M. Kiupel); Michigan State University Department of Entomology, Lansing (E.D. Walker)

DOI: https://doi.org/10.3201/eid2704.202400

The Study

In 2019, the southwest region of Michigan experienced high incidence of EEEV exposure in humans and nonhuman animals, including wild deer and domestic horses (*7*,*8*,*12*). Clinical human cases were reported during June 18–September 20, 2019 (*12*). Binder Park Zoo (BPZ) (Battle Creek, Michigan, USA) is on a 400-acre property, half maintained as natural wetlands with a large population of native waterfowl and passerine avian species and half as a developed zoo. The Mexican wolf exhibit is located ≈30 m from the natural wetlands. In the midst of the outbreak, EEEV was diagnosed in two 2-month old Mexican wolf (*Canis lupus baileyi*) pups at BPZ. We assumed that transmission of EEEV to the wolf pups was from a mosquito bite that occurred at their exhibit location.

Pup 1 was a 2-month-old male pup that was brought for care on September 1, 2019, after a brief entanglement with the exhibit's electric fence. The pup was noted to be increasingly ataxic, which progressed quickly to an obtunded recumbent state. On examination, the pup had decreased responsiveness to handling, increased respiratory effort and crackles, anisocoria, and pyrexia (temperature of 40°C; in adult domestic canids, pyrexia is ≥40°C) (*9*). Initial supportive care was unsuccessful; the pup died shortly thereafter. Necropsy revealed a focal area of hemorrhage along the junction of the basilar and posterior cerebral arteries. We submitted formalin-fixed tissues to Michigan State University Veterinary Diagnostic Lab-

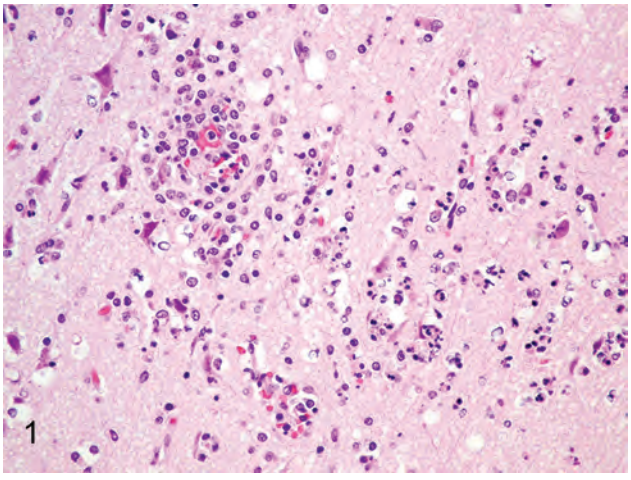

Figure 1. Brain specimen from Mexican wolf pup infected with eastern equine encephalitis virus at Binder Park Zoo, Michigan, USA. Hematoxylin and eosin stain shows severe, acute necrotizing and neutrophilic encephalitis with neuronal necrosis with pyknotic nuclei associated with perineuronal satellitosis and neutrophilic neuronophagia.

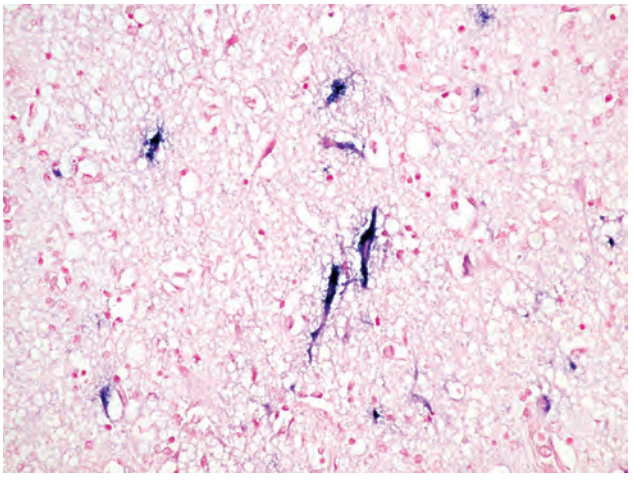

Figure 2. Brain specimen from Mexican wolf pup infected with eastern equine encephalitis virus (EEEV) at Binder Park Zoo, Michigan, USA. Blue stain shows EEEV nucleic acid in the perikaryon and dendrites of necrotic and intact neurons. Nuclear fast red counterstain shows nitro blue tetrazolium/5-Bromo-4-chloro-3-indolyl phosphate (NBT/BCIP) chromogen.

oratory (MSU VDL; Lansing, Michigan, USA) for histopathology. Throughout the cerebrum we observed expansion of the Virchow-Robin space by large numbers of lymphocytes and histocytes with extension of the inflammatory cells into the surrounding neuropil. Gray and white matter had randomly scattered foci of rarefaction and necrosis with low numbers of associated infiltrating neutrophils (Figure 1). Inflammatory cells often surrounded and occasionally phagocytize necrotic neurons in the process of neuronophagia. The meninges were expanded by edema and moderate numbers of lymphocytes and histiocytes. The cerebellum and brain stem had similar lesions. The cerebrum was positive for EEEV on SYBR green–based real-time reverse transcription PCR (rRT-PCR); EEEV nucleic acid was detected within neurons via in situ hybridization (Figure 2) (*13*,*14*). We noted a mild eosinophilic pneumonia.

Pup 2 was found deceased in the underground den the following day. This male pup had a history of healing traumatic rib fractures and delayed growth rate; he was in treatment for pneumonia and a suspected hepatic abscess and had been improving. Necropsy revealed healed rib fractures and consolidated left cranial lung lobes; the liver was firm, with a pronounced lobular pattern and prominent white interlobular septae. We sent formalin-fixed tissues for histopathology at MSU VDL. The lesions within the brain were similar to those described for pup 1. In addition, there was a moderate lymphoplasmacytic bronchointerstitial pneumonia and severe chronic fibrosing periportal hepatitis, moderate bile duct hyperplasia, moderate arteriole proliferation, and intermittent absence of periportal veins (portal vein hypoplasia), most consistent with a congenital vascular anomaly. Culture of the lung was positive for rare *Mycoplasma canis* and moderate *Escherichia coli* (negative for virulence factor genes *cnf1* and *cnf2*). The brain was positive by rRT-PCR for EEEV; in situ hybridization detected EEEV nucleic acid (*13*,*14*).

The surviving female pup (pup 3) and the dam and sire showed no clinical signs. Banked serum samples frozen at −30°C were sent to National Veterinary Services Laboratories (Ames, Iowa, USA) for plaque reduction neutralization test to evaluate timelines of exposure for pups 1, 2, and 3. Samples from pups 2 and 3 were negative, whereas serum from pup 1 tested positive for neutralizing antibodies at 1:10 dilution on the day of death (Table 1). Frozen cerebrum from the fourth littermate (pup 4) that had died a month earlier at 4 weeks of age tested negative by rRT-PCR for EEEV (*13*,*14*). Necropsy findings from

Table 1. Plaque reduction neutralization test results for eastern equine encephalitis virus in banked serum samples from 3 Mexican wolf pups at Binder Park Zoo, Michigan, USA*

Animal ID	Date	Result
Pup 1	2019 Aug 14	Negative
	2019 Sep 1	Positive
Pup 2	2019 Aug 12	Negative
	2019 Aug 22	Negative
Pup 3	2019 Aug 14	Negative
	2019 Sep 20	Negative

*Test result interpreted at 1:10. Pups were tested before (all pups), during (pup 2), and after (pup 3 only) an outbreak of eastern equine encephalitis.

Table 2. Results from 3 rounds of mosquito trapping at Binder Park Zoo, Michigan, USA*

Mosquito species	Trap date		
	2019 Sep 25	2019 Sep 27	2019 Oct 9
Aedes cinereus	1	2	0
Aedes japonicus	8	3	0
Aedes trivittatus	107	58	6
Aedes vexans	72	22	1
Anopheles punctipennis	3	1	0
Anopheles quadrimaculatus	11	9	1
Anopheles walkeri	1	0	0
Coquillettidia perturbans	8	7	0
Culex erraticus	0	7	1
Culex pipiens	4	2	0
Culiseta melanura	4	2	0
Culex territans	0	1	0
Orthopodomyia signifera	1	0	0
Psorophora ferox	21	5	0
Uranotaenia sapphirina	6	1	4
Total no. mosquitoes	247	118	13
Total species	13	13	5
Total no. traps	10	13	12
Overnight temperature, °C	16–22	19–21	11–18

*After detection of eastern equine encephalitis virus, mosquitoes were trapped with CDC miniature light traps baited with dry ice. Adulticide spray was applied between the second and third round. Data are numbers of mosquitoes except where otherwise noted.

pup 4 included thoracic rib fractures and moderate, acute, diffuse, fibrinosuppurative bacterial alveolitis and pleuritis.

We conducted mosquito surveillance throughout the zoo's property using dry ice–baited, CDC miniature light traps (John W. Hock Company, https://www.johnwhock.com) on 3 different dates (September 25 and 27, October 9). Mosquitoes were identified to species, and pools of ≤25 individuals were tested for EEEV RNA by rRT-PCR (*15*). Both the enzootic vector, *Culiseta melanura* (n = 6/378), and possible bridge vector mosquito species such as *Coquillettidia perturbans* (n = 15/378) were present (Table 2). After risk assessment, with local and state agencies, mosquito management was implemented on the property, including targeted barrier and state conducted adulticide spray over the area. All pools were negative for EEEV RNA.

Conclusions

Zoonotic disease detection, especially for reportable diseases, may have implications to a zoo beyond animal health and may require a substantial amount of time and resources. After diagnosis of EEEV cases, the zoo provided educational material on EEEV and complimentary DEET mosquito spray for staff and zoo patrons. In addition, all overnight camping safaris, evening events, and school field trip groups were canceled. Zoos can act as sentinels for disease detection in an area because of the wide variety of resident species and thorough necropsies. Since the diagnosis of EEEV, BPZ's preventative medicine measures to decrease the risk for nondomestic canids to contract EEEV include the use of a monthly topical pyrethrin-based product on all Mexican wolves starting at 8 weeks of age.

Because of the natural distribution of the Mexican wolf population in Mexico and the southwestern United States, EEEV probably has little effect on the free-ranging population. However, the translocation of animals to zoos outside of their natural range may expose them to novel diseases such as EEEV. The cases in our study provide evidence for clinicians to include EEEV as a differential for acute neurologic signs or death in young canids, both domestic and nondomestic, especially during outbreaks of EEEV.

Acknowledgments

We thank the Binder Park Zoo animal care staff for their dedication in caring for these animals. We thank the staff of the Calhoun County Public Health Department, Michigan Department of Agriculture and Rural Development, and Michigan Department of Health and Human Services for their assistance during this disease occurrence.

This work was supported in part by the Centers for Disease Control project Midwest Center of Excellence in Vector-Borne Disease (contract no. U50 723K866).

About the Author

Dr. Thompson is the staff veterinarian at Binder Park Zoo in Battle Creek, Michigan, and an adjunct professor with Michigan State University College of Veterinary Medicine. Her main research interests are infectious diseases and neonatal medicine.

References

1. Skaff NK, Armstrong PM, Andreadis TG, Cheruvelil KS. Wetland characteristics linked to broad-scale patterns in *Culiseta melanura* abundance and eastern equine encephalitis virus infection. Parasit Vectors. 2017;10:501. https://doi.org/10.1186/s13071-017-2482-0
2. Armstrong PM, Andreadis TG. Eastern equine encephalitis virus in mosquitoes and their role as bridge vectors. Emerg Infect Dis. 2010;16:1869–74. https://doi.org/10.3201/eid1612.100640
3. Molaei G, Armstrong PM, Graham AC, Kramer LD, Andreadis TG. Insights into the recent emergence and expansion of eastern equine encephalitis virus in a new focus in the Northern New England USA. Parasit Vectors. 2015;8:516. https://doi.org/10.1186/s13071-015-1145-2
4. Steele KE, Twenhafel NA. Review paper: pathology of animal models of alphavirus encephalitis. Vet Pathol. 2010;47:790–805. https://doi.org/10.1177/0300985810372508
5. McBride MP, Sims MA, Cooper RW, Nyaoke AC, Cullion C, Kiupel M, et al. Eastern equine encephalitis in a captive harbor seal (*Phoca vitulina*). J Zoo Wildl Med. 2008;39:631–7. https://doi.org/10.1638/2008-0021.1
6. Guthrie A, Citino S, Rooker L, Zelazo-Kessler A, Lim A, Myers C, et al. Eastern equine encephalomyelitis virus infection in six captive southern cassowaries (*Casuarius casuarius*). J Am Vet Med Assoc. 2016;249:319–24. https://doi.org/10.2460/javma.249.3.319
7. Schmitt SM, Cooley TM, Fitzgerald SD, Bolin SR, Lim A, Schaefer SM, et al. An outbreak of Eastern equine encephalitis virus in free-ranging white-tailed deer in Michigan. J Wildl Dis. 2007;43:635–44. https://doi.org/10.7589/0090-3558-43.4.635
8. Tate CM, Howerth EW, Stallknecht DE, Allison AB, Fischer JR, Mead DG. Eastern equine encephalitis in a free-ranging white-tailed deer (*Odocoileus virginianus*). J Wildl Dis. 2005;41:241–5. https://doi.org/10.7589/0090-3558-41.1.241
9. Farrar MD, Miller DL, Baldwin CA, Stiver SL, Hall CL. Eastern equine encephalitis in dogs. J Vet Diagn Invest. 2005;17:614–7. https://doi.org/10.1177/104063870501700619
10. Andrews C, Gerdin J, Patterson J, Buckles EL, Fitzgerald SD. Eastern equine encephalitis in puppies in Michigan and New York states. J Vet Diagn Invest. 2018;30:633–6. https://doi.org/10.1177/1040638718774616
11. Carstensen M, Giudice JH, Hildebrand EC, Dubey JP, Erb J, Stark D, et al. A serosurvey of diseases of free-ranging gray wolves (*Canis lupus*) in Minnesota, USA. J Wildl Dis. 2017;53:459–71. https://doi.org/10.7589/2016-06-140
12. Forshey TM, Byrum BA, Machesky KD, Stephen Roney C, Gomez TM, Mitchell JR, et al.; Centers for Disease Control and Prevention (CDC). Notes from the field: multistate outbreak of Salmonella Altona and Johannesburg infections linked to chicks and ducklings from a mail-order hatchery—United States, February–October 2011. MMWR Morb Mortal Wkly Rep. 2012;61:195.
13. Kiupel M, Fitzgerald SD, Pennick KE, Cooley TM, O'Brien DJ, Bolin SR, et al. Distribution of eastern equine encephalomyelitis viral protein and nucleic acid within central nervous tissue lesions in white-tailed deer (Odocoileus virginianus). Vet Pathol. 2013;50:1058–62. https://doi.org/10.1177/0300985813488956
14. Nolen-Walston R, Bedenice D, Rodriguez C, Rushton S, Bright A, Fecteau ME, et al. Eastern equine encephalitis in 9 South American camelids. J Vet Intern Med. 2007;21:846–52. https://doi.org/10.1111/j.1939-1676.2007.tb03030.x
15. Hull R, Nattanmai S, Kramer LD, Bernard KA, Tavakoli NP. A duplex real-time reverse transcriptase polymerase chain reaction assay for the detection of St. Louis encephalitis and eastern equine encephalitis viruses. Diagn Microbiol Infect Dis. 2008;62:272–9. https://doi.org/10.1016/j.diagmicrobio.2008.07.004

Address for correspondence: Kimberly A. Thompson, Binder Park Zoo, 7400 Division Dr, Battle Creek, MI, 49014, USA; email: kthompson@binderparkzoo.org

Genomic Analysis of Novel Poxvirus Brazilian Porcupinepox Virus, Brazil, 2019

Aline S. Hora, Sueli A. Taniwaki, Nathana B. Martins, Nataly N.R. Pinto, André E. Schlemper, André L.Q. Santos, Matias P.J. Szabó, Paulo E. Brandão

We obtained the complete sequence of a novel poxvirus, tentatively named Brazilian porcupinepox virus, from a wild porcupine (*Coendou prehensilis*) in Brazil that had skin and internal lesions characteristic of poxvirus infection. The impact of this lethal poxvirus on the survival of this species and its potential zoonotic importance remain to be investigated.

Poxviruses are among the best known and most feared viruses (*1*); the *Poxviridae* family includes several viruses of veterinary and medical relevance, some of them zoonotic. Emergence and reemergence of poxviruses is frequently observed (*2*–*4*). We report a systemic and lethal poxvirus infection in a wild porcupine and further characterize the virus through genomic analysis.

The Study

In March 2019, a free-ranging adult male Brazilian porcupine (*Coendou prehensilis*) in good bodily condition was captured near a park in the urban area of Uberlândia in the state of Minas Gerais in southeastern Brazil and was then referred for veterinary clinical care at the Federal University of Uberlândia. The animal had multifocal skin edema and erythema, especially on the eyelid and muzzle (Figure 1, panel A), extremity of limbs (Figure 1, panel B), and genital areas, and a penetrating skin lesion on the lateral face of the right limb near the elbow joint. We observed purulent nasal and ocular secretion. After 4 days of supportive treatment, the porcupine died and was subjected to a full necropsy for histopathologic evaluation and to collect samples for molecular investigation.

Author affiliations: Federal University of Uberlândia, Minas Gerais, Brazil (A.S. Hora, N.B. Martins, N.N.R. Pinto, A.E. Schlemper, A.L.Q. Santos, M.P.J. Szabó); University of São Paulo, São Paulo, Brazil (S.A. Taniwaki, P.E. Brandão)

DOI: https://doi.org/10.3201/eid2704.203818

On macroscopic examination, the spleen was enlarged, lungs were turgid, and the liver was pale and greyish. Standard histopathologic sections were cut from formalin-fixed, paraffin-embedded skin and organ samples and stained with hematoxylin and eosin. Histologic examination of the skin revealed several common alterations, irrespective of the location of the sample (Figure 1, panels C and D). Epidermis exhibited marked hyperplasia, parakeratotic hyperkeratosis, and moderate acantholysis. Epidermal cells were swollen, with foci of ballooning degeneration, and the cytoplasm of scattered epithelial cells contained round eosinophilic inclusions of varying size. No intranuclear inclusions were found. We also observed ulcerated epidermis with eosinophilic, amorphous keratinaceous crusts, necrosis, and numerous degenerated granulocytes. Dermal lesions included hemorrhage at the dermal–epidermal junction, severe edema, necrotic areas, and mixed inflammatory infiltrate that extended into the deep dermis. Venous blood congestion was observed in the kidneys, liver, spleen, and lungs. Hepatocytes evidenced moderate degeneration, whereas emphysema and pneumonitis were observed in the lungs.

We extracted total DNA from lesioned eyelid skin, spleen, and liver samples and subjected to a pan-pox universal PCR assay (*5*). All samples resulted in amplicons with low–GC content poxvirus primers targeting a region of the putative metalloproteinase gene. The amplicon from lesioned eyelid skin was submitted for Sanger sequencing (GenBank accession no. MK944278), and total DNA from this lesion was submitted to full-genome sequencing using the Illumina NextSeq platform (Illumina, https://www.illumina.com). We performed viral particle enrichment and next-generation sequencing (Appendix, https://wwwnc.cdc.gov/EID/article/27/4/20-3818-App1.pdf). A total of 71,507,840 pairs of 151-bp reads were obtained after

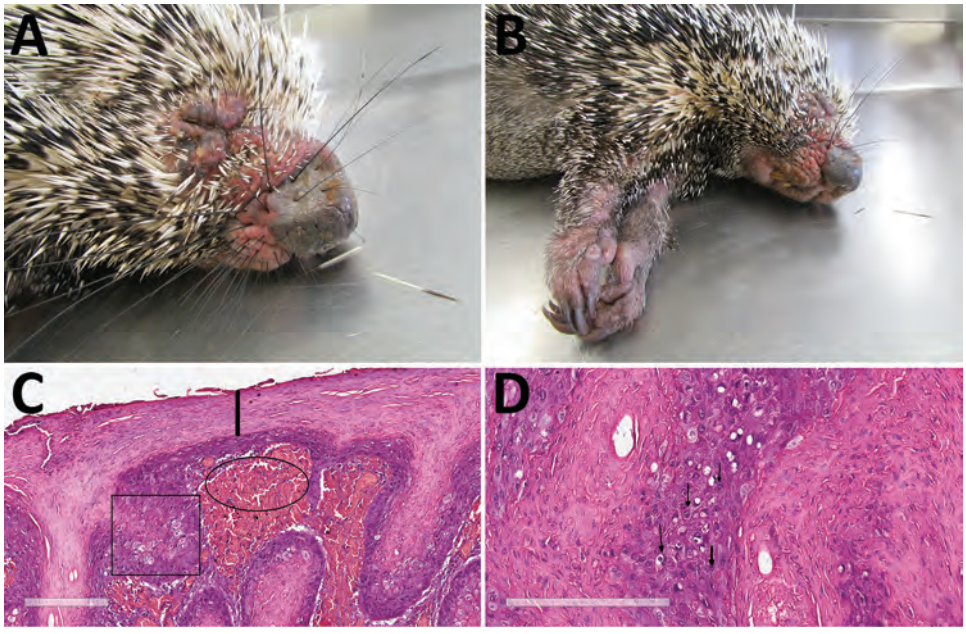

Figure 1. Photographs and histopathology of Brazilian porcupine (*Coendou prehensilis)* with novel poxvirus tentatively named Brazilian porcupinepox virus, Brazil, 2019. A) Severely swollen and erythematous skin of the eyelids, nasal region, and around oral cavity. B) Severely swollen skin of the forelimbs. C) Histopathologic examination of skin. Marked epidermal hyperplasia and swollen epithelial cells with foci of ballooning degeneration are marked with the square, and parakeratotic hyperkeratosis is indicated by the line. Dermal hemorrhage at the dermal–epidermal junction is indicated with the oval. Hematoxylin and eosin stain. Scale bar indicates 200 μm. D) Histopathologic examination of skin. Cytoplasm of several epithelial cells of epidermis with round eosinophilic inclusions is indicated by arrows. Hematoxylin and eosin stain. Scale bar indicates 200 μm.

raw data quality control using CLC Genomics Workbench 11 (QIAGEN, https://www.qiagen.com). The resulting paired-end reads were de novo assembled in CLC Genomics Workbench 11 (QIAGEN) with default parameters, resulting in a 144,504-nt genome (GenBank accession no. MN692191) with average coverage of 230.41x.

We annotated the genome (Appendix). Of 133 open reading frames (ORFs) found, only 2 (117 and 129) have no equivalents in other poxviruses, ORFs situated in the middle region of the genome encode proteins related to virion morphogenesis, the structure of virus particles, and viral DNA and RNA metabolism. We also identified the minimum essential chordopoxvirus genome, 49 genes conserved between highly diverged poxviruses families, and 41 genes conserved in chordopoxviruses (*6*). ORFs related to host range, immunomodulation, and virulence were observed in the extremities of the genome.

Alignments of 9 amino acid sequences corresponding to 9 conserved genes located in the central region were concatenated (7,956 aa) compiled from this genome with homologous sequences from different genera of chordopoxviruses with low GC content. Thus, we constructed a phylogenetic tree by using the maximum-likelihood method and Jones–Taylor–Thornton model (*7*) in MEGA X software (*8*) with the frequency matrix model (Figure 2). A nucleotide tree with complete genomes was also constructed (Appendix Figure 1).

Using the 9 concatenated sequences corresponding to the conserved central region of MN692191 and other known chordopoxviruses, we obtained nucleotide identities ranging from 69.9% to 85.2% (Appendix Figure 2) and amino acid identities ranging from 57.7% to 78.8% (Appendix Figure 3). The highest identity was observed between MN692191 and Cotia virus (CoTV) in clusters in the phylogenetic trees. In the 1960s, CoTV was isolated in Brazil from sentinel suckling mice (*9*); the natural host remains unknown and CoTV remains unclassified despite attempts to place it in a new genus of *Poxviridae* (*10*). According to the International Committee on Taxonomy of Viruses (*11*), isolates within a species exhibit >98% nucleotide identity. CoTV and MN692191 exhibit 85.2% of nucleotide identity and thus are distinct species.

We estimated maximum-likelihood distances for this region of conserved nucleotides; the distance between CoTV and MN692191 was 0.156. MN692191 belongs to a main clade that includes *Capripoxvirus, Suipoxvirus, Leporipoxvirus, Cervidpoxvirus*, and *Yatapoxvirus* (clade CSLCY). Distances ranging from 0.177 to 0.210 were observed between MN692191 and species from different genera of the CSLCY clade. In species from the same genus of this clade, distance ranged from 0.006 to 0.052, which suggests that MN692191 and CoTV (maximum-likelihood distance 0.156) do not belong to the same genus.

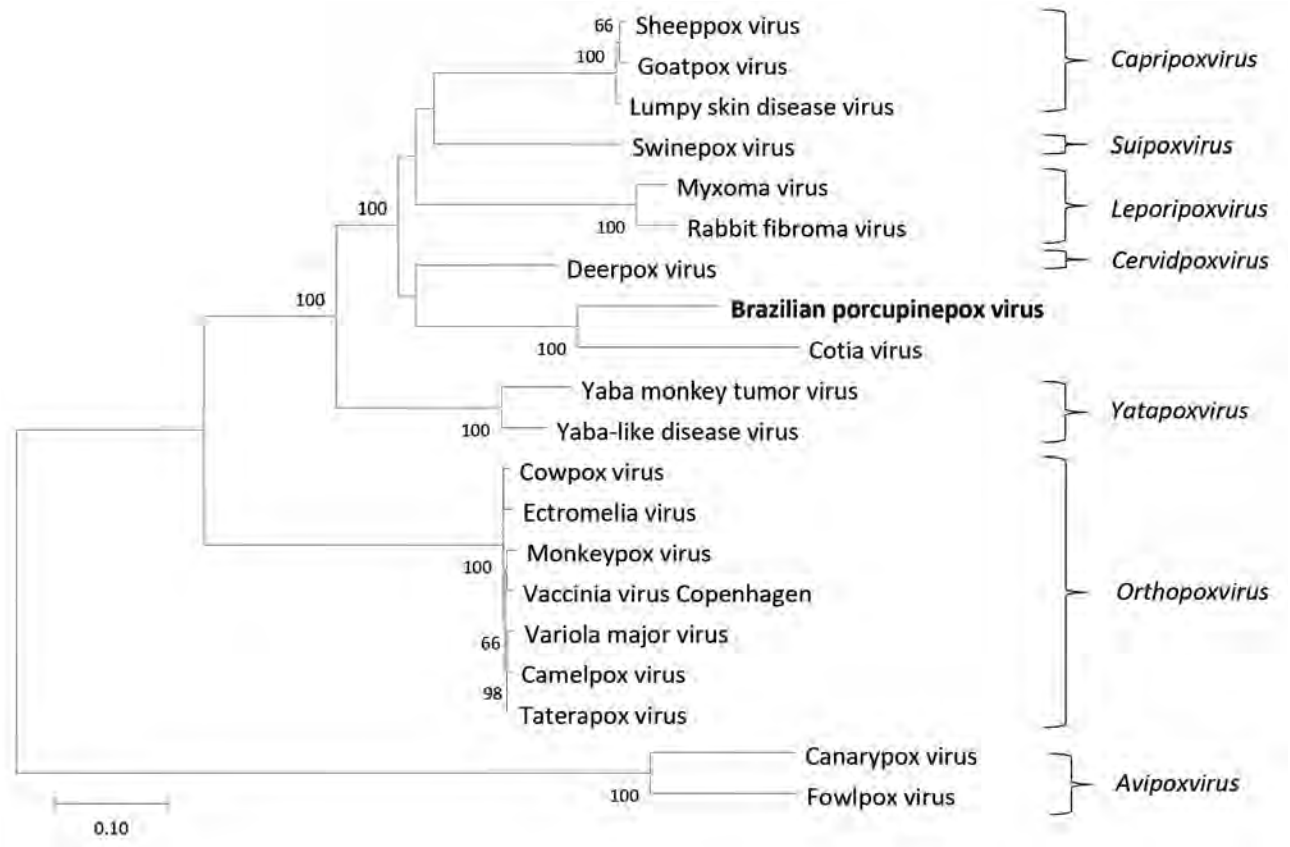

Figure 2. Phylogenetic tree constructed in genomic analysis of novel poxvirus Brazilian porcupinepox virus, Brazil, 2019 (boldface). Tree constructed by using the maximum-likelihood method and Jones–Taylor–Thornton model (*7*) with frequency model for amino acid sequence alignments of the RNA polymerase subunit RPO147, RNA polymerase subunit RPO132, RNA polymerase–associated RAP94, mRNA capping enzyme large subunit, virion major core protein P4a, early transcription factor VETFL, nucleoside-triphosphatase, DNA polymerase, and DNA topoisomerase I genes of selected strains representing different genera of chordopoxvirus with low GC contents and their respective genera. The numbers next to each node represent the values of 1,000 bootstrap repetitions, and only those >50% are shown. Evolutionary analyses were conducted in MEGA X (*8*). GenBank accession numbers are as follows: Brazilian porcupinepox virus, MK944278.1; camelpox virus, AY009089.1; canarypox virus, NC005309.1; Cotia virus, KM595078.1; cowpox virus, DQ437593.1; deerpox virus, AY689437.1; ectromelia virus, NC004105.1; fowlpox virus, NC002188.1; goatpox virus, MH381810.1; lumpy skin disease virus, NC003027.1; monkeypox virus, DQ011157.1; myxoma virus, NC001132.2; rabbit fibroma virus, NC001266.1; sheeppox virus, NC004002.1; swinepox virus, NC003389.1; taterapox virus, NC008291.1; vaccinia virus, M35027.1; variola major virus, L22579.1; Yaba monkey tumor virus, NC005179.1; Yaba-like disease virus, NC002642.1. Scale bar represents number of substitutions per site.

Conclusions

This comprehensive phylogenetic analysis supports the classification of MN692191 into a new genus in the family *Poxviridae*, subfamily *Chordopoxvirinae*. Because the virus described in this study is distinct from previously identified viruses, we propose the tentative species name Brazilian porcupinepox virus (BPoPV), according to recommendations for nomenclature of poxvirus species of the International Committee on Taxonomy of Viruses (*11*).

Wildlife veterinarians in Brazil have observed free-ranging porcupines exhibiting clinical signs compatible with those described in this study (B.S.S. Petri, CRAS Parque Ecológico do Tietê- São Paulo, pers. comm., 2019 Sep 16; I.S. Barbosa, CETAS–Goiânia, pers. comm., 2020 Jan 6) have been observed. In 2019, of 13 of these porcupine specimens reported, only 3 had fully recovered from clinical symptoms, demonstrating that this virus might be a common pathogen for this species and could have consequences for its conservation.

Brazilian porcupines have a greater distribution in Brazil but are found in 10 other countries in Latin America (*12*). This species is found mainly in forest environments (*12*) and can be observed in forest fragments in urban areas, as was the case for the specimen in this study. Housing construction nearer to forested areas has led to this porcupine sometimes being hunted for meat (*13*), which leads to human exposure to the pathogens hosted by this species.

The genus *Orthopoxvirus* includes the best-known zoonotic poxvirus species, such as cowpox, monkeypox, and vaccinia viruses (*14*); however, the zoonotic poxvirus is not restricted to this genus. The genera *Parapoxvirus* and *Yatapoxvirus* also include viral species of zoonotic importance (*15*). Furthermore, chordopoxviruses are often described as emerging zoonoses. Contact between Brazilian porcupines and humans, because of anthropized forested areas and the porcupines' broad geographic distribution and presence in urban areas, raises concerns about the zoonotic potential of BPoPV, which remains to be investigated.

In summary, our description of this novel poxvirus contributes to knowledge of viral diversity and pathogenicity of poxviruses. Some chordopoxviruses are capable of infecting multiple animal species, whereas others have a restricted host spectrum (*14*,*15*). The infection capability of BPoPV is a crucial aspect for further study.

Acknowledgments

We thank José Luiz Catão-Dias and Carlos Sacristán for kindly providing the positive control for the initial molecular screening.

This research was sponsored by the Coordenação de Aperfeiçoamento de Pessoal de Nível Superior—Brasil (finance code 001) and the Conselho Nacional de Desenvolvimento Científico e Tecnológico (grant no. 307291/2017-0).

About the Author

Dr. Hora is a professor in the School of Veterinary Medicine, Federal University of Uberlândia, Brazil. Her research interests include molecular diagnostic techniques of infectious diseases in wild and domestic animals.

References

1. Oliveira GP, Rodrigues RAL, Lima MT, Drumond BP, Abrahão JS. Poxvirus host range genes and virus–host spectrum: a critical review. Viruses. 2017;9:331. https://doi.org/10.3390/v9110331
2. Gigante CM, Gao J, Tang S, McCollum AM, Wilkins K, Reynolds MG, et al. Genome of *Alaskapox virus*, a novel orthopoxvirus isolated from Alaska. Viruses. 2019;11:708. https://doi.org/10.3390/v11080708
3. Kantele A, Chickering K, Vapalahti O, Rimoin AW. Emerging diseases—the monkeypox epidemic in the Democratic Republic of the Congo. Clin Microbiol Infect. 2016;22:658–9. https://doi.org/10.1016/j.cmi.2016.07.004
4. Abrahão JS, Campos RK, Trindade GS, Guimarães da Fonseca F, Ferreira PCP, Kroon EG. Outbreak of severe zoonotic vaccinia virus infection, southeastern Brazil. Emerg Infect Dis. 2015;21:695–8. https://doi.org/10.3201/eid2104.140351
5. Li Y, Meyer H, Zhao H, Damon IK. GC content-based pan-pox universal PCR assays for poxvirus detection. J Clin Microbiol. 2010;48:268–76. https://doi.org/10.1128/JCM.01697-09
6. Upton C, Slack S, Hunter AL, Ehlers A, Roper RL. Poxvirus orthologous clusters: toward defining the minimum essential poxvirus genome. J Virol. 2003;77:7590–600. https://doi.org/10.1128/JVI.77.13.7590-7600.2003
7. Jones DT, Taylor WR, Thornton JM. The rapid generation of mutation data matrices from protein sequences. Comput Appl Biosci. 1992;8:275–82. https://doi.org/10.1093/bioinformatics/8.3.275
8. Kumar S, Stecher G, Li M, Knyaz C, Tamura K. MEGA X: molecular evolutionary genetics analysis across computing platforms. Mol Biol Evol. 2018;35:1547–9. https://doi.org/10.1093/molbev/msy096
9. Lopesode S, Lacerda JP, Fonseca IE, Castro DP, Forattini OP, Rabello EX. Cotia virus: a new agent isolated from sentinel mice in São Paulo, Brazil. Am J Trop Med Hyg. 1965;14:156–7. https://doi.org/10.4269/ajtmh.1965.14.156
10. Afonso PP, Silva PM, Schnellrath LC, Jesus DM, Hu J, Yang Y, et al. Biological characterization and next-generation genome sequencing of the unclassified Cotia virus SPAn232 (*Poxviridae*). J Virol. 2012;86:5039–54. https://doi.org/10.1128/JVI.07162-11
11. International Committee on Taxonomy of Viruses. *Poxviridae*. 2011 [cited 2020 Jul 22]. https://talk.ictvonline.org/ictv-reports/ictv_9th_report/dsdna-viruses-2011/w/dsdna_viruses/74/poxviridae
12. Marinho-Filho J, Emmons L. *Coendou prehensilis* (Brazilian porcupine). The IUCN red list of threatened species. 2016 [cited 2020 Oct 29]. https://www.iucnredlist.org/species/101228458/22214580
13. Emmons LH, Feer F. Porcupines (*Erethizontidae*). In: Emmons LH, Feer F, editors. Neotropical rainforest mammals: a field guide. 2nd ed. Chicago: University of Chicago Press; 1997. p. 216–23.
14. Essbauer S, Pfeffer M, Meyer H. Zoonotic poxviruses. Vet Microbiol. 2010;140: 229–36.
15. Barrett JW, McFadden G. Origin and evolution of poxviruses. In: Domingo E, Parrish C, Holland J, editors. Origin and evolution of viruses. 2nd ed. Cambridge (MA): Academic Press; 2008. p. 431–46.

Address for correspondence: A.S. Hora, Avenida Ceará S/N, bloco 2D, sala 46, Campus Umuarama, Uberlândia–Minas Gerais, 38400-902, Brazil; email: alinedahora@ufu.br

Highly Pathogenic Avian Influenza Clade 2.3.4.4 Subtype H5N6 Viruses Isolated from Wild Whooper Swans, Mongolia, 2020

Sol Jeong,[1] Nyamsuren Otgontogtokh,[1] Dong-Hun Lee, Bayarmagnai Davganyam, Sun-Hak Lee, Andrew Y. Cho, Erdene-Ochir Tseren-Ochir, Chang-Seon Song

We identified clade 2.3.4.4 highly pathogenic avian influenza A(H5N6) viruses from whooper swans (*Cygnus cygnus*) found dead in Mongolia. The identification of these infections in wild birds in this area is of concern because of the potential for virus dissemination during fall migration.

Highly pathogenic avian influenza (HPAI) H5Nx viruses have been continuous threat to poultry and public health since the detection of A/Goose/Guangdong/1/1996(H5N1) (Gs/GD) in 1996 in Guangdong Province, China. The Gs/GD-lineage has evolved into 10 genetically distinct clades (0–9) and subclades (*1*). A novel clade 2.3.4.4 of H5Nx viruses bearing multiple neuraminidase subtypes, including N2, N5, N6, and N8, has been identified in China since 2008 (*2*), and the H5 genes have been phylogenetically differentiated into 4 subgroups (A–D) (*3*). Clade 2.3.4.4 H5N6 viruses have been causing worldwide epizootics in poultry and wild birds, and human cases have also been reported since 2014 (*4*). In this study, we report the identification and genetic analysis of 2 HPAI clade 2.3.4.4 H5N6 viruses isolated from whooper swan carcasses in central Mongolia during April 2020.

Wild whooper swan (*Cygnus cygnus*) carcasses were found in April 2020 on the banks of 2 small ponds (48°25′39.8″N, 102°36′09.6″E, and 47°56′22.0″N, 102°32′54.0″E) around the Orkhon River located nearby Khunt Lake (Bulgan Province, 48°25′59.8″N, 102°34′51.1″E) and Doitiin Tsgaaan Lake (Arkhangal Province, 47°34′20.1″N, 102°31′45.4″E) (Appendix 1 Figure 1, https://wwwnc.cdc.gov/EID/article/27/4/20-3859-App1.pdf). These lakes are a major stopover site of migratory wild birds in central Mongolia between their breeding sites in the north and the wintering sites in the south and are also major breeding and molting habitats of wild bird species, including whooper swan. The lakes were the outbreak sites of HPAI H5N1 in wild birds in 2005, 2006, and 2009 (*5*). Two HPAI viruses, A/Whooper swan/Mongolia/24/2020(H5N6) and A/Whooper swan/Mongolia/25/2020(H5N6), referred to as MN-H5N6/2020 viruses in this article, were isolated from 2 brain tissue samples of whooper swan carcasses. We conducted whole-genome sequencing (*6*) and phylogenetic analysis on the isolates (Appendix). The nucleotide sequences have been deposited in GenBank (accession nos. MT872354–69).

The 2 MN-H5N6/2020 viruses shared high nucleotide similarity (99.65%–100%) across all 8 gene segments. Polybasic amino acid motif on the cleavage site of hemagglutinin (HA) genes (PLRERRRKR/G) suggested that the MN-H5N6/2020 viruses are HPAI. BLAST (https://blast.ncbi.nlm.nih.gov/Blast.cgi) and GISAID (https://platform.gisaid.org) searches showed that the MN-H5N6/2020 viruses share high nucleotide identity (99.4%–99.9%) across all 8 gene segments with the HPAI H5N6 viruses, referred to as Xinjiang-H5N6/2020 viruses in this article, isolated from wild swans (mute swans [*Cygnus olor*] and whooper swans) during January 2020 in Xinjiang Province, China (Table 1) (*7*), which is located ≈4,800 km southwest of the isolation sites of the MN-H5N6/2020 viruses. These results suggested that the

Author affiliations: Konkuk University, Seoul, South Korea (S. Jeong, S.-H. Lee, A.Y. Cho, C.-S. Song); Mongolian University of Life Sciences, Ulaanbaatar, Mongolia (N. Otgontogtokh, B. Davganyam, E.-O. Tseren-Ochir); University of Connecticut, Storrs, Connecticut, USA (D.-H. Lee)

DOI: https://doi.org/10.3201/eid2704.203859

[1]These authors contributed equally to this article.

Table 1. Nucleotide sequence identities between each gene segment of MN-H5N6/2020 highly pathogenic avian influenza virus isolates from Mongolia, 2020, and the isolates with the highest homology in the GISAID and GenBank databases*

Gene	Accession no.	Virus	% Identity
PB2	EPI1718955	A/Whooper swan/Xinjiang/3/2020(H5N6)	99.74–99.83
PB1	EPI1718956	A/Whooper swan/Xinjiang/3/2020(H5N6)	99.44
PA	EPI1719034	A/Whooper swan/Xinjiang/13/2020(H5N6)	99.78
HA	EPI1718990	A/Whooper swan/Xinjiang/7/2020(H5N6)	99.60–99.66
NP	EPI1718951	A/Whooper swan/Xinjiang/3/2020(H5N6)	99.74–99.81
NA	EPI1719037	A/Whooper swan/Xinjiang/13/2020(H5N6)	99.65–99.72
MP	EPI1719033	A/Whooper swan/Xinjiang/13/2020(H5N6)	99.70
NS	EPI1719032	A/Whooper swan/Xinjiang/13/2020(H5N6)	99.54

*As of 2020 Jul 16. GISAID, https://platform.gisaid.org. HA, hemagglutinin; MP, matrix protein; NP, nucleoprotein; NS, nonstructual protein PA, acidic polymerase; PB1, basic polymerase 1; PB2, basic polymerase 2.

MN-H5N6/2020 viruses might have been introduced through the Central Asian flyway to central Mongolia most likely during early spring migration in 2020.

In the maximum-likelihood phylogenetic trees, all 8 gene segments of the MN-H5N6/2020 were closely clustered with the sequences of the Xinjiang-H5N6/2020 viruses and the H5N6 viruses of clade 2.3.4.4 group C isolated during 2016–2019 in China, Vietnam, and Russia, including human isolates (Appendix 1 Figure 2). The phylogenetic relationship and high nucleotide identity indicated that the MN-H5N6/2020 viruses possess the identical genome constellation with the Xinjiang-H5N6/2020 viruses (*7*). The time of most recent common ancestor for each gene of the MN-H5N6/2020 viruses and the Xinjiang-H5N6/2020 viruses ranged from May to December 2019, suggesting that the MN-H5N6/2020 viruses and the Xinjiang-H5N6/2020 viruses had diverged from a common ancestor most likely during the second half of the previous year (Table 2; Appendix 1 Figure 3). The time of most recent common ancestor for each gene of the MN-H5N6/2020 viruses ranged from January through March 2020. These data and understanding of waterfowl migration patterns suggest that H5N6 viruses were maintained among wild birds during fall and winter 2019 and reached Mongolia by late winter, most likely carried by long-distance flights of infected migrating wild birds during spring migration. A previous satellite-tracking study of whooper swans between northern China and Mongolia showed that the most stable period for the wintering population of whooper swans in the Sanmenxia Reservoir area was from late December to early January (*8*). For spring migration, departure dates of the wintering population of whooper swans ranged from February 17 to March 27, and arrival dates at the breeding sites in Mongolia ranged from February 27 to May 23. This spring bird migration pattern coincided with the timing and direction of H5N6 virus transmission between Xinjiang and Mongolia.

The MN-H5N6/2020 and the Xinjiang-H5N6/2020 viruses had mutations associated with increased HA receptor binding affinity to human-like receptor (α-2,6 sialic acid), including D94N, S133A, S154N, and T156A (H5 numbering) (*9*) (Appendix 2 Table 2, https://wwwnc.cdc.gov/EID/article/27/4/20-3859-App2.xlsx), although they maintained the amino acids related to the binding tropism to avian-like (α-2,3 sialic acid) receptors (222Q and 224G). Unlike 7 H5N6 human isolates of clade 2.3.4.4 group C, the MN-H5N6/2020 and the Xinjiang-H5N6/2020 viruses had amino acid substitution at HA position 188 (H5 numbering), from threonin to isoleucine, which is known to enhance receptor binding affinity to human-like receptor (*10*). In the maximum-likelihood phylogenetic tree and maximum clade credibility tree of polymerase basic 2 gene, the closest isolates of the MN-H5N6/2020 and Xinjiang-H5N6/2020 viruses were human H5N6 isolates from China (Table 2; Appendix 1 Figure 2, 3).

Table 2. tMRCA of each gene segment of H5N6 highly pathogenic avian influenza viruses from Mongolia, 2020*

	tMRCA† of MN-H5N6/2020 viruses		tMRCA of MN-H5N6/2020 and Xinjiang-H5N6/2020 viruses	
Gene	Mean	95% HPD‡ range	Mean	95% HPD range
PB2	Feb 2020	Jan–Mar 2020	Dec 2019	Dec 2019
PB1	Feb 2020	Jan–Mar 2020	May 2019	Dec 2018–Aug 2019
PA	Jan 2020	Dec 2019–Mar 2020	Sep 2019	Jun–Nov 2019
HA	Jan 2020	Oct 2019–Feb 2020	Jul 2019	Mar–Oct 2019
NP	Jan 2020	Nov 2019–Mar 2020	Nov 2019	Aug–Dec 2019
NA	Feb 2020	Dec 2019–Mar 2020	Jul 2019	Jan–Oct 2019
MP	Mar 2020	Jan–Mar 2020	Jul 2019	Feb–Oct 2019
NS	Feb 2020	Dec 2019–Mar 2020	Nov 2019	Sep–Dec 2019

*HA, hemagglutinin; HPD, highest posterior density; MP, matrix protein; NP, nucleoprotein; NS, nonstructural protein PA, acidic polymerase; PB1, basic polymerase 1; PB2, basic polymerase 2; tMRCA, time to the most recent common ancestor.
†tMRCA estimated by using Bayesian molecular clock analysis. It represents the potential existing timing of a common ancestral node.

Wild migratory birds have played an important role in disseminating and maintaining of Gs/GD lineage HPAI H5Nx viruses, as observed in the epizootics of H5N1 clade 2.2 during 2005–2006 (*11*), H5N1 clade 2.3.2 in 2009 (*12*), clade 2.3.2.1c in 2015 (*13*), and clade 2.3.4.4 since 2014 (*14*). During widespread dissemination of the HPAIV clade 2.2 during 2005–2006 and clade 2.3.2 in 2009, these viruses were also detected from wild birds at Doitiin Tsgaaan Lake and Khunt Lake, highlighting that these areas are useful locations for monitoring of HPAI in wild birds as a pathway for the spread of HPAI during migration of waterfowl. Identifying 2 H5N6 HPAI viruses in wild waterfowl in this area signifies the potential for wide spread of this clade 2.3.4.4 H5N6 viruses during the 2020 fall migration.

Since the first report of a human infection with HPAI clade 2.3.4.4 H5N6 virus in Sichuan Province, China, in April 2014 (*4*), a total of 24 cases had been reported from China as of August 2020 (*15*). The mammalian host-specific markers found in the MN-H5N6/2020 viruses suggest that these viruses are potentially infectious for mammals. Considering the possibility of future dispersal of the H5N6 HPAI viruses through wild birds and the presence of mammalian host-specific genetic markers, enhanced active surveillance in wild birds, poultry, and mammals is needed to monitor spread and understand the potential for zoonotic infection.

Acknowledgment

We would like to thank the State Central Veterinary Laboratory of Mongolia for providing Biosafety Level 3 facilities and technical support.

This research was supported by the Bio and Medical Technology Development Program of the National Research Foundation, funded by the government of South Korea (grant no. NRF-2018M3A9H4056535).

About the Author

Ms. Jeong is a PhD candidate at Konkuk University, Seoul, South Korea; her primary research interests include the molecular epidemiology and host–pathogen interaction of avian influenza viruses. Ms. Nyamsuren is a researcher and MSc student at Mongolian University of Life Sciences, Ulaanbaatar, Mongolia; her primary research interests include the molecular epidemiology and diagnosis of transboundary animal diseases.

References

1. WHO/OIE/FAO H5N1 Evolution Working Group. Toward a unified nomenclature system for highly pathogenic avian influenza virus (H5N1). Emerg Infect Dis. 2008;14:e1. https://doi.org/10.3201/eid1407.071681
2. Gu M, Liu W, Cao Y, Peng D, Wang X, Wan H, et al. Novel reassortant highly pathogenic avian influenza (H5N5) viruses in domestic ducks, China. Emerg Infect Dis. 2011;17:1060–3. https://doi.org/10.3201/eid/1706.101406
3. Lee DH, Bahl J, Torchetti MK, Killian ML, Ip HS, DeLiberto TJ, et al. Highly pathogenic avian influenza viruses and generation of novel reassortants, United States, 2014–2015. Emerg Infect Dis. 2016;22:1283–5. https://doi.org/10.3201/eid2207.160048
4. Pan M, Gao R, Lv Q, Huang S, Zhou Z, Yang L, et al. Human infection with a novel, highly pathogenic avian influenza A (H5N6) virus: virological and clinical findings. J Infect. 2016;72:52–9. https://doi.org/10.1016/j.jinf.2015.06.009
5. Gilbert M, Jambal L, Karesh WB, Fine A, Shiilegdamba E, Dulam P, et al. Highly pathogenic avian influenza virus among wild birds in Mongolia. PLoS One. 2012;7:e44097. https://doi.org/10.1371/journal.pone.0044097
6. Lee DH. Complete genome sequencing of influenza A viruses using next-generation sequencing. Methods Mol Biol. 2020;2123:69–79. https://doi.org/10.1007/978-1-0716-0346-8_6
7. Li Y, Li M, Li Y, Tian J, Bai X, Yang C, et al. Outbreaks of highly pathogenic avian influenza (H5N6) virus subclade 2.3.4.4h in swans, Xinjiang, Western China, 2020. Emerg Infect Dis. 2020;26:2956–60. https://doi.org/10.3201/eid2612.201201
8. Li S, Meng W, Liu D, Yang Q, Chen L, Dai Q, et al. Migratory whooper swans *Cygnus cygnus* transmit H5N1 virus between China and Mongolia: combination evidence from satellite tracking and phylogenetics analysis. Sci Rep. 2018;8:7049. https://doi.org/10.1038/s41598-018-25291-1
9. Suttie A, Deng YM, Greenhill AR, Dussart P, Horwood PF, Karlsson EA. Inventory of molecular markers affecting biological characteristics of avian influenza A viruses. Virus Genes. 2019;55:739–68. https://doi.org/10.1007/s11262-019-01700-z
10. Yang ZY, Wei CJ, Kong WP, Wu L, Xu L, Smith DF, et al. Immunization by avian H5 influenza hemagglutinin mutants with altered receptor binding specificity. Science. 2007;317:825–8. https://doi.org/10.1126/science.1135165
11. Chen H, Li Y, Li Z, Shi J, Shinya K, Deng G, et al. Properties and dissemination of H5N1 viruses isolated during an influenza outbreak in migratory waterfowl in western China. J Virol. 2006;80:5976–83. https://doi.org/10.1128/JVI.00110-06
12. Li Y, Liu L, Zhang Y, Duan Z, Tian G, Zeng X, et al. New avian influenza virus (H5N1) in wild birds, Qinghai, China. Emerg Infect Dis. 2011;17:265–7. https://doi.org/10.3201/eid1702.100732
13. Bi Y, Chen J, Zhang Z, Li M, Cai T, Sharshov K, et al. Highly pathogenic avian influenza H5N1 clade 2.3.2.1c virus in migratory birds, 2014–2015. Virol Sin. 2016;31:300–5. https://doi.org/10.1007/s12250-016-3750-4
14. Global Consortium for H5N8 and Related Influenza Viruses. Role for migratory wild birds in the global spread of avian influenza H5N8. Science. 2016;354:213–7. https://doi.org/10.1126/science.aaf8852
15. World Health Organization. Avian influenza weekly update number 754. 2020 [cited 2020 Aug 19]. https://www.who.int/docs/default-source/wpro—documents/emergency/surveillance/avian-influenza/ai-20200814.pdf?sfvrsn=30d65594_68

Address for correspondence: Chang-Seon Song, College of Veterinary Medicine, Konkuk University, 120 Neungdong-ro, Gwangjin-gu, Seoul 05029, South Korea; e-mail: songcs@konkuk.ac.kr

Increased SARS-CoV-2 Testing Capacity with Pooled Saliva Samples

Anne E. Watkins, Eli P. Fenichel, Daniel M. Weinberger, Chantal B.F. Vogels, Doug E. Brackney, Arnau Casanovas-Massana, Melissa Campbell, John Fournier, Santos Bermejo, Rupak Datta, Charles S. Dela Cruz, Shelli F. Farhadian, Akiko Iwasaki, Albert I. Ko, Nathan D. Grubaugh,[1] Anne L. Wyllie,[1] the Yale IMPACT Research Team[2]

We analyzed feasibility of pooling saliva samples for severe acute respiratory syndrome coronavirus 2 testing and found that sensitivity decreased according to pool size: 5 samples/pool, 7.4% reduction; 10 samples/pool, 11.1%; and 20 samples/pool, 14.8%. When virus prevalence is >2.6%, pools of 5 require fewer tests; when <0.6%, pools of 20 support screening strategies.

Limited laboratory capacity in the United States has hindered access to testing for severe acute respiratory syndrome coronavirus 2 (SARS-CoV-2) and has delayed results. To control outbreaks of coronavirus disease (COVID-19), testing capacity must be increased and maintained for the foreseeable future. One resource-saving, capacity-increasing approach is pooling samples, thereby testing multiple persons simultaneously. A negative result for the pool indicates that all samples were below the limit of detection, and a positive result for the pool requires individual retesting of all samples. Pooled testing has been widely proposed as a way to expand capacity for large-scale screening (*1*,*2*; C.M. Verdun, unpub data, https://doi.org/10.1101/2020.04.30.20085290), a proactive strategy for early pathogen detection, primarily for persons who are not yet symptomatic.

Saliva is being used as a noninvasive source for SARS-CoV-2 testing (*3*,*4*) yet can be more difficult to process than traditional swab-based samples (*5*). Given limited empirical evidence to properly inform projections of feasibility and cost-effectiveness of pooling, we explored the potential of pooling saliva to increase SARS-CoV-2 testing capacity.

The Study

Using saliva collected from COVID-19 inpatients and at-risk healthcare workers (*5*), we combined 1 SARS-CoV-2–positive sample (<38 PCR cycle threshold [C_t]) with SARS-CoV-2–negative saliva (Appendix, https://wwwnc.cdc.gov/EID/article/27/4/20-4200-App1.pdf) before RNA extraction in total pool sizes of 5 samples/pool (n = 23 pools), 10 (n = 23), and 20 (n = 31). As pool size increased, detection sensitivity decreased independent of starting viral load (pool of 5, +2.2 cycle threshold [C_t], 95% CI 1.4–3.0 C_t; 10, +3.1 C_t, 95% CI 2.3–4.0 C_t; 20, +3.6 C_t, 95% CI 2.7–4.4 C_t) (Figure 1; Appendix).

By applying the regression coefficients (C_t increase) to the C_t values from all SARS-CoV-2–positive saliva samples detected during our studies (*6*), we estimate that pool sizes will lead to detection sensitivities of 92.59% (95% CI 88.89%–95.56%) for pools of 5 samples, 88.89% (95% CI 80.00%–91.85%) for pools of 10, and 85.19% (95% CI 75.56%–91.11%) for pools of 20, relative to sensitivity of unpooled samples (Appendix Figure 1). This loss in sensitivity could be minimized through protocol modifications: increasing the volume of pooled samples tested (400 µL, n = 20 pools of each size; Appendix Figure 2) and decreasing the elution volume.

On the basis of the calculated relative sensitivity loss resulting from pooling, we modeled the number of tests required (total of pooled and individual samples from positive pools tested) for a population of 10,000 with increasing SARS-CoV-2 prevalence

Author affiliations: Yale School of Public Health, New Haven, Connecticut, USA (A.E. Watkins, D.M. Weinberger, C.B.F. Vogels, A. Casanovas-Massana, A.I. Ko, N.D. Grubaugh, A.L. Wyllie); Yale School of the Environment, New Haven (E.P. Fenichel); Connecticut Agricultural Experiment Station, New Haven (D.E. Brackney); Yale University School of Medicine, New Haven (M. Campbell, J. Fournier, S. Bermejo, R. Datta, C.S. Dela Cruz, S.F. Farhadian, A. Iwasaki, A.I. Ko); Howard Hughes Medical Institute, New Haven (A. Iwasaki)

DOI: https://doi.org/10.3201/eid2704.204200

[1]These senior authors contributed equally to this article.

[2]Team members team are listed at the end of this article.

(Figure 2, panel A). We estimate that for populations with prevalence <0.6%, pools of 20 require the fewest tests. However, for populations with prevalence >2.6%, our analyses suggest that pooling of 5 samples leads to the fewest tests. For populations with prevalence >28.1%, testing individual samples is more efficient than testing pools of any size. Thus, we suggest using an adaptive pooling strategy that accounts for SARS-CoV-2 prevalence for the population tested: as virus prevalence decreases, pool size can be increased, but as prevalence rises, pool size should be decreased.

Because sensitivity varies by pooling design (Figure 1), a different number of positive results will be detected for a given population with a given SARS-CoV-2 prevalence. As virus prevalence decreases, we estimate that cost savings of pooled testing will increase (Figure 2, panel B). For example, if SARS-CoV-2 prevalence for a 10,000-person population was 0.5%, then pooling by 20 would require only 1,318 tests, including retesting of all persons from test-positive pools. If tests cost US$30 each, the savings would be $260,453 relative to individual testing while still identifying ≈43 of 50 infected persons. The savings will vary on a scale relative to test prices. Ultimately, the net benefits of pooled testing can continue to increase even as virus prevalence decreases with increased pool sizes, which is essential for ongoing screening.

Conclusions

The cost of SARS-CoV-2 testing can be prohibitive when positive samples are rarely found, presenting a major barrier to prolonged screening strategies. Pooling of samples can help overcome this barrier. Our model demonstrates that as local outbreaks fluctuate, adapting pool sizes will have resource-savings benefits.

The benefits of pooled testing will always be accompanied by decreased detection sensitivity. However, the lower overall number of tests required and the lower associated costs expands testing capacity, permitting more frequent testing, and testing persons more often mitigates the loss of sensitivity (*7*). By enabling broader testing, pooling has the potential to identify more infected persons than more limited (or no) individual testing. Infected persons can then be isolated from the population, thus reducing the probability of contact between a susceptible and an infectious person, ultimately reducing transmission. Given our findings, we urge the US Food and Drug Administration to develop new guidelines for pooled-testing approaches. Although the first Emergency Use

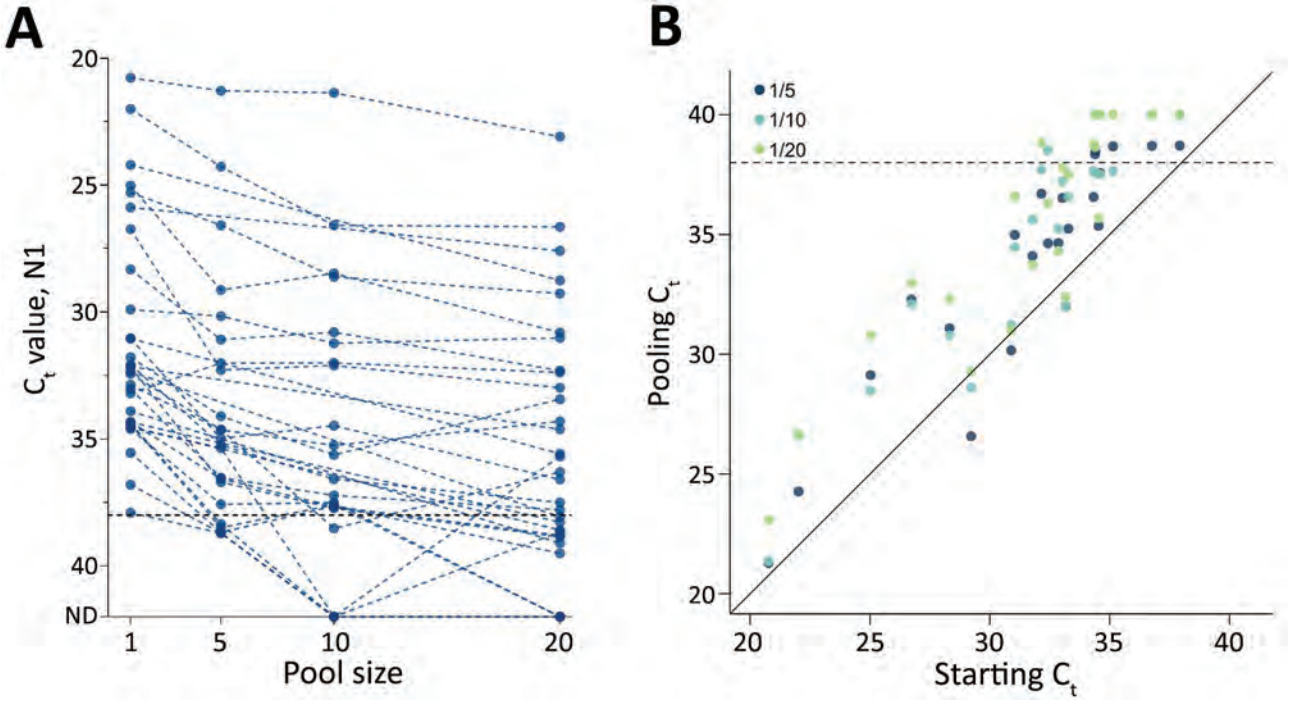

Figure 1. Effect of pooling on detection of severe acute respiratory syndrome coronavirus 2, by pool size and between samples tested. A) As the pool size increased, so did the C_t value (dotted lines connect pools comprising the same positive sample). C_t for positivity is set to 38. Samples falling on the x-axis indicated samples from which signal was not detected by reverse transcription quantitative PCR. B) As the pool size increased, so did the C_t. We equated this change by using linear regression (pool of 5 samples, dark blue, +2.2 C_t, 95% CI 1.4–3.0 C_t; pool of 10, light blue, +3.1 C_t, 95% CI 2.3–4.0 C_t; pool of 20, green, +3.6, 95% CI 2.7–4.4 C_t). Dashed lines indicate C_t 38 (cutoff for sample positivity). 1/5, pool of 5; 1/10, pool of 10; 1/20, pool of 20. C_t, cycle threshold.

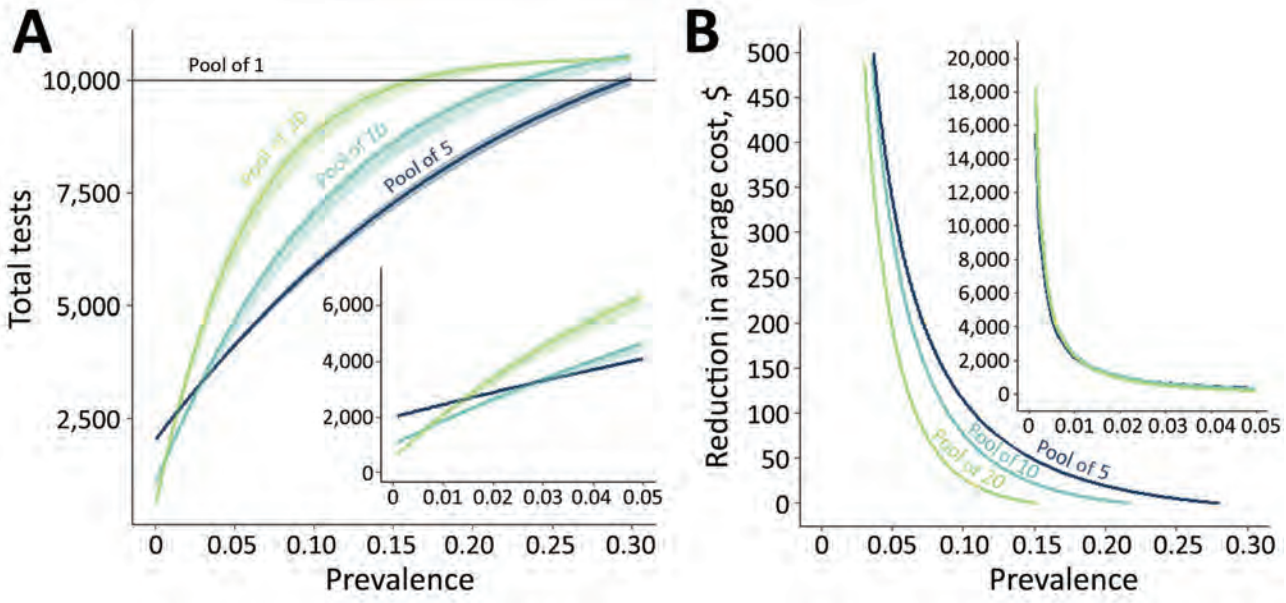

Figure 2. The resource-saving benefit of sample pooling for severe acute respiratory syndrome coronavirus 2 (SARS-CoV-2) testing, based on size of the pool and expected prevalence of SARS-CoV-2 within the population. A) We modeled the number of tests required to test 10,000 persons (results qualitatively scale with population) when pools contain 5, 10, or 20 samples (and individually retesting samples within positive pools) compared with testing samples individually (pool = 1 sample). As prevalence increases, so does the number of pools positive for SARS-CoV-2, thereby increasing the required number of confirmatory tests of individual samples. Therefore, over a prevalence of 2.6%, pooled samples of 5 result in fewer overall tests required than do larger pool sizes. B) At lower prevalence rates, such as when outbreaks have been controlled but ongoing screening is required, pools of 10 or 20 samples yield substantial cost savings for the same expected level of positive detections, after accounting for sensitivity differences. Values are shown in US$. Insets show the region with <5% prevalence.

Authorization for SARS-CoV-2 pooled testing (≤4 swab samples in 1 test) (*8*) will be most useful in high-prevalence settings, the ≈12%–15% losses in sensitivity when pooling 10–20 samples would probably not pass current authorization criteria (>95% sensitivity).

Going forward, screening strategies need to be reviewed separately from traditional diagnostic testing, taking into consideration the repeated testing of individuals performed during screening. For strategies considering twice-weekly sampling, such as in the reopening plans for many US colleges, even if larger pools have lower sensitivity per test, the probability of 2 repeated false-negative results for any person will often be less than the probability of a false-negative result for a single test from a small pool. For example, a small pool (or individual test) may have the probability of a false-negative result of 2% but cost may limit testing to once per week. Conversely, the lower per-person cost of a large pool with a per-test probability of a false-negative result of 14% is more likely to allow for testing twice per week. Therefore, persons tested twice in larger pools have a per-week false-negative probability of only 1.96%. In the context of prolonged community screening, sensitivity should be thought of as per unit time, and the testing regimen should be taken into account.

Our estimates are conservative; the number of tests required is most likely lower than predicted, especially if behavioral or geographic information can be used to stratify the population so that the adaptive pooling strategy can be applied differentially to different sampled subpopulations. However, this approach needs to be balanced with feasibility in the laboratory because pooled testing adds additional steps and complexity to the system, all of which must be reliably implemented. Furthermore, pooled approaches could incorporate retesting individual samples from pools generating any SARS-CoV-2–specific signal in quantitative reverse transcription PCR regardless of C_t (in place of those pools with the <38 C_t cutoff applied here) (*9*). Although pooling has traditionally focused on extracted nucleic acid before quantitative reverse transcription PCR (*10*–*12*), because of the expense of RNA extraction and a comparable effect on detection sensitivity (Appendix), we recommend pooling before RNA extraction. Validation of our work in additional settings and on a larger scale will help better inform our models.

The cost-savings benefits of adaptive pooling saliva for community screening for SARS-CoV-2 provides a mechanism to maintain testing as virus spread

is brought under control and to avoid resurgence. Even if prevalence is very low, it is probably desirable to increase pool sizes before stopping testing altogether. Together with the ease of saliva collection, pooling samples should be considered as an effective testing strategy for expanding the breadth of testing and continued screening during the ongoing COVID-19 pandemic.

Yale IMPACT Research Team authors: Kelly Anastasio Michael H. Askenase, Maria Batsu, Sean Bickerton, Kristina Brower, Molly L. Bucklin, Staci Cahill, Yiyun Cao, Edward Courchaine, Giuseppe DeIuliis, Rebecca Earnest, Bertie Geng, Ryan Handoko, Christina A. Harden, Chaney C. Kalinich, William Khoury-Hanold, Daniel Kim, Lynda Knaggs, Maxine Kuang, Eriko Kudo, Melissa Linehan, Peiwen Lu, Alice Lu-Culligan, Anjelica Martin, Irene Matos, David McDonald, Maksym Minasyan, Adam J. Moore, M. Catherine Muenker, Nida Naushad, Allison Nelson, Jessica Nouws, Abeer Obaid, Camila Odio, Ji Eun Oh, Saad Omer, Isabel M. Ott, Annsea Park, Hong-Jai Park, Xiaohua Peng, Mary Petrone, Sarah Prophet, Tyler Rice, Kadi-Ann Rose, Lorenzo Sewanan, Lokesh Sharma, Denise Shepard, Mikhail Smolgovsky, Nicole Sonnert, Yvette Strong, Codruta Todeasa, Maria Tokuyama, Jordan Valdez, Sofia Velazquez, Arvind Venkataraman, Pavithra Vijayakumar, Elizabeth B. White, and Yexin Yang.

Acknowledgments

We gratefully acknowledge the study participants for their time and commitment to the study. We thank all members of the clinical team at Yale-New Haven Hospital for their dedication and work, which made this study possible. We also thank S. Taylor and P. Jack for technical discussions.

This study was supported by the Huffman Family Donor Advised Fund (N.D.G.), Fast Grant funding support from the Emergent Ventures at the Mercatus Center, George Mason University (N.D.G.), the Yale Institute for Global Health (N.D.G.), and the Beatrice Kleinberg Neuwirth Fund (A.I.K.). C.B.F.V. is supported by NWO Rubicon 019.181EN.004.

About the Author

Ms. Watkins is a master's degree student and research assistant in Epidemiology of Microbial Diseases, Yale School of Public Health, in New Haven, CT. Her primary research interests are the intersection of infectious and chronic diseases with a focus on respiratory and neurologic pathogens.

References

1. Cherif A, Grobe N, Wang X, Kotanko P. Simulation of pool testing to identify patients with coronavirus disease 2019 under conditions of limited test availability. JAMA Netw Open. 2020;3:e2013075. https://doi.org/10.1001/jamanetworkopen.2020.13075
2. Abdalhamid B, Bilder CR, McCutchen EL, Hinrichs SH, Koepsell SA, Iwen PC. Assessment of specimen pooling to conserve SARS CoV-2 testing resources. Am J Clin Pathol. 2020;153:715–8. https://doi.org/10.1093/ajcp/aqaa064
3. Yokota I, Shane PY, Okada K, Unoki Y, Yang Y, Inao T, et al. Mass screening of asymptomatic persons for SARS-CoV-2 using saliva. Clin Infect Dis. 2020 Sep 25 [Epub ahead of print]. https://doi.org/10.1093/cid/ciaa1388
4. Vogels CBF, Brackney D, Wang J, Kalinich CC, Ott I, Kudo E, et al. SalivaDirect: simple and sensitive molecular diagnostic test for SARS-CoV-2 surveillance [cited 2021 Jan 27]. https://www.cell.com/med/pdf/S2666-6340(20)30076-3.pdf
5 Landry ML, Criscuolo J, Peaper DR. Challenges in use of saliva for detection of SARS CoV-2 RNA in symptomatic outpatients. J Clin Virol. 2020;130:104567. https://doi.org/10.1016/j.jcv.2020.104567
6. Wyllie AL, Fournier J, Casanovas-Massana A, Campbell M, Tokuyama M, Vijayakumar P, et al. Saliva or nasopharyngeal swab specimens for detection of SARS-CoV-2. N Engl J Med. 2020;383:1283–6. https://doi.org/10.1056/NEJMc2016359
7. Larremore DB, Wilder B, Lester E, Shehata S, Burke JM, Hay JA, et al. Test sensitivity is secondary to frequency and turnaround time for COVID-19 surveillance. Sci Adv. 2021;7:eabd5393. https://doi.org/10.1126/sciadv.abd5393
8. Quest Diagnostics. Quest SARS-CoV-2 rRT-PCR package insert [cited 2020 Aug 20]. https://www.fda.gov/media/136231
9. Pasomsub E, Watcharananan SP, Watthanachockchai T, Rakmanee K, Tassaneetrithep B, Kiertiburanakul S, et al. Saliva sample pooling for the detection of SARS-CoV-2. J Med Virol. 2020 Aug 25 [Epub ahead of print]. https://doi.org/10.1002/jmv.26460
10. Eis-Hübinger AM, Hönemann M, Wenzel JJ, Berger A, Widera M, Schmidt B, et al. Ad hoc laboratory-based surveillance of SARS-CoV-2 by real-time RT-PCR using minipools of RNA prepared from routine respiratory samples. J Clin Virol. 2020;127:104381. https://doi.org/10.1016/j.jcv.2020.104381
11. Wyllie AL, Rümke LW, Arp K, Bosch AATM, Bruin JP, Rots NY, et al. Molecular surveillance on *Streptococcus pneumoniae* carriage in non-elderly adults; little evidence for pneumococcal circulation independent from the reservoir in children. Sci Rep. 2016;6:34888. https://doi.org/10.1038/srep34888
12. Yelin I, Aharony N, Tamar ES, Argoetti A, Messer E, Berenbaum D, et al. Evaluation of COVID-19 RT-qPCR test in multi-sample pools. Clin Infect Dis. 2020;71:2073–8. https://doi.org/10.1101/2020.03.26.20039438

Address for correspondence: Anne L. Wyllie, Yale School of Public Health, 60 College St, New Haven, CT 06511, USA; email: anne.wyllie@yale.edu; Eli P. Fenichel, Kroon Hall, 195 Prospect St, New Haven, CT 06511, USA; email: eli.fenichel@yale.edu

SARS-CoV-2 Seropositivity among US Marine Recruits Attending Basic Training, United States, Spring–Fall 2020

Andrew G. Letizia, Yongchao Ge, Carl W. Goforth, Dawn L. Weir, Rhonda Lizewski, Stephen Lizewski, Alessandra Soares-Schanoski, Sindhu Vangeti, Nada Marjanovic, Stuart C. Sealfon, Irene Ramos

In a study of US Marine recruits, seroprevalence of severe acute respiratory syndrome coronavirus 2 IgG was 9.0%. Hispanic and non-Hispanic Black participants and participants from states affected earlier in the pandemic had higher seropositivity rates. These results suggest the need for targeted public health strategies among young adults at increased risk for infection.

Coronavirus disease (COVID-19) cases are increasing in young adults (*1*). In some instances, prevalence among younger adults exceeds that of older adults (*2*). Younger adults often have a paucisymptomatic or asymptomatic response to infection (*3*). The potential for rapid spread exists within this age group (*4*). Without active serologic surveillance, cases among young adults might not be identified and the cumulative incidence underestimated. Well-defined cohorts are needed to assess the proportion of young adults who have severe acute respiratory syndrome coronavirus 2 (SARS-CoV-2) antibodies (*5*). We studied the seroprevalence of SARS-CoV-2 IgG among US Marine recruits preparing for basic training at Marine Corps Recruit Depot Parris Island, South Carolina.

The Study

Before beginning basic training, recruits quarantined for 2 weeks at a hotel or college campus as previously described (*6*). Within 48 hours of arriving at the quarantine location, ≈350–500 recruits per week were offered the opportunity to volunteer for the COVID-19 Health Action Response for Marines Study, which included collecting baseline SARS-CoV-2 serologic test results.

We collected paper questionnaires and assayed serum samples for the presence of SARS-CoV-2 IgG upon participants' arrival at the quarantine location. We tested serum specimens for SARS-CoV-2 IgG by ELISA (*6*) (Appendix, https://wwwnc.cdc.gov/EID/article/27/4/20-4732-App1.pdf). The association between demographics, risk factors, and IgG-positivity variables were analyzed with logistic regression to determine the p value and odds ratio (OR).

The study protocol was approved by the Naval Medical Research Center Institutional Review Board in compliance with all applicable Federal regulations governing the protection of human subjects. All participants provided written informed consent for participation.

During May 11–September 7, 2020, we enrolled 3,249 (69.8%) volunteers out of 4,657 eligible recruits; because the minimum age was 18, 530/5,187 (10.2%) persons who were 17 years of age were ineligible. Valid IgG data were obtained for 3,196/3,249 (98.4%) participants. Most participants were from the Eastern United States or states with larger populations (Figure 1). Study participants had a median age of 19.1 (range 18–31) years, and 257 (8.0%) were women (Table 1). Participants 18–20 years of age (2,748 [86.0%]) were overrepresented in our cohort compared with 3.9% in the general US population according to 2020 Census data. When compared with 2020 Census data for persons 18–20 years of age, our cohort had a similar percentage of Hispanic participants (23.9% compared with 23.9%) and non-Hispanic Black participants (12.04% compared with 15.04%) (*7*).

Author affiliations: Naval Medical Research Center, Silver Spring, Maryland, USA (A.G. Letizia, C.W. Goforth, D.L. Weir); Icahn School of Medicine at Mount Sinai, New York, New York, USA (Y. Ge, A. Soares-Schanoski, S. Vangeti, N. Marjanovic, S.C. Sealfon, I. Ramos); Naval Medical Research Unit 6, Lima, Peru (R. Lizewski, S. Lizewski)

DOI: https://doi.org/10.3201/eid2704.204732

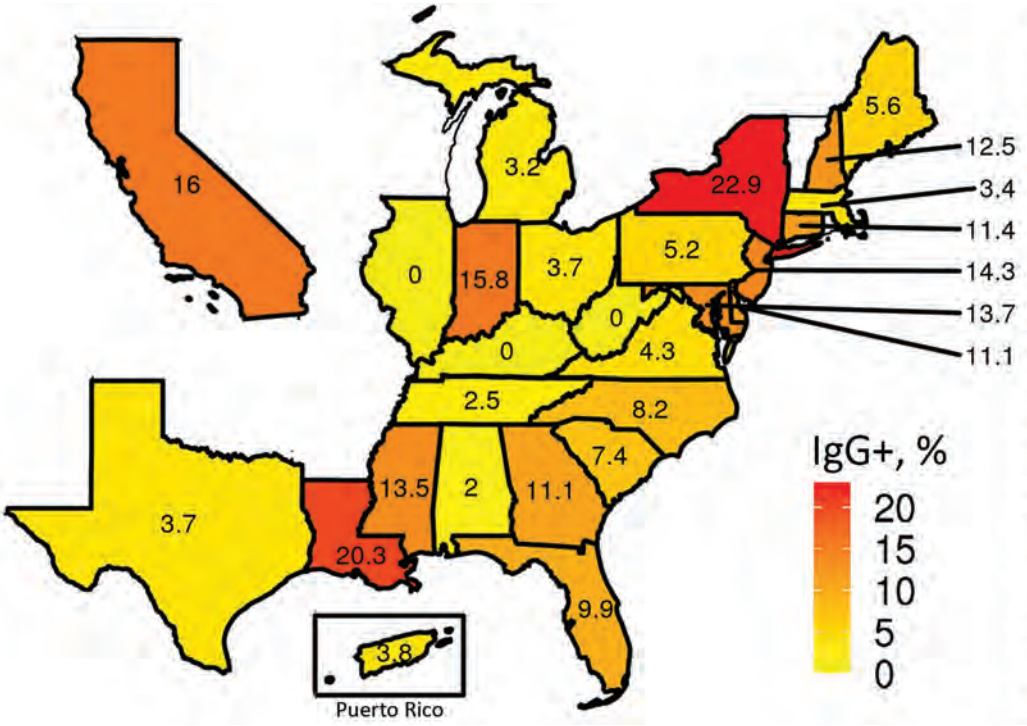

State	No.	F, %	IgG+, %
FL	434	5.3	9.9
NY	292	4.1	22.9
GA	270	4.1	11.1
OH	217	4.1	3.7
PA	192	3.6	5.2
VA	188	5.9	4.3
NC	184	3.8	8.2
MI	156	5.1	3.2
NJ	140	4.3	14.3
TN	120	5.0	2.5
AL	100	3.0	2.0
MD	95	5.3	13.7
SC	94	4.3	7.4
MA	89	4.5	3.4
LA	69	1.4	20.3
KY	65	3.1	0.0
CT	44	4.5	11.4
MS	37	2.7	13.5
WV	29	3.4	0.0
TX	27	81.5	3.7
PR	26	0.0	3.8
CA	25	84.0	16.0
NH	24	0.0	12.5
IN	19	26.3	15.8
DE	18	5.6	11.1
ME	18	11.1	5.6
IL	13	69.2	0.0

Figure 1. Percentage of severe acute respiratory syndrome coronavirus 2 IgG-positive recruits from US states or territories with ≥10 participants in the COVID-19 Health Action Response for Marines Study, May 11–September 7, 2020. The table lists the number of participants and the percentage of women.

Upon arrival at quarantine, 28/3,196 (0.9%) participants were SARS-CoV-2–positive by PCR and 289/3,196 (9.0%) were ELISA-positive for SARS-CoV-2 IgG targeting the receptor-binding domain of the spike protein. A total of 135/768 (17.6%) participants who identified as Hispanic were positive for SARS-CoV-2 IgG (Table 2), higher than the percentage of non-Hispanic White participants (80/1,817 [4.4%]) (OR 3.80, 95% CI 2.82–5.14; p<0.001). Hispanic participants also had higher rates of IgG seropositivity among weekly cohorts throughout the study period, and those rates increased with time (trend p<0.00017); seropositivity rates rose from 12.1% in May and June to 22.3% in July and August. Similarly, non-Hispanic Black participants had higher prevalence of SARS-CoV-2 IgG (62/414 [15.0%]) than non-Hispanic White participants (OR 3.54, 95% CI 2.47–5.05; p<0.001). Seropositivity was also greater in women (32/257, 12.5%) than men (257/2,939, 8.7%) (OR 1.57, 95% CI 1.02–2.33; p = 0.033).

Because participants came from states that were affected by COVID-19 at different times and in variable intensity, we grouped participants' states of origin into 3 categories on the basis of when confirmed COVID-19 cases began to increase in each state (Appendix) (*8*). The groups were early spring, for states in which the outbreak began in March; late spring, for states in which the outbreak began in early June; and summer, for states in which the outbreak began in late June–July (Figure 2, panel A). We plotted weekly IgG-positivity rates during the 17-week study period (Figure 2, panel B) and found that participants from the early spring states had higher IgG seropositivity compared with late spring and summer and maintained a similar rate for the duration of the study. Overall, SARS-CoV-2 IgG seropositivity among participants from summer states (43/994 [4.3%]) and late spring states (126/1,389 [9.1%]) was much lower than in participants from early spring states (110/701 [15.7%]); OR was 0.35 (0.23–0.50; p<0.001) for summer and late spring states and 0.61 (0.46–0.81; p = 0.001) for early spring states. Figure 2, panel C, shows the weekly IgG-positive rate by race and ethnicity.

Conclusions

By using a cross-sectional study design during a 17-week period, the baseline seroprevalence of IgG against SARS-CoV-2 in US Marine recruits primarily from the eastern United States was 9.0%. In the United States, young adults have demonstrated higher levels of SARS-CoV-2–specific antibodies than persons of other ages (*9*). Among persons 18–20 years of age, low adherence to recommendations for social distancing, wearing of masks, and other public health

measures might increase their level of exposure compared with older persons (*10*). The high rate of asymptomatic infection in this age group (*6*) likely leads to underestimates of the cumulative incidence. Subsequent spread could contribute to infections among more vulnerable populations (*11*). Therefore, this age group represents an at-risk population that should be considered for COVID-19 monitoring and other targeted public health measures.

The participants in our study did not come from a cohort of convenience, a group at high risk, or a group receiving medical care; rather, they were selected from a group of young adults for the primary purpose of assessing baseline seropositivity. This process minimized selection bias (*12*), excluding the self-selection that occurred because participants chose to join the US Marine Corps and enroll in our study. Enrollment rate (70%) was high, which increased the likelihood that we studied a representative sample of recruits.

Consistent with other reports (*13*), Hispanic participants had higher IgG seroprevalence (OR 3.80) than non-Hispanic White participants in a multivariable logistic regression. This trend was similar for non-Hispanic Black participants and participants residing in states affected earlier in the pandemic. Our cohort was primarily young adults, many of whom had never held full-time jobs and might not represent essential workers, who have been associated with higher rates of infection among minority groups (*14*). It has been proposed that the higher incidence of SARS-CoV-2 in minority communities is associated with lower socioeconomic status and the associated inability to telecommute, leading to increased workplace exposure (C.T. Rentsch, unpub. data, https://doi.org/10.1101/2020.05.12.20099135). Instead, these data could demonstrate the downstream effects of residing with an essential worker or could reflect intrinsic risk within a community.

Table 1. Demographics of 3,196 COVID-19 Health Action Response for Marines study participants with valid IgG data, United States, May 11–September 7, 2020*

Characteristic	Total
Age, y, mean (SD)	19.1 (1.9)
Sex	
M	2,939 (92.0)
F	257 (8.0)
Race or ethnicity	
Non-Hispanic White	1,817 (56.9)
Non-Hispanic Black	414 (13.0)
Non-Hispanic other†	197 (6.2)
Hispanic	768 (24.0)
IgG	
Negative	2,907 (91.0)
Positive	289 (9.0)
COVID-19 by PCR	
Negative	3,054 (95.6)
Positive	28 (0.9)
Other‡	114 (3.6)
State group§	
Early spring	701 (21.9)
Late spring	1,389 (43.5)
Summer	994 (31.1)
Other‡	112 (3.5)
Resides in a country other than the United States	
No	3,084 (96.5)
Yes	23 (0.7)
Other‡	89 (2.8)
Born in a country other than the United States	
No	2,928 (91.6)
Yes	231 (7.2)
Other‡	37 (1.2)

*Values are no. (%) except as indicated. COVID-19, coronavirus disease.
†Non-Hispanic other also includes participants with missing values.
‡Inconclusive assay or the participant left question blank or answered by marking unknown.
§Defined in Figure 2, panel A, and the Appendix (https://wwwnc.cdc.gov/EID/article/27/4/20-4732-App1.pdf).

Table 2. Association between demographic variables and SARS-CoV-2 IgG results in study of seroprevalence in US Marine recruits, United States, May 11–September 7, 2020*

	IgG result		Univariable analysis		Multivariable analysis	
Characteristic	Negative	Positive	OR (95% CI)	p value	OR (95% CI)	p value
Age, y, mean (SD)	19.1 (1.9)	19.0 (1.7)	0.99 (0.92–1.05)	0.672	0.96 (0.89–1.02)	0.212
Sex						
M	2682 (91.3)	257 (8.7)	Referent		Referent	
F	225 (87.5)	32 (12.5)	1.48 (0.99–2.17)	0.048	1.57 (1.02–2.33)	0.033
Race or ethnicity						
Non-Hispanic White	1737 (95.6)	80 (4.4)	Referent		Referent	
Non-Hispanic Black	352 (85.0)	62 (15.0)	3.82 (2.69–5.42)	<0.001	3.54 (2.47–5.05)	<0.001
Non-Hispanic Other	185 (93.9)	12 (6.1)	1.41 (0.72–2.54)	0.283	1.32 (0.67–2.39)	0.388
Hispanic	633 (82.4)	135 (17.6)	4.63 (3.47–6.22)	0.001	3.80 (2.82–5.14)	<0.001
State group						
Early spring	591 (84.3)	110 (15.7)	Referent		Referent	
Late spring	1263 (90.9)	126 (9.1)	0.54 (0.41–0.71)	<0.001	0.61 (0.46–0.81)	0.001
Summer	951 (95.7)	43 (4.3)	0.24 (0.17–0.35)	<0.001	0.35 (0.23–0.50)	<0.001
Other†	102 (91.1)	10 (8.9)	0.53 (0.25–0.99)	0.065	0.54 (0.25–1.04)	0.085

*Values are no. (%) except as indicated. Univariable odds ratio and p value were computed on the basis of the logistic regression with a single variable only. Multivariable odds ratio and p value were computed by using all 4 variables in the model. OR, odds ratio; SARS-CoV-2, severe acute respiratory syndrome coronavirus 2.
†Inconclusive assay (not residing in the United States) or participants left residence question blank or answered by marking unknown.

Our study incorporates participants from multiple states and represents a diverse mix of race, ethnicity, and backgrounds, providing a unique assessment relevant to public health concerns among persons 18–20 years of age. Conversely, the study results are not representative of the population as a whole, especially children and older adults. Even among young adults, the results are specific to persons who chose to join the US Marine Corps. Additional limitations include a lack of information regarding exposure, participant risk-taking behavior before enrollment, and lack of confirmation of COVID-19 by PCR before study enrollment.

In our study, the seroprevalence of SARS CoV-2 IgG among a cohort of predominately young men

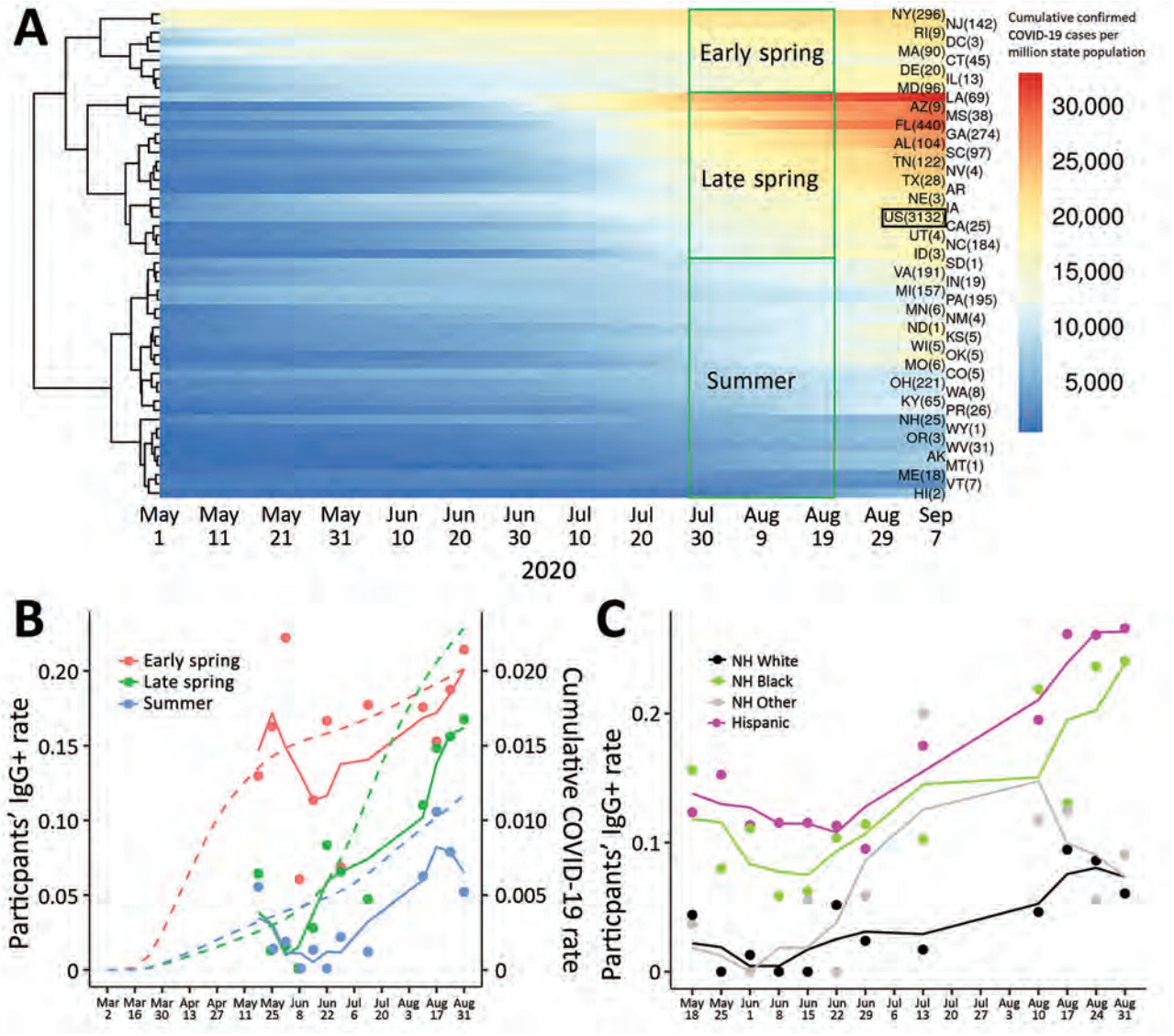

Figure 2. Confirmed COVID-19 and severe acute respiratory syndrome coronavirus 2 (SARS-CoV-2) IgG-positivity by state, race, and ethnicity, in a study of US Marine recruits, May 11–September 7, 2020. A) Heatmap of cumulated confirmed COVID-19 cases normalized by each state's population. Each row represents 1 state, and number in parentheses indicates number of participants. Color reflects cumulative PCR-confirmed cases per 1 million state population (data obtained from COVID-19 Data Repository by the Center for Systems Science and Engineering at Johns Hopkins University, https://github.com/CSSEGISandData/COVID-19). Each column indicates 1 day during May 1–September 7, 2020. The US in aggregate is shown in the black box. B) SARS-CoV-2 IgG-seropositivity rate by week of enrollment on the basis of state groupings. Colored dots indicate the weekly IgG-positivity rate for study participants grouped by state; colored solid lines show 3-week running means. Dotted lines indicate cumulative PCR-confirmed COVID-19 cases in each state grouping obtained from COVID-19 Data Repository, including data before the study commenced. C) SARS-CoV-2 IgG-positivity by race and ethnicity. Colored dots indicate weekly IgG-positivity rate for study participants; colored solid lines indicate 3-week running means. Because of the relatively small number of participants in the first study week (May 11), they are merged into May 18 data. COVID-19, coronavirus disease; NH, Non-Hispanic.

was 9.0%. Multivariable analysis showed incidence rates were significantly higher in women, Hispanic participants, Non-Hispanic Black participants, and participants from states that were affected earlier in the pandemic. These data can help inform surveillance and management strategies, as well as targeted public health interventions, for this age group.

Acknowledgments

We thank the devoted US Marine Corps recruits who volunteered for this study; Sagie Mofsowitz, Mary Anne Amper, Nitish Seenarine, Mital Vasoya, and Natalia Mendelev for technical assistance; and Russell Tracy for providing pre-COVID-19 serum samples used as negative controls. We also thank Capt. Adam Armstrong for his strategic guidance throughout the study and the many US Navy corpsmen who assisted in logistics and sample acquisition.

This work was supported by a grant (9700130) from the Defense Health Agency through the Naval Medical Research Center and by the Defense Advanced Research Projects Agency (contract no. N6600119C4022). The views expressed in this article are those of the authors and do not necessarily reflect the official policy or position of the Department of the Navy, Department of Defense, or the US Government.

About the Author

Dr. Andrew Letizia is the head of the Emerging Infectious Disease Department and Deputy Director of the Infectious Disease Directorate at the Naval Medical Research Center in Silver Spring, Maryland, USA. He is a board-certified infectious disease physician on active duty in the US Navy.

References:

1. Cunningham JW, Vaduganathan M, Claggett BL, Jering KS, Bhatt AS, Rosenthal N, et al. Clinical outcomes in young US adults hospitalized with COVID-19. JAMA Intern Med. 2020 Sep 9 [Epub ahead of print]. https://doi.org/10.1001/jamainternmed.2020.5313
2. Amorim Filho L, Szwarcwald CL, Mateos SOG, Leon ACMP, Medronho RA, Veloso VG, et al.; Grupo Hemorio de Pesquisa em Covid-19. Seroprevalence of anti-SARS-CoV-2 among blood donors in Rio de Janeiro, Brazil. Rev Saude Publica. 2020;54:69. https://doi.org/10.11606/s1518-8787.2020054002643
3. Payne DC, Smith-Jeffcoat SE, Nowak G, Chukwuma U, Geibe JR, Hawkins RJ, et al.; CDC COVID-19 Surge Laboratory Group. SARS-CoV-2 infections and serologic responses from a sample of U.S. Navy service members—USS Theodore Roosevelt, April 2020. MMWR Morb Mortal Wkly Rep. 2020;69:714–21. https://doi.org/10.15585/mmwr.mm6923e4
4. Huang L, Zhang X, Zhang X, Wei Z, Zhang L, Xu J, et al. Rapid asymptomatic transmission of COVID-19 during the incubation period demonstrating strong infectivity in a cluster of youngsters aged 16-23 years outside Wuhan and characteristics of young patients with COVID-19: a prospective contact-tracing study. J Infect. 2020;80:e1–13. https://doi.org/10.1016/j.jinf.2020.03.006
5. Lipsitch M, Swerdlow DL, Finelli L. Defining the epidemiology of Covid-19—studies needed. N Engl J Med. 2020;382:1194–6. https://doi.org/10.1056/NEJMp2002125
6. Letizia AG, Ramos I, Obla A, Goforth C, Weir DL, Ge Y, et al. SARS-CoV-2 transmission among Marine recruits during quarantine. N Engl J Med. 2020;383:2407–16. https://doi.org/10.1056/NEJMoa2029717
7. United States Census Bureau. National demographic analysis tables: 2020. 2020 [cited 2020 Dec 20]. https://www.census.gov/data/tables/2020/demo/popest/2020-demographic-analysis-tables.html
8. Dong E, Du H, Gardner L. An interactive web-based dashboard to track COVID-19 in real time. Lancet Infect Dis. 2020;20:533–4. https://doi.org/10.1016/S1473-3099(20)30120-1
9. Bajema KL, Wiegand RE, Cuffe K, Patel SV, Iachan R, Lim T, et al. Estimated SARS-CoV-2 seroprevalence in the US as of September 2020. JAMA Intern Med. 2020 Nov 24 [Epub ahead of print]. https://doi.org/10.1001/jamainternmed.2020.7976
10. Nivette A, Ribeaud D, Murray A, Steinhoff A, Bechtiger L, Hepp U, et al. Non-compliance with COVID-19-related public health measures among young adults in Switzerland: insights from a longitudinal cohort study. Soc Sci Med. 2021;268:113370. https://doi.org/10.1016/j.socscimed.2020.113370
11. Gao Z, Xu Y, Sun C, Wang X, Guo Y, Qiu S, et al. A systematic review of asymptomatic infections with COVID-19. J Microbiol Immunol Infect. 2020 May 15 [Epub ahead of print]. https://doi.org/10.1016/j.jmii.2020.05.001
12. Anand S, Montez-Rath M, Han J, Bozeman J, Kerschmann R, Beyer P, et al. Prevalence of SARS-CoV-2 antibodies in a large nationwide sample of patients on dialysis in the USA: a cross-sectional study. Lancet. 2020;396:1335–44. https://doi.org/10.1016/S0140-6736(20)32009-2
13. Martinez DA, Hinson JS, Klein EY, Irvin NA, Saheed M, Page KR, et al. SARS-CoV-2 positivity rate for Latinos in the Baltimore-Washington, DC region. JAMA. 2020;324:392–5. https://doi.org/10.1001/jama.2020.11374
14. Williams JC, Anderson N, Holloway T, Samford E III, Eugene J, Isom J. Reopening the United States: Black and Hispanic workers are essential and expendable again. Am J Public Health. 2020;110:1506–8. https://doi.org/10.2105/AJPH.2020.305879

Address for correspondence: Andrew G. Letizia, Naval Medical Research Center, 503 Robert Grant Ave, Silver Spring, MD 20910, USA; email: Andrew.G.Letizia.mil@mail.mil; Irene Ramos, Icahn School of Medicine at Mount Sinai, Annenberg 14-83, 1 Gustave L. Levy Pl, New York, NY 10029, USA; email: irene.ramos-lopez@mssm.edu

Experimental SARS-CoV-2 Infection of Bank Voles

Lorenz Ulrich,[1] Anna Michelitsch,[1] Nico Halwe,[1] Kerstin Wernike, Donata Hoffmann, Martin Beer

After experimental inoculation, severe acute respiratory syndrome coronavirus 2 infection was confirmed in bank voles by seroconversion within 8 days and detection of viral RNA in nasal tissue for up to 21 days. However, transmission to contact animals was not detected. Thus, bank voles are unlikely to establish effective transmission cycles in nature.

Severe acute respiratory syndrome coronavirus 2 (SARS-CoV-2) led to a global pandemic in the human population within months after its first reporting (*1*). Potential wildlife reservoirs of SARS-CoV-2 remain unknown; susceptibility of various animal species has been described (*2*,*3*). Among rodent species, the Syrian hamster (*Mesocricetus auratus*) (*4*) and the North American deer mouse (*Peromyscus maniculatus*) (A. Fagre et al., unpub. data, https://doi.org/10.1101/2020.08.07.241810; B.D. Griffin et al., unpub.data,https://doi.org/10.1101/2020.07.25.221291), both *Cricetidae* species, have proved to be highly susceptible. These rodents transmit SARS-CoV-2 to co-housed contact animals and therefore are likely to develop effective infection chains, which could result in independent SARS-CoV-2 transmission cycles in nature and sequential reintroduction to the human population (*4*; B.D. Griffin et al., unpub. data, https://doi.org/10.1101/2020.07.25.221291). In Europe, bank voles (*Myodes glareolus*) are a widespread *Cricetidae* species (*5*). We aimed to characterize SARS-CoV-2 infection in bank voles and their ability to maintain sustainable infection chains.

We intranasally inoculated 9 bank voles with SARS-CoV-2 strain Muc-IMB-1 and, 24 hours later, co-housed 1 contact animal with each of 3 groups of 3 inoculated animals (donor–recipient ratio [d:r] 3:1). We took swab samples regularly from all animals (Appendix, https://wwwnc.cdc.gov/EID/article/27/4/20-4945-App1.pdf); we euthanized 1 or 2 animals at predefined times (Appendix). One bank vole did not survive initial anesthesia for inoculation.

Neither inoculated nor contact animals showed clinical signs during the study. We detected seroconversion for all directly inoculated animals euthanized 8, 12, and 21 days postinfection (dpi), whereas the animals euthanized 4 dpi and the contact animals were all clearly seronegative for SARS-CoV-2 antibodies in an already validated indirect multispecies ELISA based on the receptor-binding domain (*6*).

All directly inoculated bank voles tested positive for SARS-CoV-2 by quantitative reverse transcription PCR (qRT-PCR) by oral and rhinarium swab specimens at 2 dpi. At 4 dpi, 5 of these 8 animals were positive by oral swab specimen; 2 were also positive by rhinarium swab specimen. On both sampling days, rectal swab specimens of 2 animals tested positive for SARS-CoV-2 by qRT-PCR. Groupwise collected fecal samples also tested positive by qRT-PCR at 2 and 4 dpi. All swabs collected 8, 12, and 16 dpi from directly inoculated animals and every swab from the co-housed contact animals tested negative by qRT-PCR (Table; Figure).

Two animals were euthanized at 4 dpi; nasal conchae, trachea, lung, and olfactory bulb samples tested positive for SARS-CoV-2 RNA by qRT-PCR (quantification cycle [Cq] 25.45–37.15). One animal showed viral genome in cerebrum and cerebellum samples, whereas the spleen sample from the other animal was positive for the viral genome. At 8 dpi another 2 animals were euthanized; both exhibited viral RNA only within the nasal conchae. The animal euthanized at 12 dpi was negative in all collected tissue samples. Nasal conchae of 3 inoculated animals euthanized at 21 dpi tested positive by qRT-PCR (Cq values 34.78, 34.97, 36.25), whereas all 3 contact animals euthanized at the same time tested negative in the nasal conchae.

Reisolation of viable virus from tissue materials in cell culture (Vero E6) was successful for 1 nasal conchae sample taken at 4 dpi. However, isolation

Author affiliation: Friedrich-Loeffler-Institut, Greifswald–Insel Riems, Germany

DOI: https://doi.org/10.3201/eid2704.204945

[1]These authors contributed equally to this article.

Table. Quantitative reverse transcription PCR results of swab sampling for all inoculated and contact bank voles in experimental study of SARS-CoV-2 transmission*

Box	Status	Swab	−1 dpi	2 dpi	4 dpi	8 dpi	12 dpi	16 dpi
Box 1	Inoculated	Oral	Neg	32.45	Neg	Neg	Neg	Neg
		Nasal	Neg	32.29	Neg	Neg	Neg	Neg
		Rectal	Neg	Neg	Neg	Neg	Neg	Neg
	Inoculated	Oral	Neg	NA	NA	NA	NA	NA
		Nasal	Neg	NA	NA	NA	NA	NA
		Rectal	Neg	NA	NA	NA	NA	NA
	Inoculated	Oral	Neg	32.09	28.16	Neg	Neg	Neg
		Nasal	Neg	31.72	34.03	Neg	Neg	Neg
		Rectal	Neg	36.54	36.39	Neg	Neg	Neg
	Contact	Oral	Neg	Neg	Neg	Neg	Neg	Neg
		Nasal	Neg	Neg	Neg	Neg	Neg	Neg
		Rectal	Neg	Neg	Neg	Neg	Neg	Neg
	Collected feces		Neg	36.58	37.66	Neg	Neg	Neg
Box 2	Inoculated	Oral	Neg	29.40	32.41	NA	NA	NA
		Nasal	Neg	32.68	34.72	NA	NA	NA
		Rectal	Neg	Neg	Neg	NA	NA	NA
	Inoculated	Oral	Neg	30.46	32.54	Neg	NA	NA
		Nasal	Neg	32.30	Neg	Neg	NA	NA
		Rectal	Neg	36.67	Neg	Neg	NA	NA
	Inoculated	Oral	Neg	32.72	37.07	Neg	Neg	Neg
		Nasal	Neg	34.74	Neg	Neg	Neg	Neg
		Rectal	Neg	Neg	Neg	Neg	Neg	Neg
	Contact	Oral	Neg	Neg	Neg	Neg	Neg	Neg
		Nasal	Neg	Neg	Neg	Neg	Neg	Neg
		Rectal	Neg	Neg	Neg	Neg	Neg	Neg
	Collected feces		Neg	36.06	36.65	Neg	Neg	Neg
Box 3	Inoculated	Oral	Neg	30.98	Neg	Neg	NA	NA
		Nasal	Neg	31.63	Neg	Neg	NA	NA
		Rectal	Neg	Neg	Neg	Neg	NA	NA
	Inoculated	Oral	Neg	30.66	34.32	NA	NA	NA
		Nasal	Neg	34.52	Neg	NA	NA	NA
		Rectal	Neg	Neg	34.89	NA	NA	NA
	Inoculated	Oral	Neg	32.64	Neg	Neg	Neg	NA
		Nasal	Neg	35.46	Neg	Neg	Neg	NA
		Rectal	Neg	Neg	Neg	Neg	Neg	NA
	Contact	Oral	Neg	Neg	Neg	Neg	Neg	Neg
		Nasal	Neg	Neg	Neg	Neg	Neg	Neg
		Rectal	Neg	Neg	Neg	Neg	Neg	Neg
	Collected feces		Neg	36.62	37.02	Neg	Neg	Neg

*Positive results are given as quantification cycle values. dpi, days postinoculation; NA, not applicable; Neg, negative; SARS-CoV-2, severe acute respiratory syndrome coronavirus 2.

from samples with Cq >28 failed, in line with findings of other groups (*3*,*7*).

Overall, bank voles proved to be susceptible to infection with SARS-CoV-2 but did not transmit the virus to co-housed direct contact animals (initial d:r 3:1), in contrast to highly susceptible hamsters or deer mice, which transmit SARS-CoV-2 to each contact animal (d:r 1:1) within 5 days (*4*; B.D. Griffin et al., unpub. data, https://doi.org/10.1101/2020.07.25.221291). Our results suggest a tissue tropism for SARS-CoV-2 replication in bank voles to the upper respiratory tract, as seen for other species, such as ferrets, fruit bats, and raccoon dogs (*3*,*7*). The persistence of viral genome for at least 3 weeks in nasal tissue of directly inoculated animals was unexpected, especially because the last positive sample was retrieved 4 dpi from the respective bank voles (Table). This finding is most likely the result of the suspected clustering of SARS-CoV-2 infection foci in narrow areas of the upper respiratory tract (L.M. Zaeck et al., unpub. data, https://doi.org/10.1101/2020.10.17.339051). Considering that virus isolation from these 21 dpi samples was not successful, the persistence of SARS-CoV-2 is unlikely to lead to the same shedding of infectious virus as it was shown previously for deer mice (A. Fagre et al., unpub. data, https://doi.org/10.1101/2020.08.07.241810; B.D. Griffin et al., unpub. data, https://doi.org/10.1101/2020.07.25.221291). Deer mice also seem to shed virus through the rectum. However, in bank voles, the SARS-CoV-2 genome could not be detected in the intestines. Although rectal swabs and fecal samples were qRT-PCR positive, the detected Cq values were high, indicating low viral RNA levels. Therefore, the detected viral RNA likely represents residues, which might have resulted from extensive grooming behavior and therefore do not correspond with actual virus shedding from the rectum or feces.

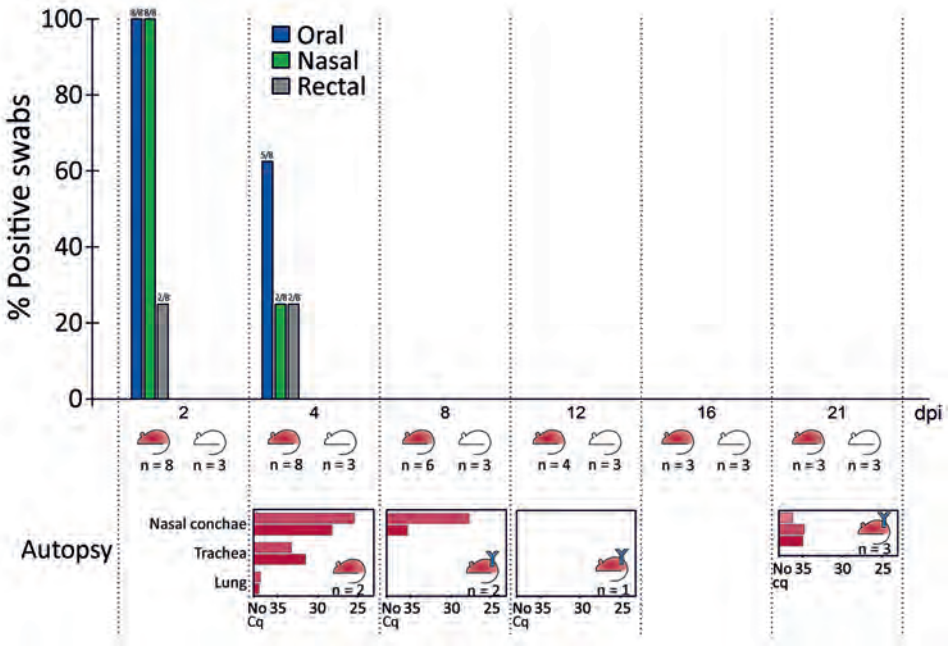

Figure. Percentage of swab specimens positive by quantitative reverse transcription PCR for SARS-CoV-2 on all sampling time points in study of experimental infection of bank voles. The red mouse symbols symbolize inoculated bank voles; the white mouse symbols represent co-housed contact bank voles. Blue Y symbols stand for detected antibodies against SARS-CoV-2 in the respective bank vole group. Quantitative reverse transcription PCR results for the sampled organs of the euthanized, inoculated bank voles are given below the main chart for each time point. Cq, quantification cycle; dpi, days postinoculation; n, number of bank voles; SARS-CoV-2, severe acute respiratory syndrome coronavirus 2.

This study proves a general susceptibility of bank voles toward SARS-CoV-2 infection. However, bank voles did not transmit SARS-CoV-2 to contact animals, making them unlikely to maintain sustainable infection chains in nature. Therefore, the risk of bank voles becoming a reservoir for SARS-CoV-2 in nature (for example, after contact with infected cats) is low.

Acknowledgments

We thank Mareen Lange, Anke Eggert, Bianka Hillmann, Frank Klipp, Doreen Fiedler, and Harald Manthei for their excellent assistance in the lab and dedicated animal care. We are very grateful to Markus Keller for managing the bank vole colony at the Friedrich-Loeffler-Institut and to Roman Wölfel (German Armed Forces Institute of Microbiology) for providing the SARS-CoV-2 isolate used in this study.

This research was supported by intramural funding of the German Federal Ministry of Food and Agriculture provided to the Friedrich-Loeffler-Institut and partial funding from the European Union Horizon 2020 project (Versatile Emerging Infectious Disease Observatory, grant no. 874735).

The experimental protocol was assessed and approved by the ethics committee of the State Office of Agriculture, Food Safety, and Fisheries in Mecklenburg-Western Pomerania (permission no. MV/TSD/7221.3-2-010/18).

About the Author

Mr. Ulrich and Dr. Michelitsch are veterinarians and Mr. Halwe is a biologist at the Friedrich-Loeffler-Institut, Greifswald–Insel Riems, Germany. Their research interests include pathogenesis and prevention of zoonotic viruses.

References

1. Zhu N, Zhang D, Wang W, Li X, Yang B, Song J, et al.; China Novel Coronavirus Investigating and Research Team. A novel coronavirus from patients with pneumonia in China, 2019. N Engl J Med. 2020;382:727–33. https://doi.org/10.1056/NEJMoa2001017
2. Muñoz-Fontela C, Dowling WE, Funnell SGP, Gsell PS, Riveros-Balta AX, Albrecht RA, et al. Animal models for COVID-19. Nature. 2020;586:509–15. https://doi.org/10.1038/s41586-020-2787-6
3. Freuling CM, Breithaupt A, Müller T, Sehl J, Balkema-Buschmann A, Rissmann M, et al. Susceptibility of raccoon dogs for experimental SARS-CoV-2 Infection. Emerg Infect Dis. 2020;26:2982–5. https://doi.org/10.3201/eid2612.203733
4. Sia SF, Yan LM, Chin AWH, Fung K, Choy KT, Wong AYL, et al. Pathogenesis and transmission of SARS-CoV-2 in golden hamsters. Nature. 2020;583:834–8. https://doi.org/10.1038/s41586-020-2342-5
5. Michelitsch A, Wernike K, Klaus C, Dobler G, Beer M. Exploring the reservoir hosts of tick-borne encephalitis virus. Viruses. 2019;11:669. https://doi.org/10.3390/v11070669
6. Wernike K, Aebischer A, Michelitsch A, Hoffmann D, Freuling C, Balkema-Buschmann A, et al. Multi-species ELISA for the detection of antibodies against SARS-CoV-2 in animals. Transbound Emerg Dis. 2020;tbed.13926. https://doi.org/10.1111/tbed.13926
7. Schlottau K, Rissmann M, Graaf A, Schön J, Sehl J, Wylezich C, et al. SARS-CoV-2 in fruit bats, ferrets, pigs, and chickens: an experimental transmission study. Lancet Microbe. 2020;1:e218–25. https://doi.org/10.1016/S2666-5247(20)30089-6

Address for correspondence: Martin Beer, Institute of Diagnostic Virology, Friedrich-Loeffler-Institut, Südufer 10, 17493 Greifswald–Insel Riems, Germany; email: martin.beer@fli.de

Surveillance of COVID-19–Associated Multisystem Inflammatory Syndrome in Children, South Korea

Young June Choe, Eun Hwa Choi, Jong Woon Choi, Byung Wook Eun, Lucy Youngmin Eun, Yae-Jean Kim, Yeo Hyang Kim, Young A. Kim, Yun-Kyung Kim, Ji Hee Kwak, Hyuk Min Lee, Hyunju Lee, Joon Kee Lee, June Dong Park, Eun-Jin Kim, Young Joon Park, Jin Gwack, Sang Won Lee

A concerning development during the coronavirus disease pandemic has been multisystem inflammatory syndrome in children. Reports of this condition in East Asia have been limited. In South Korea, 3 cases were reported to the national surveillance system for multisystem inflammatory syndrome in children. All case-patients were hospitalized and survived with no major disease sequelae.

Amid the coronavirus disease (COVID-19) pandemic, multisystem inflammatory syndrome in children (MIS-C) has emerged as a major concern globally (*1*). MIS-C features clinical characteristics that overlap with Kawasaki disease, including high fever, mucocutaneous involvement, and affecting of coronary arteries. Yet, reports of MIS-C have been limited in East Asia countries, where the incidence of Kawasaki disease is high (*2*).

Although South Korea was one of the countries struck early in the COVID-19 pandemic, spread of the virus there has been relatively contained. However, reports on MIS-C from other countries has necessitated the monitoring of COVID-19–associated MIS-C at the national level. In May 2020, the Korean Society of Pediatric Infectious Diseases, Korean Society of Kawasaki Disease, and Korean Society of Pediatric Critical Care Medicine, with support from the Korea Disease Control and Prevention Agency, created a strategic framework for prospective surveillance of MIS-C in South Korea. In this study, we describe the development of the MIS-C surveillance system and report the clinical characteristics of children meeting the case definition of MIS-C in South Korea.

The Study

First, the Case Assessment Committee (CAC) was established, consisting of 4 pediatric infectious disease specialists, 3 pediatric cardiologists, 3 pediatric intensivists, 1 clinical microbiologist, and 1 epidemiologist. A case reporting form was created, and members of the Korean Pediatric Society (n = 5,891) were contacted to provide assistance with data collection and reporting.

Once a suspected MIS-C case was reported, CAC members quickly assessed whether the case met the clinical criteria for MIS-C case definition. In accordance with the Infectious Disease Control and Prevention Act (chapter 4, article 18), the public health officers then conducted an epidemiologic investigation of all suspected MIS-C cases. For all reported cases, the Korea Disease Control and Prevention Agency performed serologic assays for severe acute respiratory syndrome coronavirus 2 (SARS-CoV-2), including neutralizing antibody tests and the Anti-SARS-CoV-2 ELISA Assay for detection of IgG (EUROIMMUN, https://www.euroimmun.com). CAC meetings were held on an ad hoc basis for case ascertainment,

Author affiliations: Korea University Anam Hospital, Seoul, South Korea (Y.J. Choe); Seoul National University College of Medicine, Seoul (E.H. Choi, H. Lee, J.D. Park); Bundang Jesaeng General Hospital, Seongnam, South Korea (J.W. Choi); Eulji University School of Medicine, Seoul (B.W. Eun); Yonsei University College of Medicine, Seoul (L.Y. Eun, H.M. Lee); Sungkyunkwan University School of Medicine, Seoul (Y.-J. Kim, J.H. Kwak); School of Medicine Kyungpook National University, Daegu, South Korea (Y.H. Kim); Pusan National University Children's Hospital, Yangsan, South Korea (Y.A. Kim); Korea University College of Medicine, Seoul (Y.-K. Kim); Chungbuk National University Hospital, Cheongju, South Korea (J.K. Lee); Korea Disease Control and Prevention Agency, Cheongju (E.-J. Kim, Y.J. Park, J. Gwack, S.W. Lee)

DOI: https://doi.org/10.3201/eid2704.210026

treatment consultation, and exchange of knowledge. The study was approved by the Institutional Review Board of Seoul National University Hospital (approval no. 2012–136–118).

During May–November 2020, a total of 2,287 COVID-19 cases in persons 0–19 years of age were reported (Figure). During the surveillance period, 9 suspected cases of MIS-C were reported to the surveillance system. Of the reported cases, 3 (33%) case-patients had evidence of COVID-19 exposure (positive for SARS-CoV-2 by PCR, SARS-CoV-2 antibody detection, or exposure history), and their illness was assessed as COVID-19–associated MIS-C, which likely occurred 3–4 weeks after the diagnosis of COVID-19 (Table).

The age of case-patients ranged from 11 to 14 years, 2 were boys, and none had preexisting conditions. All case-patients had fever and abdominal symptoms (abdominal pain, nausea, vomiting, or diarrhea) at admission. Mucocutaneous symptoms and signs (mucosal changes, skin rash, extremity changes) occurred in 2 patients, and all patients had documented hypotension (<50th percentile, adjusted for age, sex, and height). All case-patients had marked leukocytosis or elevated inflammatory markers. Echocardiography showed coronary artery dilatation (z-scores 1.64–3.98 mm for left coronary arteries), mitral regurgitation, or left ventricular dysfunction. Chest radiography or computed tomography showed pulmonary edema or pleural effusion. Abdominal ultrasound or computed tomography showed mesenteric lymphadenopathies, hyperechoic liver, or hypertrophic gall bladder. All 3 case-patients received intravenous immunoglobulin (IVIg); 1 patient (case 3) received methylprednisolone pulse therapy and immunomodulatory agent (Anakinra) because of persistent hypotension after initial IVIg treatment. Two patients received inotropic agents and required transfer to the intensive care unit (ICU), but no patients required mechanical ventilation. The duration of hospitalization was 10–19 days, and duration of ICU admission was 6–7 days. All 3 patients received aspirin and have survived to date with no major disease sequelae.

Conclusions

We describe MIS-C surveillance results from South Korea, an East Asia country with high incidence of Kawasaki disease. As of December 15, 2020, COVID-19 had been diagnosed in 4,107 children and adolescents 0–19 years of age in South Korea, which translates roughly to 0.07% of all childhood COVID-19 cases reported in South Korea (*3*). Concern about MIS-C was raised after episodes of increased incidence of Kawasaki-like disease were noted in children after COVID-19 diagnosis in Europe and the United States (*4*,*5*). In South Korea, there was no substantial increase in Kawasaki disease–related hospitalizations in 2020 compared with 2016–2019 (*6*). There might be ethnic differences in susceptibility; only 5% of MIS-C cases in New York (USA) occurred in Asian persons (*7*). Reports from India (*8*), Pakistan (*9*), and Iran (*10*) underscore the importance of monitoring MIS-C cases; however, surveillance data have not yet been reported for East Asia countries. Alongside genetic susceptibility, the

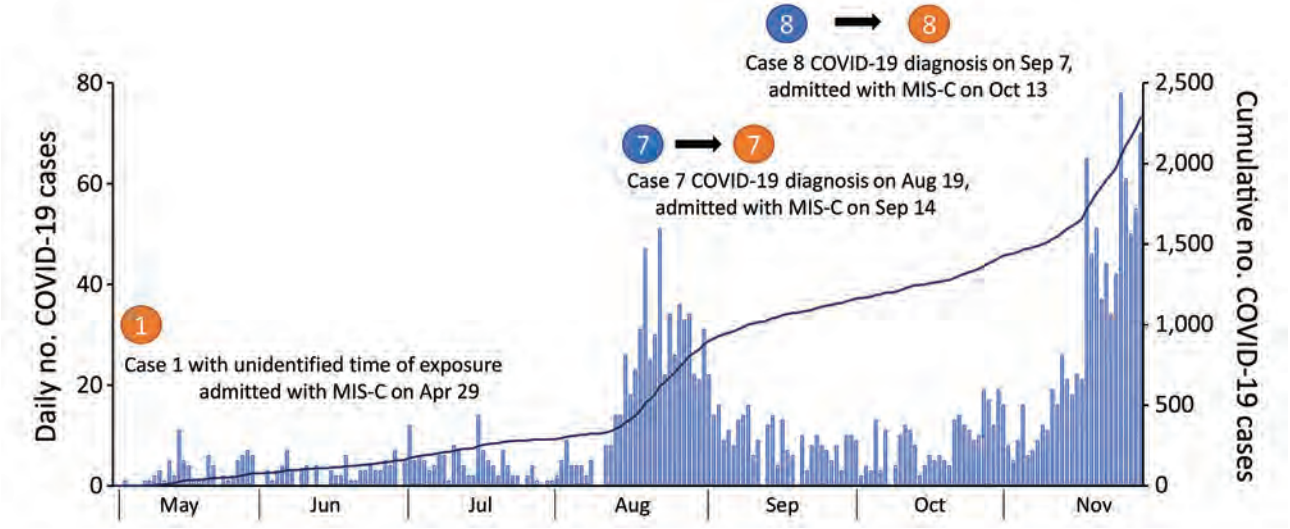

Figure. Daily number (bars) and cumulative number (line) of COVID-19 cases among children 0–19 years of age, South Korea, May–November 2020. The occurrences of the 3 cases of multisystem inflammatory syndrome are indicated. COVID-19, coronavirus disease; MIS-C, multisystem inflammatory syndrome in children.

Table. Demographics, clinical features, treatments, and outcomes of the 3 COVID-19–associated MIS-C case-patients, South Korea, May–November 2020*

Characteristics	Case 1	Case 2	Case 3
Age, y	11	11	14
Sex	Boy	Boy	Girl
Underlying disease	None	None	None
Clinical signs and symptoms			
Initial symptoms	Fever, abdominal pain	Fever, abdominal pain, headache, nausea, vomiting	Fever, abdominal pain, diarrhea
Fever	Present	Present	Present
Conjunctival injection	Present	Present	Present
Mucosal change	Present	None	Present
Skin rash	Present	None	Present
Extremity changes	Present	None	Present
Lymphadenopathy	None	None	None
Gastrointestinal symptoms	Present	Present	Present
Hypotension	Present	Present	Present
Inflammatory markers (peak)			
Leukocyte (neutrophil %), 10^3/μL	7.55 (87)	9.55 (82.8)	26.56 (93)
ESR, mm/h	NT	82	77
CRP, mg/L	18.95	10.36	>30
Fibrinogen, mg/dL	633	NT	NT
Procalcitonin, ng/mL	14.55	1.54	9.62
D-dimer, μg/mL	894	2.5	3.95
Ferritin, μg/mL	NT	2485	663
IL-6, pg/mL	NT	NT	2410
Abnormal imaging studies			
Echocardiography	Coronary dilatation	Mitral regurgitation	Coronary dilatation, left ventricle dysfunction
Chest radiography or CT	Bilateral pleural effusion, pneumonic infiltration	Suspected pulmonary edema	Bilateral pulmonary edema, pleural effusion
Abdominal ultrasound or CT	Abdominal lymphadenopathy	Mesenteric lymphadenopathy	Hyperechoic liver, gallbladder hypertrophic edema, peripancreatic fluids, splenomegaly, scant pelvic ascites
Treatment			
IVIg	Provided	Provided	Provided
ASA	Provided	Provided	Provided
Steroids	Not provided	Not provided	Provided
Immunomodulatory	Not provided	Not provided	Provided (Anakinra)
Inotropic agent	Provided	Not provided	Provided
ICU care	Provided	Not provided	Provided
Mechanical ventilator	Not provided	Not provided	Not provided
Outcome			
Hospitalization, d	12 d	10 d	19 d
ICU admission, d	6 d	NA	7 d
Prognosis	Improved, discharged	Improved, discharged	Improved, discharged

*MIS-C clinical case definition is as follows: age ≤19 y, fever ≥38.0°C for ≥24 h, laboratory evidence of inflammation (i.e., elevation of ESR, CRP, fibrinogen, procalcitonin, d-dimer, ferritin, LDH, IL-6, neutrophilia, lymphopenia, hypoalbuminemia), multisystem involvement (≥2 organ systems involved), severe illness requiring hospitalization, and no other plausible microbial cause of inflammation (i.e., bacterial sepsis, staphylococcal/streptococcal toxic shock syndromes, enteroviral myocarditis). Evidence of SARS-CoV-2 exposure history defined as positive SARS-CoV-2 by RT-PCR, positive serology (neutralizing antibody or anti-SARS-CoV-2 IgG), or exposure to individual with COVID-19 ≤4 weeks before onset of symptoms (epidemiologic linkage with individual or cluster). ASA, acetylsalicylic acid; COVID-19, coronavirus disease 2; CRP, c-reactive protein; CT, computed tomography; ESR, erythrocyte sedimentation rate; ICU, intensive care unit; IL-6, interleukin 6; IVIg, intravenous immunoglobulin; LDH, lactate dehydrogenase; MIS-C, multisystem inflammatory syndrome in children; NA, not applicable; NT, not tested; RT-PCR, reverse transcription PCR; SARS-CoV-2, severe acute respiratory syndrome coronavirus 2.

background incidence of SARS-CoV-2 infection might play a critical role in the occurrence of MIS-C.

Although estimates of risk for MIS-C after SARS-CoV-2 infection are not yet available, we report a rough estimate in South Korea, where COVID-19 testing is widely accessible (*11*). Our findings suggest that the incidence of MIS-C is low among children with COVID-19 in this country. However, COVID-19–associated MIS-C might cause serious clinical outcomes requiring ICU care and might require immunomodulatory agents.

All 3 MIS-C case-patients experienced gastrointestinal symptoms, which is consistent with reports from Italy (*5*), the United States (*12*), and the United Kingdom (*13*) that indicate gastrointestinal symptoms appear to be the most prominent

clinical manifestation of MIS-C. Gastrointestinal involvement might also be a predictor of severe COVID-19. A systematic review of 83 studies showed that diarrhea (odds ratio 1.50, 95% CI 1.10–2.03; p = 0.01) was observed more often in patients with severe COVID-19 compared with patients with nonsevere COVID-19 (*14*). Previously, syndromic involvement of the gastrointestinal system has been associated with higher risk for IVIg resistance and coronary aneurysms in patients with Kawasaki disease (*15*). These features indicate the possibility of a mechanism linking gastrointestinal involvement and syndromic features for MIS-C and Kawasaki-like illness, which needs further elucidation.

The first limitation of this study is that, given the intrinsic properties of a passive surveillance system, only a fraction of actual MIS-C cases might have been reported. Pediatricians are more likely to report cases that result in serious conditions; nonetheless, the case definition included hospitalization. Second, a large proportion of SARS-CoV-2 infections in children are asymptomatic; therefore, passive surveillance that relies on the presence of symptoms might underestimate the actual incidence of MIS-C. Despite these limitations, this study suggests that enhanced passive surveillance, including frequent outreach to pediatricians through academic societies, was a manageable scheme to monitor MIS-C in South Korea. Given that the level of SARS-CoV-2 community transmission was low during the surveillance period, passive surveillance was considered a robust plan to capture MIS-C cases at a national level.

Despite the introduction of vaccines, the global COVID-19 pandemic could continue for months. Therefore, surveillance is a critical tool for the detection and evaluation of serious complications in vulnerable population. Our experience offers a possible surveillance model for other countries concerned about COVID-19–associated MIS-C. MIS-C surveillance data in South Korea call for enhanced monitoring through syndromic and laboratory-based combination surveillance approaches.

Acknowledgments

We thank members of the Korean Pediatric Society who were involved in direct clinical service to children. We also thank public health officials for their cooperation and critical feedback.

About the Author

Dr. Choe is a pediatrician specializing in infectious diseases and epidemiology. His research addresses quantifying of and understanding the mechanisms of immunization programs' impact on public health, focusing on studies of respiratory virus transmission in the community and the effectiveness of control measures.

References

1. Kaushik A, Gupta S, Sood M, Sharma S, Verma S. A systematic review of multisystem inflammatory syndrome in children associated with SARS-CoV-2 infection. Pediatr Infect Dis J. 2020;39:e340–6. https://doi.org/10.1097/INF.0000000000002888
2. Singh S, Vignesh P, Burgner D. The epidemiology of Kawasaki disease: a global update. Arch Dis Child. 2015;100:1084–8. https://doi.org/10.1136/archdischild- 2014-307536
3. Korea Disease Control and Prevention Agency. Coronavirus disease-19 dashboard [cited 2020 Jan 5]. http://ncov.mohw.go.kr/en/
4. Dufort EM, Koumans EH, Chow EJ, Rosenthal EM, Muse A, Rowlands J, et al.; New York State and Centers for Disease Control and Prevention Multisystem Inflammatory Syndrome in Children Investigation Team. Multisystem inflammatory syndrome in children in New York State. N Engl J Med. 2020;383:347–58. https://doi.org/10.1056/NEJMoa2021756
5. Verdoni L, Mazza A, Gervasoni A, Martelli L, Ruggeri M, Ciuffreda M, et al. An outbreak of severe Kawasaki-like disease at the Italian epicentre of the SARS-CoV-2 epidemic: an observational cohort study. Lancet. 2020;395:1771–8. https://doi.org/10.1016/S0140-6736(20)31103-X
6. Kim YJ, Park H, Choi YY, Kim YK, Yoon Y, Kim KR, et al. Defining association between COVID-19 and the multisystem inflammatory syndrome in children through the pandemic. J Korean Med Sci. 2020;35:e204. https://doi.org/10.3346/jkms.2020.35.e204
7. Lee EH, Kepler KL, Geevarughese A, Paneth-Pollak R, Dorsinville MS, Ngai S, et al. Race/ethnicity among children with COVID-19-associated multisystem inflammatory syndrome. JAMA Netw Open. 2020;3:e2030280. https://doi.org/10.1001/jamanetworkopen.2020.30280
8. Jain S, Sen S, Lakshmivenkateshiah S, Bobhate P, Venkatesh S, Udani S, et al. Multisystem inflammatory syndrome in children with COVID-19 in Mumbai, India. Indian Pediatr. 2020;57:1015–9. https://doi.org/10.1007/s13312-020-2026-0
9. Clark BC, Sanchez-de-Toledo J, Bautista-Rodriguez C, Choueiter N, Lara D, Kang H, et al. Cardiac abnormalities seen in pediatric patients during the SARS-CoV2 pandemic: an international experience. J Am Heart Assoc. 2020;9:e018007. https://doi.org/10.1161/JAHA.120.018007
10. Mamishi S, Movahedi Z, Mohammadi M, Ziaee V, Khodabandeh M, Abdolsalehi MR, et al. Multisystem inflammatory syndrome associated with SARS-CoV-2 infection in 45 children: a first report from Iran. Epidemiol Infect. 2020;148:e196. https://doi.org/10.1017/S095026882000196X
11. Huh HJ, Hong KH, Kim TS, Song SH, Roh KH, Lee H, et al. Surveillance of coronavirus disease 2019 (COVID-19) testing in clinical laboratories in Korea. Ann Lab Med. 2021;41:225–9. https://doi.org/10.3343/alm.2021.41.2.225
12. Miller J, Cantor A, Zachariah P, Ahn D, Martinez M, Margolis KG. Gastrointestinal symptoms as a major presentation component of a novel multisystem inflammatory syndrome in children that is related to coronavirus disease 2019: a single center experience of 44 cases. Gastroenterology.

2020;159:1571–1574.e2. https://doi.org/10.1053/j.gastro.2020.05.079
13. Tullie L, Ford K, Bisharat M, Watson T, Thakkar H, Mullassery D, et al. Gastrointestinal features in children with COVID-19: an observation of varied presentation in eight children. Lancet Child Adolesc Health. 2020;4:e19–20. https://doi.org/10.1016/S2352-4642(20)30165-6
14. Aziz M, Haghbin H, Lee-Smith W, Goyal H, Nawras A, Adler DG. Gastrointestinal predictors of severe COVID-19: systematic review and meta-analysis. Ann Gastroenterol. 2020;33:615–30.
15. Fabi M, Corinaldesi E, Pierantoni L, Mazzoni E, Landini C, Bigucci B, et al. Gastrointestinal presentation of Kawasaki disease: A red flag for severe disease? PLoS One. 2018;13:e0202658. https://doi.org/10.1371/journal.pone.0202658

Address for correspondence: Eun Hwa Choi, Professor of Pediatrics, Seoul National University College of Medicine, 101 Daehak-ro, Jongno-gu, Seoul 110-769, South Korea; email: eunchoi@snu.ac.kr

Low-Level Middle East Respiratory Syndrome Coronavirus among Camel Handlers, Kenya, 2019

Peninah M. Munyua, Isaac Ngere, Elizabeth Hunsperger, Adano Kochi, Patrick Amoth, Lydia Mwasi, Suxiang Tong, Athman Mwatondo, Natalie Thornburg, Marc-Alain Widdowson,[1,2] M. Kariuki Njenga[1]

Although seroprevalence of Middle East respiratory coronavirus syndrome is high among camels in Africa, researchers have not detected zoonotic transmission in Kenya. We followed a cohort of 262 camel handlers in Kenya during April 2018–March 2020. We report PCR-confirmed Middle East respiratory coronavirus syndrome in 3 asymptomatic handlers.

Since the first human case of Middle East respiratory syndrome coronavirus (MERS-CoV) was identified in 2012, the World Health Organization has reported 2,494 infections and 858 deaths (case-fatality ratio 34.4%) in persons across 27 countries in the Middle East, Europe, Asia, and North America (*1*). Dromedary camels (*Camelus dromedarius*) are the known reservoirs of the virus (*2*,*3*). Most human cases result from direct or indirect transmission of virus from camels or human-to-human transmission in healthcare settings; researchers have also documented limited secondary transmission to household contacts (*4*). Occupational direct contact with camels is a risk factor for primary MERS-CoV infection (*5*). Camel workers and herders have a 0%–50% seroprevalence of MERS-CoV, generally higher than that of the general population in Saudi Arabia (*4*,*6*).

Although infection is widespread among dromedary camels, zoonotic transmission from camels to humans is sporadic, and disease prevalence among humans is not directly proportional to potential exposure to infected camels (*4*,*5*,*7*). Although >65% of the world's dromedary camels live in Africa, on that continent MERS-CoV seroprevalence in humans is low (0.2%), with no documented cases of acute human infection (*8*,*9*). Furthermore, studies in the Africa region have identified MERS-CoV RNA in 11%–16% of camels and in 80%–95% of seropositive camels (*9*–*11*). To determine whether MERS-CoV infections occur in humans in a region with high seroprevalence among camels, we studied a cohort of 262 camel handlers in Kenya.

The Study

During April 2018–March 2020, we enrolled participants on a rolling basis from 32 camel-owning households in Marsabit County, northern Kenya (Figure 1). We defined a camel handler as any person in the household who had contact with camels (Figure 2). This study was approved by the Scientific and Ethical Review Committee of Kenya Medical Research Institute (approval no. SSC3472), the Institutional Review Board of Washington State University (approval no. 16245), and the US Centers for Disease Control and Prevention (approval no. 7065). We obtained written informed consent from all participants.

We conducted monthly visits with the participants. At each visit, we collected nasopharyngeal and oropharyngeal swab samples from each participant. We also administered a questionnaire to each participating camel handler to identify signs and symptoms of possible respiratory illness during the previous 30 days. In addition, we recorded occurrences of respiratory illness among their household members. Participants belonged to 32 households with a median of 6

Author affiliations: US Centers for Disease Control and Prevention, Nairobi, Kenya (P.M. Munyua, E. Hunsperger, M.A. Widdowson); University of Nairobi, Nairobi (I. Ngere); Washington State University, Nairobi (I. Ngere, M.K. Njenga); County Government of Marsabit, Marsabit, Kenya (A. Kochi); Kenya Ministry of Health, Nairobi (P. Amoth, A. Mwatondo); Kenya Medical Research Institute, Nairobi (L. Mwasi); US Centers for Disease Control and Prevention, Atlanta, Georgia, USA (S. Tong, N. Thornburg)

DOI: https://doi.org/10.3201/eid2704.204458

[1]These senior authors contributed equally to this article.

[2]Current affiliation: Institute of Tropical Medicine, Antwerp, Belgium.

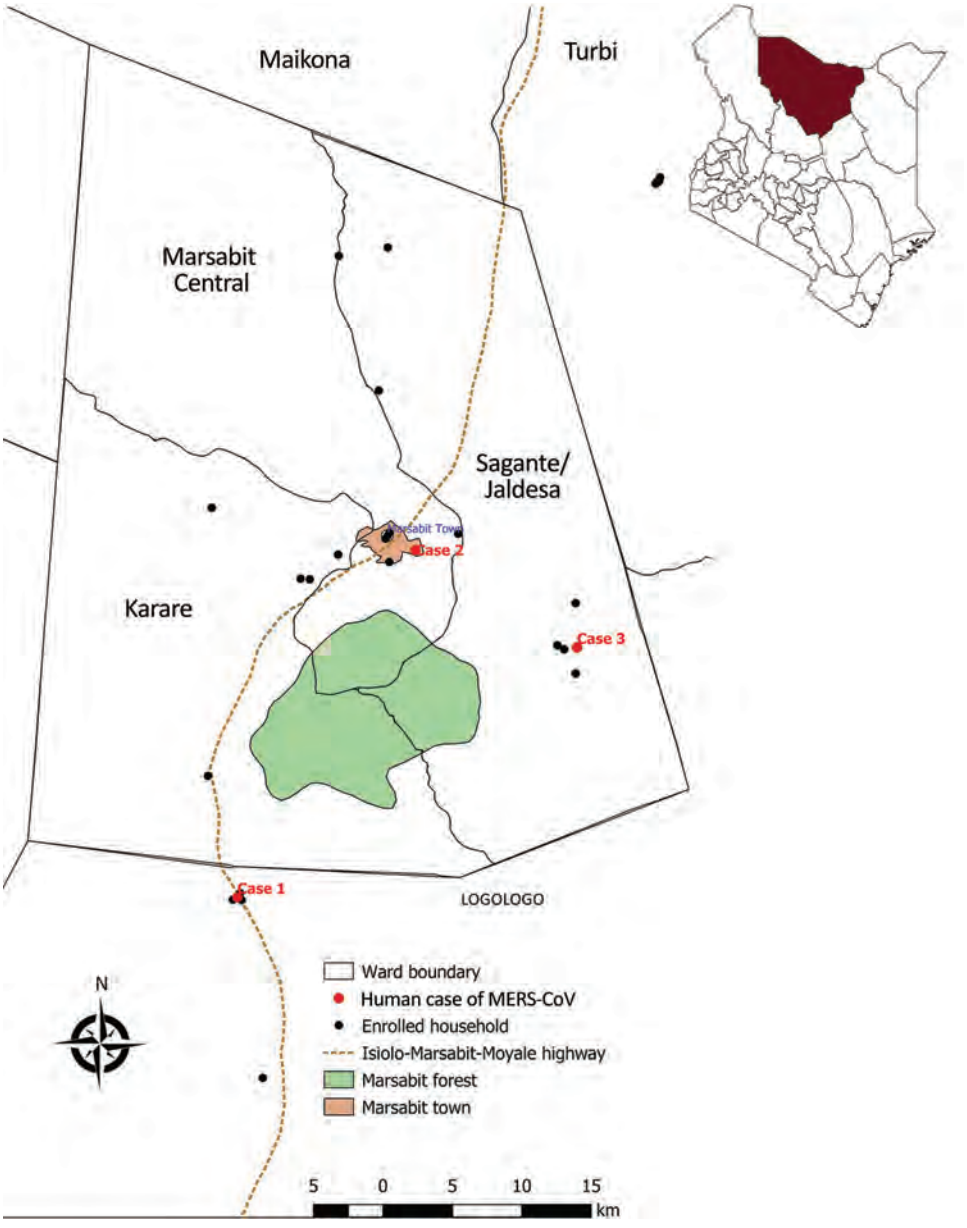

Figure 1. Locations of enrolled households in study on MERS-CoV, Marsabit County, Kenya, 2018–2020. Black circles indicate participating households; red circles indicate households with cases. Inset shows location of Marsabit County within Kenya. MERS-CoV, Middle East respiratory syndrome coronavirus.

persons (interquartile range [IQR] 1–8 persons) and 32 camels (IQR 2–48 camels) at enrollment. The median age of these participants was 19 years (IQR 11–38 years). Most (67.2%) participants were male, of whom 39.3% were employed as camel workers and 38.2% were school going household members (Table 1). All participants handled camels. The most frequent interactions were herding (74.4%), cleaning barns (67.9%), feeding (67.6%), and milking (63.7%) (Figure 2).

We stored the swab samples in virus transport media and tested them for MERS-CoV by reverse transcription PCR (RT-PCR) at the Kenya Medical Research Institute (Nairobi, Kenya) as described previously (*12*). We conducted real-time RT-PCR selective for the upstream region envelope and 2 distinct regions of nucleocapsid genes on total nucleic acid extracted from 200 μL of sample. We defined a positive sample by positivity of all 3 PCRs.

We tested 1,369 samples from 262 camel handlers during the 2-year follow-up period. Participants had a median of 43.6% of monthly follow-up visits (IQR 8%–75%). Three (1.1%) participants (cases 1–3) tested positive for MERS-CoV by RT-PCR. The cycle threshold (C_t) values for case 1 were 38.9 for the upstream envelope, 37.7 for the nucleocapsid 2, and 39.3 for the nucleocapsid 3 genes; for case 2, the values were 39.7 for the upstream envelope, 36.9 for the nucleocapsid 2, and 39.8 for the nucleocapsid 3 genes; for case 3,

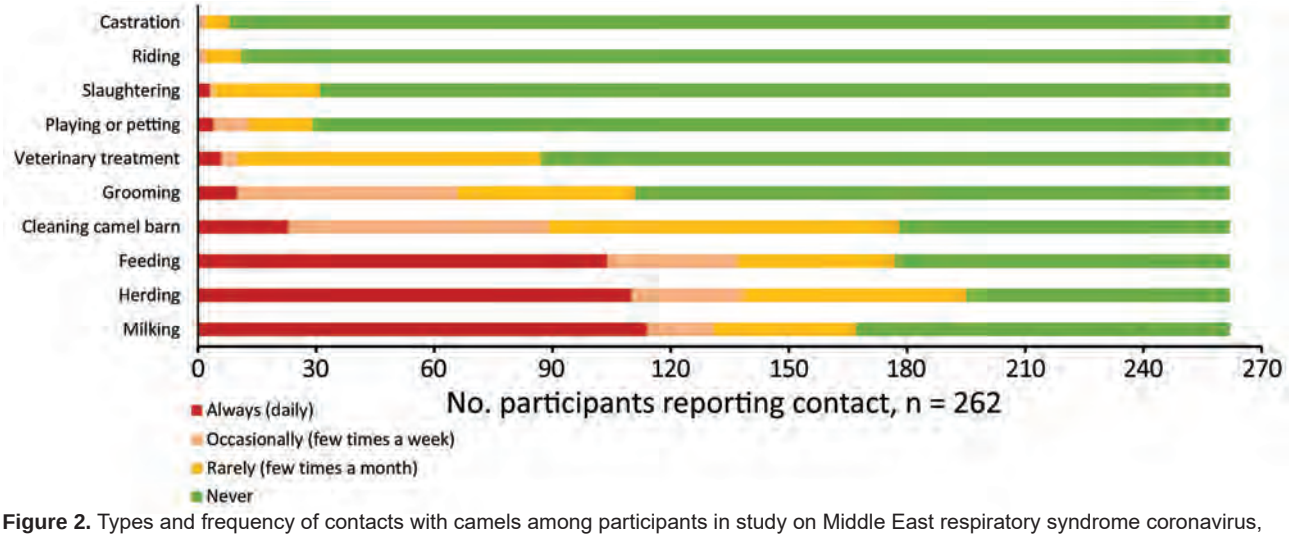

Figure 2. Types and frequency of contacts with camels among participants in study on Middle East respiratory syndrome coronavirus, Marsabit County, Kenya, 2018–2020.

the values were 35.6 for the upstream envelope, 36.0 for the nucleocapsid 2, and 36.8 for the nucleocapsid 3 genes. We detected all 3 cases during July–September 2019 (Table 2).

Table 1. Characteristics of camel handlers enrolled in a study on Middle East respiratory syndrome coronavirus, Marsabit, Kenya, 2018–2020*

Characteristic	Value, n = 262
Sex	
M	176 (67.2)
F	86 (32.8)
Age, y	
≤19	131 (50)
20–39	73 (27.9)
40–59	41 (15.6)
≥60	17 (6.5)
Median participant age, y (IQR)	19 (11–38)
Work engagement in the previous 30 d	
Camel farm worker	103 (39.3)
Primary/secondary school student	100 (38.2)
Housewife	28 (10.7)
Farm owner	22 (8.4)
Pastoralist	6 (2.3)
Not currently engaged	2 (0.8)
Retiree	1 (0.4)
Median household size (IQR)	6 (1–8)
Median camel herd size (IQR)	32 (2–48)
History of chronic respiratory symptoms†	5 (1.9)
History of other chronic conditions‡	1 (0.4)
History of travel in the previous 5 y	0
Past tobacco use	72 (27.5)
Current tobacco use	72 (27.5)
Respiratory symptoms during the 2-year follow-up period	25 (9.5)
Fever	5 (1.9)
Running nose	39 (14.9)
Cough	25 (9.5)
Nasal stuffiness	23 (8.8)
Sore throat	16 (6.1)
Chest pain	2 (0.8)

*Values are no. (%) except as indicated.
†Respiratory symptoms include cough, sore throat, running nose, nasal stuffiness, chest pain.
‡Other chronic medical conditions include diabetes, cancer, liver disease, kidney disease, and tuberculosis.

Case 1 was in a woman 20 years of age who enrolled in June 2019 and had 9 monthly follow-up visits. She participated in the study with 11 other members of the household, all of whom tested negative for MERS-CoV throughout the follow-up period. Case 2 was in a man 49 years of age who enrolled in May 2019 and had 7 monthly follow-up visits. He participated in the study with 6 of his 10 household members; all the participants in his household tested negative for MERS-CoV. Case 3 was in a man 22 years of age who enrolled in May 2018 and had 12 monthly follow-up visits. He participated in the study with 3 of his 9 household members; the participants in his household tested negative for MERS-CoV. None of the 3 with positive results tested positive for MERS-CoV in the subsequent months.

All of the 3 with positive results were asymptomatic at diagnosis and had no concurrent conditions or history of travel outside of the county or country in the previous month. None of them or their household members had respiratory illness before or after diagnosis.

Conclusions

We report 3 PCR-confirmed cases of MERS-CoV in humans in Kenya; these cases met the World Health Organization case definition of MERS-CoV infection (*13*). All 3 persons were asymptomatic before and after diagnosis; this finding supports previous data suggesting that the virus causes no or mild disease in Africa compared with the Middle East and Asia, perhaps because of the younger age of most camel herders in Africa (*4*,*8*,*9*). Our findings are limited by the high C_t values (>35) of all

Table 2. Characteristics of persons with Middle East respiratory syndrome coronavirus, Kenya, 2019

Case	Age, y/sex	Occupation	No. household members in study	No. of camels owned by household	Enrollment date	Diagnosis date	Type of camel contact at time of positive sample
1	20/F	Spouse to herder	11	37	2019 Jun 23	2019 Jul 31	Herding, milking, feeding, petting/playing, grooming, cleaning barn
2	49/M	Herder	6	2	2019 May 21	2019 Aug 13	Herding, milking, feeding, grooming, cleaning barn, administering medications
3	22/M	Herder	3	32	2018 May 2	2019 Sep 12	Herding, milking, feeding, grooming, cleaning barn, assisting in birth

cases, a level which some experts might not consider to be positive. However, because these cases had C_t values <40 for 3 distinct MERS-CoV genes, we feel confident that these are unlikely to be false positive results. Researchers have observed low upper respiratory tract RNA concentrations in asymptomatic patients and contacts of MERS-CoV patients (*14*). In contrast to studies conducted in the Middle East, we found no evidence of human-to-human transmission; a total of 20 household members of the 3 patients tested negative for MERS-CoV before and after their household member's diagnosis. However, we might have missed some infections that occurred between follow-up visits. Furthermore, not all household members were enrolled in the study. In addition, serologic assessment of MERS-CoV T-cell responses might detect mild and asymptomatic MERS-CoV cases (*15*). Finally, the low (0.2%) seroprevalence among participants who had high exposure to camel herds with MERS-CoV circulation suggest a low level of zoonotic camel-to-human transmission. We previously found no antibodies against MERS-CoV in camel herders despite high seroprevalence among camels in this community (*9*).

In conclusion, we confirmed zoonotic transmission of MERS-CoV from camels to handlers in Kenya. Focused surveillance is needed to detect these rare infections when they occur.

Acknowledgments

We thank Arithi Mutembei, Jack Omolo, Diba Denge, Boru Dub Wato, Millicent Minayo, Moshe Alando, Doris Marwanga, and Cynthia Awuor for their contribution to data and specimen collection. We appreciate the camel herders in Marsabit who participated in this study. We also thank the administrative team at the Washington State University Global Health Program for facilitating all study logistics.

This project was funded by the US Centers for Disease Control and Prevention under the research co-operative agreement with Washington State University (grant no. 1U01GH002143).

About the Author

Dr. Munyua is an epidemiologist within the Division of Global Health Protection, Global Health, US Centers for Disease Control and Prevention, Nairobi. Her research interests include infectious and zoonotic diseases.

References

1. World Health Organization. Middle East respiratory syndrome coronavirus (MERS-CoV) summary updates, November 2019. 2019 [cited 2020 Jul 6]. https://www.who.int/emergencies/mers-cov/en
2. Ali MA, Shehata MM, Gomaa MR, Kandeil A, El-Shesheny R, Kayed AS, et al. Systematic, active surveillance for Middle East respiratory syndrome coronavirus in camels in Egypt. Emerg Microbes Infect. 2017;6:1. https://doi.org/10.1038/emi.2016.130
3. Reusken CB, Farag EA, Jonges M, Godeke GJ, El-Sayed AM, Pas SD, et al. Middle East respiratory syndrome coronavirus (MERS-CoV) RNA and neutralising antibodies in milk collected according to local customs from dromedary camels, Qatar, April 2014. Euro Surveill. 2014;19:20829. https://doi.org/10.2807/1560-7917.ES2014.19.23.20829
4. Grant R, Malik MR, Elkholy A, Van Kerkhove MD. A review of asymptomatic and subclinical Middle East respiratory syndrome coronavirus infections. Epidemiol Rev. 2019;41:69–81. https://doi.org/10.1093/epirev/mxz009
5. Hui DS, Azhar EI, Kim YJ, Memish ZA, Oh MD, Zumla A. Middle East respiratory syndrome coronavirus: risk factors and determinants of primary, household, and nosocomial transmission. Lancet Infect Dis. 2018;18:e217–27. https://doi.org/10.1016/S1473-3099(18)30127-0
6. Alshukairi AN, Zheng J, Zhao J, Nehdi A, Baharoon SA, Layqah L, et al. High prevalence of MERS-CoV infection in camel workers in Saudi Arabia. MBio. 2018;9:e01985-18. https://doi.org/10.1128/mBio.01985-18
7. Hemida MG, Al-Naeem A, Perera RA, Chin AW, Poon LL, Peiris M. Lack of Middle East respiratory syndrome coronavirus transmission from infected camels. Emerg Infect Dis. 2015;21:699–701. https://doi.org/10.3201/eid2104.141949
8. Liljander A, Meyer B, Jores J, Müller MA, Lattwein E, Njeru I, et al. MERS-CoV antibodies in humans, Africa, 2013–2014. Emerg Infect Dis. 2016;22:1086–9. https://doi.org/10.3201/eid2206.160064
9. Munyua P, Corman VM, Bitek A, Osoro E, Meyer B, Müller MA, et al. No serologic evidence of Middle East respiratory syndrome coronavirus infection among camel farmers exposed to highly seropositive camel herds: a household linked study, Kenya, 2013. Am J Trop Med Hyg. 2017;96:1318–24. https://doi.org/10.4269/ajtmh.16-0880

10. Chu DKW, Hui KPY, Perera RAPM, Miguel E, Niemeyer D, Zhao J, et al. MERS coronaviruses from camels in Africa exhibit region-dependent genetic diversity. Proc Natl Acad Sci U S A. 2018;115:3144–9. https://doi.org/10.1073/pnas.1718769115
11. Corman VM, Jores J, Meyer B, Younan M, Liljander A, Said MY, et al. Antibodies against MERS coronavirus in dromedary camels, Kenya, 1992–2013. Emerg Infect Dis. 2014;20:1319–22. https://doi.org/10.3201/eid2008.140596
12. Corman VM, Ölschläger S, Wendtner CM, Drexler JF, Hess M, Drosten C. Performance and clinical validation of the RealStar MERS-CoV Kit for detection of Middle East respiratory syndrome coronavirus RNA. J Clin Virol. 2014;60:168–71. https://doi.org/10.1016/j.jcv.2014.03.012
13. World Health Organization. Middle East respiratory syndrome case definition for reporting to WHO. 2017 [cited 2020 Oct 2]. https://www.who.int/csr/disease/coronavirus_infections/mers-interim-case-definition.pdf
14. Drosten C, Meyer B, Müller MA, Corman VM, Al-Masri M, Hossain R, et al. Transmission of MERS-coronavirus in household contacts. N Engl J Med. 2014;371:828–35. https://doi.org/10.1056/NEJMoa1405858
15. Mok CKP, Zhu A, Zhao J, Lau EHY, Wang J, Chen Z, et al. T-cell responses to MERS coronavirus infection in people with occupational exposure to dromedary camels in Nigeria: an observational cohort study. Lancet Infect Dis. 2020;S1473-3099(20)30599-5. https://doi.org/10.1016/S1473-3099(20)30599-5

Address for correspondence: Peninah Munyua, US Centers for Disease Control and Prevention, PO Box 606, Nairobi 00621, Kenya; email: ikg2@cdc.gov

Emergence and Polyclonal Dissemination of OXA-244–Producing *Escherichia coli*, France

Cecile Emeraud, Delphine Girlich, Rémy A. Bonnin, Agnès B. Jousset, Thierry Naas, Laurent Dortet

Since 2016, OXA-244–producing *Escherichia coli* has been increasingly isolated in France. We sequenced 97 OXA-244–producing *E. coli* isolates and found a wide diversity of sequence types and a high prevalence of sequence type 38. Long-read sequencing demonstrated the chromosomal location of $bla_{OXA-244}$ inside the entire or truncated Tn*51098*.

Carbapenems are the last line antimicrobial drugs for treating infections caused by multidrug-resistant *Enterobacterales*. The global dissemination of carbapenemase-producing *Enterobacterales* (CPE; formerly known as carbapenemase-producing *Enterobacteriaceae*) pose a serious threat to public health (*1*). Oxacillin (OXA) 244, a single amino-acid variant of OXA-48 (Arg-222-Gly) (*2*), is an emerging carbapenemase variant in several countries in Europe (*3*–*7*). During 2013–2019, the French National Reference Center received a continuously increasing number of OXA-244–producing isolates for antimicrobial resistance (AMR) testing. OXA-244–producing isolates increased from 0 in 2012 to 72 in 2019. In France, OXA-244–producing *Enterobacteriaceae* represent 2.4% of all CPE and represented 3.4% of OXA-48–like producing CPE in 2019 (*8*). In addition, this tendency might represent only a fraction of OXA-244–producing *Enterobacteriaceae* because this variant is difficult to detect on CPE screening media due to the low hydrolytic activity of this carbapenemase (*8*). OXA-244 is found mainly in *Escherichia coli* isolates (*6*). The $bla_{OXA-244}$ gene is described in only 1 type of transposon, Tn*51098*, a 21.9-kb IS*1R*-based composite transposon that includes a truncated Tn*1999.2* (ΔTn*1999.2*) and a fragment of the archetypal IncL bla_{OXA-48}–carrying plasmid, pOXA-48 (*2*).

Previous studies analyzed only a limited number of OXA-244–producing *E. coli* of an epidemic clone belonging to sequence type (ST) 38 that spread in countries in Europe (*3*,*5*,*7*,*9*). More data on the epidemiology and genetics of OXA-244 are required to understand its spread in Europe. We used whole-genome sequencing (WGS) to characterize the epidemiology of OXA-244–producing *E. coli* circulating in France during 2016–2019.

The Study

During 2016–2019, the French National Reference Center identified 97 OXA-244–producing *E. coli* isolates. We performed WGS on all isolates by using the HiSeq (Illumina Inc., https://www.illumina.com) sequencing platform (GenBank accession nos. in Appendix 1 Table, https://wwwnc.cdc.gov/EID/article/27/4/20-4459-App1.xlsx). We performed in silico multilocus sequence typing (MLST) by using the MLST 2.0 server (https://cge.cbs.dtu.dk/services/MLST). We identified 12 different sequence types (STs); the 5 most prevalent were ST38 (n = 37), ST361 (n = 17), ST69 (n = 12), ST167 (n = 11), and ST10 (n = 8) (Figure 1). Among OXA-244–producing *E. coli* isolates, the prevalence of ST38 rose from 12% in 2016 and to 47% in 2019.

On all 97 genomes of OXA-244–producing *E. coli*, we used a core genome single-nucleotide polymorphism (SNP)–based approach to create a phylogenetic tree by using CSIPhylogeny (https://cge.cbs.dtu.dk/services/CSIPhylogeny). To identify clades within STs, we performed a nested phylogenetic analysis with isolates of each ST to construct a SNP matrix. Isolates within the same clade would be highly suggestive of patient-to-patient cross-transmission of the same strain. We considered 2 strains to be part of the same clade if they were separated by <100 SNPs along their common genome

Author affiliations: INSERM, University Paris-Saclay, Le Kremlin-Bicêtre, France (C. Emeraud, D. Girlich, R.A. Bonnin, A.B. Joussett, T. Naas, L. Dortet); Bicêtre Hospital, Le Kremlin-Bicêtre (C. Emeraud, A.B. Jousset, T. Naas, L. Dortet); French National Reference Center for Antibiotic Resistance, Le Kremlin-Bicêtre (C. Emeraud, R.A. Bonnin, A.B. Jousset, T. Naas, L. Dortet)

DOI: https://doi.org/10.3201/eid2704.204459

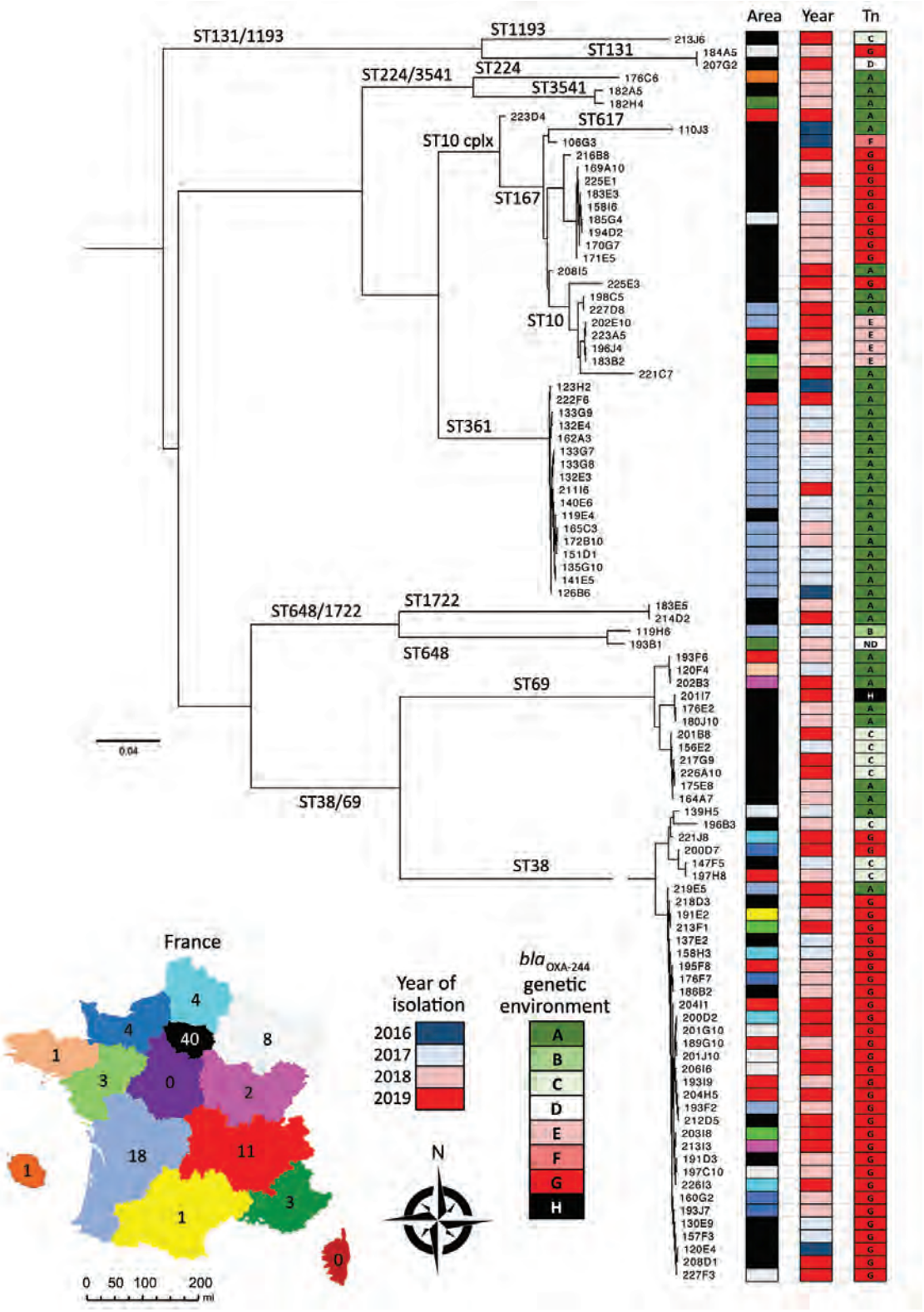

Figure 1. Phylogenetic relationship and geographic distribution of the 97 OXA-244–producing *Escherichia coli* isolates recovered in France, 2016–2019. Inset map shows regions of France; colors correspond to areas from which OXA-244–producing *E. coli* isolates were collected. The phylogenetic tree was constructed using CSIPhylogeny version 1.4 (https://cge.cbs.dtu.dk/services/CSIPhylogeny). Scale bar indicates nucleotide substitutions per site. ND, not detected; OXA, oxacillin; ST, sequence type.

(Appendix 2 Figure, https://wwwnc.cdc.gov/EID/article/27/4/20-4459-App2.pdf). We identified large clades corresponding to clonal dissemination of a single strain in the same area, including 5/12 isolates of ST167 and 15/17 isolates of ST361. We identified ≤7 different clades of ST38, and most (30/37) isolates belonged to the same clade (Appendix 2 Figure). However, these 30 ST38 isolates were collected in 9 different areas of France and 25 were isolated during 2018–2019 (Figure 1).

Because assembly of regions with repeated sequences was difficult with Illumina WGS data, we sequenced some isolates by using long read nanopore technology by using a MinIon (Oxford Nanopore, https://nanoporetech.com) sequencer (*10*). We performed WGS on 3 isolates belonging to the most prevalent STs: isolate

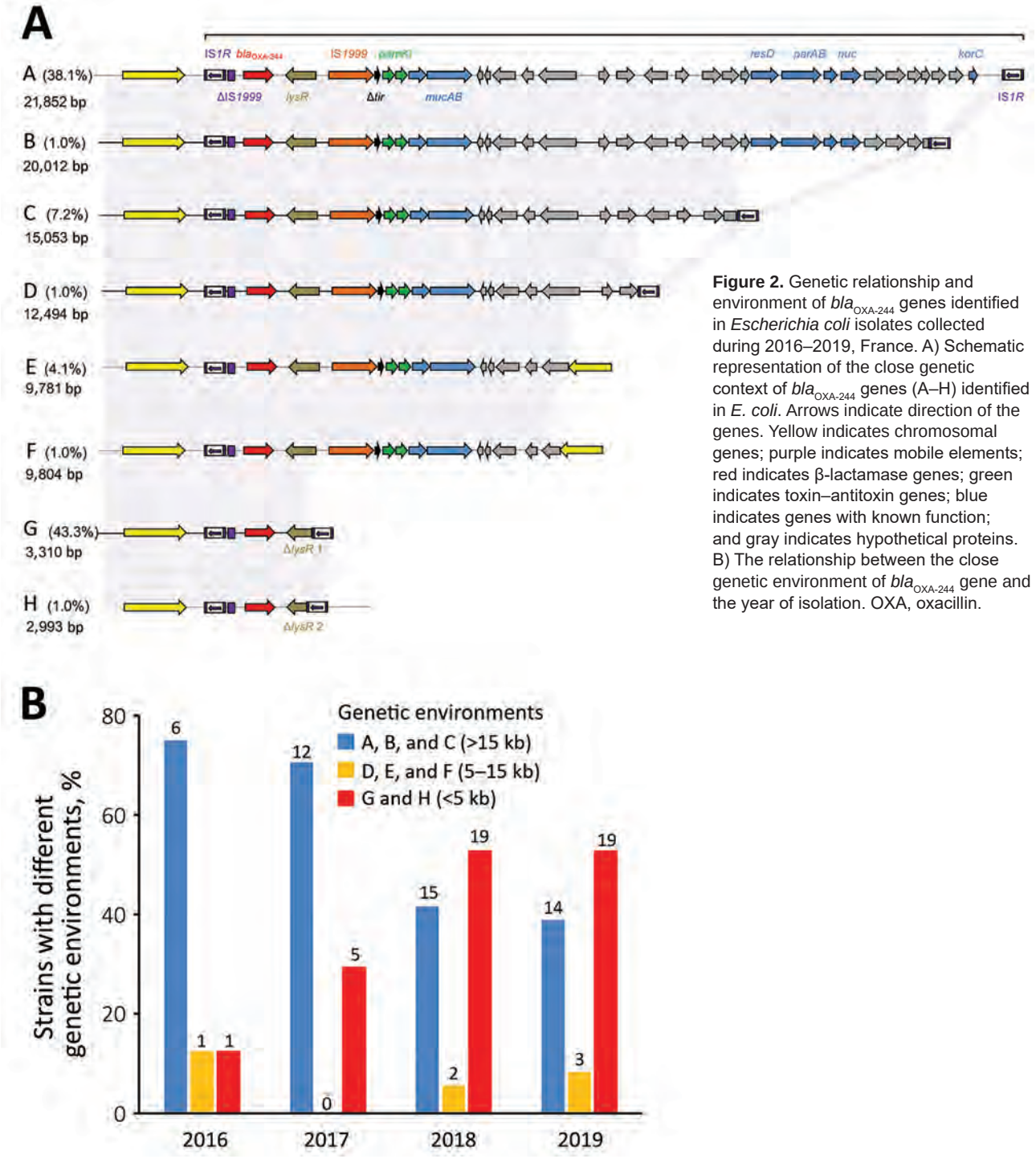

Figure 2. Genetic relationship and environment of *bla*$_{OXA-244}$ genes identified in *Escherichia coli* isolates collected during 2016–2019, France. A) Schematic representation of the close genetic context of *bla*$_{OXA-244}$ genes (A–H) identified in *E. coli*. Arrows indicate direction of the genes. Yellow indicates chromosomal genes; purple indicates mobile elements; red indicates β-lactamase genes; green indicates toxin–antitoxin genes; blue indicates genes with known function; and gray indicates hypothetical proteins. B) The relationship between the close genetic environment of *bla*$_{OXA-244}$ gene and the year of isolation. OXA, oxacillin.

119E4 (ST361), isolate 120E4 (ST38), and isolate 156E2 (ST69) (Appendix 1 Table). We found a chromosomal localization of $bla_{OXA-244}$ gene in the 3 isolates. By combining data obtained by both WGS technologies, we reconstructed the different genetic environments of $bla_{OXA-244}$ gene and annotated the assembled sequences by using CLC Genomics Workbench version 12.0 software (QIAGEN, https://www.qiagen.com).

We detected 8 different genetic environments in our collection (Figure 2, panel A). Among the 97 *E. coli* isolates, 37 (38.1%) possessed the $bla_{OXA-244}$ gene in Tn*51098*, a previously described transposon (*2*,*11*) (Figure 2, panel A). Among the other 60 (61.9%) isolates, we found $bla_{OXA-244}$ in the shorter form of Tn*51098* (2,933–20,012 bp) (Figure 2, panel A). The $bla_{OXA-244}$ gene still was systematically included in a truncated Tn*1999.2* (ΔTn*1999.2*), as described in *E. coli* VAL (*2*). For 44.3% of isolates, the remnant Tn*51098* was reduced in size (42 isolates with genetic environment G and 1 with genetic environment H) (Figure 2, panel A). We noted, the $bla_{OXA-244}$ gene was included in a ΔTn*1999.2* where the *lysR* gene was truncated by the IS*1R* element. Of the 42 isolates sharing the genetic environment G, 32 (76.1%) belonged to ST38. By separating the type of genetic environment according to the date of isolation, we noticed that the short forms were isolated during 2018–2019 (38/44 strains, 86%) (Figure 2, panel B).

Discussion

Dissemination of ST38 OXA-244–producing *E. coli* has been observed in many countries in Europe (*3*–*7*) and a few other countries around the world (*12*,*13*). However, most of these studies focused on ST38. Our results confirm the phenomenon of OXA-244–producing *E. coli* isolates in France because 38% of isolates in our study belonged to ST38. In addition, we observed an increased number of ST38 isolates during 2018–2019. Phylogenetic analysis identified a substantial clade inside ST38 (Appendix 2 Figure), but massive dissemination of this clone in France likely does not correspond to cross transmission of a single strain in different areas. The few SNP differences identified among ST38 isolates suggest this clade emerged recently. Accordingly, inside this compact ST38, the <100 SNP cutoff used to discriminate between 2 clades might be lowered because it was recently described for another high-risk clone, *Klebsiella pneumoniae* carbapenemase–producing *K. pneumoniae* ST258 (*14*).

The other common STs noted in our study are ST361, ST167, ST69 and ST10. In Europe, OXA-244–producing *E. coli* of ST69, ST167, and ST361 have been reported in Denmark (*6*), and ST69 and ST10 in Switzerland. Unlike what we observed with ST38, clones observed inside ST167 and ST361 mostly correlate with the same geographic area suggesting patient-to-patient cross-transmission.

As previously described for ST38 *E. coli* VAL (*2*), we demonstrated the chromosomal location of the $bla_{OXA-244}$ gene in 3 isolates belonging to the 3 main STs, ST38, ST361, and ST69. The chromosomal localization of $bla_{OXA-244}$ together with the intrinsic lower hydrolytic activity of OXA-244, compared with OXA-48, contribute to the difficulties in accurately detecting OXA-244–producing *E. coli* using classical screening media (*8*,*15*), suggesting a large underestimation of the real spread of OXA-244 producers.

In 2013, the $bla_{OXA-244}$ gene initially was reported to be embedded in a 21,852-bp transposon Tn*51098*, which contains ΔTn*1999.2* (*2*). This structure still is present in 38.1% of OXA-244–producing *E. coli*. To our knowledge, Tn*51098* is the sole genetic structure reported for $bla_{OXA-244}$. In our collection, $bla_{OXA-244}$ was embedded in truncated forms of Tn*51098* in most isolates. Of note, in most (86.5%) ST38 OXA-244–producing *E. coli* the close genetic context of the $bla_{OXA-244}$ gene was reduced to a small 3,310-bp fragment matching Tn*51098* and corresponding to a truncated form of the Tn*1999.2*. In addition, the most recently collected isolates possess short versions of the Tn*51098* compared with the isolates collected earlier (Figure 2, panel B). The effect on the clonal dissemination of this genome reduction around $bla_{OXA-244}$ gene (e.g., better fitness) remains undetermined. Further analysis on the $bla_{OXA-244}$ close genetic environment could elucidate the effects of this genome reduction.

About the Author

Dr. Emeraud is an assistant professor at the INSERM, Le Kremlin-Bicêtre, France. Her main research interests include epidemiology, genetics, and biochemistry of β-lactamases in gram negative bacteria.

References

1. Nordmann P, Dortet L, Poirel L. Carbapenem resistance in *Enterobacteriaceae*: here is the storm! Trends Mol Med. 2012;18:263–72. https://doi.org/10.1016/j.molmed.2012.03.003
2. Potron A, Poirel L, Dortet L, Nordmann P. Characterisation of OXA-244, a chromosomally-encoded OXA-48-like β-lactamase from *Escherichia coli*. Int J Antimicrob Agents. 2016;47:102–3. https://doi.org/10.1016/j.ijantimicag.2015.10.015
3. Masseron A, Poirel L, Falgenhauer L, Imirzalioglu C, Kessler J, Chakraborty T, et al. Ongoing dissemination of OXA-244 carbapenemase-producing *Escherichia coli* in Switzerland and their detection. Diagn Microbiol Infect Dis. 2020;97:115059. https://doi.org/10.1016/j.diagmicrobio.2020.115059
4. European Centre for Disease Prevention and Control. Increase in OXA-244-producing *Escherichia coli* in the European Union/European Economic Area and the UK

since 2013. Stockholm: the Centre; 2020 [cited 2020 Feb 18]. https://www.ecdc.europa.eu/sites/default/files/documents/RRA-E-coli-OXA-244-producing-E-coli-EU-EEA-UK-since-2013.pdf.
5. Kremer K, Kramer R, Neumann B, Haller S, Pfennigwerth N, Werner G, et al. Rapid spread of OXA-244-producing *Escherichia coli* ST38 in Germany: insights from an integrated molecular surveillance approach; 2017 to January 2020. Euro Surveill. 2020;25:2000923. https://doi.org/10.2807/1560-7917.ES.2020.25.25.2000923
6. Hammerum AM, Porsbo LJ, Hansen F, Roer L, Kaya H, Henius A, et al. Surveillance of OXA-244-producing *Escherichia coli* and epidemiologic investigation of cases, Denmark, January 2016 to August 2019. Euro Surveill. 2020;25. https://doi.org/10.2807/1560-7917.ES.2020.25.18.1900742
7. Falgenhauer L, Nordmann P, Imirzalioglu C, Yao Y, Falgenhauer J, Hauri AM, et al. Cross-border emergence of clonal lineages of ST38 *Escherichia coli* producing the OXA-48-like carbapenemase OXA-244 in Germany and Switzerland. Int J Antimicrob Agents. 2020;56:106157. https://doi.org/10.1016/j.ijantimicag.2020.106157
8. Emeraud C, Biez L, Girlich D, Jousset AB, Naas T, Bonnin RA, et al. Screening of OXA-244 producers, a difficult-to-detect and emerging OXA-48 variant? J Antimicrob Chemother. 2020;75:2120–3.
9. Oteo J, Hernández JM, Espasa M, Fleites A, Sáez D, Bautista V, et al. Emergence of OXA-48-producing *Klebsiella pneumoniae* and the novel carbapenemases OXA-244 and OXA-245 in Spain. J Antimicrob Chemother. 2013;68:317–21. https://doi.org/10.1093/jac/dks383
10. Bonnin RA, Jousset AB, Gauthier L, Emeraud C, Girlich D, Sauvadet A, et al. First occurrence of the OXA-198 carbapenemase in *Enterobacterales*. Antimicrob Agents Chemother. 2020;64:e01471-19. https://doi.org/10.1128/AAC.01471-19
11. Pitout JDD, Peirano G, Kock MM, Strydom K-A, Matsumura Y. The global ascendency of OXA-48-type carbapenemases. Clin Microbiol Rev. 2019;33:e00102-19. https://doi.org/10.1128/CMR.00102-19
12. Abril D, Bustos Moya IG, Marquez-Ortiz RA, Josa Montero DF, Corredor Rozo ZL, Torres Molina I, et al. First report and comparative genomics analysis of a $bla_{OXA-244}$-harboring *Escherichia coli* isolate recovered in the American continent. Antibiotics (Basel). 2019;8:222. https://doi.org/10.3390/antibiotics8040222
13. Soliman AM, Ramadan H, Sadek M, Nariya H, Shimamoto T, Hiott LM, et al. Draft genome sequence of a bla_{NDM-1}- and $bla_{OXA-244}$-carrying multidrug-resistant *Escherichia coli* D-ST69 clinical isolate from Egypt. J Glob Antimicrob Resist. 2020;22:832–4. https://doi.org/10.1016/j.jgar.2020.07.015
14. David S, Reuter S, Harris SR, Glasner C, Feltwell T, Argimon S, et al.; EuSCAPE Working Group; ESGEM Study Group. Epidemic of carbapenem-resistant *Klebsiella pneumoniae* in Europe is driven by nosocomial spread. Nat Microbiol. 2019;4:1919–29. https://doi.org/10.1038/s41564-019-0492-8
15. Hoyos-Mallecot Y, Naas T, Bonnin RA, Patino R, Glaser P, Fortineau N, et al. OXA-244-producing *Escherichia coli* isolates, a challenge for clinical microbiology laboratories. Antimicrob Agents Chemother. 2017;61:e00818-17. https://doi.org/10.1128/AAC.00818-17

Address for correspondence: Laurent Dortet, Service de Bactériologie-Hygiène, Hôpital de Bicêtre, 78 rue du Général Leclerc, 94275 Le Kremlin-Bicêtre CEDEX, France; email: laurent.dortet@aphp.fr

Fatal Case of Crimean-Congo Hemorrhagic Fever Caused by Reassortant Virus, Spain, 2018

Anabel Negredo, Rafael Sánchez-Arroyo, Francisco Díez-Fuertes, Fernando de Ory, Marco Antonio Budiño, Ana Vázquez, Ángeles Garcinuño, Lourdes Hernández, César de la Hoz González, Almudena Gutiérrez-Arroyo, Carmen Grande, Paz Sánchez-Seco

In August 2018, a fatal autochthonous case of Crimean-Congo hemorrhagic fever was confirmed in western Spain. The complete sequence of the viral genome revealed circulation of a new virus because the genotype differs from that of the virus responsible for another case in 2016. Practitioners should be alert to possible new cases.

A fatal case of Crimean-Congo hemorrhagic fever (CCHF) detected in Spain in 2018 was caused by a different genotype, a reassortant virus, than the genotype of a previous case detected in 2016. This unexpected variability contrasts with the situation in other CCHF-endemic countries. Because CCHF is a zoonotic disease and animal migratory routes between Europe and Africa usually pass through Spain, data about genetic sequences are crucial for monitoring infections in humans, developing suitable detection tools, and providing information about the dynamics of virus circulation and spread.

The Case

On July 31, 2018, a 74-year-old man sought care at Nuestra Señora de Sonsoles Hospital (Ávila, Spain) with fever (39.2°C), pain in the sacroiliac area, chills, shivering, and a feeling of dizziness without loss of consciousness. No relevant physical findings or analytical parameters were detected (Table 1). While in the hospital, the patient remained stable and in good general condition. He was discharged for observation at home, afebrile, with a diagnosis of febrile syndrome with bacteremia and a prescription of amoxicillin/clavulanic acid and instructions to take acetaminophen if fever redeveloped.

On August 4, the man returned to the hospital with general discomfort and no improvement. He reported increased stools that he (a retired physician) assumed were associated with the antimicrobial drug and reported probably having been bitten by a tick while participating in boar hunting on July 24 in Helechosa de los Montes (Badajoz, Spain) (Figure 1). The patient had skinned the boar and came into close contact with abundant blood. Physical examination on his return to the hospital was unremarkable, but because of persistent symptoms and the appearance of petechiae and thrombocytopenia, the man was hospitalized for laboratory testing (Table 1) and imaging.

On August 7, infection with CCHF virus (CCHFV) was considered. The patient progressively worsened and died at the end of the day. On August 8, a blood sample was collected into an EDTA tube and sent to the National Center for Microbiology (Madrid, Spain) for CCHFV diagnostic testing. The sample was inactivated in the Biosafety Level 3 facility by using a QIAamp viral RNA kit (QIAGEN, https://www.qiagen.com) and after addition of ethanol was sent to the Biosafety Level 2 facility. Diagnostic testing was performed by using a RealStar CCHFV RT-PCR Kit 1.0 (Altona Diagnostics, https://altona-diagnostics.com), and CCHFV infection was confirmed by 2 methods: reverse transcription PCR (*1*) (slightly modified to incorporate an internal control for amplification) and a nested reverse transcription PCR (*2*). Results were further confirmed by a World Health Organization Collaborating Center (Public Health England, London, UK).

Molecular and serologic virus detection testing was also performed on additional serum samples. At

Author affiliations: National Center of Microbiology, Madrid, Spain (A. Negredo, F. Díez-Fuertes, F. De Ory, A. Vázquez, L. Hernández, P. Sánchez-Seco); Complejo Asistencial de Ávila, Ávila, Spain (R. Sánchez-Arroyo, M.A. Budiño, A. Garcinuño, C. de la Hoz González, C. Grande); CIBERESP, Madrid (A. Vázquez); La Paz Hospital, Madrid (A. Gutiérrez-Arroyo)

DOI: https://doi.org/10.3201/eid2704.203462

6 days after symptom onset, the patient's viral load (standards kindly provided by Altona Diagnostics) was >10^8 copies/mL. Specific IgG and IgM against CCHFV were detected by using a commercial indirect immunofluorescence assay (Crimean-Congo Fever Virus Mosaic 2 IFA; Euroimmun, https://www.euroimmun.com), according to the manufacturer's instructions (Table 2). IgM was detected on day 6 and IgG on day 7, both at very low titers.

Sequencing of small (S), medium (M), and large (L) segments was performed by using primers previously described (*3*). Complete genome sequences were obtained (GenBank accession nos. MN689738 [S segment], MN689740 [M segment], and MN689741 [L segment]).

Phylogenetic analyses with neighbor-joining and Bayesian (Figure 2) approaches that used MEGA7 (https://www.megasoftware.net) and the Beauti/Beast 1.75 package (https://beast.community) programs show similar results. The strain, Badajoz 2018, belongs to genotype III if the L and M segments are analyzed; however, the S segment

Table 1. Serial hematologic and biochemical parameters, vital signs, and treatments administered for Crimean-Congo hemorrhagic fever patient, Spain, 2018*

Variable	Jul 31	Aug 4	Aug 5	Aug 6	Aug 7
Hematologic parameters					
Hemoglobin, g/dL	13.5	14.5	12.9	12.4	9.4
Hematocrit, %	39.4	42.9	37.7	36.4	28
Leukocytes, $\times 10^{-3}$ cells/mm^3	10.7	4.1	3.6	4.6	5.9
Neutrophils, $\times 10^{-3}$ cells/mm^3	9.5	2.7	2.4	2.8	3.6
Lymphocytes, $\times 10^{-3}$ cells/mm^3	0.4	0.9	0.8	1.1	1.3
Platelets, $\times 10^{-3}$/mm^3	229	19	12	16	71
Internal normalized ratio	0.97	0.91	0.94	NT	1.27
Prothrombin time, s	10.7	9.9	10.2	NT	14
Prothrombin activity, %	104	115	110	NT	71
Partial thromboplastin time, s	26.2	46.7	47.5	NT	Not coagulable
Functional fibrinogen, mg/dL	320	274	268	NT	172
D-dimer, ng/mL	NT	NT	1123	NT	1781
Biochemical parameters					
Aspartate aminotransferase, U/L	20	197	527	961	3,129
Alanine aminotransferase, U/L	9	52	155	269	755
Bilirubin, mg/dL	0.5	0.6	0.5	0.7	0.9
Gamma-glutamyl transferase, U/L	22	229	303	388	545
Alkaline phosphatase, U/L	43	187	289	456	679
Lactate dehydrogenase, U/L	172	1,017	1,188	1,801	3,864
Creatinine, mg/dL	0.83	0.6	0.96	0.8	0.77
Sodium, mmol/L	138	136	134	134	137
Potassium, mmol/L	4.3	5.4	4.5	4.5	4.9
Ionic calcium, mmol/L	1.1	NT	1.15	1.06	1.06
Albumin, g/dL	3.9	NT	2.8	2.4	2.3
Glucose, mg/dL	83	87	97	100	117
Uric acid, mg/dL	NT	NT	NT	3.7	NT
C-reactive protein, mg/dL	0.51	1.77		3.77	NT
Procalcitonin, ng/L	0.17	0.22	0.63	NT	NT
Bicarbonate, mmol/L	23.2	NT	21.6	20.8	20
Lactate, mmol/L	1.1	3	1.4	1.2	2.5
Ferritin, ng/dL	NT	NT	NT	>40,000	NT
Ammonia, μmol/L	NT	NT	NT	NT	60
Spontaneous urine protein, g/L	Neg	1.41	NT	NT	**NT**
Erythrocytes in urine, cells/μg	Neg	50	NT	NT	NT
Vital signs					
Temperature, °C	39.2	38.3	37.1	37.2	37.1
Blood pressure, mm Hg	122/59	116/66	110/65	100/60	90/45
Heart rate, beats/min	110	87	70	76	89
Treatments received, IV					
Physiologic serum	N	Y	Y	Y	Y
Doxycycline	N	Y	Y	Y	Y
Piperacillin–tazobactam	N	Y	Y	Y	Y
Levofloxacin	N	Y	N	N	Y
Platelets, 1 pool	N	Y	N	N	Y
Vitamin K	N	N	N	N	Y
Tranexamic acid	N	Y	N	N	Y
Fresh frozen plasma	N	N	N	N	Y
Methylprednisolone	N	Y	Y	Y	Y

*IV, intravenous; neg, negative; N, not collected/administered that day; NT, not tested, Y, yes, collected/administered that day.

Figure 1. Regions where human infections with Crimean-Congo hemorrhagic fever virus (CCHFV) or infected ticks have been found in Spain. 1, CCHFV hyperendemic focus; 2, human infected by a tick bite in 2016 (Ávila); 3, human infected by a tick bite in 2018 (Badajoz). Red circle indicates area where infected ticks were detected during a surveillance study in 2016.

is closely related to sequences of genotype IV and shares the highest identity with the strains BT 958 (92.62%) from Central African Republic and IbAn7620 (92.58%) from Nigeria.

Conclusions

Phylogenetic analysis of the virus responsible for a fatal case of CCHF in 2018 showed reassortment, indicating a new CCHFV circulating in Spain. The patient was probably infected by a tick bite obtained while hunting. The incubation period for this patient was longer (7 days) than that typical after a tick bite (1–3 days) (*6*); however, the patient also participated in skinning the boar. The geographic location of the hunting site is very close to a natural park, bordering regions where the CCHFV genome has been detected in ticks (*7*) (Figure 1). After returning home, the patient felt ill, but CCHFV was not suspected until 7 days after symptoms appeared, just before he died. No specific treatment was administered. Despite the hospital being located within the region where the first case of CCHFV in Spain was detected, clinician awareness was not high enough to suspect CCHFV infection, partially because the patient diverted attention away from his possible contact with ticks or infected animals. The analytical parameters and the microbiological data are in accordance with described parameters for CCHFV in patients who have died (*8*), although partial thromboplastin time (and not prothrombin time) was altered in the final hemorrhagic phase, in contrast with parameters for the 2016 CCHF patient in Spain (*2*).

Table 2. Microbiological test results for Crimean-Congo hemorrhagic fever patient, Spain, August 2018

Result	Days after symptom onset	Viral load, copies/mL	C_t	IgG		IgM	
				GPC C	N	GPC	N
Serum	6	$2{,}82\ 10^8$	22	Neg	Neg	Neg	Pos (1/10)
Serum	7	$1{,}54\ 10^7$	25	Neg	Pos (1/40)	Neg	Pos (1/10)
Blood in EDTA	7	$1{,}58\ 10^7$	25	NT	NT	NT	NT

*C_t, cycle threshold; GPC, glycoprotein C; N, nucleoprotein; neg, negative; NT, not tested; pos, positive.

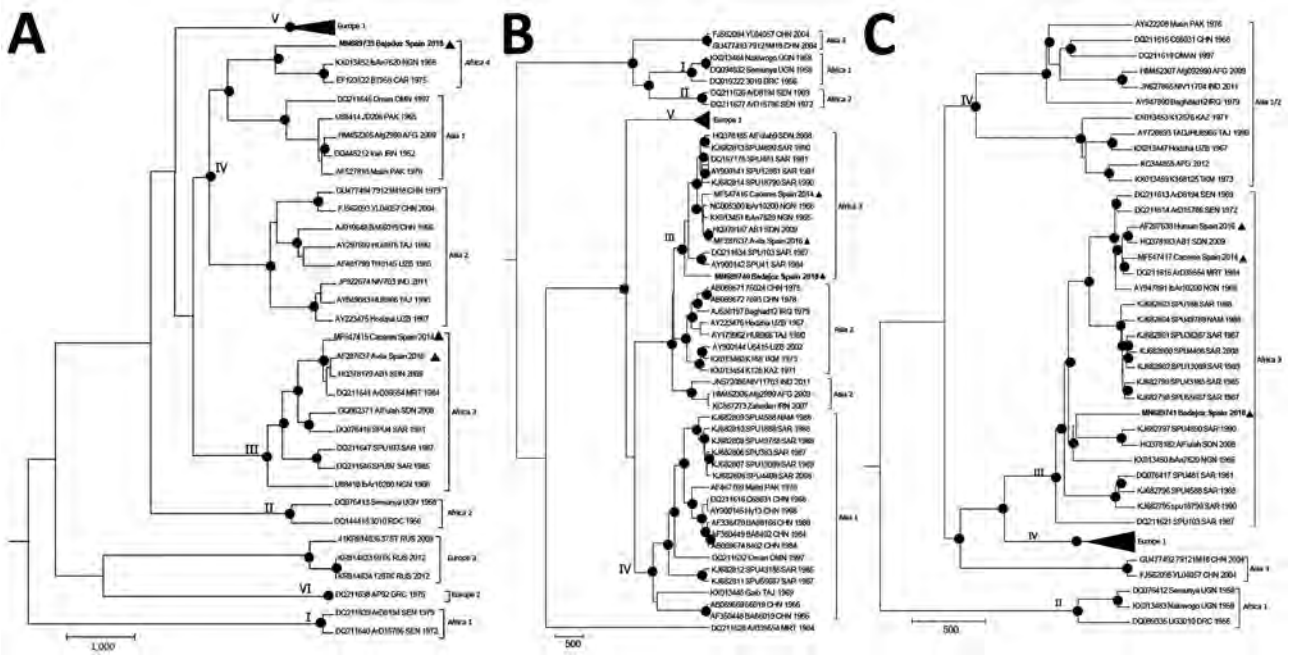

Figure 2. Bayesian phylogenetic trees showing genetic relationships among Crimean-Congo hemorrhagic fever (CCHFV) viruses based on complete small (A), medium (B), and large (C) segment sequences. In the medium segment, the hypervariable mucin-like domain was excluded. We used CIPRES Science gateway (http://www.phylo.org) to implement Bayesian analyses. Black dots indicate nodes with posterior probabilities >0.95; boldface indicates CCHFV strain Badajoz 2018 from Spain; arrowheads indicate other isolates from Spain. Other sequences are named by GenBank accession number, strain, geographic origin, and sampling year. Sequences from this study are included in EMBL/GenBank databases. Roman numerals indicate genotypes, named according to (*4*) with the equivalent clade nomenclature according to (*5*) indicated by brackets: I, West Africa (Africa 1); II, Central Africa (Africa 2); III, South and West Africa (Africa 3); IV, Middle East/Asia, divided in 2 groups corresponding to groups Asia 1 and Asia 2; V, Europe/Turkey (Europe 1); VI, Greece (Europe 2). Italics indicate the proposed new lineage, Africa 4. Scale bars indicate time in years.

Sequence analysis revealed circulation of a CCHFV very different genetically than the one previously described in Spain in humans or ticks (*2*,*3*,*9*,*10*). Complete sequences of viruses detected in humans (2016) and in ticks (2014) have indicated circulation of genotype III viruses, but the virus detected in 2018 is a reassortant in the S segment. Badajoz 2018 L and M segments group within genotype III (with sequences quite different than other sequences from Spain) and the S segment is similar to genotype IV. This S segment is close to the IbAn 7620 strain, isolated from the serum of a goat in 1965 in Nigeria, and the BT 958 strain from the Central African Republic, detected in 1975 and considered by Lukashev et al. (*11*) as an outlier of genotype IV. Genotype IV is formed by 2 genetic lineages, Asia 1 and Asia 2. Because the differences of Badajoz 2018 and related sequences with the Asia strains of genotype IV are remarkable, obtaining more related sequences from Spain or Africa may enable us to split this genotype into other genetic lineages by defining new genetic groups, probably with an origin in Africa. To date, this new genetic lineage contains sequences from 3 geographic regions detected 3 times.

The sequencing results showing 2 virus genetic lineages circulating in Spain indicate that at least 2 introductions have occurred. This situation seems to be distinct from that of the Balkans region, where only 1 virus was introduced from Asia and the virus causing human cases has remained genetically stable for decades (*11*). In fact, circulation of different variants of 1 virus in a small region where it is hyperendemic (Figure 1) in Spain in different years has been described (*10*), showing that the variability of CCHFV in Spain deserves special attention and efforts to get more sequence information.

Because of the high pathogenicity of CCHFV, a detailed medical history of the patient, including travel history and possible risk factors, is crucial for prompt diagnosis to ensure that appropriate infection control measures can be implemented in a timely manner. For the patient that we report, lack of immediate information regarding the tick bite in combination with the nonspecific initial symptoms meant

that CCHF was not suspected until day 8 of illness. The public health services performed contact tracing to identify all persons exposed, and none contracted symptomatic CCHF. This case and the description of a new virus do not modify the risk for infection by CCHFV in Spain. Risk is still considered low, although clinicians at hospitals and general practitioners need to be alert to the possibility of new cases.

Acknowledgment

We thank Amir Gacem for reviewing the grammar. We thank Roger Hewson and staff from Public Health England for their support with confirmation and isolation of the virus.

This study was partially funded by ISCIII, RD-16CIII/0003/0003, "Red de Enfermedades Tropicales," Subprogram RETICS Plan Estatal de I+D+I 2013-2016, and co-funded by FEDER "Una manera de hacer Europa."

About the Author

Dr. Negredo is a senior researcher at the Arbovirus and Imported Viral Diseases Laboratory of the National Centre for Microbiology (Madrid, Spain). Her primary research interests are viral hemorrhagic fevers and detection of emerging viruses that circulate in Spain.

References

1. Atkinson B, Chamberlain J, Logue CH, Cook N, Bruce C, Dowall SD, et al. Development of a real-time RT-PCR assay for the detection of Crimean-Congo hemorrhagic fever virus. Vector Borne Zoonotic Dis. 2012;12:786–93. https://doi.org/10.1089/vbz.2011.0770
2. Negredo A, de la Calle-Prieto F, Palencia-Herrejón E, Mora-Rillo M, Astray-Mochales J, Sánchez-Seco MP, et al.; Crimean Congo Hemorrhagic Fever@Madrid Working Group. Autochthonous Crimean-Congo hemorrhagic fever in Spain. N Engl J Med. 2017;377:154–61. https://doi.org/10.1056/NEJMoa1615162
3. Ramírez de Arellano E, Hernández L, Goyanes MJ, Arsuaga M, Cruz AF, Negredo A, et al. Phylogenetic characterization of Crimean-Congo hemorrhagic fever virus, Spain. Emerg Infect Dis. 2017;23:2078–80. https://doi.org/10.3201/eid2312.171002
4. Carroll SA, Bird BH, Rollin PE, Nichol ST. Ancient common ancestry of Crimean-Congo hemorrhagic fever virus. Mol Phylogenet Evol. 2010;55:1103–10. https://doi.org/10.1016/j.ympev.2010.01.006
5. Chamberlain J, Cook N, Lloyd G, Mioulet V, Tolley H, Hewson R. Co-evolutionary patterns of variation in small and large RNA segments of Crimean-Congo hemorrhagic fever virus. J Gen Virol. 2005;86:3337–41. https://doi.org/10.1099/vir.0.81213-0
6. Ergönül O. Crimean-Congo haemorrhagic fever. Lancet Infect Dis. 2006;6:203–14. https://doi.org/10.1016/S1473-3099(06)70435-2
7. Gobierno de España, Ministerio de Sanidad, Consumo y Bienestar Social. Evaluación rápida. Informe de situación y evaluación del riesgo de transmisión del virus de Fiebre Hemorrágica de Crimea-Congo (FHCC) en España [cited 2019 Jul 12]. https://www.mscbs.gob.es/profesionales/saludPublica/ccayes/analisisituacion/doc/ER_FHCC.pdf
8. Cevik MA, Erbay A, Bodur H, Eren SS, Akinci E, Sener K, et al. Viral load as a predictor of outcome in Crimean-Congo hemorrhagic fever. Clin Infect Dis. 2007;45:e96–100. https://doi.org/10.1086/521244
9. Cajimat MNB, Rodriguez SE, Schuster IUE, Swetnam DM, Ksiazek TG, Habela MA, et al. Genomic characterization of Crimean-Congo hemorrhagic fever virus in *Hyalomma* tick from Spain, 2014. Vector Borne Zoonotic Dis. 2017;17:714–9. https://doi.org/10.1089/vbz.2017.2190
10. Negredo A, Habela MA, Ramírez de Arellano E, Diez F, Lasala F, López P, et al. Survey of Crimean-Congo hemorrhagic fever enzootic focus in Spain, 2011–2015. Emerg Infect Dis. 2019;25:1177–84. https://doi.org/10.3201/eid2506.180877
11. Lukashev AN, Klimentov AS, Smirnova SE, Dzagurova TK, Drexler JF, Gmyl AP. Phylogeography of Crimean Congo hemorrhagic fever virus. PLoS One. 2016;11:e0166744. https://doi.org/10.1371/journal.pone.0166744

Address for corresponding Ana Negredo, National Center of Microbiology, Arbovirus and Imported Viral Diseases Laboratory, Crta. Majadahonda–Pozuelo Km 2, 28220-Majadahonda, Madrid, Spain; email: anabelnegredo@isciii.es

High Case-Fatality Rate for Human Anthrax, Northern Ghana, 2005–2016

Jason K. Blackburn, Ernest Kenu, Franklin Asiedu-Bekoe, Badu Sarkodie, Ian T. Kracalik,[1] William A. Bower, Robyn A. Stoddard, Rita M. Traxler

The human cutaneous anthrax case-fatality rate is ≈1% when treated, 5%–20% when untreated. We report high case-fatality rates (median 35.0%; 95% CI 21.1%–66.7%) during 2005–2016 linked to livestock handling in northern Ghana, where veterinary resources are limited. Livestock vaccination and access to human treatment should be evaluated.

Despite being one of the earliest diseases described, anthrax, caused by infection with the bacterium *Bacillus anthracis*, remains a global public health concern, especially in resource-limited, rural agricultural areas, including West Africa (*1*). Cutaneous anthrax, the most common human form, is readily treatable with antimicrobials and has a case-fatality rate (CFR; annual anthrax deaths/annual anthrax cases) ≈1%. Left untreated, CFR increases to 5%–20% for cutaneous anthrax and 25%–60% for gastrointestinal anthrax (*1*,*2*). However, Ghana has a history of human anthrax associated with high CFRs. One study reported that nearly 1,000 persons died from anthrax in Ghana during 1980–2000 (*3*). Most cases occurred in northern Ghana and were attributed to spillover from infected livestock. A 2017 study modeling the geographic distribution of anthrax risk in Ghana corroborated those findings and identified Northern, Savannah, Upper West, North East, and Upper East regions (using the current nomenclature for regions) as the areas of greatest risk for anthrax persistence in livestock and associated risk to humans (*4*). A 2000 study (*3*) focusing on Tamale, a major livestock production and trading center in northern Ghana, identified behaviors that increased risk for acquiring anthrax infection. These behaviors included neglecting livestock vaccination despite local vaccine production and availability, slaughtering, butchering, and distributing the meat from livestock that were sick or had died from anthrax, and believing that cooking the meat with specific herbs makes it safe to consume. In addition, the use of untested herbal or holistic treatments to cure anthrax has increased CFR; use of plants to treat anthrax has also been described in Nigeria (*5*).

Whereas human and livestock anthrax outbreaks are reported nearly annually in Ghana (*3*,*4*), most available studies are dated or limited to the distribution of human cases within specific communities or over short time periods (*6*). Here we describe human anthrax cases and resulting deaths reported across northern Ghana during 2005–2016.

The Study

We obtained data for the study through a One Health collaboration of the Ghanaian Ministries of Statistics, Health and Veterinary Services, and Agriculture, as part of anthrax surveillance capacity building aimed at integrating livestock and human reporting (*4*). Data included field reports not previously aggregated in national reports, reviews of national reports filed with the appropriate ministries, and outbreak investigations captured in gray literature or peer-reviewed articles. We used livestock data published elsewhere (*4*,*7*). Ethics approval was received by the Noguchi Memorial Institute for Medical Research in Accra.

Human anthrax cases were reported by district in Upper East region and a single district in Northern region. Data from Upper East were limited to aggregated annual counts per district for 2005–2015; limited line list data were available for 2016. Case-patient age and sex were available in Upper East for a subset of years, 2008–2014; other regions included

Author affiliations: University of Florida, Gainesville, Florida, USA (J.K. Blackburn, I.T. Kracalik); University of Ghana, Accra, Ghana (E. Kenu); Ghana Health Service, Accra (F. Asiedu-Bekoe, B. Sarkodie); Centers for Disease Control and Prevention, Atlanta, Georgia, USA (W.A. Bower, R.A. Stoddard, R.M. Traxler)

DOI: https://doi.org/10.3201/eid2704.204496

[1]Current affiliation: Centers for Disease Control and Prevention, Atlanta, Georgia, USA.

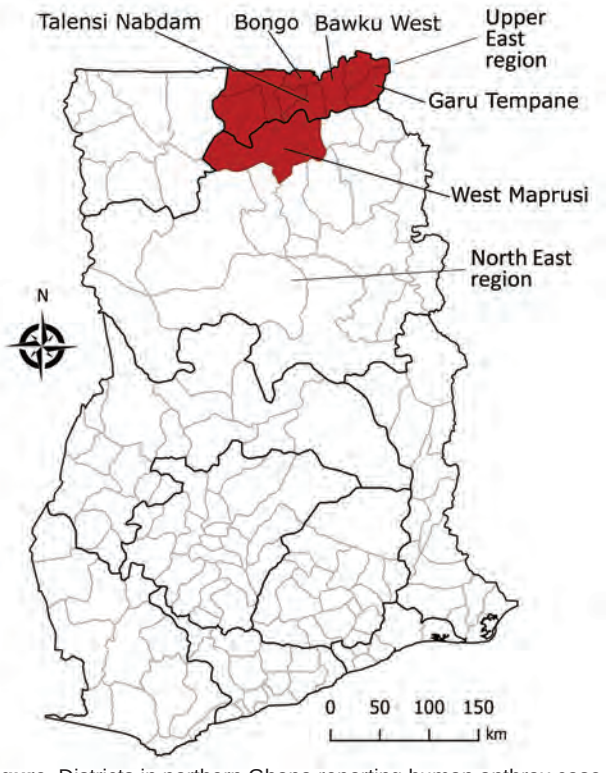

Figure. Districts in northern Ghana reporting human anthrax case and mortality data during 2005–2016.

human anthrax fatalities by month and year during 2005–2016. Deaths were aggregated by month and by year for comparison to livestock reports. No information was available on the form of infection (e.g., cutaneous, gastrointestinal).

We calculated CFRs and exact binomial CIs using the epitools package in the R software package (The R Project for Statistical Computing, https://www.r-project.org). We calculated median CFRs with bias-corrected and accelerated CIs with 10,000 replicates using the boot package in R. Because Upper East data were more complete, we calculated CFRs by district and year.

During 2005–2016, a total of 38 human deaths from anthrax were reported in Ghana, 30 from Upper East and 8 from Northern regions. For 8 cases with month of occurrence documented, deaths were reported in March, April, June, and December. Four deaths occurred during March and April, and in the Upper East, corresponding to seasonal peaks and geographic concentrations of livestock anthrax (*4*,*7*).

District-level data reported 30 (36.1%) deaths from 83 human anthrax cases in Upper East, including 1 district, West Mamprusi (now part of North East; Figure). During 2005–2016, Bawku West reported outbreaks in 4 years, Talensi Nabdam in 3 years, and other districts in 1 year. Cases of human anthrax peaked in 2006, 2008, and 2014 (Table). One study reported 43 livestock anthrax outbreaks in Northern region during 2005–2012; in 6 (14.0%) of those outbreaks, human cases were reported (*8*). From the 28 cases of cutaneous human anthrax in those 6 outbreaks, 6 (22.2%) persons died. However, neither case counts nor mortality rates could be directly associated with other reported livestock outbreaks. This disconnection of data on human anthrax cases from livestock outbreaks has been documented elsewhere (*9*). In data from Upper East with information on the age and sex of case-patients, 75.6% (31/41) of patients were men, consistent with rates in a previous report (*6*). Of the 31 men, 48.4% (15/31) died compared with 40.0% (4/10) of women. For all cases with age data, median age was 38 years (range 7–81 years) for men and 39.5 years (range 4–61 years) for women.

Conclusions

We found CFRs from recurrent anthrax outbreaks associated with human deaths in northern Ghana exceeded expected global CFRs for treated and untreated cutaneous anthrax and were likely untreated gastrointestinal anthrax. Evidence of the consumption of anthrax-contaminated meat in the region

Table. Annual human mortality by district for Upper East region and a single district from what is now North East region (formerly part of Northern region), Ghana, 2006–2016

Region and district	Year	Cases	Deaths	Case-fatality rate (95% CI)
Upper East				
Bawku West	2006	27	6	22.2 (8.6–42.3)
	2012	3	2	66.7 (9.4–99.2)
	2013	7	6	85.7 (42.1–99.6)
	2014	1	1	100.0 (2.5–100.0)
Garu-Tempane	2008	10	3	30.0 (6.7–65.2)
Talensi Nabdam	2008	6	1	16.7 (0.4–64.1)
	2009	9	2	22.2 (2.8–60.0)
	2014	10	6	60.0 (26.2–87.8)
Bongo	2012	5	2	40.0 (5.3–85.3)
North East*				
West Mamprusi	2007	5	1	20.0 (0.5–71.6)

*Current region for this district

suggests gastrointestinal anthrax is probably underrecognized in Ghana (*1*,*2*,*10*). The very high death rates may indicate that gastrointestinal anthrax is frequent in Ghana (*1*), which is supported by findings regarding beliefs in the same area about what meat is safe to consume (*3*). A study in Tamale, Ghana, found that livestock dying from anthrax are considered a ready source of meat for local community members, potentially leading to high human case numbers from relatively few animals (*3*). More education about the risks of consuming meat from animals that die suddenly is needed to counteract this belief.

The form of anthrax in cases identified here was undocumented. However, CFRs for human anthrax in Ghana were higher than for outbreaks in Thailand (CFR = 4%) and Zambia (CFR = 19%) involving gastrointestinal anthrax (*10*,*11*). High anthrax CFRs highlight 2 challenges. First, access to treatment may be limited, requiring long-distance travel in some settings (*11*). Second, anthrax underreporting is common, particularly for gastrointestinal anthrax because symptoms are atypical. There is insufficient awareness among healthcare providers and limited diagnostic capacity in rural endemic areas; anthrax should be included in differential diagnoses.

Although not captured in the data here, 2 deaths in March 2016 in Ghana were reported as suspected anthrax in the human health reporting system but could not be laboratory confirmed (data not shown). Both were reported as anthrax based on clinical signs and an epidemiologic link to livestock clinically diagnosed by the veterinary reporting system. This incident, coupled with findings from our analyses, illustrates the need for joint evaluation of records and uniformity in case definitions between human and animal reporting systems.

Early treatment is crucial for recovery from anthrax; prophylactic antimicrobial drugs are recommended for persons with known or suspected exposure to anthrax-contaminated meat or livestock. Livestock vaccination remains the most effective control method for reducing anthrax burden in livestock and humans (*12*,*13*); however, minimal vaccination uptake persists because of beliefs about its effectiveness and limited veterinary services and because underreporting associated with diagnostic capacity hinders vaccination campaigns. Recent models prioritized geographic areas for prevention and control (*1*,*4*).

Our findings highlight the need for education about the risks of consuming meat from sick or dead animals and the benefits of livestock vaccination, increased healthcare provider awareness, and evaluation of accessibility to anthrax treatment. These findings support ongoing efforts in Ghana to coordinate human and livestock anthrax reporting and to improve and expand diagnostic capacity.

Acknowledgments

We thank the Ghana FELTP, Noguchi Medical Research Institute, and Sean Shadomy. We are grateful to the data management team in the Disease Surveillance Department, Ghana Health Service led by Isaac Beffoe-Nyarko.

This work was funded by the Centers for Disease Control and Prevention, National Center for Emerging and Zoonotic Infectious Diseases, Division of High-Consequence Pathogens and Pathology.

About the Author

Dr. Blackburn is an associate professor of medical geography in global health and principal investigator at the Emerging Pathogens Institute, University of Florida. His research interests are focused on the spatiotemporal patterns and ecology of pathogens found in environmental reservoirs, particularly those that cause zoonoses.

References

1. Carlson CJ, Kracalik IT, Ross N, Alexander KA, Hugh-Jones ME, Fegan M, et al. The global distribution of *Bacillus anthracis* and associated anthrax risk to humans, livestock and wildlife. Nat Microbiol. 2019;4:1337–43. https://doi.org/10.1038/s41564-019-0435-4
2. Doganay M, Metan G. Human anthrax in Turkey from 1990 to 2007. Vector Borne Zoonotic Dis. 2009;9:131–40. https://doi.org/10.1089/vbz.2008.0032
3. Opare C, Nsiire A, Awumbilla B, Akanmori BD. Human behavioural factors implicated in outbreaks of human anthrax in the Tamale municipality of northern Ghana. Acta Trop. 2000;76:49–52. https://doi.org/10.1016/S0001-706X(00)00089-9
4. Kracalik IT, Kenu E, Ayamdooh EN, Allegye-Cudjoe E, Polkuu PN, Frimpong JA, et al. Modeling the environmental suitability of anthrax in Ghana and estimating populations at risk: Implications for vaccination and control. PLoS Negl Trop Dis. 2017;11:e0005885. https://doi.org/10.1371/journal.pntd.0005885
5. Alawa JP, Jokthan GE, Akut K. Ethnoveterinary medical practice for ruminants in the subhumid zone of northern Nigeria. Prev Vet Med. 2002;54:79–90. https://doi.org/10.1016/S0167-5877(01)00273-2
6. Awoonor-Williams JK, Apanga PA, Anyawie M, Abachie T, Boidoitsiah S, Opare JL, et al. Anthrax outbreak investigation among humans and animals in northern Ghana: case report. Int J Trop Dis Health. 2015;12:1–11. https://doi.org/10.9734/IJTDH/2016/22359
7. Nsoh AE, Kenu E, Forson EK, Afari E, Sackey S, Nyarko KM, et al. Mapping as a tool for predicting the risk of anthrax outbreaks in Northern Region of Ghana. Pan Afr Med J. 2016;25(Suppl 1):14. https://doi.org/10.11604/pamj.supp.2016.25.1.6205

8. Ayamdooh EN. Mapping as a tool for predicting the risk of anthrax outbreaks in Northern Region of Ghana [thesis]. Accra (Ghana): University of Ghana; 2015.
9. Sirisanthana T, Brown AE. Anthrax of the gastrointestinal tract. Emerg Infect Dis. 2002;8:649–51. https://doi.org/10.3201/eid0807.020062
10. Siamudaala VM, Bwalya JM, Munang'andu HM, Sinyangwe PG, Banda F, Mweene AS, et al. Ecology and epidemiology of anthrax in cattle and humans in Zambia. Jpn J Vet Res. 2006;54:15–23.
11. Kracalik I, Malania L, Tsertsvadze N, Manvelyan J, Bakanidze L, Imnadze P, et al. Human cutaneous anthrax, Georgia, 2010–2012. Emerg Infect Dis. 2014;20:261–4. https://doi.org/10.3201/eid2002.130522
12. Kracalik I, Abdullayev R, Asadov K, Ismayilova R, Baghirova M, Ustun N, et al. Changing patterns of human anthrax in Azerbaijan during the post-Soviet and preemptive livestock vaccination eras. PLoS Negl Trop Dis. 2014;8:e2985. https://doi.org/10.1371/journal.pntd.0002985
13. Kracalik I, Malania L, Broladze M, Navdarashvili A, Imnadze P, Ryan SJ, et al. Changing livestock vaccination policy alters the epidemiology of human anthrax, Georgia, 2000–2013. Vaccine. 2017;35:6283–9. https://doi.org/10.1016/j.vaccine.2017.09.081

Address for correspondence: Jason K. Blackburn, Spatial Epidemiology and Ecology Research Laboratory, Department of Geography, 3141 Turlington Hall, University of Florida, Gainesville, FL 32611, USA; email: jkblackburn@ufl.edu

Postvaccination COVID-19 among Healthcare Workers, Israel

Sharon Amit, Sharon Alexsandra Beni, Asaf Biber, Amir Grinberg, Eyal Leshem,[1] Gili Regev-Yochay[1]

Coronavirus disease (COVID-19) symptoms can be mistaken for vaccine-related side effects during initial days after immunization. Among 4,081 vaccinated healthcare workers in Israel, 22 (0.54%) developed COVID-19 from 1–10 days (median 3.5 days) after immunization. Clinicians should not dismiss postvaccination symptoms as vaccine-related and should promptly test for COVID-19.

Large-scale vaccination of risk groups and later the general population is the single most effective public health measure for mitigation of the coronavirus disease (COVID-19) pandemic. National COVID-19 vaccination programs started during December 2020 in several countries and prioritized healthcare workers (HCWs) (*1*). In some countries the vaccination programs coincided with a surge in detected COVID-19 cases and increased burden on the healthcare system (*2*).

During December 2020–January 2021, Israel experienced a surge in COVID-19 incidence that resulted in the third national lockdown imposed since the pandemic began in early 2020 (*3*). Concomitantly, during December 2020, Israel's Ministry of Health approved the Pfizer-BioNTech COVID-19 vaccine (BNT162b2; Pfizer Inc., https://www.pfizer.com) and prioritized HCWs for immunization (*4*).

Sheba Medical Center is a large hospital with 9,069 staff members in Ramat-Gan, Israel. The hospital started its personnel vaccination program on December 20, 2020, and excluded workers who had recovered from COVID-19. During the first week of the campaign, 4,081 (45%) eligible staff members received the first dose of BNT162b2. Concurrently, the national COVID-19 positivity rate rapidly increased to >6% on January 3, 2021 (*2*).

The Study

The hospital's Infection Prevention and Control Unit conducted active and passive surveillance of vaccinated staff by using daily health questionnaires, hotlines, on-call infectious disease unit staff, and post-vaccination web-based questionnaires to identify and test symptomatic HCWs. Among 4,081 HCWs vaccinated in the first week of the campaign, 22 (0.54%) later had laboratory-confirmed COVID-19 (Table). The average age among COVID-19–positive vaccinated HCWs was 45.3 years (±9.85 years), and they belonged to different healthcare sectors and worked on various wards.

Among the 22 vaccinated HCWs who tested positive for COVID-19, 13 were tested because they had symptoms, most commonly an influenza-like illness that included fever, chills, cough, headache, myalgia, and sore throat. Two vaccinated HCWs were tested because of exposure to confirmed or suspected COVID-19 cases yet reported symptoms upon questioning. Asymptomatic COVID-19 cases were identified among HCWs as part of postexposure screening. Among the 22 COVID-19–positive HCWs, 11 had presumable community-related exposures, 4 of whom reported exposure incidents that occurred before or on the date of vaccination. An investigation conducted by the hospital's Infection Control and Prevention Unit identified 10 healthcare-related secondary exposures. However, we did not identify any point-source exposures or COVID-19 clusters linked to the immunization process.

Among the 11 vaccinated HCWs who reported COVID-19 symptoms, the median time between the first dose of BNT162b2 immunization and symptom onset was 3.5 (range 0–10) days; we excluded 1 vaccinee from our calculation and analysis because the HCW had symptoms before immunization (Table). The median time between the onset of symptoms and testing was 1 day, demonstrating the high level of suspicion for COVID-19 during the vaccination campaign.

Of note, apart from the need for early detection, persons who test positive for COVID-19 after receiving the first vaccine dose (whether asymptomatic and tested following exposure or tested because they are symptomatic) are not eligible to receive the second dose, according to Ministry of Health policy. However, depending on availability of vaccines, this policy might change when further data are collected.

Authors affiliation: Chaim Sheba Medical Center, Ramat-Gan, Israel

DOI: https://doi.org/10.3201/eid2704.210016

[1]These authors equally contributed to the study.

Conclusions

COVID-19 in HCWs is a major concern for health authorities worldwide. HCWs, especially acute and chronic care facility personnel, are at high risk for contracting symptomatic and asymptomatic COVID-19 and might become infected at home or nosocomially while caring for patients or interacting with other staff members (*5*–*7*). Infections among HCWs have an immediate effect on their close occupational environment and the overall healthcare system. Secondary exposures, isolation, and infections of staff can substantially impair the capacity of a single ward to care for patients, creating a snowball effect with collateral damage to both the functional resilience of the facility and morale of staff. Consequently, as soon as COVID-19 vaccines were deployed in Israel, HCWs were the first group to receive it.

We report 22 cases of early, postimmunization, laboratory-confirmed COVID-19 among HCWs during the launch of the vaccination campaign in a large hospital in Israel. BNT162b2 is not likely to exert protection against clinical disease during the first days after receipt of the first dose. Efficacy of the BNT162b was 52% a week after the first dose, and positive COVID-19 cases were described among vaccinees even early after the second dose (*8*). Thus, during a large-scale immunization campaign coinciding with rapid national increase in COVID-19 cases, some immunized persons likely will develop clinical disease.

The co-occurrence of vaccination deployment with the rapidly climbing COVID-19 spread in many parts of the world is a confusing period in which hope is mixed with great vulnerability. The phenomenon of pandemic fatigue, in which the population tires of constant safety precautions, testing, isolation, and restrictions, could lead to less social distancing and personal protection. Pandemic fatigue coupled with the availability of a vaccine, might give the population a false sense of reassurance and consequently lead to a brisk increase in COVID-19 cases. Thus, almost every physical complaint after vaccination poses a true diagnostic dilemma as to whether an adverse reaction or a new COVID-19 infection is the cause. Undetected COVID-19 cases among HCWs could be hazardous for patients and other staff.

Table. Coronavirus disease cases among healthcare workers in the early postvaccination period, Israel, December 20, 2020–January 2, 2021*

Case no.	Age, y/sex	Ward	Healthcare sector	Indication for testing	Presumed exposure source	Exposure day	Day of symptom onset†	Day tested	No. days from symptom onset to testing	No. secondary isolations
1	42/F	General surgery	Physician	Symptoms	Unknown	Unknown	−4	+5	Excluded‡	0
2	54/F	Transportation	Secretary	Symptoms	Unknown	Unknown	0	+9	9	1
3	34/M	Geriatrics	Physician	Symptoms	Unknown	Unknown	+1	+1	0	1
4	31/F	Cardiovascular surgery	Nurse	Symptoms	Community	Unknown	+1	+1	0	1
5	49/F	Psychiatry	Cleaning services	Symptoms	Unknown	Unknown	+1	+3	2	0
6	43/F	Laundry	Laundry handler	Symptoms	Community	−3	+2	+3	1	3
7	43/F	Laboratory	Scientist	Exposure	Community	−3	+2	+6	4	0
8	60/F	ED	Nurse assistant	Symptoms	Community	0	+3	+5	2	0
9	50/F	Eye clinic	Technologist	Symptoms	Unknown	Unknown	+4	+6	2	0
10	33/M	Psychiatry	Psychologist	Exposure	Community	+2	+6	+6	0	0
11	36/M	Operating room	Logistics	Symptoms	Community	+4	+7	+8	1	0
12	54/M	Pulmonology	Physician	Symptoms	Community	+4	+7	+7	0	0
13	37/M	ED	Physician	Symptoms	Unknown	+3	+7	+9	2	0
14	32/M	Rehabilitation	Nurse	Symptoms	Unknown	Unknown	+9	+10	1	1
15	40/M	Laboratory	Physician	Symptoms	Unknown	Unknown	+10	+10	0	1
16	52/F	Radiotherapy	Secretary	Exposure	Unknown	Unknown	Asymp	+5	NA	3
17	55/F	General surgery	Phlebotomist	Exposure	Unknown	Unknown	Asymp	+8	NA	4
18	55/F	Kitchen	Food handler	Exposure	Community	−5	Asymp	+2	NA	1
19	61/F	Radiology	Physician	Exposure	Community	+4	Asymp	+11	NA	0
20	40/F	ED	Secretary	Exposure	Community	+6	Asymp	+11	NA	2
21	45/F	Internal medicine	Nurse	Exposure	Unknown	Unknown	Asymp	+8	NA	0
22	39/M	Internal medicine	Nurse	Exposure	Community	+2	Asymp	+8	NA	0

*All persons with cases were vaccinated during the first week of campaign, December 20–27, 2020. Asymp, asymptomatic; ED, emergency department; NA, not applicable.
†Considering day of vaccination as day 0.
‡Excluded from calculations of mean time from vaccination to symptom onset because symptoms began before vaccination.

Clinicians should have a high level of suspicion of reported symptoms and avoid dismissing complaints as vaccine-related until true infection is ruled out and vaccinees are tested. Active and passive surveillance that enables rapid testing and initiation of infection control measures are essential in preventing possible diagnostic delays and secondary exposures. Therefore, healthcare-related indications for testing should not be altered until systematic and exhaustive data are gathered regarding vaccine effectiveness in healthcare settings.

About the Author

Dr. Amit is a certified internist, infectious disease specialist, and clinical microbiologist, and is the director of the Clinical Microbiology Laboratory Department at Sheba Medical Center, Israel. Her fields of research include clinical microbiology and communicable diseases epidemiology.

References

1. Dooling K, McClung N, Chamberland M, Marin M, Wallace M, Bell BP, et al. The Advisory Committee on Immunization Practices' interim recommendation for allocating initial supplies of COVID-19 vaccine—United States, 2020. MMWR Morb Mortal Wkly Rep. 2020;69:1857–9. https://doi.org/10.15585/mmwr.mm6949e1
2. Johns Hopkins University Center for Systems Science and Engineering. COVID-19 dashboard. 2020 [cited 2021 Jan 3]. https://coronavirus.jhu.edu/map.html
3. Leshem E, Afek A, Kreiss Y. Buying time with COVID-19 outbreak response, Israel. Emerg Infect Dis. 2020;26:2251–3. https://doi.org/10.3201/eid2609.201476
4. State of Israel Ministry of Health. Coronavirus (COVID-19) vaccines [in Hebrew]. 2020 [cited 2021 Jan 3]. https://www.health.gov.il/UnitsOffice/HD/PH/epidemiology/td/docs/365_Corona.pdf
5. Calcagno A, Ghisetti V, Emanuele T, Trunfio M, Faraoni S, Boglione L, et al. Risk for SARS-CoV-2 infection in healthcare workers, Turin, Italy. Emerg Infect Dis. 2021;27:303–5. https://doi.org/10.3201/eid2701.203027
6. Feaster M, Goh YY. High proportion of asymptomatic SARS-CoV-2 infections in 9 long-term care facilities, Pasadena, California, USA, April 2020. Emerg Infect Dis. 2020;26:2416–9. https://doi.org/10.3201/eid2610.202694
7. Akinbami LJ, Vuong N, Petersen LR, Sami S, Patel A, Lukacs SL, et al. SARS-CoV-2 seroprevalence among healthcare, first response, and public safety personnel, Detroit metropolitan area, Michigan, USA, May–June 2020. Emerg Infect Dis. 2020;26:2863–71. https://doi.org/10.3201/eid2612.203764
8. Polack FP, Thomas SJ, Kitchin N, Absalon J, Gurtman A, Lockhart S, et al.; C4591001 Clinical Trial Group. Safety and efficacy of the BNT162b2 mRNA Covid-19 vaccine. N Engl J Med. 2020;383:2603–15. https://doi.org/10.1056/NEJMoa2034577

Address for correspondence: Sharon Amit, Clinical Microbiology, The Chaim Sheba Medical Center, Ramat Gan, Israel; email: sharon.amit@sheba.health.gov.il

Genomic Characterizations of Clade III Lineage of *Candida auris*, California, USA

Travis K. Price, Ruel Mirasol, Kevin W. Ward, Ayrton J. Dayo, Evann E. Hilt, Sukantha Chandrasekaran, Omai B. Garner, Annabelle de St Maurice, Shangxin Yang

Candida auris is an emerging multidrug-resistant yeast. We describe an ongoing *C. auris* outbreak that began in October 2019 in Los Angeles, California, USA. We used genomic analysis to determine that isolates from 5 of 6 patients belonged to clade III; 4 isolates were closely related.

Candida auris was isolated from a patient in Tokyo, Japan in 2009 (*1*), although clinical isolates have been retrospectively identified from as early as 1996 (*2*). Since then, bloodstream and other invasive infections caused by *C. auris* have been reported worldwide (*3*–*5*). Many strains of *C. auris* are multidrug-resistant; some strains require elevated MICs to azoles, echinocandins, and polyenes. In 2019, the US Centers for Disease Control and Prevention (CDC) listed *C. auris* as an urgent threat to public health (*6*), highlighting the need for active surveillance and appropriate infection prevention.

Whole-genome sequencing (WGS) and phylogenetic analyses have revealed ≥4 major clades of *C. auris*; each clade covers a distinct geographic area, giving *C. auris* a global distribution (*7*,*8*). Researchers have documented several *C. auris* outbreaks in the United States, mostly caused by strains belonging to clades I and IV (*9*). We describe several cases of *C. auris* colonization and infection in patients of long-term acute-care (LTAC) facilities in and around Los Angeles, California, USA.

The Study

We screened patients at high risk for drug-resistant infections who were transferred to University of California, Los Angeles (UCLA)–affiliated hospitals from LTAC and skilled nursing facilities (SNFs). We analyzed swab samples of patients' axilla and groin and yeast isolates from positive fungal culture of clinical specimens using PCR selective for the ITS2 region of the *C. auris* genome. We conducted antifungal susceptibility testing using broth microdilution; WGS using Illumina MiSeq (Illumina, https://www.illumina.com); and k-mer and single-nucleotide polymorphism (SNP) analyses using CLC Genomics Workbench (QIAGEN, https://www.qiagen.com) and Geneious Prime (Geneious, https://www.geneious.com) (Appendix 1, https://wwwnc.cdc.gov/EID/article/27/5/20-4361-App1.pdf).

During September 2019–September 2020, we screened 113 patients using in-house PCR selective for *C. auris* according to Los Angeles County Public Health and CDC guidelines (Appendix 1). Six patients tested positive for *C. auris* with cycle threshold (C_t) values of 22.6–39.7 (Table 1). Patient A tested positive in October 2019; patients B–F tested positive during July–September 2020.

The 6 patients were residents of 4 LTAC facilities in Los Angeles County. All 6 had a history of tracheostomy. Patients A and F had prior history of *C. auris* colonization; patient F had active infection of a bronchopulmonary fistula. Patient D had *C. auris* and severe acute respiratory syndrome coronavirus 2 co-infection (Table 1). We cultured *C. auris* isolates from inguinal and axillary swab samples of patients A, C, D, and E; pleural fluid of patient F; and tracheal aspirate of patient A. The sample from patient A produced few colonies; we treated the patient for bacterial pneumonia. We were not able to isolate *C. auris* from patient B (C_t = 39.5).

All *C. auris* isolates were resistant to amphotericin B (MIC = 2 μg/mL) and fluconazole (MIC >64 μg/mL) but susceptible to echinocandins (Table 2). We conducted k-mer analysis using 261 *C. auris* sequences available on GenBank, most of which were described previously (*10*) (Appendix 2 Table 1, https://wwwnc.cdc.gov/EID/article/27/5/20-4361-App2.xlsx). All 6

Author affiliation: University of California, Los Angeles, California, USA

DOI: https://doi.org/10.3201/eid2705.204361

UCLA isolates belonged to clade III (Appendix 2 Table 1). We conducted a phylogenetic analysis of clade III isolates using k-mers (Appendix 1 Figure).

In the United States, researchers have identified isolates belonging to all 4 clades; although these isolates show geographic relationships (*9*), clade I is predominant across the country. Clade III isolates have been identified in Indiana, Texas (*11*), and Florida. We conducted a k-mer–based phylogenetic analysis of *C. auris* isolates in the United States (Figure). SNP analysis showed that 5 of the UCLA isolates were closely related (3–12 SNPs); isolate F1 was genetically distinct (77–79 SNPs). All 6 isolates were distinct from isolates from Indiana (65–139 SNPs) and Florida (47–117 SNPs) (Appendix 1 Table 1).

We also analyzed the sequences of 2 genes associated with antifungal resistance: *erg11* (lanosterol 14-α demethylase) and *fks1* (subunit of 1,3-β-D-glucan synthase). Sequences of *erg11* were identical among all isolates, with 99.6% pairwise nucleotide identity to the reference (GenBank accession no. CP043531) and 2 amino acid substitutions: V125A and F126L

Table 1. Characteristics of patients with *Candida auris* infection, Los Angeles, California, USA, 2019–2020*

Patient	Date of positive PCR	Cycle threshold	*C. auris* isolate (specimen type)	Approximate age, y	Clinical history	Current signs, symptoms, and diagnosis
A	2019 Oct 8	22.6	UCLA_A1 (inguinal–axillary); UCLA_A2 (tracheal, deemed colonization)	65	Coronary artery disease, stroke, chronic respiratory fracture, tracheostomy and ventilator dependence, gastrostomy tube dependence, urinary incontinence, multiple ulcers, heart failure, atrial fibrillation, and previous carbapenem-resistant *Enterobacteriaceae* bacteremia. This patient had a prior history of *C. auris* colonization at the long-term acute-care facility.	Septic shock caused by methicillin-resistant *Staphylococcus aureus* bacteremia and multifocal pneumonia. *C. auris*, *Candida albicans*, and *Candida parapsilosis* were isolated from tracheal suction culture.
B	2020 July 28	39.5	Not isolated†	45	Anoxic brain injury caused by MRSA endocarditis and pulseless electrical activity arrest, stroke, and gastrostomy tube dependence.	Hemoptysis, upper gastrointestinal bleeding, hypotension, and tachycardia. MRSA, *Escherichia coli*, *Providencia stuartii*, *Proteus mirabilis*, and *Acinetobacter baumanii* grew on blood cultures. *Candida glabrata* grew on lower respiratory culture.
C	2020 Aug 12	22.6	UCLA_C1 (inguinal–axillary)	65	Hypertension, hyperlipidemia, intracranial hemorrhage and ventriculoperitoneal shunt, tracheostomy, and gastrostomy tube dependence.	Respiratory failure caused by pulmonary edema. *P. mirabilis* grew on urine cultures.
D	2020 Aug 19	39.7	UCLA_D1 (inguinal–axillary)	55	Hypertension, hyperlipidemia, type 2 diabetes, aplastic anemia, stroke, pulmonary embolism, pneumothorax, and coronavirus disease–related pneumonia causing respiratory failure, tracheostomy, and gastrostomy tube dependence.	Elevated liver enzymes and gastrointestinal bleeding complicated by *Enterococcus* bacteremia and *E. coli* urinary tract infection.
E	2020 Aug 31	28.3	UCLA_E1 (inguinal–axillary)	65	Hypertension, hyperlipidemia, tracheostomy, and gastrostomy tube dependence.	Worsening generalized weakness possibly caused by chronic intermittent demyelinating polyneuropathy.
F	2020 Sep 3	30.6	UCLA_F1 (pleural fluid, active infection)	85	Subarachnoid hemorrhage, tracheostomy, gastrostomy tube dependence, stage IV sacral decubitus ulcer, and chronic kidney disease. This patient had a prior history of *C. auris* colonization at the long-term acute-care facility.	Bronchopulmonary fistula. *C. auris*, *Pseudomonas aeruginosa*, and *Enterococcus faecalis* grew on pleural fluid cultures.

*MRSA, methicillin-resistant *Staphylococcus aureus*.
†*C. auris* was not isolated from the inguinal–axillary surveillance swab of patient B.

Table 2. Antifungal susceptibility results for *Candida auris* isolates, Los Angeles, California, USA, 2019–2020*

	MIC, μg/mL (interpretation)†					
Antifungal	UCLA_A1	UCLA_A2	UCLA_C1	UCLA_D1	UCLA_E1	UCLA_F1
Amphotericin B	2 (R)	2 (R)	2 (R)	2 (R)	2 (R)	2 (R)
Fluconazole	>64 (R)	>64 (R)	>64 (R)	>64 (R)	>64 (R)	>64 (R)
Voriconazole	2	1	1	0.5	0.5	2
Itraconazole	1	1	0.5	0.25	0.25	1
Posaconazole	0.06	0.12	≤0.03	≤0.03	0.06	0.06
Anidulafungin	0.5 (S)	0.12 (S)	0.25 (S)	0.12 (S)	0.06 (S)	1 (S)
Caspofungin	0.5 (S)	0.12 (S)	0.5 (S)	0.5 (S)	0.12 (S)	0.5 (S)
Micafungin	0.25 (S)	0.25 (S)	0.25 (S)	0.12 (S)	0.25 (S)	0.25 (S)

*I, intermediate; R, resistant; S, susceptible.
†MIC testing was conducted on panels prepared in-house in accordance with Clinical and Laboratory Standards Institute guidelines (https://standards.globalspec.com/std/10266416/CLSI%20M27). Interpretive breakpoints were defined by the CDC Antifungal Susceptibility Testing and Interpretation guidelines for *C. auris* (https://www.cdc.gov/fungal/candida-auris/c-auris-antifungal.html), which were adapted from interpretive criteria for closely related *Candida* spp. Tentative breakpoints for the following antifungal drugs were: amphotericin B (≥2 μg/mL), fluconazole (≥32 μg/mL), anidulafungin (≥4 μg/mL), caspofungin (≥2 μg/mL), and micafungin (≥4 μg/mL).

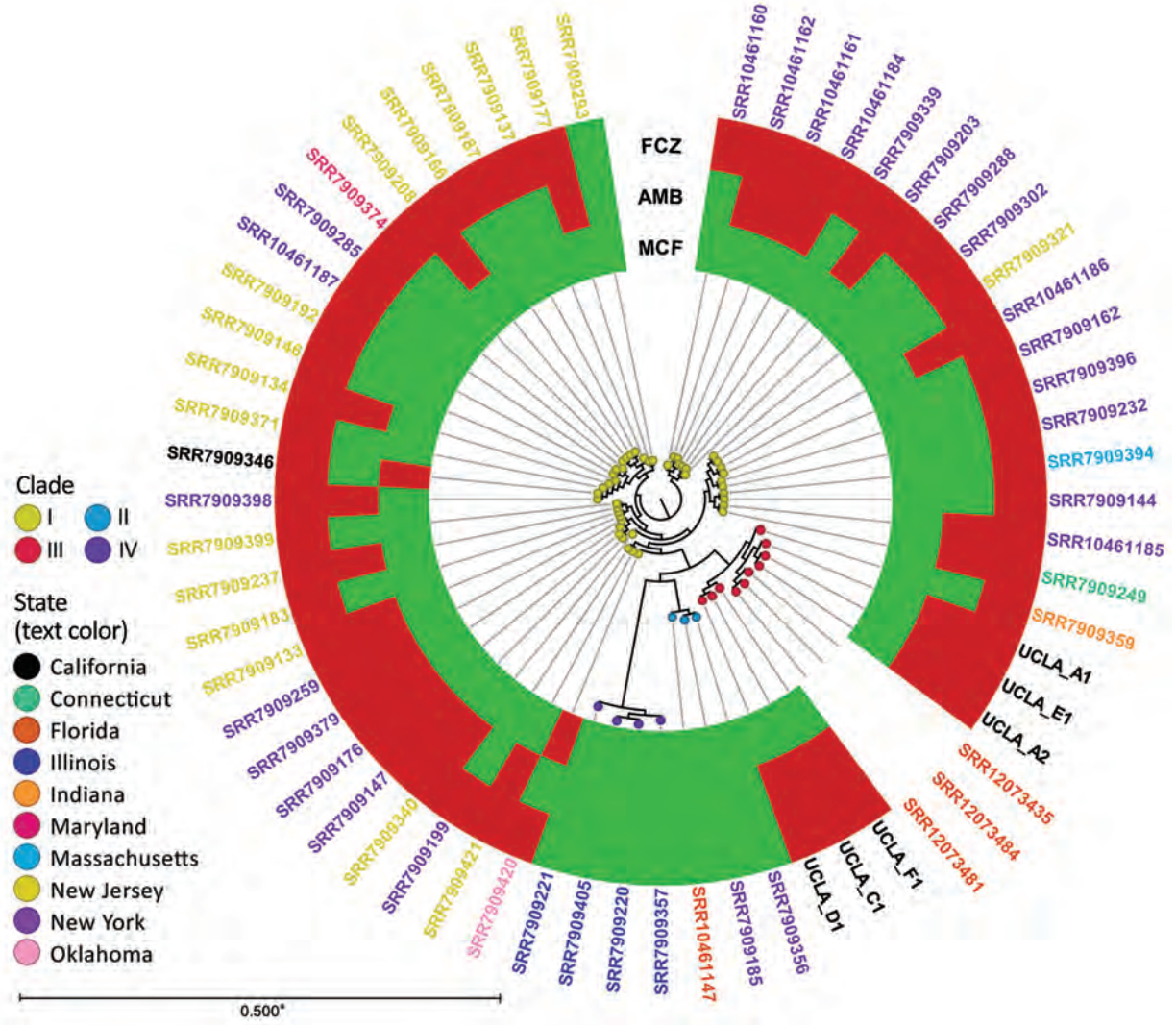

Figure. K-mer analysis of *Candida auris* isolates, United States, 2009–2020. K-mer analysis was conducted with CLC Genomics Workbench (QIAGEN, https://www.qiagen.com) using genome sequences from patients in Los Angeles, California, USA during 2019–2020 (i.e., UCLA_A1, UCLA_A2, UCLA_C1, UCLA_D1, UCLA_E1, and UCLA_F1) and 55 publicly available *C. auris* strains in GenBank (Appendix 2 Table 2, https://wwwnc.cdc.gov/EID/article/27/5/20-4361-App2.xlsx). Each node represents a unique isolate. Node color indicates clade. The color of the isolate name (i.e., label text color) indicates state of origin. The metadata shows the susceptibility of each isolate (if available) to fluconazole (FCZ), amphotericin B (AMB), and micafungin (MCF); red indicates resistant, green indicates susceptible. Asterisk indicates that branches shorter than 0.0050 are shown as 0.0050.

(Appendix 1 Table 2). Mutations at aa 126 are associated with increased azole resistance in *C. auris* (*7*) and are a common feature of clade III isolates (*12*). The F126L mutation appears to be exclusive to clade III (*10*). These findings are consistent with results of antifungal susceptibility testing, which showed that all isolates were resistant to fluconazole (Table 2). Sequences of *fks1* were identical in 5 isolates (A1, A2, C1, D1, E1), with 99.9% pairwise nucleotide identity to the reference (GenBank accession no. CP043531); these isolates had 1 amino acid substitution: I1572L (Appendix 1 Table 2). Isolate F1 had the same substitution in addition to I1095L. All isolates had a wild-type serine at aa 639; mutations at this location are linked to echinocandin resistance in *C. auris* (*13*). All isolates were susceptible to caspofungin, micafungin, and anidulafungin.

Conclusions

To identify and prevent the spread of *C. auris* in this hospital system, we used an in-house PCR to screen patients for this pathogen. WGS of isolates from patients transferred from LTAC facilities revealed that these isolates are closely related, suggesting an ongoing outbreak with community spread in the Los Angeles area.

The isolates described here were all resistant to fluconazole and amphotericin B but susceptible to echinocandins according to the CDC tentative breakpoints (https://www.cdc.gov/fungal/candida-auris/c-auris-antifungal.html). In addition, all isolates had an F126L mutation in the *erg11* gene, which is unique to clade III strains and associated with fluconazole resistance (*10*).

Patient D was admitted to an SNF after complications from pneumonia caused by coronavirus disease (COVID-19). Few cases of *C. auris* and COVID-19 co-infection have been reported (*14*,*15*). After COVID-19 infection, patient D had multiple complications requiring a tracheostomy and enteral feeding tube; the patient was subsequently transferred to an LTAC for rehabilitation. A substantial portion of adult patients who recover from severe COVID-19 have long-term sequelae and might require admission to SNFs or LTACs. Therefore, the COVID-19 pandemic might lead to increased transmission of *C. auris* in SNFs because of increased admissions and shortages of personal protective equipment. During critical shortages, CDC guidelines permit extended use of isolation gowns for patients who are known to be infected with the same infectious disease if there are no additional known coinfections transmitted through contact (https://www.cdc.gov/coronavirus/2019-ncov/hcp/non-us-settings/emergency-considerations-ppe.html#ppe-specific-strategies). To encourage appropriate use of personal protective equipment and prevent transmission, it is essential that facilities screen patients for *C. auris*.

One limitation of this study is the lack of additional epidemiologic history of the patients, especially in the context of travel-related exposures. The ability to track cases to a location with known outbreaks of clade III *C. auris* strains is essential to determining the origin of the current outbreak. Further investigation is needed to explain why patient F had a genetically distinct isolate, suggesting a separate introduction.

In conclusion, we identified a unique clade III *C. auris* strain in an ongoing outbreak in LTAC facilities since 2019. These findings indicate active community spread of multidrug-resistant *C. auris* in the Los Angeles area.

About the Author

Dr. Price is a clinical microbiology fellow at the David Geffen School of Medicine at University of California, Los Angeles in Los Angeles, California, USA. His research interests include microbial genomics, fungal species identification, and antimicrobial resistance mechanisms.

References

1. Satoh K, Makimura K, Hasumi Y, Nishiyama Y, Uchida K, Yamaguchi H. *Candida auris* sp. nov., a novel ascomycetous yeast isolated from the external ear canal of an inpatient in a Japanese hospital. Microbiol Immunol. 2009;53:41–4. https://doi.org/10.1111/j.1348-0421.2008.00083.x
2. Forsberg K, Woodworth K, Walters M, Berkow EL, Jackson B, Chiller T, et al. *Candida auris*: the recent emergence of a multidrug-resistant fungal pathogen. Med Mycol. 2019;57:1–12. https://doi.org/10.1093/mmy/myy054
3. Calvo B, Melo AS, Perozo-Mena A, Hernandez M, Francisco EC, Hagen F, et al. First report of *Candida auris* in America: clinical and microbiological aspects of 18 episodes of candidemia. J Infect. 2016;73:369–74. https://doi.org/10.1016/j.jinf.2016.07.008
4. Armstrong PA, Rivera SM, Escandon P, Caceres DH, Chow N, Stuckey MJ, et al. Hospital-associated multicenter outbreak of emerging fungus *Candida auris*, Colombia, 2016. Emerg Infect Dis. 2019;25:1339–46. https://doi.org/10.3201/eid2507.180491
5. Rhodes J, Abdolrasouli A, Farrer RA, Cuomo CA, Aanensen DM, Armstrong-James D, et al. Genomic epidemiology of the UK outbreak of the emerging human fungal pathogen *Candida auris* [Erratum in: Emerg Microbes Infect. 2018;7:104]. Emerg Microbes Infect. 2018;7:43. https://doi.org/10.1038/s41426-018-0045-x
6. Centers for Disease Control and Prevention. Antibiotic resistance threats in the United States, 2019. 2019 [cited 2019 Nov 1]. https://www.cdc.gov/drugresistance/pdf/threats-report/2019-ar-threats-report-508.pdf
7. Lockhart SR, Etienne KA, Vallabhaneni S, Farooqi J, Chowdhary A, Govender NP, et al. Simultaneous emergence of multidrug-resistant *Candida auris* on 3 continents confirmed by whole-genome sequencing and

epidemiological analyses. Clin Infect Dis. 2017;64:134–40. https://doi.org/10.1093/cid/ciw691
8. Chow NA, de Groot T, Badali H, Abastabar M, Chiller TM, Meis JF. Potential fifth clade of *Candida auris*, Iran, 2018. Emerg Infect Dis. 2019;25:1780–1. https://doi.org/10.3201/eid2509.190686
9. Chow NA, Gade L, Tsay SV, Forsberg K, Greenko JA, Southwick KL, et al.; US Candida auris Investigation Team. Multiple introductions and subsequent transmission of multidrug-resistant *Candida auris* in the USA: a molecular epidemiological survey. Lancet Infect Dis. 2018;18:1377–84. https://doi.org/10.1016/S1473-3099(18)30597-8
10. Chow NA, Muñoz JF, Gade L, Berkow EL, Li X, Welsh RM, et al. Tracing the evolutionary history and global expansion of *Candida auris* using population genomic analyses. mBio. 2020;11:e03364–19. https://doi.org/10.1128/mBio.03364-19
11. Long SW, Olsen RJ, Nguyen HAT, Ojeda Saavedra M, Musser JM. Draft genome sequence of *Candida auris* strain LOM, a human clinical isolate from greater metropolitan Houston, Texas. Microbiol Resour Announc. 2019; 8:e00532–19. https://doi.org/10.1128/MRA.00532-19
12. Healey KR, Kordalewska M, Jiménez Ortigosa C, Singh A, Berrío I, Chowdhary A, et al. Limited ERG11 mutations identified in isolates of *Candida auris* directly contribute to reduced azole susceptibility. Antimicrob Agents Chemother. 2018;62:e01427–18. https://doi.org/10.1128/AAC.01427-18
13. Chowdhary A, Prakash A, Sharma C, Kordalewska M, Kumar A, Sarma S, et al. A multicentre study of antifungal susceptibility patterns among 350 *Candida auris* isolates (2009–17) in India: role of the ERG11 and FKS1 genes in azole and echinocandin resistance. J Antimicrob Chemother. 2018;73:891–9. https://doi.org/10.1093/jac/dkx480
14. Chowdhary A, Tarai B, Singh A, Sharma A. Multidrug-resistant *Candida auris* infections in critically ill coronavirus disease patients, India, April–July 2020. Emerg Infect Dis. 2020;26:2694–6. https://doi.org/10.3201/eid2611.203504
15. Rodriguez JY, Le Pape P, Lopez O, Esquea K, Labiosa AL, Alvarez-Moreno C. *Candida auris*: a latent threat to critically ill patients with COVID-19. Clin Infect Dis. 2020 Oct 18 [Epub ahead of print]. whttps://doi.org/10.1093/cid/ciaa1595

Address for correspondence: Shangxin Yang, UCLA Clinical Microbiology Laboratory, 11633 San Vicente Blvd, Los Angeles, CA 90049, USA; email: shangxinyang@mednet.ucla.edu

Inguinal Ulceroglandular Tularemia Caused by *Francisella tularensis* Subspecies *holarctica*, Canada

Carl Boodman, Quinlan Richert, Sylvain Lother, Ken Kasper, Sergio Fanella, Philippe Lagacé-Wiens, Yoav Keynan

Author affiliations: University of Manitoba, Winnipeg, Manitoba, Canada; Shared Health Inc., Winnipeg (P. Lagacé-Wiens)

DOI: https://doi.org/10.3201/eid2704.203262

Tularemia is a zoonotic disease caused by the gram-negative coccobacillus *Francisella tularensis*, a Biosafety Level 3 pathogen and potential agent of bioterrorism. We describe 2 cases of perigenital ulcer disease caused by *Francisella tularensis* subspecies *holarctica* in Manitoba, Canada. These cases caused inadvertent exposure among laboratory personnel.

In July 2018, a previously healthy girl 4 years of age was brought to the Health Sciences Centre at University of Manitoba (Winnipeg, Manitoba, Canada) for fever, right inguinal swelling, and dysuria. The patient's symptoms had worsened despite completing a 5-day course of trimethoprim/sulfamethoxazole prescribed by her family doctor for a presumed urinary tract infection 1 week before admission. The patient lived on a rural property bordered by forest in southern Manitoba, Canada. She enjoyed playing with her dogs and cats and often returned from the yard with ticks embedded in her skin.

At admission, her vital signs were within normal limits. We noted a small ulcer lateral to the right labia majora. This shallow nonpurulent ulcer was <1 cm long, surrounded by erythema, and accompanied by tender local lymphadenopathy. We took a swab sample of the ulcer for bacterial culture and prescribed ceftriaxone for presumed cellulitis.

Three days after admission, the culture revealed pinpoint growth of *Francisella tularensis* on chocolate agar, identified by matrix-assisted laser desorption/ionization-time of flight mass spectrometry (Bruker, https://www.bruker.com) (*1*). However, because a Biosafety Level 3 (BSL-3) pathogen had not been suspected, the culture was manipulated outside a biosafety cabinet (BSC). The exposed laboratory technologist was prescribed oral doxycycline (100 mg 2×/d for 14 days) as postexposure prophylaxis; the technician showed no signs or symptoms of tularemia. The bacterial isolate was classified as a UN2814, category A infectious substance; it was mailed in a sealed container with polystyrene foam-insulated packaging and an established Emergency Response Assistance Plan and placed in a box displaying the biohazard symbol to Canada's National Microbiology Laboratory (NML) for subspeciation. The NML identified the isolate as *Francisella tularensis* type B subspecies *holarctica*. We treated the patient for ulceroglandular tularemia (20 mg/kg of oral ciprofloxacin 2×/d for 14 days), prompting a complete recovery.

In August 2019, a woman 60 years of age arrived at Brandon Regional Health Centre (Brandon, Manitoba, Canada) with acute onset of hypotension and an ulcer beside her right labia majora. She had had chills for several days before seeking care. She had end-stage renal disease managed by hemodialysis and sick sinus syndrome managed by a pacemaker. The patient lived in a rural area of southern Manitoba and had found a tick attached to her abdomen ≈1 week before admission. She was not sure how long the tick had been attached; she removed it upon discovery.

At admission, the patient was hypotensive (70/25 mm Hg). She had a paced heart rate of 60 bpm and oxygen saturation of 99% on room air. She did not have a fever. We noted a 2 cm long ulcer beside the right labia majora with surrounding erythema and bilateral inguinal lymphadenopathy. We found a 2 cm long necrotic eschar with surrounding erythema at the site of tick attachment.

The gram stain cultured from the perivulvar ulcer showed no organisms. However, faint growth appeared on chocolate agar on day 3. We identified *F. tularensis* using matrix-assisted laser desorption/ionization-time of flight mass spectrometry (*1*). Before speciation, the culture had been manipulated outside a BSC, resulting in the exposure of 1 technologist; this technologist received doxycycline for 14 days as prophylaxis and had no signs or symptoms of infection. The NML identified the sample as *F. tularensis* subspecies *holarctica*. The patient was treated with gentamicin (2 mg/kg 1×/d for 7 days) and oral ciprofloxacin (500 mg 1×/d for 14 days) and symptoms resolved. We did not conduct serologic tests on samples from either patient. We notified the medical health officer of both cases.

The low infectious dose and easy dissemination of *F. tularensis* pose a substantial risk for laboratory-acquired infections when manipulated outside of a BSC (*2*,*3*). The perigenital localization of tularemia in these cases produced an especially hazardous situation for laboratory exposure; in contrast to blood, lymph node, and bone marrow samples, genital lesions are not usually suspected to harbor BSL-3

pathogens. A history of animal or arthropod exposure is a risk factor that can alert laboratory staff to the possibility of tularemia, enabling the application of appropriate precautions (*4*). Pinpoint colonies of gram-negative coccobacilli growing aerobically on chocolate agar 48 hours after plating might indicate the presence of *F. tularensis* and should prompt BSL-3 precautions, as emphasized by the Centers for Disease Control and Prevention's Laboratory Response Network in affiliation with the American Society for Microbiology (*5*,*6*). Of 42 cases of laboratory-acquired tularemia documented by Overholt et al. (*7*), 16 were unsuspected by microbiologists and occurred outside of a known exposure.

These 2 cases caused by *F. tularensis* subspecies *holarctica* support veterinary studies suggesting that this subspecies might be more common in the Canadian prairies than the more virulent *F. tularensis* subspecies *tularensis* identified elsewhere in North America (*8*–*10*). The milder symptoms associated with *F. tularensis* subspecies *holarctica* might require a higher index of clinical suspicion, especially among patients with exposure to arthropods or wild mammals.

About the Author

Dr. Boodman is an infectious disease and medical microbiology resident doctor at the University of Manitoba, Winnipeg. His research interests include neglected infectious diseases and the interplay between infectious disease and socioeconomic disparities.

References

1. Rudrik JT, Soehnlen MK, Perry MJ, Sullivan MM, Reiter-Kintz W, Lee PA, et al. Safety and accuracy of matrix-assisted laser desorption ionization–time of flight mass spectrometry for identification of highly pathogenic organisms. J Clin Microbiol. 2017;55:3513–29.
2. Shapiro DS, Schwartz DR. Exposure of laboratory workers to *Francisella tularensis* despite a bioterrorism procedure. J Clin Microbiol. 2002;40:2278–81. https://doi.org/10.1128/JCM.40.6.2278-2281.2002
3. Centers for Disease Control and Prevention. Managing potential laboratory exposures to *Francisella tularensis*. 2018 [cited 2020 Oct 04]. https://www.cdc.gov/tularemia/laboratoryexposure/index.html
4. Singh K. Laboratory-acquired infections. Clin Infect Dis. 2009;49:142–7. https://doi.org/10.1086/599104
5. Miller JM, Astles R, Baszler T, Chapin K, Carey R, Garcia L, et al. Guidelines for safe work practices in human and animal medical diagnostic laboratories: recommendations of a CDC-convened, biosafety Blue Ribbon Panel. [Erratum in: MMWR Surveill Summ. 2012;61:214]. MMWR Suppl. 2012;61:1–102.
6. Craft D, Kijek T. Sentinel level clinical laboratory guidelines for suspected agents of bioterrorism and emerging infectious diseases: *Francisella tularensis*. 2016 [cited 2020 Oct 3]. https://asm.org/ASM/media/Policy-and-Advocacy/LRN/Sentinel%20Files/tularemia.pdf
7. Overholt EL, Tigertt WD, Kadull PJ, Ward MK, David CN, Rene RM, et al. An analysis of forty-two cases of laboratory-acquired tularemia: treatment with broad spectrum antibiotics. Am J Med. 1961;30:785–806. https://doi.org/10.1016/0002-9343(61)90214-5
8. Wobeser G, Ngeleka M, Appleyard G, Bryden L, Mulvey MR. Tularemia in deer mice (*Peromyscus maniculatus*) during a population irruption in Saskatchewan, Canada. J Wildl Dis. 2007;43:23–31. https://doi.org/10.7589/0090-3558-43.1.23
9. Wobeser G, Campbell GD, Dallaire A, McBurney S. Tularemia, plague, yersiniosis, and Tyzzer's disease in wild rodents and lagomorphs in Canada: a review. Can Vet J. 2009;50:1251–6.
10. Antonation KS, Bekal S, Côté G, Dallaire A, Corbett CR. Multiple-locus variable-number tandem-repeat analysis of *Francisella tularensis* from Quebec, Canada. Lett Appl Microbiol. 2015;60:328–33. https://doi.org/10.1111/lam.12371

Address for correspondence: Carl Boodman, Room 543, Basic Medical Sciences Building, 745 Bannatyne Avenue, Winnipeg, MB R3E 0J9, Canada; email: boodmanc@myumanitoba.ca

Risk for Fomite-Mediated Transmission of SARS-CoV-2 in Child Daycares, Schools, Nursing Homes, and Offices

Alicia N.M. Kraay, Michael A.L. Hayashi, David M. Berendes, Julia S. Sobolik, Juan S. Leon, Benjamin A. Lopman

Author affiliations: Emory University, Atlanta, Georgia, USA (A.N.M. Kraay, J.S. Sobolik, J.S. Leon, B.A. Lopman); University of Michigan, Ann Arbor, Michigan, USA (M.A.L. Hayashi); Centers for Disease Control and Prevention, Atlanta (D.M. Berendes)

DOI: https://doi.org/10.3201/eid2704.203631

Severe acute respiratory syndrome coronavirus 2 can persist on surfaces, suggesting possible surface-mediated transmission of this pathogen. We found that fomites might be a substantial source of transmission risk, particularly in schools and child daycares. Combining surface cleaning and decontamination with mask wearing can help mitigate this risk.

Severe acute respiratory syndrome coronavirus 2 (SARS-CoV-2), the causative agent of coronavirus disease, can be transmitted through close contact. However, the virus also persists for up to 28 days on surfaces (*1*–*3*), suggesting that surface-mediated (e.g., fomite) transmission might also occur.

Conventional epidemiologic studies cannot distinguish between competing transmission pathways (e.g., droplet or fomite) when they act simultaneously. Therefore, we used a transmission model to explore the potential for fomite transmission without other pathways. We adapted a published fomite transmission model (*4*) for SARS-CoV-2 (Appendix Figure 1, https://wwwnc.cdc.gov/EID/article/27/4/20-3631-App1.pdf). In our model, persons are classified as susceptible, infectious, or recovered. We explicitly tracked contamination on hands, which is independent of whether or not a person is currently infected. Infectious persons shed pathogens onto fomites or hands, but only a fraction of surfaces (λ) are accessible for contamination. Hands might become contaminated from viral excretion or from touching virus-contaminated fomites. Susceptible persons might become infected through touching their face and mouth with contaminated hands (Appendix).

By using this model, we explore how fomite transmission varies by location (comparing child daycares, schools, offices, and nursing homes), disinfection strategy, and surface type. Although precise values likely vary on a case-by-case basis, child daycares are assumed to have higher frequency of fomite touching (ρ_T) and the fraction of surfaces susceptible to contamination (λ) than offices, whereas schools are likely intermediate for both factors (*4*). Nursing homes are assumed to have similar amounts of surfaces susceptible to contamination to offices, but higher fomite touching rates.

We considered the following surface cleaning and disinfection frequencies: every 8 hours (1×/workday), every 4 hours (2×/workday), and hourly. We also considered handwashing interventions, but they had minimal impact in our model and were not included in our main results (Appendix). Because SARS-CoV-2 persistence varies by surface, we compared transmission for stainless steel, plastic, and cloth. As a sensitivity analysis, we also varied viral shedding rates in our analysis for 2 reasons: initial data are uncertain because of small sample sizes (*5*), and shedding rates are likely to vary on the basis of mask-wearing practices (*6*,*7*; Appendix). In our model, situations in which the basic reproduction number (R_0) for the fomite route exceeds 1 could sustain ongoing transmission in a given setting, whereas transmission could be interrupted when R_0 falls below 1. We explored what interventions could interrupt fomite transmission.

Our estimates suggest that fomite transmission could sustain SARS-CoV-2 transmission in many settings. The fomite R_0 ranged from 10 in low-risk venues (offices) to ≈25 in high-risk settings such as child daycares. SARS-CoV-2 transmission risk is generally higher than influenza and rhinovirus (Appendix Figure 6).

We found that hourly cleaning and disinfection alone could interrupt fomite transmission in some office settings, particularly combined with reduced shedding, but would be inadequate in child daycares and schools (Figure; Appendix Figure 3). If shedding is reduced through mask wearing, transmission from surfaces became unlikely, even with infrequent surface decontamination. Decay rates were similarly low for plastic and stainless steel (Appendix Table 2), leading to substantial transmission potential (Figure). Decay rates on cloth were high and were unlikely to sustain transmission. Therefore, cleaning and disinfection frequencies could vary by surface, with hourly interventions being helpful for frequently touched nonporous surfaces and with porous surfaces (such as plush toys) being cleaned and sanitized less frequently. In child daycares, intervening directly after high-risk shedding

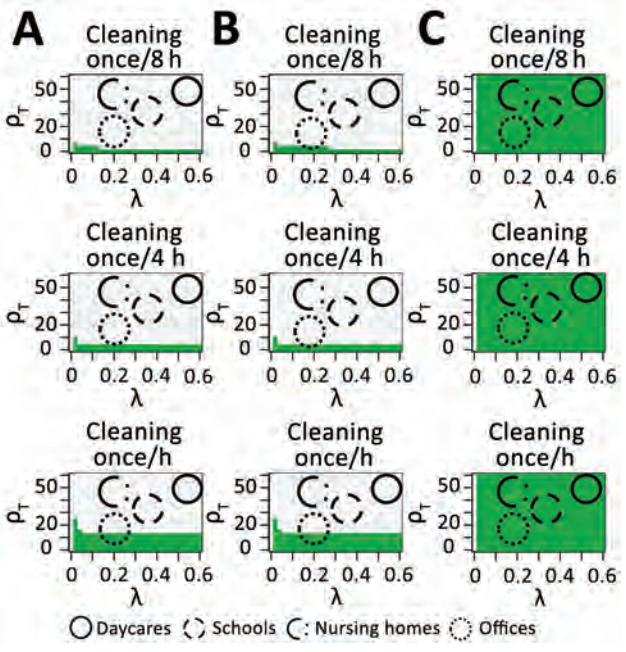

Figure. Reductions in the basic reproduction number for the fomite pathway for severe acute respiratory syndrome coronavirus 2 on stainless steel (A), plastic (B), and cloth surfaces (C), by setting (defined by hourly fomite touching rates [$\rho_T$and proportion of accessible surfaces [λ). For areas in green, the projected reproduction number from fomite transmission is <1. For comparison, cleaning every 2 hours was considered as a sensitivity analysis.

events (e.g., a feverish person coughs directly on a surface) in addition to intervening at standard intervals (such as hourly) would be beneficial.

Because of our emphasis on the basic reproduction number rather than simulating infection dynamics, these results describe transmission potential if outbreaks begin with a single case as opposed to many cases being introduced simultaneously, which could occur when transmission is high. Thus, these results apply when SARS-CoV-2 incidence is low, which might be achievable in individual locations even if community incidence is high. Near the epidemic peak, more detailed simulations are needed because environmental contamination might exceed the linear range of the dose-response curve (*8*), which could lead to an overestimate of the risk for fomite transmission. Because our objective was to assess the potential impact of fomite transmission alone, we did not account for direct transmission through direct droplet spray, aerosols, or hand-to-hand contact, all of which are likely major contributors to transmission in many settings (*9*). Our model suggests fomites can also transmit virus, which is important for indirect exposures. For simplicity, we assume that fomite transmission is similar for symptomatic and asymptomatic infections (Appendix). We also assume that the dose-response curve for fomite transmission is the same as other transmission routes, which might lead to an overestimate of fomite transmission if pathogens from surfaces are less efficiently absorbed into the lungs from hands when they are not aerosolized.

In summary, fomite transmission might be an important source of risk for SARS-CoV-2. However, both mask wearing and frequent cleaning and disinfection can reduce this risk.

This research was funded by the National Institutes of Health (grant supplement no. R01GM124280 to A.N.M.K. and B.A.L.; grant no. 2T32ES012870-16 to J.S.S.) and the National Institute of Food and Agriculture at the US Department of Agriculture (grant no. 2018-07410 to J.S.L. and B.A.L,; grant no. 2020-67034-31728).

B.A.L. reports grants and personal fees from Takeda Pharmaceuticals and personal fees from the World Health Organization outside the submitted work.

About the Author

Dr. Kraay is a postdoctoral fellow in the Epidemiology Department at Emory University. She is interested in environmental transmission of infectious diseases and how public health interventions, including vaccination, can help mitigate disease risk.

References

1. Riddell S, Goldie S, Hill A, Eagles D, Drew TW. The effect of temperature on persistence of SARS-CoV-2 on common surfaces. Virol J. 2020;17:145. https://doi.org/10.1186/s12985-020-01418-7
2. Chin AWH, Chu JTS, Perera MRA, Hui KPY, Yen HL, Chan MCW, et al. Stability of SARS-CoV-2 in different environmental conditions. Lancet Microbe. 2020;1:e10. https://doi.org/10.1016/S2666-5247(20)30003-3
3. van Doremalen N, Bushmaker T, Morris DH, Holbrook MG, Gamble A, Williamson BN, et al. Aerosol and surface stability of SARS-CoV-2 compared with SARS-CoV-1. N Engl J Med. 2020;382:1564–7. https://doi.org/10.1056/NEJMc2004973
4. Kraay ANM, Hayashi MAL, Hernandez-Ceron N, Spicknall IH, Eisenberg MC, Meza R, et al. Fomite-mediated transmission as a sufficient pathway: a comparative analysis across three viral pathogens. BMC Infect Dis. 2018;18:540. https://doi.org/10.1186/s12879-018-3425-x
5. Bullard J, Dust K, Funk D, Strong JE, Alexander D, Garnett L, et al. Predicting infectious SARS-CoV-2 from diagnostic samples. Clin Infect Dis. 2020 May 22 [Epub ahead of print].
6. Leung NHL, Chu DKW, Shiu EYC, Chan KH, McDevitt JJ, Hau BJP, et al. Respiratory virus shedding in exhaled breath and efficacy of face masks. Nat Med. 2020;26:676–80. https://doi.org/10.1038/s41591-020-0843-2
7. Fischer EP, Fischer MC, Grass D, Henrion I, Warren WS, Westman E. Low-cost measurement of face mask efficacy for filtering expelled droplets during speech. Sci Adv. 2020;6:eabd3083. https://doi.org/10.1126/sciadv.abd3083
8. Brouwer AF, Weir MH, Eisenberg MC, Meza R, Eisenberg JNS. Dose-response relationships for environmentally mediated infectious disease transmission models. PLOS Comput Biol. 2017;13:e1005481. https://doi.org/10.1371/journal.pcbi.1005481
9. Lai CC, Shih TP, Ko WC, Tang HJ, Hsueh PR. Severe acute respiratory syndrome coronavirus 2 (SARS-CoV-2) and coronavirus disease-2019 (COVID-19): the epidemic and the challenges. Int J Antimicrob Agents. 2020;55:105924. https://doi.org/10.1016/j.ijantimicag.2020.105924

Address for correspondence: Alicia Kraay, Emory University, 1518 Clifton Rd NE, Atlanta, GA, 30322, USA; email: alicia.nicole.mullis.kraay@emory.edu

Tula Virus as Causative Agent of Hantavirus Disease in Immunocompetent Person, Germany

Jörg Hofmann, Stephanie Kramer, Klaus R. Herrlinger, Kathrin Jeske, Martin Kuhns, Sabrina Weiss,[1] Rainer G. Ulrich, Detlev H. Krüger

Author affiliations: Institute of Virology, Charité–Universitätsmedizin Berlin, Berlin, Germany (J. Hofmann; S. Weiss, D.H. Krüger); Asklepios Klinik Nord, Hamburg, Germany (S. Kramer, K.R. Herrlinger); Institute of Novel and Emerging Infectious Diseases, Friedrich-Loeffler-Institut, Federal Research Institute for Animal Health, Greifswald-Insel Riems, Germany (K. Jeske, R.G. Ulrich); Institute of Diagnostic Virology, Friedrich-Loeffler-Institut, Federal Research Institute for Animal Health, Greifswald-Insel Riems (K. Jeske); Medilys Laborgesellschaft mbH, Hamburg (M. Kuhns)

DOI: https://doi.org/10.3201/eid2704.203996

We report molecular evidence of Tula virus infection in an immunocompetent patient from Germany who had typical signs of hantavirus disease. Accumulating evidence indicates that Tula virus infection, although often considered nonpathogenic, represents a threat to human health.

Hantavirus disease, also called hemorrhagic fever with renal syndrome and hantavirus cardiopulmonary syndrome, is a zoonosis; hantaviruses are transmitted from their reservoirs (rodents) to humans. The clinical course is characterized by initial high fever and body pain, potentially proceeding to renal, pulmonary failure, or both. The case-fatality rate depends on the causal virus species and can reach up to 50% (*1*).

Tula virus (TULV), a member of the family *Hantaviridae*, genus *Orthohantavirus*, has been isolated from common voles (*Microtus arvalis*) (*2*). TULV, a broadly distributed virus in different parts of Eurasia, is hosted by common voles but has also been found in related vole species (*3*). Clinical findings of TULV pathogenicity are very rare. In 2003, a case of TULV-associated hantavirus disease was diagnosed by serologic and molecular epidemiologic means (*4*). So far, direct molecular evidence for TULV infection has only been found in 2 cases (1 in an immunocompromised patient who had severe hantavirus disease [*5*], the other in an immunocompetent person without preexisting illness who had mild hantavirus disease [*6*]).

We report molecular evidence of TULV infection in a 21-year old immunocompetent man who originated from a small village near Hamburg, northern Germany. He was admitted to hospital for sudden fever, sickness, severe headache, abdominal pain, and limb pain since the day before. His medical history was unremarkable. The patient worked as a sanitary and heating engineer in the northern part of Germany. Except for elevated body temperature, the physical examination did not reveal any abnormalities. Blood testing at the day of admission revealed thrombocytopenia (63 platelets/nL), markedly elevated C-reactive protein (63.6 mg/L), and borderline leukocyte (9.8 cells/nL) and serum creatinine (1.2 mg/dL) values. Because of biochemical signs of infection, ultrasound findings of a moderate enlargement of spleen and cervical lymph nodes as well as hints of a small lung infiltration, an antibiotic regime (ampicillin/sulbactam and clarithromycin) was initiated. Over the next few days, the fever resolved.

At day 4, biochemical signs of disturbed retention function indicated acute kidney injury. An enhanced serum creatinine value (1.6 mg/dL) and impaired (59 mL/min) glomerular filtration rate (GFR), determined using the CKD-EPI method, were noted; thrombocytopenia and an elevated C-reactive protein level persisted. The GFR, determined using the cystatin method, as measured at day 5, was reduced to 48 mL/min. The patient did not observe signs of oliguria. Under calculated intravenous fluid intake, the creatinine, GFR, and platelet values normalized until day 8, and the C-reactive protein declined to 12.1 mg/L. The patient was discharged from hospital at day 8 in good general condition.

Initial laboratory diagnostics were based on hantavirus serologic test results (on day 4 of hospitalization) using the Hantavirus Profile 1 immunoblot (Euroimmun, https://www.euroimmun.com). This assay does not contain TULV antigen, but the patient's serum showed strong IgG reactivity with Dobrava–Belgrade virus (DOBV), Hantaan virus (HTNV), and Puumala virus (PUUV) antigens as well as strong band intensity on PUUV in the IgM assay. The recomLine HantaPlus IgG and IgM assays (Mikrogen, https://www.mikrogen.de) revealed strong IgG reactivity to PUUV and in the IgM blot strong band intensities on PUUV, Sin Nombre virus, and DOBV. On the basis of these serologic findings, a PUUV infection of the patient was suspected.

At day 5, serum was obtained for molecular virus detection. Using the primers of the Pan Hanta PCR (*7*),

[1]Current affiliation: Robert Koch Institute, Centre for International Health Protection, Berlin, Germany.

a 392-nt long region of the large genome segment was amplified and sequenced. The molecular phylogenetic analysis of the large segment sequence demonstrated TULV, but not PUUV, infection of the patient. Within the phylogenetic tree, the new sequence (named H18045/Winsen/19 and deposited in GenBank under accession no. MT993951) clustered with vole-derived TULV sequences from Germany and, in a more refined analysis, with those from the central north (CEN.N) clade, which consists of sequences from the northern, eastern, and central parts of the country (Figure).

Previous studies from northeast Germany have shown that TULV is able to infect humans. Out of 563 serum samples from forest workers investigated, 22 samples (3.9%) reacted exclusively with TULV diagnostic antigen (*8*). In a survey of 6,537 serum samples representing the average population of Germany, 1 sample showed its highest neutralizing titer to TULV compared with PUUV, DOBV, HTNV, and Seoul virus (*9*).

A reason for the rare finding of TULV-associated hantavirus disease might be the close genetic and antigenic relationship to another vole-associated hantavirus, PUUV, which is carried by bank voles (*Myodes glareolus*) and is a well-known pathogenic agent broadly distributed in Europe and parts of Asia (*1*). Because anti-TULV and anti-PUUV seroreactivities cannot be distinguished using the usual serologic techniques (i.e., without neutralization assays) (*2*,*10*), TULV infections might be misdiagnosed as PUUV infections during routine diagnostics.

The ability of TULV to cause hantavirus disease even in a previously healthy person shows the pathogenic potential of this virus. Therefore, the vole species hosting TULV should be considered as infection sources in their respective geographic ranges. Because of the broad distribution (https://www.iucnredlist.org/search?query%20=%20microtus&searchType%20=%20species)

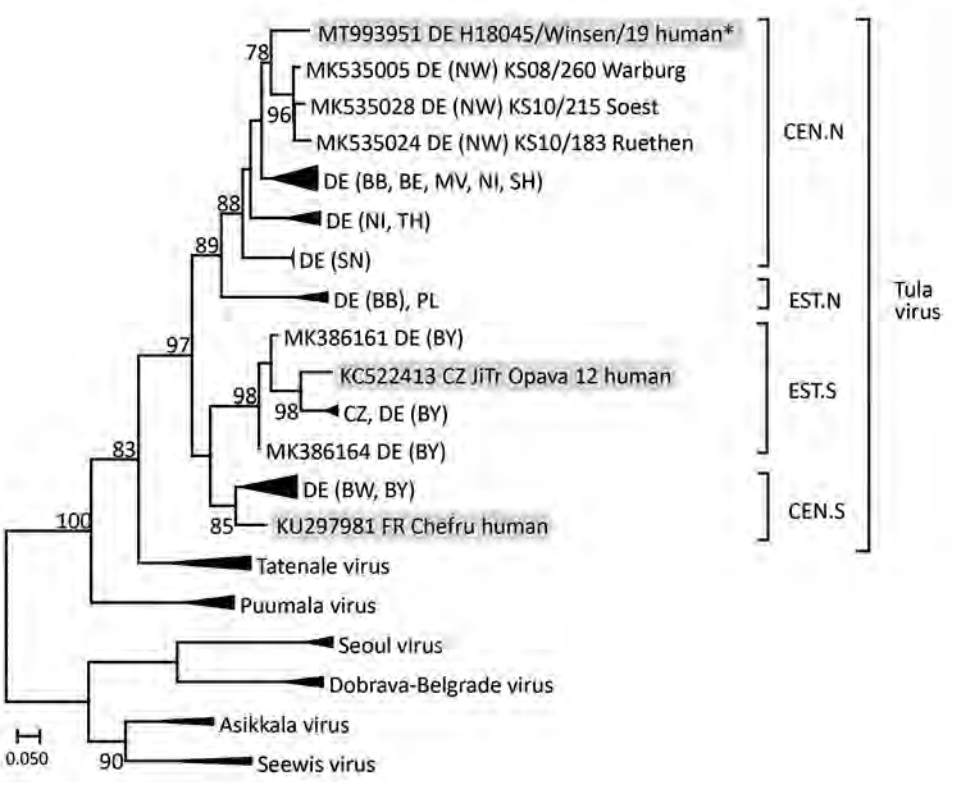

Figure. Maximum-likelihood tree of TULV from an immunocompetent patient in Germany (strain H18045/Winsen/19, marked with an asterisk [*]). Tree is based on partial large segment sequences (nucleotide position 2996–3291, according to TULV strain Moravia [GenBank accession no. NC_005226.1]). Designations of patient-derived sequences are shaded in gray. The alignment was constructed using the ClustalW Multiple Alignment algorithm implemented in Bioedit 7.2.3 (https://bioedit.software.informer.com). Maximum-likelihood analyses with 1,000 bootstraps and 50% cutoff using the general time-reversible substitution model with invariant sites and a gamma-distributed shape parameter was performed using FastTreeMP 2.1.10 (http://www.microbesonline.org) on CIPRES Science Gateway 3.3 (http://www.phylo.org). Bootstrap values >75 are given at the supported nodes. Geographic origin of TULV sequences are indicated by countries (Germany, DE; Czech Republic, CZ; France, FR; Poland, PL) and specified for Germany by adding the federal states (BE, Berlin; BB, Brandenburg; BW, Baden-Wuerttemberg, BY, Bavaria; MV, Mecklenburg-Western Pomerania, NI, Lower Saxony; NW, North Rhine-Westphalia; SH, Schleswig-Holstein; SN, Saxony; and TH, Thuringia). Triangles indicate condensed branches of TULV clades central north (CEN.N; DE: BB, GenBank accession nos. MK53017, MK53034, MK53036; BE, MK53003; MV, MK53004, MK53022; NI, MK53011, MK53032; SH, MK53033; SN HQ728453, HQ728454; TH, HQ728456, HQ728461, MK53007), eastern north (EST.N; PL: MK535037; DE: BB, MK535014–MK535015), eastern south (EST.S; CZ: MK386155–MK386156; DE: BY, MK386154, MK386161, MK386164), and central south (CEN.S; DE: BW, HQ728457, HQ728458; BY, HQ728462–HQ728464, HQ728466), as well as Puumala virus (KJ994778, MN026167, MN026168), Tatenale virus including its strain Traemmersee virus (MK542664, MK883760, MK883761, MN267824), Dobrava–Belgrade virus (JQ026206, KJ182937, KJ182938), Asikkala virus (KC880348, KC880349), Seewis virus (JQ425312, JQ425320), and Seoul virus (MG386252, KJ502300, KJ502303).

and mass reproduction of common voles in several parts of Europe, TULV should be considered as a threat to human health.

Acknowledgments

We gratefully acknowledge the expert technical assistance by Christine Stephan, Susanne Schwarz, and Dörte Kaufmann and helpful discussions with Stefan Drewes.

This work was supported by the German Federal Ministry of Public Health through Robert Koch Institute (grant nos. 1369-382/435 and 1362-924/980) and the Bundesministerium für Bildung und Forschung through the Research Network Zoonotic Infectious Diseases (grant nos. FKZ 01KI1721A and FKZ 01KI1721C).

About the Author

Dr. Hofmann is the chair of the National Consultation Laboratory for Hantaviruses, Institute of Virology, Charité–Universitätsmedizin Berlin, Germany. His primary research interest is human infections with viral pathogens.

References

1. Kruger DH, Figueiredo LT, Song JW, Klempa B. Hantaviruses—globally emerging pathogens. J Clin Virol. 2015;64:128–36. https://doi.org/10.1016/j.jcv.2014.08.033
2. Vapalahti O, Lundkvist A, Kukkonen SK, Cheng Y, Gilljam M, Kanerva M, et al. Isolation and characterization of Tula virus, a distinct serotype in the genus *Hantavirus*, family *Bunyaviridae*. J Gen Virol. 1996;77:3063–7. https://doi.org/10.1099/0022-1317-77-12-3063
3. Schmidt S, Saxenhofer M, Drewes S, Schlegel M, Wanka KM, Frank R, et al. High genetic structuring of Tula hantavirus. Arch Virol. 2016;161:1135–49. https://doi.org/10.1007/s00705-016-2762-6
4. Klempa B, Meisel H, Räth S, Bartel J, Ulrich R, Krüger DH. Occurrence of renal and pulmonary syndrome in a region of northeast Germany where Tula hantavirus circulates. J Clin Microbiol. 2003;41:4894–7. https://doi.org/10.1128/JCM.41.10.4894-4897.2003
5. Zelená H, Mrázek J, Kuhn T. Tula hantavirus infection in immunocompromised host, Czech Republic. Emerg Infect Dis. 2013;19:1873–5. https://doi.org/10.3201/eid1911.130421
6. Reynes JM, Carli D, Boukezia N, Debruyne M, Herti S. Tula hantavirus infection in a hospitalised patient, France, June 2015. Euro Surveill. 2015;20:30095. https://doi.org/10.2807/1560-7917.ES.2015.20.50.30095
7. Klempa B, Fichet-Calvet E, Lecompte E, Auste B, Aniskin V, Meisel H, et al. Hantavirus in African wood mouse, Guinea. Emerg Infect Dis. 2006;12:838–40. https://doi.org/10.3201/eid1205.051487
8. Mertens M, Hofmann J, Petraityte-Burneikiene R, Ziller M, Sasnauskas K, Friedrich R, et al. Seroprevalence study in forestry workers of a non-endemic region in eastern Germany reveals infections by Tula and Dobrava–Belgrade hantaviruses. Med Microbiol Immunol (Berl). 2011;200:263–8. https://doi.org/10.1007/s00430-011-0203-4
9. Ulrich R, Meisel H, Schütt M, Schmidt J, Kunz A, Klempa B, et al. Prevalence of hantavirus infections in Germany [in German]. Bundesgesundheitsblatt Gesundheitsforschung Gesundheitsschutz. 2004;47:661–70. https://doi.org/10.1007/s00103-004-0858-8
10. Sibold C, Meisel H, Lundkvist A, Schulz A, Cifire F, Ulrich R, et al. Short report: simultaneous occurrence of Dobrava, Puumala, and Tula hantaviruses in Slovakia. Am J Trop Med Hyg. 1999;61:409–11. https://doi.org/10.4269/ajtmh.1999.61.409

Address for correspondence: Jörg Hofmann, Institute of Virology, Helmut-Ruska-Haus, Charité University Medicine, Charitéplatz 1, 10117 Berlin, Germany; email: joerg.hofmann@charite.de

Rapid Spread and Control of Multidrug-Resistant Gram-Negative Bacteria in COVID-19 Patient Care Units

Ashka Patel, Michele Emerick, Marie K. Cabunoc, Michelle H. Williams, Michael Anne Preas, Gregory Schrank, Ronald Rabinowitz, Paul Luethy, J. Kristie Johnson, Surbhi Leekha

Author affiliations: University of Maryland Medical Center, Baltimore, Maryland, USA (A. Patel, M. Emerick, M.K. Cabunoc, M.H. Williams, M.A. Preas); University of Maryland School of Medicine, Baltimore (G. Schrank, R. Rabinowitz, P. Luethy, J.K. Johnson, S. Leekha)

DOI: https://doi.org/10.3201/eid2704.204036

We describe rapid spread of multidrug-resistant gram-negative bacteria among patients in dedicated coronavirus disease care units in a hospital in Maryland, USA, during May–June 2020. Critical illness, high antibiotic use, double occupancy of single rooms, and modified infection prevention practices were key contributing factors. Surveillance culturing aided in outbreak recognition and control.

Bacterial colonization and secondary infection have been described in patients hospitalized with coronavirus disease (COVID-19) (*1*,*2*). We report a single-center experience with spread of multidrug-resistant (MDR) gram-negative bacteria (GNB) in COVID-19 patients in Maryland, USA, during May–June 2020.

This investigation was determined to be non–human subjects research by the University of Maryland's Institutional Review Board.

At University of Maryland Medical Center (Baltimore, MD, USA), an 800-bed tertiary-care hospital, since early April 2020, critically ill COVID-19 patients had been housed in 3 dedicated units (3), which included 2 intensive care units (ICUs) (units A and B, unit A providing extracorporeal membrane oxygenation support) and 1 intermediate-care unit (unit C). Units were designed as closed, negative-pressure areas where staff remained in the same personal protective equipment while providing care to multiple patients. To accommodate the COVID-19 surge, single-patient ICU rooms in units A and B frequently housed 2 patients. Unit C rooms remained single-occupancy and received patients for step-down care from units A and B. Hospital policy required staff to change gloves and perform hand hygiene (or glove hygiene if wearing 2 layers of gloves) between patients and to wear 2 layers of gowns for patients with resistant organisms and remove the outer gown before moving to the next patient. A team nursing model was used, in which multiple nurses shared responsibilities for each patient during a shift.

For routine surveillance, the hospital defined MDR GNB as Enterobacterales, *Acinetobacter baumannii*, or *Pseudomonas aeruginosa* nonsusceptible to ≥2 of piperacillin/tazobactam, cefepime, and a carbapenem. Before COVID-19, we performed admission and weekly surveillance for MDR Enterobacterales and *A. baumannii* using perirectal swab specimens on medical and surgical ICU patients and monitored hospitalwide MDR GNB incidence by using the first positive clinical or surveillance culture >48 hours postadmission.

In mid-May 2020, a cluster of 4 patients with MDR *Escherichia coli* was identified on unit A. Hospitalwide data showed increase in MDR GNB incidence from baseline (Figure, panel A) (weeks 9–11), driven by *E. coli* cases on units A and B (Figure, panel B). Further review also revealed several patients with cefepime-resistant *E. coli* (not meeting institutional MDR criteria), MDR *P. aeruginosa*, and MDR *A. baumannii*. Surveillance screens (perirectal swab specimens on all and sputum on ventilated patients) in the 3 units in week 12 identified 18/29 (62%) additional patients with resistant GNB (MDR GNB, cefepime-resistant *E. coli*, or both). Public health authorities were notified and observations of practice and discussions with leadership were conducted. Twice-weekly surveillance culturing among patients still negative for resistant GNB was instituted (Figure).

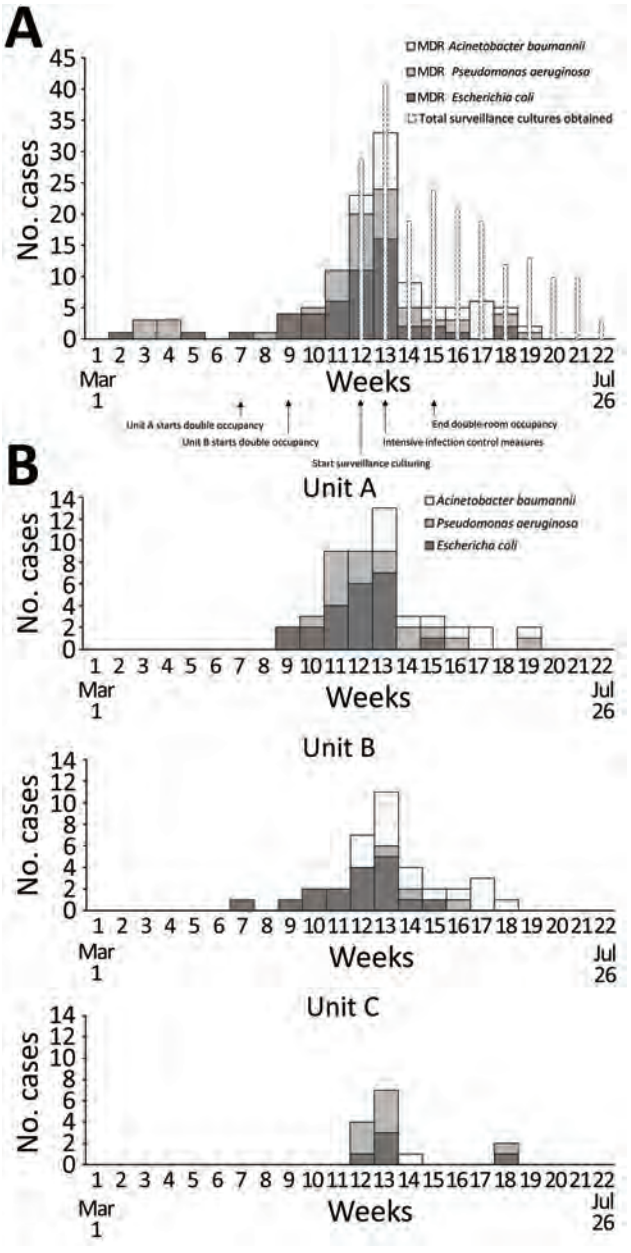

Figure. Incidence of patients with a clinical or surveillance culture-positive result indicating MDR or cefepime-resistant *Escherichia coli*, MDR *Acinetobacter baumannii*, or MDR *Pseudomonas aeruginosa* >48 hours after admission to a hospital in Maryland, USA, by week, March 1–July 31, 2020. A) Overall hospitalwide incidence (118 total cases, with 98 positive cultures belonging to outbreak units). Narrow white bars represent the number of surveillance cultures obtained during the outbreak and shaded bars show positive cultures by organism. Arrows show timing of relevant events for transmission and control. B) Incidence of outbreak cases (n = 98) stratified by the 3 units affected by the outbreak. Organisms nonsusceptible to ≥2 of piperacillin/tazobactam, cefepime, or carbapenem are considered MDR. Patients are included for the first positive culture per organism and therefore might be included more than once. MDR, multidrug-resistant.

During April 16–July 15, a total of 71 unique patients had positive clinical or surveillance cultures for resistant GNB, including 44 *E.coli* (33 MDR and 11 cefepime-resistant), 27 MDR *P. aeruginosa*, and 27 MDR *A. baumannii* (Appendix Table 1, https://wwwnc.cdc.gov/EID/article/27/4/20-4036-App1.pdf). Twenty-four patients (34%) were co-colonized with >1 resistant GNB. Of the 71 patients, 69 (97%) had received antibiotics before first positive resistant GNB culture, 30 (42%) required extracorporeal membrane oxygenation support, 27 (38%) required renal replacement therapy, 52 (73%) received corticosteroids, 25 (35%) received remdesivir, and 14 (20%) received tocilizumab. Twenty-three (32%) patients ultimately died.

Relatedness of early *E. coli* isolates was assessed by pulsed-field gel electrophoresis (PFGE) (n = 13, weeks 7–11) and genetic β-lactamase determination by Verigene gram-negative blood culture nucleic acid test (Luminex Corporation, https://www.luminexcorp.com) (n = 38, weeks 7–14) (*4*; Appendix). PFGE revealed 3 groups. Groups 1 and 2 (n = 7) were considered related and were negative for β-lactamases; these and 8/10 additional β-lactamase-negative isolates were from unit B. Group 3 (n = 6) isolates did not produce bands but were positive for CTX-M; these and 14/15 additional CTX-M positive isolates (including 10/11 phenotypically cefepime-resistant but not MDR) were from unit A and considered related, suggesting rapid patient-to-patient transmission (Appendix Table 1). MDR *P. aeruginosa* transmission occurred predominantly in unit A, whereas MDR *A. baumannii* was largely in unit B. Resistant GNB were likely introduced into unit C from both units A and B (Figure, panel B).

Key infection control findings (*5*) included tight physical spaces and close proximity of patients in double occupancy (*6*), multiple staff in contact with each patient in the team nursing model, and low compliance with hand and glove hygiene and gown changes between patients. To limit staff exposure to COVID-19 patients, the unit had less support from ancillary services; instead, daily room and equipment cleaning and stocking of medications and supplies were performed by unit-based clinical staff.

Outbreak control interventions included discontinuation of double occupancy, frequent infection prevention rounds to promote hand hygiene and glove and gown changes between patients, increased environmental services support, and attention to disinfection of reusable equipment and high-touch surfaces (Appendix Table 2) (*7*). Surveillance culturing showed a decrease in positive cultures over time (Figure).

Prolonged critical illness, high antibiotic and corticosteroid use, double occupancy, the team nursing model, and modified infection prevention practice were considered contributors to transmission, underscoring the importance of vigilance to MDR organisms in this setting (*5*,*7*–*10*). Surveillance culturing aided with recognizing the extent of spread and informed early intervention.

Acknowledgments

We would like to thank Richard Brooks and Heather Saunders for guidance on outbreak management, and Gwen Robinson for assistance with creating the figure.

About the Author

Dr. Patel is a second-year infectious diseases fellow at the University of Maryland Medical Center. She is interested in infection prevention and hospital epidemiology and has worked on projects involving hospital- acquired *Clostridium difficile* infections as well as hospital-onset bloodstream infections.

References

1. Rawson TM, Moore LSP, Castro-Sanchez E, Charani E, Davies F, Satta G, et al. COVID-19 and the potential long-term impact on antimicrobial resistance. J Antimicrob Chemother. 2020;75:1681–4. https://doi.org/10.1093/jac/dkaa194
2. Nori P, Cowman K, Chen V, Bartash R, Szymczak W, Madaline T, et al. Bacterial and fungal coinfections in COVID-19 patients hospitalized during the New York City pandemic surge. Infect Control Hosp Epidemiol. 2021;42:84–8. https://doi.org/10.1017/ice.2020.368
3. Centers for Disease Control and Prevention. Coronavirus disease 2019 (COVID-19). 2020 [cited 2020 Aug 20]. https://www.cdc.gov/coronavirus/2019-ncov/hcp/infection-control-recommendations.html
4. Hill JT, Tran K-DT, Barton KL, Labreche MJ, Sharp SE. Evaluation of the nanosphere Verigene BC-GN assay for direct identification of Gram-negative bacilli and antibiotic resistance markers from positive blood cultures and potential impact for more-rapid antibiotic interventions. J Clin Microbiol. 2014;52:3805–7. https://doi.org/10.1128/JCM.01537-14
5. Donà D, Di Chiara C, Sharland M. Multi-drug-resistant infections in the COVID-19 era: a framework for considering the potential impact. J Hosp Infect. 2020;106:198–9. https://doi.org/10.1016/j.jhin.2020.05.020
6. Kaier K, Mutters NT, Frank U. Bed occupancy rates and hospital-acquired infections—should beds be kept empty? Clin Microbiol Infect. 2012;18:941–5. https://doi.org/10.1111/j.1469-0691.2012.03956.x
7. Getahun H, Smith I, Trivedi K, Paulin S, Balkhy HH. Tackling antimicrobial resistance in the COVID-19 pandemic. Bull World Health Organ. 2020;98:442–442A. https://doi.org/10.2471/BLT.20.268573
8. Rawson TM, Moore LSP, Zhu N, Ranganathan N, Skolimowska K, Gilchrist M, et al. Bacterial and fungal

co-infection in individuals with coronavirus: a rapid review to support COVID-19 antimicrobial prescribing. Clin Infect Dis. 2020;71:2459–68.
9. Vincent J-L, Sakr Y, Singer M, Martin-Loeches I, Machado FR, Marshall JC, et al.; EPIC III Investigators. Prevalence and outcomes of infection among patients in intensive care units in 2017. JAMA. 2020;323:1478–87. https://doi.org/10.1001/jama.2020.2717
10. Prestel C, Anderson E, Forsberg K, Lyman M, de Perio MA, Kuhar D, et al. *Candida auris* outbreak in a COVID-19 specialty care unit—Florida, July–August 2020. MMWR Morb Mortal Wkly Rep. 2021;70:56–7. https://doi.org/10.15585/mmwr.mm7002e3

Address for correspondence: Surbhi Leekha, University of Maryland School of Medicine, 10 South Pine St, MSTF 334F, Baltimore, MD 21201, USA; email: sleekha@som.umaryland.edu

Cetacean Morbillivirus and *Toxoplasma gondii* Co-infection in Mediterranean Monk Seal Pup, Italy

Antonio Petrella, Sandro Mazzariol, Iolanda Padalino, Gabriella Di Francesco, Cristina Casalone, Carla Grattarola, Giovanni Di Guardo, Camilla Smoglica, Cinzia Centelleghe, Claudia Gili

Author affiliations: Istituto Zooprofilattico Sperimentale della Puglia e della Basilicata, Foggia, Italy (A. Petrella, I. Paladino); University of Padova, Padua, Italy (S. Mazzariol, C. Centelleghe); Istituto Zooprofilattico Sperimentale dell'Abruzzo e del Molise, Teramo, Italy (G. Di Francesco); Istituto Zooprofilattico Sperimentale del Piemonte, Liguria e Valle d'Aosta, Turin, Italy (C. Casalone, C. Grattarola); University of Teramo Faculty of Veterinary Medicine, Teramo (G. Di Guardo, C. Smoglica); Stazione Zoologica Anton Dohrn, Naples, Italy (C. Gili)

DOI: https://doi.org/10.3201/eid2704.204131

A Mediterranean monk seal (*Monachus monachus*) pup from the southern Adriatic coast of Italy showed cetacean morbillivirus (CeMV) and disseminated *Toxoplasma gondii* co-infection, which probably resulted from CeMV-induced immunosuppression. These findings are of concern for the conservation of this critically endangered species.

The Mediterranean monk seal (*Monachus monachus*), the most rarely occurring pinniped worldwide, ranks among the most endangered marine mammal species. A few breeding colonies remain along the shores of Greece, Turkey, and Cyprus as well as in Atlantic waters close to Cabo Blanco, Mauritania, and Madeira (*1*).

Monk seals are deemed to be officially extinct in many countries, including Italy. A monk seal pup was found alive along the southern Adriatic coast of Italy; it died after rehabilitation attempts. We performed a detailed necropsy on January 28, 2020, within 12 hours after death. Postmortem examination confirmed the animal was a female weaning pup; it had a poor body condition score. During necropsy, we collected samples from the animal's brain, spinal cord, lungs, liver, kidneys, lymph nodes, spleen, intestine, muscles, and tonsils for biomolecular analyses against viral and nonviral pathogens, with special emphasis on cetacean morbillivirus (CeMV) (*2*,*3*) and *Toxoplasma gondii* (*4*) (Appendix, https://wwwnc.cdc.gov/EID/article/27/4/20-4131-App1.pdf). We fixed all the tissue samples promptly in 10% neutral buffered formalin and routinely processed them for conventional histology and for morbillivirus and *T. gondii* immunohistochemistry. We used a commercially available monoclonal antibody against canine distemper virus (CDV) nucleoprotein (Veterinary Medical Research and Development, https://vmrd.com) and a rabbit polyclonal antibody against *T. gondii* (MyBioSource, https://www.mybiosource.com) (*5*,*6*).

We found extensive multifocal brain hemorrhages, most likely caused by a severe arteritis that also involved major cardiac vessels. The brain showed a multifocal, severe, nonsuppurative meningoencephalitis, closely associated with extensive and multifocal hemorrhages. We detected a diffuse, bilateral, chronic, and moderate interstitial pneumonia associated with a marked bronchiolar epithelial hyperplasia; we observed positive immunohistochemistry labeling for morbilliviral antigen within hyperplastic epithelial cells (Figure). Round, variably sized protozoan cysts positively stained with the *T. gondii* antibody were visible in the lung, within myocardial inflammatory foci, and in the tunica media of the aorta and pulmonary vessels. Lymphoid tissues exhibited a widespread and severe immune cell depletion.

Through biomolecular analyses (*2*,*3*), we detected CeMV genetic fragments in brain, lung, and spleen tissues preserved in RNAlater solution (ThermoFisher, https://www.thermofisher.com) and frozen lung tissue. Fragments showed a strong homology with a CeMV isolate (complete genome GenBank

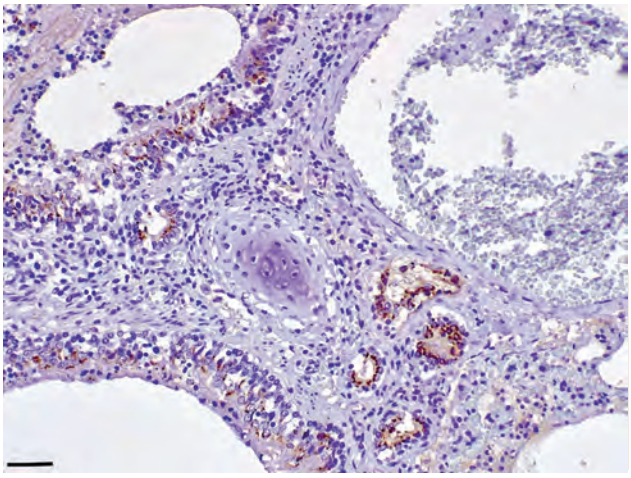

Figure. Lung tissue from a Mediterranean monk seal pup that died shortly after it was found along the southern Adriatic coast of Italy, showing positive immunostaining for morbillivirus antigen in bronchial/bronchiolar and alveolar epithelial cells, both normal and hyperplastic. Immunohistochemical analysis using an antibody against the nucleoprotein antigen of canine distemper virus (1:100 dilution), Mayer hematoxylin counterstained. Scale bar indicates 100 μm.

accession no. MH430938.1): the brain fragment (GenBank accession no. MW266078) was 397 bp long and was 98.25% homologous; the lung fragment (GenBank accession no. MW266077), 402 bp long, was 98.5% homologous; and the spleen fragment (GenBank accession no. MW266079), 152 bp long, was 99.3% homologous. In addition, we detected biomolecular positivity for *T. gondii* in skeletal muscle and lymph nodes, which supports immunohistochemical evidence.

Co-infections by morbilliviruses and *T. gondii* are well known among terrestrial and aquatic mammals, yet they have been rarely described in pinnipeds. Seals are known to be susceptible to CDV as well as to phocine distemper virus (*7*); CeMV infection has also been reported in monk and harbor seals (*Phoca vitulina*) (*6*). In 1997, half of the Mediterranean monk seals inhabiting the shores of Mauritania died and were found to have been infected with a CeMV-like agent; a similar virus was subsequently identified in a few monk seals from Greek waters (*6*). The cause of the die-off in 1997 remains unclear; biotoxins were also detected in dead seals (*8*).

The meningoencephalitic and pneumonic lesions found in the monk seal we investigated could also be associated with severe infection by *T. gondii.* Indeed, *T. gondii*–associated deaths have been reported as a significant threat to the health and conservation of Hawaiian monk seals (*Neomonachus schauinslandii*) (*9*). In the Mediterranean region, no similar cases have been previously reported other than in cetaceans, in which *T. gondii* has been recognized as a possible cause of death either alone or in association with CeMV (*6*). The young age of this monk seal suggests that CeMV or *T. gondii* infections could have been vertically acquired; the range of the severity and chronicity of *T. gondii*–associated lesions further suggest a prolonged persistence of the protozoan agent in the animal's circulation.

Previous *T. gondii* infection seems a plausible explanation for a subsequently acquired CeMV infection causing immunosuppression that led to disseminated toxoplasmosis. Nevertheless, we cannot exclude the possibility that CeMV acted as a primary pathogen. Previous reports of CeMV in Hawaiian monk seals, coupled with putative vertical transmission of *T. gondii,* indicate the need for careful evaluation of *T. gondii* and CeMV as potential threats to the health and conservation of Mediterranean monk seals. We recommend adequate and thorough seroepidemiologic and postmortem pathologic surveillance to assess the real risk posed by these 2 pathogens (*10*). An ad hoc infectious risk analysis protocol would enable investigators to address CeMV and *T. gondii* infections either separately or in combination by developing specific immunization protocols, such as those successfully employed on the Hawaiian monk seal population.

Acknowledgments

We thank the Italian National Institute for Environmental Protection and Research (ISPRA) for the support in the logistic operations before, during, and after necropsy.

About the Author

Dr. Petrella is a veterinary pathologist in the diagnostic laboratory of the Istituto Zooprofilattico Sperimentale della Puglia e Basilicata, Foggia, Italy, and serves as the regional focal point for the Italian Stranding Network. His research interests include investigations on stranded marine vertebrates.

References

1. Karamanlidis AA, Dendrinos P, Larrinoa PF, Gücü AC, Johnson WM, Kiraç CO, et al. The Mediterranean monk seal *Monachus monachus:* status, biology, threats, and conservation priorities. Mammal Rev. 2016;46:92–105. https://doi.org/10.1111/mam.12053</jrn>
2. Centelleghe C, Beffagna G, Zanetti R, Zappulli V, Di Guardo G, Mazzariol S. Molecular analysis of dolphin morbillivirus: a new sensitive detection method based on nested RT-PCR. J Virol Methods. 2016;235:85–91. https://doi.org/10.1016/j.jviromet.2016.05.005
3. Beffagna G, Centelleghe C, Franzo G, Di Guardo G, Mazzariol S. Genomic and structural investigation on dolphin morbillivirus (DMV) in Mediterranean fin whales (*Balaenoptera physalus*). Sci Rep. 2017;7:41554. https://doi.org/10.1038/srep41554

4. De Craeye S, Speybroeck N, Ajzenberg D, Dardé ML, Collinet F, Tavernier P, et al. *Toxoplasma gondii* and *Neospora caninum* in wildlife: common parasites in Belgian foxes and Cervidae? Vet Parasitol. 2011;178:64–9. https://doi.org/10.1016/j.vetpar.2010.12.016
5. Cruickshank JJ, Haines DM, Palmer NC, St Aubin DJ. Cysts of a *Toxoplasma*-like organism in an Atlantic bottlenose dolphin. Can Vet J. 1990;31:213–5.6. Van Bressem MF, Duignan PJ, Banyard A, Barbieri M, Colegrove KM, De Guise S, et al. Cetacean morbillivirus: current knowledge and future directions. Viruses. 2014;6:5145–81. https://doi.org/10.3390/v6125145
7. Duignan PJ, Van Bressem MF, Baker JD, Barbieri M, Colegrove KM, De Guise S, et al. Phocine distemper virus: current knowledge and future directions. Viruses. 2014;6:5093–134. https://doi.org/10.3390/v6125093
8. Hernández M, Robinson I, Aguilar A, González LM, López-Jurado LF, Reyero MI, et al. Did algal toxins cause monk seal mortality? Nature. 1998;393:28–9. https://doi.org/10.1038/29906
9. Barbieri MM, Kashinsky L, Rotstein DS, Colegrove KM, Haman KH, Magargal SL, et al. Protozoal-related mortalities in endangered Hawaiian monk seals *Neomonachus schauinslandi*. Dis Aquat Organ. 2016;121:85–95. https://doi.org/10.3354/dao03047
10. Robinson SJ, Barbieri MM, Murphy S, Baker JD, Harting AL, Craft ME et al. Model recommendations meet management reality: implementation and evaluation of a network-informed vaccination effort for endangered Hawaiian monk seals. Proc Biol Sci. 2018; 285:20171899. https://doi.org/10.1098/rspb.2017.1899

Address for correspondence: Sandro Mazzariol, Department of Comparative Biomedicine and Food Science, Viale dell'Università 16, 35020, Legnaro (PD), Italy; email: sandro.mazzariol@unipd.it

Increased Likelihood of Detecting Ebola Virus RNA in Semen by Using Sample Pelleting

Courtney M. Bozman, Mosoka Fallah, Michael C. Sneller, Catherine Freeman, Lawrence S. Fakoli III, Bode I. Shobayo, Bonnie Dighero-Kemp, Cavan S. Reilly, Jens H. Kuhn, Fatorma Bolay, Elizabeth Higgs, Lisa E. Hensley

Author affiliations: National Institutes of Health, Frederick, Maryland, USA (C.M. Bozman, B. Dighero-Kemp, J.H. Kuhn, L.E. Hensley); National Public Health Institute of Liberia, Monrovia, Liberia (M. Fallah, C. Freeman, L.S. Fakoli III, B.I. Shobayo, F. Bolay); National Institutes of Health, Bethesda, Maryland, USA (M.C. Sneller, E. Higgs); University of Minnesota, Minneapolis, Minnesota, USA (C.S. Reilly)

DOI: https://doi.org/10.3201/eid2704.204175

Ebola virus RNA can reside for months or years in semen of survivors of Ebola virus disease and is probably associated with increased risk for cryptic sexual transmission of the virus. A modified protocol resulted in increased detection of Ebola virus RNA in semen and improved disease surveillance.

During 2013–2016, Ebola virus (EBOV; family *Filoviridae*, genus *Ebolavirus*, species *Zaire ebolavirus*) caused an unprecedented outbreak of Ebola virus disease (EVD) that began in Guinea and subsequently affected Liberia, Sierra Leone, and, to a much lesser degree, several other countries in West Africa. Due in part to the lack of medical infrastructure and response preparedness in these countries, the outbreak ultimately involved 28,652 human infections and 11,325 deaths (*1*,*2*).

The large number of EVD survivors enabled detailed studies, such as the Partnership for Research on Ebola Virus (PREVAIL) III study (*3*), which aimed at characterizing potential EVD sequelae and EBOV persistence in a cohort of 1,144 EVD survivors in Liberia over the course of 5 years. An unexpected observation of these studies was the persistence of EBOV RNA and sometimes-replicating EBOV in the brain, eyes, and semen of survivors (*4*). EBOV RNA persistence in semen of EVD survivors, measurable up to 40 months (*3*,*5*), has been associated with rare events of sexual EBOV transmission and EVD outbreak flareups (*6*).

Assuming a causal relationship between EBOV RNA and EBOV presence in semen, we collaborated with the overseas response team to initiate an ongoing (and unpublished) trial, PREVAIL IV, to counter sexual EBOV transmission from survivors through reduction of viral RNA concentrations in semen by using the candidate medical countermeasure remdesivir. However, interpretation of data obtained in studies such as PREVAIL IV is crucially dependent on the sensitivity of EBOV RNA detection in semen samples.

The GeneXpert Systems (Cepheid, https://www.cepheid.com) are diagnostic platforms that implement single-use cartridges to simultaneously extract and detect RNA by using reverse transcription PCR. During PREVAIL III (*3*), the GeneXpert IV System was applied to standard processing of EBOV survivor semen

Table. Number of positive samples detected in whole semen samples versus pelleted semen samples for detection of Ebola virus RNA*

Method: replicate	No. samples	No. invalid samples	No. (%) Ebola virus RNA positive samples
Whole sample: A	1,661	66	50 (3.1)
Whole sample: B	1,661	112	45 (2.9)
Pellet sample: A	1,661	85	84 (5.3)
Pellet sample: B	1,661	69	73 (4.6)

*Also included are no. invalid samples (i.e., those that did not pass 1 or both of the controls (sample processing control and probe check control).

samples using EBOV nucleoprotein and glycoprotein RNA-specific GeneXpert cartridges Cepheid) (*7*): 100 μL of semen sample was transferred directly into 2.5 mL of lysis buffer provided in the kit and incubated for 10 min, followed by a second incubation of 5 min in presence of 100 μL of 1 M dithiothreitol (Sigma-Aldrich, https://www.sigmaaldrich.com). Within 30 min of processing, 1 mL of this solution was then loaded into the cartridge, run according to the manufacturer's instructions, and analyzed with GeneXpert Diagnostic Software (*8*).

We sought to further increase the EBOV RNA detection sensitivity (then 3.1% and 2.9% with whole samples) of this protocol for semen. For this experiment, 1,661 EVD survivor samples and nonsurvivor controls from PREVAIL III and IV with sample volumes ≥1.6 mL were divided into 2 cohorts and processed either as described above (whole sample) or first pelleted (pellet sample) by using 2 replicate experiments each (A and B).

For pelleting, we centrifuged 300 μL of each semen sample at 10,000 × *g* for 10 min. After pelleting, we discarded supernatants, resuspended pellets by pipetting in 100 μL of kit-provided lysis buffer and incubated for 10 min, and incubated for 5 min in presence of 100 μL of 1 M dithiothreitol. Then, we loaded 100 μL of each sample onto cartridges and processed the same way as the standard, unpelleted control sample. Samples were considered valid and positive when both the kit-provided sample processing control and probe check control passed kit criteria and EBOV nucleoprotein or glycoprotein RNA was detected.

Overall, an average of 3.0% of the whole sample-cohort was positive, compared with an average of 5.0% of the pellet-sample cohort, thereby almost doubling the detection rate ($p<0.0001$) (Table). We observed variability among replicates A and B (0.7% for the pellet and 0.2% for the whole sample), but this difference was not significant ($p = 0.35$) according to the F-test for the equality of 2 variances.

Mixed-effects logistic regression models appropriate to the study design (with random effects for specimens and random effects for replicates nested within specimens) yielded an estimated relative sensitivity of 2.24 (95% CI 1.51–2.98; $p<0.0001$) in favor of the pellet-based procedure. Thus, when semen sample volumes from EVD survivors are >300 μL, we recommend pelleting 300 μL to increase the EBOV RNA detection rate and using the GeneXpert IV System.

Acknowledgment

We thank Anya Crane for critically editing the manuscript.

This study was supported in part by the Laulima Government Solutions prime contract with the US National Institute of Allergy and Infectious Diseases (contract no. HHSN272201800013C to C.M.B. and B.D.-K.).

J.H.K. performed this work as an employee of Tunnell Government Services, a subcontractor of Laulima Government Solutions (contract no. HHSN272201800013C).

About the Author

Ms. Bozman is a response support scientist at the National Institute of Allergy and Infectious Diseases, National Institutes of Health, Frederick, MD. Her primary research interest is outbreak response in an international setting.

References

1. Decroo T, Fitzpatrick G, Amone J. What was the effect of the West African Ebola outbreak on health programme performance, and did programmes recover? Public Health Action. 2017;7(Suppl 1):S1–2. https://doi.org/10.5588/pha.17.0029
2. Bullard SG. A day-by-day chronicle of the 2013–2016 Ebola outbreak. Springer: Cham (Switzerland); 2018 [cited 2021 Jan 1]. https://link.springer.com/chapter/10.1007/978-3-319-76565-5_8
3. Sneller MC, Reilly C, Badio M, Bishop RJ, Eghrari AO, Moses SJ, et al.; PREVAIL III Study Group. A longitudinal study of Ebola sequelae in Liberia. N Engl J Med. 2019;380:924–34. https://doi.org/10.1056/NEJMoa1805435
4. Jacob ST, Crozier I, Fischer WA II, Hewlett A, Kraft CS, Vega MA, et al. Ebola virus disease. Nat Rev Dis Primers. 2020;6:13. https://doi.org/10.1038/s41572-020-0147-3
5. Keita AK, Vidal N, Toure A, Diallo MS, Magassouba N, Baize S, et al.; PostEbogui Study Group. A 40-month follow-up of Ebola virus disease survivors in Guinea (PostEbogui) reveals long-term detection of Ebola viral ribonucleic acid in semen and breast milk. Open Forum Infect Dis. 2019;6:ofz482. https://doi.org/10.1093/ofid/ofz482
6. Schindell BG, Webb AL, Kindrachuk J. Persistence and sexual transmission of filoviruses. Viruses. 2018;10:683. https://doi.org/10.3390/v10120683

7. Loftis AJ, Quellie S, Chason K, Sumo E, Toukolon M, Otieno Y, et al. Validation of the Cepheid GeneXpert for detecting Ebola virus in semen. J Infect Dis. 2017;215:344–50.
8. Pettitt J, Higgs E, Fallah M, Nason M, Stavale E, Marchand J, et al. Assessment and optimization of the GeneXpert diagnostic platform for detection of Ebola virus RNA in seminal fluid. J Infect Dis. 2017;215:547–53.

Address for correspondence: Lisa E. Hensley, Integrated Research Facility at Fort Detrick, Division of Clinical Research, National Institute of Allergy and Infectious Diseases, National, Institutes of Health, B-8200 Research Plaza, Fort Detrick, Frederick, MD 21702, USA; email: lisa.hensley@nih.gov

Polyresistant *Mycobacterium bovis* Infection in Human and Sympatric Sheep, Spain, 2017–2018

Bernat Pérez de Val, Beatriz Romero, María Teresa Tórtola, Laura Herrera León, Pilar Pozo, Irene Mercader, Jose Luís Sáez, Mariano Domingo, Enric Vidal

Author affiliations: Institut de Recerca i Tecnología Agroalimentàries-Centre de Recerca en Sanitat Animal, Barcelona, Spain (B. Pérez de Val, M. Domingo, E. Vidal); VISAVET-Universidad Complutense de Madrid, Madrid, Spain (B. Romero, P. Pozo); Vall d'Hebron Research Institute, Barcelona (M.T. Tórtola); Instituto de Salud Carlos III, Majadahonda, Madrid (L.H. León); MAEVA SERVET, S.L., Madrid (P. Pozo); Department d'Agricultura, Ramaderia, Pesca i Alimentació de la Generalitat de Catalunya, Barcelona (I. Mercader); Ministerio de Agricultura, Pesca y Alimentación, Madrid (J.L. Sáez); Universitat Autònoma de Barcelona, Barcelona (M. Domingo)

DOI: https://doi.org/10.3201/eid2704.204467

The main etiologic agent of tuberculosis (TB) in livestock is *Mycobacterium bovis*; human TB cases caused by *M. bovis* are rare. Analysis of a TB outbreak caused by polyresistant *M. bovis* involving a human and sympatric sheep in Spain suggests local circulation of drug-resistant *M. bovis* strains among livestock.

The main etiologic agent of tuberculosis (TB) in livestock and wildlife is *Mycobacterium bovis*. This species also infects humans through inhalation or ingestion and causes TB that is clinically indistinguishable from that caused by *M. tuberculosis*.

In 2017, a case of pulmonary TB caused by *M. bovis* in a human was detected in the Vall d'Hebron Hospital in Barcelona, Spain. Bacteriological culture of clinical specimens in Löwenstein-Jensen and 7H9 media (BD Diagnostics, https://bd.com), followed by antimicrobial resistance testing (BACTEC MGIT 960; BD Diagnostics), revealed a strain resistant to 2 first-line anti-TB drugs: pyrazinamide (100 μg/mL) and isoniazid (0.1 μg/mL). A complementary analysis, performed by using the proportion method, confirmed resistance to isoniazid (0.2 μg/mL), elucidating a polyresistant case of TB (resistance to >1 first-line anti-TB drug other than both isoniazid and rifampin); the strain was also resistant to ethionamide (30 μg/mL), an antimicrobial drug specifically used to treat active multidrug-resistant TB (resistance to at least both isoniazid and rifampicin). Molecular characterization by direct variable repeat (DVR)-spoligotyping identified the isolates as *M. bovis* spoligopattern SB0124 (http://www.mbovis.org).

The patient worked as a farmer on cattle and small ruminant farms in his county. Therefore, the epidemiologic investigation included the livestock he was in contact with, particularly the herd of sheep and goats he was currently managing. In 2018, a total of 34 (25%) ewes and 3 (18%) goats had positive results to a single intradermal tuberculin test, interferon gamma release assay (IDvet, https://www.id-vet.com), or both. Animals with positive test results were slaughtered, and tissues from 23 (21 sheep and 2 goats) were examined postmortem. TB-compatible lesions were found in the lungs and thoracic, mesenteric, or ileocecal lymph nodes of 13 animals (12 sheep, 1 goat). Tissues with lesions were cultured in Löwenstein-Jensen with pyruvate and Coletsos and in 7H9 media by using BACTEC MGIT 320 (all BD Diagnostics). Culture indicated growth of *M. tuberculosis* complex in 9 sheep samples, and *M. avium* subspecies *avium* was isolated from another sheep and the goat. DVR-spoligotyping was performed for the 9 *M. tuberculosis* complex isolates, and *M. bovis* SB0124 was identified in all. This unusual spoligopattern had also been identified in a cattle herd in the same county in 2005 (Spanish Database of Animal Mycobacteriosis; https://www.visavet.es/mycodb); the patient had no known connection to that herd.

Genome sequence analysis based on assessment of single-nucleotide polymorphisms (SNPs)

was conducted for 2 isolates from sheep (2018) and the isolate from the human patient (2017) and for 2 isolates collected from cattle in 2005–2006. Results showed an extremely close phylogenetic relationship between the isolates from the sheep and human (<5 SNPs), leading us to conclude that they were the same strain; they differed from the strains from cattle by 35–38 SNPs (Figure). Of note, the isolates from the sheep and human showed resistance to pyrazinamide, isoniazid, and ethionamide, and isolates from the cattle showed resistance to pyrazinamide and isoniazid. These results suggest that although strains from cattle and from the sheep and human were not closely related enough to be considered the same strain, they might have evolved from a common ancestral isoniazid-resistant strain. However, mutations associated with pyrazinamide resistance were found only at the *pncA* (C169G) gene and with isoniazid/ethionamide resistance at the *inh*A (T280G) gene, although the *inhA* modification was detected only in the isolates from cattle.

Human TB caused by *M. bovis* is usually associated with occupational exposure and is infrequently reported in Spain; cases of multidrug-resistant (MDR) TB are even more rare (*1*,*2*). However, zoonotic cases could be underestimated because the need for relatively sophisticated laboratory methods hinders estimation of zoonotic TB occurrence, particularly in low-income areas, and epidemiologic relationships between TB patients and sympatric livestock are rarely investigated.

Although only a few cases of TB in sheep have been reported in Spain (*3*,*4*), these reports suggest that sheep can play a role as maintenance hosts of *M. bovis* and *M. caprae* in certain epidemiologic situations. TB progression in sheep appears to be similar to that in cattle or goats (*5*).

M. bovis is naturally resistant to pyrazinamide (*6*), but our findings reveal circulation of polyresistant strains in livestock in the outbreak area. In contrast, a previous study reported absence of polyresistant *M. bovis* strains isolated from livestock in the Iberian Peninsula (*7*). Similarly, cases of TB in humans caused by isoniazid-resistant *M. bovis* are infrequent in Spain (*8*), although a nosocomial outbreak caused by MDR *M. bovis* involving HIV-infected patients has been described (*9*). Only a few studies have examined treatment of isoniazid polydrug resistance (*10*), which is particularly dangerous because of the high risk that resistance to rifampin will develop, requiring full MDR TB treatment.

Distinguishing between TB causative organisms is crucial for epidemiologic investigation and adequate treatment of TB in humans. The One Health approach should be implemented in contact investigations for TB cases through coordination of public and animal health authorities to prevent spread of TB between humans and livestock. Controlling TB in small ruminants and studying drug resistance in strains circulating among livestock should also be considered.

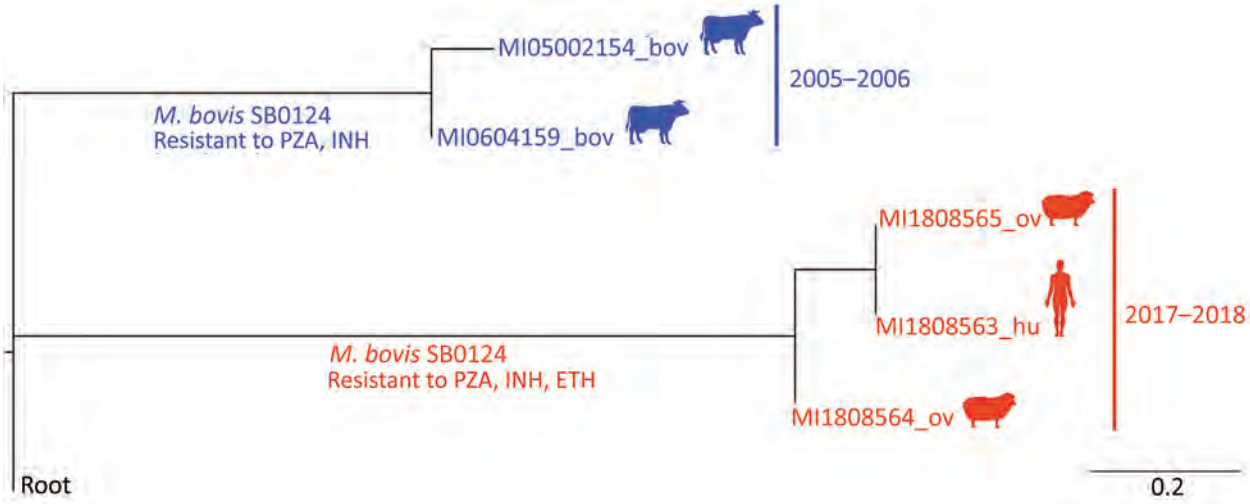

Figure. Rooted phylogenetic tree based on the maximum-likelihood method (RAxML; https://academic.oup.com/bioinformatics/article/30/9/1312/238053), showing the average number of nucleotide substitutions per site of a *Mycobacterium bovis* strain isolated in Spain from a human in 2017 (red) and with *M. bovis* strains isolated from sheep in 2018 (red), and with 2 strains isolated from cattle in the same county in 2005 and 2006 (blue). Spoligopattern SB0124 was identified in all strains. Strains from the human and the sheep showed resistance to pyrazinamide, isoniazid, and ethionamide; strains from the cattle showed resistance to pyrazinamide and isoniazid. Root: *M. bovis* AF 2122/97 reference strain sequence (National Center for Biotechnology Information accession no. NC_0002945). Bov, bovine; ETH, ethionamide; hu, human; INH, isoniazid; PZA, pyrazinamide; ov, ovine.

Acknowledgments

We are grateful to Maite Martín and Mónica Pérez for their outstanding technical assistance and to the Mycobacteria Section of the National Veterinary Services Laboratories (US Department of Agriculture, Animal and Plant Health Inspection Service) for the sequencing service and technical support.

This work was supported by the Department of Agriculture, Livestock Fisheries and Food of the Government of Catalonia and by the Spanish Ministry of Agriculture, Fisheries and Food. The Institute of Agrifood Research and Technology is supported by Centres de Recerca de Catalunya Programme/Generalitat de Catalunya.

About the Author

Dr. Pérez de Val is a researcher at the Institut de Recerca i Tecnología Agroalimentàries-Centre de Recerca en Sanitat Animal, Barcelona, Spain, where he conducts research on control and surveillance of TB.

References

1. Samper S, Iglesias MJ, Rabanaque MJ, Gómez LI, Lafoz MC, Jiménez MS, et al.; Spanish Working Group on MDR-TB. Systematic molecular characterization of multidrug-resistant *Mycobacterium tuberculosis* complex isolates from Spain. J Clin Microbiol. 2005;43:1220–7. https://doi.org/10.1128/JCM.43.3.1220-1227.2005
2. Rodríguez E, Sánchez LP, Pérez S, Herrera L, Jiménez MS, Samper S, et al. Human tuberculosis due to *Mycobacterium bovis* and *M. caprae* in Spain, 2004-2007. Int J Tuberc Lung Dis. 2009;13:1536–41.
3. Muñoz Mendoza M, Juan L, Menéndez S, Ocampo A, Mourelo J, Sáez JL, et al. Tuberculosis due to *Mycobacterium bovis* and *Mycobacterium caprae* in sheep. Vet J. 2012;191:267–9. https://doi.org/10.1016/j.tvjl.2011.05.006
4. Vidal E, Grasa M, Perálvarez T, Martín M, Mercader I, Pérez de Val B. Transmission of tuberculosis caused by *Mycobacterium caprae* between dairy sheep and goats. Small Rumin Res. 2018;158:22–5. https://doi.org/10.1016/j.smallrumres.2017.11.010
5. Balseiro A, Altuzarra R, Vidal E, Moll X, Espada Y, Sevilla IA, et al. Assessment of BCG and inactivated *Mycobacterium bovis* vaccines in an experimental tuberculosis infection model in sheep. PLoS One. 2017;12:e0180546. https://doi.org/10.1371/journal.pone.0180546
6. Scorpio A, Collins D, Whipple D, Cave D, Bates J, Zhang Y. Rapid differentiation of bovine and human tubercle bacilli based on a characteristic mutation in the bovine pyrazinamidase gene. J Clin Microbiol. 1997;35:106–10. https://doi.org/10.1128/JCM.35.1.106-110.1997
7. Romero B, Aranaz A, Bezos J, Alvarez J, de Juan L, Tariq Javed M, et al. Drug susceptibility of Spanish *Mycobacterium tuberculosis* complex isolates from animals. Tuberculosis (Edinb). 2007;87:565–71. https://doi.org/10.1016/j.tube.2007.08.004
8. Nebreda-Mayoral T, Brezmes-Valdivieso MF, Gutiérrez-Zufiaurre N, García-de Cruz S, Labayru-Echeverría C, López-Medrano R, et al. Human *Mycobacterium bovis* infection in Castile and León (Spain), 2006-2015 [in Spanish]. Enferm Infecc Microbiol Clin. 2019;37:19–24. https://doi.org/10.1016/j.eimc.2017.11.018
9. Samper S, Martín C, Pinedo A, Rivero A, Blázquez J, Baquero F, et al. Transmission between HIV-infected patients of multidrug-resistant tuberculosis caused by *Mycobacterium bovis*. AIDS. 1997;11:1237–42. https://doi.org/10.1097/00002030-199710000-00006
10. Menzies D, Benedetti A, Paydar A, Royce S, Madhukar P, Burman W, et al. Standardized treatment of active tuberculosis in patients with previous treatment and/or with mono-resistance to isoniazid: a systematic review and meta-analysis. PLoS Med. 2009;6:e1000150. https://doi.org/10.1371/journal.pmed.1000150

Address for correspondence: Bernat Pérez de Val, Institut de Recerca i Tecnologia Agroalimentaries Centre de Recera en Sanitat Animal Edifici CReSA. Campus of the Autonomous University of Barcelona, 08193-Bellaterra, Barcelona, Spain; email: bernat.perez@irta.cat

Novel SARS-CoV-2 Variant in Travelers from Brazil to Japan

Takahisa Fujino, Hidetoshi Nomoto, Satoshi Kutsuna, Mugen Ujiie, Tetsuya Suzuki, Rubuna Sato, Tsuguto Fujimoto, Makoto Kuroda, Takaji Wakita, Norio Ohmagari

Author affiliations: National Center for Global Health and Medicine, Tokyo, Japan (T. Fujino, H. Nomoto, S. Kutsuna, M. Ujiie, T. Suzuki, R. Sato, N. Ohmagari); Tohoku University, Miyagi, Japan (H. Nomoto, T. Suzuki, N. Ohmagari); National Institute of Infectious Diseases, Tokyo (T. Fujimoto, M. Kuroda, T. Wakita)

DOI: https://doi.org/10.3201/eid2704.210138

Multiple severe acute respiratory syndrome coronavirus 2 (SARS-CoV-2) variants with higher transmission potential have been emerging globally, including SARS-CoV-2 variants from the United Kingdom and South Africa. We report 4 travelers from Brazil to Japan in January 2021 infected with a novel SARS-CoV-2 variant with an additional set of mutations.

Coronavirus disease (COVID-19), caused by severe acute respiratory syndrome coronavirus 2 (SARS-CoV-2) (*1*), has wreaked havoc worldwide. SARS-CoV-2 causes severe respiratory failure, often rapidly in susceptible patients. Moreover, new variants with estimated higher transmission rates have begun circulating globally, such as Variant of Concern 202012/01 (VOC-202012/01) from the United Kingdom and variant 501Y.V2 from South Africa (*2*). The virulence, reinfection potential, antibody response to, and efficacy of vaccines against these strains, are still unknown, posing a risk for future pandemics. We detected a previously unreported SARS-CoV-2 variant strain in a family arriving in Japan from Brazil.

On January 2, 2021, a healthy man in his 40s arrived at Haneda Airport, Tokyo, Japan, from Amazonas state in Brazil via Istanbul, Turkey. At the airport quarantine station, he and the 3 family members traveling with him tested positive for SARS-CoV-2 by quantitative real-time reverse transcription PCR. All 4 were asymptomatic and were accommodated in a government-designated quarantine facility to wait out the required 14-day quarantine.

On day 2 of their visit, a fever of 37.6°C developed in the man; on day 4, the man had a cough. On day 6, his oxygen saturation (SpO_2) dropped to 93% on ambient air, and he was transferred to the National Center for Global Health and Medicine, a tertiary care hospital in Tokyo, for respiratory failure. The remaining 3 family members remained asymptomatic and continued to stay at the government-designated accommodation.

At admission, the patient had a cough and mild malaise. Physical examination was almost normal except for late inspiratory crackles in the bilateral lower lung fields. The patient's body temperature was 37.4°C; blood pressure was 113/69 mm Hg and pulse rate 108 beats/min. The patient had a regular respiratory rate of 18 breaths/min and an SpO_2 of 93% on ambient air. Laboratory tests showed a high C-reactive protein level of 10.47 mg/dL (reference range 0.00–0.14 mg/dL), but complete blood counts, renal function, liver function, and coagulation tests all were within reference ranges. Chest radiography and computed tomography showed ground-glass opacities in the lower lobes of both lungs.

We started the patient on treatment with 200 mg remdesivir, a subcutaneous injection of unfractionated heparin, and 6 mg oral dexamethasone on day 1 of admission. On day 2 of admission, the patient's fever subsided, and his general condition improved marginally. On day 3, oxygen therapy was not needed, blood tests showed a decrease in C-reactive protein levels, and no adverse side effects of treatment were observed. He continued treatment with 100 mg/d remdesivir and unfractionated heparin until day 5 of admission and dexamethasone until day 7, during which time we observed no flare-up of symptoms.

We subjected the SARS-CoV-2 detected in the case-patient and in his family to whole-genome sequencing. Phylogenetic analysis suggested a novel variant (GISAID [https://www.gisaid.org] reference no. EPI_ISL_792681) belonging to pangolin lineage P.1 with 12 nonsynonymous mutations including K417T, E484K, and N501Y in the receptor-binding domain of the spike protein (N.R. Faria et al., unpub data, https://virological.org/t/genomic-characterisation-of-an-emergent-sars-cov-2-lineage-in-manaus-preliminary-findings/586). In addition, the variant strain we detected in the travelers had the N501Y mutation in the receptor-binding site of the spike protein, as noted in VOC-202012/01 and 501Y.V2, and the E484K mutation, similar to that noted in the 501Y strain.

We did not observe any remarkable difference in the clinical course of this case-patient compared with COVID-19 cases caused by other known SARS-CoV-2 strains. According to multiple modeling analyses, the new VOC-202012/01 variant could be more infectious than previous strains and might have ≤70% increased transmissibility (*3*–*5*). Moreover, PCR testing and genomic analysis for this strain suggested an increased viral load in VOC-202012/01 variant. Another strain, 501Y.V2 from South Africa, also has been suggested to have increased transmissibility (H. Tegally et al., unpub. data, https://doi.org/10.1101/2020.12.21.20248640). However, to date, no definitive evidence has shown that either VOC-202012/01 or 501Y.V2 are associated with more severe COVID-19 cases.

The symptoms in this patient were relatively mild, although short-term oxygen administration was necessary. Onset of pneumonia a week after the onset of disease also followed the conventional clinical course. However, because the patient was young and had no underlying conditions, this case cannot be generalized.

In conclusion, we identified a novel variant strain of SARS-CoV-2 in 4 travelers from Brazil. Variant strains are appearing across the world now, and quarantine systems need to be strengthened. We hope to elucidate the infectivity, pathogenicity, and relationship of SARS-CoV-2 variants to vaccines while continuing to take conventional precautions against novel variant strains.

Acknowledgments

We thank Tsuyoshi Sekizuka, Kentaro Itokawa, Masanori Hashino, Nozomu Hanaoka, Nobuo Koizumi, and Tsuguto Fujimoto for assistance with PCR testing and whole-genome sequencing, and we thank the clinical staff at the National Center for Global Health and Medicine for their dedicated clinical practice and patient care.

This work was supported by the Health, Labor, and Welfare Policy Research Grants, Research on Emerging and Re-emerging Infectious Diseases and Immunization (grant no. 20HA1006).

About the Author

Dr. Fujino is a physician at the National Center for Global Health and Medicine in Shinjuku-ku, Tokyo, Japan. His main research interest is hematology.

References

1. World Health Organization. Coronavirus disease (COVID-19) situation reports. Weekly epidemiological update—19 January 2021 [cited 2021 Jan 21]. https://www.who.int/emergencies/diseases/novel-coronavirus-2019/situation-reports
2. World Health Organization. SARS-CoV-2 variant [cited 2021 Jan 21]. https://www.who.int/csr/don/31-december-2020-sars-cov2-variants/en/
3. European Centre for Disease Prevention and Control. Rapid increase of a SARS-CoV-2 variant with multiple spike protein mutations observed in the United Kingdom; December 20, 2020 [cited 2021 Jan 21]. https://www.ecdc.europa.eu/sites/default/files/documents/SARS-CoV-2-variant-multiple-spikeprotein-mutations-United-Kingdom.pdf
4. The New and Emerging Respiratory Virus Threats Advisory Group (NERVTAG). NERVTAG meeting on SARS-CoV-2 variant under investigation VUI-202012/01. 2020 Dec 18 [cited 2021 Jan 21]. https://app.box.com/s/3lkcbxepqixkg4mv640dpvvg978ixjtf/file/756963730457
5. New and Emerging Respiratory Virus Threats Advisory Group. NERVTAG/SPI-M Extraordinary meeting on SARS-CoV-2 variant of concern 202012/01 (variant B.1.1.7). Note of meeting 2020 Dec 21 [cited 2021 Jan 21]. https://app.box.com/s/3lkcbxepqixkg4mv640dpvvg978ixjtf/file/756964987830

Address for correspondence: Satoshi Kutsuna, Disease Control and Prevention Center, National Center for Global Health and Medicine, 1-21-1 Toyama, Shinjuku-ku, Tokyo 162-8655, Japan; email: sonare.since1192@gmail.com

Isolation of *Rickettsia rickettsii* in Rocky Mountain Spotted Fever Outbreak, Panama

Yamitzel Zaldívar, Michelle Hernández, Lillian Domínguez, Lisseth Saénz, Santiago Montilla, Maria E. Barnett de Antinori, Felipe S. Krawczak, Sergio Bermúdez

Author affiliations: Gorgas Memorial Institute for Health Research, Panama City, Panama (Y. Zaldívar, M. Hernández, L. Domínguez, L. Saénz, S. Montilla, M.E.B. de Antinori, S. Bermúdez); School of Veterinary Medicine and Animal Science, Federal University of Goiás–UFG, Goiânia, Brazil (F.S. Krawczak); Coiba Scientific Station, Panama City (S. Bermúdez)

DOI: https://doi.org/10.3201/eid2704.201606

We report new cases of Rocky Mountain spotted fever in patients from Kinkantu, Ngäbe-Bugle indigenous comarca, Panama. We isolated *Rickettsia rickettsii* in cell culture after intraperitoneal inoculation of guinea pigs with tissues from a deceased patient. Our results indicate that Rocky Mountain spotted fever is emerging in this region.

Rocky Mountain spotted fever (RMSF) causes severe cases of rickettsiosis and is considered a principal tickborne pathogen in the Americas (*1*). Clinical suspicion is crucial for timely therapy with doxycycline to prevent severe illness and death (*1*). In Panama, 5 cases of RMSF were reported during 1950–1953, of which 2 were fatal; since 2004, a total of 19 new cases have been reported in Panama, with 13 fatal cases (*2*). We report new cases of RMSF from Piedra Roja, a rural village of Kankintu, Ngäbe-Bugle indigenous comarca, located at 750 m above sea level in the western mountainous region of Panama without road access.

In February 2019, a total of 7 persons 3–20 years of age from a family cluster had a clinical picture characterized by temperatures of 39°C–41°C (100%), generalized exanthema (100%), diarrhea and vomiting (86%), headaches (71%), severe dehydration (57%), abdominal pain (43%), and hepatomegaly and jaundice (29%). The patients reported no history of recent tick bites or attachment; according to each patient, the duration of symptoms varied from 9 to 11 days. Of these 7 patients, 2 recovered after treatment with doxycycline, 1 recovered without treatment with doxycycline, and 4 died.

We diagnosed rickettsiosis by PCR on blood and samples of spleen, liver, brain and lung, using the

Rr190.70p and Rr190.602n primers, which amplify a ≈532 bp fragment of outer membrane protein gene (*ompA*) (*3*). Samples of blood, liver, and spleen from 6 patients yielded *ompA* amplicons, of which 3 generated DNA sequences 100% identical to *R. rickettsii* were deposited in GenBank (accession nos. MF678551.1, KX363464.1, and CP006010.1).

Tissue samples were recovered during the autopsy of 1 patient and stored at −40°C. Because this temperature is higher than that recommended to keep *Rickettsia* viable, we inoculated 1 guinea pig (*Cavia porcellus*) with tissue homogenate to avoid rickettsial load loss at the moment of isolation. These animals have been reported as amplifier hosts for *R. rickettsii* (*4*,*5*). Therefore, we inoculated a homogenate of spleen, liver, and lung tissues into an adult male guinea pig before starting the isolation through cell culture. The animal did not have a fever (rectal temperature ≤39.6°C) but died on the 7th day postinoculation (dpi). We extracted and macerated the liver, spleen, brain, and lungs to inoculate 5 additional guinea pigs (second passage), following Krawczak et al. (*4*). Of these, 2 animals died <24 hours later and were eliminated from the study, 1 developed high fever (≥40.0°C) at 4 dpi that persisted until 6 dpi, and 2 remained afebrile but died at 4–5 dpi. We isolated rickettsiae in cell culture from a febrile (>39.6°C) guinea pig that was euthanized at 6 dpi. We inoculated fragments of liver, spleen, and lungs into flasks containing a monolayer of Vero cells, as previously described (*5*,*6*). We considered a rickettsial isolate to be established in the laboratory after third passages, each reaching an infected cell level >90% (*6*,*7*). We successfully isolated rickettsiae in Vero cells of homogenate derived from a 3-guinea-pig passage.

We extracted DNA from infected cells following Krawczak et al. (*4*) using a PCR targeting *gltA* (401 bp), *ompA* (532 bp), and *ompB* (511 bp) (*3*,*6*). Sequenced PCR products showed a 100% identity with *R. rickettsii gltA* (GenBank accession nos. CP018914.1, CP018913.1, CP006010.1, CP006009.1, and CP000766.3), *ompA* (GenBank accession nos. MF678551.1 and MF988095.1), and *ompB* (GenBank accession nos. CP018914.1, CP018913.1, CP006010.1, CP006009.1, and CP000766.3). We deposited DNA of an isolate in GenBank (accession no. MT814706 for the *gltA* gene, MT268770 for the *ompA* gene, and MT814707 for the *ompB* gene). We designated the *R. rickettsii* isolate as strain NB, for Ngäbe Bugle, and deposited it in the Gorgas Memorial Institute at Biosafety Level 3.

The diagnosis of severe cases of RMSF in Piedra Roja represents a new locality for this disease in Panama. RMSF has been reported previously from the provinces of Panama, Panama Oeste, and Colon, associated with the distribution of *Amblyomma mixtum* and *Rhipicephalus sanguineus* s.l. ticks (*2*,*8*). More studies will be needed to determine the ecology related to these cases.

We were able to isolate *R. rickettsii* from infected tissues stored at −40°C, which is higher than the recommended temperature of −80°C for preserving tissues (*9*). Because of the relevance of *R. rickettsii* as a pathogen, the isolation of strains favors obtaining antigens for serologic tests and for further studies to determine the genetic and pathogenic differences between strains. Currently, >30 genotypes of *R. rickettsii* exist, with different degrees of pathogenicity; therefore, a more representative sample of isolates may make it possible to estimate variations among different populations (*10*).

In summary, we investigated an outbreak of RMSF in Piedra Roja, a rural village in western Panama, an area where this disease had not previously been reported. Clinicians should remain aware of the possibility of *R. rickettsii* infection in this region.

Acknowledgments

We thank Hermes Santos, Doristela Isaza, Brechla Moreno, and Claudia Gonzalez for their assistance; Sebastián Muñóz-Leal for his contributions to sequencing; Joao Varela-Petrucelli for his comments; Hector Cedeño for the information provided on the outbreak; and Lance Durden for corrections in English.

This work was authorized by the Gorgas Memorial Institute's Bioethics Committee of Investigation (no. 582/CBI/ICGES/19) and Institutional Animal Care and Use Committee (no. 01-2020), and financed with US HHS-ASPR Cooperative Agreement funds (IDSEP 170040) coordinated by Maria E. Barnett de Antinori.

About the Author

Ms. Zaldívar is a medical technologist and head of the Department of Research-Surveillance and Biological Risk 3, Gorgas Memorial Institute for Health Research, Panama City, Panama. Her primary research interest is molecular biology and genetics.

References

1. Oliveira SV, Caldas EP, Colombo S, Gazeta GS, Labruna MB, Santos FC, et al. A fatal case of Brazilian spotted fever in a non-endemic area in Brazil: the importance of having health professionals who understand the disease and its areas of transmission. Rev Soc Bras Med Trop. 2016;49:653–5. https://doi.org/10.1590/0037-8682-0088-2016

2. Bermúdez S, Domínguez L, Suárez J, Daza C, Cumbrera A, González J. Past and present of rickettsiosis in Panamá [in Spanish]. Panama City: Instituto Conmemorativo Gorgas de Estudios de la Salud, Panamá; 2018.
3. Regnery RL, Spruill CL, Plikaytis BD. Genotypic identification of rickettsiae and estimation of intraspecies sequence divergence for portions of two rickettsial genes. J Bacteriol. 1991;173:1576–89. PubMed https://doi.org/10.1128/JB.173.5.1576-1589.1991
4. Krawczak FS, Nieri-Bastos FA, Nunes FP, Soares JF, Moraes-Filho J, Labruna MB. Rickettsial infection in *Amblyomma cajennense* ticks and capybaras (*Hydrochoerus hydrochaeris*) in a Brazilian spotted fever–endemic area. Parasit Vectors. 2014;7:7. https://doi.org/10.1186/1756-3305-7-7
5. Stokes J, Walker D, Varela-Stokes A. The guinea pig model for tick-borne spotted fever rickettsioses: a second look. Ticks Tick-borne Dis. 2020;11:101538. https://doi.org/10.1016/j.ttbdis.2020.101538
6. Paddock, C.D., Allerdice, M., Karpathy, S.E., Nicholson, W.L., Levin, M.L., Smith, T.C. et al. Unique strain of *Rickettsia parkeri* associated with the hard tick *Dermacentor parumapertus* Neumann in the western United States. Appl Environ Microbiol. 2017;83:e03463-16. https://doi.org/10.1128/AEM.03463-16
7. Labruna MB, Santos FC, Ogrzewalska M, Nascimento EM, Colombo S, Marcili A, et al. Genetic identification of rickettsial isolates from fatal cases of Brazilian spotted fever and comparison with *Rickettsia rickettsii* isolates from the American continents. J Clin Microbiol. 2014;52:3788–91. https://doi.org/10.1128/JCM.01914-14
8. Bermúdez SE, Castro AM, Trejos D, García GG, Gabster A, Miranda RJ, et al. Distribution of spotted fever group rickettsiae in hard ticks (Ixodida: Ixodidae) from Panamanian urban and rural environments (2007–2013). EcoHealth. 2016;13:274–84. https://doi.org/10.1007/s10393-016-1118-8
9. Ammerman N, Beier-Sexton M, Azad A. Laboratory maintenance of *Rickettsia rickettsii*. Curr Protoc Microbiol. 2008;11:3A.5.1–21. https://doi.org/10.1002/9780471729259.mc03a05s11
10. Eremeeva ME, Dasch GA. Closing the gaps between genotype and phenotype in *Rickettsia rickettsii.* Ann N Y Acad Sci. 2009;1166:12–26. https://doi.org/10.1111/j.1749-6632.2009.04526.x

Address for correspondence: Sergio Bermúdez, Medical Entomology Department, Gorgas Memorial Institute for Health Research, Panama; email: sbermudez@gorgas.gob.pa; Felipe Krawczak, Preventive Veterinary Medicine Department, Federal University of Goiás, Goiânia-GO, Brazil; email: felipekvet@ufg.br

Co-infection with Severe Fever with Thrombocytopenia Syndrome Virus and *Rickettsia japonica* after Tick Bite, Japan

Tatsuya Fujikawa, Tomoki Yoshikawa, Takeshi Kurosu, Masayuki Shimojima, Masayuki Saijo, Kyoko Yokota

Author affiliations: Mitoyo General Hospital, Kanonji, Japan (T. Fujikawa); National Institute of Infectious Diseases, Tokyo, Japan (T. Yoshikawa, T. Kurosu, M. Shimojima, M. Saijo); Kagawa Prefectural Central Hospital, Takamatsu, Japan (K. Yokota)

DOI: https://doi.org/10.3201/eid2704.203610

Severe fever with thrombocytopenia syndrome was diagnosed in a febrile woman in Japan after a tick bite. However, *Rickettsia japonica* DNA was retrospectively detected in the eschar specimen, suggesting co-infection from the bite. Establishment of the severe fever with thrombocytopenia syndrome virus infection might have overpowered the *R. japonica* infection.

Severe fever with thrombocytopenia syndrome (SFTS) is caused by SFTS virus (SFTSV), a novel phlebovirus in the family *Bunyaviridae* (*1*). It has been reported that SFTS is endemic to Japan (*2*). SFTS is classified as a viral hemorrhagic fever, and its case-fatality rate in Japan is ≈30% (*3*).

Japanese spotted fever (JSF) is an acute tickborne rickettsiosis caused by *Rickettsia japonica* and is endemic to Japan (*4*). Most cases of SFTS in Japan have been reported in southwestern Japan, and the JSF-endemic area overlaps the areas to which SFTS is endemic. Because the *Haemaphysalis longicornis* tick is a vector for both SFTSV and *R. japonica* (*4*,*5*), co-infection events might occur in patients with SFTS or *R. japonica* infection.

A woman 84 years of age was bitten on her lower right back by a tick while working in a field. She became febrile on day 1, experienced mild delirium on day 2, and visited the emergency department of Mitoyo General Hospital (Kanonji, Japan) on day 5, where she had low-grade fever but was alert and lucid. Physical examination revealed an eschar surrounded by exanthema on her lower right back (Figure). She had noticed the eschar on the day after the bite, and her family removed it. We observed no other skin exanthema on her body. Laboratory analysis revealed thrombocytopenia and leukocytopenia (Table). Serum chemistry analyses revealed elongation of the activated partial thromboplastin time and an

Figure. Eschar at site of tick bite surrounded by exanthema on lower right back of patient with severe fever with thrombocytopenia syndrome and positive *Rickettsia japonica* DNA in eschar, Japan.

increase in the D-dimer level, suggesting coagulopathy. Because increases in aspartate transaminase and blood urea nitrogen were noted, liver and renal functions might have been impaired transiently (Table).

Because of the fever, thrombocytopenia, history of tick bite, and eschar with localized exanthema, we suspected JSF. The patient's blood samples and the crust of the eschar were tested by PCR assays for *R. japonica*, *Orientia tsutsugamushi*, and SFTSV. The serum sample tested positive for SFTSV by a conventional 1-step reverse transcription PCR reported previously (*6*). *R. japonica* DNA was also detected in the eschar sample through the methods described previously (*7*), but it was not detected in serum samples. We empirically administered 100 mg of minocycline intravenously for 7 days, after which minocycline was administered orally every 12 hours for 3 days. Her symptoms resolved without complications by day 6, the second day of admission. After discharge from the hospital on day 12, outpatient follow-up was uneventful.

We analyzed blood specimens to examine paired serum antibody titers against SFTSV in the acute phase and convalescent phase with indirect immunofluorescence assay (IFA) (*8*), which indicated a substantial increase in the antibody to SFTSV from <10 to 640. A relatively low level of viremia (154 copies/mL) was also confirmed in the acute phase (day 4) of the disease by quantitative PCR assays (*6*). We tested paired serum from the acute phase (day 4) and the convalescent phase (day 27) for IgG and IgM titers against *R. japonica* by IFA as described previously (*9*). IgG and IgM against *R. japonica* were not detected in either the acute-phase or convalescent-phase serum samples. This result suggests that a general *R. japonica* infection had not established itself and that infection was localized to the eschar, in which erythematous lesions were present, and *R. japonica* DNA was detected only in the eschar sample (Figure). Unfortunately, the nucleotide sequence of the *R. japonica* genome amplified from the eschar was not determined.

The clinical course and laboratory results of this patient, with the exception of the eschar, were consistent with SFTS but not JSF. It has been reported that a tick bite scar could not be found in 56% of SFTS patients (*6*), whereas skin eruptions appear in 100% of patients with JSF and tick bite eschar appear in 90% of patients

Table. Laboratory findings in patient with severe fever with thrombocytopenia syndrome and positive *Rickettsia japonica* DNA in eschar at site of tick bite, Japan*

Parameter	Values	Reference range
Total blood cell counts		
Leukocytes	17.1 × 10^2/μL	33–86 × 10^2/μL
Erythrocytes	410 × 10^4/μL	380–500 × 10^4/μL
Hemoglobin	12.4 g/dL	11.5–15.0 g/dL
Hematocrit	35.2%	35.0%–45.0%
Platelets	7.4 × 10^4/μL	15–35 × 10^4/μL
Neutrophils	58%	35.0%–75.0%
Coagulation-associated tests		
PT	10.3 s	9.9–11.8 s
APTT	45.9 s	23.0–39.0 s
FDP	4.3 μg/mL	0.0–5.0 μg/mL
D-dimer	1.2 μg/mL	0.0–1.0 μg/mL
Serum chemistry		
CRP	<1.0 mg/dL	0.00–0.14 mg/dL
AST	42 U/L	13–30 U/L
ALT	18 U/L	7–23 U/L
ALP	170 U/L	106–322 U/L
γ-GT	14 U/L	9–32 U/L
Total bilirubin	0.5 mg/dL	0.4–1.5 mg/dL
LDH	200 U/L	124–222 U/L
CK	63 U/L	59–248 U/L
Total protein	7.1 g/dL	6.6–8.1 g/dL
Albumin	3.9 g/dL	4.1–5.1 g/dL
BUN	26 mg/dL	8–20 mg/dL
Creatinine	0.76 mg/dL	0.46–0.79 mg/dL
eGFR	54.5 mL/min	80–100 mL/min
Ccr	41.8 mL/min	NA
Uric acid	3.7 mg/dL	2.6–5.5 mg/dL
Sodium	127 mmol/L	138–145 mmol/L
Potassium	3.8 mmol/L	3.6–4.8 mmol/L
Chloride	92 mmol/L	101–108 mmol/L

*ALP, alkaline phosphatase; ALT, alanine transaminase; APTT, activated partial thromboplastin time; AST, aspartate transaminase; BUN, blood urea nitrogen; Ccr, calculated creatinine clearance; CK, creatine kinase; CRP, C-reactive protein; eGFR, estimated glomerular filtration rate; FDP, fibrin/fibrinogen degradation products; LDH, lactate dehydrogenase; PT, prothrombin time; SFTS, severe fever with thrombocytopenia syndrome; γ-GT, γ-glutamyl transpeptidase.

with JSF (*10*). The patient showed no other skin eruptions besides the eschar at the site of the tick bite (Figure). It is highly possible that the eschar on this patient could have been caused by an inflammatory response induced by the local *R. japonica* infection. *R. japonica* did not induce systemic symptoms in this patient for 2 possible reasons. First, the incubation time for SFTS might be shorter than that of JSF. Second, the initiation of antimicrobial drugs in the early phase of disease might have ameliorated the clinical course of the diseases.

In conclusion, we describe a patient with a generalized SFTSV infection and a localized skin lesion caused by *R. japonica* at the site of a tick bite. This study suggests that SFTS patients with eschar at the site of a tick bite should be treated with appropriate antimicrobial drugs, such as doxycycline and minocycline.

The study was carried out partially with financial support from the Japan Agency for Medical Research and Development (AMED, 19fk0108081j and 20fk0108081j). The funders had no role in study design, data collection and analysis, decision to publish, or preparation of the manuscript.

T.F. and K.Y. contributed to clinical management and writing of the manuscript. M.S. contributed to writing of the manuscript. T.Y., T.K., and M.S. contributed to the virological diagnosis. All authors had full access to all data in the study and all take responsibility for the integrity of the data and the accuracy of the data analysis.

About the Author

Dr. Fujikawa is a chief director in the Department of General Internal Medicine, Kagawa, Mitoyo General Hospital, Japan. His research interests include general internal medicine and medical education.

References

1. Yu XJ, Liang MF, Zhang SY, Liu Y, Li JD, Sun YL, et al. Fever with thrombocytopenia associated with a novel bunyavirus in China. N Engl J Med. 2011;364:1523–32. https://doi.org/10.1056/NEJMoa1010095
2. Takahashi T, Maeda K, Suzuki T, Ishido A, Shigeoka T, Tominaga T, et al. The first identification and retrospective study of severe fever with thrombocytopenia syndrome in Japan. J Infect Dis. 2014;209:816–27. https://doi.org/10.1093/infdis/jit603
3. Kato H, Yamagishi T, Shimada T, Matsui T, Shimojima M, Saijo M, et al.; SFTS epidemiological research group-Japan. Epidemiological and clinical features of severe fever with thrombocytopenia syndrome in Japan, 2013–2014. PLoS One. 2016;11:e0165207. https://doi.org/10.1371/journal.pone.0165207
4. Yamaji K, Aonuma H, Kanuka H. Distribution of tick-borne diseases in Japan: Past patterns and implications for the future. J Infect Chemother. 2018;24:499–504. https://doi.org/10.1016/j.jiac.2018.03.012
5. Saijo M. Circulation of severe fever with thrombocytopenia syndrome virus (SFTSV) in nature: transmission of SFTSV between mammals and ticks. In: Saijo M, editor. Severe fever with thrombocytopenia syndrome. Singapore: Springer Nature Singapore Pte Ltd.; 2019. p. 151–72.
6. Yoshikawa T, Fukushi S, Tani H, Fukuma A, Taniguchi S, Toda S, et al. Sensitive and specific PCR systems for detection of both Chinese and Japanese severe fever with thrombocytopenia syndrome virus strains and prediction of patient survival based on viral load. J Clin Microbiol. 2014;52:3325–33. https://doi.org/10.1128/JCM.00742-14
7. Furuya Y, Katayama T, Yoshida Y, Kaiho I. Specific amplification of *Rickettsia japonica* DNA from clinical specimens by PCR. J Clin Microbiol. 1995;33:487–9. https://doi.org/10.1128/JCM.33.2.487-489.1995
8. Fukuma A, Fukushi S, Yoshikawa T, Tani H, Taniguchi S, Kurosu T, et al. Severe fever with thrombocytopenia syndrome virus antigen detection using monoclonal antibodies to the nucleocapsid protein. PLoS Negl Trop Dis. 2016;10:e0004595. https://doi.org/10.1371/journal.pntd.0004595
9. Uchiyama T, Zhao L, Yan Y, Uchida T. Cross-reactivity of Rickettsia japonica and Rickettsia typhi demonstrated by immunofluorescence and Western immunoblotting. Microbiol Immunol. 1995;39:951–7. https://doi.org/10.1111/j.1348-0421.1995.tb03298.x
10. Mahara F. Japanese spotted fever: report of 31 cases and review of the literature. Emerg Infect Dis. 1997;3:105–11. https://doi.org/10.3201/eid0302.970203

Address for correspondence: Tatsuya Fujikawa, Department of General Internal Medicine, Mitoyo General Hospital, 708 Himehama Toyohama, Kanonji, Kagawa 769-1695, Japan; email: tfujikawa-gi@umin.ac.jp

Imported SARS-CoV-2 Variant P.1 in Traveler Returning from Brazil to Italy

Fabrizio Maggi, Federica Novazzi, Angelo Genoni, Andreina Baj, Pietro Giorgio Spezia, Daniele Focosi, Cristian Zago, Alberto Colombo, Gianluca Cassani, Renee Pasciuta, Antonio Tamborini, Agostino Rossi, Martina Prestia, Riccardo Capuano, Lorenzo Azzi, Annalisa Donadini, Giuseppe Catanoso, Paolo Antonio Grossi, Lorenzo Maffioli, Gianni Bonelli

Author affiliations: ASST Sette Laghi, Varese, Italy (F. Maggi, F. Novazzi, A. Baj, C. Zago, A. Colombo, G. Cassani, R. Pasciuta, A. Tamborini, A. Rossi, M. Prestia, R. Capuano, L. Azzi, P.A. Grossi, L. Maffioli, G. Bonelli); University of Insubria, Varese (F. Maggi, A. Genoni, A. Baj, P.A. Grossi); University of Pisa, Pisa, Italy (P.G. Spezia); North-Western Tuscany Blood Bank, Pisa (D. Focosi); ATS Insubria, Varese (A. Donadini, G. Catanoso)

DOI: https://doi.org/10.3201/eid2704.210183

We report an imported case of severe acute respiratory syndrome coronavirus 2 (SARS-CoV-2) variant P.1 detected in an asymptomatic traveler who arrived in Italy on an indirect flight from Brazil. This case shows the risk for introduction of SARS-CoV-2 variants from indirect flights and the need for continued SARS-CoV-2 surveillance.

Severe acute respiratory syndrome coronavirus 2 (SARS-CoV-2) variant P.1 currently is causing a major outbreak of coronavirus disease (COVID-19) in the Amazonas province of Brazil (N.R. Faria et al., unpub. data, https://virological.org/t/genomic-characterisation-of-an-emergent-sars-cov-2-lineage-in-manaus-preliminary-findings/586). The P.1 variant also is known as B.1.1.28 in the Phylogenetic Assignment of Named Global Outbreak Lineages (https://cov-lineages.org/pangolin.html) and as 20J/501Y.V3 in NextStrain (https://nextstrain.org). Preliminary reports have associated several spike protein mutations harbored in the P.1 variant with escape from neutralizing monoclonal antibodies (mAb) and P.1 was detected in convalescent serum collected during previous epidemic waves (Z. Liu et al., unpub. data, https://www.biorxiv.org/content/10.1101/2020.11.06.372037v1; S. Jangra et al., unpub. data, https://www.medrxiv.org/content/10.1101/2021.01.26.21250543v1).

The B.1.1.28 lineage emerged in Brazil during February 2020, and 2 subclades recently evolved separately (C.M. Voloch et al., unpub. data, https://doi.org/10.1101/2020.12.23.20248598; N.R. Faria, et al., unpub. data, https://virological.org/t/genomic-characterisation-of-an-emergent-sars-cov-2-lineage-in-manaus-preliminary-findings/586). During January 2021, SARS-CoV-2 variant P.1 was reported in 4 travelers returning to Japan from Amazonas state in Brazil (*1*). The strain identified in the travelers was associated with E484K, K417N, and N501Y mutations as noted in the the B.1.351 line 20I/501.V2 clade of South African lineage (*1*). In addition, 1 case of reinfection has been documented months after a B.1 primary infection (F. Naveca et al., unpub. data, https://virological.org/t/sars-cov-2-reinfection-by-the-new-variant-of-concern-voc-p-1-in-amazonas-brazil/596). Another lineage, P.2, was reported in Rio de Janeiro, Brazil, but has been associated with spike mutations only in E484K; ≥2 cases of reinfection have been documented several months after primary B.1.1.33 infections (P. Resende et al., unpub. data, https://virological.org/t/spike-e484k-mutation-in-the-first-sars-cov-2-reinfection-case-confirmed-in-brazil-2020/584; C.K. Vasques Nonaka et al., unpub. data, https://doi.org/10.20944/preprints202101.0132.v1). Among the spike mutations, E484K is considered the main driver of immune evasion to mAbs and convalescent serum (A.J. Greaney et al., unpub. data, https://doi.org/10.1101/2020.12.31.425021). Of note, many of the most potent mRNA vaccine-elicited mAbs were 3- to 10-fold less effective at neutralizing pseudotyped viruses carrying E484K (K. Wu et al., unpub. data, https://doi.org/10.1101/2021.01.25.427948), which has unknown implications for protection. We report an asymptomatic traveler from Brazil who tested positive for the SARS-CoV-2 P.1 variant in a screening nasopharyngeal swab sample.

After visiting São Paulo, Brazil, during November 23, 2020–January 16, 2021, a family, including a 33-year-old man, his 38-year-old wife, and his 7-year-old daughter, flew back to their home in Italy. During their time in Brazil, the family did not travel outside of São Paulo, which is >2,000 miles from Amazonas. The family took an indirect return flight; they flew from São Paulo/Guarulhos International Airport in Brazil to Madrid, Spain, and from there flew to Milan Malpensa Airport in Italy. Molecular tests were performed on all 3 family members at the departure airport in Brazil, and all were SARS negative.

The family arrived in Milan on the afternoon of January 17 and took a train and a car to their home, 30 miles from Milan. Under current recommendations in Italy, all persons entering the country can decide to be screened for SARS-CoV-2. After consulting a general practitioner on January 21, the father went to the hospital for a screening nasopharyngeal swab sample. The sample was tested by using the Alinity platform (Abbott, https://www.abbott.com), which returned a positive result for SARS-CoV-2 RNA with a cycle threshold of 23. Reverse transcription PCR (RT-PCR) fragments corresponding to the receptor-binding domain (RBD) in the spike gene of SARS-CoV-2 were amplified from purified viral RNA by using a OneStep RT-PCR Kit (QIAGEN, https://www.qiagen.com). We used a reference sequence from GSAID (https://www.gisaid.org; accession no. EPI_ISL_402124) and

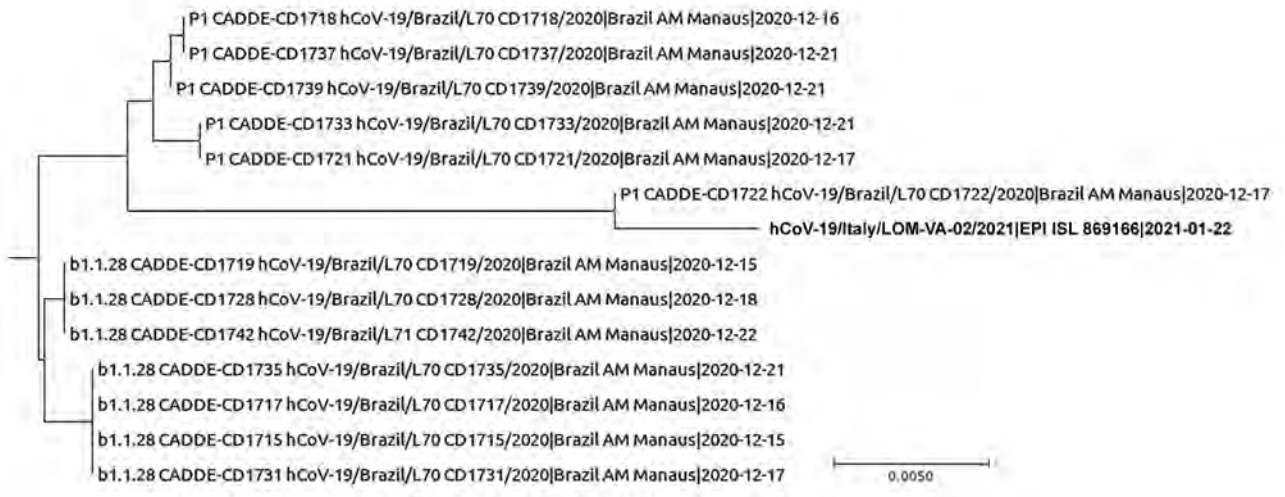

Figure. Phylogenetic tree of severe acute respiratory syndrome coronavirus 2 variant P.1 sequences from a male traveler returning from Brazil to Italy and reference sequences from Brazil. Bold text indicates sequence from the traveler. Scale bar indicates nucleotide substitutions per site.

nucleotide sequences of primer sets to map genome locations (Figure; Appendix, https://wwwnc.cdc.gov/EID/article/27/4/21-0183-App1.pdf). The sequence of RBD from the patient included the P.1 barcoding mutations K417T, E484K, and N501Y. We deposited these data in GenBank (accession no. MW517286) and GISAID (accession no. EPI-ISL-869166).

SARS-CoV-2 variant P.1 is characterized by K417N, but K417T also has been reported in several cases before our patient (*1*), suggesting ongoing evolution. On January 22, 2021, after we reported the sequencing results, the patient was admitted to the infectious and tropical diseases unit of ASST dei Sette Laghi–Ospedale di Circolo e Fondazione Macchi (Varese, Italy) for observation. The patient remained asymptomatic and was discharged on January 29. The patient's spouse also tested positive for SARS-CoV-2 RNA via a nasopharyngeal swab sample. Antibody tests conducted by using Liaison Analyzer (DiaSorin, https://www.diasorin.com) were negative for SARS-CoV-2 S1/S2 IgG in serum of both the man and his wife, suggesting a primary infection.

Direct flights from Brazil to Italy were canceled upon the unilateral decision of the government of Italy on January 16, 2021, but our findings confirm the risk for introducing SARS-CoV-2 variants from indirect flights if no surveillance measures are implemented at arrival. This case also suggests wider circulation of SARS-CoV-2 variant P.1 in areas other than Amazonas in Brazil. P.1-specific primer sets recently have been designed (A. Lopez-Rincon et al., unpub. data, https://doi.org/10.1101/2021.01.20.427043) and will aid in development of large-scale screening programs for this variant.

About the Author

Prof. Maggi is on the Faculty of Medicine at the University of Insubria and directs the Virology Unit of Ospedale di Circolo and Fondazione Macchi in Varese, Lombardia, Italy. His primary research interest is emerging viral pathogens.

Reference

1. National Institute of Infectious Diseases, Japan. Brief report: new variant strain of SARS-CoV-2 identified in travelers from Brazil. 2021 Jan 21 [cited 2021 Jan 27]. https://www.niid.go.jp/niid/images/epi/corona/covid19-33-en-210112.pdf

Address for correspondence: Andreina Baj and Fabrizio Maggi, University of Insubria Faculty of Medicine and Surgery, Varese, Italy; email: andreina.baj@uninsubria.it and fabrizio.maggi@uninsubria.it

Understanding Coronavirus

Raul Rabadan; Cambridge University Press, Cambridge, UK, 2020; ISBN 9781108826716 (paperback); ISBN 9781108920254 (e-book); Pages: 136; Price: $11.99 (paperback); $8.99 (e-book)

DOI: https://doi.org/10.3201/eid2704.210152

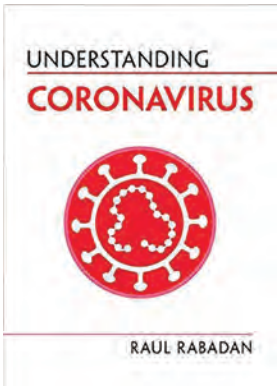

Accounts of pandemic illness are found throughout history (*1*). Despite advances in scientific knowledge and medical resources, society found itself repeating history with the global coronavirus pandemic. Though we have learned much about severe acute respiratory syndrome coronavirus 2 (SARS-CoV-2), many facts remain unknown and questions unanswered. In an age when information is easily shared globally, a demand for intelligent, understandable, and unbiased information exists, without which society experiences (and social media spreads) confusion, anxiety, and possibly panic.

Raul Rabadan, a professor at Columbia University and an expert and leading researcher in the field of genomics and systems biology, sought to provide much-needed accurate information. Understanding Coronavirus is a concise look at the recent history and epidemiologic, immunologic, and scientific concepts related to the pandemic. Organized as a series of questions and answers, his new book discusses many hot topics. Rabadan uses questions such as "How do we track back the origin of SARS-CoV-2?" to review the biology and epidemiology of coronavirus, the evolution and transmission of SARS-CoV-2, and key concepts involved in the ongoing pandemic and to offer comparison to previous pandemics, as well as those treatment and prevention options known at the time of publication.

Helping the reader to better understand viruses, Rabadan describes the basics of their biologic structures, origin, evolution, and spread in the first 4 chapters. He seeks to answer questions such as "What is a coronavirus?" and "How does the coronavirus enter cells and replicate?" Although he simplifies concepts as much as possible through illustrations and figures, it may still be a difficult read for those with little background knowledge.

Chapter 5 details the coronavirus disease (COVID-19) outbreak by explaining the symptoms, at-risk populations, infection-fatality rate, case-fatality rates, and mortality rates. Other chapters are devoted to comparing and contrasting COVID-19 with the 2002–2003 severe acute respiratory syndrome outbreak and pandemic influenza, in particular the 1918 Spanish influenza. This historical information provides a sobering reminder that what is occurring is not unique to our generation. At the time the disease was beginning to spread in the United States, comparisons of coronavirus disease to seasonal influenza focused on similarities as contagious respiratory illnesses; further information revealed many differences between COVID-19 and influenza (*2*).

The text concludes with a summary of common misunderstandings and suggestions for further reading for those interested in learning more about specific topics. We particularly liked the summary of common misunderstandings, which offers clear, straightforward answers to prevalent misinformation. However, the section "Updates at Press" could be improved by providing more context and citing specific sources for each finding.

Overall, Understanding Coronavirus is a well-written, well-organized, and informative book that would appeal to a broad range of readers, including epidemiologists, public health workers, university and medical students, physicians, and others interested in public health. Although the book lacks current details about treatment and vaccines, the scientific foundations introduced will be of great benefit for conceptualizing the pandemic now and in the future.

References

1. History. Pandemics that changed history. January 30, 2020 [cited 2021 Jan 6]. https://www.history.com/topics/middle-ages/pandemics-timeline
2. Maragakis LL. Coronavirus disease 2019 vs. the flu. Johns Hopkins Medicine [cited 2021 Jan 6]. https://www.hopkinsmedicine.org/health/conditions-and-diseases/coronavirus/coronavirus-disease-2019-vs-the-flu

Xin Yin, Nicole M. Hackman

Author affiliations: Pennsylvania State University College of Medicine, Hershey, Pennsylvania, USA (X. Yin, N.M. Hackman)

Address for correspondence: Nicole M. Hackman, Department of Pediatrics, Pennsylvania State University College of Medicine, 500 University Dr, Hershey, PA, 17033, USA; email: nhackman@pennstatehealth.psu.edu

Johan Christian Dahl (1788–1857), *Eruption of the Volcano Vesuvius*, 1821. Oil on canvas, 38.7 in × 54.1 in/98.3 cm × 137.5 cm. Public domain digital image courtesy of National Gallery of Denmark, Sølvgade 48–50, 1307 Copenhagen, Denmark.

An Interesting and Horribly Wondrous Sight

Byron Breedlove

Volcanoes—active, dormant, and extinct—are found on every continent on Earth. Many lay submerged below the oceans, and others exist as islands. Volcanic explosions, upheavals, and lava flows, coupled with eons of weathering, have formed mountains and plateaus, created craters, and etched valleys. Approximately 80 percent of Earth's surface was created by volcanic activity. The United States Geological Survey notes, "Gaseous emissions from volcanic vents over hundreds of millions of years formed the Earth's earliest oceans and atmosphere, which supplied the ingredients vital to evolve and sustain life."

Ancient to modern eyewitness accounts document the devastation and spectacle associated with volcanic eruptions. For centuries, artists have depicted in their works both the sublime beauty and unthinkable destruction of volcanic eruptions. Among them is the Norwegian painter Johan Christian Claussen Dahl. Considered the first great Romantic painter in Norway and among the greatest European artists of all time, Dahl traveled to Italy during the fall of 1820. He visited Naples in late December of that year and observed firsthand Vesuvius erupting, an event he called an "interesting and horribly wondrous sight." This month's cover image, *Eruption of the Volcano Vesuvius, 1821,* is the first in a series of paintings he created after that experience.

Dahl's up-close portrayal reverses the more common artistic perspective of placing volcanoes in the background. In this painting, clouds of smoke and steam flecked with lava billow and whirl skyward from the glowing red fissures and caldera of Mount Vesuvius, obscuring much of the sky and water in the

Author affiliation: Centers for Disease Control and Prevention, Atlanta, Georgia, USA

DOI: https://doi.org/10.3201/eid2704.AC2704

left half of the painting. Near the edge of the crater, a pair of visitors (perhaps one represents Dahl) appear as tiny silhouettes and convey a sense of scale. A panoramic view of Naples receding in the background and hugging the shore of its namesake gulf in the Mediterranean Sea fills the right side of the painting. More mountain ridges rise and jut into the bay under a panoramic, calm sky. Nearly hidden in the foreground, a local guide waits and watches, clutching the tethers of a pair of donkeys.

Art historian Maia Heguiaphal writes, "The vast smoke coming out of the incandescent lava immediately attracts the viewer's eyes, but the background of the volcano intensifies the effect of destruction carried by the eruption. Dahl makes us see the landscape that the volcano will destroy: The lava flows in its direction. We are therefore confronted with the imminent destruction of idyllic nature."

Worldwide, approximately 1,500 volcanoes are potentially active, and on any given day, about a dozen may be erupting. The World Health Organization estimates that during 1998–2017, volcanic activities and the wildfires they spawned affected 6.2 million people and caused nearly 2,400 deaths. Geosciences professor Erik Klemetti notes, "With our modern ability to monitor volcanoes in many remote locations thanks to satellites, and the speed with which news travels around the globe today, an eruption that might have gone unnoticed 100 years ago is bound to make headlines in 2018. The world is not more volcanically active, we're just more volcanically aware."

Volcanic eruptions are among the most dramatic, unpredictable, and dangerous threats from Mother Nature. But unseen threats, arriving more stealthily via emerging and reemerging high-consequence pathogens, are much more deadly. High-consequence pathogens cause diseases that typically have a high case-fatality rate, are often difficult to recognize and detect rapidly, may spread rapidly and cause epidemics, and lack effective measures for prophylaxis or treatment. For example, the 2014–2016 Ebola outbreak in West Africa alone caused more than 11,000 deaths.

Among the diseases caused by high-consequence pathogens are Middle East respiratory syndrome, Nipah virus infection, monkeypox, and a cluster of hemorrhagic fever diseases (in addition to Ebola, including Marburg hemorrhagic fever, Crimean-Congo hemorrhagic fever, and Rift Valley fever). Such pathogens are also responsible for many diseases that have been known for centuries, such as anthrax, melioidosis, rabies, and smallpox.

Although many pathogenic agents may be circulating at any given time, disease outbreaks (or even small numbers of cases) caused by high-consequence pathogens can have serious public health, economic, and even security consequences. That point is underscored by the current COVID-19 pandemic. Although the case-fatality rate associated with SARS-CoV-2 infection is lower than that of many other viruses (i.e., is less deadly at the individual level), the enormous number of persons infected and the ability of SARS-CoV-2 to spread rapidly results in many more deaths.

CDC-based scientists Belay and Monroe state that "ongoing surveillance and public health research of high-consequence pathogens are critical for identifying their natural reservoirs, developing diagnostic tests, and devising appropriate control and prevention measures." Though the world is now more pathogenically aware than ever before, high-consequence pathogens are, like volcanoes, predictably unpredictable, and they are an ongoing public health concern.

Bibliography

1. Belay ED, Monroe SS. Low-incidence, high-consequence pathogens. Emerg Infect Dis. 2014;20:319–21. https://doi.org/10.3201/eid2002.131748
2. Centers for Disease Control and Prevention. Division of High Consequence Pathogens and Pathology [cited 2021 Feb 8] https://www.cdc.gov/ncezid/dhcpp/index.html
3. European Centre for Disease Prevention and Control. Health emergency preparedness for imported cases of high-consequence infectious diseases. Stockholm: The Centre; 2019 [cited 2021 Feb 17]. https://www.ecdc.europa.eu/sites/default/files/documents/Health-emergency-preparedness-imported-cases-of-high-consequence-infectious-diseases.pdf
4. Heguiaphal M. When Romanticism meets eruptions: volcanoes in paintings. Daily Art Magazine [cited 2021 Feb 4]. https://www.dailyartmagazine.com/volcanoes-in-paintings
5. Klemetti E. Five myths about volcanoes. Washington Post [cited 2021 Feb 8]. https://www.washingtonpost.com/outlook/five-myths/five-myths-about-volcanoes/2018/05/23/9d18fea6-5e07-11e8-9ee3-49d6d4814c4c_story.html
6. National Gallery of Denmark. Eruption of the volcano Vesuvius, 1821, J.C. Dahl [cited 2021 Feb 17]. https://www.smk.dk/en/highlight/eruption-of-the-volcano-vesuvius-1821
7. United States Geological Survey. How much of the Earth is volcanic? [cited 2021 Feb 2]. https://www.usgs.gov/faqs/how-much-earth-volcanic?qt-news_science_products=0#qt-news_science_products
8. United States Geological Survey. Volcano hazards program. About volcanoes [cited 2021 Feb 2]. https://www.usgs.gov/natural-hazards/volcano-hazards/about-volcanoes
9. Wei-Haas M. Volcanoes, explained. National Geographic [cited 2021 Feb 2]. https://www.nationalgeographic.com/environment/natural-disasters/volcanoes
10. World Health Organization. Volcanic eruptions [cited 2021 Feb 4]. https://www.who.int/health-topics/volcanic-eruptions#tab=tab_1

Address for correspondence: Byron Breedlove, EID Journal, Centers for Disease Control and Prevention, 1600 Clifton Rd NE, Mailstop H16-2, Atlanta, GA 30329-4027, USA; email: wbb1@cdc.gov

EMERGING INFECTIOUS DISEASES®

Upcoming Issue

- Coccidioidomycosis and COVID-19 Co-Infection, United States, 2020
- Successful Control of an Onboard COVID-19 Outbreak Using the Cruise Ship as a Quarantine Facility, Western Australia
- Active Case Finding of Current Bornavirus Infections in Human Encephalitis Cases of Unknown Etiology, Germany, 2018–2020
- Serologic Screening of Severe Acute Respiratory Syndrome Coronavirus 2 Infection in Cats and Dogs during First Coronavirus Disease Wave, the Netherlands
- SARS-CoV-2 Susceptibility of Cell Lines and Substrates Commonly Used in Diagnosis and Isolation of Influenza and Other Viruses
- Symptom Diary–Based Analysis of COVID-19 Disease Course, Germany, 2020
- Prevalence and Clinical Profile of Severe Acute Respiratory Syndrome Coronavirus 2 Infection among Farmworkers, California, June–November 2020
- Herd Immunity against Severe Acute Respiratory Syndrome Coronavirus 2 Infection in 10 Communities, Qatar
- Monitoring SARS-CoV-2 Circulation and Diversity through Community Wastewater Sequencing, the Netherlands and Belgium
- Characteristics and Clinical Implications of Carbapenemase-Producing *Klebsiella pneumoniae* Colonization and Infection, Italy
- Epidemiologic History and Genetic Diversity Origins of Chikungunya and Dengue Viruses, Paraguay
- Use of Genomics to Track Coronavirus Disease Outbreaks, New Zealand
- Global Trends in Norovirus Genotype Distribution among Children with Acute Gastroenteritis
- Longevity of Middle East Respiratory Syndrome Coronavirus Antibody Responses in Patients, Saudi Arabia
- Whole-Genome Sequencing of Shiga Toxin–Producing *Escherichia coli* OX18 from a Fatal Hemolytic Uremic Syndrome Case
- Introduction of ORF3a-Q57H SARS-CoV-2 Variant Causing Fourth Epidemic Wave of COVID-19, Hong Kong, China
- Racial and Ethnic Disparities in Incidence of SARS-CoV-2 Infection, 22 US States and DC, January 1–October 1, 2020
- Detecting COVID-19 Clusters at High Spatiotemporal Resolution, New York City, NY, USA, June–July 2020
- Prescribing Antimicrobial Drugs for Acute Gastroenteritis, Primary Care, Australia, 2013–2018
- Severe Acute Respiratory Syndrome Coronavirus 2 Serial Interval Variation, Montana, USA, March 1–July 31, 2020
- Upper Respiratory Infections in Schools and Childcare Centers Reopening after COVID-19 Dismissals, Hong Kong
- Undocumented Migrants Reintroducing COVID-19, Yunnan Province, China
- Genomic Evidence of SARS-CoV-2 Reinfection Involving E484K Spike Mutation, Brazil

Complete list of articles in the May issue at http://www.cdc.gov/eid/upcoming.htm

Earning CME Credit

To obtain credit, you should first read the journal article. After reading the article, you should be able to answer the following, related, multiple-choice questions. To complete the questions (with a minimum 75% passing score) and earn continuing medical education (CME) credit, please go to http://www.medscape.org/journal/eid. Credit cannot be obtained for tests completed on paper, although you may use the worksheet below to keep a record of your answers.

You must be a registered user on http://www.medscape.org. If you are not registered on http://www.medscape.org, please click on the "Register" link on the right hand side of the website.

Only one answer is correct for each question. Once you successfully answer all post-test questions, you will be able to view and/or print your certificate. For questions regarding this activity, contact the accredited provider, CME@medscape.net. For technical assistance, contact CME@medscape.net. American Medical Association's Physician's Recognition Award (AMA PRA) credits are accepted in the US as evidence of participation in CME activities. For further information on this award, please go to https://www.ama-assn.org. The AMA has determined that physicians not licensed in the US who participate in this CME activity are eligible for AMA PRA Category 1 Credits™. Through agreements that the AMA has made with agencies in some countries, AMA PRA credit may be acceptable as evidence of participation in CME activities. If you are not licensed in the US, please complete the questions online, print

Article Title

Blastomycosis Surveillance in 5 States, United States, 1987–2018

CME Questions

1. You are advising a public health department in Wisconsin regarding anticipated cases of blastomycosis. According to the analysis by Benedict and colleagues of combined 1987–2018 surveillance data from the 5 states where blastomycosis is reportable, which of the following statements about epidemiologic features of blastomycosis is correct?

A. Mean annual incidence was < 1 case/100,000 population in most areas and > 20 cases/100,000 in some northern Wisconsin counties
B. Most patients were female, aged > 65 years, and White
C. Incidence increased in all 5 states during 2007–2017 (years with data available from all 5 states)
D. Most cases were associated with spring outbreaks

2. According to the analysis by Benedict and colleagues of combined 1987–2018 surveillance data from the 5 states where blastomycosis is reportable, which of the following statements about clinical features of blastomycosis is correct?

A. One-quarter of patients were hospitalized and 4% died
B. Median time from symptom onset to diagnosis was 12 days
C. Chest pain was the most common symptom
D. Factors significantly associated with death were older age (median 61 vs 44 years; P < .001) and positive microscopy test (relative risk [RR] = 1.76 [95% CI: 1.34, 2.38])

3. According to the analysis by Benedict and colleagues of combined 1987–2018 surveillance data from the five states where blastomycosis is reportable, which of the following statements about public health and clinical implications of the epidemiologic and clinical features of blastomycosis is correct?

A. Surveillance is likely to reflect the true number of cases
B. More in-depth surveillance in additional states would help improve understanding of blastomycosis and inform strategies to increase clinician and public awareness
C. Blastomycosis is limited to the states where reporting is required
D. Currently available diagnostic methods for blastomycosis are sufficient for optimal case detection

Earning CME Credit

To obtain credit, you should first read the journal article. After reading the article, you should be able to answer the following, related, multiple-choice questions. To complete the questions (with a minimum 75% passing score) and earn continuing medical education (CME) credit, please go to http://www.medscape.org/journal/eid. Credit cannot be obtained for tests completed on paper, although you may use the worksheet below to keep a record of your answers.

You must be a registered user on http://www.medscape.org. If you are not registered on http://www.medscape.org, please click on the "Register" link on the right hand side of the website.

Only one answer is correct for each question. Once you successfully answer all post-test questions, you will be able to view and/or print your certificate. For questions regarding this activity, contact the accredited provider, CME@medscape.net. For technical assistance, contact CME@medscape.net. American Medical Association's Physician's Recognition Award (AMA PRA) credits are accepted in the US as evidence of participation in CME activities. For further information on this award, please go to https://www.ama-assn.org. The AMA has determined that physicians not licensed in the US who participate in this CME activity are eligible for AMA PRA Category 1 Credits™. Through agreements that the AMA has made with agencies in some countries, AMA PRA credit may be acceptable as evidence of participation in CME activities. If you are not licensed in the US, please complete the questions online, print

Article Title

Systematic Review of Reported HIV Outbreaks, Pakistan, 2000–2019

CME Questions

1. Which of the following groups has the highest prevalence of human immunodeficiency virus (HIV) infection in Pakistan?

A. Transgender people
B. People who inject drugs
C. Men who have sex with men
D. General population

2. Which of the following was the most common cause of HIV outbreaks in Pakistan in the current study?

A. Increasing homelessness
B. Unsafe healthcare practices
C. Reduced availability of condoms
D. Increasing contact with sex workers

3. Which of the following statements regarding limitations on reports of outbreaks of HIV infection in Pakistan is most accurate?

A. All authors were directly affiliated with the primary data
B. 20% of authors used media reports as a primary source of information
C. All 7 outbreaks included a detailed investigation
D. Most reports included phylogenetic data on HIV infection

4. All of the following variables might help contribute to unsafe injection practices in Pakistan except:

A. Patient preference for oral medications
B. Financial incentives for providers
C. No monitoring to ensure safe injection practices
D. Injectable medicines accessible without a prescription

Earning CME Credit

To obtain credit, you should first read the journal article. After reading the article, you should be able to answer the following, related, multiple-choice questions. To complete the questions (with a minimum 75% passing score) and earn continuing medical education (CME) credit, please go to http://www.medscape.org/journal/eid. Credit cannot be obtained for tests completed on paper, although you may use the worksheet below to keep a record of your answers.

You must be a registered user on http://www.medscape.org. If you are not registered on http://www.medscape.org, please click on the "Register" link on the right hand side of the website.

Only one answer is correct for each question. Once you successfully answer all post-test questions, you will be able to view and/or print your certificate. For questions regarding this activity, contact the accredited provider, CME@medscape.net. For technical assistance, contact CME@medscape.net. American Medical Association's Physician's Recognition Award (AMA PRA) credits are accepted in the US as evidence of participation in CME activities. For further information on this award, please go to https://www.ama-assn.org. The AMA has determined that physicians not licensed in the US who participate in this CME activity are eligible for AMA PRA Category 1 Credits™. Through agreements that the AMA has made with agencies in some countries, AMA PRA credit may be acceptable as evidence of participation in CME activities. If you are not licensed in the US, please complete the questions online, print the AMA PRA CME credit certificate, and present it to your national medical association for review.

Article Title

CME Questions

1. Which of the following statements regarding ticks assessed in the current study is most accurate?

A. >99% of ticks collected were *Ixodes ricinus*
B. The most common developmental stage was adult
C. Most ticks were male
D. Most patients collected >1 tick

2. Which of the following statements regarding molecular screening of ticks in the current study is most accurate?

A. ≈60% of ticks examined harbored a tickborne pathogen (TBP)
B. *Borrelia burgdorferi* was detected in 15% of ticks
C. *B. burgdorferi* sensu stricto was the most common genospecies isolated in the current series
D. *Rickettsia* spp. was the most common TBP isolated

3. What approximate percentage of patients in the current series with tick bites were positive for *Borrelia* infection?

A. 0.1%
B. 1%
C. 5%
D. 17%

4. Which of the following variables was most associated with a significantly higher risk for *Borrelia* infection in the current study?

A. Female sex and older age
B. Older age and tick bite on the head or neck
C. A higher number of ticks and confirmation of *Borrelia* infection in ticks
D. Tick engorgement and confirmation of *Borrelia* infection in ticks